Horák Jiří
Hlásny Tomáš
Růžička Jan
Halounová Lena
Čerba Otakar (Eds.)

GIS Ostrava 2011

Eight International Symposium
Ostrava, Czech Republic, January 2011
Proceedings

Auspices

International Society of Photogrammetry and Remote Sensing
Czech Association for Geoinformation
Slovak Association for Geoinformatics

HORAK Jiri, HLASNY Tomas, RUZICKA Jan, HALOUNOVA Lena, CERBA Otakar
(Eds.)

GIS Ostrava 2011, Eight International Symposium, Proceedings

Ostrava, Czech Republic

January 24th - 26th 2011

Auspices
International Society of Photogrammetry and Remote Sensing
Czech Association for Geoinformation
Slovak Association for Geoinformatics

VŠB - Technical University of Ostrava

Editors

Jiri Horak
VSB - Technical University of Ostrava
Faculty of Mining and Geology
Institute of Geoinformatics
17. listopadu 15, 708 33 Ostrava 8, Czech Republic
jiri.horak@vsb.cz

Tomas Hlasny
National Forest Centre
Forest Research Institute
T. G. Masaryka 22, 960 92 Zvolen, Slovak Republic
hlasny@nlcsk.org

Jan Ruzicka
VSB - Technical University of Ostrava
Faculty of Mining and Geology
Institute of Geoinformatics
17. listopadu 15, 708 33 Ostrava 8, Czech Republic
jan.ruzicka@vsb.cz

Lena Halounova
Czech Technical University in Prague
Faculty of Civil Engineering
Department of Mapping and Cartography
Thakurova 7, 166 29 Prague 6, Czech Republic
halounov@fsv.cvut.cz

Otakar Cerba
University of West Bohemia in Plzen
Faculty of Applied Sciences
Department of Mathematics
Univerzitni 8, 306 14 Plzen, Czech Republic
ota.cerba@seznam.cz

Cover design: Petr Vavroš
Technical editing, typesetting: Katerina Sanetrnikova, Peter Bobaľ

Production:

Institute of Geoinformatics
VSB - Technical University of Ostrava
17.listopadu 15
708 33 Ostrava-Poruba
Czech Republic
dagmar.adamkova@vsb.cz

ISBN 978-80-248-2406-2

GIS Ostrava 2011, Eight International Symposium, Proceedings

January 24th - 26th 2011, Ostrava, Czech Republic

Printed by:	VŠB - TU Ostrava, 17.listopadu 15, 708 00 Ostrava 8, Czech Republic
Bound by:	OFTIS Ostrava, Chelčického 693/7, 702 00 Ostrava, Czech Republic
Edition:	First edition, 2011
Number of pages:	435

Preface

GIS Ostrava 2011 was the 18th event of the series of conferences and symposia held in Ostrava in the fields of geographical information systems, geoinformatics, geomatics, remote sensing and spatial modelling. The aim of the symposia is to provide an international forum for presenting and discussing results of the latest research. The symposium was organised in four main research workshops, a national application session and accompanying events.

The workshop “Advances in Remote Sensing” was concentrated on new methods, new data, new sensors, and new applications in remote sensing. The new methods are focused on synergy effect of different data types including GIS data to bring new tools for analysis of complex tasks in studying mutual relations among natural changes, global changes, anthropogenetical influence, etc. New data types and new sensors can present advances in application of spectral imaging, polarimetry, interferometry and/or optical and microwave remote sensing for land use/land cover performed from, forestry, agriculture, geology, risk/hazard management, hydrology/wetlands, etc.

The workshop “Advances in Spatial Modelling” was aimed at delivering the recent knowledge about the advances in spatial analyses and modelling, emphasizing the benefits of Geographic Information Science. Three sections included theoretical aspects of spatial modelling, applied environmental modelling, and socio-economy and technical systems modelling. The first section focused on new methods in spatial statistics, geostatistics, spatio-temporal modelling, relief analysis and other fields of spatial science. The Applied Environmental Modelling section focused on case studies on climatology, hydrology and water management, forestry and agriculture, landscape ecology, etc. Social-economy and technical systems section primarily aims at urban geography, transportation, mining industry, oil and gas industry.

The aim of the workshop “Geoinformation technologies Challenges” was to bring together experts of geoinformation technologies that are interested in design and development of geoinformation technologies and technical background necessary for making geoinformation technologies more efficient. The workshop was mainly focused on systems' interoperability that allows system integration inside an enterprise or across countries including closed source software, open source software, open languages, open standards, efficiency of the systems, technologies for speeding up current software and improving software reliability.

The workshop “Harmonization and Integration Tools supporting INSPIRE implementation” was focused on description of selected tools intended for modification of spatial data and its model to be compliant with requirements of INSPIRE directive. Introduced tools were mostly developed within the scope of European project (e.g. Humboldt).

Authors registered almost 110 papers. Part of them (44 papers) was invited for reviewing process. Each paper was peer reviewed by the members of programming committee and external reviewers. Finally only 30 papers were selected for publication in these proceedings.

The proceedings cover the following topics: spatial data alignment, data modelling, spatial data harmonisation, edge-matching polygons using a constrained triangulation, generalization, cadastral data model, spatial data infrastructure, catalogue services, crowdsourcing, spatial planning, spatial data mining, landform classification, digital elevation models, geomorphological analysis, terrain analysis, visibility analysis, historical georelief reconstruction, design of model mesh, cellular automata for flow simulation, flood hazard assessment, simulation of avalanches, risk mapping, spatial interpolation, spatial measures of segregation, fractal analysis of urban growth and land cover, archaeological predictive modelling, spatial epidemiology, ontology design, multi-agent system, intelligent transport system, traffic simulation on intersections, mine image transformation, assessment of chlorophyll-a concentration, variables influencing radar based precipitation, differential radar interferometry, image segmentation and hyperspectral data.

We would like to thank International Society for Photogrammetry and Remote Sensing, Czech Association for Geoinformation and Slovak Association for Geoinformatics for their auspices.

Our special thanks go to Ivo Vondrák (rector of the VSB-Technical University of Ostrava), Vladimír Slivka (dean of the Faculty of Mining and Geology, VSB-TU Ostrava), Jaroslav Palas (president of the Moravian-Silesian Region) and Gottfried Konecny (emeritus professor of the Hannover University) for their kind support.

We cordially thank to the members of programming committee and additional external reviewers for their effort in the selection of best contributions and demanding reviewing process which will help us to provide to our audience best oral presentations and selected papers for these proceedings.

Finally we would like to thank to our sponsors for their substantial support and thank all participants to create friend and collaborative atmosphere promoting a fruitful discussion and knowledge sharing.

Jiří Horák

Program Committee

Jiri Horak	VSB-Technical University Ostrava, Czech Republic
Branislav Bajat	University of Belgrade, Serbia
Rolf de By	ITC Enschede, Netherlands
Ales Cepek	Czech Technical University Prague, Czech Republic
Otakar Cerba	University of West Bohemia, Czech Republic
Daniela Durakova	VSB-Technical University Ostrava, Czech Republic
Filip Hajek	Forest Management Institute, Frydek-Mistek, Czech Republic
Lena Halounova	Czech Technical University Prague, Czech Republic
Anneli Heimbürger	University of Jyväskylä, Finland
Tomas Hlasny	National Forest Centre Zvolen, SAGI, Slovakia
Jaroslav Hofierka	University of Presov, Slovakia
Bronislava Horakova	INTERGRAPH CS, Czech Republic
Christine Giger	ETH Zurich, Switzerland
Karel Charvat	Czech Centre for Science and Society, Czech Republic
Karel Janecka	University of West Bohemia, Czech Republic
Jaromir Kolejka	Masaryk University Brno, Czech Republic
Gottfried Konecny	Leibniz University, Hannover, Germany
Miroslav Kozuch	Komensky University, Bratislava, Slovakia
Petr Kubicek	Masaryk University Brno, Czech Republic
Dagmar Kusendova	Komensky University, Bratislava, SAGI, Slovakia
Csaba Matyas	University of West Hungary, Sopron, Hungary
Marcus Neteler	Fondazione E. Mach - Research & Innovation Centre, Trento, Italy
Branislav Niznansky	Catholic University in Ruzomberok, Slovakia
Tomas Penaz	VSB-Technical University Ostrava, Czech Republic
Katarzyna Juda-Rezler	Warsaw University of Technology, Poland
Jan Ruzicka	VSB-Technical University Ostrava, Czech Republic
Frantisek Stanek	VSB-Technical University Ostrava, Czech Republic
Michal Seliga	T-Mapy, Czech Republic
Jan Unucka	VSB-Technical University Ostrava, Czech Republic
Vit Vozenilek	Palacky University Olomouc, Czech Republic

Content

Part I

Advances in Remote Sensing

MEASUREMENT OF LANDSLIDES IN DOUBRAVA USING RADAR INTERFEROMETRY

LAZECKY Milan and KACMARIK Michal

Institute of Geoinformatics, Faculty of Mining and Geology, VSB-TU Ostrava, 17. listopadu 15, 708 00, Ostrava, Czech republic
milan.lazecky@vsb.cz, michal.kacmarik@vsb.cz

Abstract

Landslides monitoring is one of the main areas of satellite radar interferometry usage. This project aims on application of the method for measurement of landslides in Moravian-silesian region. A slope in Doubrava city is monitored that is known for a slow landslide due to erosion activity of water. A dense vegetation cover on the slope is causing decorrelation in the interferometrical processing of the Envisat ASAR images that degrades the phase values of the images. For this reason three specially designed corner reflector of the radar signal were installed on place, attached to hydrogeological boreholes that measure a changes of ground water level in time on the place. To enhance the precision of the landslide evaluation, phase values of the images are corrected by influence of signal delay through atmosphere using GPS meteorology method. Five acquisitions from the period of May until September 2010 from the Envisat ASAR sensor were processed using Permanent Scatterers method combined with other described methods for processing using very low number of images. Corner reflectors distributed in the slope surroundings were always rotated in a slightly different way by manipulation – that caused a different amount of their reflectivity and a phase shift of the radar signal corresponding to detected position change in order of millimeters. Due to slowing down of the landslide during the year 2010 this error had a significant impact on the quality of the results, anyway the methodology was confirmed as correct and it can be used in similar incoming projects.

Keywords: landslides, radar interferometry, Envisat, corner reflectors

INTRODUCTION

A hill in Doubrava with a height of 282 m and a slope of relative lift 70 m with steepness of about 30 m per 100 m distance is known to be sliding mostly due to the groundwater activity. The groundwater level is being monitored regularly by Geotest Corp. using hydrogeological drills. The landslide activity is gradually decelerating but seems to be still active. The groundwater activity is at its peak during strong rains and floods that occasionally happen in the area.

The idea of this project is to detect and measure the velocity of the landslide using satellite data. Since the hill is covered by vegetation, the radar interferometry (InSAR) results from Envisat ASAR images are totally depreciated by temporal decorrelation and therefore it cannot be monitored this way. The aim of this project was to overcome this limitation by installing corner reflectors on the site and so evaluate the slope movement during the year 2010. The hill wasn't monitored geodetically, unfortunately it wasn't possible to compare the interferometrical results with a ground truth. Anyway, in several scientific publications the methodology has been proven as reliable and the results could achieve a centimeter match (supposing high signal-to-noise ratio) in comparison with the levelling data in the areas of a slow deformation activities that are similar to expectations of this project area of interest.

This paper includes only preliminary results that need to be further enhanced.

CORNER REFLECTORS

Usage of corner reflectors was already documented in many papers as a technique with successful results. Corner reflector is an object designed to reflect the received radar wave in the exactly same direction. Several types of corner reflectors exist. The optimal reflection is ensured by appropriate geometrical setting and orientation of the reflector and a smooth material with a high dielectric constant. As a material, the aluminum with a dielectric constant of around 9 (enough to avoid penetration of the radar wave) was chosen to create a trihedral corner reflector with square sides of 80x80 cm (see Fig. 1). The computed theoretical radar cross section (RCS) of the reflector using Eq. 1 (Hanssen, 2001) is RCS=36.92 dB. To detect the corner reflector on the SAR image, at least 15 dB difference amongst surrounding pixels should be ensured. The corner reflector is designed to be as smallest as possible with keeping its proper functionality to allow its economically effective reproduction on other projects.

Eq. 1

$$RCS = \frac{12\pi \cdot a^4}{\lambda^2} \tag{1}$$

The corner reflector (CR) is designed to be mountable directly on a hydrogeological drill. Three CRs have been constructed to be deployed on two drills on the observed hill and third on a stable place in the center of Doubrava city as a reference point. Because the drills are situated on an unsecured area that is visible from a nearby road, the CRs couldn't be installed permanently during the whole year. Because its construction enables to mount the CRs again on the identical location, the CRs were always mounted on place only in the acquisition day and were carried away afterwards. It wasn't practically possible to orientate the CRs identically in every installation. That's why we have to count with a lower precision of the interferometrically estimated landslide velocity, even that the theoretical tolerance of the CR orientation to the satellite line of sight to achieve its strong reflection is relatively broad – even 5 degrees difference between the CR centerline and the satellite line of sight in the azimuth direction will provide sufficient reflection (Norris et al., 2004).

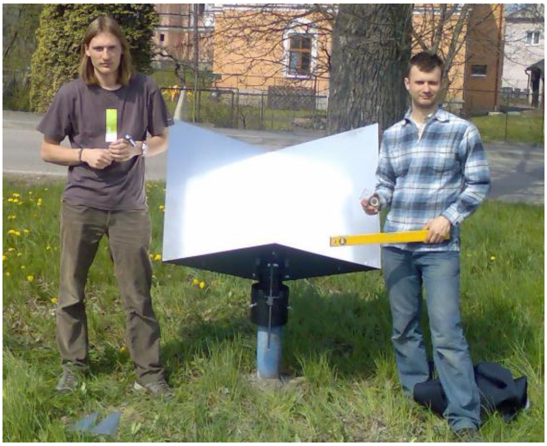

Fig. 1. Corner reflector mounted on a hydrogeological drill

CORNER REFLECTORS IN SAR DATA ACQUISITIONS

Only five Envisat ASAR acquisitions of Doubrava surroundings could be planned for the year 2010. On 22nd October 2010 Envisat has changed its orbit descending of 17.4 km. There is no inclination drift control anymore, the perpendicular baselines can reach values even 20 km, while the limit for InSAR is around 1 km. Only areas in 38 degrees of latitude are covered by InSAR available acquisitions (Miranda, 2010).

Acquisitions were planned in advance for the year 2010 (until the October). Because of conflict with projects of higher priorities, the acquisitions of 15th February and 22nd March couldn't be ordered and the acquisition of 26th April had to be achieved in H/H polarization mode (means sent and received horizontally oriented radar wave) while other executed acquisitions at 31th May, 5th July, 9th August and 13th September had to be ordered in polarization V/V. In the end, only 5 acquisitions could be ordered that will include installed corner reflectors. Normally it is not eligible to combine images with different polarization interferometrically since the physical objects reflect such waves in different ways, based mostly on different geometrical orientation. But in the case of corner reflectors this is theoretically of no concern because if the reflectors are oriented correctly, they would reflect the waves identically.

An example of a corner reflector visibility in a radiometrically calibrated intensity SAR image is Figd on Fig. 2. The value of reflectance in dB is 35.9 dB. Because of coarse resolution of ASAR data (approximately 30x30 m per pixel) the intensity of pixels containing CRs is influenced also by other surrounding strong reflectors. The georeference errors could easily overcome 100 m and the surroundings contain other sources of quite strong reflectance (possibly a nearby water well etc.), therefore it is sometimes not possible to certainly identify the location of CRs.

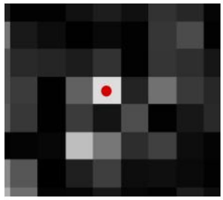

Fig. 2. Corner reflector visibility in a 31-05-2010 Envisat ASAR image.

INSAR PROCESSING

Theoretically, the radar interferometry has the abilities to evaluate terrain deformations in the order of millimeters but the radar phase measurements can be influenced by many factors increasing noise and can often discredit their successful interferometrical combinability. The applied Doris interferometrical processor includes several modules to filter out main noise and decorrelation errors. In addition, to maximally improve the InSAR evaluation accuracy, the errors caused by radar wave delay through the atmosphere are to be removed by GPS meteorology - modeling of the amount of atmospheric moisture and evaluating of thereby delay. The atmosphere moisture phase contribution appears in interferograms as a false terrain deformation of a relatively large scale. It can be modeled and removed also by using algorithms working with a stack of many radar images, such as Permanent Scatterers technique. Unfortunately, during 2010 only 5 images are available. This count is not sufficient for certain model of atmospheric errors. Another ongoing project will model the atmospheric influence using 6 more images of 2009 and the results will be compared to that from GPS meteorology attempt.

All available Envisat ASAR images were combined using Differential InSAR technique (creating an interferogram from two images and subtracting a DEM to remove topography phase contribution). The achieved results were affected by temporal decorrelation so much that they couldn't be interpreted, as it was expected. Because of a longer wavelength (that penetrates through the vegetation) Alos PALSAR data were also available, we have created an interferogram from them presented in Fig. 3 b. The interferogram shows a relative terrain changes in the period between 27-01-2008 and 13-03-2008 (46 days) with a scale of 11,8 cm per one colour cycle. The monitored hill is located in the area visible as a reddish mark in the north-west part of the image. This can be interpreted as a detected slope movement of several centimeters towards the satellite line of sight, i.e. the landslide could be moving slightly to the west or it can be an uplift. Unfortunately, due to relatively large perpendicular baseline between acquiring satellite position (493 m) the interferogram is more sensitive to the topography. Therefore this artifact will be interpreted as caused only by a DEM error.

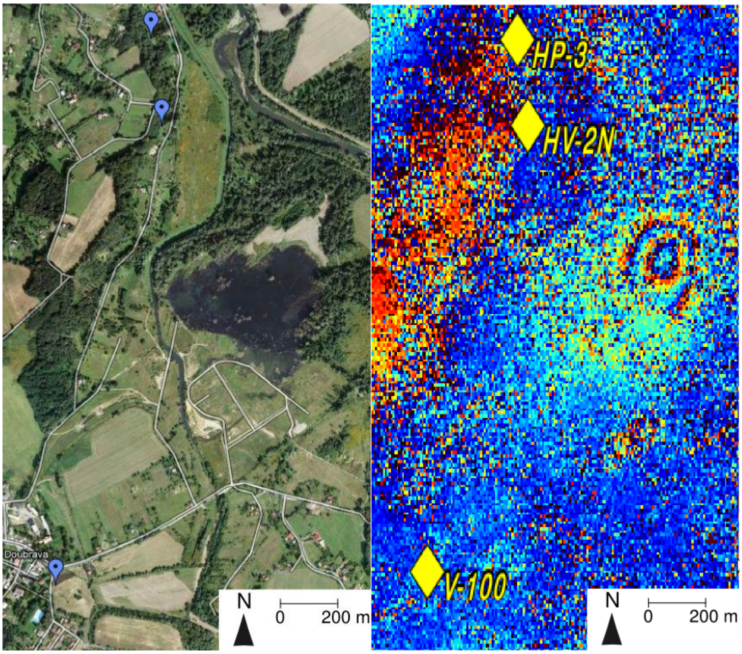

Fig. 3. Locations of installed corner reflectors in Doubrava. Right part represents Alos PALSAR interferogram between 27-01-2008 and 13-03-2008.

The main processing has been performed by StaMPS software package. As expected, a very few (and not very reliable) evaluated points called persistent scatterers were found on the monitored hill. Because of a very small number of 4 images processed it seems not possible to correctly evaluate DEM error and atmospheric phase screen. More processing will take place using earlier datasets without installed corner reflectors. The configuration of processed images with regard of their Doppler centroid used for focusing and perpendicular baselines of the satellite position between the images (see Fig. 4) seems optimal to achieve good results. The outlying image taken at 26-04-2010 was included only for processing of pixels containing corner reflectors since its polarization is H/H while the other images are polarized on V/V.

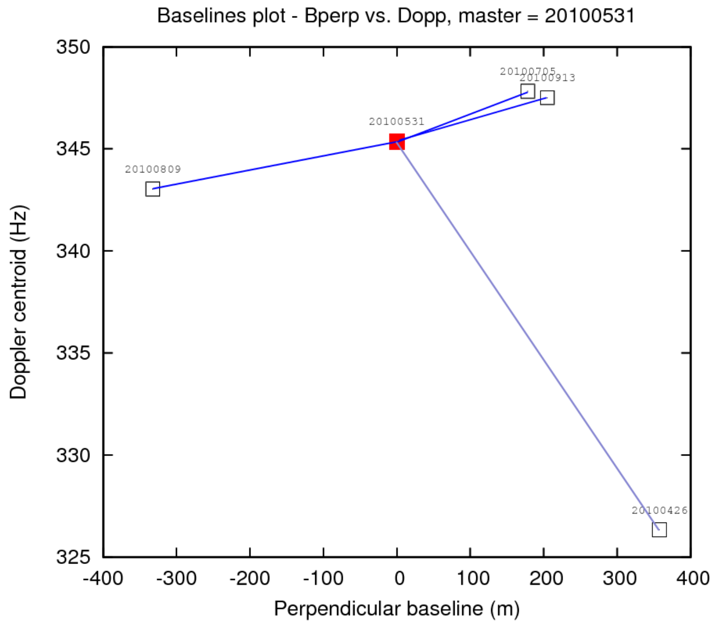

Fig. 4. Baseline plot – configuration of acquisitions used for corner reflectors InSAR processing

Unfortunately the corner reflectors were not detected or removed after their manual addition by the StaMPS algorithms. This seems to be a problem with installation of the reflectors on place or setting of higher confidence of adjacent persistent scatterers by StaMPS that caused the reflectors removal in the weeding stage. At the moment, there are no successful results that can be presented in this paper.

GPS METEOROLOGY FOR ATMOSPHERE DELAY CORRECTION

There exists an unquestionable fact that signals emitted by InSAR passing through the atmosphere are being affected by it and a delay of the signal occures. Total delay of the signal in the zenith angle can be separated in two parts - larger quantity which is caused by the hydrostatic part of the atmosphere (zenith hydrostatic delay) and smaller quantity caused by the wet part of the atmosphere (zenith wet delay, ZWD). The hydrostatic part is dependent mainly on the surface pressure and temperature and the wet part on the water vapour. Atmospheric water vapor effects represent one of major limitations to accuracy in InSAR applications mainly due its large spatial and time variability. Knowledge of ZWD values would help to reduce this limitation to minimum. In general, the atmosphere and water vapor in particular affects GPS and InSAR signals similarly. From this reason it is possible to determine delays from GPS measurements and use them as a correction for InSAR. (Xiaogang et al., 2008, Onn, 2006). GPS measurements are being succesfully used for water vapour determinations for long time. Those products can be used in numerical weather prediction models. Processing GPS ground measurements in proper software like Bernese GPS SW give zenith total delay values for location of GPS receiver in chosen time steps. For subsequent ZWD determination atmospheric pressure and temperature values measured at the same location and time are neccesary. (Bevis et al., 1992, Duan et al., 1996). Better results are acquired when differenced ZWD value from different times is applied on interferogram instead of using absolute values of ZWD for individual InSAR image. (Li et al., 2006).

In the time of writing this paper the GPS meteorology method wasn't applied to the processing for correction of radar wave delay through the atmosphere. During several radar acquisitions the atmosphere contained a strong moisture, only in the 13-09-2010 there was no rain over the area of interest. It is necessary to correct interferograms for this delay to achieve reasonable results.

CONCLUSIONS

Because of a short time dedicated to the processing, the project is not finished yet. Because of manipulation of corner reflectors between the acquisitions, some extra errors could have been caused lowering the expected precision of measurement evaluation. Furthermore, only 5 acquisitions are hard to investigate with standard multitemporal methods that assume usually 15 or more acquisitions to achieve a reasonable overview about terrain deformation in time. The project will continue developing a methodology of using define pixels to evaluate the rate of terrain deformation even from a few acquisitions. Most probably it will be in the form of a custom scripts using StaMPS processing software.

ACKNOWLEDGMENTS

We would like to thank doc. Pavel Bláha from Geotest Corp. for his assistance. Thanks goes also to Prof. Eric Pottier, a specialist in the field of polarimetric SAR processing that has given us several valuable informations which helped us with the project. Authors thank for the SAR data provided by ESA via project C1P.4578. The presented research was partially supported from SGS grant SP/2010149.

REFERENCES

Bevis, M., Businger, S., Herring, T.A., Rocken, C., Anthes, R.A., Ware, R. H. (1992) GPS meteorology – remote-sensing of atmospheric water-vapor using the global positioning system. Journal of Geohysical Research-Atmospheres, Vol. 97, Issue D14, pp. 15787-15801.

Duan, J., Bevis, M., Fang, P., Bock, Y., Chiswell, S., Businger, S., Rocken, C., Solheim, F., van Hove, T., Ware, R., McClusky, S., Herring, T., King, R. (1996) GPS meteorology: Direct estimation of the absolute value of precipitable water. Journal Appl. M., 24, 830–838.

Hanssen, R. F. (2001) Radar Interferometry: Data Interpretation and Error Analysis. Dordrecht: Kluwer Academic Publishers. 328 p. ISBN: 0792369459.

Hooper, A. (2008) A Multitemporal InSAR Method Incorporating Both Persistent Scatterer and Small Baseline Approaches. Geophysical Research Letters. doi:10.1029/2008GL034654. ISSN: 00948276.

Kampes, B. M., Hanssen, R. F., Perski, Z. (2003) Radar interferometry with public domain tools. Third International Workshop on ERS SAR Interferometry, `FRINGE03'. Frascati, Italy, 15 Dec 2003, ESA ESRIN, Italy. 6 p.

Ketelaar, G. (2009) Satellite Radar Interferometry: Subsidence Monitoring Techniques. 1st ed. Dordrecht: Springer. 270 p. ISBN: 1402094272.

Li, Z., Fielding, E.J., Cross, P., Muller, J.P. (2006) Interferometric synthetic aperture radar atmospheric correction: GPS topography-dependent turbulence model, Journal of Geophysical research, vol. 111.

Miranda, N. Impact of the Envisat Mission Extension on SAR data. ESA. 13 pp. 23-08-2010. http://earth.esa.int/download/envisat/Impact-of-Envisat-Mission-Ext-SAR-data-aug10.pdf, 16-11-2010.

Norris, J, Vachon, P. W., Schlingmeier, D., English, R., Gallop, L. (2004) Expendable Trihedral Corner Reflectors for Target Enhancement and Position Constrol in RADARSAT-1 Fine Beam Mode SAR Imagery: Results from an Exercise Narwhal Pre-Trial Deployment - Technical Memorandum. DRDC Ottawa, Canada. 44 p.

Onn, F. (2006) Modeling Water Vapor using GPS with Application to Mitigating InSAR Atmospheric Distortions. PhD thesis, Stanford University.

Ugsang, D.M., Honda, K., Saito, G. (2001) Assessment of Small Passive Corner Reflectors for Geometric Correction of RADARSAT Fine Mode SAR Data . 22nd Asian Conference on Remote Sensing, Singapore, 5 - 9 November 2001, CRISP, SISV, AARS and National University of Singapore, Singapore, China, 6 p.

Xiaogang, S., Deren, L., Mingsheng, L. (2008) Reproduction of InSAR Atmospheric Signal using GPS Data based on Topography-dependent and Turbulent Mixing Model, Proceedings Dragon 1 Programme Final Results 2004–2007, China, 2008.

2-PASS DIFFERENTIAL INTERFEROMETRY IN THE AREA OF THE SLATINICE ABOVE-LEVEL DUMP

BORIK Milan

Department of Mathematics, Faculty of Civil Engineering, Czech Technical University in Prague, Thákurova 7, 166 29, Prague,
borikm@mat.fsv.cvut.cz

Abstract

We concentrate on areas with abandoned open brown coal mines, or undermined areas. We made analyzes of terrain deformation in the area of the Slatinice above-level dump that is monitored because of potential terrain deformations. The 2-pass differential interferometry method was used. Interferometric processing was performed in the GAMMA software. The differential interferogram for the 2-pass method was filtered and then unwrapped. Due to filtering we achieved much better coherence. Unwrapped phase of that differential interferogram can be used for a terrain-deformation detection more profitably. An important feature of this method is that all measurements are relative. Theoretically, the phase of the differential interferogram should be zero in the areas of no deformation, but there are systematic errors influencing the measurements and therefore the deformations can be determined only relatively with respect to the vicinity. Expected deformations can be described quantitatively. For decision on potential terrain deformation, the suspect areas of subsidence must be sufficiently coherent. For incoherent areas there occurs decorrelation and thus loss of data. For subsidence confirmation, we demand as continuous phase as possible with a sufficient number of neighboring pixels and lines. Further we concentrated on the Jirkov-Most route and railway that slides and is also monitoring and leveled very precisely. Especially its part called the Ervenice corridor. We cannot evidence that area of the Ervenice corridor is stable because of larger variance of the unwrapped-phase values. The results are very decorrelated. In this area, we verified no terrain deformation.

Keywords: differential interferometry, 2-pass method, undermined areas, dumps

INTERFEROMETRY

Interferometry is method (Bořík, 2010), that use coherent radiation to determine space relations on the Earth surface. Satellites with synthetic aperture radar (SAR) scan the same area under little different visual angle. SAR was developed due to bad radar resolution with the real aperture. By means of Doppler effect of frequency modulation, SAR

substitutes the length of antennas by modified measurement art. Two satellites (ERS-1, ERS-2) flies the same orbits in a given time interval. Distance between both satellites is called interferometric baseline and its perpendicular projection into the slant range is called perpendicularbaseline. Radar apertures get data containing intensity (that describes reflex possibility of the surface), and phase as well, that means information about distance of radar and exposured point on the Earth. If we do complex multiplication of the first scene with another one (pixel by pixel), we get the interferogram.

2-PASS DIFFERENTIAL INTERFEROMETRY

2-pass differential interferometry is based on an interferometric image pair and a digital elevation model (DEM). The basic idea of 2-pass differential interferometry is that a reference interferogram (interferogram with phase corresponding to surface topography) is simulated based on the DEM. In order to do this the DEM is first transformed from its original coordinate system to the reference SAR image coordinates. This is done in two steps. In a first step the geometric transformation is done based on the available information on the geometry of the DEM and the SAR image geometry used. In the same step the SAR image intensity is simulated based on the simulated local pixel resolution and incidence angle. Inaccurate DEM coordinates, orbit data, and small errors in the calculation of the geometric transformations may result in small offsets between the simulated and the real SAR image geometry. In the second step the offsets between the simulated and real SAR image intensities are estimated and used to accurately register the transformed DEM to the SAR image geometry. Based on the reference SAR geometry, the interferometric baseline model, and the transformed height map, the unwrapped interferometric phase corresponding exclusively to topography is calculated. In the following this phase will also be called topographic phase.

This method is used to remove the topographically induced phase from the interferogram containing topography, deformation and atmosphere. The temporal baseline should be long enough to allow the deformations to occur, but the deformations cannot be too large.

When used for deformation mapping, the perpendicular baseline should be as short as possible (Table 1) in order to reduce the topographic signal in the interferogram as much as possible.

An important feature of this method is that all measurements are relative. Theoretically, the phase of the differential interferogram should be zero in the areas of no deformation, but there are systematic errors influencing the measurements and therefore the deformations can be determined only relatively with respect to the vicinity.

For topographic or deformation monitoring, data selection is often performed with the purpose to eliminate rain and snow. If there is no storm in the mapped area, the atmospheric influence usually has a long-wave characteristic, i.e. it changes slowly in the area.

Interferometric processing was performed in the GAMMA software. Data from track 394 for the 2-pass were used. The interferometric pairs are described in Table 1.

Table 1. Interferometric pairs

Interferometric pair	Perpendicular baseline [m]	Sign of a deformation
12501_13503	45	+
14777_15278	8	+
15278_15779	123	+
15779_16280	64	+
23795_23294	4	-
28304_29306	41	+

Table 2. Acquisition dates

Scene	Date
12501	1997-09-10
13503	1997-11-19
14777	1998-02-16
15278	1998-03-23
15779	1998-04-27
16280	1998-06-01
23294	1999-10-04
23795	1999-11-08
28304	2000-09-18
29306	2000-11-27

The differential interferogram for the 2-pass method is filtered and then unwrapped. Due to filtering we achieved much better coherence. Unwrapped phase of that differential interferogram can also be used for a terrain-deformation detection more profitably.

ANALYZES

In Fig 1 we can see landslides in the area of the Slatinice above-level dump. We can evaluate this as 2.7cm for pair 12501_13503 and as 1.6 cm for pair 14777_15278, by means of. Coherence values for pair 12501_13503 are: less than 0.6 8%, 0.6-0.7 4%, 0.7-0.8 11%, 0.8-0.9 43%, more than 0.9 34%. Maximum is 0.964 and minimum is 0.100.

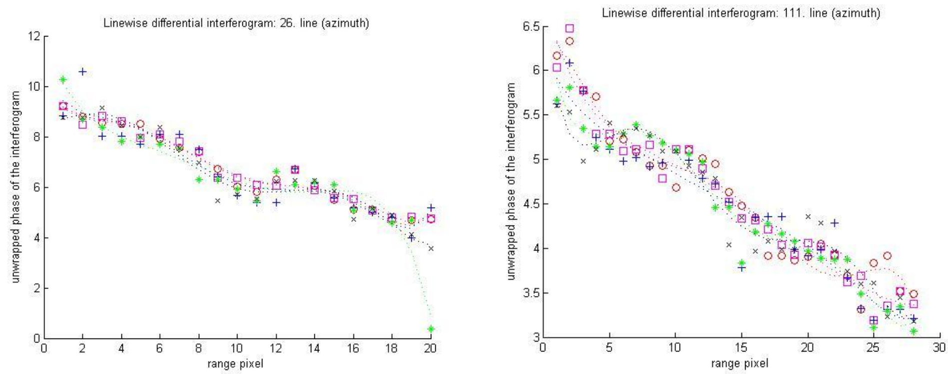

Fig. 1. Differential interferogram where vertical axis is the unwrapped phase of the differential interferogram (in radians). Landslides for interferometric pairs a) 12501_13503, b) 14777_15278.

On the left side of Fig 2a, unwrapped phase of the interferogram is continuous between 3.7 and 5.4 for lines 0-55. Thus the subsidence is 0.8cm. Coherence for these lines 0-55 is higher than 0.95. In place of the highest subsidence (line 15), coherence is 0.99. In the middle of Fig 2b, we confirmed a terrain deformation between range pixels 6 and 23. The unwrapped phase is continuous between 4.8 and 5.7. The subsidence is 0.4cm. Coherence values are between 0.96 and 0.99 for range pixels 6-23. In place of the highest subsidence (pixel 14), coherence is 0.98. Coherence values for pair 14777_15278 are: less than 0.8 0%, 0.8-0.9 1%, more than 0.9 98%. Maximum is 0.996 and minimum is 0.669.

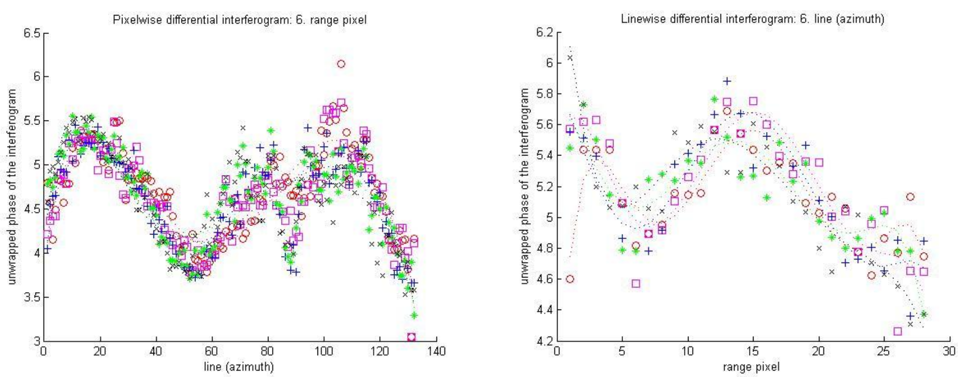

Fig. 2. Differential interferogram where vertical axis is the unwrapped phase of the differential interferogram (in radians). Subsidence for interferometric pair 14777_15278. a) pixelwise interferogram, b) linewise interferogram.

On the left side of the pixelwise differential interferogram in Fig 3a, we can see a terrain deformation. It is a subsidence because of the positive sign of the terrain deformation (Table 1). The values for unwrapped phase of the interferogram are between -9.5 and -11 for lines 0-22. The subsidence for this pair is 0.7 cm. Coherence in the highest subsidence (line 10) is 0.9. That coherence for lines 0-22 is between 0.82 and 0.96. In the linewise differential interferogram (Fig 3b), we evidenced a subsidence as well. The unwrapped phase of the interferogram is between -11.3 and -12.8 for range pixels 13-32. This subsidence is as 0.7cm as in the opposite direction. In place of the highest subsidence (pixel 22), coherence is 0.95. Coherence values are between 0.8 and 0.96 for range pixels 13-32. Coherence values for pair 15278_15779 are: less than 0.5 0%, 0.5-0.6 1%, 0.6-0.7 2%, 0.7-0.8 8%, 0.8-0.9 33%, more than 0.9 56%. Maximum is 0.975 and minimum is 0.283.

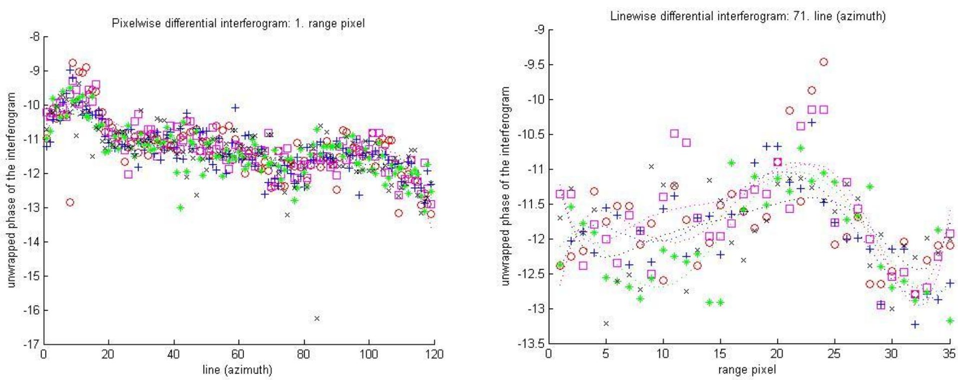

Fig. 3. Differential interferogram where vertical axis is the unwrapped phase of the differential interferogram (in radians). Subsidence for interferometric pair 15278_15779. a) pixelwise interferogram, b) linewise interferogram.

On the left side of Fig 4a, unwrapped phase of the interferogram is continuous between 3.7 and 4.7 for lines 2-55 and on the rigt side of this Fig that phase is between 4.0 and 5.7 for lines 92-130. The subsidence on the left side is 0.5cm, and on the right side 0.8cm. Coherence for lines 2-55 is between 0.75 and 0.98. Coherence for lines 92-130 is between 0.75 and 0.97. In places of the highest subsidence (line 27, and 106), coherence is 0.98, and 0.95. Coherence values for pair 15779_16280 are: less than 0.4 2%, 0.4-0.5 4%, 0.5-0.6 4%, 0.6-0.7 4%, 0.7-0.8 10%, 0.8-0.9 30%, more than 0.9 46%. Maximum is 0.988 and minimum is 0.057. In Fig 4b, we confirmed a terrain deformation between range pixels 5 and 15. The unwrapped phase is continuous between -0.8 and -2.5. Thus the subsidence is 0.8cm. Coherence values are between 0.8 and 0.9 for range pixels 5-15. In place of the highest subsidence (pixel 9), coherence is 0.9. Coherence values for pair 28304_29306 are: less than 0.3 5%, 0.3-0.4 3%, 0.4-0.5 4%, 0.5-0.6 6%, 0.6-0.7 13%, 0.7-0.8 20%, 0.8-0.9 32%, more than 0.9 17%. Maximum is 0.965 and minimum is 0.012.

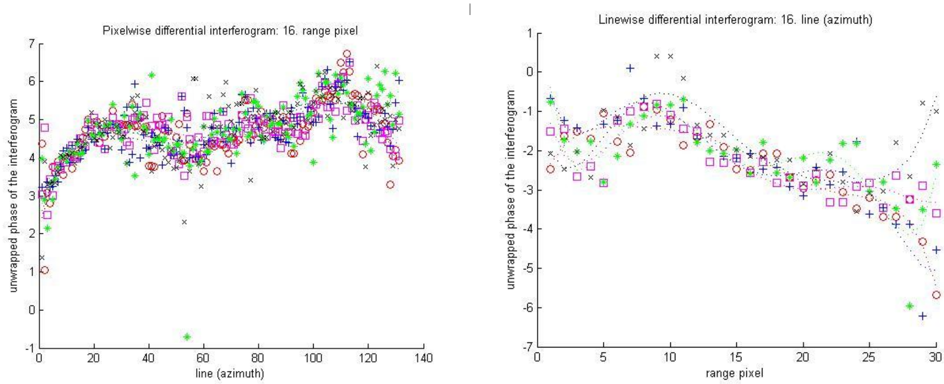

Fig. 4. Differential interferogram where vertical axis is the unwrapped phase of the differential interferogram (in radians). Subsidence for interferometric pairs a) 15779_16280, b) 28304_29306.

On the right side of the pixelwise differential interferogram in Fig 5a, we can see a terrain deformation. It is a subsidence because of the negative sign of the terrain deformation (Table 1). The values for unwrapped phase of the interferogram are between -3 and -4.4 for lines 60-95. The subsidence is 0.7 cm. Coherence in the highest subsidence (line 75) is 0.98. That coherence for lines 60-95 is between 0.96 and 0.99. In the linewise differential interferogram (Fig 5b), we evidenced a subsidence as well. The unwrapped phase of the interferogram is between -3.3 and -4.1 for range pixels 0-17. This subsidence is 0.4cm. In place of the highest subsidence (pixel 8), coherence is 0.98. Coherence values are between 0.94 and 0.99 for range pixels 0-17. Coherence values for pair 23795_23294 are: less than 0.6 3%, 0.6-0.7 2%, 0.7-0.8 3%, 0.8-0.9 8%, more than 0.9 85%. Maximum is 0.999 and minimum is 0.159.

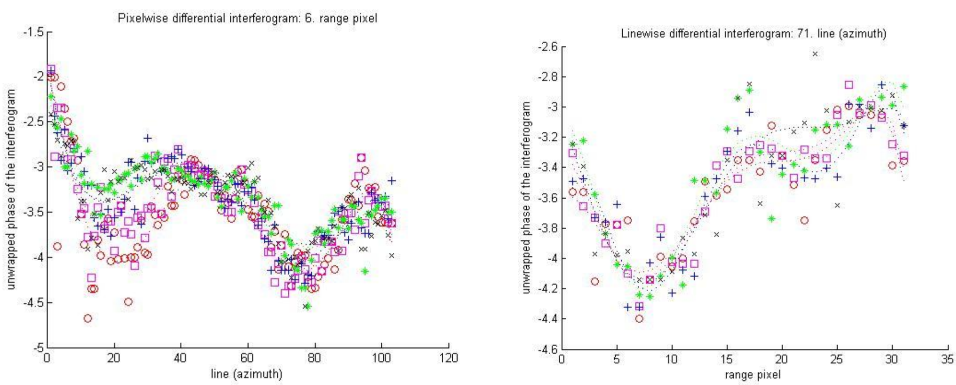

Fig. 5. Differential interferogram where vertical axis is the unwrapped phase of the differential interferogram (in radians). Subsidence for interferometric pair 23795_23294. a) pixelwise interferogram, b) linewise interferogram.

CONCLUSIONS

From our analyzes in previous section we can do some conclusions. Average subsidence in the area of Slatinice above-level dump is approximately 0.7cm per month. Maximal subsidence we evidenced was 0.8cm for pairs 14777_15278 (pixelwise), 15779_16280 (pixelwise), and 28304_29306 (linewise). These terrain deformations were confirmed by excellent coherence values (0.99, 0.95, and 0.9).

For decision on potential terrain deformation, the suspect areas of subsidence must be sufficiently coherent. For incoherent areas there occurs decorrelation and thus loss of data. We can confuse clearly visible "deformations" in differential interferograms and areas used in agriculture. There are no subsidence and landslides there but only small changes in terrain height in consequence of agricultural cultivation. Terrain could be a little covered with ice as well.

For subsidence confirmation, we demand as continuous phase as possible with a sufficient number of neighboring pixels and lines. We expect coherence values higher than 0.5. After filtering, we obtained much better coherence values. Maximal evaluated coherence was 0.999 for pair 23795_23294. Best coherences values more than 0.9, we obtained for pairs 14777_15278 and 23795_23294. Due to phase unwrapping in the end, we are able to quantify landslides higher than 2.8cm, because that phase is not more between –pi and pi and then there is no phase ambiguity. The perpendicular baseline should be as short as possible, to 50m ideally. However, that baseline for pair 15278_15779 is 123m and nevertheless, a good interference occurred. The time baseline should be as short as possible as well. That is approximately 1 month long or 2 months long exceptionally, for our purposes. When used longer time baselines or longer perpendicular baselines for scenes from stack 394, the decorrelation always occurred.

Terrain deformations (subsidence and landslides) in the area of the Slatinice above-level dump since 1997 until 2000 were evidenced. Further we concentrated on the Jirkov-Most route and railway that slides and is also monitoring and leveled very precisely. Especially its part called the Ervenice corridor. We cannot evidence that area of the Ervenice corridor is stable because of larger variance of the unwrapped-phase values. The results are very decorrelated. In this area, we verified no terrain deformation.

ACKNOWLEDGEMENTS

This article was supported by grant with No. 106/08/0403 GA ČR and by grant Interferometric Determination of Subsidence Caused by Undermining by Permanent Scatterers and Phase Unwrapping Correction within Interferometric Blocs with No. 205/08/0452 GAČR. Data were obtained from ESA within the framework of project

Interferometry Used for Landslide and Land Subsidence Detection in the Undermined Area and in the Area with Abandoned Open Brown Coal Mines.

REFERENCES

Bořík, M.: Určení terénních deformací v oblasti Ervěnického koridoru pomocí třísnímkové diferenční interferometrie. Geodetický a kartografický obzor 8/2010, 56/98, 2010, pp. 157-161.

Bořík, M.: Stanovení terénních deformací třísnímkovou diferenční interferometrií. Stavební obzor 5/2009, 2009, pp.150-153.

Bořík, M.- Čapková, I.- Halounová, L.- Kianička, J.: Qualitative distinction between terrain deformations and processing errors, and quantitative description of deformations for the 3-pass interferometry, New Developments and Challenges in Remote Sensing, Millpress, Rotterdam, 2007, pp. 113-121. ISBN 978-90-5966-053-3.

GAMMA Software - http://www.gamma-rs.ch/no_cache/software.html

Hanssen, R.F.: Radar Interferometry: Data Interpretation and Error Analysis. Dordrecht, Kluwer Academic Publishers, 2001.

Kampes, B.: Delft Object-Orientated Radar Interferometric Software: Users Manual and Technical Documentation. Delft, Delft University of Technology, 1999

INDIVIDUAL TREE CROWNS DELINEATION USING LOCAL MAXIMA APPROACH AND SEEDED REGION GROWING TECHNIQUE

NOVOTNY Jan, HANUS Jan, LUKES Petr and KAPLAN Veroslav

Institute of Systems Biology and Ecology, Academy of Sciences of the Czech Republic, Poříčí 3b, 60300, Brno, Czech Republic
jan.novotny@usbe.cas.cz

Abstract

Remote sensing applications in forestry can profit from a rapid development of optical sensors. New hyperspectral sensors have very high spatial and spectral resolution and provide continuous spectral cover in visible and infrared spectral region. Applied algorithms should be suited to the new properties of the data to achieve its maximal advantage.

Segmentation of the image into objects is a fundamental task in image processing. It is important in forestry applications of optical remote sensing as well. We are looking for a position of individual tree crowns. Such process traditionally involves two parts - 1) detection and 2) delineation phase. Local maxima approach and seeded region growing technique are presented as the key concepts. Furthermore improvements, namely histogram equalization and Voronoi diagram, are incorporated.

Two independent datasets were processed and results of the segmentation are presented. Hyperspectral data with spatial resolution of 0.8m were found as a suitable for segmentation process with 84% and 78% accuracy of detection phase and 64% and 52% accuracy in delineation phase respectively. Finally discussion of recommended settings in the algorithm is provided based on the segmentation results.

Keywords: optical remote sensing, individual tree crowns, local maxima detection, seeded region growing

INTRODUCTION

Remote sensing is a science field with a rapid development, especially when speaking about the spatial and spectral resolution. Satellite sensors with a few spectral bands (multispectral) and pixel sizes ranging from tens of meters to kilometers, are in use since 1970'. Data provided by such sensors are used for global monitoring, i.e. in weather forecast. New hyperspectral sensors (especially airborne ones) provide a data with a distinctively higher spatial and spectral resolution. Spatial resolution with a pixel size in centimeters and hundreds of narrow spectral bands within a wide range of electromagnetic spectrum are common (Goetz, 2009). This improvement in hardware implies development of appropriate software - algorithms must be suited to the data. (Gougeon et al., 2006)

In forestry remote sensing went through a long way as a tool for forest health monitoring, global biomass distribution analysis etc. New hyperspectral sensors with very high spectral resolution and continuous spectral cover provide more precise estimates of qualitative and even quantitative biophysical and biochemical parameters. (Asner, 1998, Ustin et al., 2009, Rautiainen et al., 2010)

A fundamental task of image processing — image segmentation — is important in remote sensing too. Segmentation of an image into individual objects for foresters' purposes means segmentation of individual tree crowns. Tree crown is an area with a relatively high reflectance (e.g. in NIR spectral region) compared to neighboring area. Therefore the crowns can be found around a local maximum of brightness. Successful detection of a tree crown position as well as delineation of a whole tree crown area depends on several conditions. Specific tree species, age and height, stand density must be taken into consideration as well as variation in these parameters across the region of interest. Secondly, the radiometric, spatial and spectral resolution of the sensor differs for specific sensor-tree-sun geometry present during data acquisition and therefore must be treated as well.

In this paper we present the evaluation of a modified crown segmentation algorithm on hyperspectral data with spatial resolution better than 1 meter and spectral resolution lower than 20nm.

MATERIAL

Study sites

We tested the segmentation algorithms on several data sets acquired over Šumava Mts. with airborne hyperspectral and spectrozonal sensors, Study site "Černá Hora" (48.59N; 13.35E; mean elevation of 1200 m.a.s.l.) was selected for our purposes. The dominant tree species is a mature Norway spruce (Picea Abies, L. Karst) influenced by various stressors (e.g. massive wind-fall after hurricane "Kirril" or bark beetle outbreak), thus we expected different health conditions of trees within the area. However, the canopies were still relatively closed (canopy cover about 80 %). The data used in this study were acquired during a flight campaigns in September 2009 and July 2010.

Remote sensing data

Two different datasets were used for the purposes of the study. First, the airborne hyperspectral data of AISA Dual system (Specim, Finland) were collected over the site on 1st September 2009. AISA Dual is a combination of VNIR Eagle (Hanuš et al., 2008) and SWIR Hawk sensors, with capabilities to acquire the data in spectral range from 400nm to 2500nm with maximal spatial resolution of 0.8m and full-width-half maximum (FWHM) of 12nm. This configuration was used in our study. Acquired image lines were georeferenced using the IMU/GPS navigation data, converted from raw DN values into at-sensor radiance (using sensor-specific calibration files) and further converted into real reflectance values using ATCOR-4 atmospheric correction module (ReSe, UZH, Switzerland). Such radiometrically and geometrically corrected data were used as an algorithm inputs.

Secondly, large format digital spectrozonal camera UltraCamX data were acquired on 7th July 2010. The camera produces images in high resolution of 136 Mpix (spatial resolution up to 0.2m) with RGB, Grayscale or CIR outputs. These data were used for validation of crowns identification / delineation performed on hyperspectral datasets.

METHODS

Segmentation process traditionally involves two main parts: 1) tree crowns detection and 2) tree crowns delineation. Several approaches are possible for both tasks. We tested the most suitable procedures for our data. In this paper we present a segmentation process based on broadly used approaches with several improvements.

In case of crowns detection, we applied a local maxima approach with variable window size for a detection of different crown size combined with adaptive equalization for highlighting of shaded crown parts. For tree crowns delineation we applied a seeded region growing technique with Voronoi diagrams used as primary mesh and several stopping conditions enabled.

From data to image

From the nature of hyperspectral data, we have information about reflectance in hundreds of spectral bands. This can be useful for detailed spectral analyses but tree crown detection and delineation is a question of texture and structure rather than its spectral features.

The input of a segmentation algorithm is an average brightness image computed from original data. Averaging can be performed over all available bands. That is convenient for multispectral data with several spectral bands. However, when using hyperspectral data with many narrow bands, such approach would lead to the loss of specific spectral characteristic of vegetation. We selected several wavelengths, where spectral characteristic of vegetation plays a major role. Average brightness image is then computed over selected bands. (See Table 1, Fig 1.)

Table 1. Selected spectral bands

AISA Eagle, 65 bands		AISA Dual, 359 bands	
band n.	wavelength	band n.	wavelength
13	497.5 nm	24	502.2 nm
19	551.3 nm	35	551.7 nm
25	606.6 nm	48	612.1 nm
33	680.7 nm	63	681.8 nm
37	717.8 nm	71	719.1 nm
43	773.9 nm	82	770.9 nm
51	849.4 nm	99	851.8 nm

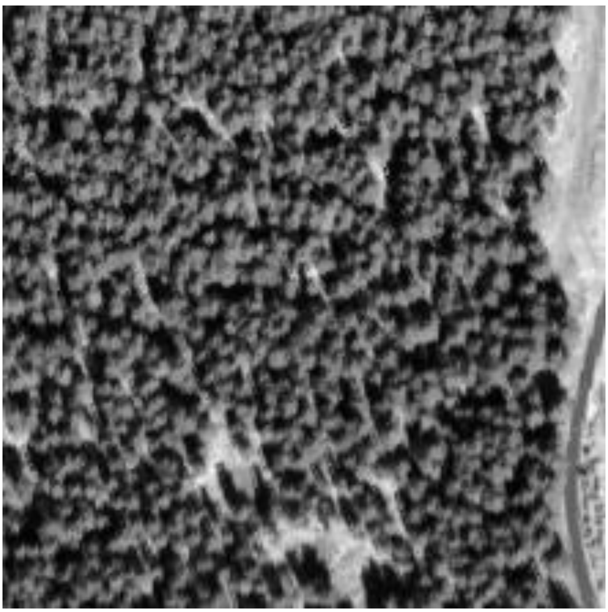

Fig 1. Average brightness image

Adaptive equalization

When talking about the trees in average brightness image, we distinguish the individual tree crowns as brighter parts surrounded by shadows. Depending on actual sun angle, certain parts of the crowns are usually shaded. This would cause inaccuracy especially in delineation phase. Shaded parts can be effectively highlighted using adaptive equalization.

Histogram equalization is well-known technique used in image processing - its main goal is to provide a uniform distribution of pixel values. Adaptive approach applies a transformation on single pixel using cumulative histogram calculated from particular pixel neighborhood as transforming function. This procedure results in better contrast of the image, in our case shaded parts of the crowns are highlighted.

Average brightness image is saved as a 2D matrix of floating point numbers ranging between 0 and 1. For the equalization, we selected a specific number of subintervals between 0 and 1. Then we transformed pixel values in such way, that percent occurrence of pixel values from particular neighborhood in selected subintervals should be uniform.

Crucial input parameter of histogram equalization is the neighborhood size entering the calculations. It should correspond with the expected size of tree crowns; therefore it directly depends on a spatial resolution of processed data (see Fig 2). Moreover, crown sizes can vary significantly over regions of interest as well.

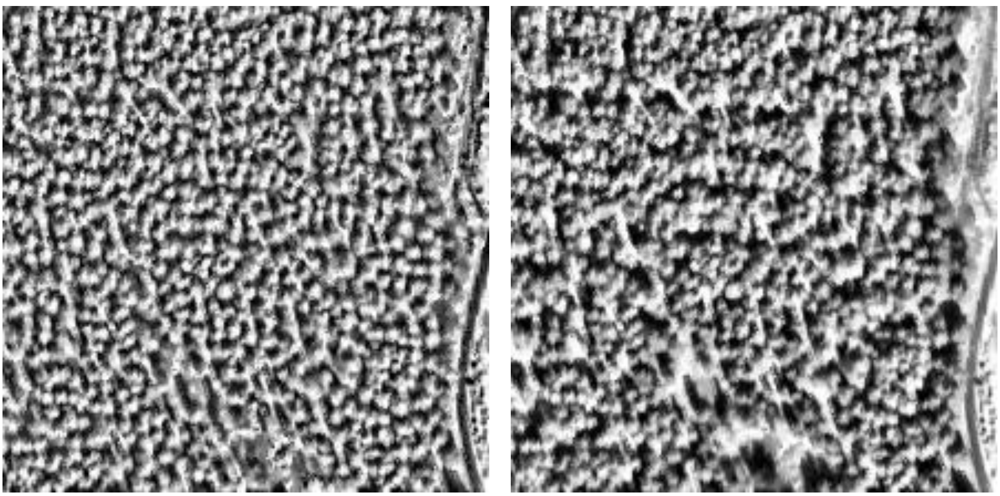

Fig 2. Equalized images, effects of different neighborhood sizes. The results obtained for region of interest using following set up: Pixel size is 80 cm, 100 subintervals were defined over the range from 0 to 1 and size of pixel neighborhood was 11 pixels for the left image and 31 pixels for the right image.

Using filters and masks

Average brightness image (both before and after equalization) holds structural information of higher as well as lower frequency. Higher frequency information represents in-crown details, understory structures and noise. Tree crowns and superior canopy structures are present in lower frequency information. While higher frequency information can be amplified by equalization, the lower frequency information is more important for segmentation process.

Therefore prior to the crown detection (with local maxima approach) use of some low-pass filter is advisable. Most common low-pass filters are so called Gaussian kernels, where again appropriate kernel size is a key factor. Example of results is shown in Fig 3.

There are also other structures inside the region of interest beyond the tree crowns itself. It is therefore advisable to exclude non-tree structures from the next steps of delineation process. Binary image mask can be applied on non-tree areas to find local maxima of sole tree crowns. Automatic supervised / unsupervised classification of the image can be applied, focusing mainly on exposed crown tops. Such mask is then applied before local maxima locating, local maxima found outside the tree tops are rejected.

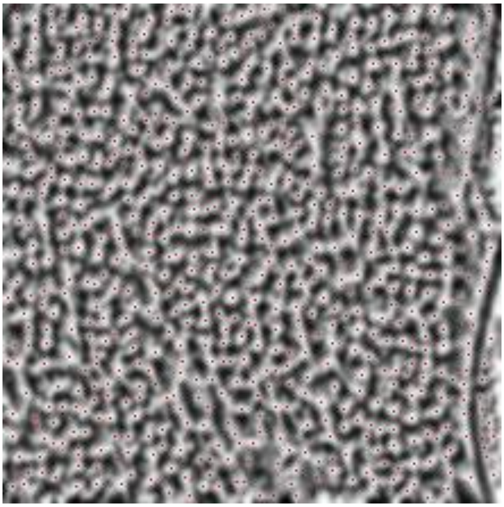

Fig 3. Filtered image with local maxima marked. Gaussian filter was used with kernel size 7 and sigma = 2

Identification of local maximal

In average brightness image the brightest pixels represent tree crown top points. However, the brightest point of the tree is not necessarily the crown top, while it depends on actual sun and sensor angle configuration too. Still, the local maxima approach works well for tree location estimates and local maxima are useful as seeds for tree crown delineation.

It is important to have only one local maxima found in each crown for following steps. We have to make a decision about each pixel, whether or not it could be a maximum inside some neighborhood. Size of this neighborhood should correspond to expected crown size, but crown sizes can vary significantly over the region of interest. The use of statistical and topological analysis of a pixel neighborhood can help us with decision about appropriate local-maxima-window size. Semivariograms calculated in eight directions from analyzed pixel tell us about pixel self-similarity against the neighborhood, while slope breaks searching for local minima in eight directions tell us about expected distances to the between-tree edge. (Wulder, 2000) These two values are then averaged to obtain a representative window size for local maxima check. (See Fig 3)

Seeded region growing

Seeded region growing is an iterative process started in a pixel from the set of seeds. Pixels from the seed neighborhood are subsequently classified whether or not they are part of the same crown as the seed. (Hirschmugl et al., 2007)

Many classification criteria are possible and useful to apply, such as:

1) Absolute distance from the seed. We set the limit according to an estimation of maximal tree crown size and classify a pixel as acceptable while its distance from the seed is within set distance limits.
2) Brightness agreement. Seed pixels are found as the brightest ones. Whole crown area should hold at least part of the brightness of the seed, but appropriate threshold have to be set up. A brightness of classified pixel can be compared with brightness of the seed or with brightness of all pixels assigned to the crown so far.
or 3) Spectral agreement - Whole spectrum (or some part) of the seed and the classified pixel can be compared. Appropriate threshold should be set up, according to comparison approach. This approach is especially suited to hyperspectral data. Possible applications are further described in (Ustin et al, 2009).

The above mentioned criteria apply to individual tree crowns. However, the trees groups in a forest and therefore shares common forest area. The boundaries between the forests should be respected and somehow included. Starting from all the seeds simultaneously and growing the regions in equivalent steps is the first important approach. Meanwhile, it is useful to have some preliminary conception of forest area division. For this purpose, the Voronoi diagram based on a position of the seeds is build. Forest boundaries found by using these two approaches should not be crossed during the region growing process.

Final corrections can be made in the last phase of delineation process. Obviously incorrect classification of some pixels can be corrected or nullified and regions under some size threshold can be removed.

RESULTS AND DISCUSION

Rectangular region of interest with a side of 176 meters was selected in a Černá Hora site. Subsets of a data from three available datasets were made. Two datasets of the same area acquired within 1 month with spatial resolution of 80 cm were used as inputs to segmentation process. Image from RGB aerial digital camera with pixel size of 20 cm was used to manually validate the results.

Region of interest covers approximately 3 hectares of closed forest stand of Norway spruce. Most of the trees are mature individuals. (See Fig 4.)

In case of AISA Eagle campaign (Eagle), the region of interest is represented by a rectangular subset with a side of 220 pixels. We have 65 spectral bands available in a range from 400 to 1000 nm with a spatial resolution of 80 cm. In AISA Dual campaign (Dual) the region of interest is represented by a rectangular subset with a side of 220 pixels. We have 150 spectral bands available in range from 400 to 1150 nm with a spatial resolution of 80 cm.

Fig 4. RGB image of the region of interest, subset from digital camera data with 20 cm spatial resolution, exported from ENVI software

Average brightness image was computed using selected bands (see Table 1.). Adaptive equalization of brightness image was performed with 11 pixels size of a floating window and normalized brightness interval 0 to 1 divided into 100 classes. Filtration of the equalized image was done by a Gaussian kernel with size of 7 pixels. The supervised classification of the image was performed in ENVI software using a neural net with image classes of exposed tree crowns, shaded parts, grass fields and roads. Resulting mask (masking out everything but the exposed tree tops) was applied in segmentation software. Then, the local maxima detection was performed.

Table 2. Tree crown detection settings

Average brightness image	averaging over selected bands
Equalization kernel size	11 pixels
Equalization classes	100 classes over range from 0 to 1
Image filtering	Gaussian kernel, size 7 pixels, sigma = 2
Local maxima detection	variable window size

Tree crown detection results

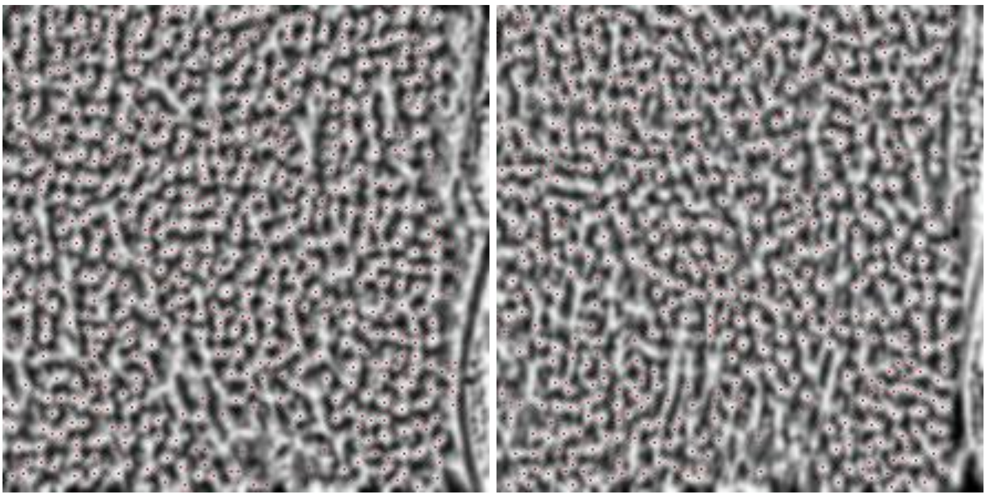

Fig 5. Local maxima = tree crown positions detected in the images (Eagle – left, Dual – right)

Identified local maxima were manually evaluated whether or not they fit to the actual tree positions. Very high spatial resolution image (pixel size 20 cm) acquired by UltraCamX was used as a reference about exact tree positions. Local maxima and tree positions were rated with the following three categories. A) If one local maximum stands for one tree crown we judge it as successful tree detection. B) If local maximum is found where no tree occurs, we judge it as incorrect tree detection. C) And if there is no local maximum found over a tree crown area we judge it as omitted tree detection.

We looked on the Eagle data first. In a rectangular region of interest of approximate size 176 x 68 meters (first 85 lines of the image above) 257 trees and 233 local maxima were located. It includes 223 successfully detected, 10 incorrectly detected and 34 omitted trees. That means nearly 84% efficiency of tree detection phase. For the Dual data we took the same part of the image, it covers nearly the same area. Again 257 trees and 213 local maxima were located, including 206 successfully detected, 7 incorrectly detected and 51 omitted trees. That means 78% efficiency of tree detection phase.

Numbers of both omitted and incorrectly detected trees depend on classification mask used. Without a mask more incorrect “trees” would be found in grass fields, roads, etc. On the other hand probably no trees would be omitted, aside from the problematic category. It is question of a coincidence (and a spatial resolution to be fair), whether or not two very closely standing trees would be distinguished.

Tree crown delineation phase was started with local maxima found in the first phase as the seeds. Seeded region growing was performed with the following initial settings. We expect maximal crown diameter of 12 meters, therefore with 80 cm pixel size maximal distance from seed is 7 pixels. Minimal agreement in brightness required was set to 40 percent compared to seed brightness value and 50 percent compared to the average of previously accepted crown pixels. Borders set up by a Voronoi diagram were modified three times and it was allowed to cross the border at most by two pixels. Foreign territories made by previously accepted pixels are not allowed to be crossed. Step by step in radial direction all seeds were developed simultaneously.

Table 3. Seeded region growing settings

Distance from seed	7 pixels
Brightness agreement with seed	40 %
Brightness agreement with average	50 %
Spectral agreement	not required
Voronoi boundaries	modified 3 times
Boundary crossing	at most 2 pixels

Tree crown delineation results

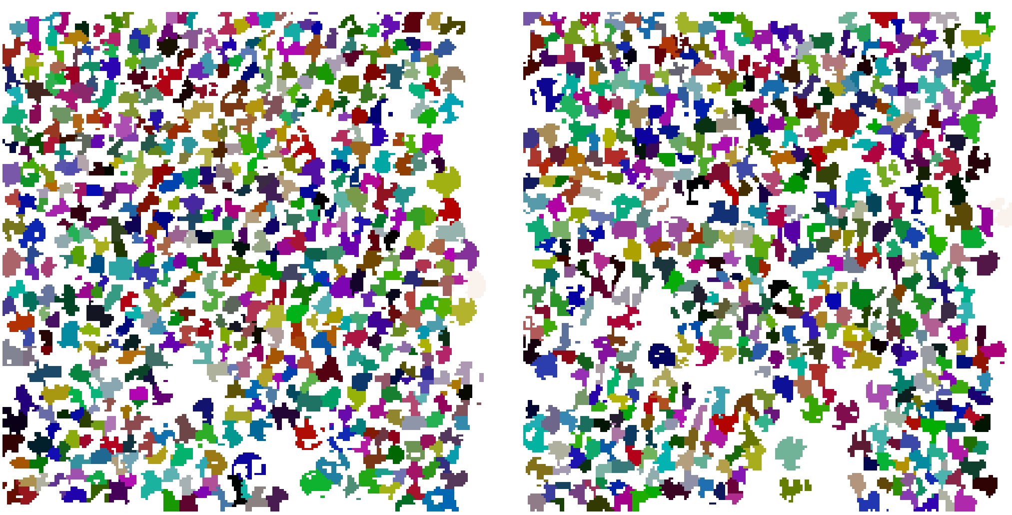

Fig 6. Results of seeded region growing (Eagle – left, Dual – right)

The results of a delineation phase were evaluated manually by direct comparison with very high spatial resolution image as well. Agreement between delineated crown area and actual tree crown was rated using scale from 0 to 4 with the following meaning. Rating 0 means 0% agreement or more precisely strong disagreement between a delineated area and a tree crown in size and shape. Very good agreement in size and shape, denoted as 100% agreement, is rated with 4.

We worked with the first 85 lines of the images again. For the Eagle data 230 delineated areas were evaluated with average 64% agreement, 90 areas rated 2 or less and 140 areas rated 3 or 4. For the Dual data 211 delineated areas were evaluated with average 52% agreement, 109 areas rated 2 or less, 102 areas rated 3 or 4.

We can see an agreement between tree crown detection and tree crown delineation results. More omitted trees in a detection phase on the Dual data implied worse segmentation results. It is understandable; typically when one of the two trees standing close to each other is not detected, the crown of the other is grown over both of them and would be rated as unsatisfactory. Improvements in both parts of algorithm are important and should be done to achieve better results.

There were minor differences between Eagle and Dual campaign, for example slightly in possition and geometry of the flight operating lines or in the post processing corrections (especially geometric ones). The differences in the results after the same segmentation process are expectable. On the other hand in both cases the applicability of 80cm optical data for tree crown segmentation was demonstrated.

What do influence the results?

There is a lot of interaction between the data and all the parameters of a segmentation algorithm, mainly the spatial and spectral resolution, or the differences in crown sizes.

Spatial resolution influences the size of a crown in the image. With the size of the crown under 4-5 pixels it is impossible to identify the crowns correctly. This is the first (lower) boundary of spatial resolution. But with the spatial resolution being too high, inadequate details occur and local maxima approach fails with several maxima found within single crown. So there is the second (upper) spatial resolution boundary. Pixel size of 80 cm used in our study is serving well — however pixel size of 20 cm used for the validation is too high for the presented algorithm.

Spectral resolution is less important for the segmentation because we averaged the bands into grayscale image. However it is a valuable opportunity to have spectral bands that include vegetation spectral information. Spectral agreement was not taken into consideration in the described analyses, more studies are needed.

Primary individual tree detection algorithms were proposed for relatively homogenous stands of coniferous species. We deal with heterogeneousness using masks and adaptive approach. The applicability of the results is obviously not universal and specific site characteristics must be taken into consideration.

Differences in tree crown sizes according to tree age composition are caught up well with adaptive approach. Both histogram equalization and local maxima detection are performed using a variable window size. It provides suitable results for different tree crown sizes and shapes. On the other hand the computational time increases significantly when different parameters are needed for each pixel.

After the above-mentioned input conditions, let’s discuss the internal conditions of the segmentation process. Computation of the average brightness image over selected spectral bands, as well as using the classification mask has the aim to suppress or even to mask out the non-tree areas. These are still uncertainties present in the input conditions; especially the quality of the classification mask, which is however not a question of this paper. On the other hand better classification mask implies better tree crown detection results.

Adaptive approach used in the following steps of tree crown detection depends on appropriate choices of variable window size. Recommendations for equalization, filtering and local maxima detection are mentioned in the Methods chapter. Expected tree crown size and spatial resolution play the major role.

In the seeded region growing process a distance from a seed is a last stopping condition. It stops the growing in cases when the other conditions fail to work correctly. We can’t expect entirely circular tree crowns, so a distance from a seed should be set slightly higher than the expected tree crown radius.

Brightness agreement is a fundamental condition to be fulfilled to identify tree crowns. After histogram equalization we have a uniform brightness distribution over both exposed and shaded crown parts. Lower limit for brightness agreement covers wider range of brightness over the region of interest and has the strong effect on the other stopping conditions. But the brightness distribution should be uniform after the equalization; the tree tops should have the highest brightness possible everywhere over the image and that’s why higher brightness agreement limit is recommended. Values of 40 and 50 percent worked well in our example.

Spectral agreement was not required in our example. It can help when a significant difference in brightness is missing on the edge of the crown. That’s why selected spectral bands are recommended to evaluate a spectral agreement.

Voronoi diagram is used as a preliminary conception of forest area division. It is necessary to distinguish two trees standing next to each other. Corrections made on the original Voronoi diagram are recommended to comprehend different tree sizes and shapes. Final post-processing depends on expected output needed for subsequent usage of the results.

ACKNOWLEDGEMENTS

This work has been supported by the Czech Ministry of Environment (ForChange SP/2d1/70/08, MŽP) and the research intention AV0Z60870520 ISBE AV ČR, v. i. i.

REFERENCES

Asner, G. (1998) Biophysical and Biochemical Sources of Variability in Canopy Reflectance. Remote Sensing of Environment, 64, 234–253.

Goetz, A. (2009) Three decades of hyperspectral remote sensing of the Earth: A personal view. Remote Sensing of Environment, 113, S5–S16.

Gougeon, F. A., Leckie, D. G. (2006) The Individual Tree Crown Approach Applied to Ikonos Images of a Coniferous Plantation Area. Photogrammetric Engineering & Remote Sensing, Vol. 72, No. 11, pp. 1287–1297.

Hanuš, J., Malenovský, Z., Homolová, L., Kaplan, V., Lukeš, P., Cudlín, P. (2008) Potentials of the VNIR airborne hyperspectral system AISA Eagle. Symposium GIS Ostrava 2008, (CZ), 27-30 January, 2008, Proceedings-CD.

Hirschmugl, M., Ofner, M., Raggam, J., Schardt, M. (2007) Single tree detection in very high resolution remote sensing data. Remote Sensing of Environment, 110, 533–544.

Novotný, J. (2009) Multispektrální analýza obrazových dat. Faculty of Mechanical Engineering, Brno University of Technology, Diploma Thesis.

Rautiainen, M., Heiskanena, J., Eklundhb, L., Mõttusc, M., Lukeš, P., Stenberg, P. (2010) Ecological applications of physically based remote sensing methods. Scandinavian Journal of Forest Research, volume 25, issue 4, 325–339.

Ustin, S., Gitelson, A. A., Jacquemoud, S., Schaepman, M., Asner, G. P., Gamon, J. A., Zarco-Tejada, P. (2009) Retrieval of foliar information about plant pigment systems from high resolution spectroscopy. Remote Sensing of Environment, 113, S67–S77.

Wulder, M., Niemann, K. O., Goodenough, D. G. (2000) Local Maximum Filtering for the Extraction of Tree Locations and Basal Area from High Spatial Resolution Imagery. Remote Sensing of Environment, 73, 103-114.

TRANSFORMATION AND CALIBRATION OF PICTURES IN THE FOTOM SYSTEM

LICEV Lacezar and KRAL Jan

Department of Computer Science, FEECS, VŠB - Technical University of Ostrava
708 33, Ostrava, Czech republic
Contact: lacezar.licev@vsb.cz

Department of Computer Science, FEECS, VŠB - Technical University of Ostrava
708 33, Ostrava, Czech republic
Contact: jn.kral@gmail.com

Abstract.

The FOTOM system developed at the Department of Computer Science FEECS VŠB TU Ostrava is used for digital image processing. FOTOM 2008 was created in the programming language C++. In 2009, a new, revolutionary version of the system, FOTOM 2009, was designed. This new system has new kernel and provides a more universal and easily extensible architecture with newly solved calibration and transformation images.

Mine image transformations consist of conversion data from snapshots to the three - dimensional coordinate system. Calibration images and acquired variables are used for corrective projection allowing for easier measuring of observed objects. Calibration images also support the transformation of objects recumbent on the inner wall of a cylindrical object.

Keywords: architecture, photogrammetry, FOTOM 2000, 2008, 2009, Java, calibration, Netbeans platform, projection, transformation, XML, interest object, image processing.

INTRODUCTION

This report addresses modern methods used for processing images and, in particular, measuring the objects present in them. Using the program / module for calibration and transformation of images within the framework of FOTOM 2008 and 2009 systems, a new generation of the FOTOM system has been created.

Data is converted from snapshots to 3D coordinate systems during the transformation of mine images. When calibrating images, we acquire variables that are useful in corrective projection and allow us to measure observed objects more easliy. Calibrating images also aids in the transformation of objects recumbent on the inner wall of a cylindrical object

These images can be used to measure objects found on inner wall of a mine - 2D image.

IMAGING METHODS AND MINE MEASURING

Measuring methods used at VVUÚ Ostrava-Radvanice and BMZ VŠB TUO

The method used in diagnosing pits presents a single-image photogrammeric method making use of two luminary plains at the same time, see Fig..1. In both images, there are two horizontal profiles displayed with a common constant vertical distance D. This principle rests upon the fact that in the original profile we regulate the photogrammetric set so that the higher of the two luminary plains is at the exact same level as the initial profile. We then select at least two appropriate points in the profile whose mutual position we determine. Following exposure, not only will the initial image be displayed, but the following image will be displayed as well. Once the entire set is activated with value D, the upper luminary plain level will be at the level of profile No. 2, and profile No. 3 will be decreased by the value of D. This process is repeated through all depths of the pit being measured.

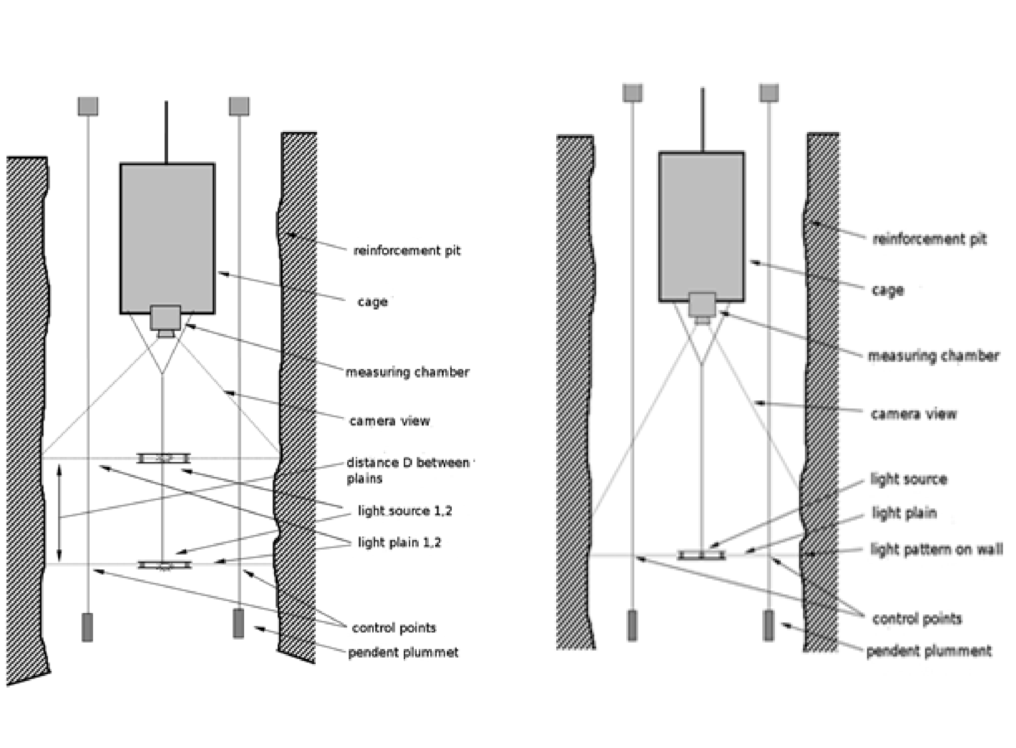

VVUÚ Ostrava-Radvanice BMZ VŠB TU Ostrava

Fig. 1: 2D projection point.

The method used at BMZ VŠB TUO, which was implemented to diagnose pits, presents a single-image photogrammetric method using one luminary plain (see picture No. 2.1.) In each image, not only are the given profile pits, guide, and pipeline captured, but the intersection luminary plains with wire plumb lines are captured as well. The distances of the photochambers and plain are constant, therefore the scale of all images is the same.

Prior to measuring, it is neccessary to select an acceptable interval of survey profiles (etc. 10 m) and mark their position in the pit. The disadvantage in using this method lies in the difficulty of manipulating when using plumb lines, resulting in the necessity for longer pauses in movement within the pit. At larger depths, a laborious stabilization or rehanging of plumb lines is necessary.

Imaging is processed with the aid of the photogrammetric kit developed by BMZ VŠB TU Ostrava and VVUÚ Ostrava-Radvanice. The kit (see picture No. 1) is pieced together by a surveying camera (aerial photogrammetry chamber AFP 21 Soviet production format 13x18 cm.), which is hung below the cage. The upper light source is hung 6m below the camera (D = 6m). This is special flash equipment equipped with an orbicular lens that generates a luminous plain (designed at the former Ore Research Institute of Prague). When measuring, a control panel is placed inside the container, upon which a metal sheet cover attached is placed simultaneously attached to a 24V accumulator battery. This control panel ensures the entire process. The total length of the device below the cage is about 18m.

A 1m measuring wheel is placed in the engine room to measure the distance traveled.

Transformation of mine images in the FOTOM system

The method used to analyze mine images belongs to the single-image photogrammetry category. This means that we can only determine 2D coordinates in the plain of the photographed object based on the position of the photo-station and orientation of the photographed object plain. In our case, this subject is the above-mentioned light plain which leaves a light-footprint on the profile pits and other devices. If we observe only the lit places (points), belonging to the light-footprint, we can clearly identify their position in the global coordinate system.

Now we need to determine transformation relations, which will transfer data from a local (snapshot) coordinate system to a global coordinate system. These transformations belong to the category of planar affine transformations. If images are produced as described, the following conditions are met:

- luminary plain and projection plain are parallel
- the image axis is perpendicular to the plain

- distortion in the special camera lens is insignificant

turn: $$\mathbf{R} = \begin{pmatrix} r_x & r_y & 0 \\ -r_y & r_x & 0 \\ 0 & 0 & 1 \end{pmatrix} \quad (1)$$

shift: $$\mathbf{T} = \begin{pmatrix} 1 & 0 & 0 \\ 0 & 1 & 0 \\ t_x & t_y & 1 \end{pmatrix} \quad (2)$$

scaling: $$\mathbf{S} = \begin{pmatrix} 1 & 0 & 0 \\ 0 & 1 & 0 \\ 0 & 0 & \frac{1}{s} \end{pmatrix} \quad (3)$$

The transformation point is then expressed by the matrix equation

$$\mathbf{X}' = \mathbf{X} \cdot \mathbf{Tr} \quad (4)$$

where X′ is the row vector representing the position of the transformed point after the transformation, X is a row vector representing the position of the transition point and Tr is the transformation matrix.

Then the overall transformation matrix is represented as:

$$\mathbf{Tr} = \mathbf{R} \cdot \mathbf{S} \cdot \mathbf{T} = \begin{pmatrix} r_x & r_y & 0 \\ -r_y & r_x & 0 \\ 0 & 0 & 1 \end{pmatrix} \cdot \begin{pmatrix} 1 & 0 & 0 \\ 0 & 1 & 0 \\ 0 & 0 & \frac{1}{s} \end{pmatrix} \cdot \begin{pmatrix} 1 & 0 & 0 \\ 0 & 1 & 0 \\ t_x & t_y & 1 \end{pmatrix} = \begin{pmatrix} r_x & r_y & 0 \\ -r_y & r_x & 0 \\ \frac{t_x}{s} & \frac{t_y}{s} & \frac{1}{s} \end{pmatrix} \quad (5)$$

We now need to determine the coefficients r_x, r_y, t_x, t_y a s. Let us set an auxiliary function of the two variables **atg2**, from which the parameters *x* and *y* calculate the deflection line angle of points [*0, 0*] and [*x, y*] from the positive half x-axis. It is now a function with field values (-p, p⟩.

The transformation is dereved from the knowledge of the two pairs of corresponding control points. Local control points are designate as L1 and L2, corresponding to the global control points G1 and G2. Further, let us introduce ΔL as the distince between points L1 and L2:

$$\Delta\mathrm{L} = \sqrt{\left(\mathrm{L2_x} - \mathrm{L1_x}\right)^2 + \left(\mathrm{L2_y} - \mathrm{L1_y}\right)^2} \tag{6}$$

Likewise, ΔG is the distance between points G1 and G2. The angle rotation is designated as ψ:

$$\psi = \mathrm{atg}\,2\left(\mathrm{G2_y} - \mathrm{G1_y}, \mathrm{G2_x} - \mathrm{G1_x}\right) - \mathrm{atg}\,2\left(\mathrm{L2_y} - \mathrm{L1_y}, \mathrm{L2_x} - \mathrm{L1_x}\right) \tag{7}$$

Then the transformation coefficients are:

$$s = \frac{\Delta\mathrm{G}}{\Delta\mathrm{L}} \tag{8}$$

$$r_x = \cos(\psi) \tag{9}$$

$$r_x = \sin(\psi) \tag{10}$$

$$t_x = \mathrm{G1_x} - s \cdot \left(\mathrm{L1_x}\, r_x - \mathrm{L1_y}\, r_y\right) \tag{11}$$

$$t_y = \mathrm{G1_y} - s \cdot \left(\mathrm{L1_y}\, r_x + \mathrm{L1_x}\, r_y\right) \tag{12}$$

Factors affecting measurement accuracy

This issue is relatively vast, therefore, we shall limit our enumeration to single factors. The most important factor affecting the accuracy of measurement (Ličev, Holusa, 1998), is to set a plumb line for the exact location of control points. Any major error can also cause a deflection of luminary plains from projection plains. Ideally, both of these plains should be horizontal. Other factors affecting accuracy include the cameras themselves (photo laboratory, lens distortion,) and the use of photographic materials (film, glass plates, …). Other errors may occur when determining the coordinate points on an image (resolution of the equipment – digitizer, scanner, monitor, ...).

In conclusion, photogrammetric accuracy for measurement of vertical mine workings is primarily dependent on the quality of facilities, the photography itslef and the setting positions of points on the images.

CALIBRATION AND TRANSFORMATION OF IMAGES IN THE FOTOM SYSTEM

FOTOM 2008

The Department of Computer Science FEECS VŠB TU Ostrava has been developing the FOTOM system for use in computer processing of digital image since 1998. At first, the system was designed to measure mine pits, but over time it has expanded into a powerful system with many modules offering advanced detection and visualization of objects of interest measurements. The architecture of this development branch carries the name FOTOM 2008 and consists of modules:

Calibration is a set of operations, which under specific conditions determine the relationship between value quantities that are indicated by a measuring system or a measuring instrument.

Rotation - Rotation templates run in virtual 3D space and correspond to rotations on the main axis object. The location calibration pattern is set using the center template, or by clicking on the image.

Camera – The camera can be moved in virtual space (X,Y,Z camera coordinates); the rotation of the camera is fixed in the program. The size of the resulting picture may be adjusted using the zoom function.

Screening:

Perspective projection – projection rays are derived from a single point. Perspective projection respects the optical model, which reflects what we see in the real world. At increasing distances from the observer, we model proportional changes in the objects we see, which provides a good 3D perception of a plain of projection.

The central projection is a special case where projection rays converge in a concentric circle in the center of an image

This projection is described by the following parameters:

$\mathbf{a}_{x,y,z}$ – point in 3D space scene

$\mathbf{c}_{x,y,z}$ – camera location

$\theta_{x,y,z}$ – camera rotation (for $\mathbf{c}_{x,y,z} = \langle 0,0,0 \rangle$ a $\theta_{x,y,z\ z} = \langle 0,0,0 \rangle$, a

3D vector $\langle 1,2,0 \rangle$ displayed in a 2D vector $\langle 1,2 \rangle$)

$\mathbf{e}_{x,y,z}$ – placement of an observer in the camera space

$\mathbf{b}_{x,y}$ – 2D projection of point **a**

First we define the point $\mathbf{d}_{x,y,z}$ as the point of translation **a** to the coordinate system defined by **c**.

This is achieved by subtracting **c** from **a** and then applying the result of the rotation matrix θ.

$$\begin{bmatrix} d_x \\ d_y \\ d_z \end{bmatrix} = \begin{bmatrix} 1 & 0 & 0 \\ 0 & \cos-\theta_x & \sin-\theta_x \\ 0 & -\sin-\theta_x & \cos-\theta_x \end{bmatrix} \begin{bmatrix} \cos-\theta_y & 0 & -\sin-\theta_y \\ 0 & 1 & 0 \\ \sin-\theta_y & 0 & \cos-\theta_y \end{bmatrix} \begin{bmatrix} \cos-\theta_z & \sin-\theta_z & 0 \\ -\sin-\theta_z & \cos-\theta_z & 0 \\ 0 & 0 & 1 \end{bmatrix} \left(\begin{bmatrix} a_x \\ a_y \\ a_z \end{bmatrix} - \begin{bmatrix} c_x \\ c_y \\ c_z \end{bmatrix} \right) \quad (13)$$

Upon breaking down the values we obtain d_x, d_y, d_z.

A thusly transformed point may be *projected*as a 2D plain implementing the following conversion:

$$\begin{bmatrix} f_x \\ f_y \\ f_z \\ f\omega \end{bmatrix} = \begin{bmatrix} 1 & 0 & 0 & -e_x \\ 0 & 1 & 0 & -e_y \\ 0 & 0 & 1 & 0 \\ 0 & 0 & 1/-e_z & 0 \end{bmatrix} \begin{bmatrix} d_x \\ d_y \\ d_z \\ 1 \end{bmatrix} \quad (14)$$

$$\begin{aligned} b_x &= f_x / f_\omega \\ b_y &= f_y / f_\omega \end{aligned} \quad (15)$$

after the transcript:

$$\begin{aligned} b_x &= (d_x - e_x)(e_z / dz) \\ b_y &= (d_y - e_y)(e_z / dz) \end{aligned} \quad (16)$$

where $\mathbf{e}_z$ is the distance of the plain camera from the observer corresponding to the angle sight α

$$\alpha = 2.\tan^{-1}(1/e_z) \quad (17)$$

The resulting projection to the computer–generated image is performed with a linear interpolation of the image size.

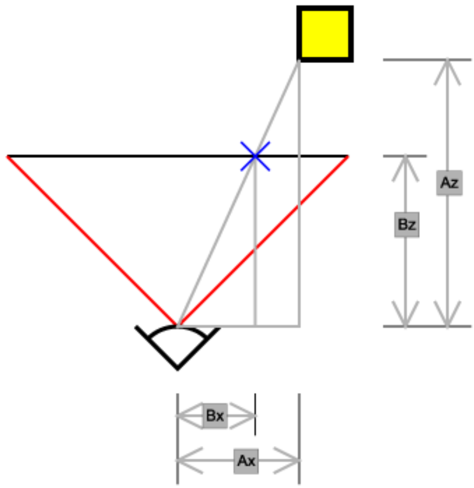

Fig. 2: 2D projection point.

Transformation image:

A calculation of the circles displayed in Fig No. 2 is follows.We have a total of 3 blue circles:

- k_0 with radius r_0 =first circles, which is entered and is closest to the center
- k_1 with radius r_1 = the largest circle in the Fig. It is presented as the second circle at the program start and should intersect with the determined starting point on the measuring axis.
- k_2 with radius r_2 = the second largest circle in Fig. This circle defines the size of first interval on the measurement axis in the pixel.

Based on these factors, the following is true:

$r_1 - r_2$ = size of the first unit of scale in pixels = U_1 (18)

As for the yellow circles displayed in the Fig, the following is true :

First, the largest yellow circle is K3 with a radius R3. This circle marks a second unit for the measuring axis.

$r_2 - r_3$ = size of the second unit pixel scale = U_2 (19)

Then the ratio

$U_2/U_1 = \Delta U$ = the coeficient for reducing circles. (20)

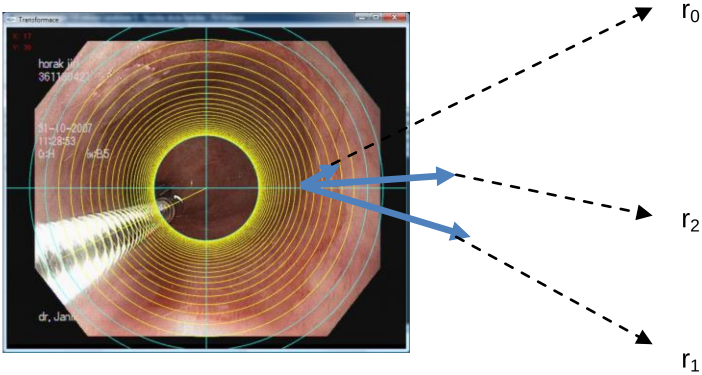

Fig. 3 Circle in image.

For the ensuing the yellow circles and their radius direction from circle k3 to the center, the following is true:

r4 = r3 – U3,   where: U3 = U2 * ΔU   (21)

r5 = r4 – U4,   where: U4 = U3 * ΔU   (22)

r6 = r5 – U5,   where: U5 = U4 * ΔU   (23)

etc.

In other words, a calculation for the size of ensuing units for

measurement = Ui = Ui-1 * ΔU   (24)

Then the radius is given by

ri = ri-1 – Ui-1   (25)

From the calculation above, we can perform the calculation of the perimeter of such circles, according to the equation:

Li = 2riπ   (26)

Scale

The size of the first unit is taken as the base. The unpacked image is read as a block of rows corresponding to the thickness of the units. Then, these unpacked rows transform into the first unit width. The principle of unpacking is presented below in Fig No. 4

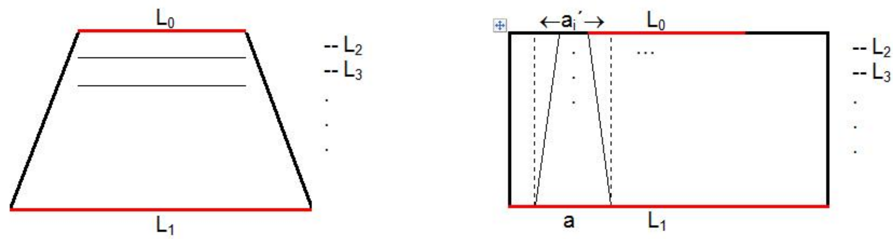

4a 4b

Fig. 4. Principle of unpacking an image.

Fig No. 4a is shows the shape of the unpacked image before the expansion and in Fig No. 4b the shape of the unpacked image after expansion is displayed. The actual expansion is performed on the basis of the calculated values of ***a*** and ***a_i´*** in equation:

$a_i´ = L_i/n$ (27)

$a = L_1/n$ (28)

where: a, a_i´ – the wide segments of L_1 and L_i,

n – the amount of sections extended.

The logic in this exercise exists within the extending the width of section ***a_i´*** to that of width ***a*.**

The result of unpacking and extending the image from Fig No. 2 is shown in Fig No.5.

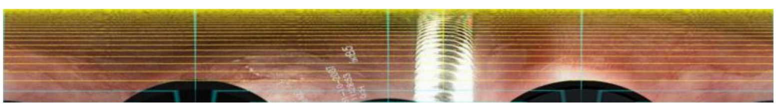

Fig. 5. Unpacking an image.

In Fig No.5, a transformed image is displayed (see Fig No. 2), except that in addition to unpacking and extending, it is also extended in length. This extension is performed by multiplying by the constant distance between each circle. Calibration of the length of the image is also performed using this last step.

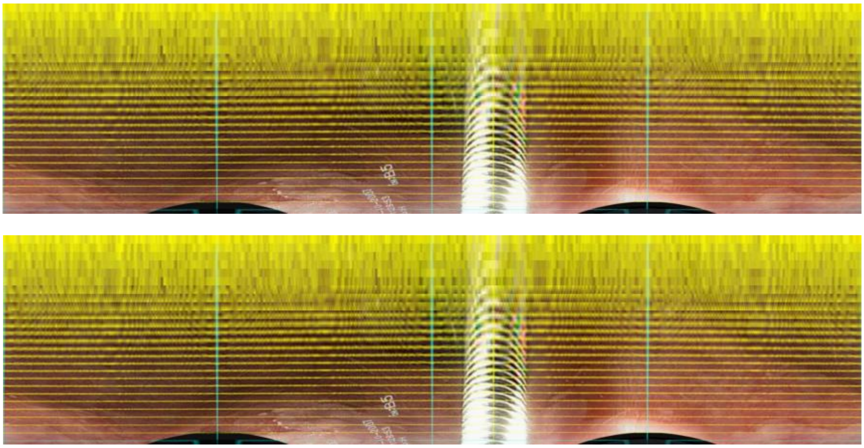

Fig. 6. Transforming the image.

The program for calibration and image transformation began with module Fotom1 of the FOTOM 2008 system. Using this program, we may project the image back onto the plain based on user defined, design projection parametrs. It is assumed that the input files are displayed using a projective view – perspective.

Using the program for calibration and image transformation

- Evaluation using image calibration and FOTOM 2008, without using a calibration image.

a. Evalution of the object as a whole

b. Evaluation of the object by dividing the object into segments

c. Evalution of the object using the standard

- Evaluation of an object by using calibration software and FOTOM 2008.

a. Using a grid-type board calibration program (see Fig No. 7)

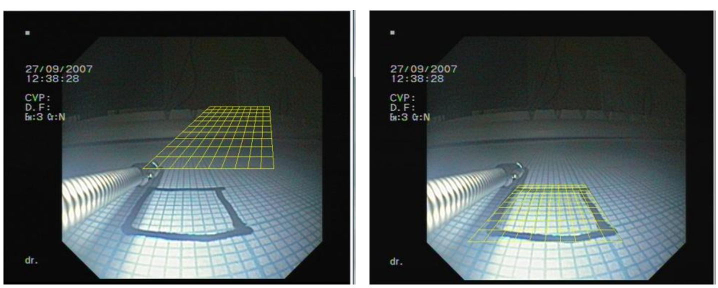

Fig. 7

b. The use of a grid–type circle calibration program.

Using a suitable grid to localize the beginning and end of the area/region of interest.

- Evaluation using the transformation system and FOTOM 2008.

Image editing for evaluations is performed by using the calibration program. To achieve the necessary repetitious accuracy, it is necessary to determine the exact center of the image/object upon which the object is analyzed. The center can be determined in several ways, as follows:

a. Using the transformation module calibration program

b. Ingestion of FOTOM 2008 and a specific Fotom1 module. Here, using tools to analyze objects in the image, we may define a polygon describing the middle/center of gravity of the object being analyzed., See Figs No.8 and No.9.

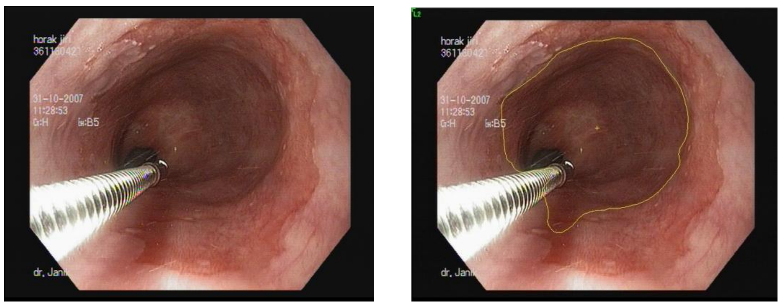

Fig. 8

The result of the transformation is show in Fig No. 9

Fig. 9

System FOTOM 2009

Over the years, the development of the system FOTOM 2008 has remained a very powerful tool for digital image processing, but has gradually ceased to meet the requirements of modern applications. Originally, this system was developed as a dedicated program and did not anticipate so many developments and the extent of possible applications. The system architecture is not composed for a modular system and all resulting modules are created as a separate application and are then integrated into the system through direct intervention in the source code. Since there is no established public communication for interface modules, each module must deal with access to image processing defined objects, etc., independantly. The consequence of these properties has resulted in an increasingly difficult expansion of the system itself, as well as individual modules.

These factors have led to the necessity to create an entirely new generation system, which would be based on a modern platform and be able to revise the system in an entirely modular way. In addition to this basic requirement, there have been other objectives introduced that have lead to the creation of a revolutionary version of FOTOM 2009.

The FOTOM 2009 application is able to export images with defined objects to the system FOTOM 2008 format, where it is possible to analyze the latest version of the system before it is implemented.

Calibration and transformation of images in the system FOTOM 2009

For simplification calibration is not considered with lens distortion, its processing only input digital image. However, lens distortion processing must be included for increase precision of calibration method into the future.

The output calibration is a two-dimensional image offering a parallel, right-angled, top view of an area of interest. 2D reduction results in an image proportionally showing only one level of space that is captured on the input image. The area captured in the image may contain an infinite number of plains. For successful reconstruction, the calibrated plain must be accurately defined. An integral part of this work is to program designed to calibrate a plain in space. It is necessary not only to define the plain to be calibrated, but also introduce a way to enter the plain: distance, angle plain and direction vector. This situation is illustrated in Fig No.10

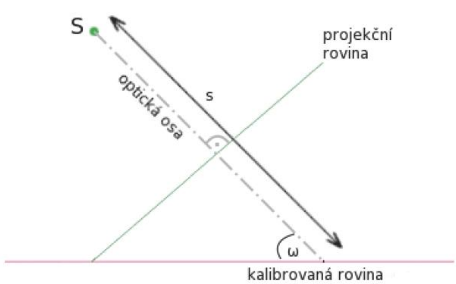

Fig. 10. Tilt and distance of a calibration plain.

Calibration process:

Calibration is focused on two kinds of images.

Flat images include the calibration of a general 3D image, when the calibrated surface on an image is captured as a plain. To apply this method, it is necessary to precisely define which plain captured on the image will be the object of calibration.

The Images cavity includes calibration of specific images created inside the hollow cylinder whose inner surface is captured on film and is the inner surface of interest intended for calibration - similar to the transformation of the image in system FOTOM 2008.

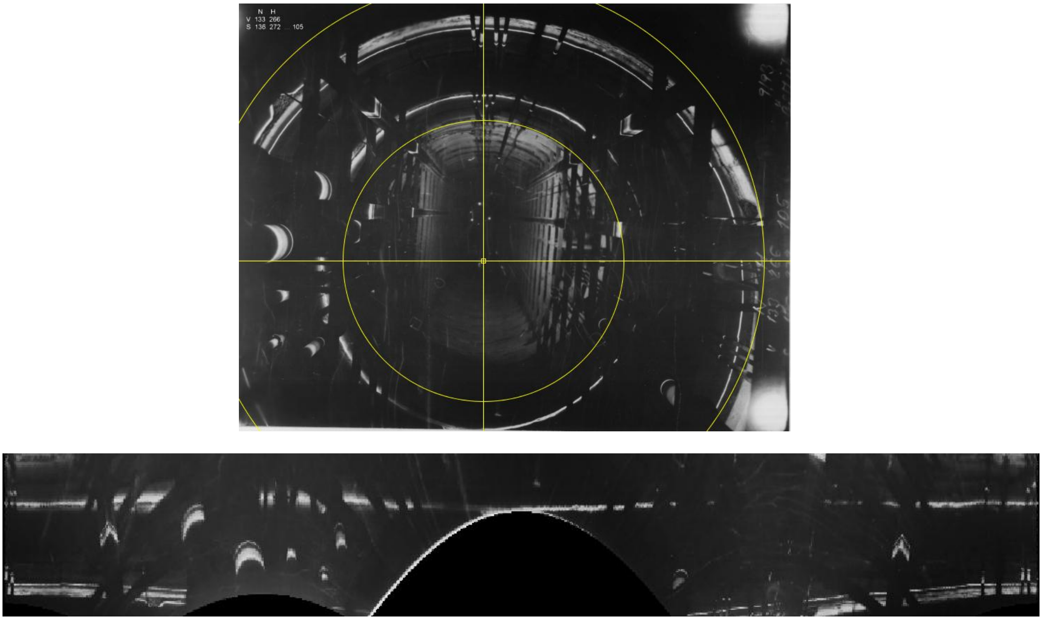

Fig. 11. Transformation of image mining.

RESULT

We have managed to create a new generation of FOTOM with the help of a program for calibration and transformation of images within the scope of systems FOTOM 2008 and 2009.

With mine images, transformations involve the conversion of a snapshot to a 3D coordinate system. With calibration, images acquire, among others things, variables that are used for corrective projections enabling easier measuring of observed objects. The calibration of images also supports object transformations recumbent on the inner wall of a cylindrical object. Using this , we can measure objects found on the inner wall of a mine with only a 2D image.

During the measurement process an aberration appears as a result of the lens geometric distortion. That is why the measurement accuracy of the objects of our interest is limited. The usability of implemented system is maintained through the calibration attributes preservation. This allows us to perform the same transformation for the same part of image with similar error. The comparison of the new result with the previous one allows the user to track changes of the object size over time.

As a result is complex system that provides processing of 3D images, which can be transformed and then continue with image processing by others implemented photogrammetric functionality. System uses modern software solutions and provides simple graphic user interface. This module/program is unique and will enable us to calibrate and transform not only mining processes. Collaboration with doctors found usage of possibility to measure an object of interest in medicine.

REFERENCES

AO 175 220 o názvu "Způsob fotogrammetrického zaměřování"

AO 235 342 o názvu "Nosné zařízení vertikální fotogrammetrické soupravy pro měření jam z těžní nádoby"

AO 241 367 o názvu "Vertikální fotogrammetrická souprava se světelnou rovinou"

Beneš B.: Počítačová grafika od 2D do 3D – 11. část, CHIP, ročník IX/1999, číslo 3, ISSN 1210-0684, 1999.

Černý I,Gavlovský E.: Odborná činnost na BMZ-referát na VIII svět. kongresu IMS v USA, IX.1991

Fojtů B., Dombrovský Z.: Coal Seam Extraction in Safety Shact Pillar, the Photogrammetric Measarument of a Shaft by the Veritikal Polygeometric traverse, září 1991, Kentucky USA

Kovář L: FOTCOUNT- Programátorská dokumentace, BMZ VŠB TU v Ostravě, 1992

Ličev L. - Holuša T.: Nové řešení důlní fotogrammetrie na PC, 2/1998, URGP Praha, 1998.

Ličev L.: New approaches to mining photogrammetry using PC, 5 nacionalna konferencija Varna ´98, MGU Sofia, 1998.

Ličev, L.: Fotogrammetrie na PC, 4/1999, Acta montanistica slovaca, Košice, SR, 1999.

Ličev L.: Fotogrammetrické měření důlních jam, 7/2001, URGP Praha, 2001.

Ličev L.: FOTOM 2000 a vizualizace procesu měření, Konference GIS '2001 VŠB-TU Ostrava, HGF, 2001.

Ličev L.: Podrobnější analýza snímků, 12. konference SDMG, Ostrava, VŠB HGF, 2005.

Ličev, L. - Holuša T.: Fotogrammetrické měření důlních jam, Konference GIS'99 VŠB TUO, HGF, 1999.

Ličev, L., Krahulec, L., Král, J.: Systém FOTOM 2009 na platformě NetBeans. In Proceedings - Symposium GIS Ostrava 2010. 2010 Hruba, Michal Podhorányi, VŠB TU Ostrava:VŠB TU Ostrava, 2010, čis. 1, Proceedings - Symposium GIS Ostrava 2010, p132-133, 8 str. VŠB TU Ostrava, ISBN 978-80-248-2171-9, 2010.

Pavelka K.: Fotogrammetrie 1/2009, 10/2003 a 20/2003, Vydavatelství ČVUT Praha

Serra, J.: Image Analysis and Matematical Morphology, Vol. 2, Academic Press, New York, 1988.

Sun Microsystems, Inc.: Modules API [online]. 2009 [citováno 2. Dubna 2009] Available at: <http://bits.netbeans.org/dev/javadoc/org-openidemodules/org/openide/modules/doc-files/api.html/>

Sojka E.: Digitální zpracování obrazu, skripta VŠB - TUO, FEECS, 1999.

Žára J. a kolektiv: Počítačová grafika – principy algoritmy, 1. vydání, GRADA, ISBN 80-85623-00-5, Praha, 1992.

Part II

Advances in Spatial Modelling

ENHANCED METHODOLOGY FOR ONTOLOGY DEVELOPMENT

RAPANT Petr, SZTURCOVA Daniela and HRUBA Lucie

Institute of Geoinformatics, Faculty of Mining and Geology, VSB – Technical University of Ostrava, 17. listopadu 15, 708 33, Ostrava – Poruba, Czech Republic, *petr.rapant@vsb.cz*

Institute of Geoinformatics, Faculty of Mining and Geology, VSB – Technical University of Ostrava, 17. listopadu 15, 708 33, Ostrava – Poruba, Czech Republic, *daniela.durakova@vsb.cz*

Department of Economy and Marketing, Regional Development Agency Ostrava, Na Jizdarne 7, 702 00, Ostrava, Czech Republic
hruba@arr.cz

Abstract

The presented paper deals with building of an initial glossary of terms, which is a preparatory phase of domain ontology building. Existing methodologies suppose to develop the initial glossary of terms by an analysis of existing documents, or using expert knowledge. There is no structured process defined for this step of the ontology building. We propose to embrace experience from object oriented analysis: to describe structure, behaviour and rules valid for a domain of interest. These three descriptions represent complex and systematic view to the domain and ensure that created glossary of terms will be exhaustive. We demonstrate our method on the domain of road transport. The method is developed as an extension of well known METHONTOLOGY, but it is general enough to be acceptable for other methodologies for the ontology building too.

Keywords: ontology design, ontology design methodology, transportation

INTRODUCTION

The research project Logic and Artificial Intelligence for Multi-agent Systems (MASS) project was carried at the Laboratory of Intelligent Systems, VSB – Technical University of Ostrava, Czech Republic, between 2004 – 2008. One of the objectives of the project was to find a solution for the communication between agents under the situated Multi-agent system (MASS), i.e. the system, in which individual agents are situated in space and spatial processes are implemented. Road transport was chosen as a test domain. The individual vehicles were employed as the MASS agents. In addressing the communication of these agents, it has proven essential to use a set of well-defined concepts with clear semantics and syntax, allowing description of both the road infrastructure itself as well as the movement of vehicles on it, including the rules which are followed in this movement. It meant to use an appropriate ontology, which describes well the domain studied and also allows clear-cut communication of the agents using clear semantics of the concepts.

DEVELOPMENT OF METHODOLOGY FOR ONTOLOGY DESIGN

Development of ontology methodologies has been addressed by many research teams. They made attempts to define the sequences of steps leading to the formation of ontology. A very good overview of different methodologies is provided at e.g. Gómez-Pérez work.

One of the first methodologies was presented in 1995. It was based on the experience drawn from the Enterprise Ontology and TOVE (TOronto Virtual Enterprise) draft, which was obtained in the field of enterprise modelling. One year later, the KACTUS project was presented at the European Conference on Artificial Intelligence, which focused on developing the ontology for the field of electric power mains. In the context of this project the methodologies for ontology development were also presented. The methodology used to design an ontology proposal within the SENSUS project is also now firmly established. From our perspective, we consider the METHONTOLOGY to be the most interesting and well organized. It is dealt with in detail below.

The common feature of most of the above noted methodologies used for the formation of ontologies is that they do not systematically describe all stages of ontology development. What still needs to be processed is often the creation of the glossary of terms. However, this stage is considered, for the formation of ontology, crucial.

METHONTOLOGY METHODOLOGY

As stated above, we sought an appropriate methodology, which would allow for the systematic ontology development. After examining the various present methodologies, we observed that none of them meet our requirements in full. Therefore, we eventually decided to use the METHONTOLOGY to start with, and to develop its enhancement for the methods used for the *specification phase*, which will result in the building of the *glossary of terms*.

We have demonstrated the basic ontological types that form the content of ontology. It's a case of attributes, taxonomies, definitions of concepts, etc. METHONTOLOGY comes from these basic ontological types. METHONTOLOGY was developed in the Laboratory of Artificial Intelligence at the Polytechnic University of Madrid. This is largely based on IEEE Std 1074-1995. We decided to follow the METHONTOLOGY because of its transparent logical structure and integrity of its steps, which reflect the process of ontology development. This includes the following tasks:

- ontology specification,
- build glossary of terms,
- build concept taxonomies,
- build relation diagrams,
- build concept dictionary,
- describe:
    - relations,
    - attributes,
    - constants,
- describe:
    - formal axioms,
    - rules,
    - instances.

The METHONTOLOGY thus describes the sequence of steps that will, in its final stage, bring us the basic ontological types. Like most of these current methodologies, this one is no different in providing no detailed guidance on how to achieve adequacy of real ontological concepts, i.e. how to select appropriate concepts with regard to the given domain and its tasks. It only contains a brief description of how to proceed in the specification phase, i.e. during the *ontology specification*.

SPECIFICATION OF ONTOLOGY

The objective of this stage is to create a specification document written in natural language, which should include at least the following information:

- the purpose of ontology, including the intended use, use case scenarios, specifications of end users, etc.
- the level of formality of the implemented ontology,
- the range, including a set of concepts to be represented in the ontology, its characteristics and granularity.

It is recommended to use a middle-out approach, which allows obtain a set of terms that should be included in the ontology, without us knowing of their significance at that time. It is also recommended to group the terms into the classification trees. All this allows us not only to verify the relevance of ontology terms and seek out missing terms at an early stage of development, but also search for synonyms, or even omit the terms that are redundant. Another advantage of this approach is that it allows you to search for terms that should be the core of future ontology. Consequently, they can be generalized or, on the contrary, specialized, if needed and only to the necessary extent. The resulting set of terms is much more stable, and will require far fewer changes in the future.

METHONTOLOGY also recommends a whole range of techniques, how to acquire the knowledge from the area of the subject, such as different interviews, document analyses, etc. Based on this knowledge a glossary of terms is to be built later. However, this methodology provides no structured process to obtain a glossary of terms. Basically, an intuitive approach is herein assumed. We have attempted to resolve this issue.

PROPOSED ENHANCEMENT OF METHONTOLOGY METHODOLOGY

Building a basic glossary of terms, which so far has not taken into account the various integrity constraints, etc., must be preceded by a number of steps. As shown in our research, the steps leading to the creation of the glossary may be (at least in general) specified and systematised. Our proposal is aimed at such a specification. We are going to describe the basic principles, whose compliance will improve the relevance of the final ontology. We will, in particular, focus on the creation of ontology for the purposes of artificial intelligence and knowledge-based systems.

At the beginning of ontology development it is necessary to specify *the purpose of ontology*. The next step is to find and collect the terms used to describe a given domain. When taking this step, we are trying to maintain the shareability of the created ontology. Identified terms are evaluated with regard to the clarified *purpose* of our ontology. Subsequently, based on the selected terms, there will be the *glossary of terms* generated, which will include a simple list of terms from the given domain. Needless to say, the process preceding the creation of the glossary is iterative.

It's a good idea to realize at the beginning of the ontology development, that the domain analyzed to meet the needs of future knowledge-based system has its static and dynamic aspects, as well as behaviour rules. Static aspects of the system include the concepts of typical objects in the given domain, i.e. they describe *its static structure*. Dynamic aspects include a description of *the system behaviour* which must respect certain *rules of behaviour*.

The analysis of systems from different perspectives is dealt with inter alia using object-oriented analysis. There are a number of different methodologies to carry out such an analysis. However, those have some general features in common. They always attempt to describe the following elements:

- structure of the system
- behaviour of the system
- rules of the system behaviour.

Our proposal is based on the same approach. We have, therefore, designed the following sequence of steps that lead to the creation of the quality glossary of terms:

1) To search the initial set of terms there is a good idea to start with building up three descriptions of the analyzed domain:

a. description of the structure
b. description of the behaviour
c. description of the behaviour rules

Description of the structure is relatively simple, and should contain all the elements of the analyzed domain, which will affect or rather will implement behaviour of the domain.

Description of the behaviour may be more complicated. It should include a description of specific issues and tasks resolved within the domain, for example in the form of use case scenarios.

Description of the behaviour rules should involve all the rules that must be respected by the system elements in the task implementation resolved within the domain.

2) The next step is focused on extracting the set of terms from each of the descriptions (both, single and multi-word terms; it will be mostly the nouns and the verbs) shown in the descriptions and bearing the information related to the domain. This way we will obtain three independent sets of terms that do not entirely agree with each other at first glance. For further processing it is important to arrange them in alphabetical order. We will maintain any duplicity between the lists in this step.

3) Consequently, we will make a comparison of these three sets of terms, such as using a table with three columns. Each column will show one list. The entire table will be then arranged alphabetically, so that each line would contain the identical terms used in multiple description. If there is no identical term for a given term in another description (i.e. in another column), we will leave this column line blank. The final table shows that if we selected only one description for the terms used, the result would never be sufficiently representative.

4) We will proceed to search the individual basic terms which form the multiple word terms, and group them into individual hierarchies. If a multiple word term is considered unique, it may be introduced as one term (e.g. *the intended direction of continuation after the intersection*). Further on, the terms that are not included in the original description, but logically belong on the list are added. The rules of addition are based on analogy (e.g. the term *to the right* can be supplemented with the term *to the left*).

5) Eventually, we will search the synonyms and homonyms and group them together. The synonyms are given in succession on one line, separated by

commas. In the first place, we will enlist the term that is preferred. Homonyms are mentioned on separate lines.

CASE STUDY

Road transport system was chosen for our case study. We have followed proposed sequence of steps. It is easy to demonstrate that our approach leads to the creation of the quality glossary of terms.

We have developed three different descriptions of transport systems. As we can see in Tab. 1, anyone of the three descriptions (if they are used separately) leads to very different set of terms, so it could lead to different ontologies, which would never be sufficiently representative. But in the case of contemporaneous use of all three descriptions much comprehensive set of terms can be generated. So combined use of all these descriptions generates synergetic effect.

Table 1: Comparison of the sets of terms.

Set of terms describing the static side	Set of terms describing the dynamic side	Set of terms describing the rules
	appropriate distance	
		at most one
		before
car	car	car
	catch up	
	continue on driving	
	cross	
	cross into the left lane	
	cross safely	
	determine	
direction of travel		direction of travel
direction of turning		
	drive	drive
dividing and/or merging section		
	endanger	
		enforced
		exceed
	give way	give way
	increase speed	
	indicate intention to cross the road	
	intended direction of continuation after an intersection	intended direction of continuation after an intersection
	intention	
intersection		intersection
junction		
		just one
	left lane	

Set of terms describing the static side	Set of terms describing the dynamic side	Set of terms describing the rules
	limit	
	main road	
		maximum car speed-limit
		currently permitted
		maximum speed limit
	merge into the right lane	
	minor road	
		motion
		move into the traffic lane
		move
		must not
one-way		
		only on
	overtake	
	pavement	
pedestrian crossing	pedestrian crossing	pedestrian crossing
pedestrian	pedestrian	pedestrian
place		place
	reduce speed	
		respect
		right-most traffic lane
road infrastructure		
road section		
	safe distance	
	section	
	side lane	
	slower moving car	
		specified
	speed	
	stop vehicle	
	straight section	
	"T"-shaped intersection	
traffic lane		traffic lane
	turn blinker off	try
	turn on a left blinker	
	turn on a right blinker	
	turn right	
	turn safely	
	turn	
		turning

Next step is searching for basic terms. We search for the individual basic terms, which serve to form the multiple-word terms. If there is a unique multiple-word collocation, it can be mentioned as one term (e.g. *the intended direction of continuation after the intersection*).

Furthermore, the terms not included in the original description, but logically belonging on the list are added. Those are added based on the analogy rule (e.g. the *„to the right“* term is to be complemented with the *„to the left“* term).

Now we identify synonyms and homonyms. Identified synonyms and homonyms are grouped together; other terms are also included in the table. In the last step, synonyms are given in succession on one line, separated by commas (see e.g. "*car*" / "*vehicle*"). The first term noted is the one preferred. Homonyms are given on separate lines (see e.g. "*turn*" / "*turn*"). The other terms are given on separate lines (see e.g. "*be located*" and "*place*").

Table 2. Grouping of synonyms and homonyms (shortened).

Term			
be located			
car, vehicle			
cross			
	- safely		
place			
speed	- maximum	- permitted	- road
			- car
	- reduce, slow down		
	- increase, speed up		
turn			
	- safely		
	- to the right		
	- to the left		
turn			
	- blinker	- on	
		- off	

The result is a glossary of terms (see Table 2), which may already serve as a sufficiently representative input into METHONTOLOGY.

CONCLUSION

Currently, there are a number of methodologies aimed at the development of ontologies. Their common disadvantage is that they do not deal with the systematic generation of the initial glossary of terms. This paper suggests the ways to extend the METHONTOLOGY methodology so that there is a clearly defined set of steps at the beginning of the ontology development, resulting in obtaining a representative set of terms which then may be already processed by traditional methods of the METHONTOLOGY methodology.

We demonstrated the usability of our proposed method on the domain of road transport. The resulting glossary of terms is more complex, systematic and therefore more exhaustive than to search the terms in professional documents or to address experts.

In addition, from the proposed set of steps, it is evident that proposed approach is very general and thus applicable within other methodologies, which, at their beginning, result from the glossary of terms.

ACKNOWLEDGEMENTS

This research has been supported by the program "Information Society" of the Czech Academy of Sciences, project No. 1ET101940420 "Logic and Artificial Intelligence for multi-agent systems."

REFERENCES

Gómez-Pérez, A., Fernández-López, M., Corcho, O. (2004) Ontological Engineering: with examples from the areas of Knowledge Management, e-Commerce and the Semantic Web. 2nd printing, Springer-Verlag, London. ISBN 1-85233-551-3.

TOVE Ontology Project. Enterprise Integration Laboratory, University of Toronto. http://www.eil.utoronto.ca/enterprise-modelling/tove/, 10.3.2010.

Wielinga, B., Schreiber, A. Th., Jansweijer, W., Anjewierden, A., van Harmelen, F. (1994) Framework and formalism for expressing ontologies. ESPRIT Project 8145 KACTUS, Free University of Amsterdam.

Ontology Creation and Use: SENSUS. http://www.isi.edu/natural-language/resources/sensus.html (10.3.2010)

Fernández, M., Gómez-Pérez, A., Juristo, N. (1997) METHONTOLOGY: From Ontological Art Towards Ontological Engineering. Spring Symposium Series, Stanford, pp. 33-40.

PRECISE EVALUATION OF PARTIAL DERIVATIVES AS AN ADVANCED TOOL FOR TERRAIN ANALYSIS

KADLEC Martin and PACINA Jan

Department of Mathematics, Geomatics Section, Faculty of Applied Sciences, University of West Bohemia, Univerzitní 22, 306 14, Plzeň, Czech Republic
kadlecm@kma.zcu.cz

Department of Informatics and Geoinformatics, Faculty of Environment, J. E. Purkyně University, Králova výšina 7, 400 96, Ústí nad Labem, Czech Republic
Jan.Pacina@ujep.cz

Abstract

In many GIS we can find tools for basic georelief analyses as the slope and orientation computation, including basic types of curvatures. For advanced terrain analyses are required layers computed from the 3rd partial derivatives. The computation of the 3rd partial derivatives is sensitive to input data (accuracy and smoothness of digital terrain model) and numerically instable and thus is not implemented in the most GIS. Within this article we introduce numerically stabile method for computation of the 3rd order partial derivatives using the weighted least square method (LSC). The most important contribution of this paper is introducing 8 various weights into the LSC evaluation of derivatives up to third order. We are testing 9 methods (unweighted LSC and 8 weights) on a model relief given as an analytical function. The test function is created so it emulates the behavior of a natural georelief – in defined interval it creates peaks, ridges and saddle points. Thanks to the explicit representation of the test function we are able to define the exact derivation values in any point. This enables usage of the test function as the etalon. The approximation preciseness is then evaluated using statistical methods on differences of the two tested surfaces – the etalon and the surface of desired partial derivative approximated by the introduced method. The usage of the 3rd order partial derivatives may be for example found at semi-automated georelief segmentation using the delimitation of elementary forms of georelief as part of Geomorphologic Information System. Here are the partial derivatives used for automatic delineation of elementary forms boundaries.

Keywords: partial derivation, 3rd order, quality test.

INTRODUCTION

Common GIS are not offering evaluation of partial derivatives of the 3rd order. Precise partial derivatives of the 3rd order are crucial for computing morphometrical variables of the 3rd order widely used in geomorphometry (Minár, (2008), Krcho, (2001)).

For the requirements of Geomorphologic Information System (GmIS) was in Pacina (2008) implemented a robust algorithm for approximation of partial derivatives up to the 3rd order with sufficient quality. This algorithm was based on weighted least squares method, however, the effect of weights was not studied in depth. This article is focused on testingthe accuracy of this method for various weights on a test polynomial function with characteristics of a topographical surface. Analytical expression of the test function allows us to compute absolutely precise partial derivatives which are further used as the *etalon*.

Approximated partial derivatives by method described in Pacina (2008), Jenčo, et al. (2009) and Pacina (2009a) are used for computation of derived morphometrical variables up to the 3rd order[1]. Surfaces of derived morphometrical variables of different orders are within the GmIS further on used for automatic delimitation of elementary forms of georelief (see Pacina,2008), Pacina (2009), ,Minár (2008), Tachikawa et al. (1993), Pike (1988)). The usage of precise partial derivatives is overall much wider. The most important contribution of this article is the study of the effect of various weights in the LSC adjustment, which was not yet studied. In all published papers are the weights either not introduced at all or it is used only one weight system without any elaboration of setting up its parameters.

Proposed method can be used for computing further morphometrical variables, namely maximal curvatures of topography with further applications e. g. in hydrology (O'Callaghan, J.F., and Mark, D.M. (1984), Chang, Y.C., Song, G.S. and Hsu, S.K. (1998) or Riazanoff, S., Cervelle, B., and Chorowicz, J. (1988)) or other geomorphologic analysis using the morphometrical variables of higher orders (Tremboš et al. (1994)).

METHODOLOGY

Tested methods for derivatives computation

This algorithm approximates the partial derivatives from a digital elevation model (DEM) given in a form of a raster. It interpolates a 5x5 neighborhood by general polynomial surface of the 3rd order, using the weighted linear least squares method. The general polynomial surface of the 3rd order is given by:

$$z_{i,j}(x,y) = a_0 + a_1(x-x_i) + a_2(y-y_j) + a_3(x-x_i)^2 + a_4(y-y_j)^2 + a_5(x-x_i)(y-y_j)$$
$$+a_6(x-x_i)^3 + a_7(y-y_j)^3 + a_8(x-x_i)^2(y-y_j) + a_9(x-x_i)(y-y_j)^2 \tag{1}$$

This formula allows to build one equation for each point with coordinates (x, y) lying in the neighborhood of the point (x_i, y_j) where we want to compute the derivatives.

[1] For example the morphometrical variables of the 3rd order: a_{gn} - change of orientation change in the direction of a fall line, A_{Ntt} – change of orientation in the direction of a contour line.

Because have used the 5x5 neighborhood of actually computed point, we can build a linear system of 25 equations and 10 unknowns a_0 … a_9. The linear system is expected to be overdetermined so we have solved the system by the least squares method.. On Fig. 1 are shown the nodes of the 5x5 neighborhood. Symbols *f* in each of the nodes represents function values in the node. Value *h* is distance between the nodes.

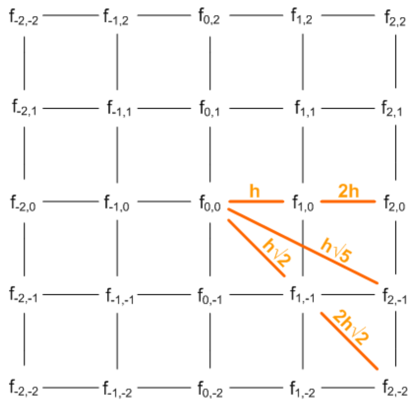

Fig. 1. Nodes of the 5x5 neighborhood for (x_i, y_j) = (0, 0)

Estimation of derivatives

Once having coefficients a_0 … a_9 of the polynomial surface for particular point (x_i, y_j), we can approximate the derivatives in the point (x_i, y_j) as derivatives of the polynomial surface. For example, partial derivative of *z* by *x* then would be:

$$\frac{\partial z}{\partial x} = a_1 + 2a_3(x - x_i) + a_5(y - y_j) + 3a_6(x - x_i)^2 + \\ +2a_8(x - x_i)(y - y_j) + a_9(y - y_j)^2. \tag{2}$$

From which results:

$$\left.\frac{\partial z}{\partial x}\right|_{(x_i, y_j)} = a_1. \tag{3}$$

And the other derivatives are:

$$\left.\frac{\partial z}{\partial y}\right|_{(x_i,y_j)} = a_2,\ \left.\frac{\partial z^2}{\partial x^2}\right|_{(x_i,y_j)} = 2a_3,\ \left.\frac{\partial z^2}{\partial y^2}\right|_{(x_i,y_j)} = 2a_4,\ \left.\frac{\partial z^2}{\partial x \partial y}\right|_{(x_i,y_j)} = a_5, \\ \left.\frac{\partial z^3}{\partial x^3}\right|_{(x_i,y_j)} = 6a_6,\ \left.\frac{\partial z^3}{\partial y^3}\right|_{(x_i,y_j)} = 6a_7,\ \left.\frac{\partial z^3}{\partial x^2 \partial y}\right|_{(x_i,y_j)} = 2a_8,\ \left.\frac{\partial z^3}{\partial x \partial y^2}\right|_{(x_i,y_j)} = 2a_9 \tag{4}$$

Weights

In unweighted least squares, all 25 points from the 5x5 neighborhood area influenced the results (third derivatives) in the same way. Therefore, the result is affected much more by 16 points that are at the boundary of the 5x5 neighborhood area than by 9 points which are close to the computational point. This fact has a smoothing effect on the derivatives computed by unweighted least squares, because distant points have together bigger weight than closer points. To encounter the higher influence of points closer to the center of approximate area, we have used the weighted least square method. We have proposed to weigh systems with weights w^{ε} and w^{δ}. Both of them give bigger weights to points closer to the computational point (center of 5x5 area) and both depend on some parameter. The first weight w^{ε} is given by

$$w_{i,j}^{\varepsilon} = \frac{\varepsilon + 2h\sqrt{2} - h\sqrt{i^2+j^2}}{2h\sqrt{2}} \tag{5}$$

Where $\varepsilon > 0$ is a parameter, $w_{i,j}$ is the weight of point x_i,y_j with respect to point x_0,y_0 and h is the distance between points x_0,y_0 and x_i,y_j. The second weigh is given by

$$w_{i,j}^{\delta} = \frac{2h\sqrt{2}}{\delta + h\sqrt{i^2+j^2}} \tag{6}$$

where $\delta > 0$ (for example 0.1), which influences the importance of the points further from the center.

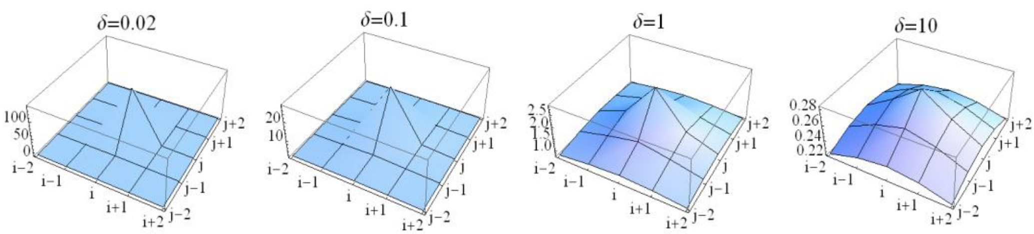

Fig. 2. Weight w^{ε} influence on the surroundings points

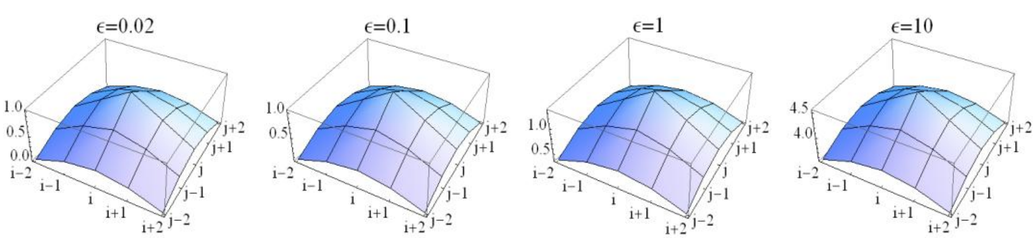

Fig. 3. Weight w^{δ} influence on the surroundings points

Both weight systems were developed to take into account the influence of the surrounding nodes, which should be decreasing with the increasing distance from the middle. Weight functions w^{ε} and w^{δ} for various parameters ε are δ and for h=1 are plotted at Fig. 2 and Fig. 3.

The weights affect the coefficients of the third order polynomial during the adjustment process in the optimization function. The only difference is that instead of using identity weight matrix, a diagonal matrix is used.

Least squares solution

The system of linear equations $\mathbf{Qa} = \mathbf{f}$ for computation of the unknown coefficients $\mathbf{a}$ can be overestimated hence in general must not have any solution and thus ee have estimated the unknown coefficients $\mathbf{a}$ by the least square method[2].

The unknown coefficients $a_0, \ldots a_9$ of the polynomial (2.3.1) are given by

$$\mathbf{a} = \mathbf{B_w f}, \tag{7}$$

where $\mathbf{B_w}$ is computed by formula

$$\mathbf{B_w} = inv(\mathbf{Q^T W^T W Q})\mathbf{Q^T W^T W}. \tag{8}$$

Size of matrix **Q** is 25×10, size of **a** is 10×1 (vector of unknown coefficients) and $\mathbf{f}$ is 25×1(vector of the nods).

The computation made in this way is very fast. The matrix $\mathbf{B_w}$ is computed only once during the first computation. We do not have to compute all the coefficients of $\mathbf{a}$, but only those we need for computation of the partial derivatives of the desired order. The matrix $\mathbf{B_w}$ was computed analytically (with the help of symbolic computations in Matlab). This helped to avoid the rounding error during computation of matrix $\mathbf{B_w}$, which made the computation even more precise.

Method presented by Florinski

Florinski (2009) introduced similar method for approximations of partial derivatives of the 3rd order based on Taylor approximating polynomial and standard least square method (without weights). The partial derivatives of the 3rd order along Florinski (2009) are computed in the following manner:

$$\frac{\partial^3 z}{\partial x^3} = \frac{z_5 + z_{10} + z_{15} + z_{20} + z_{25} - z_1 - z_6 - z_{11} - z_{16} - z_{21}}{10w^3} +$$

[2] For the whole derivation of the weighted least square method see Pacina (2008).

$$+\frac{2(z_2+z_7+z_{12}+z_{17}+z_{22}-z_4-z_9-z_{14}-z_{19}-z_{24})}{10w^3}, \qquad (9)$$

where z_i are the values from 5x5 neighborhood and w is the cell size.

Testing the methods

We have performed the accuracy test of the numerical evaluation of the derivatives on a test function with the character of topographical surface. The test function is given by mathematical formula which allows evaluation of all required derivatives and morphometrical variables analytically. Suitable test function *F(x,y)* given on a test area $A_F \subset R^2$ has to keep these properties:

- The function itself and all its partial derivatives of the first, second and third order are continuous functions in A_F .
- It is possible to express analytically all derivatives and all required morphometrical variables for any point in A_F.
- *F(x,y)* contains at least one saddle point and one peak in A_F.

We have used a polynomial function *P(x,y)* that is described in the following section as a test function

Polynomial testing function P(x,y)

We have used for testing the same function as used in Benová (2005) or Pacina (2009). This function *z = P(x,y)* is given on rectangular area A_P = (-300<x<300)×(-200<y<600) by formula

$$\begin{aligned} z &= 150+0.2y-1.5\cdot10^{-4}y^2-2\cdot10^{-7}y^3+0.1x+\\ &+1.6\cdot10^{-4}xy-1.2\cdot10^{-6}xy^2+10^{-4}x^2+\\ &+3.2\cdot10^{-6}x^2y+2\cdot10^{-12}x^2y^3-10^{-6}x^3-10^{-12}x^3y^2-\\ &-10^{-14}x^3y^3+2.5\cdot10^{-17}x^3y^4-5\cdot10^{-17}x^4y^3-10^{-19}x^4y^4. \end{aligned} \qquad (10)$$

The function is shown at **Fig. 4**. Such function is very smooth when generated in a raster with resolution 1 (i.e. raster of 600x800 cells), so the derivatives were computed very accurately even without weights. To get better insight into the influence of weights we have generated a raster Q from the same function at the same extent, but with resolution 50 (i.e. raster with only 12x16 cells).

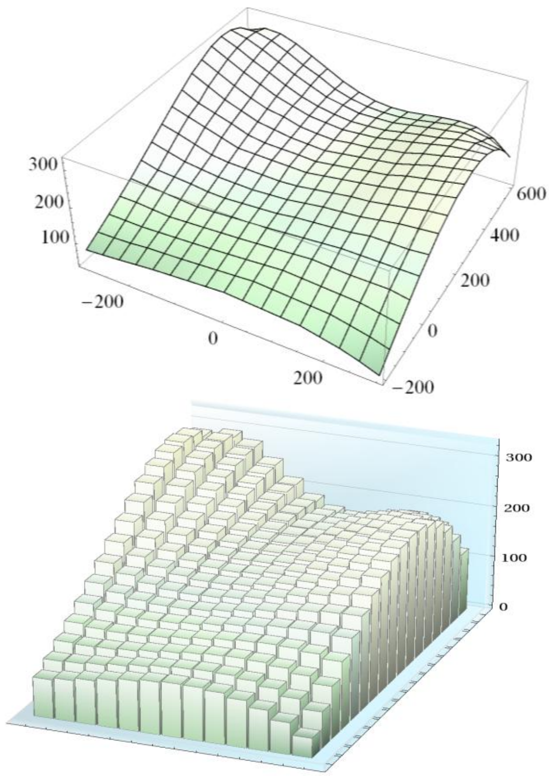

Fig. 4. Polynomial function P(x,y) plotted as a smooth surface and as raster Q with resolution h=50.

Analytical derivatives of function *P(x,y)* are given by following expressions:

$$\partial P(x,y)/\partial x = x^3 (-2.\times10^{-16}-4.\times10^{-19}\, y)\, y^3-1.2\times10^{-6} (-362.94+y) (229.606 +y)+7.5\times10^{-17} x^2 (-626.507+y) (387.984 +y) (164559. -161.477\, y+y^2)+x (0.0002 +6.4\times10^{-6}\, y+4.\times10^{-12}\, y^3) \quad (11)$$

$$\partial^2 P(x,y)/\partial x^2 = 0.0002 +6.4\times10^{-6}\, y+4.\times10^{-12}\, y^3+x^2 (-6.\times10^{-16}-1.2\times10^{-18}\, y)\, y^3+1.5\times10^{-16} x (-626.507+y) (387.984 +y) (164559. -161.477\, y+y^2) \quad (12)$$

$$\partial^3 P(x,y)/\partial x^3 = -6.\times10^{-6}-6.\times10^{-12}\, y^2+(-6.\times10^{-14}-1.2\times10^{-15}\, x)\, y^3+(1.5\times10^{-16}-2.4\times10^{-18}\, x)\, y^4 \quad (13)$$

$$\partial P(x,y)/\partial y = x (0.00016 -2.4\times10^{-6}\, y)+x^4 (-1.5\times10^{-16}-4.\times10^{-19}\, y)\, y^2+1.\times10^{-16} x^3 (-356.155+y)\, y\, (56.1553 +y)-6.\times10^{-7} (-379.153+y) (879.153 +y)+x^2 (3.2\times10^{-6}+6.\times10^{-12}\, y^2) \quad (14)$$

$$\partial^2 P(x,y)/\partial y^2 = -0.0003-2.4\times10^{-6}\, x-1.2\times10^{-6}\, y+1.2\times10^{-11} x^2\, y+x^4 (-3.\times10^{-16}-1.2\times10^{-18}\, y)\, y+3.\times10^{-16} x^3 (-229.099+y) (29.0994 +y) \quad (15)$$

$$\partial^3 P(x,y)/\partial y^3 = -1.2\times10^{-6}+1.2\times10^{-11} x^2+x^4 (-3.\times10^{-16}-2.4\times10^{-18}\, y)+x^3 (-6.\times10^{-14}+6.\times10^{-16}\, y) \quad (16)$$

$$\partial^2P(x,y)/\partial xy = 0.00016 -2.4\times10^{-6}y+x^3 (-6.\times10^{-16}-1.6\times10^{-18} y) y^2+3.\times10^{-16} x^2 (-356.155+y) y (56.1553 +y)+x (6.4\times10^{-6}+1.2\times10^{-11} y^2) \quad (17)$$

$$\partial^3P(x,y)/\partial x^2y= 6.4\times10^{-6}+1.2\times10^{-11}y^2+x^2 (-1.8\times10^{-15}-4.8\times10^{-18} y) y^2+6.\times10^{-16} x (-356.155+y) y (56.1553 +y) \quad (18)$$

$$\partial^3P(x,y)/\partial x y^2 = -2.4\times10^{-6}+2.4\times10^{-11}x y+x^3 (-1.2\times10^{-15}-4.8\times10^{-18} y) y+9.\times10^{-16} x^2 (-229.099+y) (29.0994 +y) \quad (19)$$

The workflow

We have analyzed the approximation error for both rasters $F(x,y)=P(x,y)$ with resolution $h=1$ and $F(x,y)=Q(x,y)$ with resolution $h=50$ in the following way:

1. Evaluation of raster F^A of function values $F(x,y)$ at given area with resolution h.
2. Evaluation of rasters $F^A{}_x$, $F^A{}_{xx}$, $F^A{}_{xxx}$ of analytical derivatives at given area with resolution h from analytical formulae $\frac{\partial F(x,y)}{\partial x}, \frac{\partial^2 F(x,y)}{\partial x^2}, \frac{\partial^3 F(x,y)}{\partial x^3}, \ldots$
3. Numerical evaluation of derivatives ${}^mF^N{}_x$, ${}^mF^N{}_{xx}$, ${}^mF^N{}_{xxx}$ from raster F^A by particular numerical method m.
4. Evaluation of raster of differences ${}^m\Delta F_x = F^A{}_x - {}^mF^N{}_x$ between raster of analytical derivatives $F^A{}_x$ and raster of numerical approximation ${}^mF^N{}_x$ for the first derivative $\frac{\partial F(x,y)}{\partial x}$ and similar rasters for all the other derivatives. The differences show absolute precision of various derivatives and can be used for studying of the effect of various methods for particular derivative. However, the absolute value of various derivatives significantly differs, so this absolute quantity cannot show us which derivative is computed with higher relative accuracy with respect to the other derivatives.
5. Evaluation of raster of equivalence ratios ${}^m\Pi F_x = {}^mF^N{}_x / F^A{}_x$ between raster of analytical derivatives $F^A{}_x$ and raster of numerical approximation ${}^mF^N{}_x$ for the first derivative $\frac{\partial F(x,y)}{\partial x}$ and similar rasters for all the other derivatives. This indicator is a relative quantity that allows comparing accuracy of all computed derivatives regardless their absolute value. The ideal value is 1. Because derivatives $F^A{}_x$ can be zero or small numbers, only values bigger than a chosen threshold value T are taken into account to avoid zero or small number in denominator (in tables, these values are referred as “filtered equivalence rates”). This manipulation is used only in points, where $F^A{}_x$ is small. For our purposes are more important parts, where are third derivatives high. We have chosen a very small threshold $T = 1x10^{-15}$.

6. Evaluation of statistical properties (mean, standard deviation, min and max) for rasters ${}^{m}\Delta F_x$ and ${}^{m}\Pi F_x$ for all methods and derivatives.

We have tested 9 methods with the following codes 1-9:

- Method 1: least squares (LS) without weights
- Method 2-5: LS with weights w^{δ}, $\delta = \{10, 1, 0.1, 0.02\}$
- Method 6-9: LS with weights w^{ε} , $\varepsilon = \{10, 1, 0.1, 0.02\}$

RESULTS

The results for dense (h = 1) raster P(x,y) are shown in tables Tab. 2 and Tab. 3 and results for raster Q(x,y) with the same extent, but with resolution h = 50 are shown in tables Tab. 4 and Tab. 5. Tables show, that the mean equivalence ratio is almost 1 with only negligible error for raster P(x,y). Also for raster Q(x,y), which is much more coarse, are the mean equivalence ratios between 0,95-1,25.

The minimal and maximal values of ratios look like very big in some cases, e.g. the maximal equivalence ratio of 36,76 for value ${}^{1}\Pi F_{xyy}$ means relative error 3500 % These big ratios are caused by dividing small numbers and big relative error for derivatives that are almost zero cannot much influence evaluation of important morphometrical parameters, because the wrong values will be also almost zero in absolute value. To prove that the absolute values are not too big, see statistics of ${}^{1}\Delta F_{xyy}$, where minimal and maximal differences are quite close to mean value of differences ${}^{1}\Delta F_{xyy}$.

CONCLUSIONS

- We consider the mean equivalence ratio as the main indicator of the accuracy, because it is a relative quantity, that allows comparison of all derivatives and witch can detect bias in results. The overview of all mean equivalence ratios (over whole grids) for each method and each derivative is given in table Tab. 1 (in addition to detailed results in tables **Table 2** - **Table 5**.which provide more details in-depth)
- Best method is method 9 (weight w_{ij}^{ε} with parameter ε=0.02) that gives best mean equivalence ratios which up to about 20 % better than non-weighted least squares. This method has also the biggest minimal ratio values, the smallest maximal ratios values and the smallest standard deviation of the ratios. All these parameters proof that this method is the best one.
- All numerical experiments provided in this article show that any weighted method is better than the method without any weights.

- Even though we have generated the raster Q(x,y) with really coarse grid, the agreement of numerical derivatives with etalon (analytical derivatives) is quite good. Generating a smoother raster P(x,y) resulted to even better agreement.
- The numerical results are in a good agreement with our hypothesis that the weight of closer points should be higher (even though detailed statistical test is yet not available). This method should work also for real terrains.

Table 1. Mean equivalence ratio for derivatives computed from coarse (h = 50) raster Q(x,y)

	1	2	3	4	5	6	7	8	9
dx	1,00252	1,00135	1,00125	1,00124	1,00124	1,00057	1,00128	1,00030	1,00030
dy	0,97096	0,97957	0,98078	0,98092	0,98094	0,98543	0,98924	0,98839	0,98839
dxx	1,01591	1,00482	1,00408	1,00405	1,00405	0,99934	0,99983	0,99787	0,99786
dyy	1,14498	1,07123	1,06534	1,06512	1,06511	1,04777	1,05226	1,03765	1,03762
dxy	0,97374	0,97640	0,97668	0,97671	0,97671	0,98444	0,98721	0,98658	0,98659
dxxx	0,95100	0,96804	0,96949	0,96965	0,96966	0,98195	0,98396	0,98677	0,98678
dyyy	1,25471	1,15078	1,14006	1,13886	1,13876	1,07449	1,06819	1,04560	1,04570
dxxy	0,98565	0,98712	0,98728	0,98730	0,98730	0,99169	0,99749	0,99354	0,99354
dxyy	1,22670	1,20169	1,19899	1,19869	1,19866	1,12276	1,08759	1,09227	1,09226

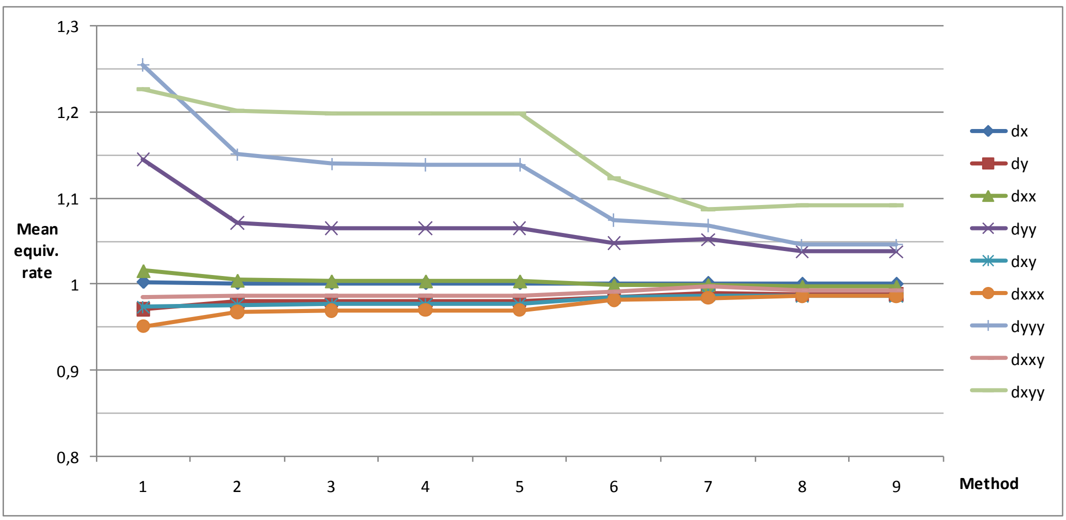

Fig. 5. Graph of mean equivalence ratios for raster Q(x,y) for various methods (weights).

REFERENCES

BENOVA, A (2005). *Georelief a modelovanie jeho geometrickej struktury pomocou KDMR*. Comenius University at Bratislava, Dissertation thesis.

O'CALLAGHAN, J.F., and MARK, D.M. (1984). *The extraction of drainage networks from digital elevation data.* Computer Vision, Graphics, and Image Processing. Volume 28, 323–344.

CHANG, Y.C., SONG, G.S. and HSU, S.K. (1998). *Automatic extraction of ridge and valley axes using the profile recognition and polygon-breaking algorithm.* Computers and Geosciences. Volume 24, 83–93.

FLORINSKY, I.V. (2009). *Computation of the third-order partial derivatives and derivation function from a digital elevation model*. International Journal of Geographical Information Science. Volume 23, Issue 2, ISSN:1365-8816

JENČO, M., PACINA, J., SHARY, P. (2009). Terrain skeleton and local morphometric variables: geosciences and computer vision technique. In Advances in Geoinformation Technologies. Ostrava: Technical University of Ostrava, s. 57-76. ISBN: 978-80-248-2145-0.

KRCHO, J. (2001). *Modelovanie georeliéfu a jeho geometrickej štruktúry pomocou DTM; polohová a numerická presnosť*. Bratislava. ISBN 80-85401-92-4

MINÁR, J.; EVANS, I., S. (2008). *Theoretical basis of elementary landform segmentation in geomorphological mapping*. Geomorphology, nr. 95, p. 236-259, ISSN: 0169-555X.

PIKE, R.J.: *The Geometric Signature: Quantifying Landslide-Terrain Types from Digital Elevation Models*. Mathematical Geology 20 (5), 491-511, 1988.

PACINA, J. (2008). *Methods for automatical delimitation of elementary forms of georelief as a part of Geomorphologic information system*. FAV ZČU Plzeň , dissertation thesis, Pilsen. On-line: www.git.zcu.cz

PACINA, J. (2009). *Possibilities of automated georelief segmentation for the requirements of Geomorphologic information system (GmIS)*. Geomorphologia Slovaca et Bohemica, 9, 2009, 2, 37 - 49. ISSN 1337-6799

RIAZANOFF, S., CERVELLE, B., and CHOROWICZ, J. (1988). *Ridge and valley line extraction from digital terrain models.* International Journal of Remote Sensing, Volume 9, 1175–1183

TACHIKAWA, Y., MICHIHARU S., TAKUMA T. (1993). Development *of a Basin Geomorphic Information System Using a Tin-Dem Data Structure.* Proceedings of the Symposium on Geographic Information Systems and Water Resources. Mobile, AL: American Water Resources Association AWRA, 1993. 1: 163-172.

TREMBOŠ, P., MINÁR,J., MACHOVÁ, Z. (1994). *Identification of Selected Natural Hazards from Viewpoint of the the Evaluation of Environmental Limits*. Acta Facultatis Rerum Naturalium Universitatis Comenianae, Geographica Nr. 34, 1994, p. 135-151.

Table 2. Methods 1-5 for raster P with resolution h=1.

Differences					*Filtered equivalence rates*			
				Method 1				
	$^{1}\Delta P_i$				$^{1}\Pi P_i$			
i	**mean**	**stdev**	**min**	**max**	**mean**	**stdev**	**min**	**max**
dx	5,1776E-11	6,0579E-10	-2,2383E-09	2,7376E-09	1,00000	0,00000	0,99974	1,00009
dy	-2,0533E-10	2,6783E-10	-1,6233E-09	2,9485E-10	1,00000	0,00000	0,99979	1,00168
dxx	9,1078E-08	1,4211E-07	-4,9185E-08	9,6619E-07	1,00000	0,01098	-3,89008	4,27598
dyy	5,7739E-08	1,0632E-07	-4,5983E-08	7,7106E-07	1,00003	0,00349	-0,10849	1,85696
dxy	-5,7089E-09	1,3218E-07	-7,4138E-07	5,8683E-07	0,99992	0,04100	-15,54950	6,27836
dxxx	-8,3282E-11	1,0600E-09	-4,7686E-09	3,9358E-09	1,00001	0,00092	0,91430	1,08996
dyyy	2,5400E-10	3,9467E-10	-5,3041E-10	2,3593E-09	1,00009	0,00034	0,97595	1,02308
dxxy	4,0827E-10	4,8268E-10	-2,7598E-10	2,5697E-09	1,00000	0,00103	0,91268	1,11756
dxyy	-6,6923E-11	6,2340E-10	-2,8549E-09	2,2650E-09	1,00002	0,00110	0,91702	1,09534
				Method 2				
	$^{2}\Delta P_i$				$^{2}\Pi P_i$			
dx	4,7629E-11	5,5465E-10	-2,0488E-09	2,5072E-09	1,00000	0,00000	0,99976	1,00008
dy	-1,9123E-10	2,4794E-10	-1,5010E-09	2,6951E-10	1,00000	0,00000	0,99981	1,00159
dxx	8,7040E-08	1,3514E-07	-4,6057E-08	9,1420E-07	1,00000	0,01043	-3,67754	4,09616
dyy	5,3930E-08	9,9309E-08	-4,2878E-08	7,2041E-07	1,00003	0,00329	-0,04250	1,80660
dxy	-5,6221E-09	1,3017E-07	-7,3012E-07	5,7791E-07	0,99992	0,04038	-15,29810	6,19819
dxxx	-7,7876E-11	9,9166E-10	-4,4610E-09	3,6821E-09	1,00001	0,00086	0,91985	1,08414
dyyy	2,3710E-10	3,6894E-10	-4,9627E-10	2,2048E-09	1,00009	0,00032	0,97750	1,02159
dxxy	4,0422E-10	4,7787E-10	-2,7073E-10	2,5389E-09	1,00000	0,00102	0,91318	1,11688
dxyy	-6,5969E-11	6,1253E-10	-2,8057E-09	2,2249E-09	1,00002	0,00109	0,91850	1,09364
				Method 3				
	$^{3}\Delta P_i$				$^{3}\Pi P_i$			
dx	3,5117E-11	4,0234E-10	-1,4847E-09	1,8204E-09	1,00000	0,00000	0,99983	1,00006
dy	-1,4689E-10	1,8699E-10	-1,1261E-09	1,9438E-10	1,00000	0,00000	0,99986	1,00127
dxx	7,1918E-08	1,0975E-07	-3,5019E-08	7,2572E-07	1,00000	0,00842	-2,87960	3,44730
dyy	3,9859E-08	7,4075E-08	-3,1940E-08	5,3809E-07	1,00002	0,00255	0,19401	1,62592
dxy	-5,3408E-09	1,2366E-07	-6,9358E-07	5,4900E-07	0,99992	0,03836	-14,48250	5,93807
dxxx	-6,1662E-11	7,8880E-10	-3,5476E-09	2,9296E-09	1,00001	0,00068	0,93643	1,06676
dyyy	1,8452E-10	2,9131E-10	-3,9533E-10	1,7351E-09	1,00007	0,00025	0,98206	1,01722
dxxy	3,9010E-10	4,6114E-10	-2,5337E-10	2,4335E-09	1,00000	0,00099	0,91504	1,11441
dxyy	-6,2746E-11	5,7636E-10	-2,6418E-09	2,0916E-09	1,00002	0,00102	0,92340	1,08800
				Method 4				
	$^{4}\Delta P_i$				$^{4}\Pi P_i$			
dx	2,7919E-11	3,1698E-10	-1,1690E-09	1,4348E-09	1,00000	0,00000	0,99986	1,00005
dy	-1,1912E-10	1,5037E-10	-9,0266E-10	1,5267E-10	1,00000	0,00000	0,99988	1,00105
dxx	5,8506E-08	8,8054E-08	-2,6083E-08	5,6641E-07	1,00000	0,00670	-2,16957	2,90291
dyy	2,7598E-08	5,3054E-08	-2,5843E-08	3,8551E-07	1,00001	0,00195	0,38119	1,47568
dxy	-5,1533E-09	1,1932E-07	-6,6923E-07	5,2972E-07	0,99993	0,03701	-13,93900	5,76470
dxxx	-5,2525E-11	6,7671E-10	-3,0423E-09	2,5143E-09	1,00001	0,00059	0,94572	1,05705
dyyy	1,5252E-10	2,4699E-10	-3,3992E-10	1,4620E-09	1,00005	0,00022	0,98455	1,01483
dxxy	3,7979E-10	4,4896E-10	-2,4201E-10	2,3592E-09	1,00000	0,00096	0,91659	1,11233
dxyy	-6,0551E-11	5,5241E-10	-2,5331E-09	2,0034E-09	1,00002	0,00098	0,92664	1,08428
				Method 5				
	$^{5}\Delta P_i$				$^{5}\Pi P_i$			
dx	2,6925E-11	3,0579E-10	-1,1277E-09	1,3842E-09	1,00000	0,00000	0,99987	1,00004
dy	-1,1522E-10	1,4535E-10	-8,7221E-10	1,4724E-10	1,00000	0,00000	0,99989	1,00102
dxx	5,7515E-08	8,6489E-08	-2,5477E-08	5,5518E-07	1,00000	0,00658	-2,11675	2,86464
dyy	2,6818E-08	5,1682E-08	-2,5953E-08	3,7552E-07	1,00001	0,00190	0,39418	1,46535
dxy	-5,1263E-09	1,1869E-07	-6,6573E-07	5,2695E-07	0,99993	0,03682	-13,86070	5,73974
dxxx	-5,1201E-11	6,6219E-10	-2,9766E-09	2,4607E-09	1,00001	0,00057	0,94695	1,05577
dyyy	1,4808E-10	2,4114E-10	-3,3280E-10	1,4254E-09	1,00005	0,00021	0,98486	1,01453
dxxy	3,7823E-10	4,4712E-10	-2,4040E-10	2,3482E-09	1,00000	0,00096	0,91684	1,11199
dxyy	-6,0227E-11	5,4898E-10	-2,5175E-09	1,9908E-09	1,00002	0,00097	0,92710	1,08375

Table 3. Methods 1 and 6-9 for raster P with resolution h=1.

	Differences				***Filtered equivalence rates***			
Method 1								
	$^{1}\Delta P_i$				$^{1}\Pi P_i$			
i	**mean**	**stdev**	**min**	**max**	**mean**	**stdev**	**min**	**max**
dx	5,1776E-11	6,0579E-10	-2,2383E-09	2,7376E-09	1,00000	0,00000	0,99974	1,00009
dy	-2,0533E-10	2,6783E-10	-1,6233E-09	2,9485E-10	1,00000	0,00000	0,99979	1,00168
dxx	9,1078E-08	1,4211E-07	-4,9185E-08	9,6619E-07	1,00000	0,01098	-3,89008	4,27598
dyy	5,7739E-08	1,0632E-07	-4,5983E-08	7,7106E-07	1,00003	0,00349	-0,10849	1,85696
dxy	-5,7089E-09	1,3218E-07	-7,4138E-07	5,8683E-07	0,99992	0,04100	-15,54950	6,27836
dxxx	-8,3282E-11	1,0600E-09	-4,7686E-09	3,9358E-09	1,00001	0,00092	0,91430	1,08996
dyyy	2,5400E-10	3,9467E-10	-5,3041E-10	2,3593E-09	1,00009	0,00034	0,97595	1,02308
dxxy	4,0827E-10	4,8268E-10	-2,7598E-10	2,5697E-09	1,00000	0,00103	0,91268	1,11756
dxyy	-6,6923E-11	6,2340E-10	-2,8549E-09	2,2650E-09	1,00002	0,00110	0,91702	1,09534
Method 6								
	$^{6}\Delta P_i$				$^{6}\Pi P_i$			
dx	4,7351E-11	5,5119E-10	-2,0360E-09	2,4916E-09	1,00000	0,00000	0,99976	1,00008
dy	-1,9032E-10	2,4665E-10	-1,4929E-09	2,6780E-10	1,00000	0,00000	0,99981	1,00158
dxx	8,6802E-08	1,3472E-07	-4,5856E-08	9,1098E-07	1,00000	0,01039	-3,66507	4,08494
dyy	5,3706E-08	9,8875E-08	-4,2677E-08	7,1727E-07	1,00003	0,00327	-0,03835	1,80343
dxy	-5,6063E-09	1,2981E-07	-7,2806E-07	5,7629E-07	0,99992	0,04026	-15,25220	6,18353
dxxx	-7,7498E-11	9,8674E-10	-4,4389E-09	3,6638E-09	1,00001	0,00086	0,92024	1,08373
dyyy	2,3604E-10	3,6717E-10	-4,9380E-10	2,1944E-09	1,00009	0,00032	0,97761	1,02149
dxxy	4,0373E-10	4,7728E-10	-2,7010E-10	2,5352E-09	1,00000	0,00102	0,91324	1,11680
dxyy	-6,5853E-11	6,1122E-10	-2,7998E-09	2,2201E-09	1,00002	0,00108	0,91867	1,09344
Method 7								
	$^{7}\Delta P_i$				$^{7}\Pi P_i$			
dx	8,3848E-12	8,1531E-11	-2,9741E-10	3,7231E-10	1,00000	0,00000	0,99997	1,00001
dy	-4,7564E-11	5,6369E-11	-3,0941E-10	3,6907E-11	1,00000	0,00000	0,99996	1,00052
dxx	4,5393E-08	6,6757E-08	-1,5219E-08	3,9173E-07	1,00000	0,00493	-1,47895	2,29338
dyy	1,6496E-08	3,0465E-08	-1,2444E-08	2,2260E-07	1,00001	0,00126	0,59108	1,30567
dxy	-3,1776E-09	7,3574E-08	-4,1267E-07	3,2664E-07	0,99996	0,02282	-8,21174	3,93802
dxxx	-2,2389E-11	2,9445E-10	-1,3220E-09	1,0954E-09	1,00000	0,00025	0,97676	1,02449
dyyy	5,7459E-11	1,0370E-10	-1,4912E-10	5,9540E-10	1,00002	0,00010	0,99318	1,00655
dxxy	2,6595E-10	3,1805E-10	-1,0390E-10	1,5130E-09	1,00000	0,00072	0,93187	1,09197
dxyy	-3,4809E-11	2,6450E-10	-1,2268E-09	9,4102E-10	1,00001	0,00048	0,96570	1,03938
Method 8								
	$^{8}\Delta P_i$				$^{8}\Pi P_i$			
dx	8,3848E-12	8,1531E-11	-2,9741E-10	3,7231E-10	1,00000	0,00000	0,99997	1,00001
dy	-4,7564E-11	5,6369E-11	-3,0941E-10	3,6907E-11	1,00000	0,00000	0,99996	1,00052
dxx	4,5393E-08	6,6757E-08	-1,5219E-08	3,9173E-07	1,00000	0,00493	-1,47895	2,29338
dyy	1,6496E-08	3,0465E-08	-1,2444E-08	2,2260E-07	1,00001	0,00126	0,59108	1,30567
dxy	-3,1776E-09	7,3574E-08	-4,1267E-07	3,2664E-07	0,99996	0,02282	-8,21174	3,93802
dxxx	-2,2389E-11	2,9445E-10	-1,3220E-09	1,0954E-09	1,00000	0,00025	0,97676	1,02449
dyyy	5,7459E-11	1,0370E-10	-1,4912E-10	5,9540E-10	1,00002	0,00010	0,99318	1,00655
dxxy	2,6595E-10	3,1805E-10	-1,0390E-10	1,5130E-09	1,00000	0,00072	0,93187	1,09197
dxyy	-3,4809E-11	2,6450E-10	-1,2268E-09	9,4102E-10	1,00001	0,00048	0,96570	1,03938
Method 9								
	$^{9}\Delta P_i$				$^{9}\Pi P_i$			
dx	8,3848E-12	8,1531E-11	-2,9741E-10	3,7231E-10	1,00000	0,00000	0,99997	1,00001
dy	-4,7564E-11	5,6369E-11	-3,0941E-10	3,6907E-11	1,00000	0,00000	0,99996	1,00052
dxx	4,5393E-08	6,6757E-08	-1,5219E-08	3,9173E-07	1,00000	0,00493	-1,47895	2,29338
dyy	1,6496E-08	3,0465E-08	-1,2444E-08	2,2260E-07	1,00001	0,00126	0,59108	1,30567
dxy	-3,1776E-09	7,3574E-08	-4,1267E-07	3,2664E-07	0,99996	0,02282	-8,21174	3,93802
dxxx	-2,2389E-11	2,9445E-10	-1,3220E-09	1,0954E-09	1,00000	0,00025	0,97676	1,02449
dyyy	5,7459E-11	1,0370E-10	-1,4912E-10	5,9540E-10	1,00002	0,00010	0,99318	1,00655
dxxy	2,6595E-10	3,1805E-10	-1,0390E-10	1,5130E-09	1,00000	0,00072	0,93187	1,09197
dxyy	-3,4809E-11	2,6450E-10	-1,2268E-09	9,4102E-10	1,00001	0,00048	0,96570	1,03938

Table 4. Methods 1-5 for raster Q with resolution h=50.

	Differences				***Filtered equivalence rates***			
	Method 1							
	$^{1}\Delta Q_i$				$^{1}\Pi Q_i$			
i	mean	stdev	min	max	mean	stdev	min	max
dx	3,8551E-04	4,3954E-03	-1,4215E-02	1,7387E-02	1,00252	0,06964	0,24013	1,49803
dy	-1,5556E-03	2,0247E-03	-1,0425E-02	1,8991E-03	0,97096	0,58189	-7,49817	2,37510
dxx	2,8727E-04	4,4579E-04	-1,2261E-04	2,4980E-03	1,01591	0,53611	-2,10224	5,30039
dyy	1,9191E-04	3,4005E-04	-1,1334E-04	1,9989E-03	1,14498	0,88616	-6,74476	9,70580
dxy	-1,8148E-05	4,0980E-04	-1,9132E-03	1,5133E-03	0,97374	1,00615	-11,70870	4,23124
dxxx	-2,4638E-07	3,0701E-06	-1,2103E-05	9,9902E-06	0,95100	1,88624	-25,61410	8,57538
dyyy	7,9215E-07	1,2016E-06	-1,3637E-06	6,0620E-06	1,25471	0,36751	-1,56791	3,39896
dxxy	1,1764E-06	1,4036E-06	-7,1205E-07	6,5566E-06	0,98565	0,81374	-4,33275	9,61478
dxyy	-1,9883E-07	1,8141E-06	-7,2533E-06	5,7550E-06	1,22670	2,65098	-5,07256	36,76390
	Method 2							
	$^{2}\Delta Q_i$				$^{2}\Pi Q_i$			
dx	2,1559E-04	2,3933E-03	-7,7252E-03	9,4804E-03	1,00135	0,03788	0,58740	1,27122
dy	-9,2505E-04	1,1729E-03	-6,0091E-03	1,0234E-03	0,97957	0,39209	-4,73816	1,88628
dxx	1,8596E-04	2,8089E-04	-6,8183E-05	1,5118E-03	1,00482	0,33660	-1,11774	3,49531
dyy	9,7091E-05	1,7781E-04	-5,9621E-05	1,0463E-03	1,07123	0,50327	-3,43836	5,87902
dxy	-1,6427E-05	3,7152E-04	-1,7352E-03	1,3725E-03	0,97640	0,91128	-10,50950	3,92711
dxxx	-1,5876E-07	2,0070E-06	-7,9094E-06	6,5371E-06	0,96804	1,23270	-16,40190	5,92395
dyyy	4,9122E-07	7,7140E-07	-8,9437E-07	3,8581E-06	1,15078	0,23808	-0,68742	2,57851
dxxy	1,0959E-06	1,3078E-06	-6,2904E-07	6,0467E-06	0,98712	0,77237	-4,10113	9,24444
dxyy	-1,8078E-07	1,6188E-06	-6,4792E-06	5,1257E-06	1,20169	2,37231	-4,46470	32,84020
	Method 3							
	$^{3}\Delta Q_i$				$^{3}\Pi Q_i$			
dx	2,0019E-04	2,2187E-03	-7,1609E-03	8,7899E-03	1,00125	0,03511	0,61765	1,25144
dy	-8,6228E-04	1,0918E-03	-5,5912E-03	9,4813E-04	0,98078	0,36804	-4,38672	1,83002
dxx	1,7710E-04	2,6699E-04	-6,3895E-05	1,4299E-03	1,00408	0,31978	-1,02746	3,34949
dyy	8,9489E-05	1,6505E-04	-5,5462E-05	9,7092E-04	1,06534	0,47259	-3,17182	5,57330
dxy	-1,6241E-05	3,6736E-04	-1,7158E-03	1,3572E-03	0,97668	0,90100	-10,37970	3,89417
dxxx	-1,5105E-07	1,9163E-06	-7,5512E-06	6,2432E-06	0,96949	1,17704	-15,61830	5,69498
dyyy	4,6240E-07	7,3313E-07	-8,5475E-07	3,6569E-06	1,14006	0,22721	-0,61376	2,50952
dxxy	1,0861E-06	1,2962E-06	-6,2019E-07	5,9871E-06	0,98728	0,76686	-4,06835	9,19182
dxyy	-1,7875E-07	1,5977E-06	-6,3951E-06	5,0578E-06	1,19899	2,34199	-4,39776	32,41670
	Method 4							
	$^{4}\Delta Q_i$				$^{4}\Pi Q_i$			
dx	1,9849E-04	2,1996E-03	-7,0990E-03	8,7141E-03	1,00124	0,03480	0,62096	1,24927
dy	-8,5527E-04	1,0828E-03	-5,5449E-03	9,3988E-04	0,98092	0,36527	-4,34635	1,82362
dxx	1,7666E-04	2,6630E-04	-6,3698E-05	1,4260E-03	1,00405	0,31895	-1,02274	3,34265
dyy	8,9198E-05	1,6452E-04	-5,5281E-05	9,6781E-04	1,06512	0,47119	-3,15954	5,55946
dxy	-1,6220E-05	3,6689E-04	-1,7136E-03	1,3555E-03	0,97671	0,89984	-10,36500	3,89045
dxxx	-1,5021E-07	1,9064E-06	-7,5120E-06	6,2111E-06	0,96965	1,17096	-15,53270	5,66992
dyyy	4,5921E-07	7,2892E-07	-8,5043E-07	3,6346E-06	1,13886	0,22603	-0,60574	2,50200
dxxy	1,0850E-06	1,2948E-06	-6,1919E-07	5,9803E-06	0,98730	0,76622	-4,06452	9,18568
dxyy	-1,7852E-07	1,5953E-06	-6,3857E-06	5,0501E-06	1,19869	2,33856	-4,39020	32,36890
	Method 5							
	$^{5}\Delta Q_i$				$^{5}\Pi Q_i$			
dx	1,9834E-04	2,1979E-03	-7,0935E-03	8,7073E-03	1,00124	0,03478	0,62126	1,24908
dy	-8,5464E-04	1,0820E-03	-5,5407E-03	9,3914E-04	0,98094	0,36503	-4,34271	1,82304
dxx	1,7663E-04	2,6625E-04	-6,3684E-05	1,4257E-03	1,00405	0,31889	-1,02237	3,34215
dyy	8,9179E-05	1,6448E-04	-5,5268E-05	9,6759E-04	1,06511	0,47108	-3,15863	5,55845
dxy	-1,6219E-05	3,6685E-04	-1,7134E-03	1,3554E-03	0,97671	0,89974	-10,36370	3,89012
dxxx	-1,5013E-07	1,9055E-06	-7,5085E-06	6,2082E-06	0,96966	1,17041	-15,52500	5,66767
dyyy	4,5892E-07	7,2855E-07	-8,5004E-07	3,6327E-06	1,13876	0,22593	-0,60502	2,50132
dxxy	1,0849E-06	1,2947E-06	-6,1911E-07	5,9797E-06	0,98730	0,76617	-4,06418	9,18513
dxyy	-1,7850E-07	1,5951E-06	-6,3848E-06	5,0494E-06	1,19866	2,33826	-4,38952	32,36470

Table 5. Methods 1 and 6-9 for raster Q with resolution h=50.

	Differences				***Filtered equivalence rates***			
				Method 1				
	${}^{1}\Delta Q_i$				${}^{1}\Pi Q_i$			
i	**mean**	**stdev**	**min**	**max**	**mean**	**stdev**	**min**	**max**
dx	3,8551E-04	4,3954E-03	-1,4215E-02	1,7387E-02	1,00252	0,06964	0,24013	1,49803
dy	-1,5556E-03	2,0247E-03	-1,0425E-02	1,8991E-03	0,97096	0,58189	-7,49817	2,37510
dxx	2,8727E-04	4,4579E-04	-1,2261E-04	2,4980E-03	1,01591	0,53611	-2,10224	5,30039
dyy	1,9191E-04	3,4005E-04	-1,1334E-04	1,9989E-03	1,14498	0,88616	-6,74476	9,70580
dxy	-1,8148E-05	4,0980E-04	-1,9132E-03	1,5133E-03	0,97374	1,00615	-11,70870	4,23124
dxxx	-2,4638E-07	3,0701E-06	-1,2103E-05	9,9902E-06	0,95100	1,88624	-25,61410	8,57538
dyyy	7,9215E-07	1,2016E-06	-1,3637E-06	6,0620E-06	1,25471	0,36751	-1,56791	3,39896
dxxy	1,1764E-06	1,4036E-06	-7,1205E-07	6,5566E-06	0,98565	0,81374	-4,33275	9,61478
dxyy	-1,9883E-07	1,8141E-06	-7,2533E-06	5,7550E-06	1,22670	2,65098	-5,07256	36,76390
				Method 6				
	${}^{6}\Delta Q_i$				${}^{6}\Pi Q_i$			
dx	1,0065E-04	1,0202E-03	-3,2422E-03	4,0364E-03	1,00057	0,01608	0,82624	1,11548
dy	-4,9575E-04	5,9731E-04	-2,9698E-03	4,1509E-04	0,98543	0,26305	-2,86052	1,55329
dxx	1,5145E-04	2,2506E-04	-4,6215E-05	1,1480E-03	0,99934	0,26766	-0,80726	2,79531
dyy	6,6400E-05	1,1876E-04	-3,8129E-05	7,0206E-04	1,04777	0,35664	-2,17464	4,41388
dxy	-1,1233E-05	2,5598E-04	-1,1979E-03	9,4787E-04	0,98444	0,62489	-6,88926	3,00910
dxxx	-8,8413E-08	1,1385E-06	-4,4834E-06	3,7098E-06	0,98195	0,69881	-8,87098	3,77339
dyyy	2,6010E-07	4,2872E-07	-5,0816E-07	2,1169E-06	1,07449	0,13531	0,04104	1,89952
dxxy	8,5216E-07	1,0236E-06	-3,6571E-07	4,4818E-06	0,99169	0,65415	-3,44538	8,19794
dxyy	-1,2471E-07	1,0039E-06	-4,0395E-06	3,1387E-06	1,12276	1,50196	-3,15264	20,46080
				Method 7				
	${}^{7}\Delta Q_i$				${}^{7}\Pi Q_i$			
dx	1,5182E-04	7,2910E-04	-1,1112E-03	2,0704E-03	1,00128	0,00938	0,89925	1,06705
dy	-4,7888E-04	2,9674E-04	-1,3929E-03	-1,1625E-04	0,98924	0,20599	-2,02586	1,41784
dxx	1,4264E-04	2,0450E-04	-3,5272E-05	1,0286E-03	0,99983	0,25289	-0,71687	2,70784
dyy	6,0891E-05	9,8556E-05	-2,9210E-05	5,8644E-04	1,05226	0,37106	-2,10374	4,58541
dxy	-9,7200E-06	2,2676E-04	-1,0666E-03	8,4416E-04	0,98721	0,55010	-5,94354	2,76991
dxxx	-9,4640E-08	8,9681E-07	-3,1151E-06	2,3306E-06	0,98396	0,62315	-7,73297	3,67021
dyyy	2,2727E-07	3,0314E-07	-2,8017E-07	1,2568E-06	1,06819	0,10064	0,58393	1,31323
dxxy	7,4089E-07	9,4023E-07	-3,0814E-07	4,0411E-06	0,99749	0,60204	-3,15404	7,73444
dxyy	-9,3041E-08	7,7691E-07	-3,2713E-06	2,5760E-06	1,08759	1,11411	-2,94535	15,06500
				Method 8				
	${}^{8}\Delta Q_i$				${}^{8}\Pi Q_i$			
dx	6,0082E-05	5,7789E-04	-1,8433E-03	2,3078E-03	1,00030	0,00910	0,90296	1,06553
dy	-3,3608E-04	4,0422E-04	-1,9353E-03	2,3135E-04	0,98839	0,20367	-1,99257	1,41370
dxx	1,3508E-04	2,0025E-04	-3,8110E-05	9,9550E-04	0,99787	0,23725	-0,64957	2,52023
dyy	5,3255E-05	9,5698E-05	-3,0369E-05	5,6631E-04	1,03765	0,29921	-1,67548	3,84190
dxy	-9,7938E-06	2,2368E-04	-1,0474E-03	8,2883E-04	0,98658	0,54524	-5,88289	2,75354
dxxx	-6,3595E-08	8,3794E-07	-3,3003E-06	2,7367E-06	0,98677	0,51367	-6,26115	3,02225
dyyy	1,7591E-07	3,0939E-07	-3,7627E-07	1,5002E-06	1,04560	0,10222	0,28792	1,67123
dxxy	7,4333E-07	8,9943E-07	-2,6587E-07	3,8155E-06	0,99354	0,59504	-3,08714	7,62325
dxyy	-1,0180E-07	7,6544E-07	-3,0921E-06	2,3727E-06	1,09227	1,16564	-2,83711	15,67250
				Method 9				
	${}^{9}\Delta Q_i$				${}^{9}\Pi Q_i$			
dx	6,0026E-05	5,7723E-04	-1,8412E-03	2,3052E-03	1,00030	0,00909	0,90307	1,06546
dy	-3,3587E-04	4,0396E-04	-1,9338E-03	2,3106E-04	0,98839	0,20360	-1,99155	1,41352
dxx	1,3501E-04	2,0015E-04	-3,8084E-05	9,9494E-04	0,99786	0,23713	-0,64880	2,51929
dyy	5,3219E-05	9,5632E-05	-3,0347E-05	5,6592E-04	1,03762	0,29902	-1,67382	3,84008
dxy	-9,7876E-06	2,2354E-04	-1,0467E-03	8,2831E-04	0,98659	0,54490	-5,87858	2,75244
dxxx	-6,3549E-08	8,3719E-07	-3,2974E-06	2,7342E-06	0,98678	0,51321	-6,25455	3,02056
dyyy	1,7590E-07	3,0917E-07	-3,7591E-07	1,4994E-06	1,04570	0,10210	0,28862	1,67059
dxxy	7,4307E-07	8,9910E-07	-2,6586E-07	3,8143E-06	0,99354	0,59479	-3,08537	7,62037
dxyy	-1,0178E-07	7,6534E-07	-3,0917E-06	2,3724E-06	1,09226	1,16544	-2,83533	15,67080

USING SPATIAL DATA MINING TO DISCOVER THE HIDDEN RULES IN THE CRIME DATA

JANECKA Karel and HULOVA Hana

Department of Mathematics, Faculty of Applied Sciences, University of West Bohemia
Univerzitni 22, 32300, Pilsen, Czech Republic
kjanecka@kma.zcu.cz

Abstract

The main of this research was to explore the possibilities of Oracle Spatial for spatial data mining. We used Oracle Spatial for finding of association rules in the crime data. In particular, we had data about robberies which happened in the Czech Republic in the year of 2008. We focused on robberies which were perpetrated by youth. The amount of crime data is increasing and needs modern and effective processing. The crime data contain both spatial and non-spatial part. It makes sense explore the crime data if there are some regional patterns. In our research the thematic crime data were offered by the Czech Police Headquarters. We obtained this source thematic data in many xls files. Extraction, transformation and loading of data into the Oracle database were the initial steps of the spatial data mining process. In addition, we applied the built-in functionality of Oracle Spatial for materialization of loaded data. In particular the spatial binning method was used. The last step was done in Oracle Data Miner. For finding of association rules the Apriori algorithm was applied. We received many important association rules. These rules show that the situation about the crime perpetrated by youth differs from region to region. The results of this research were offered to the Czech Police Headquarters. Consequently appropriate measures can be applied to remedy the situation in particular regions.

Keywords: CRISP-DM methodology, ETL process, Spatial Binning, Regional Patterns, Oracle Spatial

INTRODUCTION

Today we can hear and read more and more that young people perpetrate crime. It is a very dangerous fact. It is necessary to explore the reasons why it is so. Police is responsible for solving it. Police is collecting data which are next processed and analyzed, mostly in geographical information systems. The amount of this data is rapidly increasing. Due to this reason the using of data mining seems to be an adequate method for exploring of huge amount of crime data. But the thematic crime data are relative to positions on the Earth and therefore it is not possible to use only the methods of classical data mining. It is about using of both data and spatial data mining methods.

There are currently several methodologies for data mining which we can be used in many application fields. As an example we can mention the CRISP-DM methodology. This is an industry and tool neutral data mining process model and consists of six steps:Business Understanding

- Data Understanding
- Data Preparation
- Modelling
- Evaluation
- Deployment

The relationships between particular phases are illustrated on Fig 1. Spatial data mining is broadly used in geographical information systems, geomarketing, Earth observation, navigation and many other areas (Murray, 2010). It is used for better understanding of relationships in data, for discovering of hidden relationships between spatial and attribute data and also for optimizing of spatial queries.

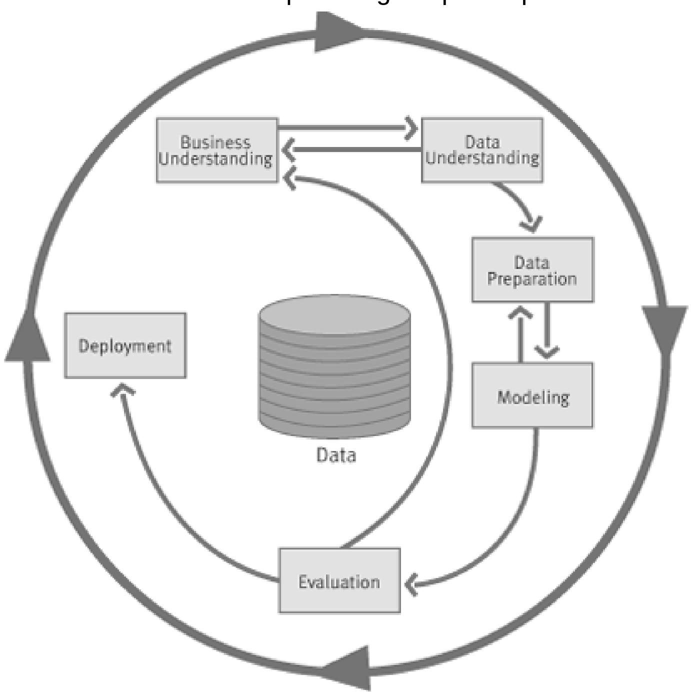

Fig. 1 The current process model for data mining provides an overview of the life cycle of a data mining project. It contains the corresponding phases of a project, their respective tasks, and relationships between these tasks. (Cross Industry Standard Process for Data Mining, 2010)

Our research was inspired by previous researches done in the field of spatial data mining and crime data in which generally the principles of the CRISP-DM model are used (McCue, 2007, Cherukuri et al, 2009, Nath, 2009). In our research we also followed the CRISP-DM model principles. However, the referenced works didn't use only the spatial database management system for spatial data mining process. Therefore one of the main aims of this research was to explore the possibilities of Oracle Spatial for spatial data mining process. We believe that describing of hidden associations in the crime data in the form of association rules is very readable for crime specialists to be able make important decisions. Therefore we strongly focused on possibilities of Oracle Spatial for generating of association rules.

SPATIAL DATA MINING

Spatial data mining can be defined as follows:

“Spatial Data Mining (SDM) is a well identified domain of data mining. It can be defined as the discovery of interesting, implicit and previously unknown knowledge from large spatial data bases.” (Witte, 2010)

The spatial data mining is more complicated than classical data mining due to the complexity of spatial data types, spatial relationships and spatial correlation among features. The spatial correlation means that the object of interest is influenced also by the neighbouring features. That is the reason why we have to also consider the attributes of “neighbours” during the spatial mining process. An effectiveness of many algorithms depends on the effective processing of relationships with surrounding.

Unsupervised Data Mining

An unsupervised data mining (UDM) is sometimes also called as “teaching without a teacher”. It means that known proved values are not available. The both methods clustering and finding of association rules belong to this group of data mining methods. Due to the reason that known patterns are not available before application of these methods we can use them for description of relationships and found patterns in data. In our research we especially concentrated on the method of finding of association rules in combination with the spatial binning for detection of regional patterns in crime data.

Spatial Data Mining in Oracle Spatial

Oracle is a relational database management system with the advanced possibilities of data processing. Oracle Spatial supports also spatial analysis and mining in Oracle Data Mining (ODM) applications. ODM allows automatic discovery of knowledge from a database. Its techniques include discovering hidden associations between different data attributes, classification of data based on some samples, and clustering to identify intrinsic patterns. Spatial data can be materialized for inclusion in data mining applications. The spatial analysis and mining features in Oracle Spatial let as exploit spatial correlation by using the location attributes of data items in several ways: for binning (discretizing) data into regions (such as categorizing data into northern, southern, eastern, and western regions), for materializing the influence of neighbourhood, and for identifying collocated data items.

The original data, which included spatial and nonspatial data, is processed to produce materialized data. Spatial data in the original data is processed by spatial mining functions to produce materialized data. The processing includes such operations as spatial binning, proximity, and collocation materialization. The ODM engine processes materialized data (spatial and nonspatial) to generate mining results. (Murray, 2009)]

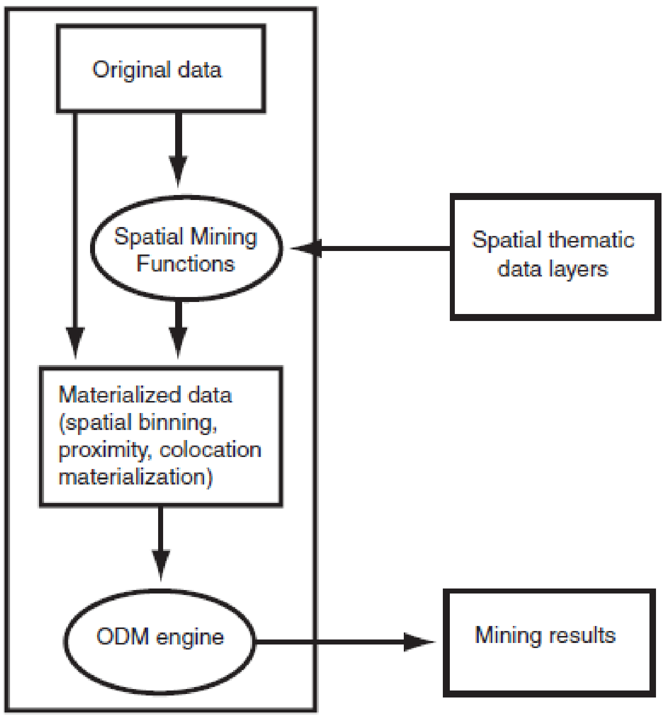

Fig. 2 A scheme of the Spatial Mining process in Oracle Spatial. The spatial materialization could be performed as a preprocessing step before the application of data mining techniques, or it could be performed as an intermediate step in spatial mining. (Murray, 2009)

Spatial binning for detection of regional patterns

Spatial binning (spatial discretization) discretizes the location values into a small number of groups associated with geographical areas. The assignment of a location to a group can be done by any of the following methods:

- Reverse geocoding the longitude/latitude coordinates to obtain an address that specifies (for United States locations) the ZIP code, city, state, and country.
- Checking a spatial bin table to determine which bin this specific location belongs in (Murray, 2009)

We were applying ODM techniques to the discretized locations to identify interesting regional patterns and association rules in the crime data.

Association

Association is a data mining function that discovers the probability of the co-occurrence of items in a collection. The relationships between co-occurring items are expressed as association rules. Association rules are often used to analyze sales transactions but association modelling has also important applications in other domains as well (Oracle Data Mining Concepts, 2008)

INPUT CRIME DATA

The thematic crime data were offered by the Czech Police Headquarters – the department of prevention. Overall we got nearly 90 xls files including among other things the source data about robberies which happened in the year 2008. Table 1 gives information about the count of robberies in the year 2008 in the Czech Republic.

Table 1 Count of all facts and robberies which were registered in the Czech Republic in the year 2008

Count of district police departments	Count of registered facts	Count of robberies
196	223 036	3 435

There are 14 main administrative regions in the Czech Republic and many district police departments belong to each region as stated on Fig 3.

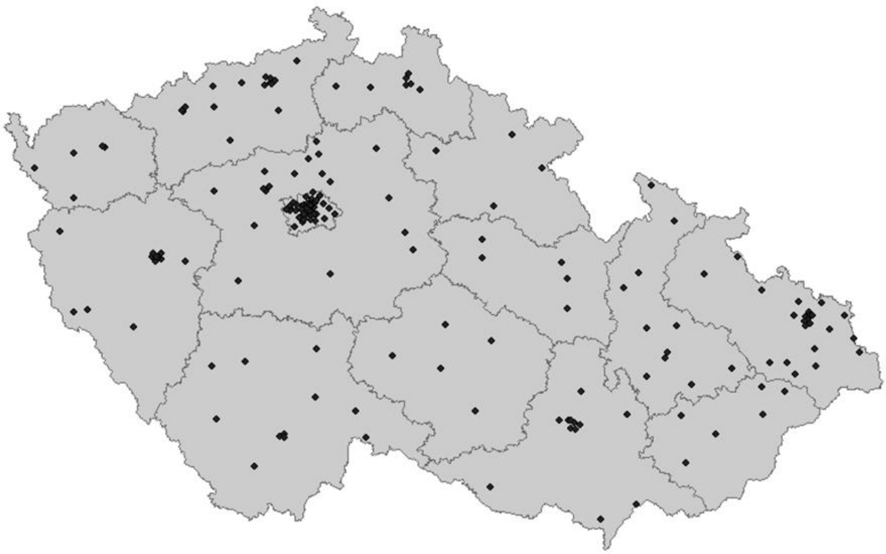

Fig. 3 The Czech Republic consists of the 14 main administrative regions. Dots represent locations of district police departments

The aim of the research was to try finding out some hidden associations in this crime data in particular main administrative regions. In particular we concentrated on robberies which were perpetrated by youth (up to 15 years of age; next as “youth<15”) and youth (between 15 and 18 years of age, according by the Czech law; next as “youth>15”) because this is a very negative social phenomenon.

PROCESSING OF INPUT DATA

To be able make spatial data mining we had to process all input data through Extraction – Transformation – Loading (ETL) process. ETL is a process that involves the following tasks:

- Extracting data from source operational or archive systems which are the primary source of data for the data warehouse;
- Transforming the data - which may involve cleaning, filtering, validating and applying business rules;
- Loading the data into a data warehouse or any other database or application that houses data (ETL-Tools, 2010)

Extraction

In addition to the aforementioned crime data, we used the locations of police departments of the Czech Republic organized in shp file. The data were extracted from the files of Land Identification Register – Basic Area Units (Czech Statistical Office (UIR-ZJS, 2010)). In addition, boundary of the Czech Republic and boundaries of 14 main administrative regions were used.

Transformation

It should be stated that not all attributes were considered during the spatial data mining. From the source thematic data we filtered out only the following attributes for each robbery: a day (Monday, Tuesday …), time of day (1 – 6 a.m., 7 – 12 a.m., noon – 6 p.m., 6 – 12 p.m.), kind of thief in accordance with his age (as described in chapter 3) and alcohol (if the robbery was done after the influence of alcohol).

The above mentioned attributes dealing with robberies were added to the dbf table of shapefile with positions of police departments. Now, we had thematic information relative to some spatial position.

Loading

First of all it was necessary to load the extracted data into the Oracle database. The tables for storing of extracted and transformed data were created. The spatial attributes like boundaries of regions were modeled as objects and stored in SDO_GEOMETRY (Murray, 2010) columns. This data type offers to model spatial features in object-relational way. All geometry description of spatial feature is then stored in one cell in spatial table. There were created two main tables:

- `BIN_TABLE_KRAJE` (for storing of 14 regions; one `SDO_GEOMETRY` column for storing of regions' boundaries),
- `LOUPEZE` (for storing of data in shapefile with thematic information; one `SDO_GEOMETRY` column for storing of positions of police departments). Fig 4 illustrates the positions of district police departments.

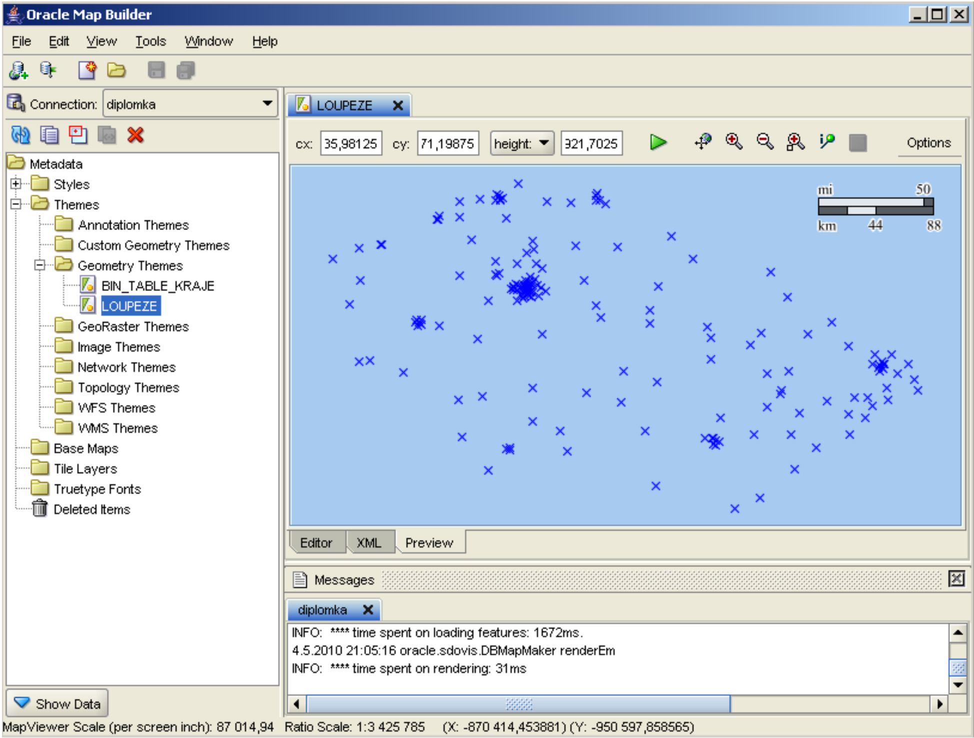

Fig. 4 Visualization of district police departments' positions

The loading of data was done by using of the Oracle Map Builder application. This application allows user to create, to maintain and to view spatial data and metadata. It allows also loading the shapefile into the Oracle database.

Application of Spatial Binning on the loaded data

As we needed to join the `BIN_TABLE_KRAJE` and `LOUPEZE` tables by using of the Spatial Binning method, we had to add some columns to the previous tables. In particular, the column `BIN` was added to the `BIN_TABLE_KRAJE` table and column `ID_BIN` to the `LOUPEZE` table.

The `SDO_SAM.BIN_GEOMETRY` function, documented in (Murray, 2010)], performs operation related to spatial binning. In particular, it computes the most-intersecting tile for geometry. After applying of this function on the `BIN_TABLE_KRAJE` table fourteen bins were created and their identifiers were stored in the `BIN` column. Finally, for spatial assigning of each police department (stored in the `LOUPEZE` table) to the appropriate bin the `SDO_SAM.BIN_LAYER` (Murray, 2010)procedure was used.

Now, we had materialized data (see Fig 2) ready for spatial data mining.

FINDING OF ASSOCIATION RULES

The Apriori algorithm was used for finding of association rules. This algorithm calculates the probability of an item being present in a frequent itemset, given that another item or items is present. The Apriori algorithm calculates rules that express probabilistic relationships between items in frequent itemsets For example, a rule derived from frequent itemsets containing A, B, and C might state that **IF** A and B are included in a transaction, **THEN** C is likely to also be included. An association rule states that an item or group of items implies the presence of another item with some probability. Unlike decision tree rules, which predict a target, association rules simply express correlation (Oracle Data Mining Concepts, 2010).

Antecedent and Consequent

The **IF** component of an association rule is known as the *antecedent*. The **THEN** component is known as the *consequent*. The antecedent and the consequent are disjoint; they have no items in common. Oracle Data Mining supports association rules that have one or more items in the antecedent and a single item in the consequent (Oracle Data Mining Concepts, 2010).

Metrics for association rules

Two main metrics are used to influence the build of an association model - *support* and *confidence*. Support and confidence are also the primary metrics for evaluating the quality of the rules generated by the model. Additionally, Oracle Data Mining supports *lift* for association rules. These statistical measures can be used to rank the rules and hence the usefulness of the predictions (Oracle Data Mining Concepts, 2010). In our work we used only support and confidence.

Support

The support of a rule indicates how frequently the items in the rule occur together. Support is the ratio of transactions that include all the items in the antecedent and consequent to the number of total transactions.

Confidence

The confidence of a rule indicates the probability of both the antecedent and the consequent appearing in the same transaction. Confidence is the conditional probability of the consequent given the antecedent. Confidence is the ratio of the rule support to the number of transactions that include the antecedent (Oracle Data Mining Concepts, 2010).

Example of computing support and confidence metrics for the rule R_1 **IF** A and B **THEN** C for the following transactions:

Transaction ID	Items
1	(A, B, C)
2	(D, A, B)
3	(A, C, D)
4	(A, B, D)

Probability of antecedent (A, B) and consequent (C) is 25% because only one transaction contains items A, B and C. Therefore the support for the rule R_1 is 25%. Transactions 1, 2 and 4 contain items A and B. It means that the confidence for the rule R_1 is 33%.

Preparation of transactional data

Unlike other data mining functions, association is transaction-based. Due to this fact it was necessary to transform our data stored in table `LOUPEZE`. To be possible to find out some regional patterns we created fourteen tables including transactional data. Each table contained transactional data for one particular administrative region. Each “transactional” table contained four columns:

- `id` – an identifier of transaction
- `id_police_department` – an identifier of district police department,
- `police_department` – a name of district police department,
- `code_of_act` – possible values are defined in chapter bellow.

Values in the `id` column were generated by database management system. Each triplet of values for the remaining columns was transformed from the `LOUPEZE` table.

Generating of association rules

The Oracle Data Miner (ODM) application was used for retrieving of hidden relationships and association rules in the crime data in the form **IF** A AND B **THEN** C. There is a five-step wizard we can use for finding of association rules (Haberstroh, 2010)in ODM. In the first step, we must select Function Type and used Algorithm. We used Association rules and the Apriori algorithm as theoretically described above. The choice of Function type and Algorithm is illustrated on Fig 5.

Next step was the selecting of source table with transactional data. All fourteen tables with the transactional data about the robberies were subsequently chosen. An identifier of each transaction was also set up in this step. In particular, the attribute `code_of_act` was used. In the third step of this process next attributes from “transactional tables” were chosen. Next, a name of the new table for storing of found association rules was entered. Finally, the association rules were generated and stored in the new table. It was necessary to enter some appropriate values for Support and Confidence parameters. We tried to set up these values repeatedly and explore the retrieved association rules. Finally, to get some predicative result we set up the Support parameter on value 30% for each region. The Confidence parameter was set up on value 20% for each region. In last step of wizard association rules were retrieved.

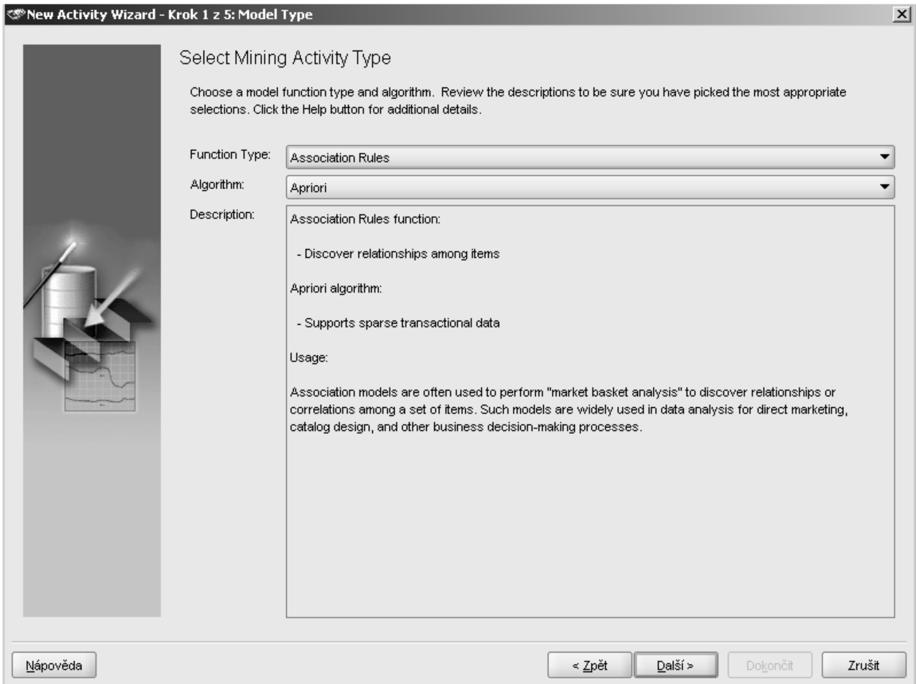

Fig. 5 The Apriori algorithm was used for retrieving of association rules

Regional patterns

It was recognized that there are differences in the retrieved association rules in different administrative regions. We concentrated on the children's and young's criminality (robberies). For example, in the South Bohemian Region, if the robbery happened on Monday in time 1 p.m. – 6 p.m., then it was committed by child in 45%! The Support for this association rule was 100%, Confidence 45%. Against this fact, the situation in the neighboring Pilsen region was quite different. The table 2 contains selected examples of association rules for particular regions with the inclusion of the values of both Support and Confidence parameters.More retrieved association rules and their description can be found in (Hulova, 2010).

Table 2 Association rules for particular regions with the highest value of Support and Confidence for the robberies perpetrated by “youth<15”

Region	Association Rule	Confidence	Support
South Bohemia	**IF** robbery on Monday AND in time 1 p.m. – 6 p.m. **THEN** committed by "youth<15"	100%	45%
Pilsen	**IF** robbery perpetrated by youth AND in time 7 p.m. – 12 p.m. **THEN** committed by "youth<15"	80%	33%
Karlovy Vary	**IF** robbery **on Tuesday AND in time 1 p.m. – 6 p**.m. **THEN** committed by "youth<15"	33%	20%
Usti nad Labem	**IF** robbery on Monday AND in time 1 a.m. – 6 a.m. **THEN** committed by "youth<15"	81%	50%
Liberec	**IF** robbery on Thursday AND in time 7 a.m. – 12 a.m. **THEN** committed by "youth<15"	50%	11%
Hradec Kralove	**IF** robbery on Wednesday AND in time 1 a.m. – 6 a.m. **THEN** committed by "youth<15"	100%	25%
Central Bohemia	**IF** robbery perpetrated by youth AND in time 7 a.m. – 12 a.m **THEN** committed by "youth<15"	50%	13%
Prague (the capital)	**IF** robbery perpetrated by youth AND on Tuesday **THEN** committed by "youth<15"	47%	18%
Vysocina	**IF** robbery perpetrated by youth AND on Sunday **THEN** committed by "youth<15"	100%	33%
Olomouc	**IF** robbery on Monday AND in time 7 p.m. – 12 p.m. **THEN** committed by youth	100%	45%
Moravian-Silesian	**IF** robbery on Thursday AND in time 7 a.m. – 12 a.m. **THEN** committed by "youth<15"	100%	62%
South Moravian	**IF** robbery on Wednesday AND in time 7 a.m. – 12 a.m. **THEN** committed by "youth<15"	100%	61%

CONCLUSION

One of the aims of this research was to explore the possibilities of Oracle database including Spatial for spatial data mining. This topic is very wide. We tried to apply the method of finding association rules in spatially materialized data. For materialization of spatial and thematic (crime) data the spatial binning was used. The results of this work were taken over by the Czech Police Headquarters. Some information rising from the research was really surprising. For example, the children’s criminality in Prague, the capitol, is not so much high as it is generally supposed to be. The work also presented the possible way how to process the huge amount of data which are collected by police. The retrieved association rules can help to adapt appropriate measures to remedy the situation in particular region. From the technical point of view we tried to describe all process of spatial data mining with the crime data. We described the ETL-processing of crime data and spatial data and the transactional structure of corresponding tables which are a base for retrieving of association rules.

REFERENCES

Cross Industry Standard Process for Data Mining. http://www.crisp-dm.org/index.htm, Cited: 10/2010

Murray, Ch. Oracle Spatial Developer's Guide 11g Release 1. Oracle, 2009. http://download.oracle.com/docs/cd/B28359_01/appdev.111/b28400.pdf, Cited: 03/2010

McCue, C. (2007) Data Mining and Predictive Analysis: Intelligence gathering and crime analysis. Butterworth-Heinemann.

Cherukuri, K.; Muralikrishna, Reddy, V. Spatial and Collateral Data Mining for Crime Detection and analysis. http://www.gisdevelopment.net/application/miscellaneous/me05_183.htm, Cited: 11/2009

Nath, S., V. Crime Pattern Detection Using Data Mining. Oracle http://www.oracle.com/technetwork/database/options/odm/overview/crime-patterns-snath-odm-134695.pdf, Cited: 11/2009

Witte, E. Spatial Data Mining. http://www1.in.tum.de/teaching/ws01/CBP-Hauptseminar/Presentations/SpatialDataMining-Pres.pdf, Cited: 03/2010

Oracle Data Mining Concepts 11g Release 1. Oracle, 2008. http://download.oracle.com/docs/cd/B28359_01/datamine.111/b28129.pdf, Cited: 04/2010

ETL-Tools.Info. http://etl-tools.info/en/bi/etl_process.htm, Cited: 10/2010

Uzemne identifikacni registr UIR-ZJS, Cesky statisticky urad. http://www.liberec.czso.cz/csu/rso.nsf/i/prohlizec_uir_zsj, Cited: 03/2010

Oracle Data Miner. http://www.oracle.com/technetwork/database/options/odm/downloads/index.html, Cited: 03/2010

Haberstroh, R. Oracle Data Mining Tutorial. Oracle, 2008 http://www2.tech.purdue.edu/cit/Courses/CIT499d/ODMr%2011g%20Tutorial%20for%20OTN.pdf, Cited: 04/2010

Hulova, H. Aplikace vybranych metod prostoroveho dolovani dat v databazovych systemech. Diploma Thesis. Pilsen, 2010

VISIBILITY ANALYSES AND THEIR VISUALIZATION

POPELKA Stanislav

Dept. of Geoinformatics, Palacky University, tř. Svobody 26, 771 46, Olomouc, Czech Republic *Standa.Popelka@gmail.com*

Abstract

Visibility analysis or Viewshed is a common function of almost all GIS systems. The aim of this paper is to find out the best solution, to compute viewshed for the Olomouc region and ensure the best way of visualization of the results. The first step to analyze the visibility is making a high quality Digital Terrain Model, choice of the best interpolation method and subsequent addition of vegetation and man-made structures layer. Not all applications are able to compute visibility for a large area, so the choice of software was also very important. Currently there are many ways to transmit the analysis results to the target user. We used Google Earth for visualization.

For the representation of results Google Earth and Google Earth API were used. The project deals with the possibilities of exporting the output from the visibility analysis from ArcGIS system to Google Earth. An important part is to optimize the size of the resulting layer using various methods of generalization so that the resulting layer is sufficiently precise and not too voluminous at the same time. The project also explores the possibilities of enrichment of visualization with multimedia content, which can be for example 3D models of buildings, photos, videos or spherical panoramas as we know from Google Street View, etc. The output of the project is an interactive application that will ensure a simple and visually attractive approach to data that represent the visibility of the most important observation points in the area of interest.

Keywords: Visibility, Visualization, Analysis, Generalization, Google Earth, Google Maps, API

INTRODUCTION

Visibility analysis based on viewsheds is one of the most frequently used GIS analysis tools. In the past, these analyses were used primarily for military purposes.

It is believed that the first recorded use of Line of Sight dates to the beginning of the 18th century when a French military engineer, Prestre de Vauban (1603-1707), created a map of the siege of the town of Ath in Belgium. The upper part of the map (Fig 1) contains Line Of Sight, the lower part contains Weapon Fan that depicts the action radius of artillery batteries. Visibility analyses can be also highly important for the reconstruction of historical military operations

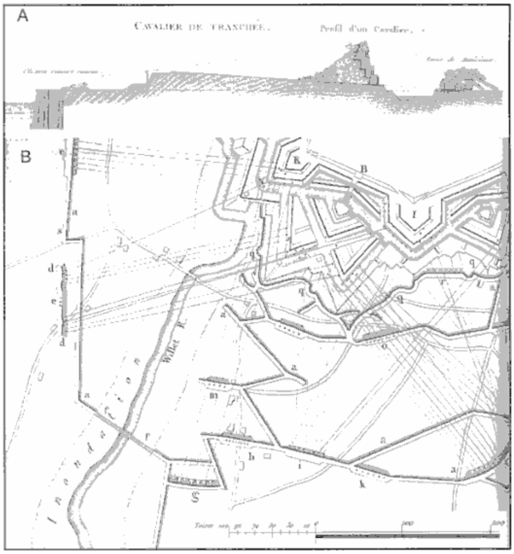

Fig. 1 One of the first examples of the use of Line Of Sight.
The siege of Ath in 1706. (Caldwell, 2004)

With the spread of GIS in the private sector there emerged a wide range of uses in many spheres of human activity. Viewshed analysis has been used in a wide range of applications, including radio communication or localization electrical generating windmills or lookout towers. Other field of use of visibility analyses is archaeology, where these methods can be used to detect archeological sites, spatial planning and many other spheres of human activity.

Sector, where the outcomes depend on the manner of visualization of the results, is use of visibility analyses in tourism. Even if we count on calculations of extreme quality, it does not necessarily mean that they can be used in practice; this is only possible when they are represented in a suitable manner and made accessible to a target group of users.

The Google Earth and Google Maps tools have become popular in the wide public in a relatively short period of time. Their big advantage is the continuous refinement of source data and the creation of new functions. These tools can be effectively used for displaying various types of information, like overlay layers, texts, pictures or videos. One example is the project of the Crisis in Darfur.

This paper deals with visibility analyses in the region of Olomouc. Results of the study should be used for the propagation of the studied region and that they can serve as a basis for the creation of new scenic view points in the landscape or the construction of new observation towers.

METHODOLOGY OF COMPUTATION OF VISIBILITY ANALYSES

The GIS environment offers three main methods of computing visibility analyses. These methods are called differently in different applications. In this study, the functionality and terminology from ArcGIS are used.

Line of Sight

Line-of-sight analysis determines whether two points in space are intervisible. In practice, only the initial and terminal points are determined, and possibly the elevation of the observer. The software divides the line into segments that are visible from the initial points and segments that are hidden behind an obstacle. Some applications combine this method with terrain profile, making a colour differentiation not only of the line segment but also of the curve that represents this profile.

Viewshed

Viewshed is created over a DTM – Digital Terrain Model using an algorithm that estimates the difference in elevation in the observer's cell and the target cell. To determine the visibility of the target cell, each cell that lies on the line connecting the observer and the target must be examined by Line of Sight. If there is a cell with a higher value between the observer and the target cell, it is blocked. In such a case the target cell is marked "Not Visible".

Visibility

Visibility is the last method offered by ArcGIS. In other applications this tool can be called Multiple Viewshed. The Visibility function provides answers to two basic questions: "What places are visible from the given observation place?" and "How many observation places is the given object/place visible from?" The Visibility command also enables a visibility analysis using a line theme.

CREATION OF A DIGITAL SURFACE MODEL

In terms of accuracy and reality of the output of visibility analyses, the quality of input digital terrain model is the most significant element. In order to get an accurate image of the Earth's surface, it would have to be scanned with the techniques of remote sensing, like laserscanning, for example (Sander, 2007). However, these methods are extremely costly, especially if it is necessary to obtain data for the range of district of Olomouc (800 km^2). That is why the terrain was interpolated from contour lines with the basic interval of 5 m, then adding man-made structures, forests and line vegetation.

Creation of a DTM

It is important to base the process on sufficiently accurate elevation data, as well as to choose a suitable interpolation method and its setting.

Comparison of interpolation methods

Sharma argues that the five most frequently cited interpolation methods are TIN with linear interpolation, Inverse Distance Weighing (IDW), Spline, Ordinary Kriging and TOPOGRID. For our purpose, IDW, Spline and Ordinary Kriging were chosen. To evaluate the DTM quality we chose the RMSE method which measures the dispersion of the frequency distribution of deviations between the original elevation data and the DTM data. Mathematically it is expressed as (Chen, 2009). A higher RMSE value shows a greater dispersion between the interpolated and input data. The ideal value should not exceed half of the value of the basic contour line interval (Svobodova, 2009). That means that in this case it should not be greater than 2.5.

$$RMSE_Z = \sqrt{\frac{1}{n}\sum_{i=1}^{n}(Z_{di} - Z_{ri})^2} \qquad (1)$$

where Z_{di} is the value of altitude from DTM surface,

Z_{ri} is the corresponding original altitude,

n is the number of samples.

The input point field used for computation of DTM was divided into two parts. 85% of points were used for creation of DTM and 15 % for determination of the Root Mean Square Error (RMSE). These points were chosen randomly using RandomSelection toolbox for ArcGIS.

First, the area of interest was divided into squares with the length of their sides of 4 km. Elevation range was calculated within each square. This way the values of relative height division were worked out in each square. Flat land and hilly areas are predominant in the area of interest, therefore, such settings of interpolation methods that showed the best results for these characteristics were chosen from the thesis. „Analýza morfometrických charakteristik různých typů reliéfu“. This thesis deals with evaluation of interpolation methods on different types of relief. With help of weighed order there were chosen the best interpolation methods and parameter setting for each type of relief (planes, downs etc.). Eight settings of interpolation methods were chosen from this thesis.

Tab 1. Setting of the spline interpolation method

Name	Type	Weight	Points
Splinet-5-20	Tension	5	20
Splinet-01-12	Tension	0,1	12
Splinet-1-20	Tension	1	20
Splinet-5-10	Tension	5	10
Splinet-20-10	Tension	20	10

Tab 2. Setting of the kriging interpolation method

Name	Method	SemiVar	Radius	Points
Krig-u-l-25	Universal	Linear	Variable	25
Krig-o-s-12	Ordinary	Spherical	Variable	12
Krig-o-s-25	Ordinary	Spherical	Variable	25

These 8 grids were interpolated using the settings mentioned above. The resulting DTMs were then tested, so that it could be found what setting is the most suitable for the studied area. To complete this evaluation we calculated the basic statistical characteristics and then applied RMSE. These values were calculated in relation to the remaining 15 % of points that were not included in the generation of the grids. This enabled us to check the accurateness of the grids in relation to the original data.

Spline with tension with weight 5 and number of points ten seems to be the most suitable method of terrain interpolation. It had the value of RMSE only 1.14. All results are shown in Table 3.

Tab 3. Comparison of interpolation methods. Sorted by RMSE.

Name	Min	Max	Mean	Range	SD	RMSE
Splinet-5-10	193	681	286	488	101	1.14
Splinet-20-10	196	681	286	484	101	1.18
Splinet-01-12	169	681	286	511	101	1.38
Krigu-l-25	92	677	286	585	101	3.01
Krig-o-s-12	199	679	286	479	101	3.09
Krig-o-s-25	199	677	286	477	101	3.71
Splinet-5-20	190	836	286	645	101	4.44
Splinet-1-20	184	681	286	496	101	4.48

Creation of DSM from DTM

The created digital terrain model must then be complemented with man-made structures and vegetation, so that it better corresponds to the reality and the results of the visibility analyses are realistic. Unavailability of data became a limiting factor in the case of man made structures (data equivalent to the various buildings were not available for the whole study area), therefore resulting Digital Surface Model - DSM is more accurate in the area of Olomouc city and less accurate in surrounding areas. In these areas, data of blocks of buildings from DMU25 were used. The height of buildings was calculated from the number of floors which was gained from address points of the Czech Republic.

Permeability in the winter

Because in the summer the vegetation presents a much greater barrier to visibility than in the period of vegetation dormancy, we took into account two alternatives of the input DSM. One for the summer when the "permeability" through vegetation is minimum, and one for the winter when leaves fall and visibility is much greater.

The best method, which would ensure data most corresponding with reality, would be creation of 3D models of separate trees in the winter and summer version. These models would be used right in the visibility analysis. Unfortunately nowadays GIS softwares don't support analyses of real 3D data and therefore some degree of generalization had to be accepted. The differences between winter and summer season were simulated by extraction of certain part of pixels from the layer of vegetation. Effect of this operation on the following analysis is quite equivalent to the reality. It is very important to find out the most suitable settings of pixels extraction. When we just chose certain percentage of pixels with cellsize 5*5 metres, the effect was hardly noticeable. Reason for this was small size of pixel in comparison with the width of the area which represents the linear vegetation. In this case shading of individual pixels appeared. Appropriate step was to resample the vegetation grid and after this extract part of pixels. Because this operation is quite timeconsuming, the season versions were made only for areas of vegetation which are not wider than 20 metres.

We created a random grid of three different cell sizes. The spatial resolution of the first variant was 25 × 25 m, the second 15 × 15 m, and the third was of the same spatial resolution as the DTM (5 × 5m). These random grids were then re-classified into several categories. In the winter alternative, we tested variants where 50, 75 and 85 % of pixels were deleted. In the summer alternative 25 and 35 % of pixels were deleted. These layers with random pixel values were then used to multiply the vegetation layer, where the permeability changes in relation to the time of the year. The total of 8 variants of the degree of permeability of vegetation were created and then compared with the reality. The CellSize setting of 15 × 15 m and the deletion of 75 % pixels was closest to the reality. In the summer alternative 35 % of cells were deleted.

To better simulate the differences between summer and winter, type of vegetation should be included when calculating results. Unfortunately, these data were not available. So it was not distinguished if the vegetation is cofinerous, broadleaved or mixed.

Results of analyses with different setting were compared with the real visibility captured by panoramic photography. On both map and photo, easily identificable points (chimneys, natural peaks, groups of trees or alleys) were marked. Then it had to be stated whether the object marked as visible in reality is also marked as visible in map and vice versa.

OBSERVATION POINTS

The Olomouc region is an area of relatively small segmentation. Nevertheless, there is a number of interesting places that can be determined as significant observation points. The selection of these points was made using the criterion of visibility from a given point, taking into account the accessibility of this point. Therefore, it was necessary to choose a compromise between elevation of the given point and its distance from roads, etc. The total of 40 observation points was selected, with a relatively even distribution over the region of Olomouc. We elected several categories of observation points. These are: natural places, sacral and technical buildings and potential observation points. The last category corresponds to places where there is currently no view due to a vegetation barrier but where the situation would change after a construction of an observation tower.

In the case of sacral and technical buildings the elevation of the observer corresponds to the height of the observation deck, window of the church, etc. On the other hand, in the case of natural places the basic elevation of the observer is set to 2m above the ground. The work also resulted in a study on how the share of visible land would change if the elevation of the observer changed to 8, 15 and 30 metres. To better illustrate the height of the observation tower, as well as to increase the attractiveness of the visualization, we created 3D models of observation towers that correspond to the elevation of the observer and, at the same time, depict three different types of observation towers.

These models were created in freeware software Google SketchUp, which allows export of model to kmz format which can be visualized in Google Earth application.

ANALYSIS COMPUTATION AND GENERALIZATION

Most of the GIS softwares, which can work with 3D data, allow some visualization of visibility analysis. Ten freeware and commercial applications, which provide computing of visibility analyses, were chosen and compared.

Freeware aplications, used for comparison, were MicroDEM, AutoDEM, SAGA and GRASS GIS.

Difference between commercial and noncommercial applications was not in the quality of results or in the user interface (which was better arranged and provided more possibilities in noncommercial softwares). The biggest and fundamental difference was in the possibility to calculate results for large areas. Most of the noncommercial applications were not able to even display the digital terrain model of district of

Olomouc. Other aplications could not compute Viewshed for this area. Despite this fundamental insufficiency, these applications had many positives, for example possibility to export results of visibility analysis to video. This makes it possible to watch the change of visible area depending on movement of observer point.

Commercial applications which were tested were ERDAS, IDRISI and ArcGIS 9.3 There were no significant diversities in the quality of outcomes. All three applications seem to use very similar algorithm and therefore their outcomes are almost identical

ArcGIS was chosen for computatuion of visibility analyses in the distric of Olomouc. ESRI announced support of real 3D objects as input data do viewshed analysis. If this was done, it could be possible to use for example 3D models of particular buildings, vegetation etc. as input layer to the visibility analyses and the results would be more accurate. Unfortunately this feature is eventually not suported in ArcGIS 10. Differences between applications sufficinet for analyses of large areas are only in the user interface.

Ways of conversion into KMZ

As we want to present the results in the Google Earth environment, we must find a solution of how to convert data into the KMZ format. There are three ways to do it.

Raster layer

The easiest solution is to use the function Layer to KML, which is offered by ArcGIS from the version 9.3 onward. It is possible to specify the resolution of the resulting overlaying image that will be represented in Google Earth. But there is a problem: when an image is bigger than approximately 10000 pixels, kmz is created but the Google Earth application does not depict it. Lower resolution leads to the loss of detail and, therefore, this export alternative cannot be used.

Raster tiles

The problem of insufficient resolution can be solved by using the MapTiler freeware application, which cuts the raster into so called Tiles and creates Super-Overlay. It is a pyramid loading of layers, i.e. layers with a different level of detail (LOD). Using tile raster is suitable especially for the representation of old aerial photos, early maps, etc. Biggest disadvantage of this method lays in the huge amount of files which are created during export and thus make transfer of application very complicated. In our case, when the overlaying layer only has two categories, it is more advantageous to use the last possibility of export of data into KML, i.e. the conversion of vector data.

Vector layer

There are several methods to convert vector data into Google Earth. The above mentioned Layer to KML function offers the easiest solution. Various extensions can also be used. The freely accessible Export to KML is of high quality. This method also has its limits. No polygon can have more than 50 000 vertices or only outline is displayed. For the work in web environment it is also necessary to generalize output layers. However this method was the one most suitable one for our purposes (we export layer with only two categories) and therefore we chose this solution to represent visibility analyses

Generalization

As has already been mentioned above, we chose export to KMZ as a vector. First, we had to convert the layer of visibility analyses from raster to polygons. The disadvantage of this procedure is that a huge number of polygons is created. The size of such a KMZ would limit the applicability of the whole application, which is intended to work in the Internet environment. On the internet, users have certain expectations. One of them is the speed of loading content. This is why we had to use generalization. ArcGIS enables the generalization of polygons by two methods. Aggregate Polygons and Simplify Polygons. None of the methods produces a result whose quality would be sufficient but which would, at the same time, be as small as possible. Therefore, we combined the two methods.

First step of generalization was Aggregating of Polygons with Aggregation distance set to 50 m, minimum area of 50 m^2 and minimum Hole size of 100 m^2. Using this function led to the greatest reduction in the size of file. Smoothing of generalized polygons was achieved by the subsequent application of Simplify Polygons method (with setting PointRemove and Offset of 1 m). The final size of individual visibility layers ranges from 500kB and 1,5MB.

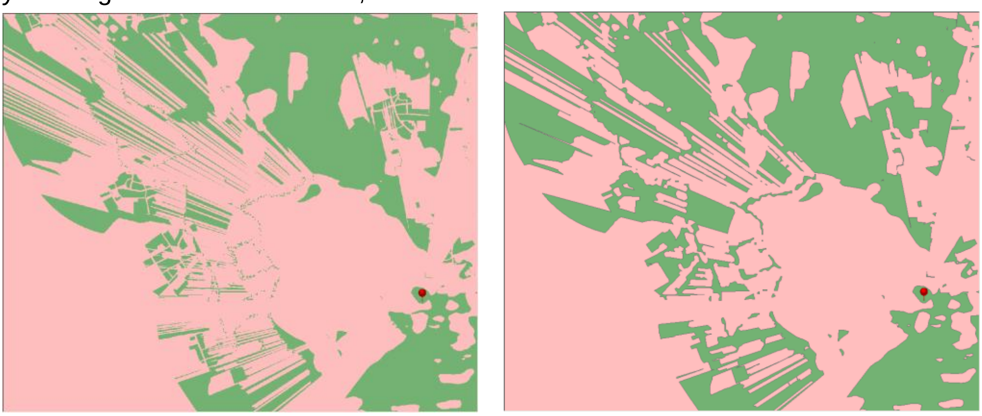

Fig. 2 Comparison of original and generalized data

VISUALIZATION OF RESULTS

Visualization capitalizes on strenghts of human perception abilities. The human brain has an impressive capacity for the understanding and assimilation of graphically presented information. The results of the viewshed analyses were visualized via Google Earth and Google API.

Google API

The use of API presents the first method of visualization of the results. We chose the combination of Maps API and Earth API. The first alternative is advantageous especially because plugin does not need to be installed; the data are depicted directly in the window of an Internet browser (Wernecke, 2008). The second advantage of this method is that there is the possibility to choose source data. To visualize information on observation points we created a point layer in the KML format. By clicking individual points the user can display basic information about the observation point and a photo gallery.

To represent the results of the visibility analyses we chose the method of JavaScript form which enables the user to select the observation point, time of the year, elevation of the observer, and whether they want circles of visibility to be displayed or not. After this selection a checkbox appears that enables the activation and deactivation of these layers. The transparency of visibility layers was set to 65%, so that the map base is visible.

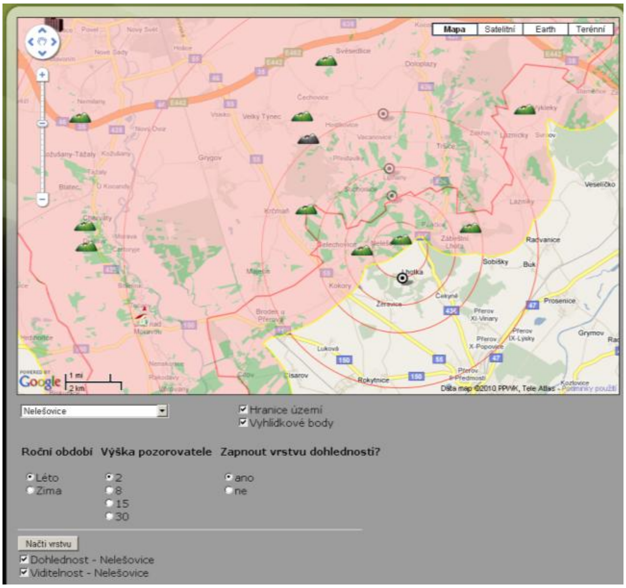

Fig. 3 Illustration of the visualization of visibility analyses in Google Maps.

Google Earth

Online tools, such as those pioneered by Google Earth, are changing the way in which scientists and the general public interact with three-dimensional geospatial data in a virtual environment. It is possible to create a complex project with various types of multimedia content in Google Earth. Apart from higher speed, in comparison to API, Google Earth offers better functionality and better interface for the user. Compared to the version for Google Maps panoramic photos and 3D models of observation towers can be displayed.

There are three possibilities how to make links to KMZ files (outcomes of visibility analyses in our case) in Google Earth.

First possibility is to create a link to external webpage in the description of observation point. This external webpage contains a javascript form which allows user to select which layer should be displayed. This layer is then downloaded and visualized in Google Earth. It would be more suitable to put the form directly into the observation point description but this is not possible for technical reasons (description cannot contain javascript, iframe, etc.). The disadvantage of this method is unnecessary burdening of user by switching to an external site where user can choose what he wants to see.

Second possibility is creation of folder structure in the left bar of Google Eearth application. This structure would contain checkboxes and radiobuttons which would help user to set the layer which he wants to see. This procedure is not suitable for large amount of layers. We have 40 observation points and thus the folder structure would be complicated and 'stretched.'

Last possibility is to put links to KMZ files directly to the description of observation points. User doesn't need to leave Google Earth environmnent. This method can only be used when there are not many outputs related to the observation point. In our case, eight visibility layers are peak value and therefore it is not a problem to insert the links into the description. If we had more layers, we would use the first possibility. In our case, third approach was chosen, thus placing a link directly to the description of each point.

After clicking the point a description is opened and the user chooses one of the links and the required layer is downloaded from the Internet and displayed. Apart from these visibility layers it is possible to display visibility circles for each point, a 3D model of one of three types of observation towers or a panorama photo. All these objects are displayed directly in the Google Earth environment as KMZ files. Example of visibility analysis visualization in Google Earth is shown on Fig 4.

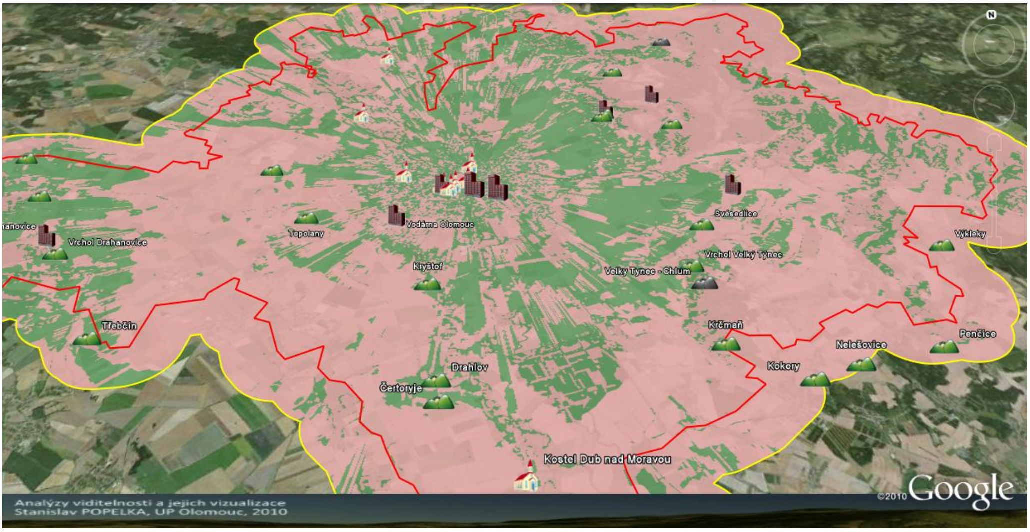

Fig. 4 Viewpoint description in Google Earth.

CONCLUSION

This extensive study deals with the computation of analyses of visibility from significant observation points in the region of Olomouc. The main prerequisite to get high-quality visibility analyses was to create a digital terrain model of sufficient accuracy and complete it with man-made structures and vegetation. Two alternatives of DTMs were created, representing the landscape in the summer and in the winter. The total of 40 observation points was selected. If these were sacral or technical buildings, the elevation of the observer corresponded to the height of the building. If it was a natural hilltop, we computed the visibility in the current situation, as well as the visibility after a construction of an observation tower of 8, 15 or 30 metres.

Central part of the work is the visualization of the results that would be attractive and easily accessible to the users. We used the Google Earth and Google Maps API tools that enable the display of the output directly in the window of an Internet browser. In the case of Google Maps, the user can find the description and photos of individual observation points, and accedes to the results of the analyses via a form. In the case of Google Earth, there is a greater functionality and, moreover, it contains panoramic photos and 3D models of observation towers. Both types of visualization are accessible to the wide public at www.OlomouckeVyhledy.upol.cz

REFERENCES

CHEN Aijun, LEPTOUKH Gregory, KEMPLER Steven (2009), Visualization of A-Train vertical profiles using Google Earth. Computers & Geosciences 35 (2009) 419–427

GERMINO Mathew J.; REINERS William A.; BLASKO Benedict J.; McLEOD Donald, BASTIAN Chris T. (2001) Estimating visual properties of Rocky Mountain landscapes using GIS. Landscape and Urban Planning 53 (2001) 71-83

GROOTHUIS Peter A.; GROOTHUIS Jana D; Whitehead John D. (2008) Green vs. green: Measuring the compensation required to site electrical generation windmills in a viewshed. Energy Policy 36 (2008) 1545–1550

OGBURN Dennis E. (2006) Assessing the level of visibility of cultural objects in past landscapes. Journal of Archaeological Science 33 (2006) 405-413

PARKS Lisa (2009), Digging into Google Earth: An analysis of ‘‘Crisis in Darfur”. Geoforum 40 (2009) 535–545

SANDER Heather A.; MANSON Steven M. (2007), Heights and locations of artificial structures in viewshed calculation: How close is close enough?. Landscape and Urban Planning 82 (2007) 257–270

SEVENANT Marjanne; ANTROP Marc (2006), Settlement models, land use and visibility in rural landscapes: Two case studies in Greece. Landscape and Urban Planning 80 (2007) 362–374

SHARMA, A.; TIWARI, K.N. (2009), Measuring the Accuracy of Contour Interpolated Digital Elevation Models, Journal of the Indian Society of Remote Sensing 37 (2009) 139-146

SVOBODOVÁ, J, TUČEK, P: Creation of DEM by kriging method and evaluation of the results. Geomorphologia Slovaca et Bohemica 9 (2009) 53-60

WINTERBOTTOM S. J.; LONG D. (2006), From abstract digital models to rich virtual environments: landscape contexts in Kilmartin Glen, Scotland, Journal of Archaeological Science 33 (2006) 1356-1367

CALDWELL, Douglas R. (2004), Studies in military geography and geology. Dordrecht : Cluver academic publishers, 348p

DODD, Howard Mannin. (2001), The Validity of Using a GIS Viewshed Function [online]. Blacksburg : Blacksburg, 49 p. Diploma thesis. Faculty of the Virginia Polytechnic Institute.

ONDRÁČKOVÁ, J. (2009), Analýza Morfometrických charakteristik různých typů reliéfu. Olomouc, 40 p. Bachelor Thesis. Palacky University Olomouc.

WERNECKE, Josie. (2008), The KML Handbook: Geographic Visualization for the Web. Addison-Wesley Professional, 368 p.

Digitální model území DMU25 [Dataset, CD-ROM] Dobruška. Vojenský topografický ústav Dobruška, 2003

Viewshed Analysis, cit. 2010-04-29. <http://en.wikipedia.org/wiki/GIS _Viewshed_ Analysis>.

Random selection, cit. 2010-11-29, <http://arcscripts.esri.com/details.asp?dbid= 15156>

CREATION OF MODEL MESHES FOR HYDROGEOLOGIC MODELING

MALA Blanka and PACINA Jan

Institute of Novel Technologies and Applied Informatics, Faculty of Mechatronics, Informatics and Interdisciplinary Studies , Technical Univerzity of Liberec, Studentská 2/1402, 461 17, Liberec, Czech Republic
blanka.mala@tul.cz

Department of Informatics and Geoinformatics, Faculty of Environment, J. E. Purkyně University, Králova výšina 7, 400 96, Ústí nad Labem, Czech Republic
jan.pacina@ujep.cz

Abstract

A number of practical problems are solved through modeling. Examples include the water flow and transport in the rock environment. They are modeled by finite element method, the solution uses software tools for which it is always necessary to process real data of the modeled area. In mathematical modeling of processes is the construction of model meshes and their filling with data significant challenge. The existence of the model mesh with required properties is a prerequisite for specific calculations in mathematical modeling of processes investigated in the study area. Processing of real world data requires the use of GIS and geoinformatic modeling approaches.

For each modeled area is always created its own model mesh or set of model meshes with different parameters. In order to address the construction of model meshes was explored methods to create a file of model geometry based on data stored in the GIS and, consequently file of model mesh, which is filled by all the necessary data and will be used for calculations. To create a model mesh and fill it with data are used real data stored in the GIS, which serves as the basis for modeling the area of interest. The model mesh must always reflect the purpose and desired characteristics of the area and at every moment during creation of model mesh must be ensured the continuity with real data in GIS. Therefore, the methodology for data preprocessing, data storing in GIS, data processing in GIS including generalization, and for transformation to geometric model and model mesh is created. Another task is to fulfill the model mesh by data from GIS.

Keywords: geometric model, model mesh, GIS, GMSH, GEO format, MSH format

INTRODUCTION

In this paper willl be explained transformation procedures of particular part of the landscape sphere (area of interest) into geometric model and model mesh, which are used in modeling of transport and flow in the rock environment, simulating the process of disseminating the risk of contamination, etc.

Area of interest is described by the geographic data. For example maps in analogue or digital form, data of watercourses, watersheds, divorces, surface relief, but also socio-economic activities that cause pollution and contamination of surface, underground geological data with rock structure, tectonic areas, physical properties of rocks, cracks in the rock properties, data describing wellsprings, wells, geological exploration (drilling), geological profiles, mine maps, hydrogeological characteristics of the territory, a number of textual and tabular data describing the area with attributes of selected objects and phenomena in the area.

Geoinformation technologies are used for processing of primary data describing the area of interest into the desired formats and geoinformatic models. For modelers – users of our geoinformatic models - a black box. From different data sources and requirements by which is final model defined, they obtain appropriate model. This model must be filled with data. Then it can be used for calculations in mathematic modeling. This is a specific set of models which are used for mathematical modeling and calculations by finite element method. Model is called model mesh. We assume models that are fully 3D, volumetric, so we work in conjunction with GIS software and software for solid modeling in which the model mesh is created.

Construction of the model mesh is not trivial, various processes and software are used. What exactly model mesh is and what is a methodology of its creation, will be explained below.

MODEL MESH AND ITS CREATION

Model mesh and geometric model of area

The model mesh is given by a finite number of two-dimensional and three-dimensional elements in 3D. These elements cover the area in accordance with established criteria and the spatial resolution.

Model mesh is model of the area in accordance with given purpose. The model of the area is the system model of the geographical area where the system elements and relationships are defined in order to carry out the analysis and calculations of data base. Conceptual model of the model mesh is created first. There are elements of the real world and their relationships defined. Both elements and relationships are essential according to the purpose of the model.

The logical model is implemented in a particular software and its file system and filled with data about a particular territory. It is appropriate to handle such models in a geographic information system (GIS) and then use GIS filled by data as the data basis for derived models creation - geometric models and model meshes.

Model mesh is essentially a model compiled from 2D and 3D elements in space. 2D elements are triangles and 3D tetrahedral elements. All surfaces and volumes in original GIS of modeled area, which is needed to be described for the mathematical model, are discretized and a finite number of triangles is created to fill the surface (eg rock interface cracks of vertical and horizontal progression, the surface relief, etc.) and a finite number of tetrahedra to fill volumes of model is created (volumes of rocks, volumes of cracks in a high-resolution, volumes of anthropogenic shapes, etc.). Exactly it is filling of areas and volumes of geometric model (will be described later). How these elements form the model is dependent on the resolution of the model and the requirements for the resulting number of elements in the model. This resolution is due to the length of the element edge and sets up the final mesh of geometric model.

The geometric model describes the entire modeled area from the view of geometry. This is a solid model, realistic 3D. It is composed by elements of geometric model: 0D – point, 1D - Line, 2D - plane, 3D - volume. 1D elements can be difficult - for example, splines, 2D element can also be ruled surfaces, space balls, etc. Then they have a special definition in the source code of the geometric model. The closest to this model is wireframe body, which requires CAD access to model creation (see fig. 1, 2). In GIS SW (ArcGIS, GRASS GIS) this volumetric vector model can not be completely created. Geometric models created on the base of real-world data are usually complex.

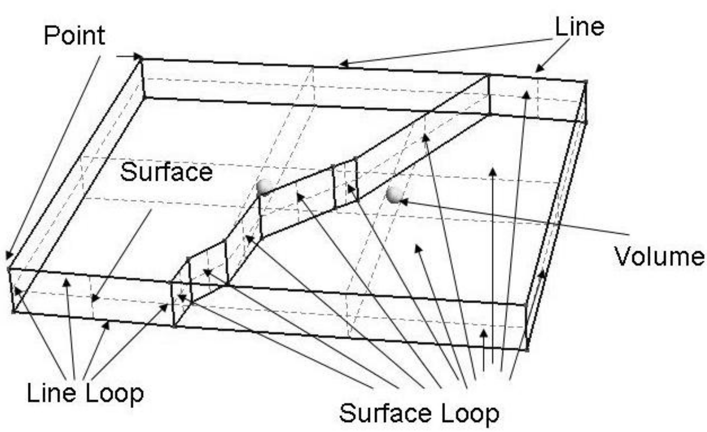

Fig. 1 Elements of geometric model

For example a block of broken rock with fissures with both vertical and horizontal direction. These fissures divide a single block of rock in many volumes. Geometry of area is affected also by many other features and phenomena - configuration of the terrain, rivers and their effect on the circulation of water, the course of the watershed, the water table and many others. Which geoobjects will be introduced into geometric model depends on purpose of the model, depends on desired resolution and accuracy of the model. The geometric model addresses not only the decomposition into sub-volumes and surfaces in space, but also defines sets of volumes and areas according to physical properties. Then one physical volume is formed by set of all volumes with particular property, which is essential in particular physical group for the subsequent model calculations. Likewise, the areas or lines or points in the model can be a part of physical group of appropriate dimension.

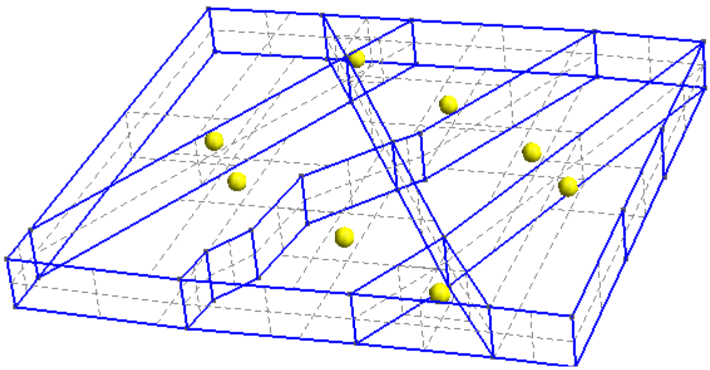

Fig. 2. Geometric model

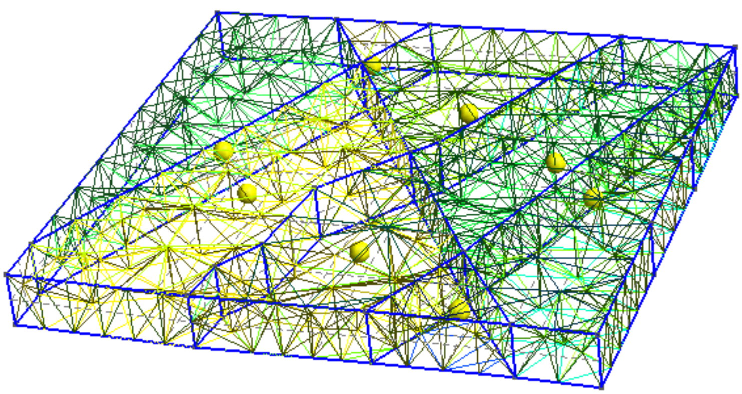

Fig. 3. Model mesh

In this paper is handled only the issue of the construction of geometric models and model meshes, solutions will be demonstrated on the model data from different areas. Creation of geoinformatic system as data base for construction of model meshes is sufficiently described for example in.

Model mesh construction

Construction of the model mesh (fig. 3) is in several successive steps. Asume that geographic information system of modelled locality is created. Next step is to determine the requirements for model mesh. Creating a conceptual model of the mesh. Conceptual model of mesh is a description future mesh in terms of size in horizontal and vertical directions, the extent of area to be modeled, the boundaries of the model - which type of elements will define the boundary, the determination of the exact boundary shape, what will be the mesh density, constant or variable length of element edge and the resulting number of mesh elements. Selected geographic features - rivers, lakes, conduct watershed, ridges, walleys. Geological elements - rock, rock boundaries, tectonic fault lines. Hydrogeological features and phenomena - springs, wells, cracks, and their permeability and groundwater level.

These all are things that affect geometry and water flow and transport in rock environment and will be included in geometric model. Their attributes will be involved. It is necessary to define context and relationships of individual phenomenon included in the geometric model and model mesh. Parameters of the future model influence generalization - selection, simplification of shapes, aggregation of object classes and attribute generalization.

The next step is geoinformation system data preprocessing to the required format of the modeling tools used in consecutive processing. This step includes preparation of geometric model and data preprocessing in GIS. It also includes generalization methods of both geometric and database. In detail, the issue is described in Malá, B., Pacina, J., Capeková, Z.. The resulting geometric model can be geometrically simplified, but it must be topologically correct. They must be well maintained neighborhood, including the relative distance of the elements that interact or have a common influence on the course of flow and transport. Further attributes are prepared for future model mesh data fulfillment. Attributes are usually exported from GIS database in text format file and it is joined with source code of the model mesh to combine element with its properties.

Since the geometric model is built from the points (0D elements), in the data preprocessing is first created a definition point set. All the elements entering into geometric model are replaced by point sets (see fig. 4, 6), and each point carries information about its absolute location in the model, belonging to the element or phenomenon, information about neighboring points, belonging to line and area, volume, and then carries the attributes of all phenomena in which it occurs (eg point lies on the boundary model, which is also a water course, lies on the surface at certain altitude, belongs to a certain volume of rock that has given physical properties, at the crack with certain characteristics, etc.). On the basis of these points can element of higher dimension obtain relevant information (eg cracks in the geometry model, the volume of rock, etc.). Such a way new data model is created. The result of data preprocessing for construction geometric model are files with data about points with their properties, which are the basis for geometric model creation. Each file can be converted to the GEO format, which is a format for geometry described in GMSH software (see below).

For construction of a geometry model of model mesh we use software GMSH. GMSH is a 3D finite element generator of spatial meshes. This SW is also used for construction of geometric models. Purpose why this software was selected was given by requirements from mathematical modeling, which require the input mesh in the MSH format, which is being generated by GMSH. Geometry is created on the basis of pre-processed data. More about building of concrete geometries is described further in examples of model mesh ceration.

Generally, geometric model always begins with points that are then connected by lines (line segments), the surface is defined by border lines, the volume is defined by its surface - a set of surfaces that make it up. Furthermore, physical groups of surfaces and volumes are defined - by the same properties (eg cracks of the same bandwidth, equal volumes of rock).

Creation of the model mesh file is in the program GMSH based on geometric model. Areas and volumes of geometric model are filled with finite number of elements (see fig. 3). You can set the mesh density, ie, the length of edge of an element. The result is a MSH file format containing a description of all nodes of the mesh and description of all elements and their types with codes of points on element.

Last step is to create files of physical and material properties and files of initial conditions for simulation. It is done on the basis of physical groups defined in the model geometry. To these files can be attached files contains the attributes of elements, which are created in GIS from the stored attribute data (rock type, geological structure, areas of the same hydraulic conductivity).

GEOINFORMATIC MODELING OF GEOMETRIC MODELS

Original geoinformatic system

Creating of geoinformatic system is an important thing (meaning mainly conceptual model of data base, which specifies the individual elements of real world and their relations in accordance with the fundamental purpose of the model created). Such geoinformation system allows multiple use for derivation of various geometric models of the area, easy data update and, ultimately, feedback for creating a model meshes - their geometry and initial conditions, which, despite on the specifics of their construction must remain in line with reality.

More about the creation and processing of GIS data layers in Maryška, J., Malá, B. Consequently, it is necessary to define which objects, phenomena, layers will be treated as the basis of geometry, then determine their range and resolution based on the requirements for future model geometry of the mesh. This is a task of creation of a conceptual model for the model mesh. On this basis, data in GIS are preprocessed for the geometric model.

Creation of model geometry – specific types of problems

Creation of a geometrical model is not trivial. It consists of different steps, depending on the character of the area and available data. Way of creating geometric model depending on requirements to geometric model and the model mesh. Furthermore, we explore different ways of preprocessing data and creation of various types of geometric models.

Preprocessing of data in GIS and creation of volumetric geometry in GMSH

All elements (meaned geographical, hydrological and geological objects) entering the geometry or affecting the geometry of the model are converted to a point sets (fig. 4, 5), every point has coordinates given in S-JTSK (czech national geodetic coordinate system). Individual objects of real world (ie original geoinformatic system) that enter the mesh model geometry, are initially described by lines and subsequently represented by point sets. Spatial objects have their boundary line, so they workare processed the same way. When creating a set of points generalization starts with selection and simplification. Line can be simplified by generalization algorithm and then the simplified line replaced with a set of points. Or the opposite approach, where the point set is reduced. The resulting set of points represents an appropriate shape and size of the object in the original model in the desired degree of resolution. Simplification is necessary because of the quantity of processed data and also in terms of purpose and resolution of model mesh. The model mesh is not important the exact shape (eg lines, which can be very complicated in their course), but maintaining above topological adjacency relations, and including, maintaining the distance between the individual elements.

At this stage, the points are exported from GIS to CSV or is appropriately adapted attribute table of points and is used DBF format. As follows files are converted to the GEO format for GMSH, it contains information about points and their position in absolute coordinates x, y, z. File describing the points in GEO format is loaded into GMSH. Next geometric model is edited in GMSH. To ensure good orientation in the GEO file during editing source code of geometry, it is essential to choose the numbering of points, lines, areas and volumes according to a certain order.

The geometry consists of a set of points, lines, surfaces and volumes. First, they are always defined points (imported points preprocessed in GIS), then lines are created by connection of points, on the basis of lines are defined surfaces and volumes ared defined on the basis of surfaces.

This process (the creation of geometry at the basis of point GIS layers) is appropriate in two cases. For small geometric models with a simple structure (Fig. 3) where the direct editing geometry in GMSH is fast. The second case is a complex geometry (fig. 5), which, however, consists of a relatively small number of elements of geometric model. In the second case it can be very difficult have algorithm for automated solutions. Such a solution can be partially automated. Then is created model mesh atomatically on the vase of geometric model in GMSH.

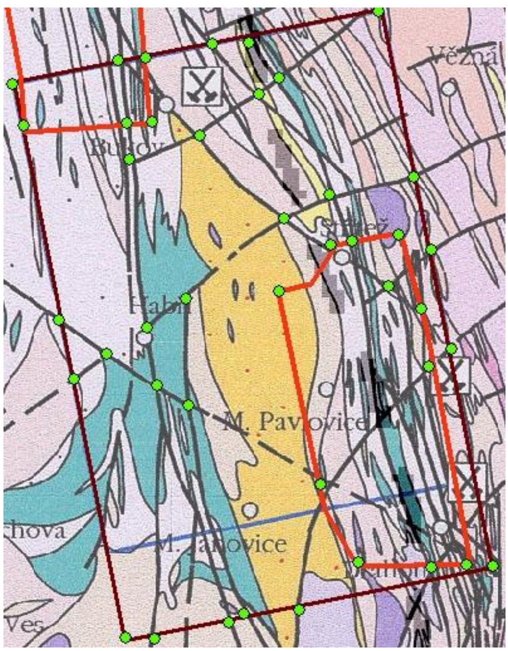

Fig. 4. Creation of part of point set in GIS – example of complex geometry

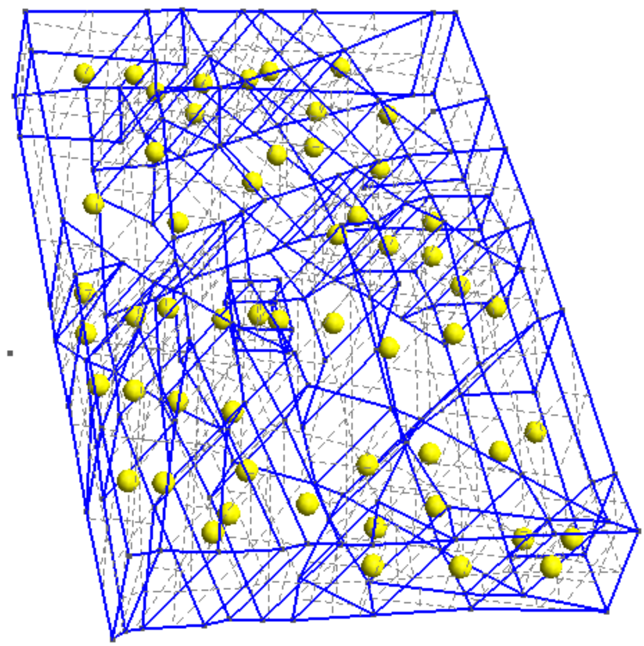

Fig. 5. Geometric model – example of geometry of locality from fig. 5

Creation of surface mesh in GIS

If working with volumes are not required, and demand is for surface model network (ie the surface in space), we use GIS tools. Preprocessing of data to generate the surface geometry in GIS means creation of a set of points representing the elements of geometry. For this purpose the line elements was replaced by points (in accordance to model resolution). See Fig. 6.

Areas between lines in model are filled with regular points (see Fig. 6, 7). Geometry is based on the point layer, which consists of a point field defining characteristics of modelled area. Each point has coordinates x, y.

Next is used a digital elevation model. On its basis is assigned altitude as the coordinates of Z to every point in point layer which was created. Point layer has attribute table, where they are recorded in addition to coordinates X, Y, Z, other characteristics - the belonging of point to the type of line (tectonics, rock interfaces, boundary), points inside the area carry information about the area in which belongs (thereby physical characteristics, such as type of rock). Attribute data of point are used to create a file of physicas properties of model mesh for subsequent mathematical model.

In the point layer is then formed triangulation (Delaunay) (Fig. 7) and the triangles are stored as lines and surfaces. It is necessary to create topology - relationships between points from point layer, lines and surfaces from triangulation and results are recorded to the database tables.

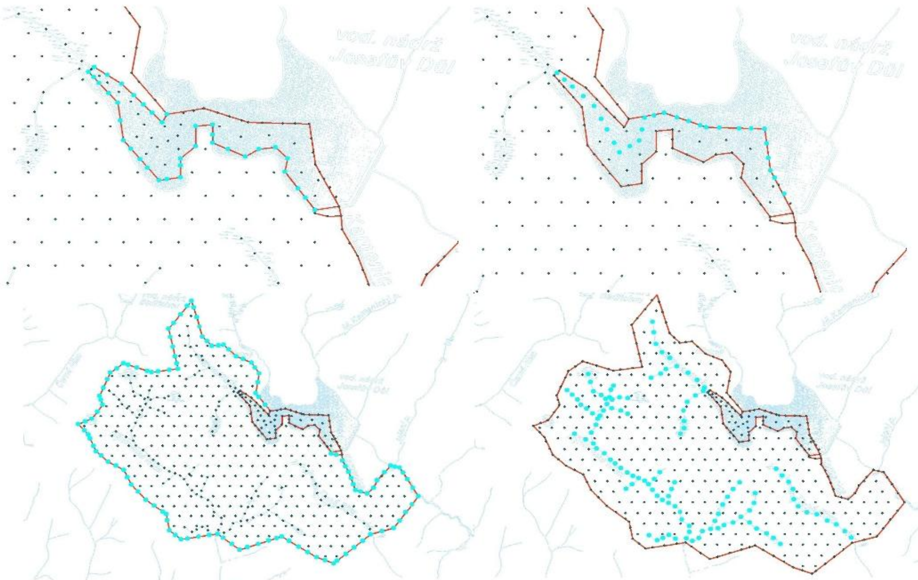

Fig. 6. Replacement a line by points and fill of resting area by regular point grid

Gradually, the information about lines is obtained (line IDs, IDs of extreme points). Then information about the area (triangular area ID, ID numbers of lines – triangle edges). Prepared table can be transformed to the format of GEO and loaded into the GMSH. Here, triangular geometry is meshed. Or directly can be created a format MSH (a mesh), where triangular elements in GIS were created diectly as elements of the model mesh. Elements (triangles) are easy assigned to the GIS features (eg. information about the type of rock, of wells, etc. associated to surface element - Fig 8).

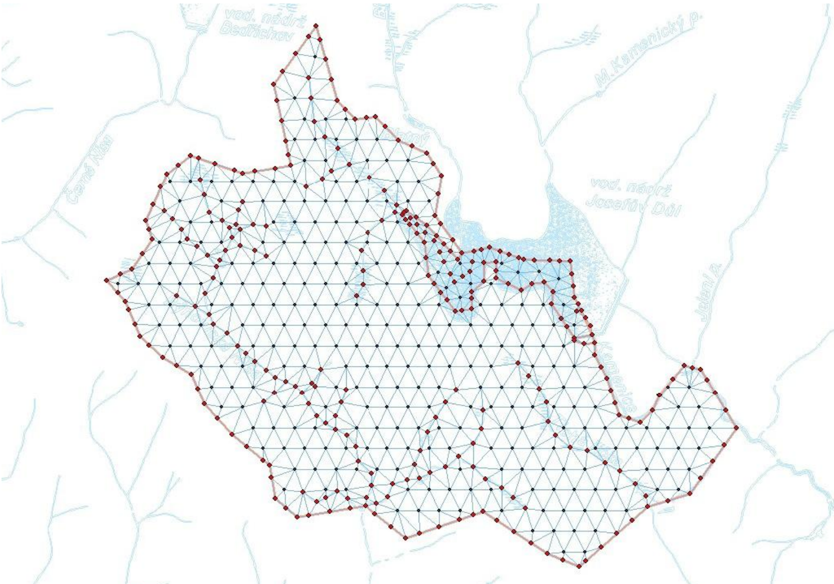

Fig. 7. Triangulation in processed point layer

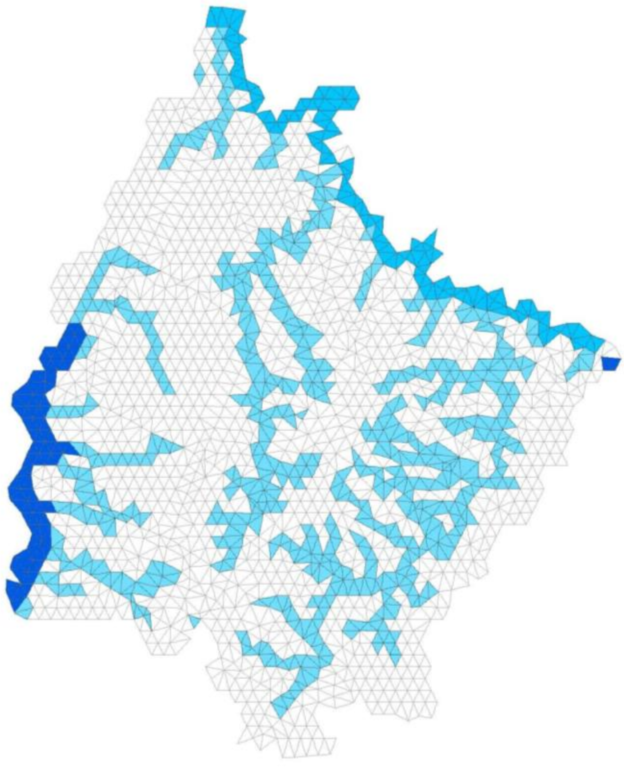

Fig. 8. Properties of surface mesh elements – elements with occurrence of water are selected

Preprocessing of data in GIS for automatic creation of geometric model

In this variant of modeling preprocessing procedure is the same as in the previous case. Triangular grid is created in GIS and relations between points, lines, areas in triangular network are described. The basis for future geometric model is formed. As follows data from GIS to dbf of desired structure are transformed. It is created a table of points (point ID, x, y, z) and table of triangular areas (area ID, ID point1, point2 ID, point3 ID). Subsequently, the dbf files are input into the application for automated processing of model geometry. For the construction of geometry, where the necessary information for the entire volume of the geometric model are contained in the surface layer, has been developed applications Convert2geo.

AUTOMATIZATION IN CREATION OF MODEL GEOMETRY

Because construction of geometric model from pre-processed data is in many cases only a matter of routine, we searched for a way to automate the construction of the geometry for such models. First, we conducted a search of available software products that are potentially capable of creating a fully automated spatial mesh. Standard GIS tools allow only so-called 2.5D interpolation (two and a half dimensional). This type of interpolation is specific in the resulting interpolated surface, which is described by a 2D matrix (grid), or possibly by using a TIN (Triangulated Irregular Network). These data types do not save the interpolated values of the two values of the same phenomena (eg height Z) to one point with coordinates [x, y]. Selected software products are fully able to interpolate the data in 3D - the ability to model overhangs, cumulus geological layers - the one where the value of the coordinates [x, y] associated with two (or more) values of Z. From the available resources was chosen three commercial products and one software distributed under the GNU Open-licensing: EVS-PRO – C-TECH company, RockWorks 2006 – RockWare company, VOXLER – Golden Software company, GRASS 6.3 – OPEN-GNU licensing.

The test results both commercial and non-commercial software products for creating a fully spatial data shows that none of these programs is able automatically create a triangulated network, which fulfill our requirements to model mesh. We proceeded to design and implement an algorithm which is capable from entry points representing geographic and geologic phenomena (as described above) to generate a mesh format for GMSH program.

The application is based on generalization of the surface geometry into space. The surface geometry of triangles means the triangular prisms in space. Thanks triangles generated in the point layer (point layer formation described in chapter Creation of surface mesh in GIS) we can describe the surface of terrain, the course of an interface of rocks, tectonic vertical lines etc. (as is reflected in the geological map). By creating triangular prisms (see fig. 10) we are able to describe the volumes, the vertical surfaces and another surface which is approximated by the triangles forming the bottom base of triangular prisms. If such prisms are used in multiple layers on each other, we are also able to describe the horizontal surfaces (cracks with horizontal direction, groundwater level or interface of horizontally laid geological layers). Each triangular prism is defined by points, points define a line, lines define the area: the two triangles, three rectangles (surface of prizm), areas define volumes (prisms).

To implement the algorithm we choose two solutions independent on platform. There were created two applications - one that uses XML database options and XSL programming and JAVA application CONVERT2GEO described in Tomčík, D., Malá, B.. The data entry for application is generated by preprocessing as described in chapter Preprocessing of data in GIS for automatic creation of geometric model.

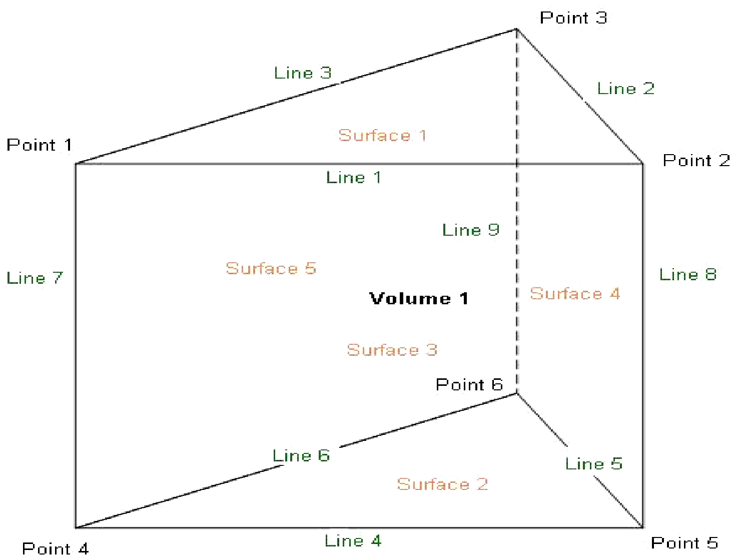

Fig. 9. Definition of triangular prism in GEO format

Data input to application issues from triangular network (fig. 11):points on each layer - contains the coordinates X, Y, Z1 and X, Y, Z 2, ..., X, Y, Zn (in the application Convert2Geo the point layers of the model levels are specified in the top bottom order) triangles - the area contains triangular identifier and references to 3 points IDs-triangle vertices.

The data triangulated in GIS are next processed in GIS to gain required data format as an input to application. Data are stored in DBF tables and are read through the user interface (see Fig. 13). Algorithm for generatig a model mesh using triangular prisms assumes corresponding nodes (peaks) in all layers have identical X and Y.

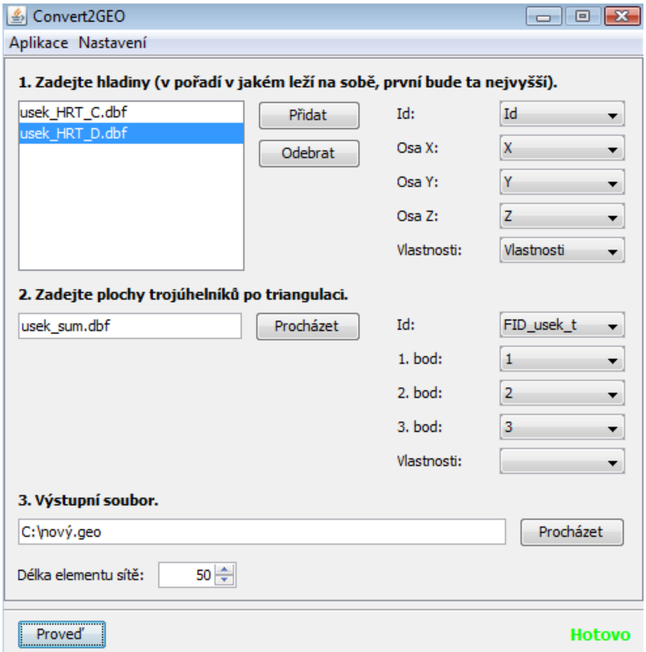

Fig. 10. Application Convert2Geo – input data dialog window

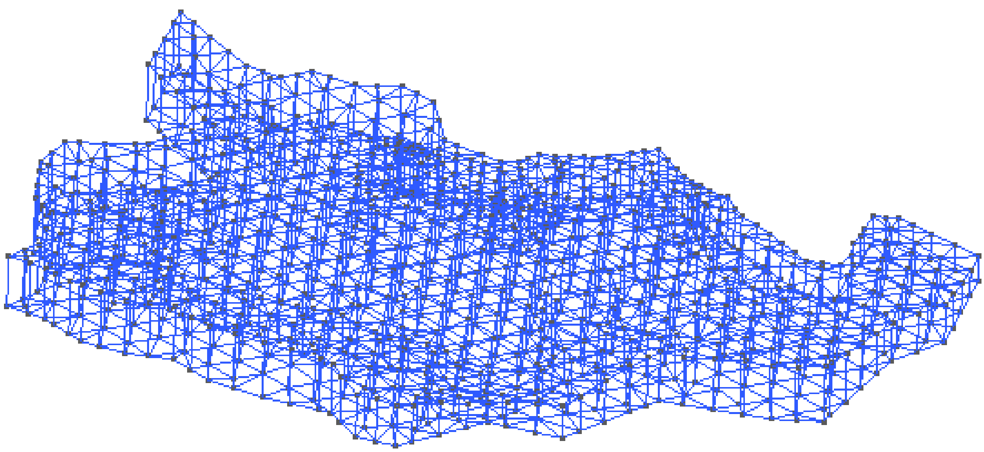

Fig. 11. Triangular prisms model geometry

This procedure allows to model complex area with number of lines projected into the surface layer in GIS. The disadvantage is that the size of triangular prisms in the model (as well as the length of triangle edge in surface geometry) must be consistent with the size of the mesh element. Model mesh is generated on the base of model geometry. The problem is for example the length of the edge of the prism 500 m and effort to generate mesh model with an element edge length of 400 m. Therefore, in data is taken into account the desired density of the model mesh.

This application now allows to create a model containing the layer between two surfaces which is filled with a single volume (Fig. 12). Another type of model geometry contains only complex boundary and single volume (Fig. 13).

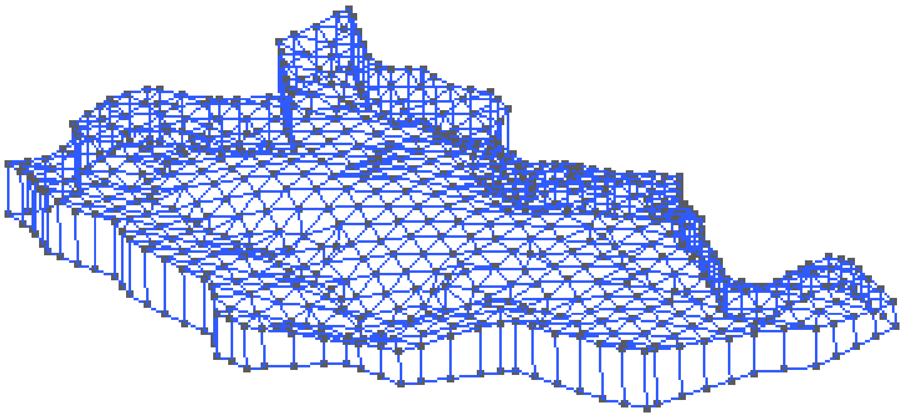

Fig. 12. Geometric model with surfaces and one volume

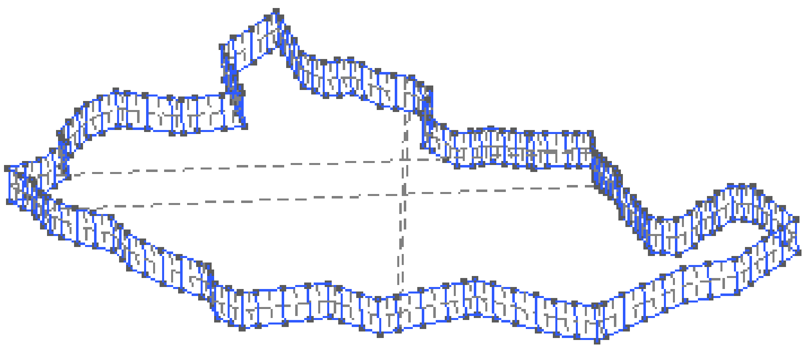

Fig. 13. Geometric model with complex boundary and one volume.

CONCLUSION

Creating of geometric models based on real data is a geoinformatic task which requires full 3D modeling and use both GIS and also other programming tools, which enable to create a geometric volume model based on data pre-processed in GIS.

Each modeled area has a different structure in shapes, but over time we created a methodology of preprocessing various data describing the various types of geographical and geological phenomena. We have also methodology of processing the geometric model and model mesh and its fulfill with data processed in GIS.

There are geometric models that we can create automatically, where preprocessed data in the required format are available. In this area we are working on automating the data preprocessing and automating control algorithms for each stage of preprocessing. Other types of models are not created automatically, for example, currently we have no automatic solution for modeling the vertical wavy surface and sloping surfaces. Automated processing allowes create model geometry in real time, quickly check the overall configuration of the mesh and assess its quality in terms of modeling requirements. Also is the possibility to quickly create a new (corrected) model geometry and mesh according to the requirements of network modeling. Automation of mesh construction also allows creation of multiple meshes based on different variants of input data. For an extensive models automated solutions enables introduce corrections in the input data and then quickly generate a new model.

A methodology and implemented algorithms were tested on several model areas, all designed model geometry and model meshes were used in the practice of mathematical modeling.

ACKNOWLEDGMENT

This article was realized under the state subsidy of the Czech Republic within the research and development project "Advanced Remediation Technologies and Processes Center" 1M0554 - Programme of Reserch Centers supported by Ministry of Education.

REFERENCES

Malá, B., Pacina, J., Capeková, Z. (2009). Účelově odvozované modely v procesu předzpracování dat pro tvorbu geometrie modelových sítí. In: SiMoNA 2009 — Simulace modelování a nejrůznější aplikace Seminář výzkumného centra ARTEC. TUL Liberec.

Tomčík, D., Malá, B. (2010) Automation in construction of 3D models and meshes. In: Petr Šaloun (ed.), DATAKON 2010, Mikulov, 16-19. 10. 2010, University of Ostrava, pp. 153 to 157.

Maryška, J., Malá, B. (2008) Creation of model mesh and its fill with data from GIS SURAO and definition of initial conditions for variations of migration. Partial final report Research of the field of remote interaction of underground storage of spent nuclear fuel and high-level waste.Technical Univerzity of Liberec, 52 pp.

Maryška, J., Královcová, J., Hokr, M., Šembera, J. (2010) Modelling of Transport Processes in Rock Environment. Technical Unversity of Liberec. 303 pp.

GMSH. http://geuz.org/gmsh/

SELECTION OF APPROPRIATE INTERPOLATION METHODS FOR CREATION DEMS OF VARIOUS TYPES OF RELIEF BY COMPLEX APPROACH TO ASSESSMENT OF DEMS

SVOBODOVA Jana

Department of Geoinformatics, Faculty of Science, Palacký University in Olomouc, tr. Svobody 26, 771 46, Olomouc,
svobodova-j@centrum.cz

Abstract

The main aim of a research presented in this paper is selection of the most suitable interpolation method and its parameter settings for creation of digital elevation models (DEMs) of base types of relief in the Czech Republic (flatlands, hilly areas, uplands and highlands) from the DMÚ 25 database. The suitability of interpolation methods and their settings was explored using the assessment of metric accuracy of resulting DEMs, i.e. difference between estimated data and reference data. The non-spatial indicators (root mean square error – RMSE, total absolute error – AE and hammock index – H) were used to assess the quality of DEM in terms of metric accuracy.

However, complex approach to the assessment of DEMs must contain also evaluation of spatial distribution of errors. For these reason, the spatial cluster analysis LISA has been used. Its sense consists in a possibility to identify the spatial clusters of statistically significant high error values. The next aim of the research was thus using of spatial assessment of metric accuracy of DEMs to verify the results of non-spatial assessment and also to find the differences in spatial behaviour (distribution) of errors in DEMs rated using weighted order as high-quality and low-quality DEMs.

It is evident from the results that if input elevation data are dense enough, non-spatial characteristics of metric accuracy can be viewed as decisive for assessing quality of DEMs and differentiation the high-quality DEMs form low-quality DEMs. The results from local cluster analysis LISA can be than used for verification of non-spatial assessment. However, when using spatial analysis LISA for assessment of DEM quality it is necessary to consider also selected non-spatial indicators in order to avoid misinterpretation.

Keywords: digital elevation models, errors, non-spatial assessment, spatial assessment

INTRODUCTION

A relief is a key factor in many environmental processes. It has a significant impact on climate variables like temperature and precipitation. It also influences a degree and spatial extent of weathering, erosion or accumulation on the Earth's surface etc. (Moore et al. 1991, Wilson and Gallangt 2000, Arrell 2005). Within a GIS environment, digital elevation models represent the real image of a relief. The most quality DEM must be used to getbest quality of the results from environmental analysis and such DEM it is possible to get only using of suitable interpolation method and setting of its parameters. The main theme of this paper is selection of suitable interpolation methods for creation the DEMs of different types of relief.

The suitability of selected interpolation method or the quality of resulting DEM is commonly described in terms of a metric accuracy of altitude values i.e. a difference between modelled values and real (referential) values. As Arrell (2007) puts it, the applications using DEMs predominantly do not require an overall metric accuracy of altitude, but they rather need accurate illustration of a surface form. In practice, however, there are no limits or definitions which enable to differentiate between DEMs of high or low shape accuracy. A shape fidelity assessment is mostly based only on a visualization of a DEM and its derived morphometric variables. From this reason, the assessment of DEMs will be further focused solely on the assessment of metric accuracy, which can be quantified more easily.

Common methods used for assessment of a metric accuracy of DEMs (like RMSE) are only global non-spatial measures. Their unquestionable advantages are their easy calculation and interpretation. However, as to environmental applications, the knowledge of spatial error variability is very important. Many authors (Desmet 1997, Erdogan 2009, Fischer 1998, Gao 1997, Hofierka et al. 2007, Hunter and Goodchild 1997, Svobodová 2008, Kyriakidis et al. 1999, Wise 2000) claim that the extent of errors in a DMR depends on a character of a terrain and is spatially variable. In the paper, the process of selection the most suitable methods for creation DEMs of various types of a relief is state and also the process of assessment of spatial distribution of errors.

SETUP OF MODEL DEMS

In the research were used 21 model areas (4×4 km large) which with regard to their relative roughness height represent four major types of a relief in the Czech Republic i.e. flatlands, hilly areas, uplands and highlands. Three model areas were selected for each type (respectively subtype) of a relief. The outline of selected areas can be seen in table 1.

Table 1. An outline of selected model areas

Type of relief	Relative roughness height [m]	Model areas	
		Czech massif	**West Carpathians**
flatland	0-30	Sadska flatland	Zerotinska flatland Cervenecka flatland
flat hilly area	30-75	Nechanicka table Ostromerska table	Orlovska table
rugged hilly area	75-150	Podjestedska hilly area Radomyslska hilly area	Vlcnovska hilly area
flat upland	150-220	Studenska upland	Divacka upland Uhricka upland
rugged upland	225-300	Bozkovska upland Kozlovska upland	Hostalkovska upland
flat highland	300-450	Ustecke highland	Rusavska highland (RH) Rusavska highland (RU)
rugged highland	450-600	Hornoopavska highland Cernohorska saddlebow Boubinsky ridge	---

A layer of contours from the DMÚ 25 database has been applied as input data in a creation of DEMs in ArcGIS Desktop v. 9.x environment. Selected interpolation methods (see below) require points as an input data. Therefore, the contours with equidistance 5 m had to be translated into points. Resulting file have been divided into two parts, points used in the process of interpolation (85 %) and referential point for calculation of root mean square error and absolute error (15 %). Taking into account the use of geostatic method kriging as one of the main interpolation methods for the creation of DEMs, dependency (autocorrelation), normality of division, and stationarity of input data have been verified.

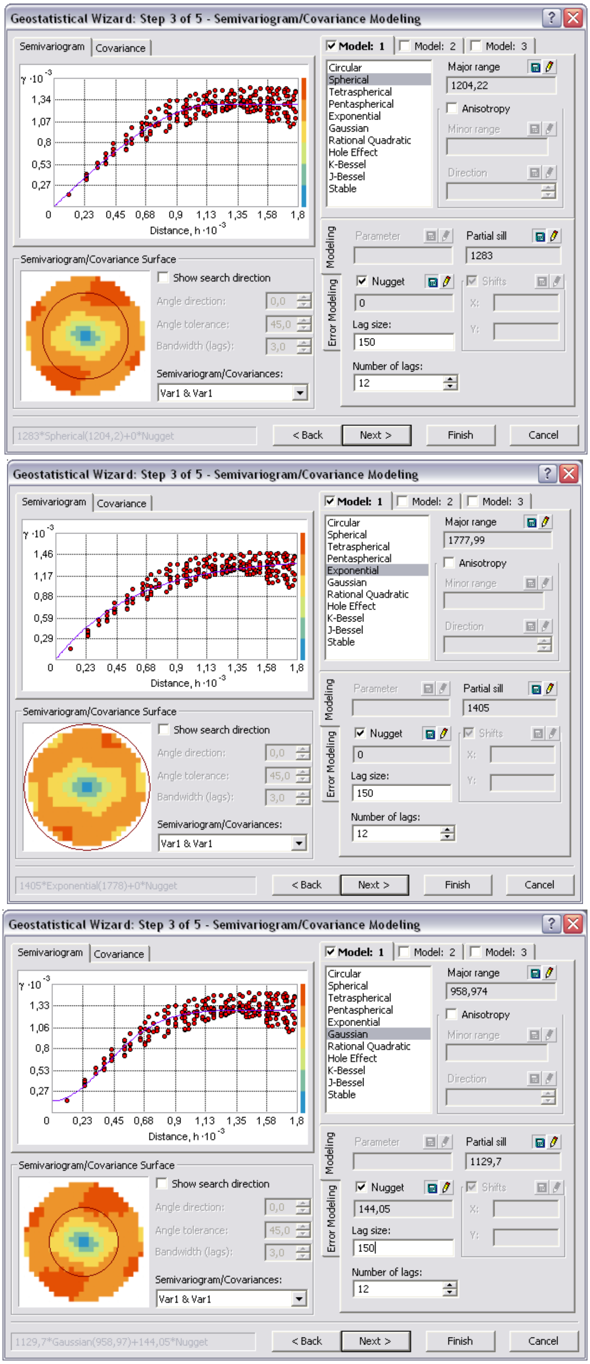

Fig. 1. Empirical semivariogram created in ArcGIS Desktop v. 9.x environment fitted by the curve of Spherical (A), Exponential (B) or Gaussian (C) theoretical semivariogram (the example of the Divacka upland)

To create DEMs, four interpolation methods have been selected: inverse distance weighting (IDW), regularized spline (RS), spline with tension (ST), and ordinary kriging (KG). These methods (or their modifications) can be found not only in ArcGIS Desktop v. 9.x software, but also in other easily accessible commercial (e.g. Idrisi, Surfer) and non-commercial software programs (e.g. GRASS GIS, QGIS). The main idea of choosing values of different parameters was to try to cover their basic (in reality applicable) spectrum. For all used methods, two most important parameters were set. Parameter *n*, expressing number of input points from the closest surroundings, was common for all the methods. Parameter *p* (power) was then applied in the inverse distance weighting method, weight parameter in spline methods, and theoretical semivariogram function in kriging (Fig. 1). The values of setting of different parameters are outlined in table 2. Kriging method includes also other parameters like range, sill and nugget effect witch are used to modify the curve of theoretical semivariogram. Values of these parameters are counted automatically in ArcGIS Desktop v. 9.x environment from the empirical semivariogram. When kriging method has been used they stayed default. The lag size has been set to 150 m and number of lags to 12. For all used interpolation methods the pixel size has been set to 10 m.

Table 2. An outline of setting of parameters for applied interpolation methods

interpolation method: parameter	**value**		
IDW: power	0,5	2,0	4,0
SR: weight	0,0	0,3	0,6
ST: weight	0,1	5,0	10,0
KG: theoretical semivariogram	spherical	exponential	gaussian
common parameter	**value**		
number of input points	10		20

The presented values of parameter power, weight parameter and theoretical semivariogram were always combined with two values of input point numbers. This setting was applied consistently in all the tested areas. All in all, 24 DEMs for each area have been created, which means 504 DEMs in total (for all 21 areas). TIN supplemented by ridge lines, valley lines and peaks were used as a reference DMR for assessment of spatial distribution of errors. It was later transformed into a grid.

NON-SPATIAL AND SPATIAL METHODS APPLIED IN ASSESSMENT OF DEM ACCURACY

Digital models of relief have been evaluated by using both the global non-spatial and local spatial methods. To draw a comparison between individual DEMs with regard to non-spatial characteristics, a weighted order based on a calculation of root mean square error, total absolute error and hammock index have been used. The root mean square error (RMSE) expresses an extent to which an interpolated value differs from a real value. A higher value corresponds to a greater difference between two datasets (Wood 1996). The total absolute error (AE) shows a real sum of all deviations from reference data in both positive and negative directions (Svobodová et al. 2009). The hammock index (H) examines the regularity of location of interpolated values between the known values, as well as excessive incidence of pixels whose altitude tally with original data values (Wood 1996). In compliance with each of the above mentioned characteristics, the order of DEMs was created. Subsequently, it was multiplied by a selected weight of individual characteristics: RMSE – 2/5, AE – 2/5, H – 1/5. The values of weights were chosen experimentally based on the author's knowledge of predicative values of individual characteristics. Values of weights can be modified by uřsing different characteristics. The total weighted order of DEMs was determined by ý,summing the individual weighted orders (see table 3). It allows for arranging DEMs qualitatively and distinguishing between DEMs of higher and lower quality.

Table 3. Calculation of weighted order - the example of the Divacka upland

Interpo-lation method	Name of DEM	RMSE [m]	Order of RMSE	AE [m]	Order of AE	H	Order of H	Weighted order	Total order
kriging	kg_sf_20	0,96	1	1288,14	1	0,25	10	2,8	1
kriging	kg_ex_20	0,97	2	1290,54	2	0,25	8	3,2	2
kriging	kg_sf_10	0,97	3	1291,04	3	0,25	7	3,8	3
…	…	…	…	…	…	…	…	…	…
IDW	iw_2_20	2,83	20	3932,76	20	0,50	21	20,2	22
kriging	kg_ga_20	4,08	24	5891,65	24	0,25	6	20,4	23
IDW	iw_0-5_10	2,91	21	4072,29	21	0,26	18	20,4	24

To assess DEMs spatially, a local cluster analysis LISA which enables to observe a spatial distribution of errors was applied. In contrast to a mere representation of size of errors in form of an accuracy surface (gained by a mere difference between estimated data and reference data), which does not allow for exact determination of boundaries between high and low error values, a local cluster analysis determines statistically significant high and low error values (or outlying values) accurately enough (Fig. 2). The accurate determination can be further used for a research into relationships between occurrence of high error values (or outlying values) in DEMs and values of morphometric parameters derived from these DEMs. For the assessment of DEMs, two DEMs of each area (the highest-quality one and the lowest-quality one selected according to a weighted order) were taken. The two very different DEMs were used in attempt to explore a concordance or difference of spatial location of errors in both high-quality and low-quality DEMs.

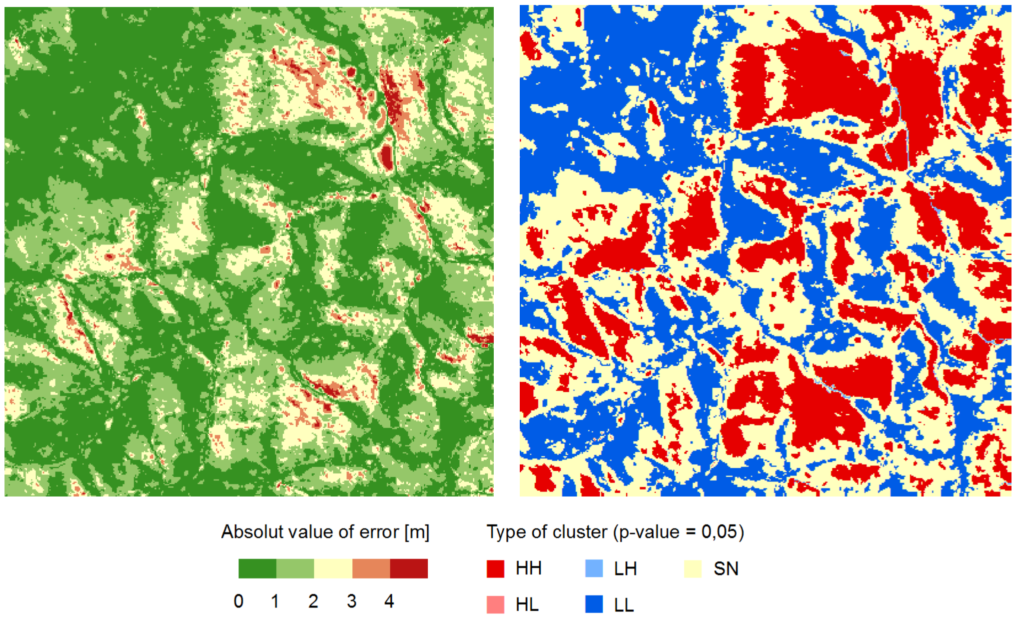

Fig. 2. Comparison of common accuracy surface with absolute error values (left) and localization of statistically significant clusters of high (HH) or low (LL) values gained by LISA (right) - the example of the Rusavská highland

COMPLEX ASSESSMENT OF DEM ACCURACY OF MODEL AREAS

Suitability of Interpolation Methods for Creation of High-quality DEMs according to Non-Spatial Indicators of Metric Accuracy

The weighted order (see chapter Non-spatial and Spatial Methods Applied in Assessment of DEM Accuracy) was used as a basis for the assessment of quality of DEMs according to non-spatial characteristics. Table 4 shows the interpolation methods with concrete setting of their parameters which were evaluated as the best ones for gaining high-quality DEMs of individual relief types. The selection was carried out with regard to their occurrence in the first three places of a weighted order within a given type of a relief. The main condition of the selection was that the same setting of a decisive parameter was applied at least twice in one interpolation method. A parameter of weight was decisive in case of spline methods. As to inverse distance method, a parameter power was taken into account. As for ordinary kriging method, a parameter representing an applied model of theoretical semivariogram was considered. A common parameter of a number of input points (n) was not regarded significant when testing values of ten and twenty points were in use. Concrete vales of the decisive parameters must be viewed as approximate since they were chosen experimentally and thus do not cover the extent of the decisive parameter values elaborately enough. Their significance lays in showing a certain area of values (area of higher and lower values from an interval of real values) from which it is advisable to choose a concrete setting of interpolation method for a given type of a relief.

Table 4 shows that ordinary kriging is the most suitable interpolation method for rough terrains like highlands, uplands (both flat and rugged) on condition that the spherical or exponential model of theoretical semivariogram are used. The suitability of these two types of mathematical functions for modelling a surface by ordinary kriging was expected and later was proved to be successful. The above mentioned theoretical models intensify the influence of the closest points to the place of estimated value and at the same time, a calculation does not cover the values of more distant input points. Thus final surfaces are not too flattened which is by rough surfaces undesirable.

In the case of highlands and uplands, interpolation method spline with tension with low value of weight parameter (about 0,1) can be used as well. The low value of weight parameter produces a high tension of a surface. Consequently, interpolated values move more within the range of input data and they do not tend to create local extremes. Output values of RMSE and AE are thus low for these DEMs.

As for flatter surfaces like hilly areas and flatlands the choice of a suitable interpolation method differs significantly. Especially for modelling of flat hilly areas and flatlands, regularized spline with weight values around 0,3 (or 0,6) has been considered the most appropriate interpolation method. Preference of weight values around 0,3 and than 0,6 signifies that these types of relief require the use of a method, which creates flattened surfaces. Flattening, however, cannot be too great even in the case of lowlands.

Speaking about flatlands, inverse distance weighting method with a high power parameter value appears to be one of the most convenient interpolation methods. It emphasises an influence of the closest points, which is useful mainly when input data are not dense enough. Due to a higher power parameter value, results are not distorted even if more distant points are included. Despite the above mentioned advantage, the use of this method is very questionable since the DEMs created by this interpolation method have been listed at the end of the weighted order covering all types of reliefs (including flatlands).

Selection of interpolation methods for rough hilly areas must be considered individually since this type of relief can be regarded a transition type between rough and flat types of relief (see table 4). Similarly to highlands and uplands, ordinary kriging (using exponential model of theoretical semivariogram) as well as spline with tension with a low weight value were successfully used. On the other hand, regularized spline that is used rather for flatter types of reliefs has been found to be suitable for this type of relief as well. In contrast to flat hilly areas and flatlands, the weight value is zero and therefore there is only a slight flattening.

Table 4. The most suitable methods for interpolation of DEMs of a given type of relief (listed according to frequency of occurrence in the first three places of a weighted order of a given type of relief, the choice was conditioned by the same setting of a decisive parameter at least twice in one interpolation method)

type of relief	interpolation method	value of parameter
rugged highland	KG	sf
	KG	ex
	ST	0,1
flat highland	KG	sf
	ST	0,1
	-	-
rugged upland	KG	ex
	KG	sf
	ST	0,1
flat upland	KG	sf
	KG	ex
	ST	0,1
rugged hilly area	KG	ex
	SR	0
	ST	0,1
flat hilly area	SR	0,3
	SR	0,6
	-	-
flatland	SR	0,3
	IW	4
	SR	0,6

Assessment of Spatial distribution of Errors in DEMs

The aim of spatial assessment of metric accuracy of DEMs was to verify the results of non-spatial assessment and also to find the differences in spatial behaviour (distribution) of errors in DEMs rated using weighted order as high-quality and low-quality DEMs. To assess the spatial metric accuracy of DEMs, the local cluster analysis LISA has been used. It came out during the evaluation of its results that when interpreting results it is desirable to focus not only on a spatial visualization of clusters of statistically significant high or low error values, but also on quantitative (or sometimes global) values of indicators like a range of values in a set of errors, a mean error value or maximal value in the clusters of high error values. On the basis of assessment of spatial extend of statistically significant clusters of errors together with using of above-mentioned quantitative indicators the rules for assessment of quality of DEM (at one area) in the terms of spatial accuracy were made and they are state in table 5.

Table 5. Evaluation of quality of DEMs according to a spatial assessment of LISA results supplemented with quantitative non-spatial indicators

Area of clusters at comparison of two DEMs by visual evaluation	Range of error values, mean value of errors, max. value in HH* clusters	Quality of DEM
bigger	higher	less-quality
	lower	more-quality
smaller	higher	less-quality
	lower	more-quality
comparable	higher	less-quality
	lower	more-quality
	comparable	comparable

*cluster of high values (high error values)

It is possible to demonstrate a need to supplement spatial assessment of quality of DEMs with quantitative non-spatial indicators by the results of local cluster analysis of highland relief (Rusavska highland RH). The results of LISA are in case of the high-quality DEM compact and aerially more extensive clusters of high or low errors. As for the low-quality DEM, the clusters are aerially less extensive and their types vary in areas more often (see Fig 3). Interpretation by visual evaluation only could lead us to the conclusion that there are more statistically significant errors in the DEM which is considered to be high-quality one than in the lower-quality DEM (Fig 4). Nonetheless, this way of differentiating between high-quality and low-quality DEM is not correct.

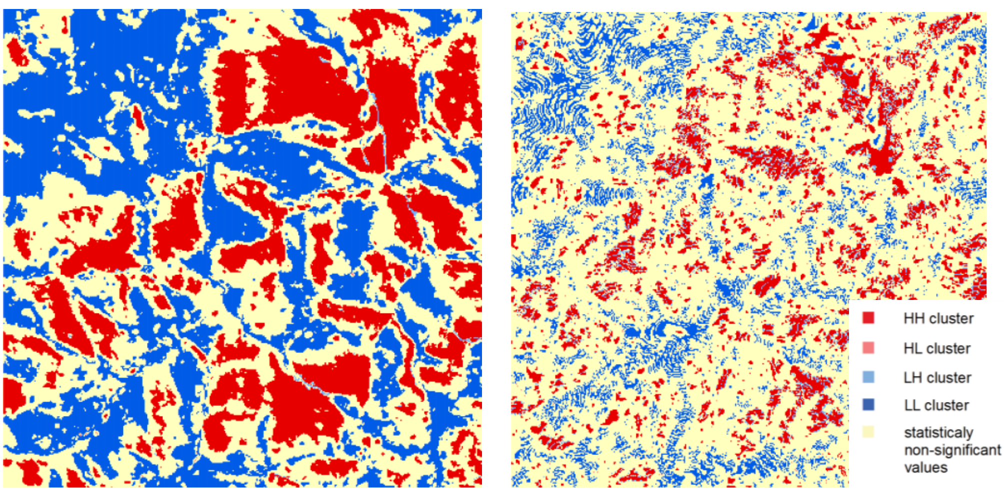

Fig. 3. Typical structure of clusters in results of LISA derived from the high-quality (left) and low-quality (right) DEMs of highlands (the example of the Rusavska highland)

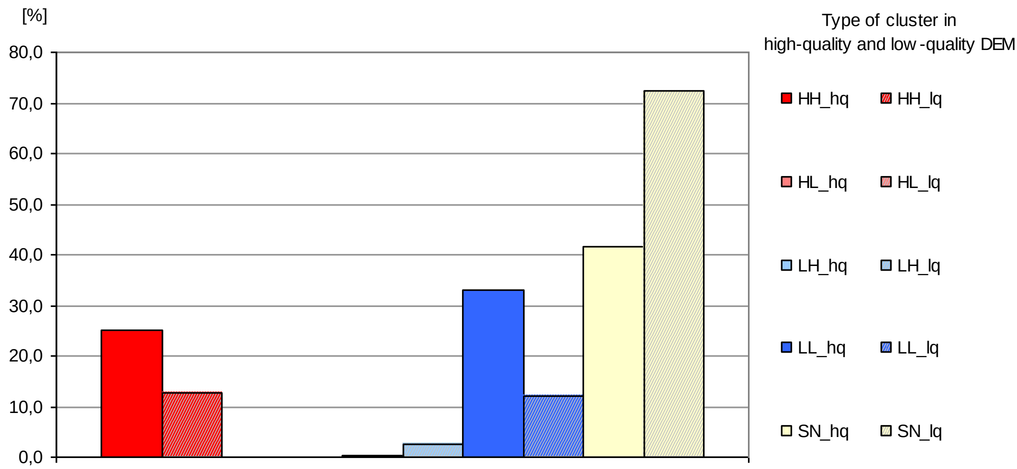

Fig. 4. Percentage rate of features that belong to the individual types of clusters with the use of high-quality and low-quality DEMs (the example of the Rusavska highland)

When considering the various extent of error values, different mean error values in files entering the local cluster analysis and different size of maximal value in the clusters of high error values (table 6), however, we find out that clusters of high errors in high-quality DEM which at first sight appear to be more extensive, in reality cover much lower values of errors than aerially smaller clusters of high errors derived from low-quality DEM. Moreover, taking into account the structure of clusters, it can be supposed that more compact shapes allow for a smoother change of error values, which can preserve shape fidelity of an actual relief. On the contrary, a frequent change of little clusters of low and high errors can bring about occurrence of local minims and maxims in DEM resulting in prevention of fluent outflow.

Table 6. Range and mean value of absolute error values gained by subtraction of high-quality (HQ) or low-quality (LQ) DEM from referential DMR and maximal value of error in clusters of statistically significant high error values (max. HH) - the example of the Rusavska highland

range [m]		**mean [m]**		**max. HH [m]**	
HQ	**LQ**	**HQ**	**LQ**	**HQ**	**LQ**
6,53	17,42	1,22	1,53	6,53	17,42

CONCLUSION

If input elevation data are dense enough, non-spatial characteristics can be viewed as decisive for assessing quality of DEMs. As for highlands, uplands as well as hilly areas, it is possible to tell apart high-quality DEMs from low-quality ones unequivocally by using a weighted order based on a calculation of RMSE, AE and H. As to flatlands, it is nearly impossible to create a high-quality DEM because of the lack of data (especially speaking about the use of contours). Therefore, the results of weighted order in flatlands seem to be considerably distorted.

For rough terrains like highlands and uplands ordinary kriging (with use spherical or exponential model of theoretical semivariogram) or spline with tension (with low value of weight parameter - about 0,1) are the most suitable interpolation methods according to non-spatial assessment of metric accuracy of DEMs. The default setting of parameters range, sill and nugget of kriging method had not negative influence on resulting interpolation. As for flatter surfaces like hilly areas and flatlands the regularized spline method (with weight values around 0,3 or 0,6) has been considered as the most appropriate interpolation method for creation of high-quality DEM. Selection of interpolation methods for rough hilly areas must be considered individually since this type of relief can be regarded a transition type between rough and flat types of relief. Similarly to highlands and uplands, ordinary kriging (using exponential model of theoretical semivariogram) as well as spline with tension (with a low weight value) is possible to use. On the other hand, regularized spline that is used rather for flatter types of relief has been found to be suitable for this type of relief as well. The selection of interpolation method is thus dependent on a segmentation of the model area.

Importance of local cluster analysis LISA lies especially in spatial determination of occurrence of statistically significant clusters of high error values, i.e. determination of places where the results from environmental analysis have to be more critically evaluated. When using spatial analysis LISA for assessment of DEM quality it is necessary to consider also selected non-spatial indicators in order to avoid misinterpretation. For this reason the base rules for assessment of metric accuracy of DEM using LISA were made. They are summarized in table 5.

ACKNOWLEDGMENTS

This work was supported by the student project of Integral Grant Agency of the Palacky University in Olomouc (project no. PrF_2010_14).

REFERENCES

Anděl, J. (1993) Statistické metody. 1. vyd. Praha, MATFYZPRESS, 246 p.

Arrell, K. (2005) Predicting glacier accumulation area distributions. Unpublished PhD thesis, Durham University.

Arrell, K., Wise, S., Wood, J., Donoghue, D. (2007) Spectral filtering as a method of visualising and removing striped artefacts in digital elevation data. In: Earth Surface Processes and Landforms. John Wiley and Sons, 33, pp. 943-961

Carlisle, B. H. (2005) Modelling the Spatial Distribution of DEM Error. In: Transaction in GIS, 9 (4), Blackwell Publishing Ltd., pp. 521-540

Desmet, P. J. J. (1997) Effects of interpolation errors on the analysis of DEMs. In: Earth surface processes and landforms, vol. 22, John Wiley & Sons Ltd., pp. 5693-580

Erdogan, S. (2009) A comparsion of interpolation methods for producing digital elevation models at the field scale. In: Earth surface processes and landforms, 34, John Wiley & Sons Ltd., pp. 366-376

Evans, I. S. (1972) General geomorphometry, derivatives of altitude, and descriptive statistics. In: Chorey, R. J. (ed.) Spatial Analysis in Geomorphology, Methuen, London. pp.17-90.

Fischer, P. (1998) Improved Modeling of Elevation Error with Geostatistics. GeoInformatica, 2, 3, pp. 215-233

Gao, J. (1997) Resolution and accuracy of terrain representation by grid DEMs at a micro-scale. International Journal of Geographical Information Science, 11, pp. 199–212

Hofierka, J., Cebecauer, T., Šúri, M. (2007) Optimisation of Interpolation Parameters Using a Cross-validation. In: Peckham R.J., Jordan G. (eds.) Digital Terrain Modelling, Development and Applications in a Policy Support Environment, Series: Lecture Notes in Geoinformation and Cartography, Springer, pp. 67-82, ISBN: 978-3-540-36730-7

Hunter, G. J., Goodchild, M. F. (1997) Modeling the uncertainty of slope and aspect estimates derived from spatial databases. Geographical Analysis, 29, pp. 35–49

Kyriakidis, P. C., Shortridge, A. M., Goodchild, M. F. (1999) Geostatistics for conflation and accuracy assessment of digital elevation models. International Journal of Geographical Information Science, 13, pp. 677–707

Moore, I. D., Grayson, R. B., Landson A. R. (1991) Digital Terrain Modelling: A Review of Hydrological, Geomorphological, and Biological Applications. Hydrological Processes, 5, pp. 3–30

Svobodová, J. (2008) Evaluation of digital elevation model accuracy. Geomorphologia Slovaca et Bohemica, ISSN: 1337-6799, pp. 76-81

Svobodová, J., Tuček, P. (2009) Creation of DEM by kriging method and evaluation of the results. Geomorphologia Slovaca et Bohemica, 9, 1

Wilson, J. P., Gallant, J. C. (eds.) (2000) Terrain Analysis: Principles and Applications, ISBN 0-471-32188-5, John Wiley & Sons, Inc.

Wise, S. (2000) Assessing the quality for hydrological applications of digital elevation models derived from contours. In: Hydrological processes, 14, pp. 1909-1929

Wood, J. D. (1996) The geomorphological characterisation of digital elevation models. [on-line], [cit. 2006-10-09]. Geography Department, University of Leicester, UK, Ph.D. thesis, 456 pp., dostupné z:
<http://www.geog.le.ac.uk/jwo/research/dem_char/thesis/>.

LANDFORM CLASSIFICATION AND ITS APPLICATION IN PREDICTIVE MAPPING OF SOIL AND FOREST UNITS

BARKA Ivan, VLADOVIC Jozef and MALIS František

Department of Ecology and Biodiversity of Forest Ecosystems, Forest Research Institute, National Forest Centre, T.G. Masaryka 22, 960 92, Zvolen, Slovakia
barka@nlcsk.org, vladovic@nlcsk.org, malis@nlcsk.org

Abstract

Georelief is one of the most important landscape components in conditions of Carpathian Mountains. The paper deals with an evaluation of georelief's influence on the other landscape and forest characteristics in selected model areas. Its aim is to evaluate the different algorithms of landform classification and their suitability for predictive mapping of soils and forests by analysis of spatial relationships between resulting landforms and selected maps of soil and forest characteristics.

Information on georelief is based on digital elevation models (DEM) and field research. The information on other landscape components was taken from existing resources (pedological map, forestry typological map) and also prepared by field research (detailed maps of forest stands).

Several algorithms of classification are tested: Hammond's (1964), Dikau's (1988 and 1991), MORAP's, estimation of topographic position index (Jenness 2006), classifications according to Iwahashi and Pike (2007) and Wood (1996), and delineation of genetically and dynamically well interpretable relief forms (Minár, Evans 2008). Algorithms were calibrated in areas with different types of terrain.

Preliminary results show that the evaluated methods can be helpful in the predictive mapping of soils and forest types. The correlations between classified landforms and soil types are lower than ones between georelief and forest types. The algorithms of landforms classification proposed by Wood and Jennes seem to be the most applicable methods from the pedological and forestry viewpoints. The Wood's approach uses a multi-scale approach by fitting a bivariate quadratic polynomial to a given window size using least squares. Jennes's classification is based on topographic position index values computed for the same location with two different scales. The future development of classification methods can bring new possibilities for predictive soil and forestry mapping.

Keywords: georelief, landform classification, predictive mapping, soil characteristics, forest stands

INTRODUCTION

Landform units have been used as basic georelief descriptors in soil and vegetation mapping for a relatively long time. Several papers document applicability of landform classification for predictive mapping of soil and vegetation properties, especially in steepland areas. Utilization of automated landform classification started in 1990s. There are new opportunities in this field, resulting from existence of relatively precise global and regional digital elevation models and methods of their automated segmentation. However, the terms and methods used in different fields of science vary in detail.

The paper deals with an evaluation of georelief's influence on other landscape and forest characteristics in selected testing regions. Its aim is to evaluate the algorithms of landform classification and their suitability for predictive mapping of soils and forests by analysis of spatial relationships between classified landforms and maps of soil and forest units. The landforms are classified at three scales – macrolandforms using global elevation products, landforms with regional digital elevation model (DEM) and local scale with attempt to define elementary landforms (or landform elements) using detailed local DEM.

MATERIALS AND METHODS

Digital elevation models (DEMs)

Several digital elevation models were used during research. The global products include SRTM DEM and ASTER GDEM (90 and 30 m resolution); at regional scale a DEM with resolution 10 m and a local DEM with 5 m resolution, both based on topographic maps.

The NASA Shuttle Radar Topographic Mission (SRTM) produced DEM with spatial resolution of 90 m. The version 4 downloaded from http://srtm.csi.cgiar.org was used. For the macrolandform classification also DEM with resolution of 200 m was prepared from SRTM DEM.

ASTER Global DEM (ASTER GDEM) is a product of METI and NASA. Tiles, covering the whole Slovakia's territory, were downloaded using WIST web application of NASA. The missing values and values for pixels with apparently wrong elevation (e.g. pixels with elevation below sea level) were interpolated from surrounding pixels, using regularized spline with tension.

Regional digital elevation model was prepared by Topographic Institute of Armed Forces of Slovak Republic, using contours from topographic maps 1:25 000. The raster spatial resolution is 10 m.

Local DEM was interpolated from contours of topographic maps 1:10 000 using spline with tension. The spatial resolution is 5 m. It covers area of 70 ha.

Methods of classification

Three methods of macrolandform classification were tested with global elevation products. Dikau et al. automated the manual identification of macrolandforms, originally proposed by Hammond. The method uses thresholds for slopes and flat plains determination (8% slope), 4 classes of slope, 6 classes of relative relief, 4 classes of profile type and a size of circular moving window. Original Hammond's subclasses of macrolandforms (96 possible) are grouped into 24 classes and 5 landform types. Similarly, the more simplified version of landform map, using a procedure suggested by Missouri Resource Assessment Partnership, was developed. All three methods (Hammonds's, Dikau's and MORAPS's) were applied to SRTM and ASTER GDEM with moving window sizes ranges between 1.6 and 10.2 km with 200 m step (radius range 0.8 – 5.1 km). The other parameters of the original methods were unchanged. All three methods were automated using bash scripts for GRASS GIS.

The method of classification, using a multi-scale approach by taking fitting quadratic parameters to mowing window, was proposed by Wood. It is scale-dependent and it identifies 6 morphometric features (peaks, ridges, passes, channels, pits and planes). The method is implemented within GRASS GISS module r.param.scale. It was applied with slope tolerance between 1° to 7° (defines flat surface), curvature tolerance ranging from 0.001 to 0.007 (defines planar surface) and mowing window-sizes from 30 to 500 m.

The landform classification following Iwahashi and Pike is based on an unsupervised nested-means algorithms and a three part geometric signature. The slope gradient, surface texture and local convexity are calculated within a given window size and classified according to the inherent data set properties. It can be characterized (in terms of thresholds) as a dynamic landform classification method. Original AML scripts for ArcINFO, published by J. Iwahashi, were rewritten for GRASS GIS. All the threshold values of parameters for classification are derived during computation from the properties of DEM raster (range of values, distribution) therefore selection of different computational region extents can lead to slightly different results.

Estimation of topographic position index (TPI) at different scales (plus slope) can classify the landscape into both slope position (i.e. ridge top, valley bottom, mid-slope, etc.) and a landform category (i.e. steep narrow valleys, gentle valleys, plains, open slopes, etc.). This method was further developed by Weiss and Jenness. The classification of slope position to 6 classes requires setting the radius of neighbourhood (mowing window) and its geometric shape. Classification of landforms is based on analyses of TPI index and slope at two different scales; therefore it requires 2 values of radius size. A computer version of this method is available as an extension for ArcView 3.x. Topographic position index maps with radius size between 50 and 1000 m with 50 m step were computed and used for landform classifications.

The classification of landform elements is probably the simplest of mentioned methods. It was applied using curvature threshold values ranging from 0,001 to 0,005 to regional and local DEM. Resulting maps were simplified by majority filter with 7x7 pixel neighbourhood. The curvature threshold sets the boundary between curved and plane forms. The method was applied within SAGA GIS (module *Curvature Classification*).

The last used method is the determination of genetically and dynamically well interpretable relief forms. An attempt to create automated procedure for delineation of forms is still solved only partially; therefore this method was applied only at local level using manual expert delineation of landforms. The results of field research were also applied for classification.

Evaluation of landform classifications

To assess the accuracy of classification results, an error matrix and a kappa index were computed for each classification map (map of classified landforms), with respect to reference maps (maps of soil and forest types). Kappa index of agreement equals 1 when agreement between reference and classification maps is perfect and kappa equals 0 when agreement is as expected by chance. The classification map with the best value of kappa index was chosen as the more appropriate combination of algorithm's input parameters (according to georelief of testing region and quality of DEM). Only those soil and forest types (e.g. scree and ravine forests - *Fraxineto-Aceretum* forest types according to Zlatník), which are typically found at certain landforms, were used for assessment.

Classifications of macrolandforms led to a division of state area into similar categories that can be found in the map of morphological-morphometrical landform types. A direct comparison of macrolandforms and soil and forest type's maps is impossible. Therefore, the accuracy of macrolandforms classification maps was assessed by comparison with mentioned map and not with the maps of soil and forest types.

Testing regions

Three types of testing regions were selected (Fig. 1). The classification of macrolandforms, based on global elevation products, was done for the whole state territory of Slovakia. Mesolandforms were classified in the south-western part of Nízke Tatry Mts. and adjacent part of Horehronské podolie basin. This region has highly diversified georelief, with almost the all expected landform classes. It covers 290 km^2.

At a local level, the elementary landforms were classified on the slopes called *Medvedia úboč (Bear's slope)* in the eastern part of testing region for landforms.

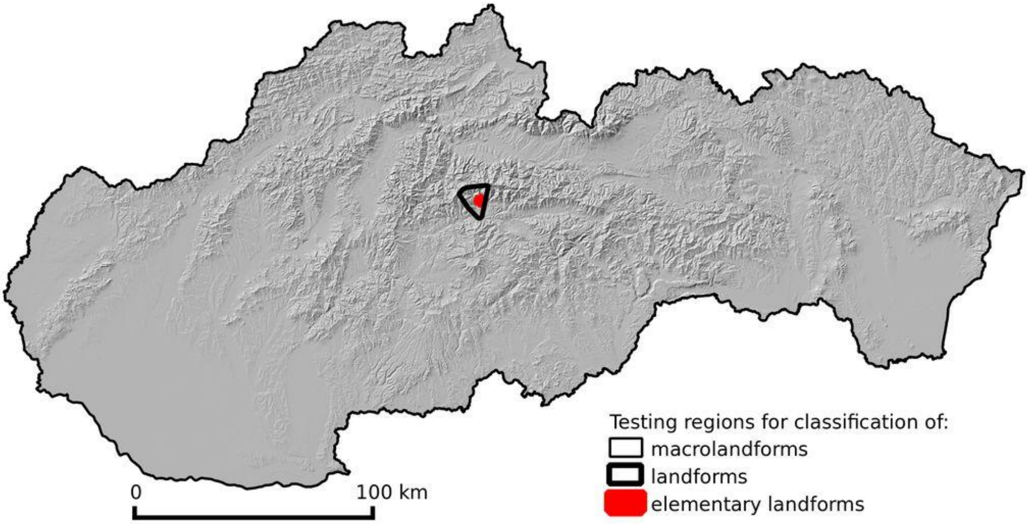

Fig. 1. Location of testing regions within Slovakia

Soil and forest type maps

The maps of soil and forest types were prepared by National Forest Centre (NFC), Zvolen, Slovakia. Their accuracy was evaluated by their cross combination and expert method considering the probability of occurrence of each combination (Fig. 2) (see Hančinský, 1972). The combinations were conforming for 87,44% of testing region's area, disputable for 5,5% and nonconforming for 7,06%. The evaluation showed that the main disproportions results mainly from different generalization levels of both maps, e.g. pedological map missed fluvisols in the narrow valleys where vegetation units of alluvial forests with *Alnus* sp. were mapped by forestry typologists.

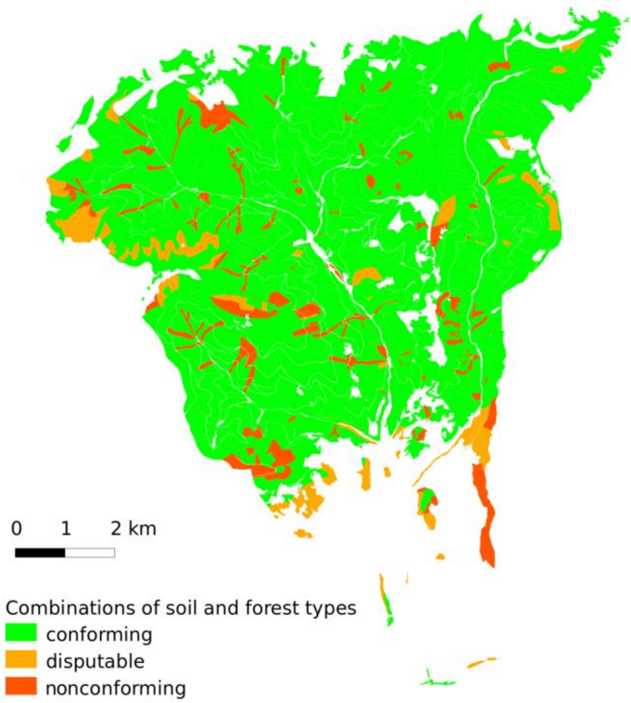

Fig. 2. Accuracy assessment of maps of soil and forest types, prepared by NFC (testing region for classification of landforms)

RESULTS

Classifications of macrolandforms

The best results were achieved using classification according to Dikau et al. with radius 3.7 km (Fig. 3, Tab. 1). This is similar to the results of further development of Dikau's algorithm presented by Brabyn. Original size of the moving window (~ 10 km) used by Hammond, Dikau and MORAP team seems to be too large for Central European conditions. The lower values of radius lead to cutting of single slopes into several landform classes. The MORAP's team algorithm is too much simplified and low number of classes is not appropriate for classification of Western Carpathian’s diversified georelief. Direct comparison of classification according to Hammond and MORAP was impossible due to the different meaning of categories in classification and reference maps.

Table 1.. Kappa index values for the classifications according to Dikau's (Dikau, 1991) algorithm. Comparison based on the high mountain categories of both classification and reference maps.

Neighborhood radius [km]	0.8	1.2	1.6	2.0	2.4	2.8	3.0	3.4	3.7	3.8	4.2	4.6	5.0	5.1
Kappa index	0.01	0.09	0.27	0.48	0.59	0.64	0.65	0.66	0.68	0.67	0.54	0.52	0.48	0.45

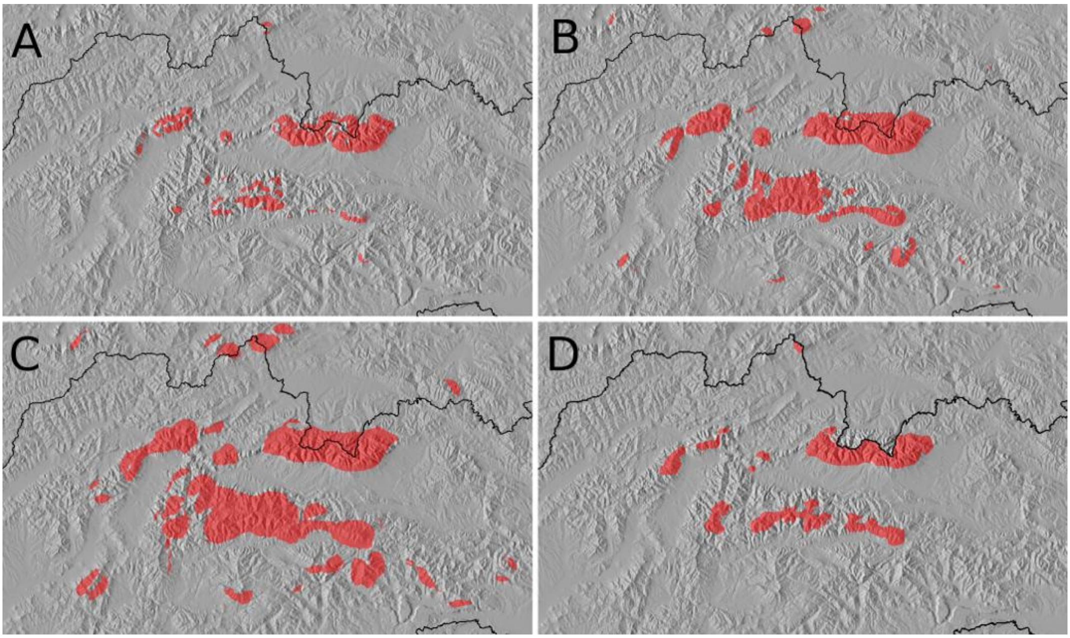

Fig. 3. Class of high mountains according to Dikau's algorithm and traditional classification. A- 2.5 km radius, B – 3.7 km radius, C – 10.2 km radius, D – high mountains according to Tremboš, Minár (2001). Central part of Slovakia. Red – high mountains.

Landform classifications (mesolandforms)

Different values of input parameters (7 for slope tolerance, 7 for curvature tolerance and 24 window sizes) led to 1176 unique classifications according to Wood. The best combination of input parameters (the highest kappa index values) determined by comparison with the soil and forest type maps (0.76 for forest types, 0.68 for soil types) is as follows: slope tolerance 1° (defines flat surface), curvature tolerance of 0.002 (defines planar surface) and window-size of 170 m. The results are shown at Fig. 4.

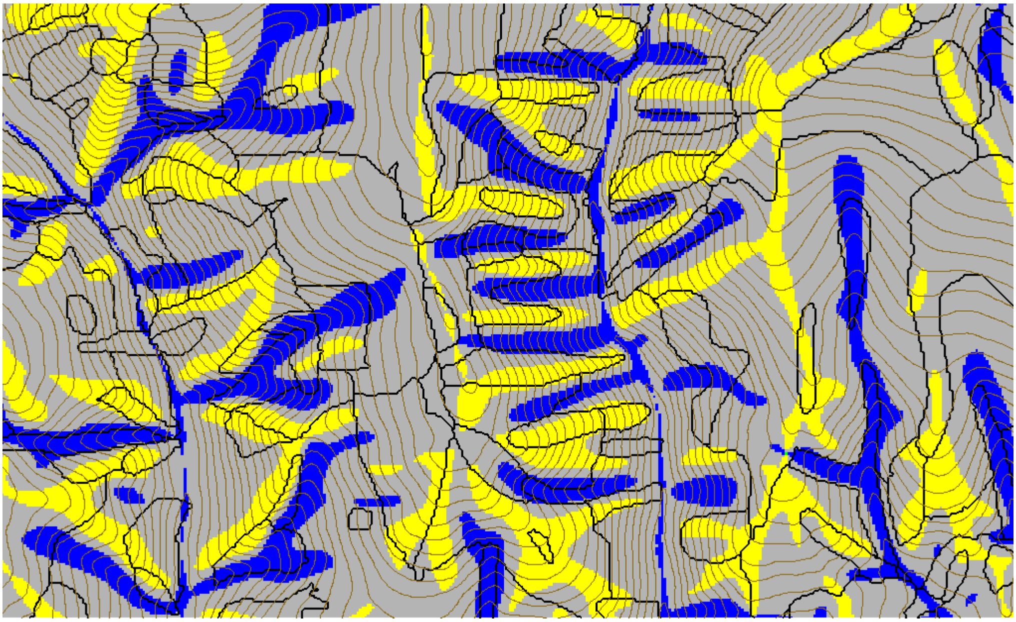

Fig. 4. Comparison of landforms according to Wood (1996) and boundaries of forest types. Central part of testing region. Blue – valleys, yellow – ridges, grey – slopes, black lines – boundaries of forest types

The method proposed by Iwahashi and Pike classifies relief into 8, 12 or 16 classes without possibility to change other input parameters. Therefore only 3 classifications were prepared with almost the same kappa index values. The Fig. 5 shows results with 8 landform classes. More detailed classifications are achieved by more precise segmentation of relatively flat areas (Fig. 6), which were not the subject of comparison. Kappa index values were the same for all 3 classifications (0.58 for forest types, 0.51 for soil types), because only steep forested parts of testing region were evaluated.

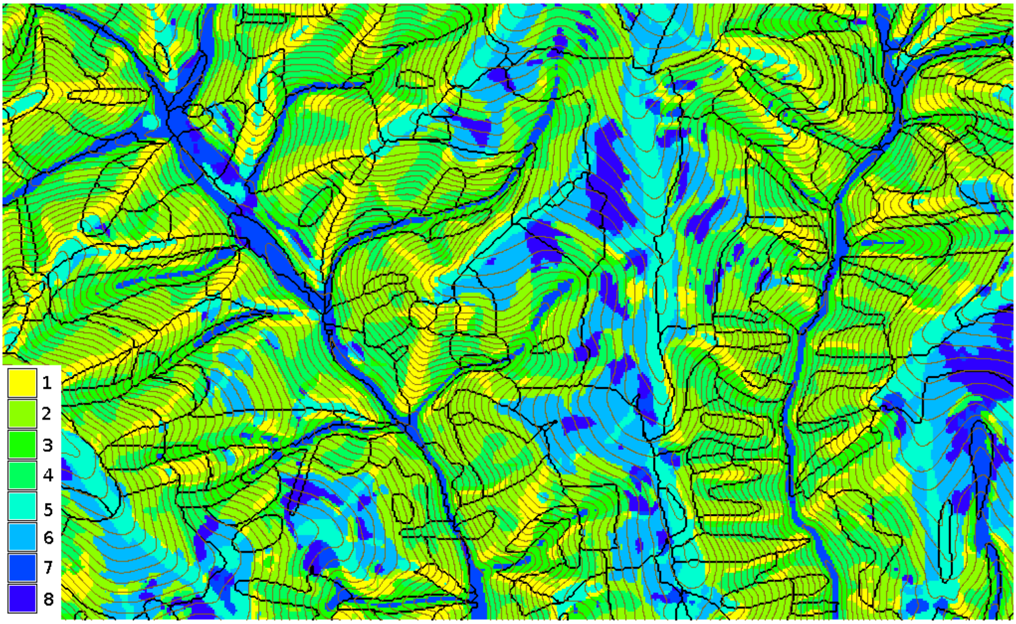

Fig. 5. Comparison of landforms according to Iwahashi and Pike (2007) and boundaries of forest types. Central part of testing region. 1 – steep, high convexity, fine texture; 2 – steep, high convexity, coarse texture; 3 – steep, low convexity, fine texture; 4 – steep, low convexity, coarse texture; 5 – gentle, high convexity, fine texture; 6 – gentle, high convexity, coarse texture; 7 – gentle, low convexity, fine texture; 8 – gentle, low convexity, coarse texture

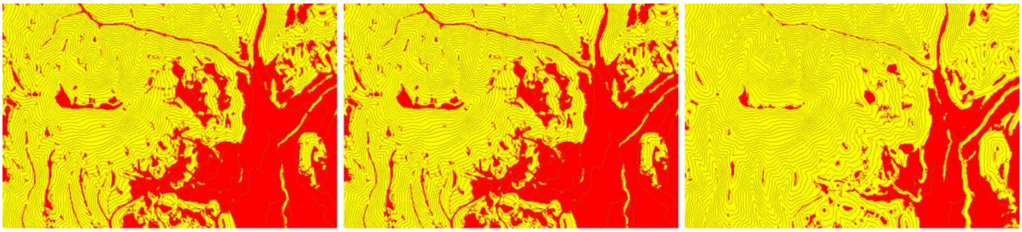

Fig. 6 . Differences between three types of landform classification according to Iwahashi and Pike (2007). Southern part of testing region. From left to right: differences between maps with 8 and 12 classes, between 8 and 16 and between 12 and 16 classes. Red – difference, yellow – agreement

The best results for algorithm according to Jennes were achieved using 2 circular neighbourhoods 100 and 900 m in diameter with kappa index 0.73 (Fig. 7). With these settings, the algorithm was able to distinguish between shallow valleys on side slopes and main valleys of mountain ranges. However, it was not possible to set one setting appropriate for both mountainous and hilly land georelief.

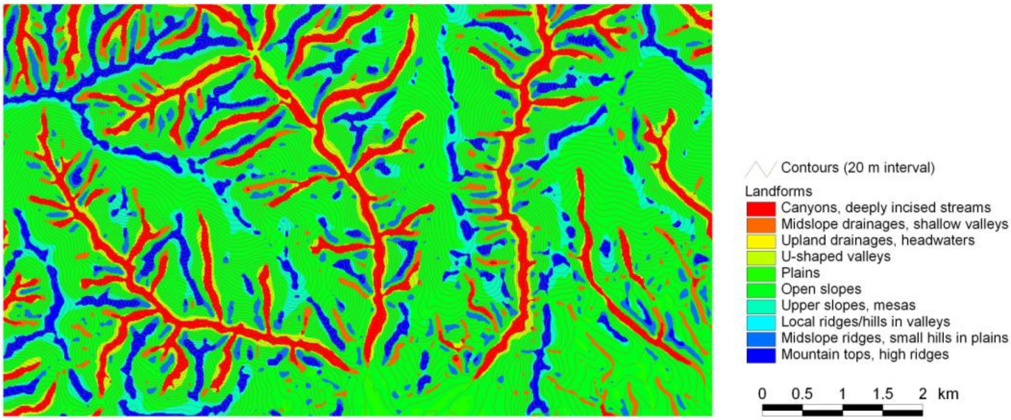

Fig. 7. Landform classification according to Jennes. Central part of testing region.

Landform elements, elementary landforms

The classification of landforms elements according to Dikau was not able to identify bottoms of wider valleys (Fig. 8). The wider bottoms are classified as linear slopes or planes combined with concave slopes at valley sides. Classification of steeper shallow valleys is more successful. The best threshold value of curvature tolerance in testing regions and DEMs was 0.003, but the kappa index values were very low – only 0.42. The better results were achieved for 10 m resolution DEM with kappa index 0.51. Results for local DEM with 5 m resolution were partially influenced by artificial undulations caused by interpolation method.

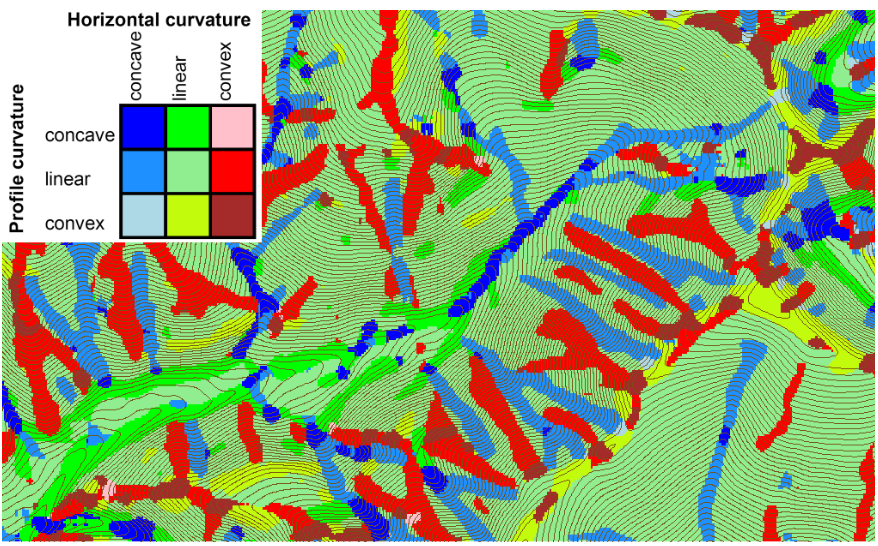

Fig. 8. Landform elements (Dikau 1988). Valley bottom (lower right part) classified as plains and concave slopes. Upper part of Lomnistá dolina valley.

Elementary landforms defined by manual expert method following Minár, Evans were compared with forest types mapped by detailed field research of the smallest testing region. This comparison gave the highest kappa index value (0.87) comparing with all other methods at all three scales. However, this is probably influenced by the methodology of field research, when forestry typologists for mapping of forest types used the geomorphological maps prepared specifically for testing region.

DISCUSSION

The main reason why the classification of macrolandforms was tested is the possibility the define regions (using classes of macrolandforms) for which the different values of another algorithm's input parameters can be set when classifying landforms and elementary landforms (at regional or local level). However, the evaluation of this possibility will require the modification of used computer programmes and algorithms and therefore it will be a task of the future research. The most promising classification method from this viewpoint seems to be the one of Dikau et al. Its main problem – a progressive zonation when landform changes from plains to mountains could be solved according to Brabyn.

The computed correlations between classified landforms and soil properties at regional and local level were lower than ones between georelief and forest cover properties. This is probably due to the more simplified soil map comparing with map of forest types.

Method of J. Wood is the most promising algorithm for classification of landforms for forestry and pedological predictive mapping. It is highly configurable and this increases its applicability in different types of relief. The number of resulting landform classes (Dikau, 1991) is usually adequate; however incorporation of other relief characteristics (e.g. aspect) can significantly help to predict spreading of specific units.

Estimation of topographic position index according to Jennes is also of high interest, because of variability of input parameters and simple user interface.

From the viewpoint of forestry and pedological predictive mapping, Iwahashi's algorithm is less usable, because it can not be parameterized by modifications of input values.

The parameter for method of Dikau is highly dependent on the type of relief and DEM quality, especially if it is computed from vectorised contours. In the mountainous relief of Nízke Tatry Mts. the best results with regional DEM were achieved with curvature threshold set to 0.004, which is significantly more than standard value of 0.001 set as default. This high threshold filtered out the influence of microrelief (either natural or artificial resulting from the DEM interpolation method) and allowed clear identification of small valleys and steep ridges (spurs) on large valley slopes (Fig. 8). Even higher values of threshold led to discontinuous classification of forms. The lower thresholds resulted in extremely dissected map affected by microrelief. However, the lower values (0.002 or 0.001) were usable in Horehronské podolie basin with gentle slopes and wide valleys. This simple method is also unable to define terrain context and uses hard classifiers. The bottoms of major valleys are classified only as concave forms at the bottom of side slopes, bottoms of wider valleys are classified as plains. The main purpose for which it could be used is the delineation of soil and forest types typically occupying bottoms of small side valleys (Fig. 8) or steep ridges (spurs) on valley sides within a small region with relatively simple relief.

The best results were achieved by expert manual delineation of elementary landforms using detailed topographic maps and field research. However, its application is time consuming which makes it unsuitable for mapping of larger areas.

Setting the best values of input parameters for each classification method is dependent on spatial resolution, quality of DEM, characteristics of georelief in study area and spreading of pedological or forestry units, which are to be predicted. Moreover, specifically in this study the correctness of reference maps is a little bit questionable. At this stage of research the question is how the low values of kappa index should be understood: (i) the values of input parameters are not optimal, (ii) the selected method is not appropriate or (iii) the accuracy of reference maps is low. An answer should be based on results of detailed field research and mapping of geomorphological, pedological and forestry units.

CONCLUSIONS

It is supposed that maps of soil and forest types can be improved using more detailed information on abiotic environment. A terrain classification is one of the methods which can significantly help in boundary delineation of pedological and forestry units. It is clear that the landforms themselves, without information on other landscape components, can not successfully predict distribution of specific soil and forest types. It is necessary to incorporate other characteristics of abiotic environment (e.g. geology) and other characteristics of georelief itself (elevation, slope and aspect with respect to solar radiation, wetness index and other). However, the map of landforms, based on DEM, can significantly help in predictive mapping of soil and forest types.

The presented paper is the introductory study of future research and application of relief classification in predictive pedological and forestry mapping in Slovakia. The future research will concern on detailed specification of input parameters of selected methods suitable for predictive mapping of specific soil and forest types (groups of forest types resp.).

ACKNOWLEDGMENT.

This work was supported by the Slovak Research and Development Agency under the contract No. APVT-27-009304 and APVV-0632-07.

REFERENCES

Barka, I. (2009) Remote sensing and GIS in geoecological research: a case study from Malá Fatra Mts., Slovakia In: Horák, J., Halounová, L., Kusendová, D., Rapant, P., Voženílek, V. (eds.): Advances in Geoinformation Technologies. Ostrava : VŠB - Technical University of Ostrava, 2009, s. 77-88. ISBN 978-80-248-2145-0

Brabyn, L. (1996) Landscape Classification using GIS and National Digital Databases. PhD Thesis. University of Canterbury, New Zealand. Available on-line at: http://www.waikato.ac.nz/wfass/subjects/geography/people/lars/phd/main.htm

Brabyn, L. (1998) GIS Analysis of Macro Landform. Proceedings of the Spatial Information Research Centre's 10th Colloqium. University of Otago, New Zeealand, 16-19 November, 1998. p. 35-48.

Čurlík, J., Šubrina, B. (1998) Príručka terénneho prieskumu a mapovania pôd. Bratislava: VÚPÚ. 134 p.

Dikau, R. (1988) Entwurf einer geomorphographisch-analytischen Systematik von Reliefeinheiten. Vol. 5. Heidelberg: Heidelberger Geographische Bausteine, 1988.

Dikau, R., Brabb, E. E., Mark, R. M. (1991) Landform Classification of New Mexico by Computer. Open File report 91-634. U.S. Geological Survey.

Guisan, A., Weiss, S. B., Weiss, A. D. (1999) GLM versus CCA spatial modeling of plant species distribution. Kluwer Academic Publishers. Plant Ecology. 143:107-122.

Hammond, E.H. (1954) Small scale continental landform maps. Ann. Assoc. Am. Geogr. 44, 32–42.

Hammond, E.H. (1964) Analysis of properties in landform geography: an application to broadscale landform mapping. Ann. Assoc. Am. Geogr. 54, 11–19.

Hančinský, L. (1972) Lesné typy Slovenska. Príroda, Bratislava 178 p.

Iwahashi, J., Pike, R.J. (2007) Automated classifications of topography from DEMs by an unsupervised nested-means algorithm and a three-part geometric signature. Geomorphology, 86, p. 409-440.

Jenness, J. (2006) Topographic Position Index (tpi_jen.avx) extension for ArcView 3.x, v. 1.3a. Jenness Enterprises. Available at: http://www.jennessent.com/arcview/tpi.htm

Križová, E. (1995) Fytocenológia a lesnícka typológia. (Učebné texty). Vydavateľstvo TU vo Zvolene, 203 pp.

Lillesand, M.T., Kiefer R.W. (1994) Remote Sensing and Image Interpretation, John Wiley & Sons, New York

MacMillan, R. A., Pettapiece, W. W., Nolan, S. C., Goddard, T. W. (2000) A generic procedure for automatically segmenting landforms into landform elements using DEMs, heuristic rules and fuzzy logic. Fuzzy Sets and Systems, 113, 1, 81 – 109

Meybeck, M., Green, P., Vorosmarty, Ch. (2001) A New Typology for Moutains and other relief Classes. Moutain Research and Development, Vol. 21, 1, p. 34-45

Minár, J., Evans, I. S. (2008) Theoretical basis of elementary landform segmentation in geomorphological mapping. Geomorphology, nr. 95, p. 236-259, ISSN: 0169-555X.

Minár, J. et al. (2001) Geoekologický (komplexný fyzickogeografický) výskum a mapovanie vo velkých mierkách. Geografika Bratislava, ISBN: 80-968146-3-X.

Minár, J., Mentlík, P., Jedlička, K., Barka, I. (2005) Geomorphological information system: idea and options for practical implementation. In Geografický časopis. 2005, roč.57, č.3, s.247-266, ISSN 0016-7193

Morgan, J.M., Lesh, A.M. (2005) Developing Landform maps using ESRI'S ModelBuilder. 2005 Esri International User Conference Proceedings. 11 p., proceedings.esri.com/library/userconf/proc05/papers/pap2206.pdf

Neteler, M., Mitášová, H. (2008) Open Source GIS: A GRASS GIS Approach. Third Edition. The International Series in Engineering and Computer Science: Volume 773. Springer, New York. 406 p. ISBN: 038735767X

Pacina, J. (2008) Metody pro automatické vymezování elementárních forem georeliéfu jako součást Geomorfologického informačního systému. disertační práce. Plzeň: Západočeská univerzita, Fakulta aplikovaných věd.

Ratajczak, M., Jasiewicz, J. (2009) Application of free open-source software tools to automatic and semiautomatic classification of landforms in lowland areas. Geomorphologia Slovaca et Bohemica, 9, 2009, 1, p. 43-52

Schmidt, J., Hewitt, A. (2004) Fuzzy land element classification from DTMs based on geometry and terrain position, Geoderma, 121, p. 243–256.

Straumann, R. K., Purves, R. S. (2008) Delineation of Valleys and Valley Floors. In: T.J. Cova et al. (Eds.): GIScience 2008, LNCS 5266, Springer-Verlag Berlin Heidelberg 2008. pp. 320–336

Tremboš, P., Minár, J. (2001) Morphological-morphometrical landform types. 1:500 000. Landscape Atlas of the Slovak Republic. Bratislava, Banská Bystrica: MŽP SR, SAŽP. p. 90-91.

Weiss, A. (2001) Topographic Position and Landforms Analysis. Poster presentation, ESRI User Conference, San Diego, CA

Wood, J. (1996) The geomorphological characterisation of digital elevation models. PhD Thesis, University of Leicester, UK. Web publication available at this URL address http://http://www.soi.city.ac.uk/~jwo/phd/.

Zhong T., Cang X., Li R., Tang G. (2009) Landform Classification Based on Hillslope Units from DEMs. Asian Conference on Remote Sensing (ACRS) proceedings 2009., http://www.a-a-r-s.org/acrs/proceeding/ACRS2009/Papers/Poster%20 Presentation/ Session%202/PS2-19.pdf

Zlatník, A. (1976) Lesnická fytocenologie. Praha, SZN.

GEORELIEF RECONSTRUCTION AND ANALYSIS BASED ON HISTORICAL MAPS AND AERIAL PHOTOGRAPHS

PACINA Jan and WEISS Lukas

Department of Informatics and Geoinformatics, Faculty of Environment, J. E. Purkyně University, Králova výšina 7, 400 96, Ústí nad Labem, Czech Republic
Jan.Pacina@ujep.cz,weiss.lukas@email.cz

Abstract

During the last century were done many significant georelief changes caused by the human activity. The biggest influence on the landscape character change within the frame of the Czech Republic has undoubtedly the brown coal opencast mining. During the mining activity were removed a lot of cubic meters of material and placed elsewhere which resulted in dramatic changes of the georelief.

One of the ways how to reconstruct the original shape of the landscape is the usage of historical maps and old aerial photographs made in the period before the dramatic georelief changes. The maps of the 3rd Military survey 1:25 000 after reambulation (partly before reambulation) and aerial photographs taken in years 1938 and 1995 were used for this purpose. Historical maps were georeferenced using the method of Coonse plating using a huge amount of identical points (ESRI 2010). The reambulated maps contain clearly readable elevation data (contour lines), which were used for reconstructing the original georelief and as well as the base elevation layer used for aerial photographs orthorectification. Thanks to processing of the aerial photographs we can obtain the Digital Surface Model of the coal mines.

Comparing the elevation data obtained by photogrammetric methods with the elevation grid constructed from vectorized contour lines we may try to evaluate the preciseness of the old maps elevation data. The volumetric analysis was used to calculate the georelief differences done during the selected years. Within the Bílina mine we almost reach the amount of 1 bilion m^3 of transferred material.

Keywords: georelief reconstruction, 3rd Military survey, aerial photographs, digital surface model, volumetric analysis.

INTRODUCTION

The area between the towns Kadaň and Duchcov (North-west Bohemia, the Czech Republic) is a part of so called Black Triangle (ECM 2010) with active coal mining activity. The Brown coal has been mined in this area for ages, but the mining has become very intense in the last 80 years. Brown coal is not located to deep in the coal basin, so the technology of open-cast mines is widely used in this area. The open-cast mining is a rathercheap technology of coal mining giving access to huge loads of brown coal, but with a destructive effect on the surrounding environment.

This region used to be focused on agriculture, with towns and little villages spread all over the basin. The coal mining followed by the heavy industry has changed the look and shape of this region a lot. The open-cast mines are covering ca 3800 ha within the Area of interest (see **Fig. 5**). The original landscape, including settlement, infrastructure and ecosystems has been destroyed in this area.

The purpose of this paper is to visualize the original state of the georelief and to calculate some interesting statistics using the GIS technologies. Old maps and historical aerial photographs may be a good resource for reconstructing the original state of the destructed landscape. This reconstructed georelief has a wide range of use – historical purposes, recultivations, hydrological modeling, landscape planning. Obtaining the original georelief gives us a chance to calculate how much material have been so far mined (removed) and how much have been poured into the dumps.

The georelief reconstruction requires elevation data from the period before the intensive coal mining activity. This area has been closely mapped in 1930’ thanks to its geographic location (which is close to the border with Germany) and the huge brown coal reserves. The maps of the 3rd Military survey 1:25 000 of this region have been reambulated in the period 1934 – 1938 and in 1938 was the region covered with aerial photographs. The current state of the georelief within the coal mines cannot be easily obtained and the coal mining companies are not a well accessible data source at all. Here we have to use the aerial photographs for Digital Surface Model (DSM) and further on Digital Elevation Model (DTM) creation as well.

Fig. 1 Georelief change in the Basin of Most - 1960' and 2000. Štýs (2000)

DATA AND METHODS

We will work with old maps and historical/current aerial photographs. Old maps used for this project are the maps of the 3rd Military survey 1:25 000 after reambulation. Historical aerial photographs originate from the year 1938 and the recent aerial photographs from the year 1995.

Old maps

The old maps in this region were reambulated in 1930’ apparently for the strategic purposes with upcoming of the 2nd World war. Elevation data are clearly readable in these maps in the form of contour lines and elevation points. These maps are covering almost the whole Area of interest with contour interval varying from 20m in flat areas to 5m in hilly areas. Only in some parts we had to use a non-reambulated map - the elevation here is expressed by the Lehman’s hachure.

Hachures are an older model of representing the georelief. They show orientation of slope, and by their thickness and overall density they provide a general sense of steepness. Being non-numeric, they are less useful to a scientific survey than contours, but can successfully communicate quite specific shapes of terrain. They are a form of shading, although different from the one used in shaded maps. Hachure representation of relief was standardized by the Austrian topographer Johann Georg Lehmann in 1799. (Kennelly & Kimerling 2001)

All maps covering the Area of interest have to be georeferenced. Spline transformation implemented in ArcGIS was used to georeference the data. The spline transformation is a true rubber sheeting method and is optimized for local accuracy but not global accuracy. It is based on a spline function - a piecewise polynomial that maintains continuity and smoothness between adjacent polynomials. (ESRI 2010)

The spline transformation was chosen as it fulfills the position accuracy of the transformed requested for the DTM creation in this project. Approximately 150 to 250 identical points were chosen in each map sheet (dependently on the input data) to secure the local accuracy. The transformation accuracy has been visually tested with the MapAnalyst application (Jenny & Weber 2010) by applying a regular square network on the transformed data (see **Fig. 2**).

Contour lines and elevation point have been hand-vectorized and further on used for DTM creation. More complicated was to obtain the elevation data from the non-reambulated maps. Here are the contour lines created based on the Lehman’s hachure.

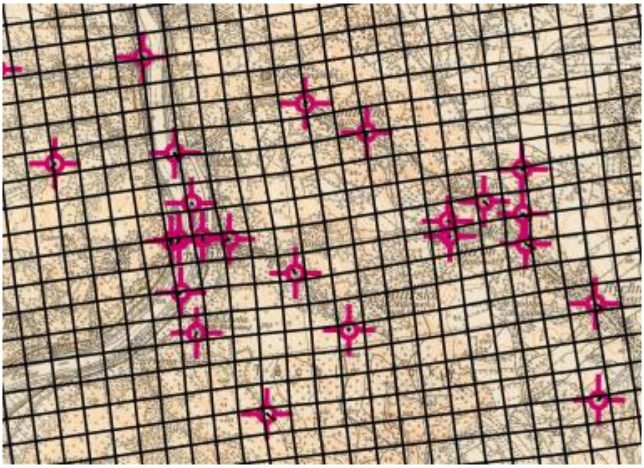

Fig. 2 Detail of the regular square network (and its distortion) applied on the transformed data

Aerial photographs

The *Area of interest* (see **Fig. 5**) is covered by 15 aerial photographs for the year 1995 and 17 for 1938. So far have been processed for the *Sample testing area* 5 aerial photographs for the year 1995 and 7 for 1938. All the images have at least 60% overlap.

Aerial photographs were processed using the Leica Photogrammetric Suite. The characteristics of processed images are following:

Table 1 Aerial photographs parameters

Year	1995	1938
Focal length	152.16	211.59
Scale factor	1 : 29450	Unknown (ca 1 : 18000)
Flight height [m]	4481	Unknown (ca 4000)
Resolution [DPI]	1016	1016
Resolution [µm]	25.00	25.00

The aerial photographs were processed in the standard way of photogrammetry. The images were at first tight together with 30 TIE points for each stereo-pair and then were added the Ground Control Points (GCP) covering the whole block. GCP's require georeferenced data, including the elevation information.

To create the GCP's for the year 1995 were used the standard accessible data – orthophoto available at http://geoportal.cenia.cz and ZABAGED® (ČUZK 2010) for the elevation data.

On the aerial images from the year 1938 are in the *Sample testing area* large parts of the landcape that has changed a lot. The recent data are practically useless for processing the GCP's in these areas. Here we have used partially the old maps (3rd Military survey) to locate the object on the historical aerial photographs, recent orthophoto for the surrounding areas without a significant change and the orthophoto from 1952 accessible at http://kontaminace.cenia.cz for the other areas.

The 1938 images are not of a very good visual quality. The images are noisy, scratched, and affected by the contemporary technology of creation – this affects especially the selection of GCP's and the automatic DSM creation from aerial images.

Vectorized contour lines from the maps of the 3rd Military survey were used for DTM creation – giving the Z coordinate for the GCP's. The contour interval of the 3rd Military survey maps is from 20m to 5m, depending on the slope of the terrain.

DTM interpolation was done using the Regularized Spline with Tension, implemented in GIS GRASS. See Mitas & Mitasova (1988) and (1993), Neteler (2004) for more information.

Triangulation of the aerial photographs was performed with respect to the quality of the processed images and to the minimum RMSE of the resulting data.

DTM and DSM creation

Several DTM's and DSM's were created under processing of the *Area of interest* - at first the DTM's defining the GCP's elevation and consequently the DSM derived from the aerial images. The method for processing the DTM's from ZABAGED® and 3rd Military survey contour line is described in the previous text.

We will use the following labeling for the further text:

- DTM_1936 – interpolated from the 3rd Military mapping contour lines,
- DSM_1938 – derived from the aerial photographs – year 1938,
- DSM_1995 – derived from the aerial photographs – year 1995.

DSM_1938 and DSM_1995 were created by automatic image correlation. This method is used for automatic DSM extraction from aerial images with known orientation parameters with image overlap (in our case 60%).

Produced DSM_1995 has no visible errors and is well corresponding to the aerial image. Quality of DSM_1995 can be evaluated by visual control of the DSM_1995 contour lines compared with ZABAGED® contour lines (in the areas outside the mines) – see **Fig. 3**.

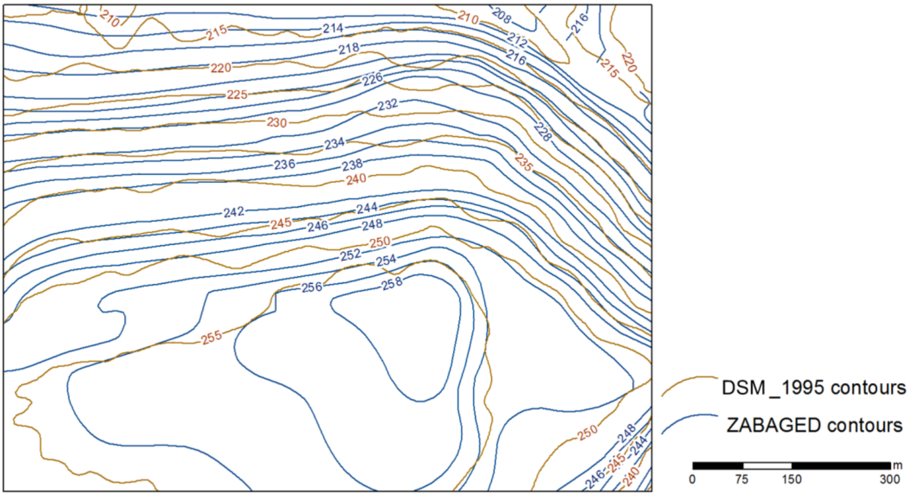

Fig. 3 Comparison of Digital Surface Model – year 1995 (DSM_1995) and ZABAGED® contour lines

The automatic DSM_1938 extraction has to deal with the following problems:

- the camera's focal length is 211.59 and the image scale is ca 1:18 000,
- old technology of original picture creation and processing,
- long term warehousing = scratched images.

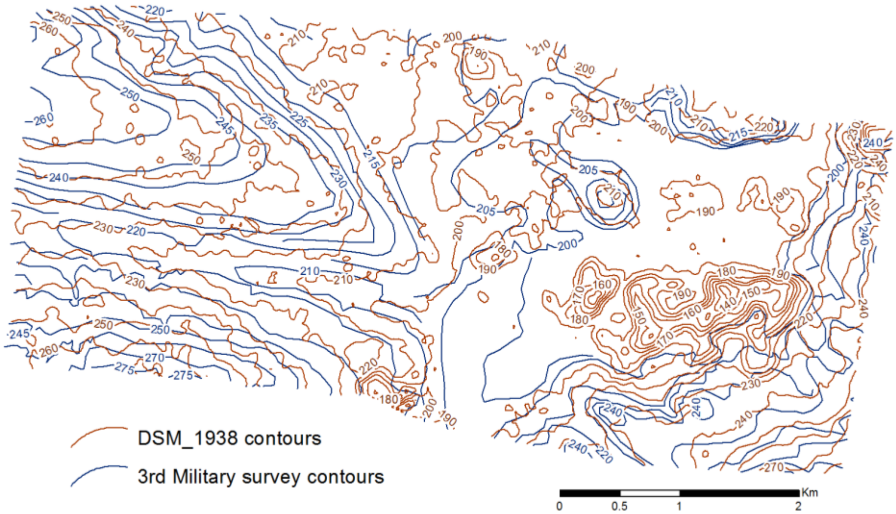

Fig. 4 Comparison of Digital Terrain Model – year 1936 (DTM_1936) contour lines based on the 3rd Military survey and Digital Surface Model – year 1938 (DSM_1938) contour lines

Our area of interest is located around the town Bílina (see **Fig. 5**) covering the open-cast mine Bílina and the Dumb Radovesice. Processing the historical aerial photographs is problematic and thus a *Sample testing area* was defined. Here we will test the so far processed data and prepare the testing methodology for the whole Area of interest. The *Sample testing area* contains locations with active mining activity (= the material being taken away) and areas recultivated from previous mining (= filled with material).

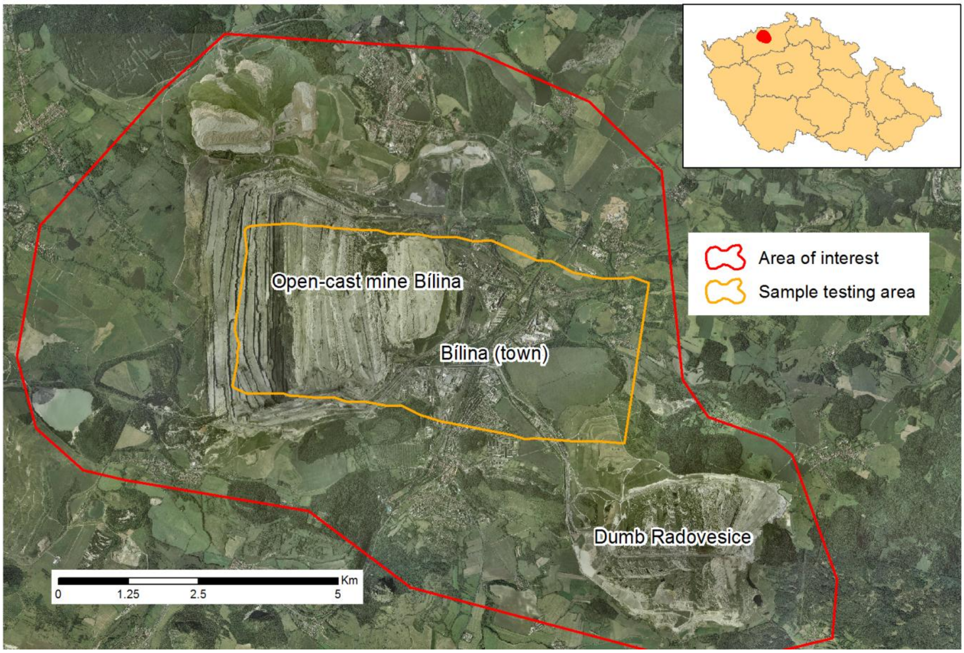

Fig. 5 The *Area of interest* overview

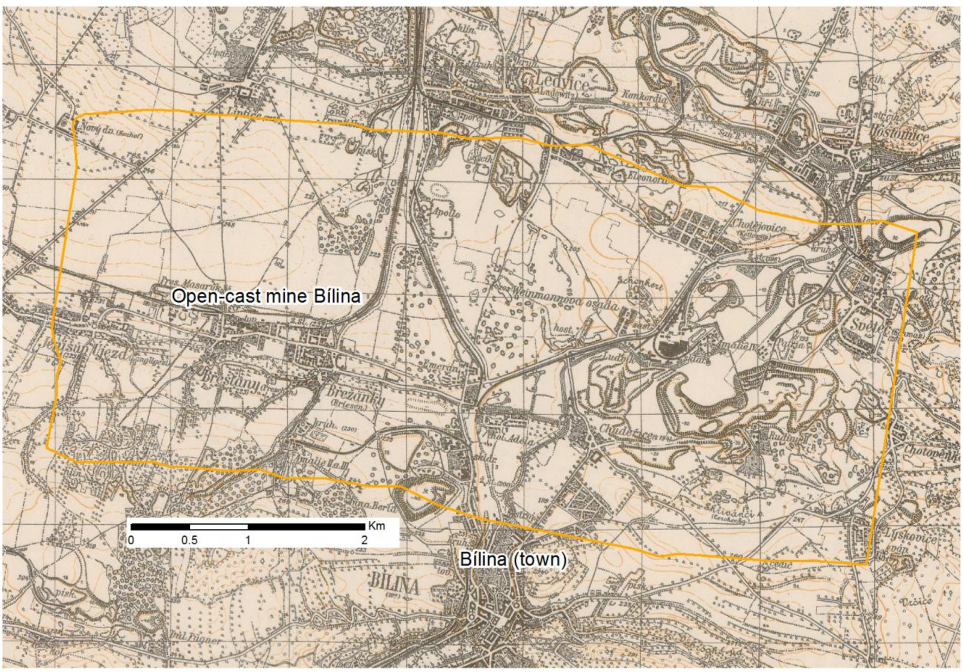

Fig. 6 Delimitation of the *Sample testing area* using the 1936 basemap

The terrain in our Sample testing area differs a lot between the year 1938 and 1995 – this is the result of mining activity, recultivations, and anthropogenic effects on the landscape (construction of houses, highway, and industrial areas). To depict the areas with the terrain change caused by the mining activity we performed an analysis computing the differences between the DSM_1938 DTM and the DSM_1995. The result shows areas with the highest terrain change (see **Fig. 7**). Areas with the highest terrain change were selected based on this analysis for further testing – to obtain more precise results the "Sub-area" was delineated in the Area 2.

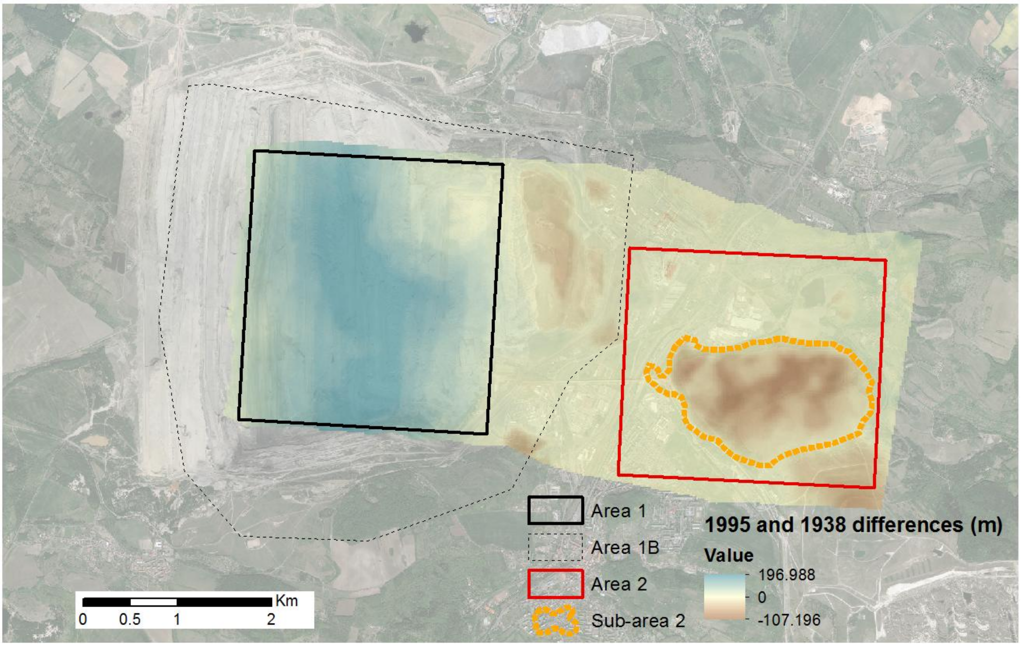

Fig. 7 Digital surface model differences (year 1938 and 1995) and areas of interest delimitation

ANALYSIS

One of the tasks of this project is to evaluate the material amount that was mined from the selected areas or transported into the dumb (deposit). The material amount is in this case equal to the volume of the upper and lower surface difference. Here we get the so called *Positive Volume (Cut)* and the *Negative Volume (Fill)*. The cut portion is the volume between the upper and lower surface when the upper surface is above the lower surface. The fill portion is the volume between the upper and lower surfaces when the upper surface is below the lower surface (see **Fig. 8**).

The volume calculation was performed using the double integral:

$$Volume = \int_{xmin}^{xmax} \int_{ymin}^{ymax} f(x,y)dxdy.$$

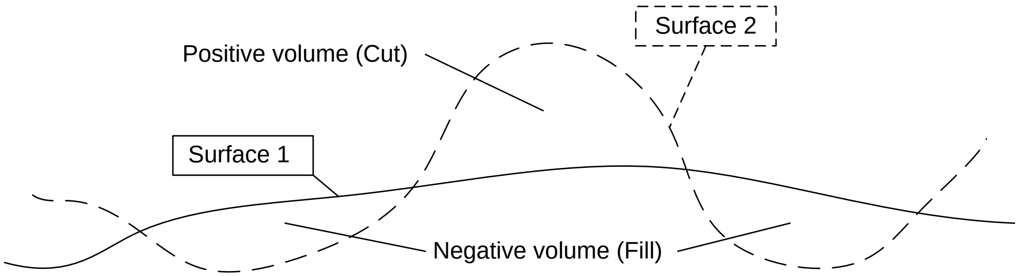

Fig. 8 Principle of Positive and Negative volume

Analysis of Area 1 (open-cast mine)

The Area 1 is covering part of the open-cast mine Bílina. Only a part of the historical aerial photographs of the Area of interest has been so far processed and thus is the created DSM_1938 not covering the whole mine. In this case we will perform the calculation of the mine volume as well from the DTM_1936 – which will overgrow the Sample testing area boundaries. The volume calculation from DTM_1936 would be proximate, as the DTM was interpolated from hand-vectorized contour lines.

The total Positive Volume (Cut) of Area 1B is 44 363 951m^3 and the Negative Volume (Fill) is 930 015 080m^3. One railway transport wagon can store up to 75m^3 - this means (based on this computation) that to transport the material and coal from the Bílina mine (until the year 1995) could be used ca 12 400 200 wagons. Detailed difference grid of DTM_1936 and DSM_1995 is shown on **Fig. 8**. Visualization of the area is presented on **Fig. 10** and **Fig. 11**.

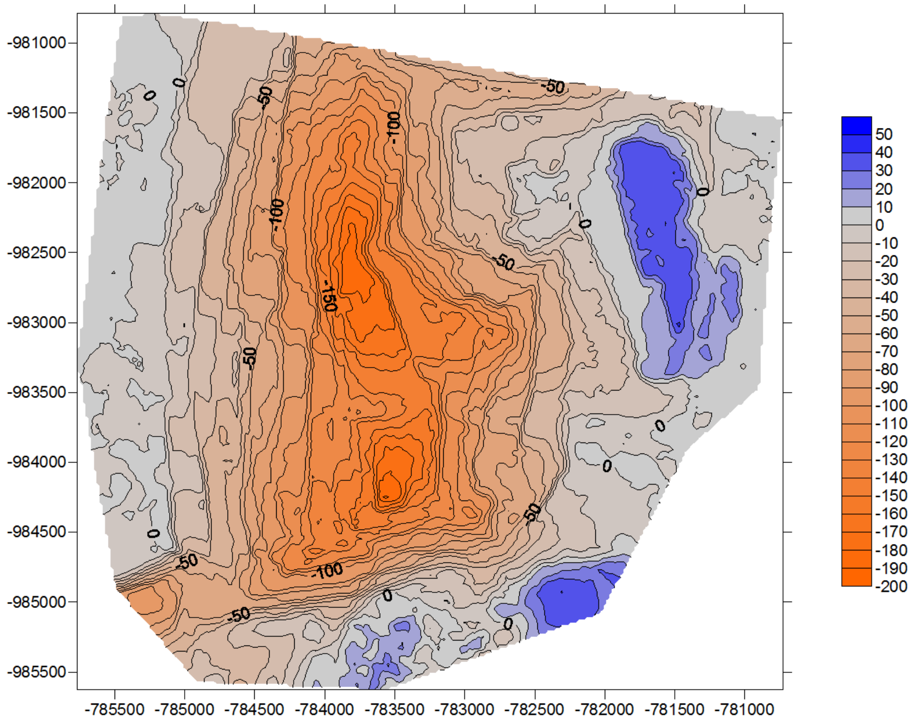

Fig. 9 Area 1B - Detailed difference grid of Digital Terrain Model – year 1936 (DTM_1936) and Digital Surface Model – year 1995 (DSM_1995)

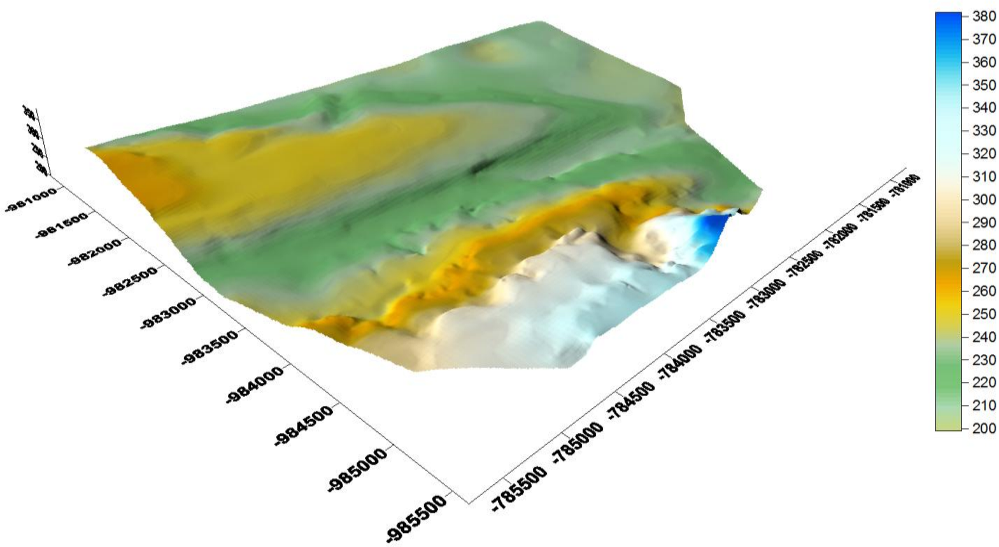

Fig. 10 Visualization of Area 1B – Digital Terrain Model – year 1936 (DTM_1936)

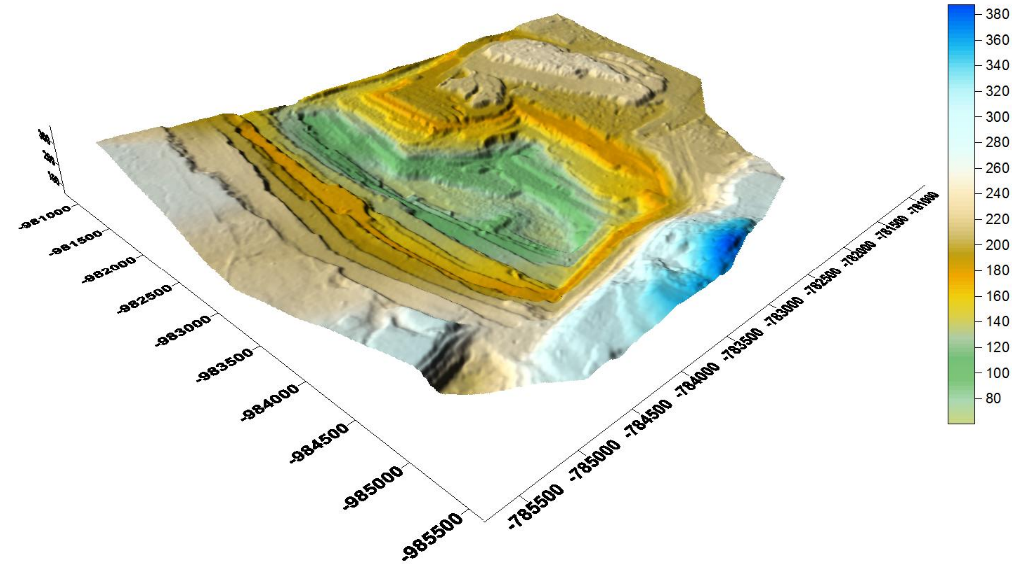

Fig. 11 Visualization of Area 1B – Digital Surface Model – year 1995 (DSM_1995)

We can compare the result of the volumetric analysis within the Area 1 using DTM_1936 and DSM_1938 in combination with DSM_1995. The DSM_1938 is more detailed but may be affected by the DSM creation method (see Fig. 12).

Calculated volumes using DSM_1938:

- Positive Volume (Cut): 487 188m^3,
- Negative Volume (Fill): 692 776 510m^3.

Calculated volumes using DTM_1936:

- Positive Volume [Cut]: 53 379m^3,
- Negative Volume [Fill]: 681 691 618m^3.

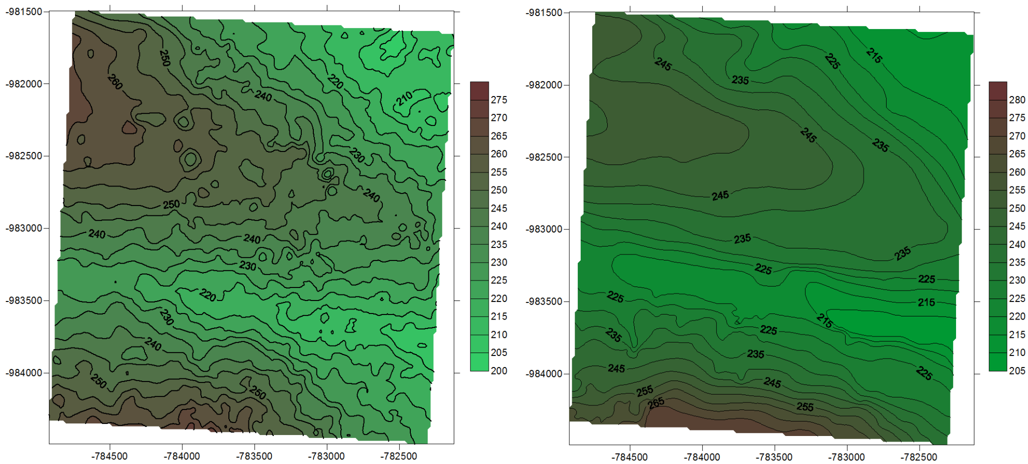

Fig. 12 Contour lines generated from Digital Surface Model – year 1936 (DSM_1938) and Digital Terrain Model – year 1936 (DTM_1936)

The contour lines generated from DSM_1938 and DTM_1936 are presented on **Fig. 12**. Here we may see the differences of the two datasets. The cartographically generalized contour lines from the map of the 3rd Military survey have the same trend as the contour lines generated from the DSM_1938. The DSM_1938's contour lines are more detailed in describing the terrain. The automatically generated DSM is based on a Triangulated Irregular Network and thus the contour lines should be further on cartographically generalized.

Analysis of Area 2 (recultivated mine)

Area 2 is covering a previous mine turned into forest/leisure-time recultivation (see **Fig. 13** and **Fig. 14**). This type of recultivation is made by filling up the old mine with the material mined in an active mine or with ashes from a coal power plant. This area is fully covered by the processed new and old aerial images. The DTM_1936 was not taken into the computation, as the mine is not well described by the contour lines.

Differences of DSM_1995 and DSM_1938 are shown on **Fig. 15**. The volumetric analysis was performed on the Sub-area 2 as here was determined our field of interest. The total volume of added material is in this case 101 282 997m^3, which equals to ca. 1 350 440 wagons.

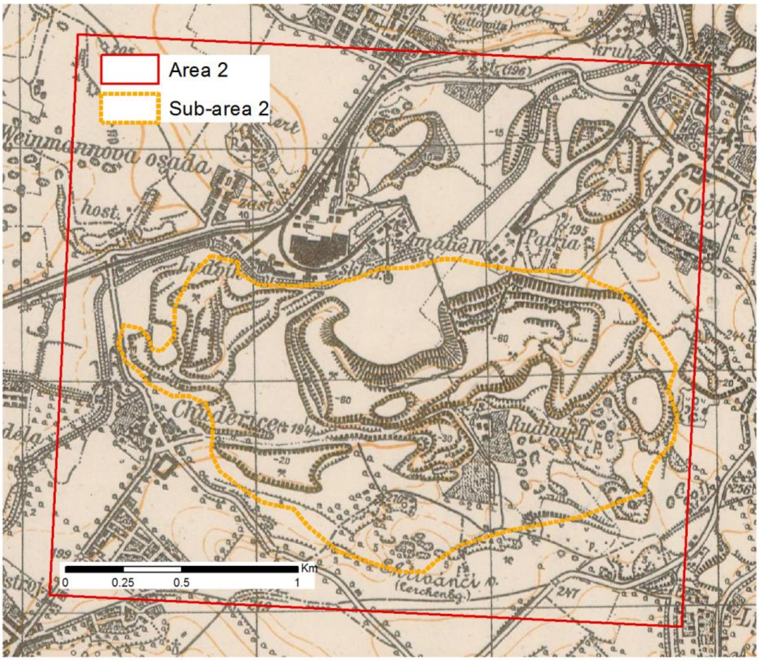

Fig. 13 The original state of Area 2 in the year 1936

Fig. 14 The current state of Area 2 in the year 2008

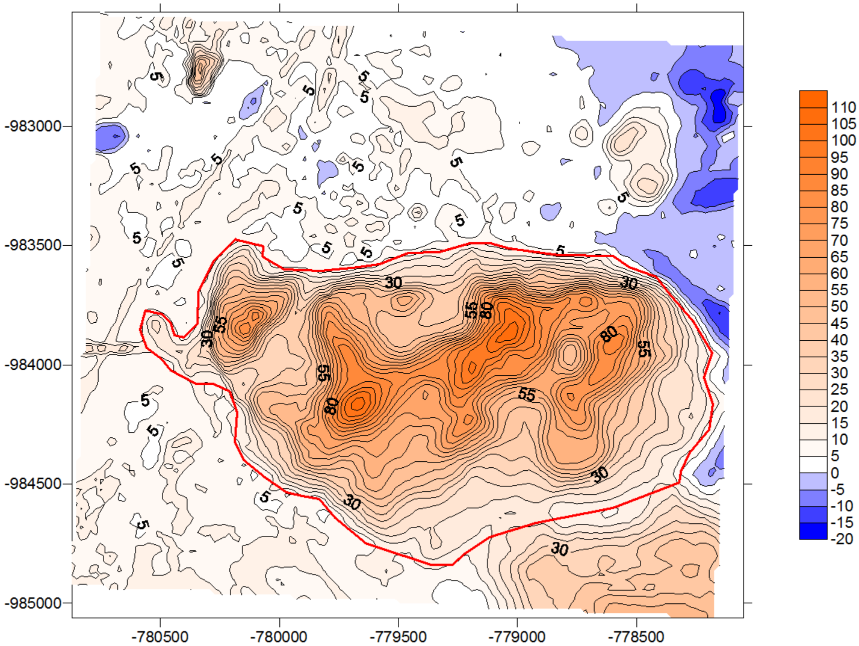

Fig. 15 Differences of Digital Surface Model – year 1995 (DSM_1995) and Digital Surface Model – year 1938 (DSM_1938) with delineated Sub-area 2

CONCLUSION

In this paper are presented possibilities for reconstruction of irreversibly changed georelief, using aerial images and old maps. We have selected the Sample testing areas in the center of our study region Bílina to test the proposed methodology.

The old maps are used as a source of elevation data in areas with a large change of the landscape. In this paper were the old maps georeferenced using a spline transformation (rubber sheeting) with a huge number of identical points – 150 to 250 per map sheet. This transformation method provides sufficient accuracy for the purpose of this project. A Digital Terrain Model (DTM) was interpolated from the hand-vectorized contour lines of the 1936 map.

The historical and recent aerial photographs were photogrammetrically processed. All of the images have a 60% overlap, thus we were able to create the automatically generated Digital Surface Model (DSM) for the year 1938 and 1995. The automatic DSM creation based on pixel correlation is not producing absolutely precise results for the year 1938, as the images are scratched and influenced by the technology of original picture creation (camera's focal length 211.59mm and the image scale ca. 1:18 000). We have as well faced the problems with identifying the Ground Control

Points (GCP) in areas with the large land use and georelief change. The produced DSM for the year 1995 is precise.

The amount of material that has been mined or added in the depicted areas during the period 1938 – 1995 can be computed from created DTM's and DSM's using a volumetric analysis. The material amount is 930 015 080m^3 of material mined from area 1B and 101 282 997m^3 material added into Area 2.

The results have shown that the computation may be refined by the usage of DTM's instead of DSM's - especially for the year 1938. This will require manual DTM extraction from recent and historical aerial images. This methodology will be applied of the whole Area of interest and the final result of our analysis will show us in numbers the effect of mining activity in the Bílina region.

REFERENCES

ČUZK, Základní báze geografických dat ZABAGED ® *[online].[cit 2010-20-10]*. URL: http://www.cuzk.cz/Dokument.aspx?PRARESKOD=998&MENUID=0&AKCE=DOC:30-ZU_ZABAGED

ESRI ArcGIS Desktop 9.3 Help *[online].[cit 2010-20-10]*. URL: http://webhelp.esri.com/arcgisdesktop/9.3/

Ekologické centrum Most pro Krušnohoří: Černý trojúhelník [online]. [cit. 2010-20-10] URL: http://www.ecmost.cz/ver_cz/aktualni_sdeleni/cerny_trojuhelnik.htm

Jenny, B., Weber, A. (2010) Map Analyst *[online]. [cit 2010-20-10] URL:* http://mapanalyst.cartography.ch/

Kennelly, P., Kimerling, A. (2001) Hillshading Alternatives *[online].[cit 2010-20-10]*. URL: http://www.esri.com/news/arcuser/0701/althillshade.html

Mitas, L., Mitasova, H. (1988) General variational approach to the interpolation problem. Computers and Mathematics with Applications,16, p.983-992.

Mitas, L., Mitasova, H. (1993) Interpolation by regularized spline with tension: I. Theory and implementation. Mathematical Geology 25, p. 641- 655.

Neteler, M. (2004) Open Source GIS: a GRASS GIS approach, Kluwer Academic Publishers, USA. ISBN: 1-4020-8064-6

Štýs, S. (2000) The Region of Most – A New Born Landscape, Ecoconsult Pons Most. Most, CZE.

USING MODERN GIS TOOLS TO RECONSTRUCT THE AVALANCHE: A CASE STUDY OF MAGURKA 1970

RICHNAVSKY Jozef, BISKUPIC Marek, MUDRON Ivan, DEVECKA Branislav, UNUCKA Jan, CHRUSTEK Pawel, LIZUCH Milan, KYZEK Filip and MATEJICEK Lubos

Institute of Geoinformatics, Faculty of Mining and Geology, VŠB – Technical Univerzity of Ostrava, 17. listopadu 15, 708 00, Ostrava Poruba, Czech Republic
jozef.richnavsky@vsb.cz, ivan.mudron@vsb.cz, branislav.devecka@vsb.cz, jan.unucka@vsb.cz

Institute of Environmental studies, Faculty of Science, Charles University in Prague, Benátská 2, 12801, Praha 2, Czech Republic
mabis@seznam.cz, lubos.matejicek@gmail.com

Avalanche Prevention Centre of Mountain Rescue Service, Jasná 84, 032 51 Demänovská dolina, Slovak Republic
slp@hzs.sk

Institute of Geography and Spatial Management, Faculty of Biology and Earth Sciences, Jagiellonian University, Gronostajowa 7, 30-387, Cracow, Poland
p.chrustek@annapasek.org

Abstract

A huge avalanche released on 14 March 1970 from the saddleback of Ďurková below the Low Tatras mountain ridge, which ran down through the whole valley and stopped close to the settlement of Magurka. The length and height of the avalanche path was enormous reaching 2,2 km and 22 meters high respectively. Taking other parameters into consideration (the length of the avalanche, the height of the avalanche release zone, total volume of snow) it can be categorised among the greatest avalanches ever observed in Slovakia. The major causes for such a big avalanche were unfavourable long-lasting snow and weather conditions. However, the starting mechanism was, as in most cases, a man. RAMMS model was used for avalanche reconstruction. It allows modelling the height of avalanche deposition, the speed of an avalanche flow and also the maximum pressure that was reached. All the required input data were derived from historical information, photographs and maps and also from the statements of the witnesses of this avalanche event. The avalanche has been successfully simulated and reconstructed. The total volume of deposited snow (relative deviation 0.16%) revealed that the simulated released area and other input parameters were precisely approximated. Small deviation between simulated and measured avalanche runout zone refers to good calibration of friction parameters. The result of the modelling will enable us a better understanding of the complete progress and action of this avalanche during its motion. The results can be also applied to planning and

constructing of anti-avalanche structures and to minimizing the negative consequences of similar avalanche in the future.

Keywords: avalanche, modelling, reconstruction, Magurka, runout zone

INTRODUCTION

For centuries, people have been altering the Earth's surface to produce food and gain material or energy through various activities. The urban areas are being enlarging backcountry skiing areas spreading fast etc. Over the last years, more people are coming to the mountains, building new cottages and cabins underneath, spending more time in the countryside. Magurka surroundings are no exceptions. The mountains are becoming overcrowded and the fact that people are dramatically enhancing the avalanche risk is well known. This was also the case of the Magurka 1970 tragedy, when four skiers triggered the avalanche. Three of them died. To avoid the risk of tragedies in the mountains of Slovakia, it is important to undertake more studies involving GIS. This paper deals with avalanche reconstruction applying the avalanche dynamics program RAMMS. Modern numerical simulation tools are frequently used for avalanche prevention in USA, Canada and some alp countries, especially in Switzerland and Austria. On the other side, in Slovak Republic as well as in Czech Republic, these tools have not been used yet. The aim of the paper is to show that this historical process can be reconstructed with modern technologies and give some useful information, which can be used nowadays

DESCRIPTION OF AVALANCHE EVENT

Weather conditions were good on March 14, 1970. Four skiers came to the saddleback of Ďurková passing the main ridge from Chopok. One of them was slightly injured, so they decided to go down all the way to Magurka settlement. They started to traverse to the right crest, and so releasing one of the greatest avalanches in Slovak history. The total amount of deposited snow was 65 000 m3, i.e. about 200,160 tons of snow. This snow deposition was stretching over 1.8 km and the front was from 20 to 25 m high. This mass of snow did not melt the following summer. The avalanche was 2.2 km long and was extending on the total area of 35.8 ha. The release area was 340 metres wide and the vertical drop between the top of the release and avalanche front was 620 m. The released snow layer varied from 1.8 metres on side ridges to 12 metres in gullies. In this mass of snow the rescue team (517 rescuers) could not find the victims for 26 days. The last victim's body was found on 6 June.

AVALANCHE SIMULATION

Modern numerical simulation software package RAMMS was used for avalanche simulation. RAMMS (*RApid Mass MovementS*) model calculates the motion of geophysical mass movements (including snow avalanches) from initiation to runout in three-dimensional terrain (Christen, 2010). It has been developed at the WSL Institute for Snow and Avalanche Research SLF in Davos. Model RAMMS can be used for accurate prediction of avalanche runout distances, flow velocities and impact pressures of avalanches. For this case of study, we have used this model for calculating the snow height in avalanche deposition and for understanding the avalanche motion. Input data were gained from historical records, studies and photos. The same data were used also for calibrating the model (calibration of friction parameters) to obtain sufficiently accurate simulation. Required input data for model RAMMS are mentioned below. Well prepared data are essential for the quality of the model results.

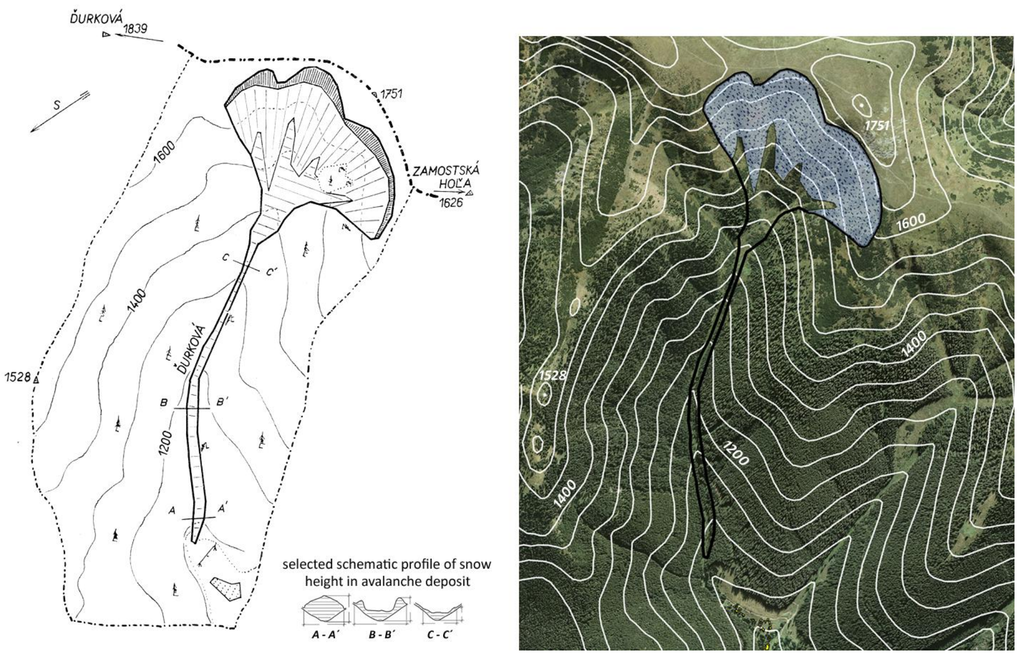

Fig. 1. Schematic location outline and its presentation in ArcMap software

Release zone

Sufficiently precise reconstruction of avalanche release's parameters has the biggest influence on exactness of simulated result. The characteristics of release determine directly the volume of avalanche snow mass. They determine the velocity of avalanche and the kinetic energy of avalanche together with the influence of terrain attributes. Hence, the reconstructed allocation of release, its shape and length of the avalanche has to be done correctly not to derive incorrect inputs. The reconstruction was deduced from schematic location outline, historical records and pictures. The main attributes of avalanche release are mentioned in Table 1. The maximum of 12 m height release were recorded in the channel due the weather conditions. Snow accumulation is taking place, especially in channels or smaller gullies under the main range. So, 12 m height is not a rare value. According to the attributes, primarily to the length, it is one of the largest avalanches observed in Slovakia. Fig. 1. shows the location outline of avalanche area, which was geotransformed and subsequently vectorised in ArcMap.

Table 1. Basic parameters of avalanche release

length of fracture line	maximal snow height	minimal snow height
1500 m	**12 m**	**1.8 m**

One of the fundamental problems in avalanche modelling is an accurate definition of release zones. It is very difficult to define release areas with responsible release heights in three-dimensional terrain. In avalanche modelling, it is common to set one release height for whole release area because of ease, simplicity and rate of calculation. In this case we have tried to simulate and reconstruct historical avalanche with big span of threshold release heights (1.8 m – 12 m). With consideration to the biggest approximation to the reality, our approach the release area was to divide it into few smaller areas with different release heights.

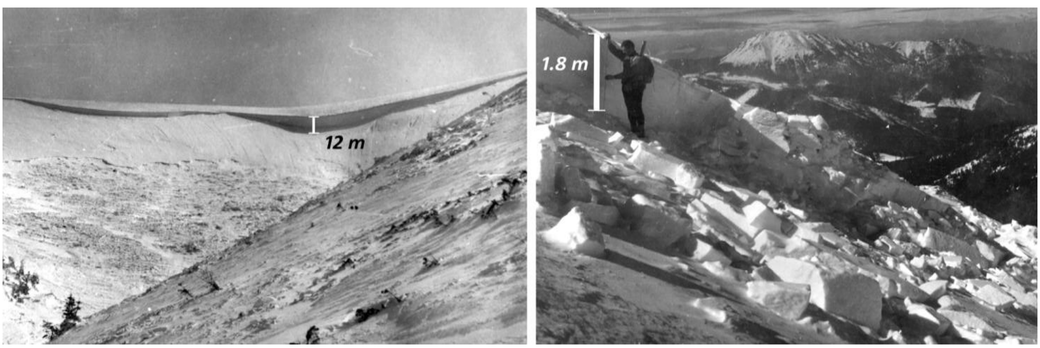

Fig. 2. Big differences in release snow height in range 1.8 up to 12 m

Terrain parameters

A terrain is considered to be a permanent, stationary factor in avalanche forecasting. So, we can use present terrain parameters also for simulation of historical avalanche events. We do not assume that there were some considerable changes in terrain proportions between years 1970 and 2010. We used digital elevation model of the study area for simulation in model RAMMS. It was derived from contours in a basic topographic map of research area with scale 1:10 000. Spatial resolution of DEM was set to 2 m (this is the value recommended for detailed avalanche simulation in RAMMS). This is accurate enough for including small terrain features, like big boulders, gullies, needles and depressions into the simulation. A good digital representation of the topography is crucial for the accuracy of the model results, especially in sensitive areas, such as small gullies and mountain ridges (Haeberli, 2004). In this case, interpolation method Topo to Raster in ArcMap software was used to determine the digital terrain model of study area.

Forest cover

The forest cover significantly inhibits or even stops avalanche flow. Thus, it significantly influences avalanche flow direction, flow velocity, and subsequently also the resulting shape of an avalanche path. To reach the most precise reconstruction of the avalanche, impact of the given forest cover was also needed to be included into the simulation. But, when the impact pressure of avalanche is more than about 100 kPa (threshold value for uproot mature spruce), inhibiting effect of the forest cover become insignificant. Large avalanches often break trees and develop into a mixed flow of snow and trees, creating greater mass with increasing damage potential. As we wanted to include information about the forest cover into the simulation, we needed to obtain this information from the date before March 1970. For this purpose the basic topographic map from the year 1956 was used. The comparison between the forest cover before simulated avalanche and the present state of the forest cover is shown in Fig. 3. Forty years are quite a long term and differences in the forest cover are significant. Therefore it is so important to use adequate information about the forest cover for avalanche modelling. Other important factors related with the forest cover (cover density, height of trees, species diversity) have influence, but the forest occurrence is sufficient for precise modelling results using model RAMMS (boolean raster layer: 0 for no forest, 1 for forest areas).

Fig. 3. Differences in forest cover in years 1956 and 2010

Inhibiting and obstacle effect of dwarf pine was not considered into this calculation due to extensive height of snowpack. The dwarf pine cover influences avalanche formation only in case, when the height of the snowpack is smaller than the height of the dwarf pine cover.

Snow density of release area

The density of released snow is another important factor linked with avalanche modelling and with model RAMMS. There are no precise measurements of snow density in historical records. However, it can be assumed that reconstructed avalanche was a hard dry slab avalanche. This precondition was derived on the grounds of historical photos (Fig. 4). A hard slab usually has large chunks of debris in the deposit. They are evidently recognized on these photos. A sharp bounded breakaway wall of top periphery of the slab is another characteristic feature for dry slab avalanches. It is also visible on these Figs. Large amount of snow in gullies is the result of snow transporting due to blowing wind. Wind packing can produce dense, cohesive snow, which aids in slab formation (McLung & Schaerer, 2006). These slabs are usually very brittle with low cohesion with the snow layer beneath. Generally speaking, most slabs consist of cohesive wind-deposited or well-bonded old snow. Average density for such snow is about 200 kg/m^3 with the range of 50 to 450 kg/m^3 (McLung & Schaerer, 2006). From the sample on Fig. 4., nearly 90% of these avalanches have average densities between 100 and 300 kg/m^3. Densities below and above this range are rare. The value 200 kg/m^3 was set as the best estimation and was used in the avalanche simulation in model RAMMS. Dry slabs are responsible for most of the damage and fatalities from avalanches. According to world injury statistics, 90 % of these slab avalanches were triggered by mountain visitors themselves.

Fig. 4. Large chunks of debris in the deposit, typically for dry slab avalanches

SIMULATION ACCURACY

Simulation accuracy is given by comparison of the simulated results with the real measured data obtained by the field research in 1970. The differences between the simulated results and the measured values are shown in the Table 2. It is necessary to mention that the precise measurement of parameters (volume, area) in 1970 was difficult. Still, it is impossible today to make precise measurements of such a big avalanche without using GIS technologies (LIDAR, modelling, etc.). Due to proper calibration method close approximation of real measured avalanche runout zone (Fig. 5.) was reached. The deviation from the real measured runout zone was statistically insignificant as well as the deviation of total avalanche volume. In spite of this, the height of avalanche front was not successfully restored (Fig. 6.). The real height of avalanche front exceeds simulated value considerably. The difference in the total avalanche area is observed mainly on the upper right part of the slope. This is due to inaccuracies in DEM representation and in localization of release area. Comparisons of all simulated results with real measured data are shown in Table 2. The relative deviation from the measured data was calculated as the ratio of difference to the measured value in 1970. The value of total area was set to recalculated data from 1970 using GIT (39.1 ha). Sequences of avalanche simulation in different computing time steps are shown in Fig. 7. A single sequence is showing the maximum height of moving snow. Profile B (Fig. 5.) is revealing a significant unevenness in the deposit surface. It was testified by eyewitnesses and historical photos.

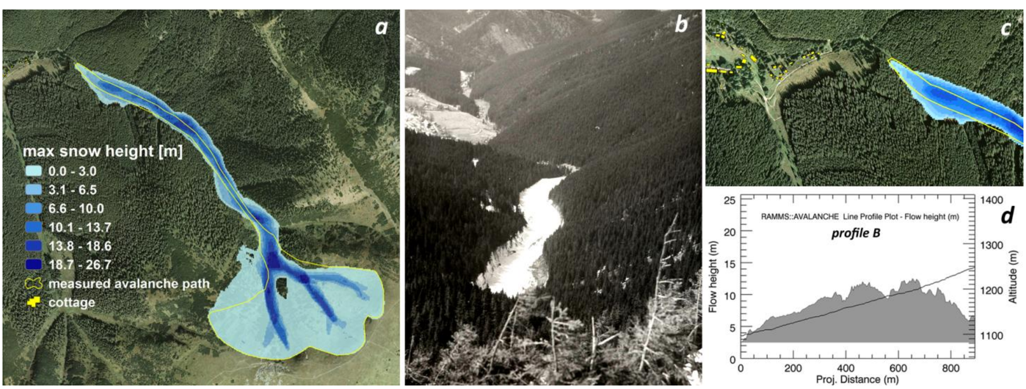

Fig. 5. Maximal snow height from avalanche simulation (a) and comparison of its runout zone with real measured data (c). Simulated snow height in longitudinal profile of avalanche deposit (d), which is captured in the historical photo (b)

Table 2. Comparison of the simulated results with real measured data

Parameter name	Measured 1970	Simulated 2010	Difference	Relative deviation
Avalanche length	2 200 m	2 221 m	21 m	0.95 %
Snow deposition length	1 800 m	1 725 m	75 m	4.17%
Snow deposition volume	625 000 m^3	626 028.7 m^3	1028.7 m^3	0.16 %
Front height	20 – 25 m	4 – 5 m	16 – 20 m	80.00%
Total area	35.8 ha (39.1 ha)	51.38 ha	12.28 ha	31.41 %
Vertical drop	620 m	622 m	2 m	0.32 %

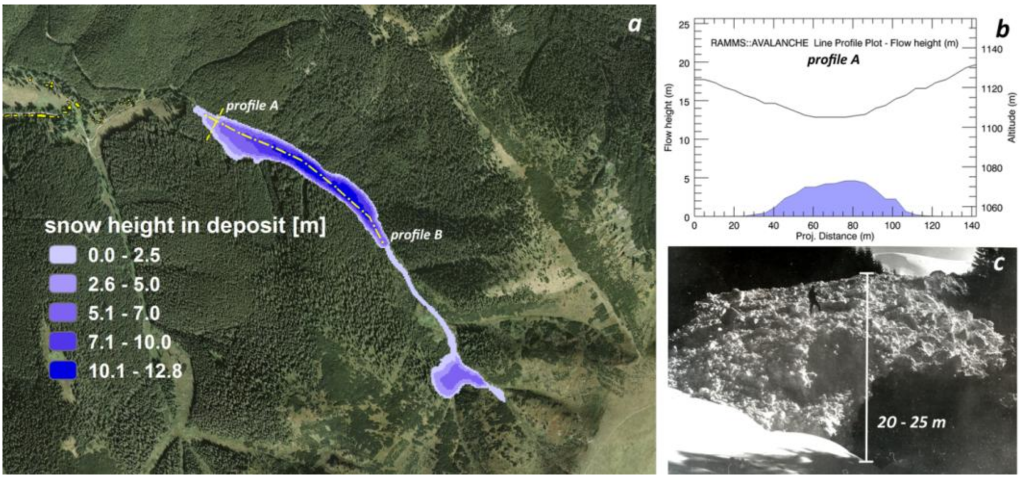

Fig. 6. Snow height in avalanche deposit and lines of cross and longitudinal profiles A and B (a). Real snow height of avalanche front (c) exceeds simulated value in profile A (b) considerably

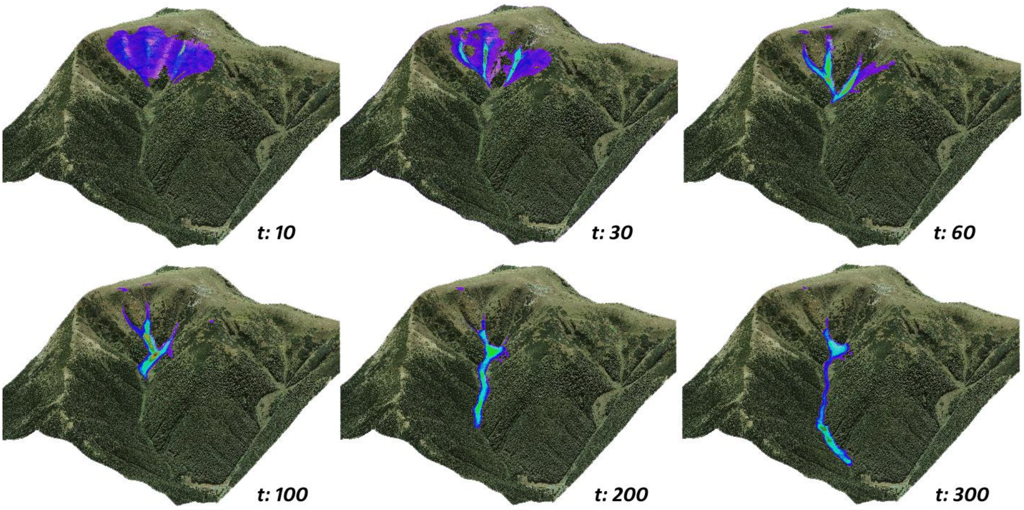

Fig. 7. Sequences of simulation in different time steps of calculation (t: 10 – t: 300)

RESULTS APPLICATIONS

One way of simulation results applications is determining established calibration friction coefficients (*Mu, Xi*). These friction coefficients determine the surface friction in different heights. Coefficients, which were determined and used in one valley, can also be used in avalanche simulations in the adjacent valleys. There is a big probability that surface resistance to the avalanche flow will be similar in adjacent valleys as well. This piece of knowledge was used for modelling potential avalanche events in the valley of Viedenka, which is situated to the west of Ďurková valley. In contrast with the reconstructed avalanche in the Ďurková valley, similarly great avalanche in the valley of Viedenka will affect significantly the urban space of Magurka settlement. Many cottages in this settlement will be damaged or ruined as a consequence of destructive power of a similar avalanche. In this locality, some experimental simulations were calculated with different heights of potential release zones. Fig. 8. shows results of particular cases of these simulations. It is obvious that a fracture height more than 2 m causes a significant spreading of the runout and more cabins are endangered.

We have alluded to prevention until now. Now, we turn to the usage of avalanche reconstruction when endangered areas are revealed. In practice, there are cases, when infrastructure, important facilities or parts of urban sprawl are a part of an endangered area. Model RAMMS can be a useful tool for designing and allocating anti-avalanche barriers, such as an avalanche dam. Parameters of these dams can be included into the digital representation of topology. Avalanche simulation can be undertaken in different scenarios with or without these barriers. A well-placed and designed avalanche dam manages to stop or divert the direction of the potential avalanche flow in order to protect the lower situated infrastructure. For facilities placed in avalanche path, it is the only way of protection.

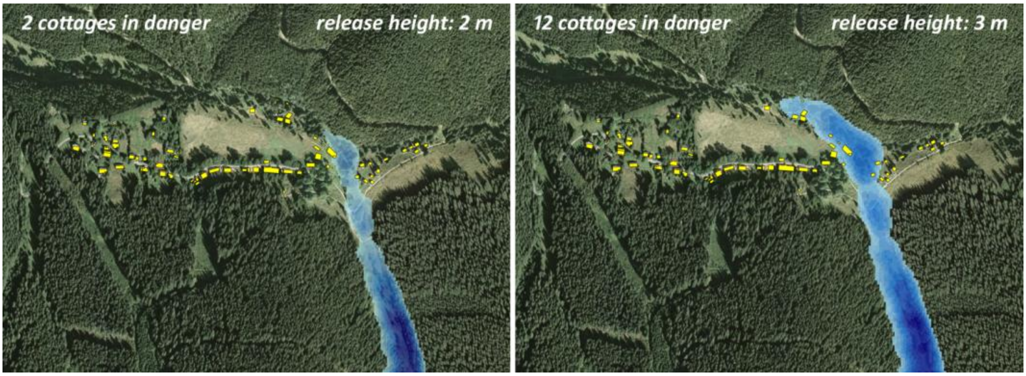

Fig. 8. Comparison of conclusions from potential avalanche with different release heights

CONCLUSION

The introduction of GIS technology opened up new perspectives to mapping and assessing hazards from snow avalanches. The purpose of mapping snow avalanche hazards is to consider avalanche risks with respect to land use planning (Haeberli, 2004). Numerical models (like RAMMS), coupled with field observations and historical records are especially helpful in understanding avalanche flow in complex terrain (Christen et al., 2008). They are very helpful in avalanche research in the given region. Simulations, like this in this case of study, are useful in understanding of all processes and actions, which are connected with avalanche. The avalanche modelling is particularly important and applicable in the avalanche protection. The results can be applied to planning and constructing of anti-avalanche structures and in this way they can minimize the negative results of a similarly destructive avalanche in the future. It is obvious that the simulated result differs from the phenomenon measured in 1970, although the deviation is not serious. The most important attribute for the avalanche hazard mapping is the length of the avalanche, which was successfully modelled. There are more reasons why differences in other attributes appeared. First of all, we have to mention that RAMMS simulation result is a model, which cannot include whole complex reality. The next reason is the input data; especially, the digital elevation model uncertainties leading to greater divergence. There will never be a model as same as the true state of nature. It is impossible to include every small bush, the precise distances between the trees etc. in the forest cover, or include every small depression in the valley, which is filled by additional snow. Next is the fundamental modelling problem such as definition of release areas in three-dimensional terrain. The difficult estimation of snow entrainment, which greatly affects overall snow mass, contributes too. One of the other drawbacks is the estimation of the height of stauchwall and the other heights (volume) of released snow. Just because of these drawbacks, it is impossible to make a perfect fit. There are much more reasons, which influence the result e.g. the historical documents (sketches, sampling etc.) were made in the era, when no computers and other advanced tools could help. Despite all these reasons, modern GIS numerical tools are able to truly reconstruct an avalanche event and this research was a good demonstration of it.

ACKNOWLEDGEMENTS

We would like to acknowledge the SGS project SV5480051/2101 from VSB TU-Ostrava. Special acknowledge belongs also to the Avalanche Prevention Centre of Mountain Rescue Service in Jasná and to Mr. Ladislav Milan for provision of historical photos and records of this avalanche event.

REFERENCES

Gruber, U. (2001) Using GIS for avalanche hazard mapping in Switzerland. *Proceedings of the 2001 ESRI International User Conference*, San Diego, s. 21.

Haeberli, W., et al. (2004): GIS applications for snow and ice high-mountains areas: Examples for the Swiss Alps in Geographic Information Science and Mountain Geomorphology. Chichester, UK, pp. 381 - 402

Christen, M, et al. (2010) *RAMMS User manual v 1.01 : A modeling system for snow-avalanches in research and practice.* Davos, Švajčiarsko.

Christen, M, et al. (2010) Back calculation of the In den Arelen avalanche with RAMMS: interpretation of model result. In Annals of Glaciology, vol. 52 issue 54, International Glaciological Society. 161 – 168.

Christen, M, et al. (2008) Calculation of dense snow avalanches in three-dimensional terrain with the numerical simulation program RAMMS. In *International Snow Science Workshop.* Whistler, BC, CAN, pp. 192 - 211.

McLung, D; Schaerer, P. (2006) *Avalanche Handbook*. The mountaineers book, Seattle, USA.

ANALYZING RADAR-MEASURED RAINFALL VS. RAIN GAUGES IN GIS

MÜLLER Arnost

Department of Mapping and Cartography, Faculty of Civil Engineering, Czech Technical University, Thákurova 7, 166 29 Praha 6 – Dejvice
arnost.muller@fsv.cvut.cz

Abstract

Rainfall data are traditionally collected at discrete point locations in space, at meteorological stations (rain gauges). Values at any other point must be interpolated or can be remotely sensed by ground-based radar, which can detect the areal distribution of precipitation at more detailed spatial scale. Nevertheless, radar measurements are affected by various types of errors and the transformation of measured radar reflectivity into rain rates is far from accurate. This study provides a deeper analysis of the influence of topography on radar measured precipitation.

By the means of linear regression analysis residuals between 134 rain gauges and corresponding radar estimated rainfalls were calculated, and then studied using residual regression analysis with the following independent variables: altitude, longitude, latitude, aspect, slope, curvature, distance from the radar antenna, aspect perpendicular to the radar beam referred to as directional difference, mean air temperature, and solar radiation. The independent variables were derived from the 90 m SRTM DEM in ArcGIS. A multivariate second order polynomial regression model was developed with three topographic and locational variables as the best predictors: altitude, distance, and latitude, which can explain up to 74% of variance of the residual errors. This means that radar measurement errors are not only a cause of random variation, but can be partially predicted, which may allow for some type of correction and improvement in radar's accuracy.

Keywords: rainfall, rain gauge, radar, GIS, regression, terrain analysis

INTRODUCTION

Precipitation, as one of the basic climatological factors, is used as an input in various models in hydrologic modeling, e.g. flood prediction, in agriculture applications for estimating yields, in land management, or in atmospheric simulation models. Rainfall data are traditionally collected at meteorological stations (rain gauges), which are discrete point locations in space. Values at any other point must be derived from neighboring meteorological stations or can be remotely sensed, e.g. by ground-based radar. The main advantage of rain gauges is a fine temporal resolution. In fact, gauges record continuously and are able to detect even short (minute) rainfalls. Rain gauge observations are still considered as close to true rainfall as we can get at present state of art technologies.

While rain gauges measure at discrete locations, weather radar samples at discrete time instances (e.g. every 10 minutes). Radar's main advantage is that it can 'see' much larger atmospheric space than rain gauges located on the ground. Radar can detect the areal distribution of precipitation at more detailed spatial scale than rain gauge network and therefore, the final rain field pattern should be determined by radar, as recommended by Krajewski. However, precipitation obtained only from radar data cannot be directly used because radar measurements are affected by various types of errors and the transformation of measured radar reflectivity into rain rates is far from accurate.

The objective of this study is to test the influence of following topographic, locational and atmospheric variables on residual errors: altitude, longitude, latitude, aspect, slope, curvature, distance from the radar antenna (DIST), aspect perpendicular to the radar beam referred to as directional difference (DIF), mean air temperature and solar radiation. Residual errors are calculated as the difference between radar-estimated rainfall and rain gauges observations, which are considered as a good approximation of the true ground rainfall. If some factors influencing residual errors are found significant, this would mean radar errors are not random and therefore can be removed by some type of correction.

DATA AND METHODS

Radar images can be imported into a Geographic Information System (GIS), which provides a standard means to display, overlay, and combine the data with other layers, e.g. topographic, for analysis. Regression analysis is applied to determine the relationship between rain gauges and radar estimates. Residual analysis using regression approach is then applied to study factors influencing residuals, which provides insight into radar measurement errors. According to the data provided by the Czech Hydrometeorological Institute (CHMI), the analysis is performed with annual estimates of 134 meteorological stations in the year 2008.

Study area is the area of the whole Czech Republic. The Czech radar network (CZRAD), operated by the CHMI, consists of two polarization C-band Doppler radars. Optimal location of the radars with respect to topography causes reflectivity to be significantly influenced by terrain blockage of radar echo only in small areas of the CR. Monthly raw radar rainfall sums (already combined from both radars) for the year 2008 were obtained in two-dimensional binary format (.RPD), were imported into ArcGIS and visualized (fig. 1.) using the same color schema as CHMI uses for radar estimated rainfall representations.

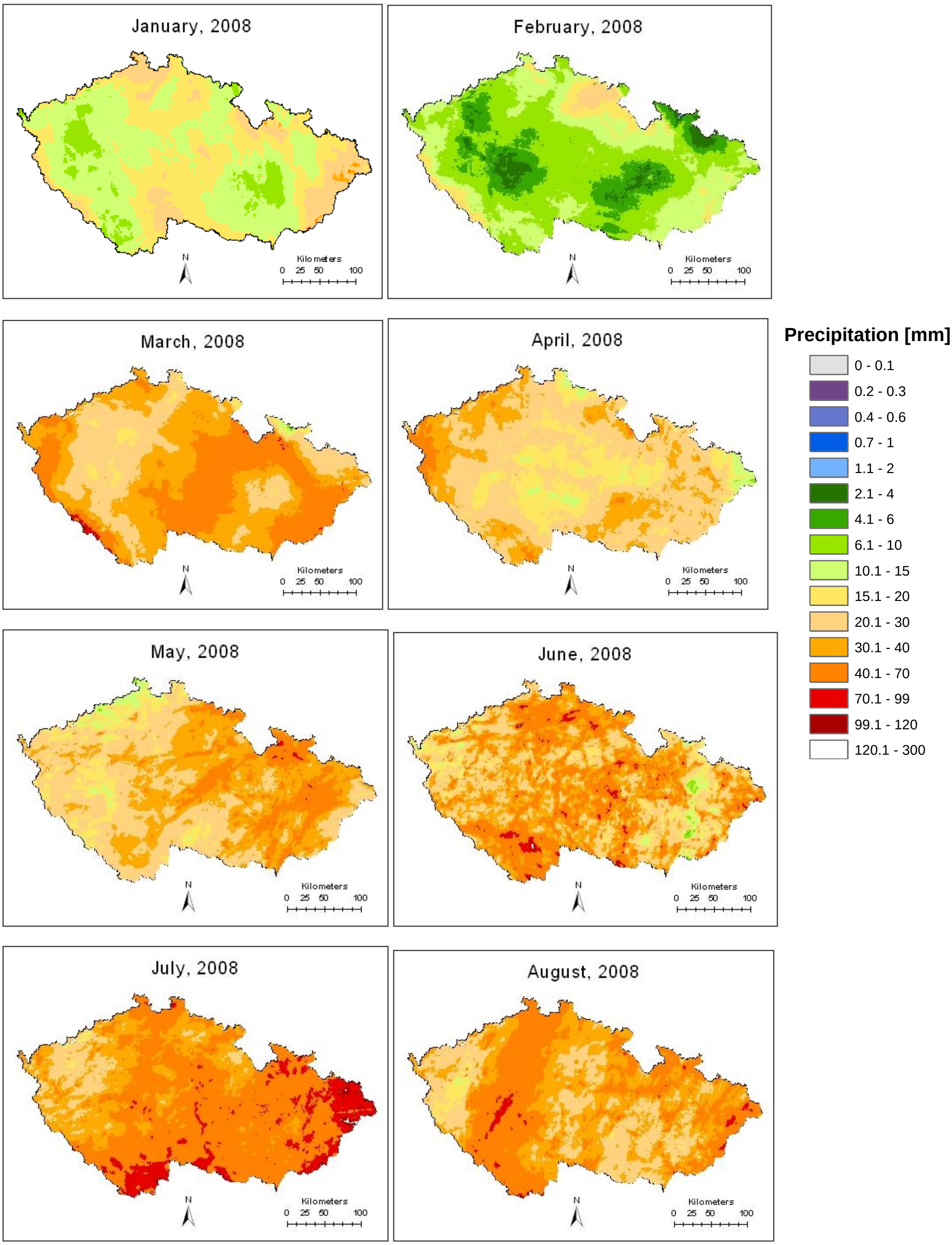
January, 2008
February, 2008
March, 2008
April, 2008
May, 2008
June, 2008
July, 2008
August, 2008
N
Kilometers
0 25 50 100
Precipitation [mm]
0 - 0.1
0.2 - 0.3
0.4 - 0.6
0.7 - 1
1.1 - 2
2.1 - 4
4.1 - 6
6.1 - 10
10.1 - 15
15.1 - 20
20.1 - 30
30.1 - 40
40.1 - 70
70.1 - 99
99.1 - 120
120.1 - 300

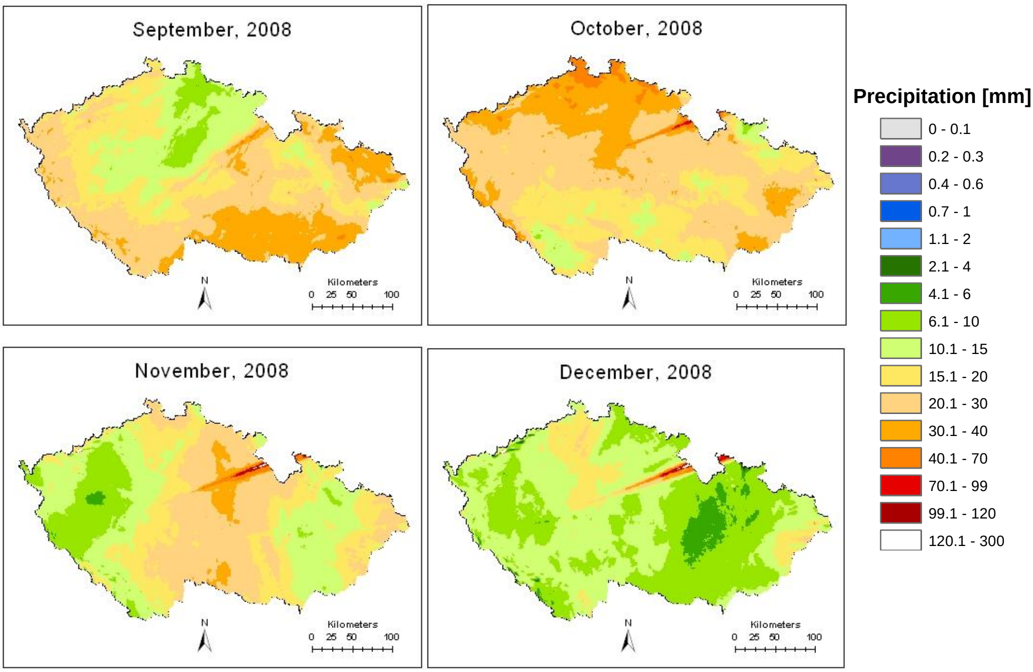

Fig. 1. Vizualisation of input data (monthly radar sums of precipitation in 2008)

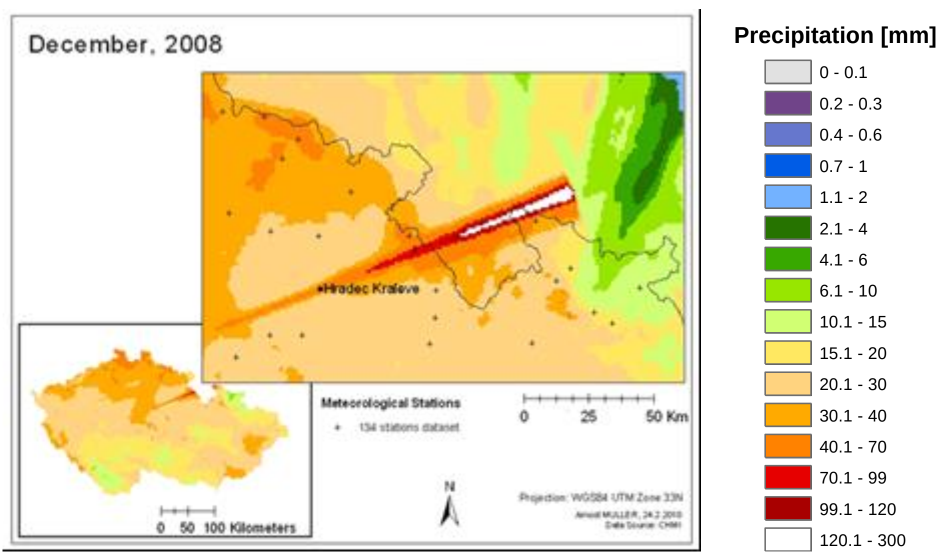

Fig. 2. The artificial 'precipitation beam' pattern caused by a microwave telecommunication link interfering with radar signal.

Fig. 2. displays a 'precipitation artifact', which appears in the data from September till November 2008. It is caused most likely by a microwave telecommunication link

(probably by Wireless Local Area Network, WLAN) interfering with radar signal. Stations lying within this artifact are discussed later in the Analysis section.

Topographical data come from the digital elevation model (DEM) from the NASA/NGA Shuttle Radar Topography Mission (SRTM). Horizontal resolution of SRTM global datasets is 3 arc seconds, for latitudes in the Czech Republic each pixel represents 90 x 60 m. Variables derived from the DEM have the same spatial resolution. The vertical accuracy of the DEM characterized by RMSE (calculated from differences in real altitudes of 134 meteorological stations and altitudes derived from the DEM) is 7 m. Derived topographic variables are: slope, aspect, curvature, solar radiation, distance from the radar antenna and the variable named directional difference (DIF).

Directional difference is derived from aspect using GIS techniques. The difference between direction to the radar antenna (DIR) and aspect is calculated as

DIF=| cos(ASPECT-DIR) |

The mathematical meaning of the DIF variable is illustrated in fig. 4 on the left. When ASPECT-DIR = ±90 or ±270, the aspect is perpendicular to the radar beam. When ASP-DIR = 0 or ±180, the aspect is facing the same direction as the radar beam

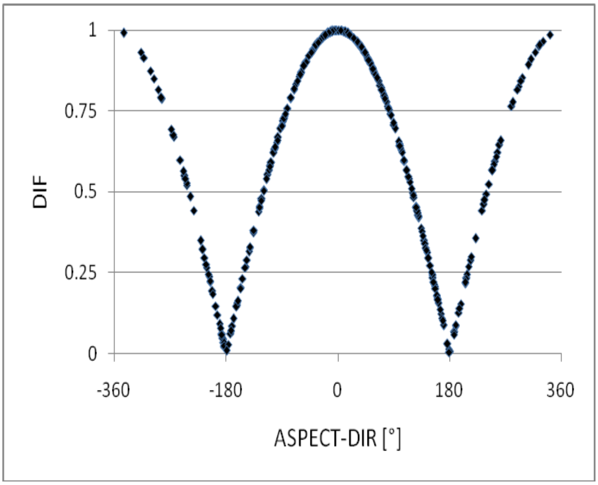

.**Fig. 4.**: Chart explaining the meaning of the variable DIF

Fig. 5. illustrates the direction of the radar beam, which is then subtracted from aspect. Fig. 6. shows the variable DIF resampled to 1 km grid. Variable DIF was resampled from 90 m spatial resolution to 1 km as well as 10 km.

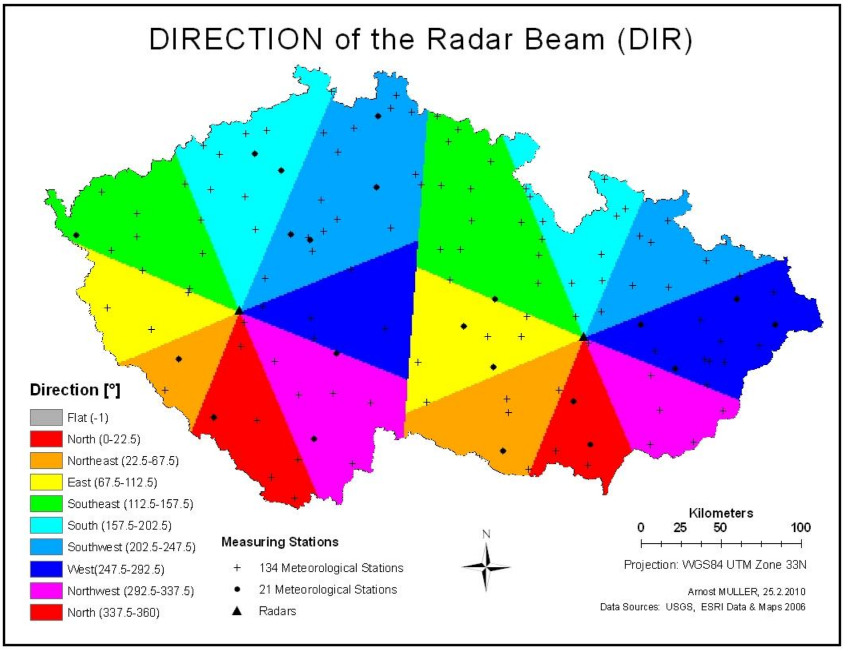

Fig. 5.: Direction of the radar beam (DIR)

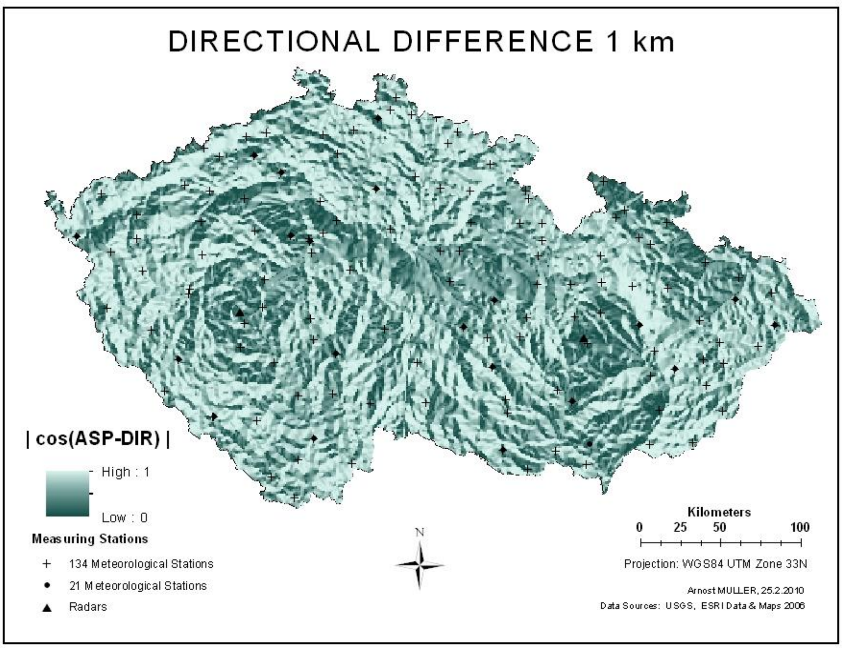

Fig. 6: Directional Difference (DIF)

ANALYSIS

Gauge measurements enter the regression analysis as dependent variable and radar rainfall sums as independent variable. The regression relationship is based on the assumption that rain gauge data are true and not biased, while annual radar sums of rainfall are not accurate. The scatter plot in fig. 7. reveals some relationship between rain gauges and radar measurements. The slope coefficient of 1.74 indicates that radar underestimates the gauge rainfall by nearly twofold. The coefficient of determination for annual data R^2=0.18 is low, which means that there is low dependence between gauge and radar precipitation estimates.

One would expect a stronger relationship between the radar and the gauge data since both methods measure the same variable – precipitation. But as noted by Austin, radar samples almost instantaneously (at intervals of several minutes) a volume of atmosphere which has a surface projection of 1 square kilometer. The gauge accumulates continuously rain falling on an area which is smaller than 1 square meter. This error is known as nonrepresentative sampling. Rainfall often varies significantly over distances of less than a kilometer, while it may also change during time intervals of a minute or less. Therefore, the gauge measurements may not be representative of that in the entire area sampled by radar and similarly, radar-estimated rain rates observed instantaneously at any given measurement cell may not be representative of intensities during the intervals between observations.

Radar rainfall integrated in time to represent rainfall accumulations are typically adjusted to rain gauge-based areal average of the corresponding rainfall. The radar data used in this analysis represent raw rainfall accumulations. If those had been calibrated with the gauge measurements, we would see a random noise pattern in the plot.

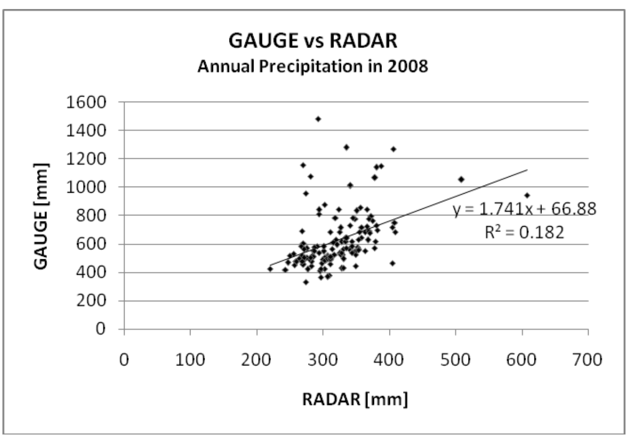

Fig. 7.: Gauge precipitation measurements of 134 meteorological stations plotted against annual radar rainfall sums over the same location

The residual analysis investigates the residuals of the regression model (illustrated in fig. 7.). Residuals (RES) are calculated as

RES = PRED – P

where PRED are predicted values by the regression model and P are rain gauge values. When the residual value is positive, the model (radar) is over-predicting the actual precipitation and vice versa. The highest residual values were found at stations situated in high altitudes where there is generally greater precipitation than in lower altitudes and where radar measurement is less accurate, primarily due to the radar beam being obstructed by mountain ridges. All of the residual values resulting from linear regression were negative, meaning that radar generally underestimates gauge rainfall. One exception was found at the station ‘Hradec Kralove‘, where the residual value was positive. Meteorological station ‘Hradec Kralove‘ lies in a ‘radar beam artifact’ caused by WLAN (refer to fig. 2.). Therefore, this station was excluded from the analysis. Stations ‘Destne v Orl.H.’ and ‘Javornik’ lying in the same ‘WLAN artifact’ did not show any outlying residuals and were not excluded.

Residuals were plotted against several variables (fig. 8.). A linear or a second order polynomial regression curve was fitted through the data to determine any underlying relationships and dependencies between residuals and other variables. This method helps to explain the variation in residuals and reveals factors which affect radar measurements.

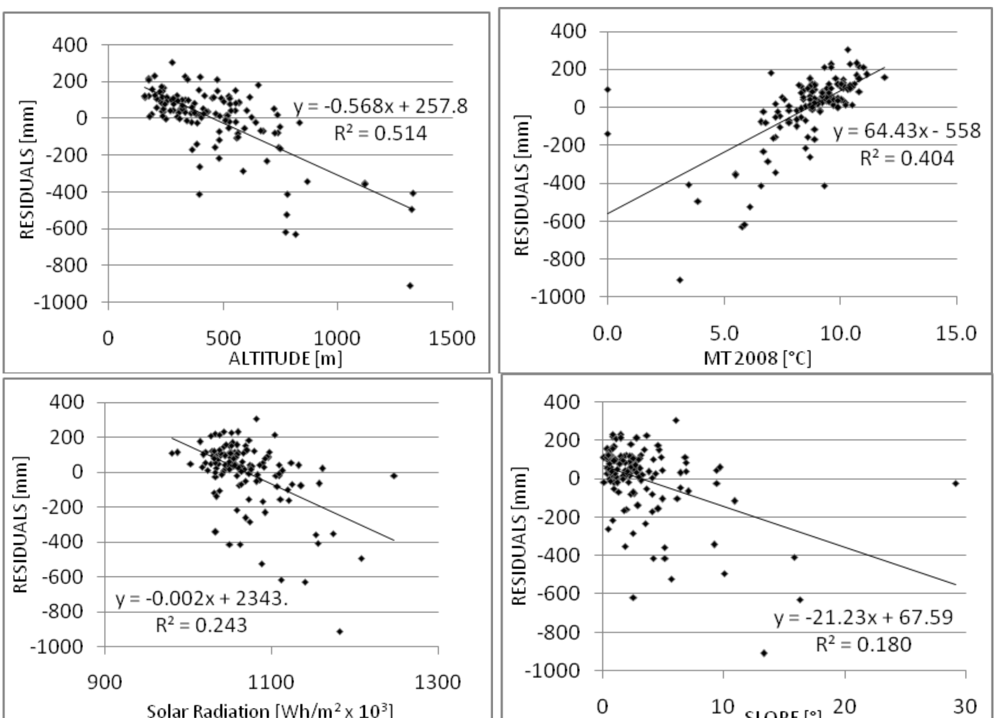

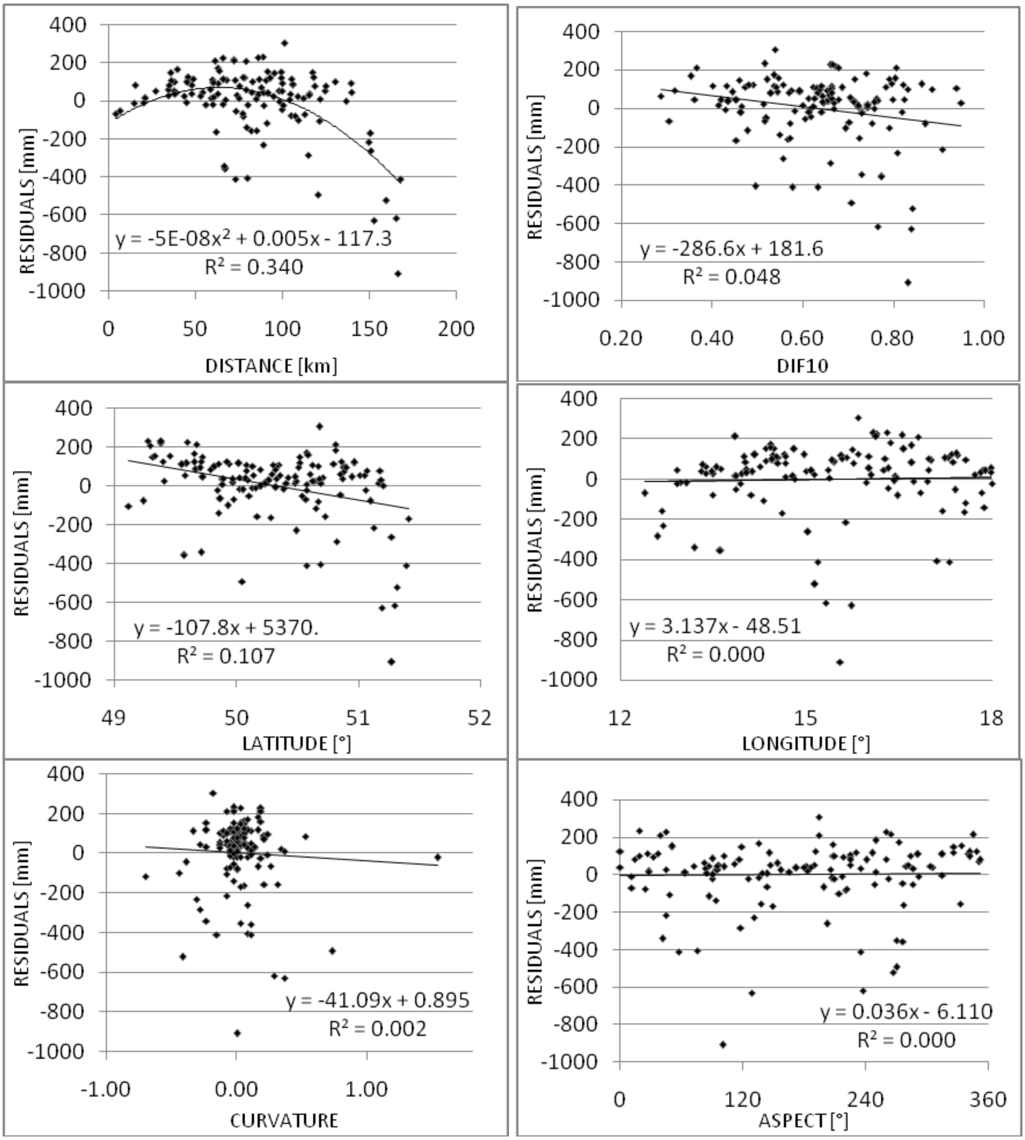

Fig. 8. Residual plots

RESULTS

Radar-derived precipitation generally underestimates gauge measurements and the underestimation increases with increasing distance from the radar. The main causes are the dispersing radar beam and its height above the curved Earths surface.

The relationship between the distance from the radar antenna and residuals is rather quadratic than linear. This can be explained by the stations situated too close or too far from the antenna resulting in higher residuals. Highest residuals (in absolute numbers negative) are associated with those stations farthest away from the radar antenna. Lowest residual values are at distances ranging from 50 to 100 km.

It is generally accepted that attitude significantly influences the spatial distribution of precipitation. The main reason for increasing precipitation with altitude is the orographic lift, which occurs on windward slopes, where the arising air mass expands and cools adiabatically which results in increasing humidity, creating clouds and precipitation. As shown in the corresponding Fig. 8. altitude has a strong influence on residuals. Altitude itself can already explain 51% of variation in residuals. The lowest residuals around 0 are in altitudes between 400 and 500 m. Altitudes lower than 400 m show generally positive residual values, while most of the altitudes above 500 m have negative residual values. The highest residuals appear at the highest altitudes.

Since mean air temperature (MT) can be interpolated over large areas with sufficient accuracy (standard deviation less than 0.5°C) (Müller, 2010), it could also be used as an independent variable in rainfall modeling. However, it should not be used together with altitude, with which it is highly correlated.

Solar radiation was calculated as a theoretical value for the year 2008 in ArcGIS using aspect and slope, and the solar angle. It does not include any actual information about cloudiness. Solar radiation in fig. 8. reveals some linear trend which considering the R^2 of 0.24 could explain ¼ of variation of residuals.

Regarding slope (fig. 8.), the majority of stations lie on flat surface of slope 5° or lower. Generally speaking, the higher the slope, the higher the residuals (in absolute numbers; when negative, it means radar is underestimating).

Directional difference (DIF) beteween the direction towards the radar antenna and aspect describes the horizontal angle of the radar beam and the reflectance area. Higher correlation, but still very low (R^2=0.048), between directional difference and residuals was found for DIF smoothed to 10 km compared to 1 km or 90 m.

Latitude does not reveal any strong relationship with residuals, but the outliers lie in latitudes above 51°, which is around the norhtern borders, where the mountains spread out. Longitude nor curvature nor aspect does not have any significant influence on residuals (R^2=0.0?). In the case of curvature, residual values around 0 spread out around curvature of 0, where the terrain is flat. In other words, higher residuals appear where the terrain is not flat, but curved.

The R^2 values obtained through the residual plots show how certain factors influence the residuals. Tab.1. summarizes the R^2 values which are sorted in descending order according to the linear regression fit.

Factors with the highest R^2 values have the highest influence on residuals and hence can bias radar measurements. Multiple regression analysis was performed with the factors in tab. 1. lying above the dashed line, which was selected arbitrary. Significant factors were identified using backward stepwise approach, which is documented in tab. 2.

Tab. 1.: Coefficients of determination between annual residuals and various factors

	R^2	
	linear	*Polynomial*
ALTITUDE	0.514	0.537
SOLARRAD	0.243	0.246
SLOPE	0.180	0.232
DISTANCE	0.156	0.338
LATITUDE	0.107	0.155
DIF10	0.048	0.051
DIF5	0.041	0.043
DIF	0.019	0.041
CURVATURE	0.002	0.013
LONGITUDE	0.000	0.032
ASPECT	0.000	0.036

Tab. 2.: Backward Stepwise Approach in Multivariate Linear Regression

			ALTITUDE		N_LAT		DIST		SOLARRAD		DIRDIFF10		MT2008		SLOPE	
R^2	**adj. R^2**	**F**	t	*prob.*	t	*prob.*	T	*prob.*	t	*prob.*	T	*prob.*	T	*prob.*	t	*prob.*
0.69	0.67	39	6.99	*0.000*	4.42	*0.000*	2.71	*0.008*	-1.70	*0.092*	1.77	*0.079*	-1.43	*0.155*	0.40	*0.687*
0.68	0.67	46	7.35	*0.000*	4.51	*0.000*	2.77	*0.006*	-1.66	*0.099*	1.76	*0.081*	-1.42	*0.159*		
0.68	0.67	54	10.3	*0.000*	4.66	*0.000*	3.00	*0.003*	-1.81	*0.073*	1.79	*0.076*				
0.67	0.66	66	10.52	*0.000*	4.45	*0.000*	3.57	*0.000*	-1.99	*0.048*						
0.66	**0.65**	**85**	**13.55**	***0.000***	**4.18**	***0.000***	**3.64**	***0.000***								
0.63	0.62	110	13.52	*0.000*	6.30	0.000										

Tab. 3.: 2nd Order Polynomial Multivariate Regression

			ALTITUDE		DISTANCE		$DISTANCE^2$		LATITUDE	
R^2	**adj. R^2**	**F**	T	*prob.*	t	*prob.*	t	*prob.*	t	*prob.*
0.74	**0.73**	**90**	**13.88**	***0.000***	**-4.52**	***0.000***	**5.99**	***0.000***	**2.57**	***0.011***
0.72	0.72	112	13.38	*0.000*	-4.94	*0.000*	7.02	*0.000*		

The best fitting model (in tab. 2. and 3.) is highlighted bold. Significant factors according to tab. 3. are altitude, latitude and DIST. Relationship between DIST and residuals is better described by a polynomial relationship rather than linear. Distance squared was therefore introduced to the regression model to simulate 2nd order polynomial (quadratic) fit, refer to tab. 3.. The results are stronger than in the linear case, since R^2 increases from 0.66 to 0.74.

The three factors included in the multivariate polynomial regression model (tab. 3.) can explain 74% of variance of residuals. This finding is important because it means that the residuals are predictable from topographic and locational variables and are not a consequence of random variation.

CONCLUSIONS AND FUTURE PLANS

By the means of regression analysis residuals between the radar predicted rainfalls and rain gauge observations were calculated and then studied using residual regression analysis. The first finding was that radar rainfall sums do not coincide nor significantly correlate (coefficient of determination R^2=0.18) with rain gauge observations due to high residual errors especially in mountainous regions. Radar underestimates annual rainfall at all gauges included in the analysis.

A multivariate second order polynomial regression model was developed with three topographic and locational variables as the best predictors: altitude, distance from the radar antenna and latitude, which can explain up to 74% of variance of the residual errors. Such findings are important in regards to radar residual errors are not random, but can be partially predicted which may allow for some type of correction and improvement in radar's accuracy.

The residual analysis was carried out at annual scale, given the data provided by CHMI. Having finer data e.g. at monthly scale could introduce some other topographic, locational or atmospheric variables and would allow us to look at seasonal variation. The main sources of radar's inaccuracy discussed here come from topography, but there is the influence of the atmosphere as well, such as the attenuation of radar's signal passing through near clouds, which blocks detection of further clouds. Such atmospheric effects are variable in time and space. Having wind direction observations it would be possible to develop and test new interactive variables mentioned in the scientific literature such as the product of slope and orientation (orientation of the prevailing winds at some specific height) or exposure of a slope with regard to wind directions. Least but not last, the radar's 'visibility' could be modeled and included as one of the independent factors in the analysis.

The 'nonrepresentative sampling' error could be reduced by interpolating rain gauge values (prior to analysis) into a grid (mean areal precipitation) matching the size of radar's pixels, as described by Sokol.

ACKNOWLEDGEMENTS

This work has been supported by grant SGS10/151/OHK1/2T/11 of the Czech Technical University (CTU).

I would like to thank Dr. Bertram Ostendorf from the School of Earth and Environmental Sciences at the University of Adelaide for his support, advice, and useful comments. I am also thankful to Tomáš Žejdlík from the Radar Department as well as Mgr. Michal Žák, Ph.D. from the Department of Climatology of the CHMI for providing me annual climatological and monthly radar data. Least but not last, I would like to thank Milan Šálek from the Regional Forecasting Office Brno, CHMI, for his corrections.

REFERENCES

Austin, P.M. (1987) Relation Between Measured Radar Reflectivity and Surface Rainfall. Monthly Weather Review, 115, 5, 1053-1071.

CHMI. http://www.chmi.cz/meteo/rad/eindex.html, CHMI Radar Network, 24.2. 2010.

Gorokhovich, Y., Villarini, G. (2005) Application of GIS for processing and establishing the correlation between weather radar reflectivity and precipitation data. Meteorological Applications, 12, 1, 91-99.

Krajewski, W.F. (1995) Rainfall Estimation Using Weather Radar and Ground Stations, International Symposium on Weather Radars, São Paulo, Brazil.

Müller, A. (2010) Spatial Modeling of Climate, Faculty of Civil Engineering, Department of Mapping and Cartography, The Czech Technical University in Prague.

Řezáčová, D., Sokol, Z., Kráčmar, J. , Novák, P. (2001) Statistical adjustment of radar-based daily precipitation to ground data from the Czech territory, Proceedings of 30th International Conf. on Radar Meteorology, 19-24 July 2001. Amer. Meteorol. Soc., Munich, 570-572.

Sokol, Z. (2003) The use of radar and gauge measurements to estimate areal precipitation for several Czech river basins. Studia Geophysica Et Geodaetica, 47, 3, 587-604.

Sokol, Z., Bližňák, V. (2009) Areal distribution and precipitation-altitude relationship of heavy short-term precipitation in the Czech Republic in the warm part of the year, Atmos. Res., 94, 652-662.

FLOOD HAZARD ASSESSMENT BASED ON GEOMORPHOLOGICAL ANALYSIS WITH GIS TOOLS - THE CASE OF LACONIA (PELOPONNESUS, GREECE)

KARAGIOZI Eleni, FOUNTOULIS Ioannis, KONSTANTINIDIS Alexandros, ANDREADAKIS Emmanouil and NTOUROS Konstantinos

[1]Department of Geoinformatics and Survey, Faculty of Applied Technology, Technological Educational Institution of Serres, Terma Magnisias str., 62124, Serres, *Greece.karagel@gmail.com*

[2] National and Kapodistrian University of Athens, School of Sciences, Faculty of Geology and Geoenvironment
Panepistimiopolis, 15784 Zografou Athens
eandreadk@geol.uoa.gr

Abstract

The aim of the study was the development of a GIS tool, to be exploited eventually in the form of a WebGIS, as a decision support tool for flood hazard (and risk) assessment. The research was conducted in Laconia Prefecture in Peloponnesus. In this work, flood hazard assessment was implemented using hydrological models into a GIS environment (Arc Hydro model) taking into account the geomorphologic characteristics of the study area. More specifically, a DEM was used as input data of the Arc hydro model in order to produce the hydrographic network and the hydrological basins layer. For each basin, the morphologic characteristics such us area, mean slope, mean elevation and total relief, were calculated. These factors, all enhancing flood hazard, were combined in a product (by simple multiplication) in order to produce the inherent flood hazard map for each water basin and enhance the spatial differentiation of the phenomena. The final flood hazard map was produced by the combination of the aforementioned map and the slope map of the study area. The results of the followed methodology were evaluated using recorded flood incidents of the study area and shown that 60% of the incidents were related with the predicted high flood risk areas, which can be considered very high, once many of the flood phenomena in the non-predicted areas were largely due to previous human activity at the sites. Ultimately, the flood hazard map was published into a web GIS environment providing a friendly GUI to the end users. Except of analyzing the static flood hazard map, the end user have also the potential to interact dynamically with the map, adding to model calculation the meteorological factor (e.g. rain intensity, mean precipitation) in order to reassess the flood hazard of the study area.

Keywords: Flood hazard assessment, geomorphological analysis, WebGIS, Arc Hydro Model.

INTRODUCTION

Natural disasters occurring all over the world have a tremendous impact on regional and global environment and economy. In recent years, disaster phenomena are believed to increase due to human activities and/or climate change. The importance of natural hazards in terms of prevention, reduction and mitigation has been brought forward by international organizations such as United Nations through the development of a framework, the International Strategy for Disaster Reduction (ISDR), aiming at the worldwide reduction of vulnerability and risk.

Natural disasters occur worldwide; however their distribution around the globe varies regarding type, frequency of occurrence and impact. According to the registered disaster data, between 1900 and 1999, 13% of the total number occurred in Europe, whereas the greatest percentage (42%) was recorded in Asia. In the European territory, 27% of the total disaster incidents of that period are related to flood phenomena. As a result, the Directive 60 of 2007 was released in the EU, to deal with flood management and achieve Flood Risk Reduction in the European Union, in connection and supplementary to the 2000/60 Directive for Water Management, also implemented by member countries. Flood Hazard and Flood Risk maps are now considered a prerequisite for flood management, throughout the EU in this framework.

In Greece, during the 20th century, earthquakes are the most often natural disaster. More specifically, between 1900 and 2004, earthquakes contribute the 35% of the total number of disasters, when floods and wildfires follow with 17% and 10% respectively. In 2007 a major part of Peloponnesus region (Southwest Greece), and large areas of Laconia prefecture within it, was seriously affected by forest fires, thereafter associated with landslides and flood incidents that occurred since in the region.

In literature, research works dealing with natural hazards focusing on understanding natural processes, analysis and forecast of hazards such as flooding, mass movement, earthquakes and volcanism, can be found. According to Alcántara – Ayala there are innumerable works related to natural hazards such as flooding associated with hydrometeorological phenomena namely tropical storms, hurricanes etc; approaches of fluvial flooding processes understanding; flood simulations and forecasting; mass movement including landslide hazard analysis and assessment as well as volcanic and seismic hazards.

The integration of GIS into hazard mapping and disaster decision support has been continually upgraded and widespread since 2000, as a result of the increased availability of spatial databases and GIS software. Several studies are cited in the literature, relating to flood hazard mapping and zonation using GIS and/or remote sensing; integration of GIS with hydrological models and flood mitigation and management decision support systems through GIS. Also, web based GIS application regarding natural hazard assessment; monitoring and forecasting were developed providing advantages against the conventional systems such as ease of data sharing across an organization; dissemination to the public; simple graphical user interface(GUI) and cost effective tools.

The aim of the study was the development of a GIS tool to be exploited through a WebGIS as a decision support tool in relation to the flood hazard (and risk) assessment. The specific objectives were i) to estimate and map flood hazard using hydrological models into a GIS environment (Arc Hydro model) on the basis of geomorphologic data , and ii) the development of a friendly GUI via Web GIS application.

METHODS

Study area

The research was conducted in Laconia Prefecture (Peloponnesus, SW Greece). The area of Laconia Prefecture is about 3.621 Km^2 with mean elevation of 460m above sea level and maximum altitude of 2500m (Taygetos Mt.). The dominant hydrological feature of the area is the basin of Evrotas River, bounded to the east and west by the mountains of Parnon and Taygetos, respectively (Fig.1). This 1.700 km^2 watershed covers most of the central and northern part of the prefecture (including the city and the plains of Sparta) and Evrotas R. discharges in the Laconic Gulf (Mediterranean Sea) to the south. Minor hydrological basins develop on the two peninsulas (Mani and Vion) at the southern extensions of the bounding mountains of the area. Evrotas valley is predominantly an agricultural region that contains many citrus and olive cultivation fields and pasture land.

Flood hazard assessment methods

Methods of flood hazard estimation have been developed, taking into account the hydrologic basins environmental characteristics, and the particularity of each basin. Most bibliographic reports refer to the methods of Frequency Analysis and Basins Flow Simulation. These methods have been applied for hydrologic systems of the Hellenic region and specifically for the prefecture of Laconia, exporting reliable results. As Basins flow simulation models, we can report the Export Coefficient Models and the Water Quality Models. The Export Coefficient Models usually calculate the loss of material in annual scale, taking into consideration the type of surface (soil, bedrock, cultivations etc), slope and mean annual precipitation. The Universal Soil Loss Equation and the Stream Power Analysis Equation can be mentioned as Export

Coefficient Models, where the erosion is calculated in small scale, with the use of simple equations without taking into consideration the spatial parameter. The Water Quality Models have been developed in order to simulate processes in environments without extreme phenomena such as flash floods, debris flows, etc.

However, these methods lead to numeric results referring to specific locations where calculations are applied, cross-sections along streambeds, or flood zones alongside the streambeds, when combined with geomorphological observations, dating and stratigraphic data regarding river terraces.

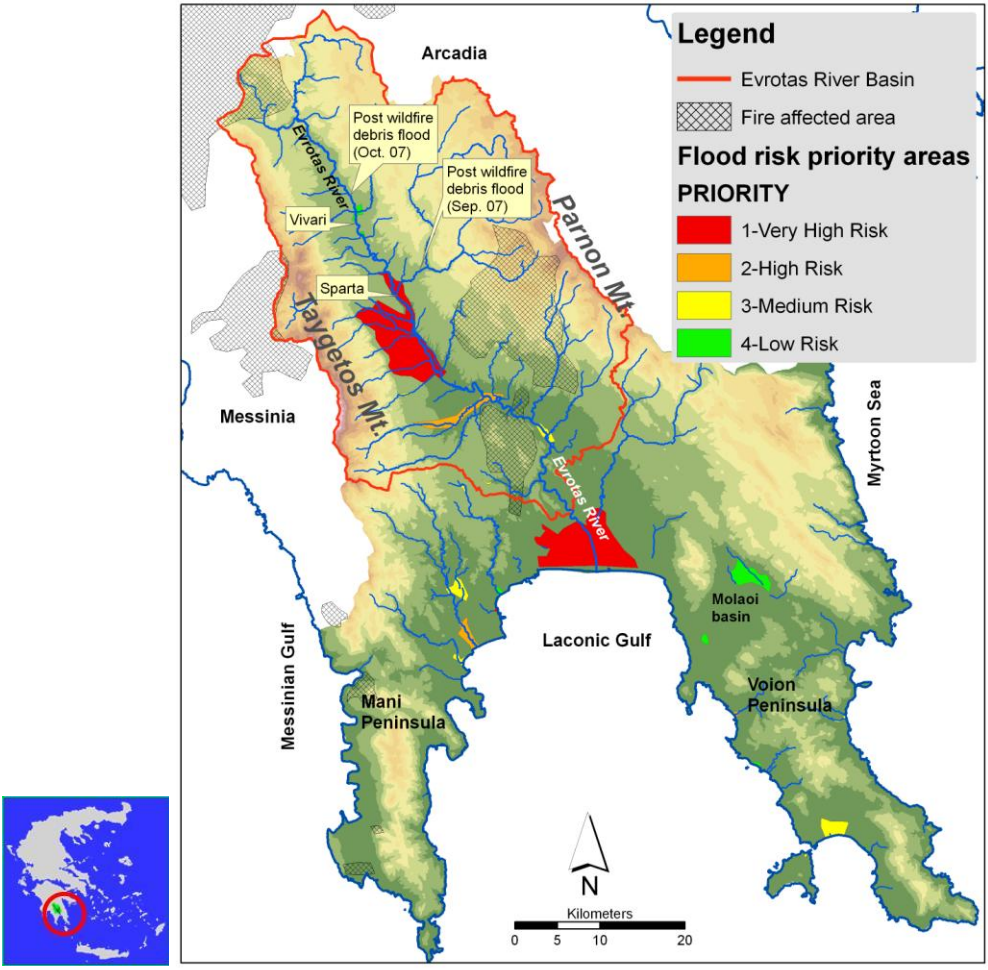

Fig1. Flood Risk Map of the study area (Andreadakis, 2008). The fire affected area of the 2007 wildfires is marked, as well as debris flood occurrences downstream, soonafter.

Methodology

The present work is attempting to cover the entire area with numeric results for a flood hazard indicator, to match the experience and observations on flooded areas as much as the active (alluvium) deposition record, which reflects flood incidents affecting areas significantly broader than the streambeds alone. The whole methodology is based on some fundamental assumptions concerning the area (so that the method can be applied with reliable results in other areas sharing similar characteristics):

- In tectonically active regions, vertical movements of tectonic blocks separated by fault zones dominate active erosion and deposition areas (and consequently, flood-prone areas)
- Drainage patterns and hydrological basin attributes (area, mean altitude, maximum and minimum altitude, mean slope etc), controlled largely by active tectonics, show a wide range of values, and create contrasts in neighbouring areas.
- Mean annual precipitation is generally proportional to altitude, as a result of the combination of atmosphere circulation with the orographic axis orientation of mountain ranges.
- The long term effects of climate are also fossilized on geomorphology (in erosion and deposition patterns, through landforms, mass transportation and accumulation etc).

Under these assumptions, it is evident that, regardless of the conditions of each extreme or regular weather event, in geological time, tectonically controlled geomorphological attributes define the flood prone areas of such regions, as well as the relative tension for flooding throughout any such area. A calculation based on these attributes shall provide a long term flood hazard indicator, which answers to a critical question for city planning, land use planning, insurance policy etc. Of course, any given precipitation event, differentiates flood hazard because of the specific rainfall spatial distribution, and then one has to overlay and run a dynamic model combining these two type of data, to switch from planning purposes to prediction, operations and emergency response.

The main aim of the study is the final production of the Flood Hazard Map of the study area, at the prefecture of Laconia, which fulfils the assumptions made previously. Flood hazard was estimated using the relief geometric characteristics in the study area and hydrologic basins. The main steps of the followed methodology are:

- calculation of a value indicating the basins and sub-basins energy level, which is determined by

- precipitation height, which is proportional to the mean elevation of the basin (factor: mean elevation)
- precipitation volume, which is proportional to mean elevation and basin area (factor: area)
- pace of transformation of runoff water dynamic energy to kinetic, in relation to the nearest baselevel (basin outlet), which is largely controlled by slope (factor: slope) and maximum and minimum altitude of the basin (factor: total relief)

- interpolation of the calculated values throughout the study area and creation of a basin energy grid
- creation of a slope grid (which is the critical factor for the water velocity reduction, the final accumulation of water in the riverbed and finally, flooding)
- combination of the basin energy grid with the slope grid, for the creation of the final hazard map.

The basin energy grid is based on a calculated parameter, referring to each basin as a single entity, which was attributed in the basin outlets, considered as relative base levels, where relative dynamic energy has been completely transformed to kinetic.

The density and frequency of basins drainage network were also calculated and evaluated, but did not provide significant differentiation of the initial results, at least for this study area. The calculation of these parameters did not result from the simple use of relative equations, but from the elaboration of the Digital Elevation Model (DEM) of the study area and the spatial and quantitative analysis of secondary data, essential factors in the process of calculation.

The production of the Digital Elevation Model was based on the elevation data of topographic maps (1:50000 scale), created by the Hellenic Military Geographic Services (HMGS). With the use of the elevation (DEM) and the relief's simulation of the study area the stream network and drainage basins in vector form (linear and polygonal representation) were produced. The intermediate products of this calculation process were the Flow Accumulation raster, the Flow direction raster, the Stream Order raster, the Drainage Line (vector form) and the Watershed (vector form). The final outputs of this process were the stream system lines (vector) and the polygons of the basins (vector) with all their geometric and geomorphologic values calculated. The results of the described process were displayed on different maps for each basin order group (from 3rd order basins up) allowing the basin analysis in comparison with their geographic placement, as it is shown in the example of the factor of Total Relief for 4th order basins in Fig. 2.

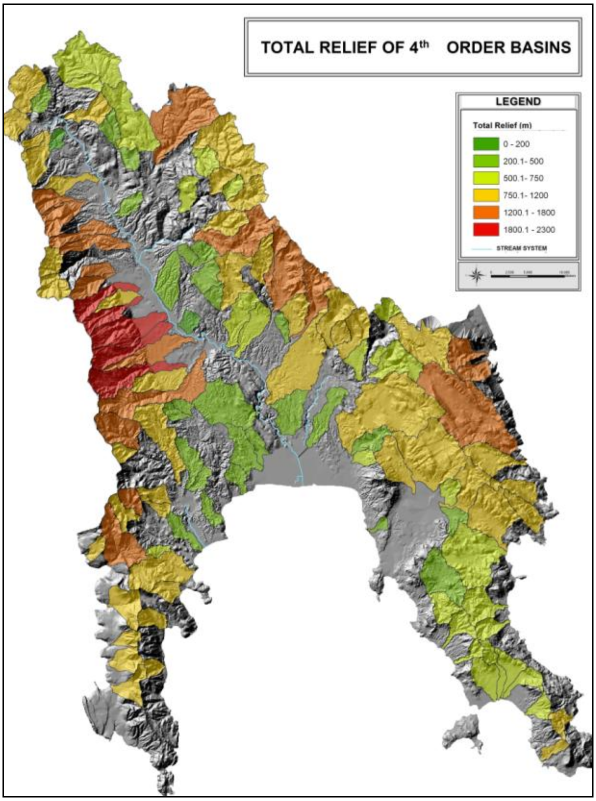

Fig2. Total Relief Map of 4th order Basins

Creation of the digital elevation model, as well as all other calculations over the study area were implemented with the use of ArcGIS software (ESRI), and the specialised toolbox ArcHydro. The Arc Hydro tools include operations for terrain processing to derive hydrologically correct terrain models to represent catchments, watersheds, and hydro networks. It also support many types of analysis such as watershed modeling, water network tracing, and flow accumulation calculations.

However, the scale of the study poses restrictions on the terrain elevation data, which derive from contour maps of 20m vertical interval. On smooth relief areas, especially in plains (be there parts of open or closed hydrological systems), detail is reduced, and one cannot rely exclusively upon the automated processes of ArcHydro tools for the creation of sub-basins and drainage network. For that reason, the resulting features of the simulated hydrological model of the area should be corrected largely in areas were they lacked primary data, while there were data about the exact connections between sub-basins and streams. A very characteristic example of possible misuse of the tools, is partly closed dolines along Parnon Mt. or Molaoi basin, where the “Fill Sinks” step of Arc Hydro would “fill” the karstic basin and continue downstream, connecting to the rest of the drainage network, which is an error by all means. In that case, runoff would accumulate in the closed basin, not to create a lake, but to be transformed to infiltration into the carbonates. Thus, the use of ArcHydro and the consequent calculations of basin features were restricted to user-defined sub-basins, determined by the STRAHLER classification, rather than running a model for the whole of the area “in blind”.

Final Flood Hazard Map production

After completion of the individual calculations for basins of all orders, the next phase is the construction of the basin energy grid map, completed in two steps, as described earlier:

- creation of the basin energy factor as an attribute for each basin, and attachment to a unique point theme containing the basin outlets of all orders,
- interpolation based on the basin energy attribute of the point theme for the creation of the basin energy grid map

Rhythm of the energy transformation on the basins outlet is proportional to dynamic energy and inverse proportional to the basins response time (it may be expressed as time of rainwater concentration or as time of flow). Both of the broadly used formulas for flow concentration time, the one of Kirpich ($t_c = 0.01947 \cdot L^{0.77} \cdot S^{-0.385}$), and the one of Giandotti ($t_c = \dfrac{4\sqrt{A} + 1.5 \cdot L}{0.8\sqrt{\Delta H}}$), take into consideration the mean slope of the basin or the total relief that are inversely proportional to the time of flow concentration In this case the rhythm of energy transformation at the basin outlets (de/dt), is increased at least proportionally to the following values (1) maximum length, (2) mean altitude, (3) mean slope, (4) total relief.

In order to maximize the spatial variation among the basin outlets into the basin energy grid, the calculated factors were put together in a product, acting as contributory factors to the total value. This product certainly does not calculate the rhythm of energy transformation itself at the basin outlet, however it is a well determined quantitative and objective indicator enhancing differences among them. This product can even be used to compare and rank areas from totally non related or non neighbouring regions. The calculating product was applied as a single value to the basins outlet in order to succeed a spatial distribution of this value to the whole study area. Although the spatial distribution of the value within 3rd orders basins close to the watersheds is practically a non-data area (it would have contributed to the map if there were calculations for the outlets of 2nd order, and so on), it depicts very well the spatial differentiation in the interior of all higher order basins (4th, 5th, 6th, etc) and of course in the intermediate area.

As mentioned before, the final step to the construction of the hazard map is the combination of the basin energy grid map with the slope grid map of the area (Fig. 3). The slope map was classified into categories according to slope values, to multiply the basin energy map, with a factor of minimum 1 for slope>10% (no flooding can take place on steeper slopes), to maximum 5 for slope<1%.

RESULTS – RISK MAP PRODUCTION

The results as shown on the final flood hazard map were considered very encouraging for further elaboration of the method. All areas with medium, high or very high flood hazard coincide with the areas of Holocene formations. This means that in these areas, where a continuous deposition action is reported for the last 10000-12000 years, as a result of flooding. For geologists, an exact geological map with explicit detail on Quaternary deposits would be enough to easily depict flood prone areas for a start. The additional advantage of this method compared to purely geological methods however, is the relative ranking of flood hazard among these areas.

Moreover, areas with high or very high flood hazard estimation are verified by the recent flood events reported by the geologists and engineers of Laconia Prefecture with a percentage greater than 60%, as was depicted by overlay of the point shape file of flooding sites over the flood hazard map (no peak discharge data were used). It is important to note that most of the non confirmed cases are locations where human intervention (e.g. roads and infrastructure, construction debris deposition) on the riverbeds, which probably rises the actual percentage of verification to quite higher levels, as far as natural factors are concerned.

A better estimation can be achieved, only if certain conditions are followed. These conditions require the execution of the selected method with great accuracy, as this was described in the previous paragraphs, but also to make calculations for the areas of the 2nd and 1st order basins, which were not included in this study. Finally, it should be pointed out that although this application was not accurate enough, it was proved particularly rapid as methodology and reliable enough for the available time and the application scale.

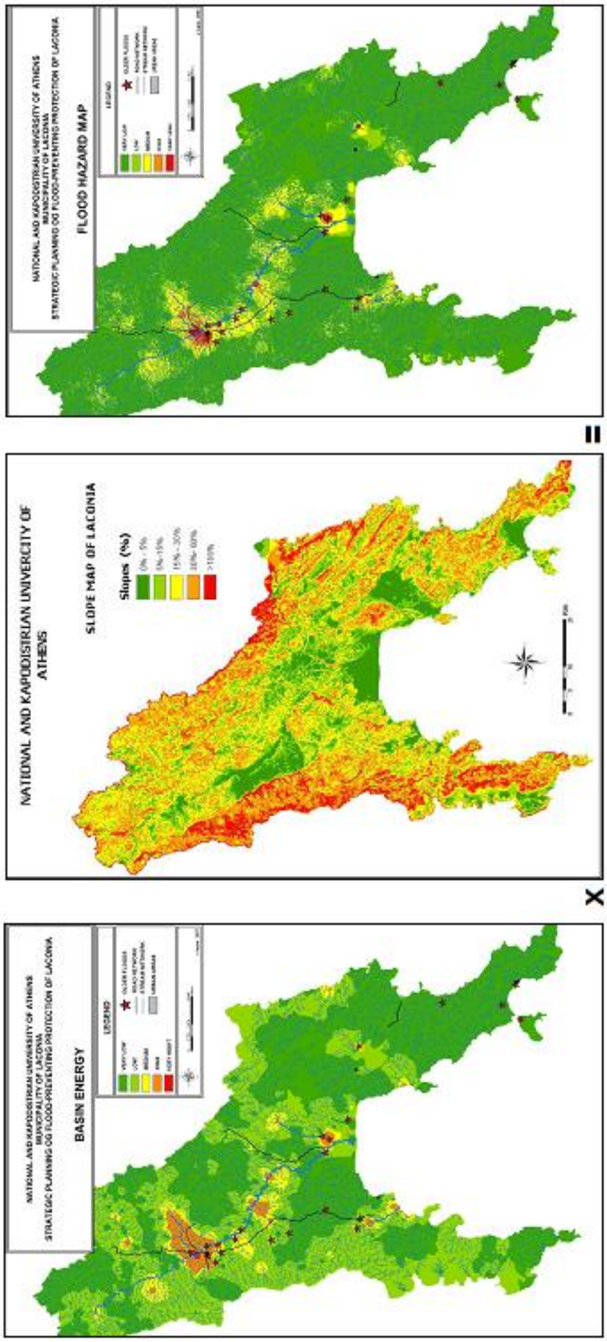

Fig. 3. Combination of Basin Energy Map with Slope map leads to the final Flood Hazard Map.

The recorded flood events of recent years (red stars) located within yellow, orange and red areas of the flood hazard map were considered positive results verifying the used methodologyMoreover, it has to be noted that the results were also verified by the debris flood phenomena following the wildfire of 2007 (depicted in Fif.1), which were included in the aftermath of an extreme disaster, at locations where no previous serious events had been recorded before, but in areas indicated as medium or high flood hazard.

The map of Fig. 1 integrates post wildfire observations about debris flow events following storms over the fire affected areas, soon after the 2007 wildfire, with a form of risk map conducted by the research team in collaboration with the scientists and administrators of Laconia Prefecture.

While Hazard maps depict the hazard potential and probability of occurrence in an area, Risk maps generally depict the form, the stakes and the vulnerability of human presence in a hazardous area, as potential severity of impact in combination with the probability or tension of the specific type of hazard to occur in the area. This relation is usually represented in the symbolic formula “(Risk)=(Hazard)x(Vulnerability)”, but reality is far more complicated than this. In order for this risk map to be created, the research team consulted with the authorities so that areas of human activity (towns and settlements, industrial zones, cultivated areas etc) are delimited and put in order of order of importance, according to their standards (land value, population density, lifelines, etc). In this way, a polygon theme with rated areas of importance was created, and risk was calculated by multiplication of flood hazard to a factor defined by importance attributed to each area. The results presented in the final map show areas where both hazard and vulnerability are high, when no values were given to the intermediate areas, once even if flood hazard was considered high, no vulnerability or value was present. Thus, areas of management priority were defined, so that measures would be taken within and in the basins upstream.

The results of this study were published via a Web GIS application with the intention to develop a useful decision support tool. The Web GIS application was developed with the use of the ArcGIS Server platform, and gives to users the desired information via a user friendly framework with all the available tools and data for a flood hazard assessment. The application is accessible from a web browser via an internet connection without requiring any additional installation, giving the opportunity to analyse dynamically (online) the available datasets regarding the flood hazards.

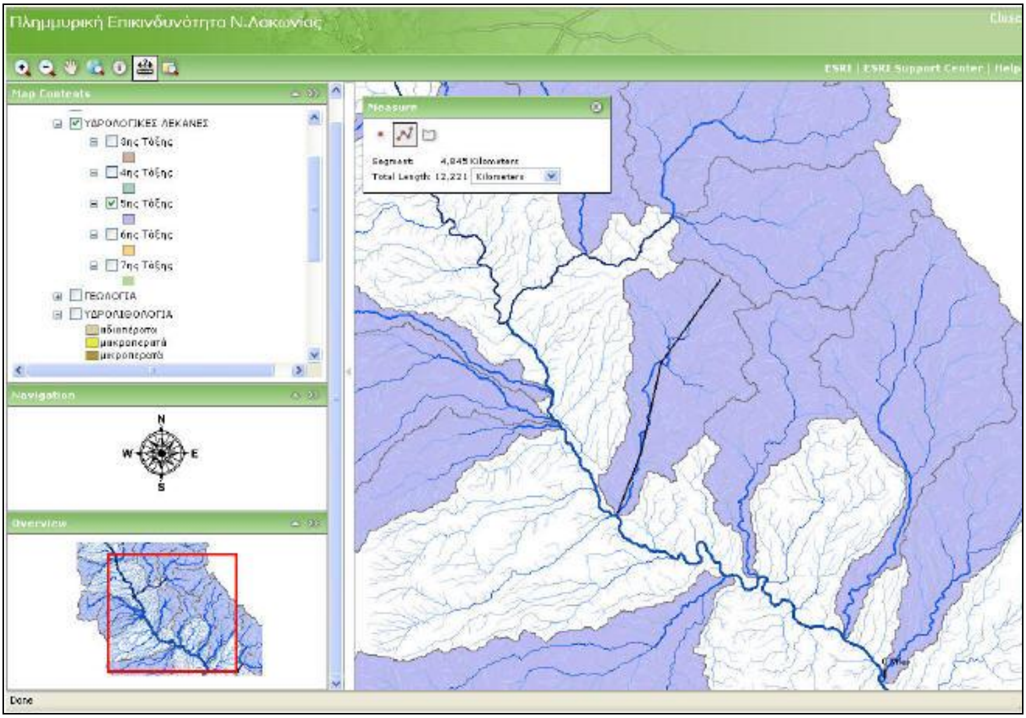

Fig4. Web GIS Applications Screen. Dynamic tool that measures the length of the basins.

CONCLUSIONS

In Laconia, as much as in many other regions of Greece and other countries, there are no time series of runoff measurements, daily precipitation or rainfall intensity data makes it impossible to use any calculation based on such data for reliable frequency estimations about floods and intensities of such phenomena. This method overcomes this obstacle, using the present picture of the long term record of the dynamic interaction of endogenous (such as tectonics) and exogenous forces (weather, climate, erosion) on the earth's surface, that is, the geomorphology.

It has to be pointed out that, such complicated and massive calculations over terrain models had been beyond scientific imagination throughout the past of earth sciences, but today they form powerful and low cost tools for difficult as much as critical tasks, such as flood hazard and risk assessment. In fact, the whole methodology presented herewith is based on topographic maps alone (geological maps are supplementary so that the results are cross checked). The only factor restricting the accuracy of the results is the accuracy of the initial topographic maps. As a first step approach to any area where the basic prerequisites of the method (about tectonic activity, precipitation etc) are met, one could hardly find a faster and more economic way to provide results for flood hazard mapping. In fact, the methodology was initially developed to respond to a specific request by the local authorities, after severe floods in Laconia by the end of 2005 and the beginning of 2006. As far as the combination of speed and low cost vs accuracy is concerned, the method met the requirements, although it was recognised that a lot of improvement can be made, and the research team has been working since and is ready to present the new results and the evolution steps of the method hereafter, also in Laconia and other regions and other scales.

On the other hand, the development of a web based application reveals that a GIS application with a simple GUI can be used from the non – GIS specialists and that the stakeholders can interact and collaborate more effectively with each other and scientists or consultants. Also, the publication of the flood hazard maps via the internet enhances the public awareness and active participation to the decision making process. Apart from that, it is a cost effective application in comparison to the traditional stand alone desktop applications, once it can be accessed with the use only of a web browser.

Ultimately, the potential of the tool in terms of the additional data interaction with the static flood hazard maps provides the capability to the experts to reassess the flood hazard introducing real time or near real time rainfall data when available and involving the spatial distribution of rainfall to provide dynamic hazard and risk maps, r even run scenarios based on hypothetical rainfall events. This is in fact one of the next steps in the process of upgrade of the methodology by the research team.

REFERENCES

Alcántara-Ayala, I. (2002) Geomorphology, natural hazards, vulnerability and prevention of natural disasters in developing countries. Geomorphology, 47, 107–124.

EM – DAT: CRED International Disaster Database, http://www.emdat.be, 2009.

Kale, V.S., Ely, L.L., Enzel, Y., Baker, V.R. (1994) Geomorphic and hydrologic aspects of monsoon floods on the Narmada and TapiRivers in central India. Geomorphology, 10, 157–168.

Enzel, Y., Ely, L.L., House, P.K., Baker, V.R., Webb, R.H. (1993) Paleoflood evidence for a natural upper bound to flood magnitudes in the Colorado River. Water Resour. Res., 29 (7), 2287 – 2297.

Baker, V.R. (1994) Geomorphological understanding of floods. Geomorphology, 10, 139–156.

Kale, V.S., Hire, P., Baker, V.R. (1997) Flood hydrology and geomorphology of monsoon-dominated rivers; the Indian Peninsula. Water Int., 22, 259– 265.

Enzel, Y., Wells, S.G. (1997) Extracting Holocene paleohydrology and paleoclimatology information from modern extreme flood events; an example from Southern California. Geomorphology, 19, 203– 226.

Bates, P.D., De Roo, A.P.J. (2000) A simple raster-based model for flood inundation simulation. J. Hydrol., 236, 54–77.

Chang, T.J., Hsu, M.H., Teng, W.H., Huang, C.J. (2000) A GIS assisted distributed watershed model for simulating flooding and inundation. J. Am. Wat. Resour. Assoc., 36 (5), 975–988.

Chowdhury, M.R. (2000) An assessment of flood forecasting in Bangladesh: the experience of the 1998 flood. Nat. Hazards, 22 (2), 139– 163.

Hansen, A. (1984) Landslide hazard analysis. In: Brunsden, D.and Prior, D.B. (Eds.), Slope Instability. Wiley, Chichester, pp. 523– 602.

Hutchinson, J.N. (1992) Landslide Hazard Assessment. Proceedings of 6th Int Symp. on Landslides, Christchurch, New Zealand, 10-14 February 1992, vol. 3, pp. 3 – 35.

Petley, D.N. (1998) Geomorphologic mapping for hazard assessment in a neotectonic terrain. Geogr. J., 164 (7), 183– 201.

Thouret, J.C. (1999) Urban hazards and risks; consequences of earthquakes and volcanic eruptions: an introduction. GeoJournal, 49 (2), 131–135.

Panizza, M. (1991) Geomorphology and seismic risk. Earth-Sci. Rev., 31 (1), 11 –20.

Zerger, A. and Smith, D.I. (2003) Impediments to using GIS for real-time disaster decision support. Computers, Environment and Urban Systems, 27, 123–141.

Merzi, N., Aktas, M.T. (2000) Geographic information systems (GIS) for the determination of inundation maps of Lake Mogan, Turkey. Water Int., 25 (3), 474–480.

Sanyal, J. and Lu, X. (2006) GIS-based flood hazard mapping at different administrative scales: A case study in Gangetic West Bengal, India. Singapore Journal of Tropical Geography, 27, 207–220.

Fernández, D.S. and Lutz, M.A. (2010) Urban flood hazard zoning in Tucumán Province, Argentina, using GIS and multicriteria decision analysis. Engineering Geology, 111, 90-98.

Islam, Md. M. and Sado, K. (2002) Development Priority Map for Flood Countermeasures by Remote Sensing Data with Geographic Information System. J. Hydrologic Engrg., 7 (5), 346-355.

He, Y.P., Xie, H., Cui, P., Wei, F.Q., Zhong, D.L. and Gardner, J.S. (2003) GIS-based hazard mapping and zonation of debris flows in Xiaojiang Basin, southwestern China. Environmental Geology, 45 (2), 286-293.

Islam, Md. M. and Sado, K. (2002) Flood hazard assessment in Bangladesh using NOAA AVHRR data with geographical information system. Hydrological Processes, 14, 605–620.

Weng, Q. (2001) Modeling Urban Growth Effects on Surface Runoff with the Integration of Remote Sensing and GIS. Environmental Management, 28 (6), 737-748.

Tralli, D.M., Blom, R.G., Zlotnicki, V., Donnellan, A. and Evans, D.L. (2005) Satellite remote sensing of earthquake, volcano, flood, landslide and coastal inundation hazards. ISPRS Journal of Photogrammetry & Remote Sensing 59, 185 – 198.

Correia, F.N., Rego, F.C., Saraiva, M.G. and Ramos, I. (1998) Coupling GIS with Hydrologic and Hydraulic Flood Modelling. Water Resources Management, 12 (3), 229-249.

Sui, D.Z. and Maggio, R.C. (1999) Integrating GIS with hydrological modeling: practices, problems, and prospects. Computers, Environment and Urban Systems, 23, 33-51.

Liu, Y.B., Gebremeskel, S., Smedt, F. De, Hoffmann, L. and Pfister, L. (2003) A diffusive transport approach for flow routing in GIS-based flood modelling. Journal of Hydrology, 283, 91–106

Rosenthal, W. D., Srinivasan, R., Arnold, J. G. (1995) Alternative River Management Using a Linked GIS-Hydrology Model. Transactions of the ASABE. 38(3), 783-790.

Zerger, A. and Wealands, S. (2004) Beyond Modelling: Linking Models with GIS for Flood Risk Management. Natural Hazards 33, (2), 191-208.

Todini, A. (1999) An operational decision support system for flood risk mapping, forecasting and management. Urban Water 1 (2), 131-143.

Al-Sabhan, W., Mulligan, M., Blackburn, G.A. (2003) A real-time hydrological model for flood prediction using GIS and the WWW. Computers, Environment and Urban Systems, 27, 9–32.

Niu, R., Zhang, L., Shao, Z. and Cheng, Q. (2007) Web-based Geological Hazard Monitoring in the Three Gorges Area of China. Photogrammetric Engineering & Remote Sensing, 73 (6), 709-719.

Wang, L. and Cheng, Q. (2007) Design and implementation of a web-based spatial decision support system for flood forecasting and flood risk mapping. Geoscience and Remote Sensing Symposium, 2007. IGARSS 2007, Barcelona, Spain, 23-28 July 2007.

Guzzetti, F. and Tonelli, G. (2004) Information system on hydrological and geomorphological catastrophes in Italy (SICI): a tool for managing landslide and flood hazards. Nat. Hazards Earth Syst. Sci., 4, 213-232.

Mansourian, A., Rajabifard, A., Valadan Zoej, M.J. and Williamson, I. (2006) Using SDI and web-based system to facilitate disaster management. Computers & Geosciences 32 (3), 303-315.

Jones P., Mullholland P.J., (1999), Streams and Groundwaters, Elsevier.

Andreadakis, Emm., Fountoulis, I., Mariolakos, I., Kapourani, E. (2008) Hydrometeorological Natural Disasters and Water Resources Management in Evrotas River Basin (Peloponnesus, Greece). *Paper presented in the 3rd International Conference "AQUA 2008" on Water Science and Technology, 16-19 October 2008, Athens. http://www.evrotas.gr/publications/16.pdf*

Fountoulis I., Mariolakos I., Andreadakis Emm., Karagiozi E., Sambaziotis E., & Kapourani E. (2008) Flood Hazard And Risk In Laconia (Peloponnesus, Greece). *Poster presented in the 3rd International Conference "AQUA 2008" on Water Science and Technology, 16-19 October 2008, Athens. http://www.evrotas.gr/publications/17.pdf*.

Andreadakis Emm. & Fountoulis, I., 2007. Flood Hazard Assessment in Tectonically Active Regions. *Tectonic Geology Symposium in Honour of Prof. I. Mariolakos, Dec. 7, 2007*. Geological Society of Greece, Athens.

Fountoulis, I., Mariolakos, I., Andreadakis, Emm., Sambaziotis, E., Karagiozi, E., 2007. Strategic Planning of Anti-Flood protection for Laconia Prefecture, App.2 in : Nikolaides et al. (2007) "Antiflood Protection Master Plan for Laconia Prefecture". (LIFE-Environment 2005, ENVIFRIENDLY). In Greek.

Karagiozi E. (2008). Natural Hazard assessment in Laconia Prefecture based on web GIS. Master thesis. Faculty of Geology and Geo-environment, National & Kapodistrian University of Athens, Athens, 160 p. (in Greek).

David V., Evelpidou N., Vassilopoulos A., Boglis A., Fountoulis I. (2009). Flood Modeling in Karlovassi Basin Area – Samos Island (Greece). Proc. Final conference COST action C22 Urban Flood Management in cooperation with UNESCO – IHP / Paris 26./ 27.11.2009. E-10, p. 1-9. http://labtect.geol.uoa.gr/pages/fountoulis/PDF%20Files/130-2009%20Paper_Paris_Conference_20090829.pdf

TICK-BORNE DISEASES RISK MODEL FOR SOUTH BOHEMIA (CZECH REPUBLIC)

HÖNIG Václav, SVEC Pavel, MASAR Ondrej and GRUBHOFFER Libor

Faculty of Science, University of South Bohemia and Institute of Parasitology, Biology Centre AS CR, Branišovská 31, 370 05 České Budějovice, Czech Republic
honig@paru.cas.cz

Institute of Geoinformatics, VSB-TU of Ostrava, 17. listopadu 15,
708 33, Ostrava – Poruba, Czech Republic
Pavel.svec1@vsb.cz, ondrej.masar@gmail.com

Faculty of Science, University of South Bohemia and Institute of Parasitology, Biology Centre AS CR, Branišovská 31, 370 05 České Budějovice, Czech Republic
liborex@paru.cas.cz

Abstract

Tick-borne diseases (TBD) like Lyme borreliosis or tick-borne encephalitis (TBE) belong to most important health threats in the Northern Hemisphere. The Czech Republic is one of the countries with highest incidence of TBD. Particularly the region of South Bohemia, with an annual average of 26 TBE cases per 100 000 inh. has been for a long time a high-risk area (mean annual TBE incidence for the whole country is 6.4 cases per 100 000 inh.). Concerning the TBD preventive measures, one of the key issues is the knowledge of disease risk distribution in time and space. Moreover, such knowledge may be helpful in revealing background mechanisms actually determining the distribution. Habitat suitability models based on remote sensing or GIS data are increasingly employed in spatial epidemiology of vector-borne diseases. We propose a model system for estimation of TBD risk based on assessment of habitat suitability for the vector –*Ixodes ricinus* tick. Land cover data (CORINE Land Cover 2006) and digital elevation model were employed for the prediction of tick activity, the main component of the biological risk of TBD. The model was validated on a dataset of field-collected data on tick activity and further on actual number of clinical cases of tick-borne encephalitis. A map of biological risk and a map of risk of TBD case occurrence were produced. Areas of high and low biological risk were identified. Areas of high biological risk were scattered mainly along the river valleys, whereas low risk areas were represented by mountainous part of the region. Highest numbers of TBD cases were predicted in surroundings of large setllements or in areas of maximum biological risk.

Keywords: GIS, cartographic model, Lyme borreliosis, tick-borne encephalitis

INTRODUCTION

Diseases transmitted by ticks – tick-borne diseases (TBD) belong to so called emerging diseases. These are diseases caused by new or altered disease agents, diseases occurring in a new context or with different intensity. An increase in the number human cases of TBD is reported from a number of European countries in last decades. Moreover, dramatic changes in the distribution of the disease cases in time and space are observed (Randolph 2001, Süss et al. 2004, Materna et al. 2008, Gray et al. 2009). Because of this dynamic nature of emergent infections, tools for disease risk assessment and monitoring are needed. In vector-borne diseases epidemiology various models are used for prediction of disease risk. Concerning the training datasates and model outputs, the risk is usually calculated based on epidemiological dat (numbers of disease cases) (e.g. Beneš et al. 2005), vector data (presence/absence, abundance) (e.g. Eisen et al. 2006, Schwarz et al. 2009), pathogen data (prevalence of pathogens, density of infected vectors) (e.g. Rizzoli et al. 2002) or on combination of above mentioned (e.g. Daniel et al. 2006). Such data are used for identification of environmental factors closely correlated to the risk of exposure. Subsequently highely correlated factors serve as predictors of exposure risk (Ostfeld et al. 2005). Each of the above-mentioned approaches influences the final model output and has certain advantages and disadvantages (summarized by Eisen and Eisen 2008).

Regarding the transmission of TBD to human, the tick *Ixodes ricinus* is the most important species in Europe. It may transmit a number of disease agents including two most widespread: tick-borne encephalitis virus and Lyme borreliosis spirochetes. This tick is mostly restricted to forested areas and prefers heterogeneous broad-leaved or mixed forests with dense undergrowth and leaf litter providing sufficient humidity. In natural foci, the pathogens circulate among ticks and their vertebrate hosts (Süss 2003; Humair et al. 2000).

Numerous woodland fragments scattered among pasture and agricultural areas, appropriate climatic and biotic conditions in the South Bohemian Region provide an especially pertinent environment for *I. ricinus* populations. An average of 160 human cases of tick-borne encephalitis and 154 cases of Lyme borreliosis occur annually in the region (data provided by the National Institute of Public Health, Prague).

The aim of our study is to assess the biological risk of TBD infection – i.e. the probability of encountering a tick in a particular area. The level of the risk depends mainly on the level of tick activity. The prevalence of pathogens was not included, because its influence on total TBD risk is minor and *I. ricinus* ticks in South Bohemia transmit multiple pathogens with variable prevalence rate. Using the habitat modeling approach a simple vector based model for assessment of tick activity was developped. Association of certain environmental variables with the biological demands of ticks was used for estimation of expected tick activity. The major advantages of this vector-based model are: risk assessment independent on human behaviour and independent on particular tick-borne pathogen.

DATA AND METHODS

Ticks are highly dependent on certain abiotic (e.g. temperature, relative air humidity) and biotic (e.g. host availability) environmental factors. These factors are numerous, often interact with each other and often are difficult to reveal and monitor. Therefore, usually complex habitat characteristics like NDVI, brightness or greennes are employed (Eisen et al. 2006, Šumilo et al. 2006). In our model, vegetation land cover was used as complex descriptor of a given area (encompassing soil type, climate, to certain extend composition of tick host fauna). Because of the partially mountainous character of the region altitude had to be included as a second predictor. The relationship between elevation and tick population activity is well described and the climatic and biotic condition covariate with altitude.

Input data, transformation

Input layers were transformed into a raster grid with uniform pixel size. Regarding the computational capacity, resolution of some of the input data and the purpose of the study, the pixel size was set 50 x 50 m. In the biological risk model, the layers were classified according to the probability of tick occurrence (based on empirical experience and literature). Intervals covering the whole range of the factor were set and rescaled to 0 – 1 scale (0 – minimum risk, 1 – maximum risk). The values of the risk index for individual categories are shown in Table 1.

<u>Vegetation cover</u>

Vegetation cover influences the probability of *I. ricinus* occurrence and level of activity essentially (Nosek and Krippel 1974). The relationship between the habitat type and distribution of the ticks was repeatidly empirically verified. Association of tick with certain habitats is commonly applied in TBD modeling studies (Daniel and Kříž 2002, Daniel et al. 2006, Eisen et al. 2006, Šumilo et al. 2006). The data on vegetation cover were obtained from CORINE Land Cover 2006 (CLC 2006) project of European Environment Agency were used (EEA, 2006). The resolution of the input data allowed us to identify even small habitat fragments, which are known to be important reservoirs of ticks. No remarkable changes in land cover are expected to occur since 2006. From a variety of land cover classes CLC 2006, only some are present in the surveyed area and only some are suitable for the survival of *I. ricinus* ticks. These classes were assigned a risk index based on own field experiments and literature (Daniel and Kříž 2002, Schwarz et al. 2009). In other classes, the probability of tick encounter is minimal, therefore these classes were merged in a single category “other”. Water courses and bodies exclude the occurrence of living ticks completely and thus were assigned a zero risk. The list of CLC 2006 vegetation cover categories and assigned risk indices is shown in Table 1.

Elevation

Altitude influences the activity of ticks and therefore was used as a second factor entering the biological risk model. The range of altitudes in the surveyed area is 330 to 1378 meters above sea level. The risk indices were inferred from the relationship between tick activity and elevation from our own field collected data and data from literature (Jouda et al. 2004; Materna et al. 2005, 2008; Danielová et al. 2010; Gilbert et al. 2010). Most studies focused on higher altitudes of 400 to 1160 m a. s. l. The activity of *I. ricinus* populations decreases rapidly in the interval of 500-850 m a. s. l. In the range 850-1160 m the activity decreases more steadily approaching the minimum values at 800-1000 m. Therefore, the risk index was assigned maximum value from zero to 500 m a. s. l. From 500 to 850 m a. s. l. the risk is decreasing continually. Above 850 m a. s. l. the index is assigned a constant value of minimum but existing risk of 0.05. The elevation values were derived from contour lines in Arc ČR500 database.

Table 1. Risk index assignment

Layer	**Category**	**Risk index** [0-minimum;1-maximum]
Vegetation cover [Corine Land Cover 2006 classification]	1.4.1. Green urban areas	0.25
	2.3.1. Pastures	0.20
	2.4.3. Land principally occupied by agriculture	0.40
	3.1.1. Broad-leaved forest	0.80
	3.1.2. Coniferous forest	0.50
	3.1.3. Mixed forest	1.00
	3.2.1. Natural grassland	0.20
	3.2.4. Transitional woodland shrub	0.60
	5.1.1. Water courses	0.00
	5.1.2. Water bodies	0.00
	other	0.05
Elevation [m a. s. l.]	< 500	1.00
	501 – 850	decreasing from 1.00 to 0.05
	> 851	0.05

Model construction

The model was compiled in ESRI ArcGIS 9.3 software. Tools and logics of map algebra were used for linking up individual map layers. Before final calculation in Single Output Map Algebra tool, necessary transformation steps including joining and cutting the input data, raster transformation and reclassification of the data (Fig. 1) were conducted. Various possibilities of the integration of individual input layers were tested in order to pick up the best representation of the real relationships among the factors.

In the proposed model the level of tick activity results from integraction of two predictors – altitude and vegetation cover. Biologically, extremely low suitability in one or another factor results in low risk regardless on the level of the second factor. For example, the occurrence of ticks is excluded in water areas independently on altitude. Similarly, very low tick activities occur in altitudes above 1000 m a. s. l., despite potentially suitable vegetation cover. On the other hand, high suitability of both factors potentiates the risk in a multiplicative manner. This behaviour was represented in the model by multiplication of the two input layers. Moreover, the final ouput value remained 0 for minimum risk and 1 for maximum risk.

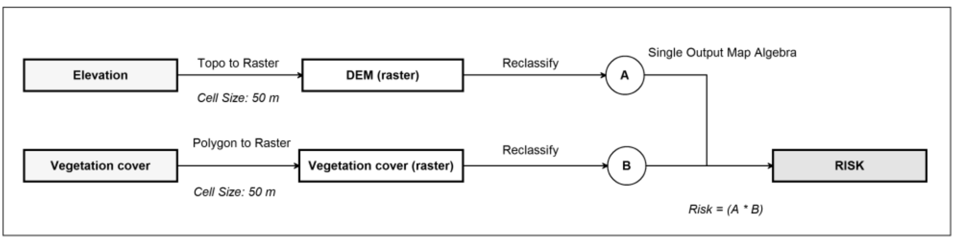

Fig. 1. The scheme of the biological risk model

Model validation

The efficiency of the model to predict tick activity was evaluated using the field-collected data. A network of 30 testing sites evenly distributed over the surveyed area was established (location indicated in Fig. 2). In each study site, the tick activity was estimated 3 times per season (May, June, September), regarding the typical seasonal pattern of *I. ricinus*. The ticks were sampled by a commonly used flagging method. The activity was calculated as a mean number of ticks per 100 m^2. In each sampling event 600 m^2 were flagged (compare Vassalo et al. 2000). The estimated activity of ticks was compared with the model output by Spearman rank order correlation test STATISTICA 9.1 software (StatSoft. Inc., USA).

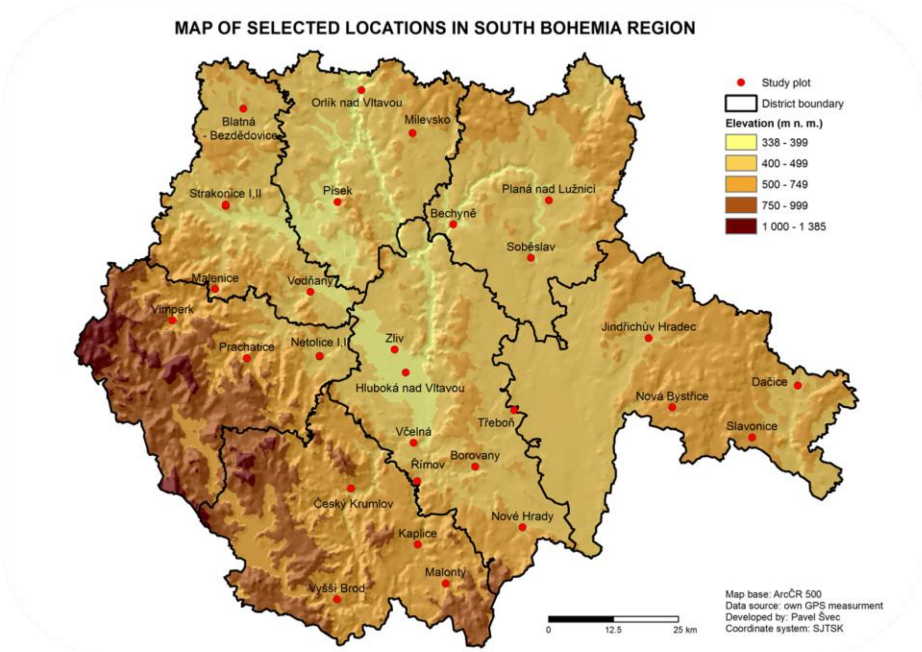

Fig. 2. Distribution of testing localities

Occurence of a disease case as a realisation of the biological risk is strongly influenced by human activity. Therefore, estimate of human activity was included in the model. The level of human occurrence was inferred from the number of inhabitants. Because of highly active tourist traffic particularly in the Region of South Bohemia tourist activity data were included. Data on number of inhabitants at the level of municipality were used (compare Estrada-Pena and Venzal 2007). The data were acquired from the Czech Statistical Office (valid to 1.1.2009) and expressed as population density per km^2 (range 1.23 - 1708.29).

No direct data on the number of tourists were available in sufficient resolution. Therefore, numbers of accomodation beds were used as a rough estimate of tourist activity. The data were obtained from The Atlas of Tourism of the Czech Republic (Vystoupil et al. 2006) and recalculated per km^2 (range 20 - 411).

Total human activity was obtained as a sum of number of inhabitants and number of tourists. All people were considered as susceptible to TBD infection and thus potential disease cases. The biological risk (activity of ticks) was multiplied by the level of human activity (probability of human occurence) resulting in a probability of disease case occurrence (Fig. 3). The model output was compared with the actual number of tick-borne encephalitis (TBE) cases per municipality and the correlation was statistically tested by the means of Spearman correlation ranking test. TBE was selected because of its precise case definition and reliable reporting system. Total numbers of disease cases for the 2001-08 period were acquired from the Institute of Public Health, Prague, Czech Republic.

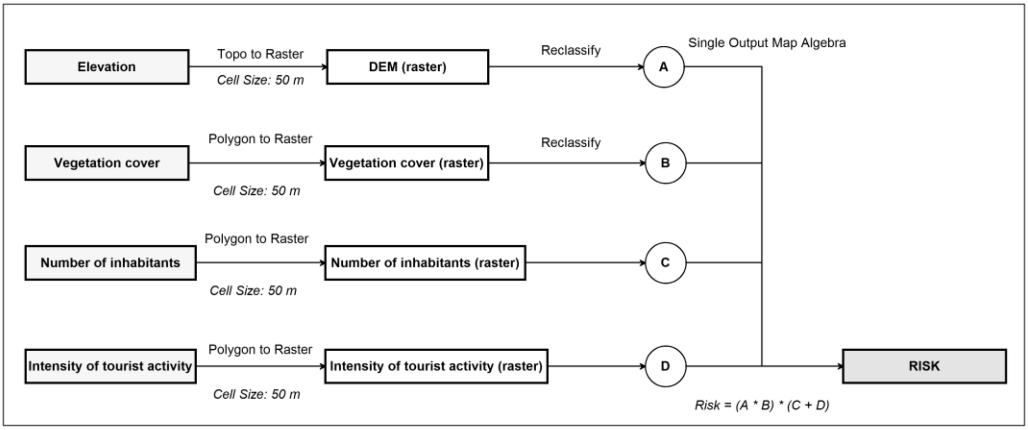

Fig. 3. The scheme of the model of disease case occurence

RESULTS

The biological risk model was transferred to a map output (Fig. 4). The biological risk represents the predicted activity of ticks.

The majority of the surveyed area falls in low risk categories. The largest compact area of minimum risk is located in the southwestern mountainous part of the region (Šumava Mountains). The maximum and high-risk areas are scattered along the valeys of the rivers Vltava, Otava and Blanice from the center of the region northwards. Large area of increased risk stretches from the town Třeboň southwards and westwards to the border. The summary of the proportional representation of the individual risk categories over the whole area is shown in Table 2.

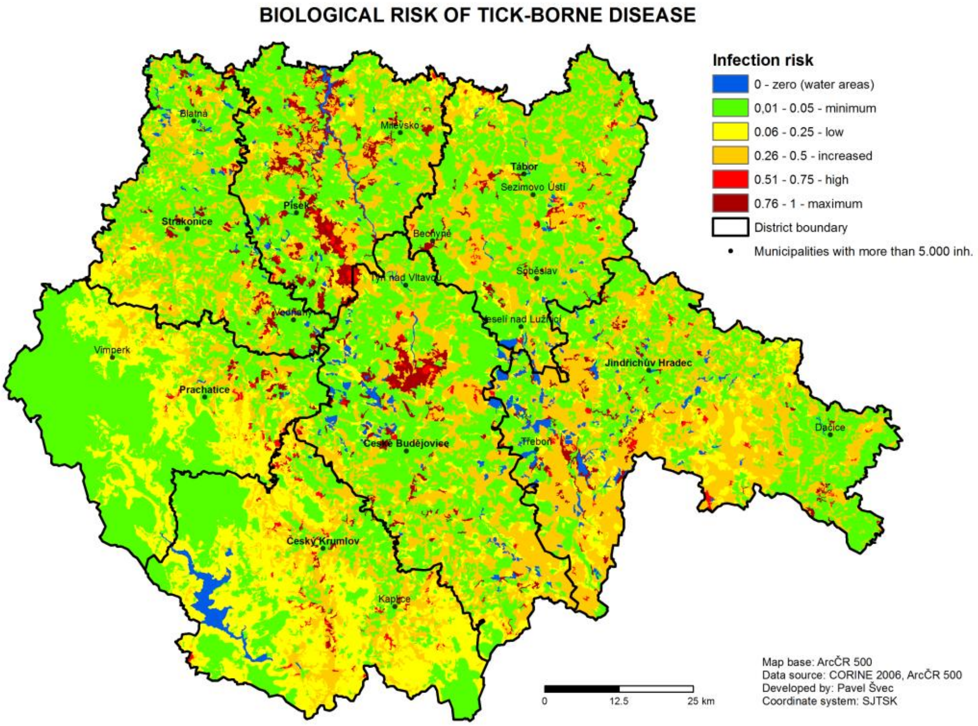

Fig. 4. Biological risk of tick-borne diseases

Table 2. Proportional representation of risk categories

Risk category	Proportion of pixels [%]
zero (0)	2.0
minimum (0.01 - 0.05)	19.1
low (0.06 - 0.25)	45.2
increased (0.26 - 0.5)	29.7
high (0.51 - 0.75)	1.0
maximum (0.76 - 1)	3.0

The model output was compared with the data on tick density assessed in 30 testing sites dispersed over the Region of South Bohemia (Fig. 2). Significant correlation was confirmed in Spearman rank order correlation test ($p<0.05$) and Pearson correlation test ($r = 0.36$, $p<0.05$) between risk predicted by model and mean density of ticks.

After addition of human activity to the model, the output was compared with the total number of TBE cases (2001-08). A strong correlation was confirmed by Spearman rank order correlation test ($p<0.05$) and Pearson correlation test ($r = 0.76$, $p<0.01$)

between risk predicted by model and total number of disease cases. A map of risk TBD case occurrence was constructed (Fig. 5).

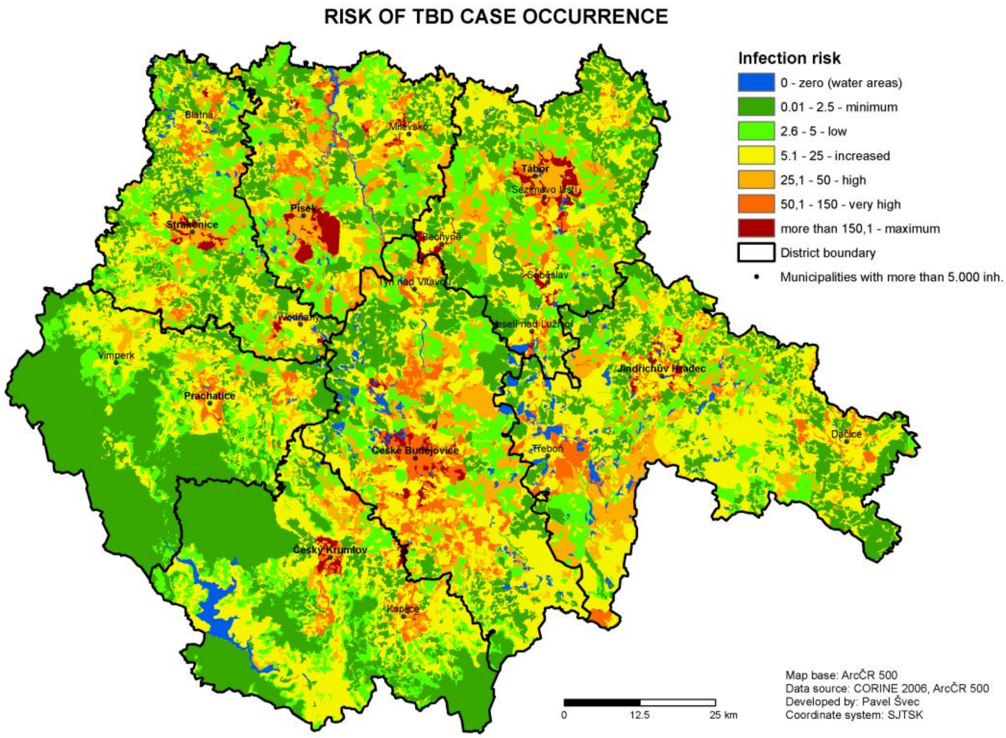

Fig. 5. Map of risk TBD cases occurence

The high-risk areas shifted considerably into the surrounding of larger settelements. Two high-risk areas remained in sparsely populated areas of the region: near Orlik dam (northern part of the region) and between the towns České Budějovice and Týn nad Vltavou.

DISCUSSION AND CONCLUSIONS

For modelling of vector-borne diseases distribution various factors are evaluated as possible predictors: macro-, microclimatic conditions, type of vegetation cover, level of urbanization etc. (Šumilo et al. 2006, Eisen et al. 2006, Estrada-Pena and Venzal 2007). In our case, a simple model predicting suitable habitats of ticks based on vegetation cover and elevation was developed. The data from CORINE Land Cover 2006 seemed sufficient for our purpose in the respect of resolution as well as number and composition of vegetation cover categories. This source was also used in the study of Šumilo et al. (2006). According to numerous experimental data, the activity of ticks is influenced by elevation (e.g. Materna et al. 2008). Altitude plays a particularly important role in our model because it allows us to classify the mountainous regions correctly as low risk areas, although the vegetation cover might be suitable.

The predictions produced by the model were significantly correlated with the actual tick activity. The valleys of large rivers were considered the areas of increased risk. This migth be possibly due to presence of deciduous and mixed forests as well as relatively low altitude. By contrast the Šumava mountain range was classified as low risk area, apparently due to high elevation. Indeed, the tick activity in this region is considerably lower when compared with the rest of the region (Danielová at al. 2002, 2006).

Human activity was included to the model, to be able to compare the model output with actual number of tick-borne encephalitis cases. Although the distribution of TBE in nature is highly focal and influenced by other factors besides simple tick activity (Danielová 2002), high degree of correlation was found. The probable reason is high correlation of human activity with number of disease cases. The high-risk areas were concentrated in the surroundings of larger settlements, indicating again the importance of human population density. The tourist activity seems to play an important role in the recreational areas of Orlik and Lipno dam and in the area of Třeboň. Nevertheless, in the map of risk TBD case occurrence some sparsely populated areas remained classified as high risk. These areas co-incided with areas of maximum biological risk. These facts indicate that high numbers of clinical cases may be caused either by high human activity or by high tick activity in poorly inhabited areas.

Concerning the overall proportional representation of different risk categories, minimum to increased risk categories cover 94 % of the area under survey. Only 4 % of the pixels were assigned to high or maximum risk indicating, that the biological risk is almost homogenously spread over the whole region with only several small areas reaching the extreme values.

The model of biological risk has a technical limitation in its resolution. In the map outputs is the lack of resolution presented in the case of smaller water courses, which are not depicted. Similar situation will be in the case of small areas of different vegetation type than the surrounding areas. However, the probability of survival of a stable tick population in a fragment of suitable habitat smaller than the model resolution 50x50 m is negligible. Therefore, we consider the resolution of the model still sufficient, although not perfect.

When compared with disease case based models, the proposed model has several advantages. Due to the vegetation cover layer is the identification of the risk areas more accurate by the model. Furthermore, the number of cases does not include the cases without any clinical signs, cases that do not occur because of immunity acquired by previous infection or vaccination. In regions with high vaccination rate, the risk for an unvaccinated person may be actually much higher than predicted from disease case mapping.

The presented model is one of the working versions and will be further optimized. The possibility of integration of climatic data, field-collected data on tick activity and pathogen prevalence will be considered. The predictors and their combinations will be selected by their statistical evaluation on a trining dataset. The human activity model could be refined by data on urbanization and land use (Estrada-Pena and Venzal 2007).

ACKNOWLEDGEMENT

The authors would like to thank for the data kindly provided by the Region of South Bohemia, Faculty of Economics and Administration, MU Brno, National Institute of Public Health, Prague and for collaboration to Dr. Danielová and Dr. Daniel. The research is co financed by the European Development Fund of the European Union, by the Region of South Bohemia and by following grants: SP/2010184 and GAČR 206/09/H026.

REFERENCES

Randolph, S.E. (2001) The shifting landscape of tick-borne zoonoses: tick-borne encephalitis and Lyme borreliosis in Europe. Phil. Trans. R. Soc. Lond. B. 386: 1045-1056.

Süss, J., Schrader, C., Falk, U., Wohanka N. (2004) Tick-borne encephalitis (TBE) in Germany – epidemiological data, development of risk areas and virus prevalence in field-collected ticks and in ticks removed from human. Int. J. Med. Microbiol. 293 Suppl 37: 69-79.

Materna, J., Daniel, M., Metelka, L., Harčarik, J. (2008) The vertical distribution, density and the development of the tick *Ixodes ricinus* in mountain areas influenced by climate changes (The Krkonoše Mts., Czech Republic). Int. J. Med. Microbiol., 298, S1, 25-37.

Gray, J.S., Dautel, H., Estrada-Pena, A., Kahl, O., Lindgren, E. (2009) Effects of climate change on ticks and tick-borne diseases in Europe. Interdiscip. Perspect. Infect. Dis. 2009:593232.

Beneš, V., Bodlák, K., Moller, J., Waagepetersen, R. (2005) A case study on point process modeling in disease mapping. Image. Anal. Stereol. 24: 159-168.

Eisen, R.C., Eisen, L., Lane R. S. (2006) Predicting density of *Ixodes pacificus* nymphs in dense woodland in Mendoncino county, California, based on geographic information systems and remote sensing versus field-derived data. Am. J. Trop.Med. Hyg. 74:632-640.

Schwarz, A., Maier, W.A., Kistemann, T., Kampen, H. (2009) Analysis of the distribution of the tick *Ixodes ricinus* L. (Acari: Ixodidae) in a nature reserve of western Germany using geographic information systems. Int. J. Hyg. Environ. Health 212: 87-96.

Rizzoli, A., Merler, S., Furlanello, C., Genchi, C. (2002) Geographical information system and bootstrap aggregation (bagging) of tree-based classifiers for Lyme disease risk prediction in Trentino, Italian Alps. J. Med. Entomol. 39: 485-492.

Daniel, M., Zítek, K., Danielová, V., Kříž, B., Valter. J., Kott, I. (2006) Risk assessment and prediction of *Ixodes ricinus* tick questing activity and human tick-borne encephalitis infection in space and time in the Czech Republic. Int. J. Med. Microbiol., 296 Suppl. 40: 41-47.

Ostfeld, R.S., Glass, G.E., Keesing, F. (2005) Spatial epidemiology: an emerging (or re-emerging) discipline. Trends Ecol. Evol., 20, s. 328-336.

Eisen, R.J. and Eisen L. (2008) Spatial modeling of human risk of exposure to vector-borne pathogens based on epidemiological versus arthropod vector data. J. Med. Entomol. 45: 181-192.

Süss, J. (2003) Epidemiology and ecology of TBE relevant to the production of effective vaccines. Vaccine: 21:S1 19-35.

Humair, P.-F. and Gern, L. (2000) The wild hidden face of Lyme borreliosis in Europe. Microbes Infect. 2: 915-922.

Šumilo, D., Bormane, A., Asoklien, L., Lucenko, I., Vasilenko, V., Randolph, S. (2006) Tick-borne encephalitis in the Baltic States: Identifying risk factors in space and time. Int. J. Med. Microbiol., 296, 76-79.

Nosek, J. and Krippel, E. (1974) Mapping of ixodid ticks. Report Inst. Geogr. Czechoslov. Acad. Sci., 111, 9-19.

Daniel, M. and Kříž, B. (2002) Klíšťová encefalitida v České republice. SZÚ. Praha.

EEA 2006 (European Environment Agency), http://www.eea.europa.eu/data-and-maps/data/corine-land-cover-2006-clc2006-100-m-version-12-2009, 29.10.2010.

Jouda, F., Perret, J., Gern, L. (2004) *Ixodes ricinus* density and distribution and prevalence of *Borrelia burgdorferi* sensu lato infection along an altitudinal gradient. J. Med. Entomol., 41, 162–169.

Materna, J., Daniel, M., Danielová, V. (2005) Altitudinal distribution limit of the tick *Ixodes ricinus* shifted considerably towards higher altitudes in Central Europe: results of three years monitoring in the Krkonoše Mts. (Czech Republic). Cent. Eur. J. Pub. Hlth., 13, 24-28.

Danielová, V., Daniel, M., Schwarzová, L., Materna, J., Rudenko, N., Golovchenko, M., Holubová, J., Grubhoffer, L., Kilian P. (2010) Integration of a tick-borne encephalitis virus and *Borrelia burgdorferi* sensu lato into mountain ecosystems, following a shift in the altitudinal limit of distribution of their vector, *Ixodes ricinus* (Krkonoše Mountains, Czech Republic). Vector Borne Zoonotic Dis., 10, 223-230.

Gilbert, L. (2010) Altitudinal patterns of tick and host abundance: a potential role for climate change in regulating tick-borne diseases. Oecologia, 162, 217-225.

Vassalo M., Pichon B., Cabaret J., Figau C., Pérez-Eid C. (2000): Methodology for sampling questing nymphs of *Ixodes ricinus* (Acari: Ixodidae), principal vector of Lyme disease in Europe. J. Med. Entomol. 37: 335-339.

Estrada-Pena, A. and Venzal, J.M. (2007) A GIS framework for the assessment of tick impact on human health in changing climate. Geospatial Health 2, 157-168.

Vystoupil, J., Holešinská, A., Kunc, J., Maryáš, J., Seidenglanz, D. Šauer, M., Tonev, P., Viturka M. (2006) Tourism Atlas of the Czech Republic. Ministerstvo pro místní rozvoj ČR, Praha.

Danielová, V., Holubová, J., Daniel, M. (2002) Tick-borne encephalitis virus prevalence in *Ixodes ricinus* ticks collected in high risk habitats of the South-Bohemian region of the Czech Republic. Exp.Appl.Acarol. 26:145-151.

Danielová, V., Rudenko, N., Daniel, M., Holubová, J., Materna, J., Golovchenko, M., Schwarzová, L. (2006) Extension of *Ixodes ricinus* ticks and agents of tick-borne diseases to mountain areas in the Czech Republic. Int.J.Med.Microbiol. 296, Suppl. 1: 48-53.

Danielová V. (2002) Natural foci of tick-borne encephalitis and prerequisites for their existence. Int. J. Med. Microbiol. 291, Suppl. 33: 183-186.

CELLULAR AUTOMATA FOR EARTH SURFACE FLOW SIMULATION

CIRBUS Juraj and PODHORANY Michal

Institute of Geoinformatics, Faculty of Mining and Geology, VŠB – TU Ostrava
17. listopadu 15, 708 00, Ostrava Poruba, Czech Republic
juraj.cirbus@vsb.cz, michal.podhoranyi@vsb.cz

Abstract

Cellular automata as a tool for modelling and simulation of processes taking place in the real world are now increasingly used, as evidenced by their use not only as a tool for creating simulations, but also by their use in areas of crisis management. Using GIS knowledge it is possible to create cellular automata, which can appropriately and authentically reflect the water flow on the Earth's surface. The issue of the water flow simulation on the surface using cellular automata is a complex problem, into which a large number of external factors enter. Some of these factors are necessary to be generalized to a great extent; some must be included in the model itself. These factors may include, for example, liquid balance equation where it is necessary to determine the amount of liquid which is located in the cell, the amount of liquid which is absorbed into the terrain (infiltration) and that which is partially evaporated (evapotranspiration). Another factor is determination of the speed of distribution of liquid amongst the cells during each step of the simulation. The project is divided into several individual parts, amongst which the preparation of test data (input layers), the design of cellular automata interface, which eventually serves for communication with the user and the core are included. The most important part of the solution is to create the core of cellular automaton, which will deal with the computation for the liquid flow. The result is then stored as a sequence of raster images that were created in a certain chronological order.

Keywords: cellular automata, model, hydrology, simulation, liquid flow

INTRODUCTION

Water drainage in the terrain is not a simple process. It is a part of a far more complex, precipitation-drainage process. In short, it can be stated that the water falls from the atmosphere in the form of precipitation, part of precipitated water is trapped on the surface of plants and objects, another part supplements the volumes in lakes, reservoirs and ponds, and part is absorbed into the ground. Previous relationship demonstrations provide a very simplified view of the complex precipitation-drainage process, whose understanding sets the basis for each analysis connected with the simulation of water mass. The aim of this paper is not "just" an understanding of the distribution of water, or liquid in nature but also its conversion into a digital format in the form of cellular automata. In terms of cellular automata for the water distribution, the contribution of the paper lies in providing information on the possibilities of using cellular automata for the simulation of hydrological processes and their implementation, or their linking with GIS applications.

CURRENT STATE

The basics of cellular automata have been given in the 1950's, inspired by the arrival of electronic computers, where some systems were equivalent to cellular automata. The cellular automata issue was first addressed by John von Neumann, who was trying to create an abstract model of self-reproduction in biology - the topic that he had to examine in cybernetics. However, the research on cellular automata began to recede due to the poor performance of computers and also due to the fact that the field of cellular automata was different from other sciences. John Horton Conway, who created a game called "Life", brought revival into this area. The *"Life"* was based on a two-dimensional field, where the cells may have only two states and 8 cells define the environment. Two states, which the cells were able to reach, were either that of dead or alive. The Conway's *"Game of Life"* scored a great popularity in all age categories. (Wolfram, 1994).

In recent years, several types of cellular automata have been created, whose use found their justification in hydrology, or in the research of hydrological processes. The most development of such simulation programs occurs because of the repeated and more frequently occurring natural disasters. The creation of simulation models, which are useful as predictive tools, helps reduce or eliminate the impacts of natural disasters. The cellular automata can be used as a simulation tool, where by using simple rules as well as physical and mathematical equations it is possible to create a comprehensive system, showing the required processes.

The cellular automata (hereinafter referred to as the CA) represent the spatial processes of uneven terrains and simulate hydrologic and hydraulic behaviour (Pearson, 2007). The authors of the each paper use similar rules to those created by Conway in his game *"Life",* and the fact that the state of the cell is influenced by the state of the previous cell. Pearson has also addressed the CA dedicated to surface drainage. His model uses the layers of a digital terrain model, the infiltration and the friction layer. The advantage of the model is that the actual outcome also incorporates the time required for the move from one cell to another. The weakness of the model could perhaps be seen in the fact that the whole cellular automaton was created in the Java programming language and thus its implementation as the programme module into already existing GIS applications is not possible.

In addressing liquid flow in the terrain it is necessary to develop such a model in which the liquid will not be distributed only through one channel, namely from the higher situated point to the point below it, but it is necessary to create the so-called multi-flow direction (MDF), where a part of the liquid is converted into nearby cells, located near the main channel. A similar case, on a larger scale, has been dealt with by the model for the simulation of braided water flow. Braided water flows are characterized by high drainage activity without the characteristic valley, cohesive banks and vegetation. In this case, the classical cellular automata rules for the water distribution could not be used. See Fig. 1.

Fig. 1: The braided river

The accuracy of the inflow is restricted by several factors. If liquid is channelled into the following three cells, the flow direction is limited to a 45° angle. As a result, the meanders which are more than 45° cannot be further monitored. Secondly, if the routing algorithm does not take into account the relationship between water drainage and water column height (amount of liquid in the cell), the complete emptying of the cell may occur. It is this example, to simulate braided water flow, which well illustrates the need of water distribution into the neighbouring cells, next to the main channel (Thomas, Nicholas, 2002).

An interesting cellular automaton that uses multi-drainage and its deployment in crisis situations is the cellular automaton for mudflow distribution. This machine uses the Moor neighbourhood concept (8 neighbouring cells). An algorithm simulates the mudflow as the liquid drainage that uses data such as the height of all points and the mud volume shown in a given period. The algorithm also uses variable percentage of the neighbours and thus ensures a random direction of drainage (Busaki, 2009).

The form-based algorithm determines the estimated flow through the digital terrain model. As a result, the form-based algorithm was compared with the results provided by the ARC / INFO programme. The algorithm has turned to provide better results than the algorithm that is used by the ARC / INFO programme. The reason is that the form-based algorithm works and divides terrain into several categories. The result of the aforementioned comparison can be seen in Fig. 2 (Pilesjö, 1998).

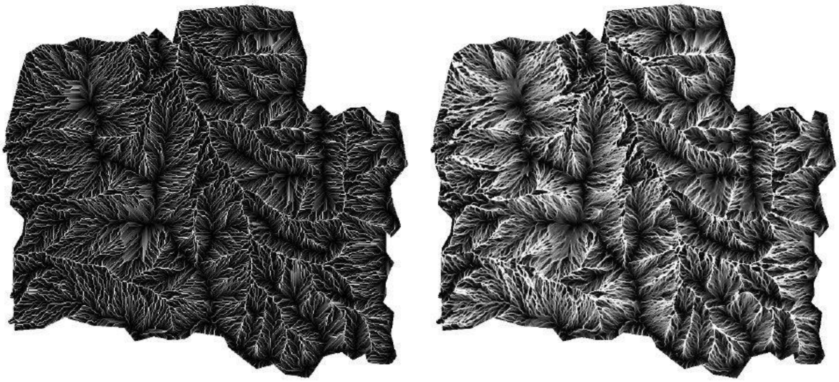

Fig. 2: Comparison between computed flow accumulation, left: flow accumulation estimated by ARC/INFO, right: flow accumulation by the form-based algorithm

WHAT IS CELLULAR AUTOMATON?

Models based on the CA principle stems from the principle of simple local interactions. The local interactions form the basis of the CA. Whether there is a change in the cell state is given by the transition rule, which is assessed using predefined neighbourhood of the cell. From this perspective the idea of using the CA to simulate liquid flow to the Earth surface is ideal. The raster data values are stored in a regular network, where both the shape and dimensions of each cell are identical. An important aspect that must be evaluated before the creation of CA is its own use in GIS.

General Principles

Cellular automata are divided into two categories, namely the CAs working with raster data, or matrix cells, which are always represented by one raster pixel, and the vector CAs (Shiyuan, 2004). In the vector CAs, the method and the work with neighbourhood is already more complex, which is so due to defining the transition rules.

The cellular automaton is a dynamic, discrete system, which works with a network of cells of the same type. Status and behaviour of the cell is determined by its current state, and the condition of the cells located in its immediate neighbourhood (Wolfram, 1984). Generally, two types of neighbourhood are used, namely the neighbourhood formed by the four closest cells (Neumann neighbourhood), see Fig. 3 (left), and the one formed by the eight cells (Moor neighbourhood), see Fig. 3 (right). An updated status of the central cell occurs during the convolution window movement, see Fig. 4, by the movement through the entire cell network. The state of the central cell varies according to defined rules, whose number is finite and the states of all cells are changing simultaneously in one instant of time. All cells use the same transition function. As a result, creating and applying the simple rules can obtain complex patterns.

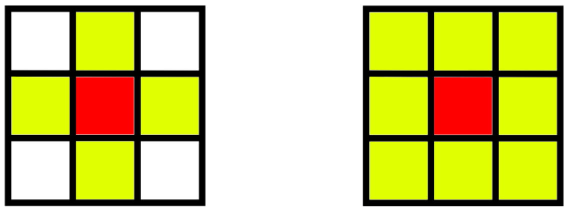

Fig. 3: The types of neighbourhood (left: Neumann´s neighbourhood, right: Moor´s neighbourhood)

The main features of cellular automata include:

- Parallelism (computations in all cells take place simultaneously, not serially)
- Location – state of the central cell depends on its current state and the state of its neighbourhood
- Homogeneity – the same rules apply to all the cells

Basic features of cellular automata are as defined below:

- Work in discrete time and space
- Formed by cells
- Each cell can have different states
- The value of the cell state is determined by the local transition function, which is the same for all cells and is defined by the rules
- Each cell has information not only about itself, but also about its neighbourhood (local information) and on this basis it makes decision what to do in the next cycle.

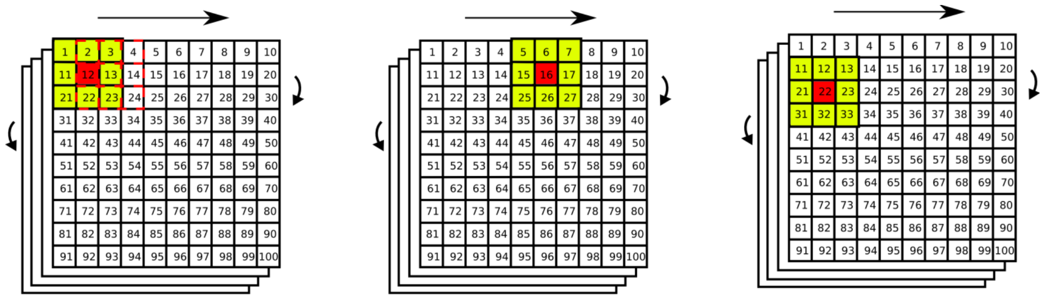

Fig. 4: Movement of convolution window

Hydrological Basis for Cellular Automata

For the simulation of hydrological processes such as the precipitation-drainage and hydrodynamic models both more and less complicated and complex simulation tools are used. These tools are used to simulate various types of spatial processes. For the model, in this case, the tool was used that is based on mathematics, whether it concerns analytical or numerical models. In the area of hydrology it generally considers complex mathematical models. These models require for its function spatial data, which must, before their use, undergo preparation (pre-processing). The data adjustment is performed by the GIS applications that are used in the final adjustment to the final data (post-processing). The GIS applications provide facilitation in the interpretation of the data with the possibility of their further use and thereby also increase their latent value.

Hydrological simulations allow us to not only study complex spatial processes that affect the water flow, but also to anticipate future situations based on the current status. Predicting hydrological processes such as directions of water spread through the terrain or an affected and contaminated area are the properties that can be used and deployed in the areas of crisis management. The issue concerning the flow of water on the Earth surface is a complex problem, into which a large number of external factors enter. Some of these factors are in the model itself necessary to be to a large extent generalized, others need to be included in the model itself. These factors may include, for example, hydrological balance equation, the amount of liquid, which is absorbed into the terrain (infiltration) and the amount, which is partially evaporated (evapotranspiration).

PROGRAMME AND DATA TOOLS

Selecting a suitable programming tool in which the cellular automaton will be created is very important. From the very beginning of the project the Python programme seemed a suitable candidate. Suitability of the Python language was confirmed by a number of reasons. First, it was the multi-platform. A script written in Python can be run in both OS Windows and Linux. For example, the Java language is also multi-platform. Another reason is that Python supports existing GIS applications. The largest representatives of the GIS software in the commercial sector include the ArcGIS programme that enables import of modules into its toolbox, developed in the Python language (Java language support is not provided). In a non-commercial area there are e.g., OpenJump, GRASS programmes that also provide a similar import.

The disadvantage of Python is a work with designing and creating a user-friendly environment. Using additional libraries solves this part. The existence of a considerable number of libraries and thus the expanding of other programming language skills are, on the other hand, again the benefits that Python provides. For working with a raster the gdal library is used. This library allows the direct download of the raster in a GeoTiff format. After downloading the raster the programme works with it as if it was a two-dimensional field (hereinafter referred to as the network of values).

The cellular automaton is programmed to be object-based. To calculate the individual elements the modules that are selected gradually and, if appropriate, are created. Modules were created gradually, as requirements and new rules for the CA have increased. The first created module was the liquid detector. It serves to detect the presence of liquid in the neighbouring cells of the matrix when the convolution window moves through the network of values. In the event of liquid detection the algorithm decides if the liquid is to be added or not to the central cell. Other models developed are as follows:

- Module for determining the outflow directions
- Module for calculating the terrain gradient
- Module for calculating the liquid distribution speed
- Module for calculating the liquid flow rate through the given cell
- Infiltration module
- Slowing of liquid movement due to ruggedness of the terrain
- Module providing an update of each network

However, the list of modules is not final and their number is with enhancement of other CA features likely to further increase.

With the development of modules there is a growing demand for storage of the calculation results. Those are recorded in the auxiliary networks. The base network is a digital terrain model and a network with the localization of liquid source. It is necessary to work on levels of several networks that are built above the base entry network. Auxiliary networks match the number created by the module, where each module stores the calculated values within its own network.

Area Studied

The base layer, which is used as a basis for simulation of the liquid flow, is in almost all analyses the digital model of terrain (DMT). DMT is most often used as a grid (in foreign literature is normally referred to as DEM). For the needs of cellular automaton generated in the following paper, a sufficient supporting input is the territory cut from DMT 25 (Digital Model of Territory). The selected territory falls within the northwestern part of Ostrava and is of the approximate area of 7.84 km^2. Selection of territories was purely accidental and not conditional by any determinants.

DMT 25 is part of the Military Information System and is generated in Toposlužba AVCR (VTOPÚ Dobruška). Information content essentially matches the 1: 25,000 topographic map (TM-25). The benefit of DMT 25 is a wider range of attachable attributes, especially in the area of communications and vegetation habitation and frequency. Some disadvantages of DMT are partial duplicity of some data and a slightly higher generalization of objects (mostly buildings and water areas).

CREATION OF CELLULAR AUTOMATON

Simulation of Liquid Flow

The base layer, which simulates the flow of liquid, is the layer of a digital model of terrain (DMT 25). Each raster cell is a carrier of information on the height. A new network of values, which contains directions of liquid distribution, is created above this layer. The values of flow directions are determined from the digital terrain model, where the central cell is assigned a value of the direction upon the movement of 3x3 convolution matrix. Directions are coded in binary manner between 1 and 128, see Fig. 5, where the following encrypted direction can be divided into liquid, if necessary, and more cells in Fig. 5. Before launching the determination of the flow and the spread of liquid it is necessary to know the location of the liquid source. Source of the liquid may be specified in either raster coordinates or information on the location can be transited through a new network of cells, which are formed above the layer of the digital model of terrain.

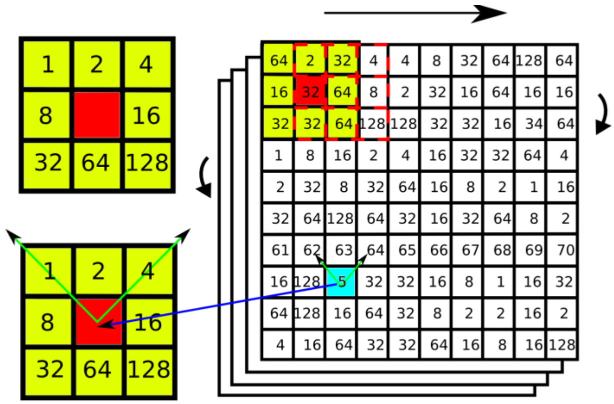

Fig. 5: Flow directions

Determination of the liquid distribution is speed calculated using the Manning roughness equation:

$$v = \frac{\sqrt[3]{depth}\,.\sqrt{s}}{n} \tag{1}$$

where *depth* is the height of the water column value, which is located in the cell, *s* stands for the gradient or slant of the terrain, which is converted from the digital model of terrain, and *n* is the value of the friction coefficient for different types of cover. The value of friction coefficient can be expressed for the whole complex area of interest or based on the cover area the friction network can be created where each cell of the network contains the determined *n* value. Roughness values used for different types of cover are listed below.

Tab. 1: Manning *n* value

Surface Description	***n* Value**
Smooth surfaces (concrete, asphalt, gravel)	0.011
Uncultivated land	0.05
Agriculturally used land	
1. Cover less than 20%	0.06
2. Cover more than 20%	0.17
Grass	
3. Short grass (prairie type)	0.15
4. Dense grass	0.24
Pastures	0.13
Forest	
5. Brushes and Scrubs	0.40
6. Dense forest	0.80

The size of the liquid volume, which will be transferred to the next cell, is calculated as follows:

$$W = depth.width.v.t \tag{2}$$

where W is the calculated volume of liquid in m^3, *depth* is the height of the water column, which appears in the cell, *width* is the pixel size, *v* is the calculated liquid distribution speed, and *t* is the time data in seconds.

After launching the cellular automaton, the user is prompted to enter time data, for a period for which output raster layers will be generated. Each iteration step corresponds to 1s. The 3x3 convolution matrix is moving through individual cells of the network. During the entered simulation period the movements of the convolution window in the network are continuously repeated, while after each movement of the network the information on elevation of terrain, outflow directions, terrain gradient and other values that are stored in the auxiliary networks must be updated. Upon exiting the simulation, the result is stored in the raster layers, which is consequently possible to simulate using a suitable software product. Simulation of raster images using the cellular automaton developed is not yet available. Fig. 6 shows the results of the simulation of the liquid distribution. The images show the results after application of cellular automaton where the input was the layer of digital model of terrain and the location of the liquid source. The value of the friction coefficient was set uniformly for the entire territory to be 0.05, which according to the table corresponds to the value of uncultivated land. After a selected time period, where one iteration corresponds to a time step of 1s there is a raster layer exported in the TIF format as an output. Each displayed image shows the result of the distribution after 5 minutes. The pixel resolution is 50x50 m. The liquid spreads from the source, which was set up as inexhaustible and still produces the same amount of liquid. The source was placed into a dry riverbed. While observing the distribution of the liquid from the source it is obvious that the liquid respects the riverbed. With an increasing amount of liquid the liquid rises in the riverbed and floods an increasing number of cells.

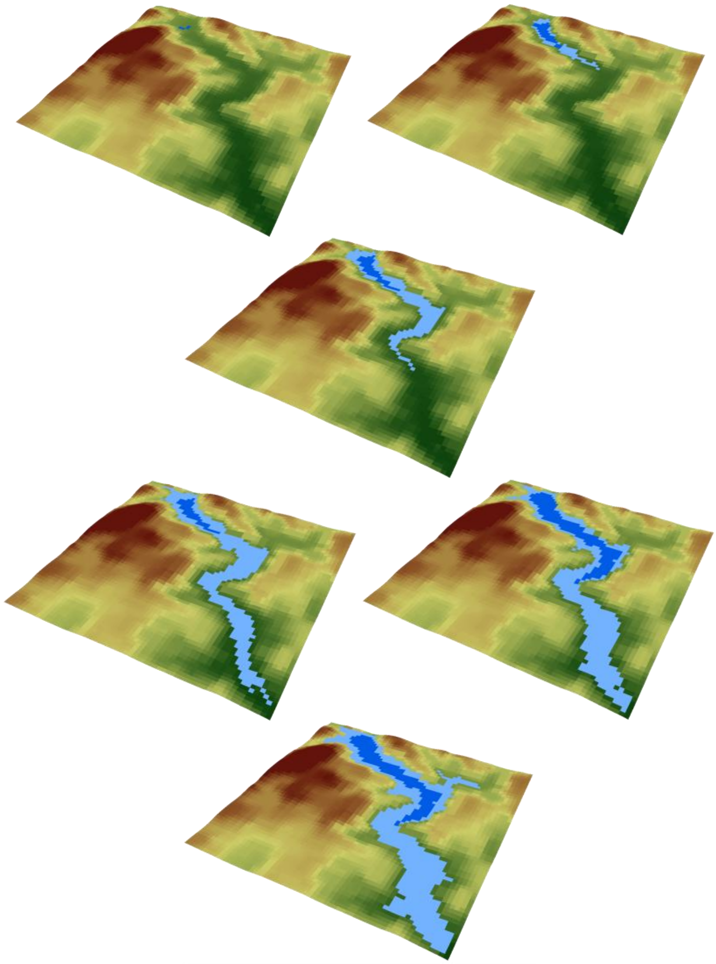

Fig. 6: Results of liquid flow simulations

CONCLUSION

To conclude, it can be stated that, although there has not been found much use for cellular automata in hydrological circles it is possible to deploy them as a tool for simulation of the liquid flow. By selecting the appropriate programming language the cellular automaton can be implemented in already existing GIS programme tools and thereby partially enhance their functionality. An important quality of the cellular automaton is in its individual approach and possibility to work independently on programme GIS applications. These arguments are already partially supported by the results obtained, which are presented at the end of the Flow Simulation chapter.

Further developments in the field of cellular automaton will be focused on the expansion of its computing parts, the capacity of the liquid infiltration as well as the possibility of entering different liquids with different densities. The results achieved will be compared and calibrated with already existing hydrodynamic models. The effort will be to get, as faithfully and accurately as possible, closer to the results obtained from comprehensive computational mechanisms that are used i.e. in hydrodynamic models.

ACKNOWLEDGEMENTS

We would like to acknowledge the SGS Project SP/2010146 from VSB TU Ostrava.

REFERENCES

Wolfram, S. (1984) Cellular automata as models of complexity, Nature. 311: 419-24.

Wolfram, S. (1994) Cellular automata and complexity: collected papers. Reading, MA: Addison – Wasley.

Thomas, R.; Nicholas, A.P. (2002) Simulation of braided river flow using a new cellular routing scheme, Geomorfology 43: 179-195.

Parson, J.; Fonstad, M. (2007) A cellular automata model of surface water flow, Hydrological Processes, 21.

Pilesjö, P. (1998), Estimating Flow Distribution over Digital Elevation Models Using a Form-Based Algorithm, Annals of GIS, 4.

Busaki, A.; Harson, T.; Arai. K. (2009) Modeling and Simulation of Hot Mudflow Movement Prediction Using Cellular Automata, Third Asia International Conference on Modelling & Simulation.

Shiyuan, H.;Deren, L. (2004) Vector Cellular Automata Based Geographical Entity, 12th Int. Conf. on Geoinformatics – Geospatial Information Research.

MICRO-SIMULATION OF DRIVER BEHAVIOUR AT UNSIGNALISED INTERSECTIONS

RAPANT Petr, SZTURCOVA Daniela *and* HRUBA Lucie

Institute of Geoinformatics, Faculty of Mining and Geology, VSB – Technical University of Ostrava,
17. listopadu 15, 708 33, Ostrava – Poruba, Czech Republic,
petr.rapant@vsb.cz

Institute of Geoinformatics, Faculty of Mining and Geology, VSB – Technical University of Ostrava,
17. listopadu 15, 708 33, Ostrava – Poruba, Czech Republic,
daniela.durakova@vsb.cz

Department of Economy and Marketing, Regional Development Agency Ostrava,
Na Jizdarne 7, 702 00, Ostrava, Czech Republic
hruba@arr.cz

Abstract

The presented paper deals with a method for the automatic evaluation of rights of way at unsignalised intersections. The method is based on (1) data describing the configuration of an intersection and its traffic signage and (2) simple rules for evaluation of rights of way based on general rules governing the road traffic. The proposed method is based on a simple procedure resulting from a table describing potential crossovers of routes for the given intersection type with priority indications for intersecting routes, intersection types and traffic signage. We have tested our method in many situations: different configurations of intersections (T-intersection, four- and five-way intersections), different configurations of traffic signage and different combinations of incoming cars. The only problem we have encountered was the deadlock. This problem can be solved quite easily. However, its solution is not included in this paper.

Keywords: traffic simulation, micro-model, Intelligent Transport System, unsignalised intersection, unprotected turn, multi-agent system

INTRODUCTION

As Intelligent Transport Systems (ITS) develop, requirements also grow for appropriate traffic simulation tools (e.g. (Mallikarjuna and Ramachandra 2005; Dailej and Taiyab 2002; Wang et al. 2007; Jost and Nagel 2003)). In terms of cooperation with Intelligent Transport Systems the *microscopic models* are the most interesting ones. These models count on interactions of individual vehicles and their independent decision-making on their further activity based on the local situation assessment (local context).

In the presented paper we deal with a proposal of a traffic situation description at an intersection so that the individual agents representing vehicles are able to evaluate the situation and correctly decide on their behaviour when passing through an intersection.

RELATED WORKS

Quite a number of authors deal with simulations of road transport. They cover in principle both the above mentioned cases, i.e. traffic simulation via cellular automata (CA) and multi-agent systems (MAS) as well. In both cases the authors solve fundamental behaviour types of vehicles within traffic infrastructure such as e.g. (Dailej and Taiyab 2002; Mallikarjuna and Ramachandra 2005; Nagel 2003; Wang and Ruskin 2002; Wang and Ruskin 2003; Wang and Ruskin 2006; Wang et al. 2007; Kozuka et al. 2001):

- speeding,
- breaking,
- free driving or optimal headway,
- car following,
- lane changing,
- takeover,
- protected turns,
- *unprotected turns*,
- roundabouts,
- bottlenecks.

From the viewpoint of the issue being solved the case of unprotected turns is of our interest.

In (Wang and Ruskin 2003) a solution of multi-lane intersections through the use of CA is described. This solution is based upon a simplified intersection type which occurs most frequently in urbanized areas of the USA and elsewhere, a two-ways stop-controlled intersection (TWSC intersection). It concerns a classical intersection of a major road and a minor road. The major road has two traffic lanes in each direction, the minor road has always a single traffic lane and before the intersection a STOP sign is located. Thereby the solution of passing through the intersection is considerably simplified.

Another approach is described in (Troutbeck and Brilon 1997; Liu et al 2005; Brilon and Bondzio 1997). The authors here work again with a TWSC intersection. All traffic lanes are ranked (see Fig. 1) and their priority is controlled by these rankings.

This un-signalled intersection has a hierarchy of traffic lanes. Some lanes have absolute priority (they have been assigned Rank 1), and the others have a lower level of priority. In the case of a TWSC intersection from Fig. 1 the traffic ranked lanes have to fit the following rules (Troutbeck and Brilon 1997):

- Rank 1 stream has absolute priority and does not need to yield right of way to another stream,
- Rank 2 stream has to yield to a Rank 1 stream,
- Rank 3 stream has to yield to a Rank 2 stream and in turn to a Rank 1 stream, and
- Rank 4 stream has to yield to a Rank 3 stream and in turn to Rank 2 and Rank 1 streams (left turners from the minor street at a cross-intersection).

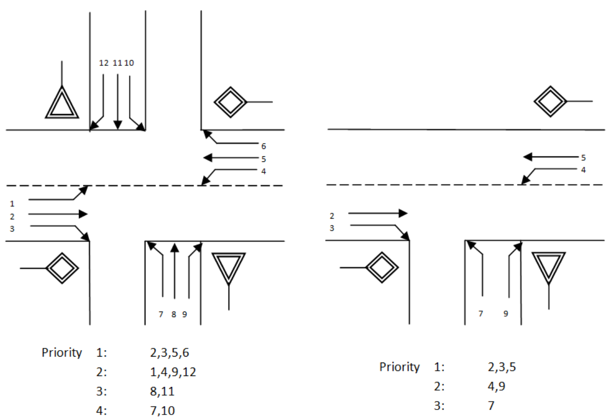

Fig. 1. The numbers beside the arrows indicate the enumeration of traffic lanes. Priority of these lanes is ranked as shown in the picture (Troutbeck and Brilon 1997).

This procedure cannot be used in the case of roundabouts (Troutbeck and Brilon 1997). Furthermore its utilization depends on an a priori evaluation of intersections. For this reason this principle of decision-making on road priority is improper for traffic modelling via MAS. On the contrary here we suppose the vehicle is able to independently evaluate the intersection it is approaching, and to decide independently on its own priority of passing through the intersection.

In (Barceló and Casas 2002) a logic of modelling the behaviour of vehicles on a road network involved in the modelling system AIMSUN is described. Among others a lane changing model and gap acceptance in the give-way zone model is also described here. Also a logic of decision-making is described in detail, whether the car driving out from a minor road manages to pass through the intersection without any danger of collision with a vehicle incoming on the major road. Thus it only concerns a partial task linked with the solution of intersections. So the question of assessment of intersections from the viewpoint of priorities is not solved here.

From this overview it is obvious that none of the authors deal with priorities assessment at a general intersection. As a rule they worked with the simplest type of intersection, at which the priorities for individual roads had been assessed a priori. The models are utilized predominantly for a statistical traffic assessment and proposals (and testing) of measures destined for improving the current state of intersection solution.

PROPOSED APPROACH AND METHODOLOGY

When approaching an intersection the vehicle attains its so-called visual assessment, i.e. visible surroundings that contains:

- an infrastructure description, in the present case the intersection layout (directed graph of entry and exit road segments),
- traffic signage, and
- the presence of cars on approach roads (cars that may immediately enter the intersection) together with their intended direction of passage (with a switched on direction indicator) and movement speed, if appropriate.

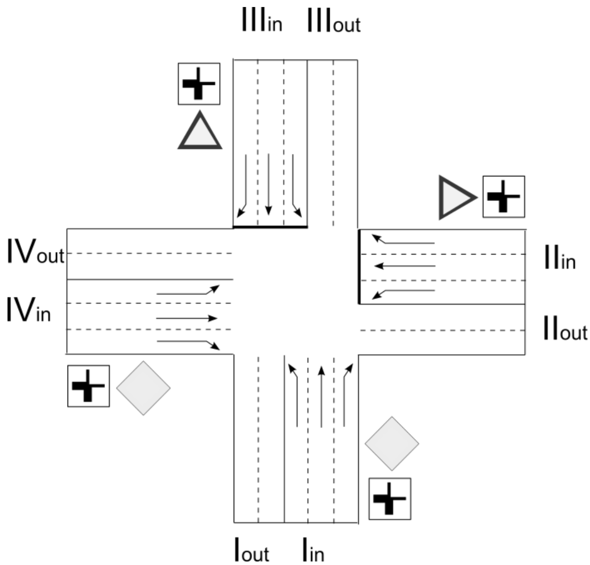

Fig. 2. Intersection of major road led at a right angle and two minor roads.

The car assesses from the data table of conflicting passages, the sequence of the cars passing through the intersection and, as soon as it is its turn, it crosses.

Fig. 2 displays an example intersection, used for our case study.

The sequence of cars passing through an intersection is governed by strict rules given by legislation regulating the local convention. In our case we proceed from states of right-hand driving. It is easy to transfer our considerations to the opposite situation, thus left-hand traffic.

INFRASTRUCTURE DESCRIPTION AND TRAFFIC SIGNAGE APPLICATION

An intersection layout is described by directed graph (see Fig. 3).

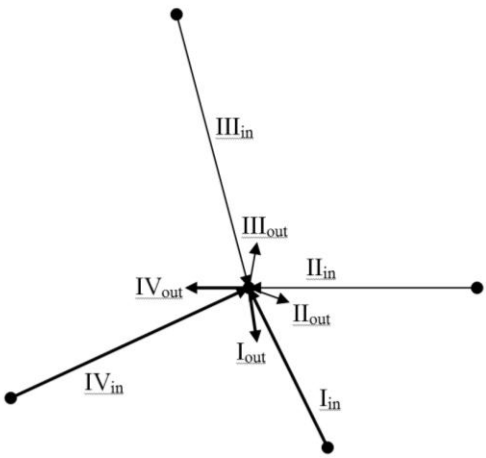

Fig. 3. Graph of intersection (subscripts are not used in tables).

While assessing priorities at an intersection we need to first assign values to the intersection graph. The graph valuation results from the traffic signage and general rules above. In the case of the presence of traffic signs the edges are assigned valuations (rank):

Table 1. Table of potential crossovers of routes for the given intersection type with indications of priorities for intersecting routes and given intersection type (see Fig. 2). (Legend: +++ means the car moving on the route stated in the row of the table gives way to the vehicle moving on the route stated in the appropriate column; --- means on the contrary the vehicle has the right of way; xxx means there is no potential crossover.)

Passage direction		I – II	I – III	I – IV	II – I	II – III	II – IV	III – I	III – II	III – IV	IV – I	IV – II	IV – III
	Rank change	M – m	M – m	M – M	m – M	m – m	m – M	m – M	m – m	m – M	M – M	M – m	M – m
I – II	M – m	xxx	xxx	xxx	xxx	xxx	xxx	xxx	---	xxx	xxx	---	xxx
I – III	M – m	xxx	xxx	xxx	---	---	---	xxx	---	xxx	xxx	---	---
I – IV	M – M	xxx	xxx	xxx	---	xxx	---	---	xxx	---	xxx	---	---
II – I	m – M	xxx	+++	+++	xxx	xxx	xxx	+++	+++	xxx	+++	+++	xxx
II – III	m – m	xxx	+++	xxx	xxx	xxx	xxx	xxx	xxx	xxx	xxx	xxx	+++
II – IV	m – M	xxx	+++	+++	xxx	xxx	xxx	+++	+++	+++	xxx	xxx	+++
III – I	m – M	xxx	xxx	+++	---	xxx	---	xxx	xxx	xxx	+++	+++	+++
III – II	m – m	+++	+++	xxx	---	xxx	---	xxx	xxx	xxx	xxx	+++	+++
III – IV	m – M	xxx	xxx	+++	xxx	xxx	---	xxx	xxx	xxx	xxx	xxx	xxx
IV – I	M – M	xxx	xxx	xxx	---	xxx	xxx	---	xxx	xxx	xxx	xxx	xxx
IV – II	M – m	+++	+++	+++	---	xxx	xxx	---	---	xxx	xxx	xxx	xxx
IV – III	M – m	xxx	+++	+++	xxx	---	---	---	---	xxx	xxx	xxx	xxx

- Edges representing elements of major roads are assigned the valuation (rank) ”major road” (abr.: M),
- The remaining edges are assigned the valuation (rank) ”minor road” (abr.: m).

In case that at the intersection no traffic signs are present, all edges are valuated as a “minor road”.

It is obvious that there are four options of changing a road element rank during passing through the intersection (in sequence: entry - exit):

1. major – major (M – M),
2. major – minor (M – m),
3. minor – minor (m – m),
4. minor – major (m – M).

We can develop Table 1, containing potential crossovers of routes for the given intersection type (see Fig. 2). Pairs of routes are indicated three x’s (xxx) that do not intersect each other, and therefore no collision can occur.

For each pair of passages threatened by a collision it is now possible to assess road priorities according to simple rules. We always proceed from the left column (the below stated rules are applied hierarchically, i.e. if it is not possible to apply the first, the second is tested etc., the rule is applied which takes effect as first):

1. If two directions intersect, starting on road elements of different ranks the one has the right of way who exits the element of the major road.
2. When incoming to the intersection on major road elements the vehicle has the right of way that stays on the major road, i.e. the one that exits the minor road must give way.
3. When both vehicles are incoming on road elements of the identical rank, usually the priority to the right is applied, or vehicle turning left must also give priority to vehicle approaching from the opposite direction.

The result for the given intersection type is stated in Table 1 too.

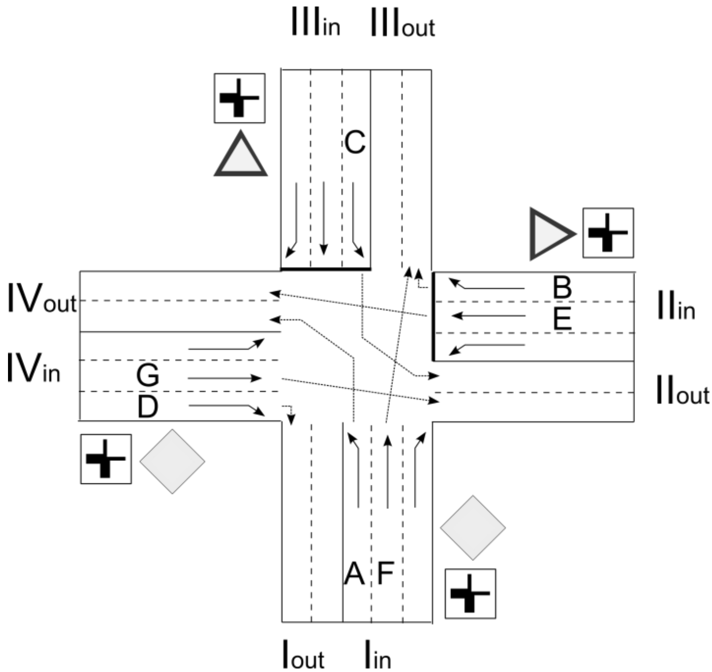

Fig. 4. Example of cars passing through the intersection; letters A to F represent cars incoming to the intersection.

ASSESSMENT OF PRIORITIES

We show the principle of the priorities assessment of the situation at the intersection from Fig. 2. For the intersection we compile a graph that is valuated and oriented, according to the above described rules (Fig. 3). We enumerate the input vertices anticlockwise. We start the numeration on one of the major roads. The numeration has a global character, i.e. all cars use identical enumeration. We validate each edge by the rank (major/minor).

For the priorities assessment we take into consideration only the cars which are first in each lane on the given road element (see Fig. 4). We have for them a given passage through the intersection that we convert to our numeration of the intersection (e.g. *I – IV* in order in – out). On the given road element then as many cars can approach the intersection as the road element has traffic lanes. At that moment we do not consider the subsequent cars in the sequence moving on the individual lanes.

Now we can compile a Table 2, representing the planned passages of cars through the intersection (according to Fig. 4).

Table 2. List of cars ready to pass through the intersection together with indicated intended routes of passages.

Car	*Passage*
A	*I – IV*
B	*II – III*
C	*III – II*
D	*IV – I*
E	*II – IV*
F	*I – III*
G	*IV – II*

In the next step we create an intersection of both above mentioned tables (i.e. we add to Table 1 cars to the routes matching to vehicles from Table 2, cancel the lines and columns without cars and exclude from the remaining lines the routes which no vehicle is moving on). The resulting table on which we are going to work further is given in Table 3.

Table 3. Resulting table after removal of all routes on which no cars are moving.

Car	Passage	Road rank	Which car theoretically to give way	Ranking
A	I – IV	M – M	---	
B	II – III	m – m	I – III	
C	III – II	m – m	IV – II, I – III,	
D	IV – I	M – M	---	
E	II – IV	m – M	I – IV, I – III, III – II,	
F	I – III	M – m	---	
G	IV – II	M – m	I – IV, I – III	

In the following step we can assess the first ranking. For some cars there are no intersecting routes. These cars thus go simultaneously as first. Further we exclude from Table 3 the routes which cars have passed and are thus already free. For cars C and G again no conflict exists in the list, so they pass through the intersection as the second in order. Further we repeat the last two steps, till the ranking of all cars is assessed. The result is given in Table 4. The result of the whole process is an empty intersection.

Table 4. Resulting table after removal of all routes on which no cars are moving.

Car	Passage	Road rank	Which car theoretically to give way	Ranking
A	I – IV	M – M	---	1
B	II – III	m – m	I – III	2
C	III – II	m – m	IV – II, I – III,	3
D	IV – I	M – M	---	1
E	II – IV	m – M	I – IV, I – III, III – II,	4
F	I – III	M – m	---	1
G	IV – II	M – m	I – IV, I – III	2

So the assessment of a static situation passes in this way, i.e. we have a set of cars which are at the entry to the intersection and assess their ranking. For the period of assessment performance the set of cars does not increase by new cars. This is however a theoretical situation only, in practice the conditions dynamically change. It is possible to modify the proposed procedure also for the case cars are coming to the intersection continuously.

CONCLUSIONS

We have developed a new approach for valuing the rights of way. Our procedure is quite simple and easily applicable. It is not data-intensive; it only needs general description of an intersection in the quality of road maps for GPS navigation. The method was tested in many situations. The only encountered trouble was the typical deadlock.

A weak point of the submitted solution (as presented above) is that it results from a static assessment of situation, i.e. it does not take into account car dynamics, like speed, period of time required to pass through an intersection, etc. Subsequent work will therefore focus on developing the approach so that it enables a dynamic assessment of priorities of cars continuously incoming to the intersection with involving gaps between cars, their speeds, needs of braking and starting and others. The involvement of the vehicle dynamics is important just for getting the simulations closer to a real traffic.

ACKNOWLEDGEMENTS

This research has been supported by the program "Information Society" of the Czech Academy of Sciences, project No. 1ET101940420 "Logic and Artificial Intelligence for multi-agent systems".

REFERENCES

Barceló, J., Casas, J. (2002) Dynamic Network Simulation With AIMSUN. *International Symposium on Transport Simulation, Yokohama*. 25 p.

Brilon, W., Wu, N., Bondzio, L. (1997) *Unisignalized Intersection in Germany – a State of the Art 1997*. Ruhr-Univerrsity Bochum. 17 p.

Dailej, D. J., Taiyab, N. (2002) *A Cellular Automata Model for Use with Real Freeway Data*. Final Research Report. Washington State Transportation Center, Seattle. 69 p.

Jost, D, Nagel, K. (2003) Probabilistic Traffic Flow Breakdown In Stochastic Car Following Models. *Transportation Research Board Annual Meeting*. Washington, D.C., paper 03-4266

Kozuka, H., Matsui, Y., Kanoh, H. (2001) Traffic Flow Simmulation Usin Cellular Automata Under Non-Equilibrium Environment. *IEEE International Conference on Systems, Man, and Cybernetics*, Vol. 2, 1341–1345.

Liu, M, Wang, R., Kemp, R. (2005) Towards a Realistic Microscopic Traffic Simulation at an Unsignalised Intersection. *Lecture Notes on Computer Science 3481*. Springer-Verlag Berlin Heidelberg, 1187–1196.

Mallikarjuna, Ch., Ramachandra Rao, K. (2005) Traffic Flow Modelling on Highways Using Celluler Automata: a Review. *Proceedings of International Conference on Structural and Transportation Engineering, (START-2005),* Elite Publishing House, N. Delhi, 912–919.

Nagel, K. (2003) Traffic Networks. In: Bornholdt, S., Schuster, H. G. (eds.): *Handbook of Graphs and Networks*. Wiley-VCH Verlag GmbH & Co. KgaA, 248–272.

Troutbeck, R. J., Brilon, W. (1997) Chapter 8: Unsignalized Intersection Theory. In: Gartner, N. H., Messer, C. J., Rathi, A. K. (eds.): *Revised Monograph on Traffic Flow Theory. A State-of-the-Art Report,* Turner-Fairbank Highway Research Center, FHWA.

Wang, R., Ruskin, H. J. (2002) Modelling trafic flow at single-lane urban roundabout. *Computer Physics Communiucations*, 147. Elsevier Science B. V., 570–576.

Wang, R., Ruskin, H. J. (2003) Modelling Trafic Flow at Multilane Intersection. *Proceedings from ICCSA*. *Lecture Notests on Computer Science*, 2667, 577–586.

Wang, R., Ruskin, H. J. (2006) Modelling Trafic Flow at Multi-Lane Urban Roundabouts. *International Journal of Modern Physics C*, 17(5), 693–710.

Wang, R., Liu, M., Kemp, R., Zhou, M. (2007) Modeling Driver Behavior on Urban Streets. *International Journal of Modern Physics*, 18(5), 903–916.

SPATIAL AND ASPATIAL MEASURES OF SEGREGATION IN THE CASE OF OSTRAVA CITY

IVAN Igor and HORAK Jiri

Institute of Geoinformatics, Faculty of Mining and Geology, VSB-Technical University of Ostrava, 17.listopadu 15/2172, Ostrava-Poruba, 70833
igor.ivan@vsb.cz

Institute of Geoinformatics, Faculty of Mining and Geology, VSB-Technical University of Ostrava, 17.listopadu 15/2172, Ostrava-Poruba, 70833
jiri.horak@vsb.cz

Abstract

Ostrava is driven by a deindustrialization process similar to other European industrial cities. Nevertheless, they are different in the stage of this process. Ostrava in this respect is unique because the process of deindustrialization started also in parallel with the end of socialism. The city partly passed a transformation which is proved in this article using selected spatial metrics on the level of basic settlement units in Ostrava city. The most common aspatial measure of segregation is index of dissimilarity. In order to incorporate the space dimension into calculations, the spatial alternatives of this index were developed and implemented in GIS SW because of its computational complexity. In addition to the application of this index of dissimilarity, spatial alternatives of this index are also introduced in this article. It does not work only within a single territorial unit, but it also considers the possibility of contact across the border into neighbouring units (based on their shared boundary, as well as its length or geometric shape of area) and multi-group measure of segregation which can accommodate more than two groups of population. These methods are applied to employment structure of the population (employment in service and industry sector, employed people over 64 years) at the basic settlement units level in the Ostrava city, derived from censuses of 1980 and 2001. Results of aspatial and spatial indices; their complementarity and appropriateness for a more comprehensive description of segregation are compared and discussed. Such type of studies has its significance especially for decision sphere and it can prepare more focused precautions to solve local problems, to provide more focused work of field workers, to provide some special help programs, to build effective community centres or even to solve problems connected to housing strategy (targeted construction of high level and social level housing in the same area).

Keywords: spatial measures, segregation, deindustrialization, GIS, Ostrava

INTRODUCTION

Ostrava represents a member of these cities where heavy industry, the engine of industrial economic growth, began to decline as in others economies of cities in developed countries in the final third of the twentieth century. As the result of closure, mechanization, suburbanization of industry and through the global shift of industrial employment from the core to semi-peripheral and peripheral countries of the world economy, these world cities have lost lot of their manufacturing employment since the mid-1960s (more in Fyfe, Kenny 2005). Ostrava became an important industrial centre of former Austria-Hungary and this fact brought a long-term influx of new population and spatial development of the city. The population of Ostrava rose continuously throughout almost all modern censuses (since 1869). The biggest waves of immigration came during the 1950s and the population of Ostrava increased about 18% (38,000 inhabitants) for 10 years. This trend continued also during the 1960s, when the positive natural change and migration gains increased the population about another 43,000 inhabitants (17%). More about industrial and modern history of Ostrava can be found in Hruška-Tvrdý et al. (2010). The changes of population within cities caused by deindustrialization can change the social status of people (in both ways) and can increase the speed and size of residential segregation. Residential segregation is defined by Massey, Denton (1988) as “the degree to which two or more groups live separately from one another, in different parts of the urban environment”. The development of demography and the rapid rate of changes in urban areas created needs for specialised measures to describe not only the level of segregation. Some of these have been adopted and accepted immediately while others continue to remain the subject of discussions (McKibben, Faust, 2004). From the spatial aspect these measures can be divided in measures which calculate with space and its specifics and those which are completely aspatial. The percentage distribution belongs to these aspatial measures as probably the simplest measure used to describe the population distribution. Other possible measures are the Gini concentration ratio and the Lorentz curve are devices for representing the inequality of two distributions (Plane, Rogerson, 1994) and these are other representatives of aspatial measures. Researchers began to develop more and more complex indices of segregation with rising availability of data and computer processing. A turning point was the research of Massey, Denton (1988) who conducted a cluster analysis of 20 indices of segregation and they grouped them into five categories of evenness, exposure, concentration, centralization and clustering with recommendation of a single best index for each group. Although some of these indices are commonly used to describe spatial segregation, they suffer from their aspatiality. This paper describe the use of selected members of these indices of residential segregation (classic index of dissimilarity and index of segregation) and developed spatial measures to describe some changes in urban environment of Ostrava caused by deindustrialization.

QUANTIFICATION OF SEGREGATION

Aspatial measures

This chapter describes selected segregation measures which do not work with space and they are not effective to differentiate different spatial distribution patterns among population groups. *Index of dissimilarity* has been found as the most useful index for the evenness dimension of segregation (Massey, Denton, 1988) and it is described by Duncan and Duncan (1955). It measures the dissimilarity of two groups in the area or the percentage of one group that would have to change residence to produce an even distribution of the two groups among areas. The index ranges from 0, indicating no residential segregation, to 1, indicating complete residential segregation.

$$D = \frac{1}{2}\sum_{i=1}^{k}\left|\frac{x_i}{X} - \frac{y_i}{Y}\right|, \tag{1}$$

where $x_i$and y_i represent the members of the studying groups X and Y in unit i, X and Y the entire population of the group X and Y in the territory (city) and k represents the number of subunits in the territory.

This measure has been one of the most popular measures of residential segregation but in recent years, it has come under criticism that it can measure only two groups at one time. So the residential segregation of university educated people can be compared to people with basic education, but university educated people cannot be compared to people with basic education and with high school education simultaneously. Nevertheless, a series of studied has revealed the inadequacies of this index from the spatial perspective and a set of spatial segregation indices has been proposed during past decades (Wong, 2003). Two key criticisms are called as the 'checkerboard' problem and the modifiable areal unit problem (MAUP) (Reardon, O'Sullivan, 2004; Wong, 2004).

Spatial measures

Spatial measures have been introduces but not been adopted widely because they are difficult to compute even within Geographic Information Systems (GIS) due to a low instant support of such operations. That is why spreadsheets or database tools are more often employed for calculations. The history of spatial dimension in segregation measuring has been started by Jakubs (1981) who incorporated distance measures to capture the proximity among population groups. The recent approach of capturing spatial dimension is to incorporate potentially relevant spatial aspects into calculations – neighbourhood relationship and the geometric characteristics of units.

To make these spatial metrics more popular, some of these measures were implemented as the set of tools in GIS environment (ArcView GIS) by David W.S. Wong (Wong, Chong, 1998; Wong, 2000, 2003, 2004). These measures can handle the traditional two-group settings or the multi-group settings.

The first spatial measure was introduced by Morill (1991) who modified the dissimilarity index with a term to compare different population in neighbouring units. This new *neighbour-adjusted* $D(adj)$ *index* solves the problem that different population groups locating next to each other should have a relatively low level of segregation.

$$D(adj) = D - \frac{\sum_i \sum_j |c_{ij} \times (z_i - z_j)|}{\sum_i \sum_j c_{ij}}, \tag{2}$$

where D is index of dissimilarity, z_i and z_j are the proportions of minority (or majority) between areal units i and j, while c_{ij} will be zero if i and j are not neighbours, and one if they are (Wong, 2003).

This index was further improved by the premise that the intensity across mutual boundary is not simple function of adjacency, but it is more dependent on the length of mutual boundary. This new *boundary-adjusted* $D(w)$ *index* was developed and defined as

$$D(w) = D - \frac{1}{2} \sum_i \sum_j w_{ij} |z_i - z_j|, \tag{3}$$

where all terms are defined as before, and

$$w_{ij} = \frac{d_{ij}}{\sum_j d_{ij}}, \tag{4}$$

where d_{ij} is the length of mutual boundary between units i and j and the denominator is basically the total length of the boundary of the unit i (Wong, 2003). Calculations of w_{ij} may be even more common and may cover different aspects of spatial adjacency including topological or distance measures (Horák, 2006).

The last improvement is based on the premise that the level of interactions is also a function of the size and shape, or the compactness of the two adjacent units. The new *index* $D(s)$ *with compactness measures* was derived and defined as

$$D(s) = D - \frac{1}{2}\sum_i \sum_j w_{ij}|z_i - z_j| \times \frac{\frac{1}{2}\left[\left(\frac{P_i}{A_i}\right)\left(\frac{P_j}{A_j}\right)\right]}{\max\left(\frac{P}{A}\right)}, \quad (5)$$

where the $\frac{P_i}{A_i}$ is the perimeter-area ration for the unit i and $\max\left(\frac{P}{A}\right)$ is the maximal perimeter-area ratio among all units in the region (Wong, 2003).

All these spatial versions has the same limitation as the classical dissimilarity index, it compares only two population groups. For multi-group comparisons, the multi-group version of dissimilarity index was introduced – *Multi-group D(m) index* and the *spatial version of multi-group index SD(m)*. More about these multi-group indices can be found in Wong (2003).

The last spatial segregation measure defined by Wong (2003) is based upon explicit spatial dissimilarity, or the concept of spatial congruence. It is based on premise that different groups do not have similar distribution patterns. To capture overall spatial distribution of each population group, a standard deviational ellipse (Lee, Wong, 2001) can be used. After construction of multiple ellipses for each population group, they are compared and combined to derive an index of segregation based upon the ratio of the intersection and union of all ellipses. This *ellipse-based measure S* is defined as

$$S = 1 - \frac{E_1 \cap E_2 \cap E_3 \cap \dots E_n}{E_1 \cup E_2 \cup E_3 \cup \dots E_n}, \quad (6)$$

where E_i is the deviational ellipse describing the distribution of population group i (Wong, 2003). A more clustered distribution will generate a smaller ellipse and more dispersed distribution will generate larger ellipse with the rotation corresponding to the orientation of the distribution.

The ellipse-based measure can be written also as *S=1-CAC*, where *CAC* is the coefficient of Areal Correspondence (Horák, 2009). It would be possible to apply also a resemblance matrix or other measures of a spatial overlay.

DATA FOR SEGREGATION AND DEINDUSTRALIZATION EVALUATION

Changes of population structure and its distribution within the city can be described and documented by above described spatial segregation measures. Data required in the segregation analysis usually specifies personal features like nationality, race, education, income or economical status (McKibben, Faust, 2004). Such complex demographical and economical data is provided by census.

Deindustrialization can be evaluated by different indirect indicators. Changes in sectoral employments are considered to be on the most important. The basic hypothesis assume the deindustrialization influence the spatial distribution of employed population in selected sectors or economical branches and this movement will be recognised by relevant changes of segregation indices.

Main aspects of deindustrialization are described by (using census data from several last periods):

- lower employment in industry (defined as the number of employees in industry),
- higher employment in service sector (defined as the number of employees in service sector[3]),
- higher employment of people older than 64 years (defined as the number of employees older than 64 years),
- employed as workers (1980) (defined as the number of workers) and employment in insurance and financial sector (2001) (defined as the number of employees in the sector).

The last aspect cannot be mutually compared but generally, while workers represent the industrial aspect of the employment situation in the city, people employed in insurance and financial sector could represent the post-industrial era of the city. The anticipated results are decreasing of spatial segregation of employment sectors due to a higher mixture of new employment possibilities. The increasing social differentiation and segregation stands against this development. This is caused by increasing level of unemployment rate (compared to 1980), more differentiated range of wages etc. and can lead even to creation of socially excluded localities (more in Horák et al., 2010).

CASE STUDY OF OSTRAVA

The case study is focused on utilization of classical index of dissimilarity and its spatial version to describe the impact of deindustrialization process on employment structure in Ostrava as it was explained in the previous chapter.

Above mentioned data from census 1980, 1991 and 2001 at the basic settlement units are applied to investigate selected aspects of deindustrialization:

The table 1 describes the main changes in population and employment situation in Ostrava for 20 years. This time series covers the most important aspects of deindustrialization in employment sectors, but in case of possible extension on results

[3] service sector is defined as the total number of employees except employees in agriculture, industry and construction

from scheduled census in 2011, the changes would be bigger and more exact and the population could be potentially more segregated. This idea of current development supports the real change of population in Ostrava. The decrease during 20 years was only 1.7%, but the decrease since 2001 to 2010 (1. 1.) is bigger than 3%. Similar situation should be in case of the change of economically active people where the decrease is slightly bigger than in case of population. So, the level of decrease in Ostrava is bigger for economically active people and the drop in the last decade should be again even bigger than the development in analyzed 20 years. While the population decrease has its peak after 2001, the change of employment structure took place during the 1990s (this is evident in Table 1). The stated aspects of deindustrialization are supported by results in table 1 – massive reduction of people employed in industry (less about almost a half) and on the other hand high increase of people employed in service sector (more than 60%) as well as the employment of people older than 64 years (more than 50%). This higher employment of older people may be caused by two factors: they are employed usually in less physically demanding positions and they simply must work to maintain their standard of living.

Table 1. Changes in population and employment in Ostrava between 1980 and 2001.

	1980	2001	change	
population	322 073	316 744	-5 329	-1.7%
economically active	164 378	160 210	-4 168	-2.5%
employed in industry sector	81 702	42 944	-38 758	-47.4%
employed in service sector	64 083	102 991	38 908	60.7%
employed and older than 64 years	3 009	4 511	1 502	49.9%

Spatial distribution of people employed in industry sector has been changed quite significantly (Fig. 1). Averagely, reduction is evident in all units of the city. While the share of economically active in industry from economically active was around 50% in 1980 with high level units placed near a geographical centre of the city, in 2001 the ratio is averagely about 20% with quite heterogeneous distribution.

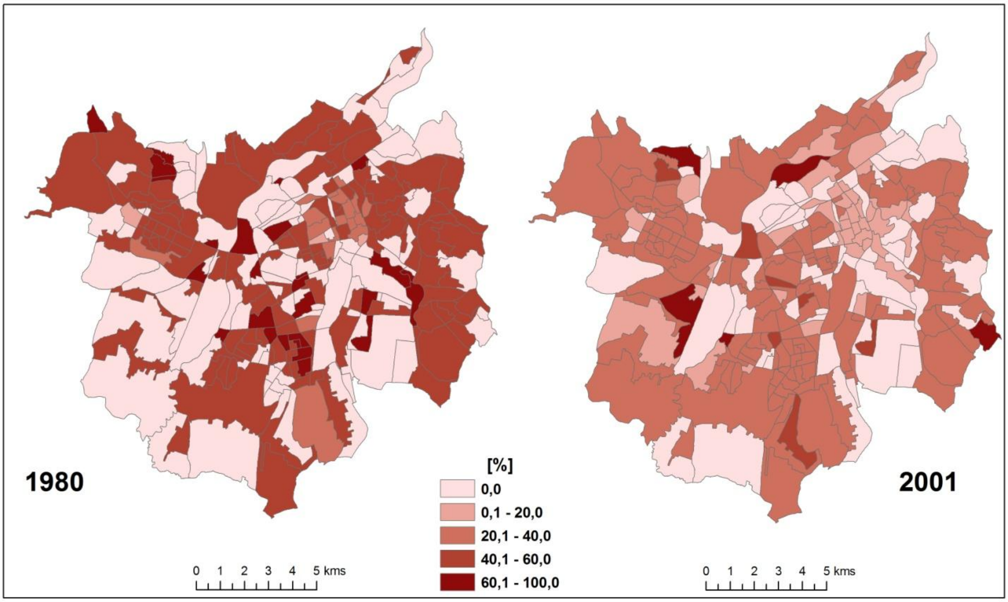

Fig. 1. Change of employment in industry (ratio of economically active in industry per 100 economically active)

Completely different development is in case of employment in service sector (Fig. 2). In 1980, a few important service areas are located around the city centre and in Poruba district (due to the presence of the Technical University of Ostrava) but others areas denote a low level of service sector. The map depicting situation in 2001 indicates much bigger ratio of economically active in services per 100 economically active and in almost all basic settlement units in Ostrava, there is more than 60% of economically active people employed in service sector.

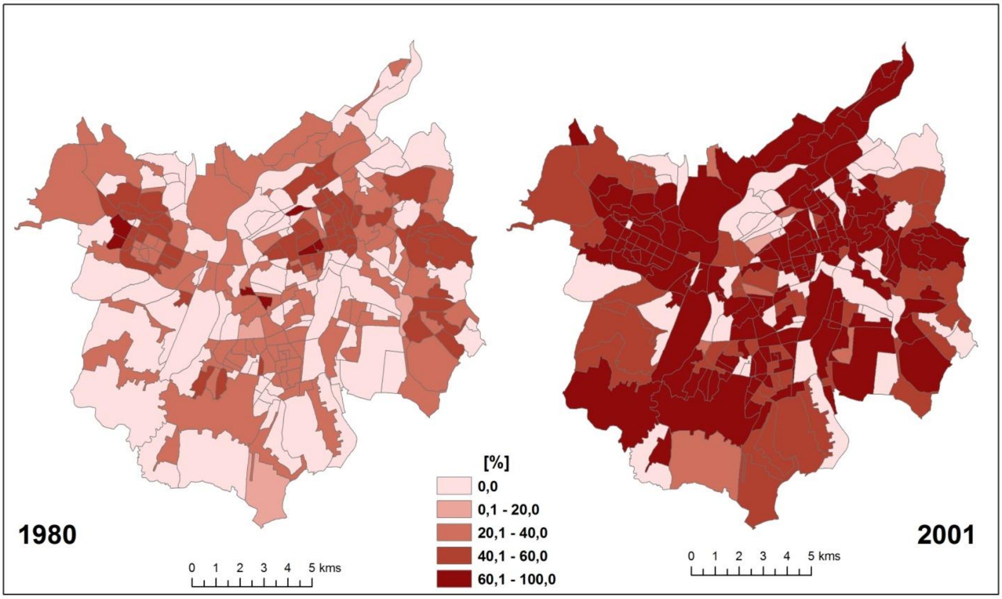

Fig. 2. Change of employment in services (ratio of economically active in services per 100 economically active)

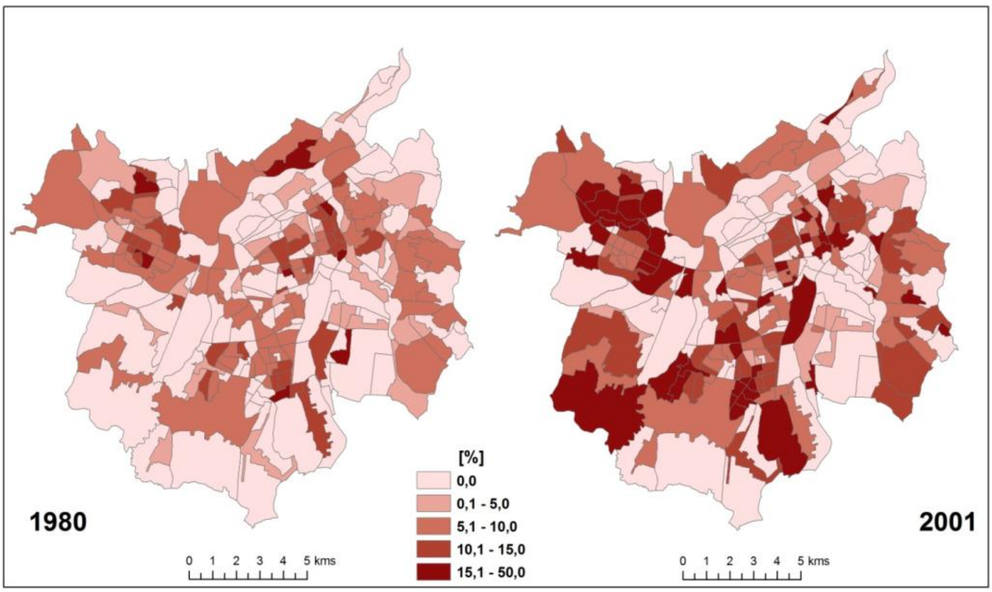

Fig. 3. Change of employed 65+ (ratio of employed 65+ per 100 people 65+)

The significant increase is evident in case of change in employment people over 64 years too (Fig. 3). Most of units have the ratio of employed 65+ per 100 people 65+

up to 10% in 1980 but in 2001 significant number of units has the ratio higher than 15%. These units are situated mainly in the west part of the city (Poruba, Pustkovec) and in the southern parts (Hrabuvka, Zabreh, Dubina, Hrabova or Polanka nad Odrou).

The changes in the share of main economical sectors are clearly depicted as well as the movement in the distribution of high and low level units. The main research question is if these significant changes are also articulated in changes of spatial segregation (uneven spatial distribution in broader sense of understanding).

Classical index of dissimilarity

The classical index of dissimilarity was used to analyze the mutual segregation of people employed in service sector, industry sector, workers and employed people older than 64 years (hereafter as employed 65+). The results from 1980 (Table 2) indicate higher segregation of employed 65+ in comparison to all other groups, the level of segregation is similar. Slightly higher segregation is between the service sector and industry sector and between workers and service sector.

Table 2. Index of dissimilarity – census 1980.

1980	industry sector	service sector	workers	employed 65+
industry sector	x	0.144	0.042	0.271
service sector	x	x	0.169	0.265
workers	x	x	x	0.274

The results of dissimilarity index based on results from 2001 indicate slight decreasing level of segregation in case of the same groups as in 1980 but the differences are quite small. The biggest decrease of segregation is between employed 65+ and service sector. The least segregation is between industry and service sector and this signifies the evenness in the geographical distribution of these groups. This approach is not quite free of the MAUP but this spatial level provides good conditions to avoid MAUP maximally. The only way to be free of the MAUP would be by the use of individual-level data what faces many problems.

Table 3. Index of dissimilarity – census 2001.

2001	industry sector	service sector	insurance and financial sector	employed 65+
industry sector	x	0.097	0.154	0.235
service sector	x	x	0.104	0.194
insurance and financial sector	x	x	x	0.262

Neighbour-adjusted D(adj) index

This first member of segregation measures yields significant decreasing level of segregation in case of all analyzed groups, thus the neighbouring effect influence positively results. This fact indicates the existence of a positive spatial association among neighbouring units but the level of this spatial association is very variable. In Ostrava, there is averagely almost 6 neighbouring units (maximum is 21 (!) units and minimum is only 2 units). The biggest smoothing effect of neighbouring units is in case of segregation between industry and service sector and workers and service sector. Here, this index does not indicate almost any segregation. Results of index between employed 65+ and others groups are in different order, compared to index of dissimilarity but still almost similar.

Table 4. Neighbour-adjusted D(adj) index – census 1980.

1980	industry sector	service sector	workers	employed 65+
industry sector	x	0.032	0.016	0.228
service sector	x	x	0.040	0.209
workers	x	x	x	0.204

In results from 2001, the influence of neighbouring units on the decrease of segregation reaches similar level as in case of the situation in 1980. This measure indicates almost no segregation between industry and service sector which is slightly lower than 20 years ago, what is anticipated development. The level of segregation has been decreased in all comparable populations between two censuses.

Table 5. Neighbour-adjusted D(adj) index – census 2001.

2001	industry sector	service sector	insurance and financial sector	employed 65+
industry sector	x	0.023	0.108	0.154
service sector	x	x	0.079	0.161
insurance and financial sector	x	x	x	0.190

Boundary-adjusted D(w) index

Theoretically this index should provide more accurate results than *D(adj)* because the impact of adjacency should be adjusted by the length of the shared boundary. The average length of shared boundary between two units is 727 metres, but the variability is quite significant (minimum is 0.6 metres and maximum over 10 kilometres). Results of this index (Table 6) yield slightly smaller values than in Table 4 with one exception. This caused the fact that longer mutual boundaries are between more homogeneity neighbouring units.

Table 6. Boundary-adjusted D(w) index – census 1980.

1980	industry sector	service sector	workers	employed 65+
industry sector	x	0.031	0.013	0.227
service sector	x	x	0.044	0.205
workers	x	x	x	0.201

This index would yield higher level of segregation than *D(adj)* if the length of shared boundaries would be longer with units with different employment structure. It is the case of segregation between industry and service where the *D(w)* indicates slightly higher level of segregation. However, the index signifies minimal level of segregation, even small increase of segregation is evident compared to 1980. The biggest impact of the length of shared boundary is in case of segregation between industry sector and employed 65+.

Table 7. Boundary-adjusted D(w) index – census 2001.

2001	industry sector	service sector	insurance and financial sector	employed 65+
industry sector	x	0.033	0.102	0.150
service sector	x	x	0.083	0.159
insurance and financial sector	x	x	x	0.192

Index D(s) with compactness measures

This index extends boundary-adjusted *D(w)* index by edge density or perimeter/area ratio of particular units. Compared to results in table 6, the level of segregation is more significant between all groups but still smaller than by using classical index of dissimilarity. The biggest influence of edge density and the biggest increase is again in case of segregation between industry and service sector. This increases are probably influenced by lower spatial compactness of particular units (boundaries follow the rivers, irregular built-up area in periphery).

Table 8. Index D(s) with compactness measures – census 1980.

1980	industry sector	industry sector	industry sector	industry sector
industry sector	x	0.105	0.023	0.256
service sector	x	x	0.126	0.244
workers	x	x	x	0.249

Similar increasing level of segregation is in 2001. The explanation is similar as previously. Compared to results in table 8, the situation of comparable groups is better what corresponds to the general development.

Table 9. Index D(s) with compactness measures – census 2001.

2001	industry sector	service sector	insurance and financial sector	employed 65+
industry sector	x	0.057	0.137	0.206
service sector	x	x	0.098	0.182
insurance and financial sector	x	x	x	0.241

CONCLUSIONS

This paper provides the description of aspatial and mainly spatial measures of segregation. These three introduced spatial indices have been already implemented into GIS environment and used to describe the change of employment structure in Ostrava between 1980 and 2001. Generally, the level of segregation decreased between 1980 and 2001 between all analyzed groups what corresponds to assumed development. Employed people over 64 years are the most segregated group; the level of segregation was the biggest between this and all other analyzed groups. Incorporation of influence of shared boundary between units or even its length caused in case of Ostrava another decrease of segregation. A practical use of the last introduced index D(s) with compactness measures is arguable because segregated localities can be separated by rectangular barriers (trunk roads, railways) as well as by curved barriers (rivers, forests) and this index favors the curved barriers. The MAUP has not been studied yet, but Wong (2004) claims, based on previous studies, that aspatial measures yield higher levels of segregation when data gathered for smaller areal units are used. This can be the next direction of this research to study the internal heterogeneity of particular municipal districts in Ostrava as well as incorporation of another attributes as describing factors of deindustrialization processes.

ACKNOWLEDGEMENT

The project is supported by the Grant Agency of the Czech Republic ("The Industrial City in a Post-Industrial Society", GA 403/09/1720) and by grant of the Technical University of Ostrava SP/2010198 "Spatial metrics of demo-social changes in urban space".

REFERENCES

DUNCAN, O.D., DUNCAN, B. (1955): A Methodological analysis of segregation indices. American Sociological review 59: 23-45.

FYFE, N. R., KENNY, J. T. (2005): The Urban Geography Reader. Routledge Taylor & Francis Group. 404p., ISBN 0-415-30702-3.

HORÁK, J. (2006): Prostorová analýza dat. Institut geoinformatiky, VŠB-Technická Univerzita Ostrava. Ostrava.

HORÁK, J. (2009): Zpracování dat v GIS. Institut geoinformatiky, VŠB-Technická Univerzita Ostrava. Ostrava.

HORÁK, J., IVAN, I., INSPEKTOR, T., TVRDÝ, L. (2010): Monitoring of Socially Excluded Localities of Ostrava City. In Proceedings of Symposium GIS Ostrava 2010, Ostrava, 14 p., ISBN 978-80-248-2171-9.

HRUŠKA-TVRDÝ, L. et al. (2010): Industriální město v postindustriální společnosti, 1. díl, Ostrava, 2010, v tisku, ISBN 978-80-248-2172-6.

JAKUBS, J.F.(1981): A distance-based segregation index. Journal of Socioeconomic Planning Sciences, Vol. 15, 129-141.

LEE, J., WONG, D. W. S. (2001): Analysis with ArcView GIS. Enviromental Systems Research Institute, Inc., 192 p.

MASSEY, D., DENTON, N. (1988): The dimensions of residential segregation. Social Forces 67: 281-315.

MORILL, R. L. (1991): On the measure of geographical segregation. Geography Research Forum, 11, 25-36.

McKIBBEN, E. N., FAUST, K. A. (2004): Population distribution: Classification of Residence. In SIEGEL, J. S., SWANSON, D. A. (eds.): The Methods and Materials of Demography. Academic Press; 2 edition. 819 p. ISBN 978-0126419559.

PLANE, D.A., ROGERSON, P.A. (1994): The Geographical Analysis of Population. With Applications to Planning and Business. John Wiley & Sons, Inc. 417 p. ISBN 0-471-51014-9.

REARDON, S.F., O'SULLIVAN, D. (2004): Measures of Spatial Segregation. Population Research Institute, The Pennsylvania State University. Working Paper 04-01.

WONG, D. W. S. (2000). Several fundamentals in implementing spatial statistics in GIS: using centro-graphic measures as examples. Geographic Information Sciences, 5(2), 163–174.

WONG, D. W. S. (2003): Implementing spatial segregation measures in GIS. Computers, Environment and Urban Systems, Vol. 27, 53-70.

WONG, D. W. S. (2004): Comparing Traditional and Spatial Segregation Measures: A Spatial Scale Perspective. Urban Geography 25(1): 66-82.

WONG, D. W. S., CHONG, W. K. (1998). Using spatial segregation measures in GIS and statistical modeling packages. Urban Geography, 19(5), 477–485.

PERSPECTIVES OF FRACTAL GEOMETRY IN GIS ANALYSES

PASZTO Vit, MAREK Lukas, TUCEK Pavel and JANOSKA Zbynek

Department of Geoinformatics, Faculty of Science, Palacký University in Olomouc, Tř. Svobody 26, 771 46 Olomouc, Czech Republic
vit.paszto@gmail.com, lukas.marek@upol.cz, zbynek.janoska@centrum.cz

Department of Mathematical Analysis and Applied Mathematics, Faculty of Science, Palacký University in Olomouc, 17. listopadu, 771 46 Olomouc, Czech Republic
pavel.tucek@upol.cz

Abstract

Together with rapid development in GI science recent decades, the fractal geometry represents a powerful tool for various geographic analyses and studies. The paper shows usage of fractal geometry in two case studies. Studied areas are Olomouc region (approx. 804 km^2) and Olomouc city itself (100.000 inhabitants). First case study concerns urban growth of Olomouc city and refers about relationship between its area and perimeter. Fractal analyses showed that Olomouc is now approximately in the middle of its growth process and especially inner parts of the city are sufficient to be developed. Second case study pointed the land cover areas with extreme values of fractal dimension in Olomouc region. This led, together with consequent statistical analyses, to result that according to fractal dimension it is possible to distinguish (or at least to assume) the origin of areas. To achieve the results, various methods were employed. For fractal dimension calculation in the first case study, the box-counting method was used. General fractal calculation method was used in the second case study. Some statistical methods were also applied to test mean values of land cover areas fractal dimension (Student's t-test and analysis of variance). Using non-integer, fractal dimension, one can analyze complexity of the shape, explore underlying geographic processes and analyze various geographic phenomena in a new and innovative way.

Keywords: fractal geometry, GIS, urban growth, land cover, geocomputation, box-counting dimension, area/perimeter relation

INTRODUCTION

When Weierstrass's continuous nonwhere-differentiable curve appeared in 1875, it was called by other mathematicians as "regrettable evil" and these types of object were known as mathematical "monsters" (HASTINGS, 1994, PENTGEIN, 1992). Nobody imagined that fundamentals of fractal geometry were just established. However, since Mandelbrot's published its basics in (MANDELBROT, 1967), fractal geometry and fractal dimension (non-integer dimension, e.g. 1.32 D) is well known as a valuable tool for describing the shape of objects. It gained large popularity in geosciences (BATTY, 1994, GOODCHILD, 1980) (among other disciplines), where the measures of object's shape are essential. Year 1994 might be considered as the beginning of exploration of cities by means of fractalgeometry (BATTY, 1994). Number of ways in which fractal geometry (and especially fractal dimension) can be used for examining the form of city and this paper's first case study follows their work in a certain way.

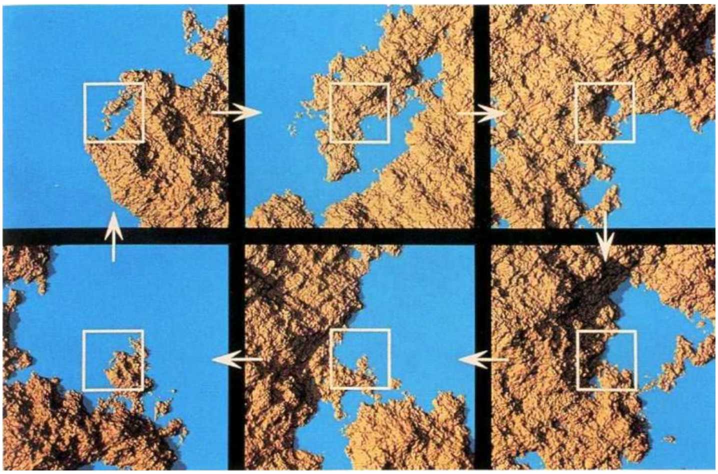

Fig. 1. Example of fractal coast and scale-invariance principle (in six steps/scales) (Peitgen, 1992)

More complex and detailed information about fractal geometry. Books provide the broad view of the underlying notions behind fractals and, in addition, show how fractals and chaos theory relate to each other as well as to natural phenomena. Especially introduction of fractals to the reader with the explicit link to natural sciences, such as ecology, geography (demography), physical geography, spatio-temporal analyses and others is in (HASTINGS, 1994). Some papers concerning topics investigated in this paper (city growth and land use pattern) were published yet, e.g. Batty and Longley's book as pioneer work. Other studies, applied different fractal methods for description of city morphology. Fractal analyses applied on land use/land cover pattern are described as well.

One of the major principles in chaos theory and descriptive fractal geometry is self-similarity and self-affinity. The most theoretical fractal objects, such as Mandelbrot set, are self-similar – this means that any part of the object is exactly similar to the whole. But these types of fractals are rarely used to approximate objects or shapes from the real world. And thus, another type of fractals is suitable for real-world object description – self-affine ones. These fractals are in fact self-similar too, but transformed via affine transformation (e.g. translation, rotation, scaling, shear mapping) of the whole or the part of fractal object. This observation is closely related to scale-invariance, which means that object has same properties in any scale, in any detail. In other words, if characteristics of some fractal object are known in certain scale, it is possible to anticipate these characteristics of another fractal object in different scale. The very typical example of this object is land cover and/or urban forms with theirs dynamics.

Concept of fractality was described in detail in many publications. Fractal dimension is a measure of complexity of shape, based on irregularity, scale dependency and self-similarily of objects. The basic property of all fractal structures is their dimension. Although there is no exact definition of fractals, the publicly accepted one, coming from Mandelbrot himself: "A fractal is by definition a set for which the Hausdorff-Besicovitch dimension strictly exceeds the topological dimension". Hausdorff-Besicovith dimension is therefore a number, which describes the complexity of an object and its value is non-integer. The bigger the value of Hausdorff-Besicovitch dimension, the more complex the shape of object and the more fills the space. In sense of Euclidean geometry, dimension is 1 for straight line, 2 for circle or square and 3 for cube or sphere, all. For real objects in plane, Hausdorff-Besicovitch dimension (fractal dimension) has values greater than 1 and less than 2. It obvious that Euclidean, integer, dimension is extreme case of fractal, non-integer, dimension. So it is claimed that regions with regular and less complex shape has lower fractal dimension (approaching to 1) and vice versa – the more irregular and complex shapes, the higher fractal dimension (approaching to 2). Values of fractal dimension of land cover regions vary between 1 and 2 because of the fact that area represented in the plane space without vertical extend is in fact enclosed curves. And fractal dimension of curves lies between 1 and 2.

As depicted in mentioned publications, fractals provide tool for better understanding the shape of given object. Furthermore, fractal geometry brings very effective apparatus to measure object's dimension and shape metrics in order to supply or even substitute other measurable characteristics of the object. Fractal dimension value is independent on area or perimeter of the object. Two objects with same area or perimeter could have absolutely different fractal dimensions. This theoretical notion is very important point, because as shown further, there is a relation between area occupied by the city and its fractal dimension. As (BATTY and LONGLEY, 1994) shows, fractals have infinite perimeter and finite area. Therefore it seems pointless to explore the perimeter of the city by means of fractal dimension. However, finding relation between area, perimeter, fractal dimension of build-up areas and fractal dimension of the boundary of the city is the scope of the analysis.

Next paragraphs do not intent to completely identify socio-economical, demographical and geographical aspects of land cover current state in Olomouc region. The case studies demonstrate the opportunity and power of fractal analyses of geographical data. Particularly, objectives are: urban structure of the city (shape of its borders) and land cover pattern and its geometric representation in GIS. In the first case, a possible explanation of city growth due to fractal analyses of its borders is stated. Land cover pattern fractal analyses, among others, identify areas with maximal and minimal fractal dimension to evaluate complexity of such areas.

DATA AND METHODS

There is a number of methods for estimating fractal dimension and as (REYNOSO, 2005) shows, results obtained by different methods often differ significantly. Also not only the method itself, but also the software, which calculates the fractal dimension may contribute to the differences (REYNOSO, 2005). In this case, Fractalyse software is used (THE FRACTALYSE, 2010).

It has to be mentioned that in case study 2 statistical testing was used. Because of its well-known formulas and characteristics, detailed description is not stated. The methods were Shapiro-Wilk test of normal distribution, Student's t-test and analysis of variance (hereafter as ANOVA).

Box-counting method

The box-counting method was used for modified data – binary pictures. Box-counting dimension of a subset *X* of the plain is defined by counting number of unit boxes which intersects *X*: for any $\Delta s > 0$, let $N(\Delta s)$ denote the minimum number of *n*-dimensional cubes of linear scale Δs (side length) needed to cover *X*. Than *X* has box dimension *D* if $N(\Delta s)$ satisfies:

$$(\Delta s) \approx c(1/\Delta s)^D, \tag{1}$$

where $\Delta s \rightarrow 0$, *c* is a constant and box-counting dimension of *X* is *D*. Formula (1) is called power law.

Dimension *D* is then be computed by:

$$= \lim_{\Delta s \to 0}\left[-\log N(\Delta s)/\log \Delta s\right], \tag{2}$$

According to formula (2), calculation of box-counting dimension is simple. For a sequence of cell size $\Delta s > 0$, the number of cells $N(\Delta s)$ needed to cover the set *S* is calculated. Box-counting dimension *D* can be also estimated by the slope of the straight line formed by plotting $\log N\Delta s$ against $\log \Delta s$ (known also as Richardson-Mandelbrot plot [3]). If the trend is linear, one can assume the observed object to be fractal.

General fractal calculation method

The same principles as in previous method employ method for calculating fractal dimension in its most general form:

$$= \frac{2 \cdot \log P}{\log A}, \tag{3}$$

where *P* is the perimeter of the space being studied at a particular length scale, and *A* is the two-dimensional area of the space under investigation (TORRENS, ALBERTI, 2000). Formula (FALCONER, 1999) was used to calculate fractal dimension for land cover regions classified by Level 1 of the hierarchy. Formula (FALCONER, 1999) can be easily computable directly within GIS, thus ESRI ArcGIS 9.x was used in order to obtain fractal dimension values.

Study region

Olomouc city is typical in many aspects. Having its center on small hill above the river Morava and surrounded by flat land, it does not have natural boundaries at all and urban growth is therefore not limited by georelief. The case study uses aerial imagery from years 1926, 1971, 1978, 1991, 2001, 2003 and 2006 to identify the boundary of the city. Both the central city and its surroundings were considered as study area, since the urbanization process of Olomouc city was heavily influenced by its surroundings. From Fig. 2, it is clear to see, that the building-up was realized primary in directions of former surrounding villages, therefore it was necessary to include those into calculation in case study 1.

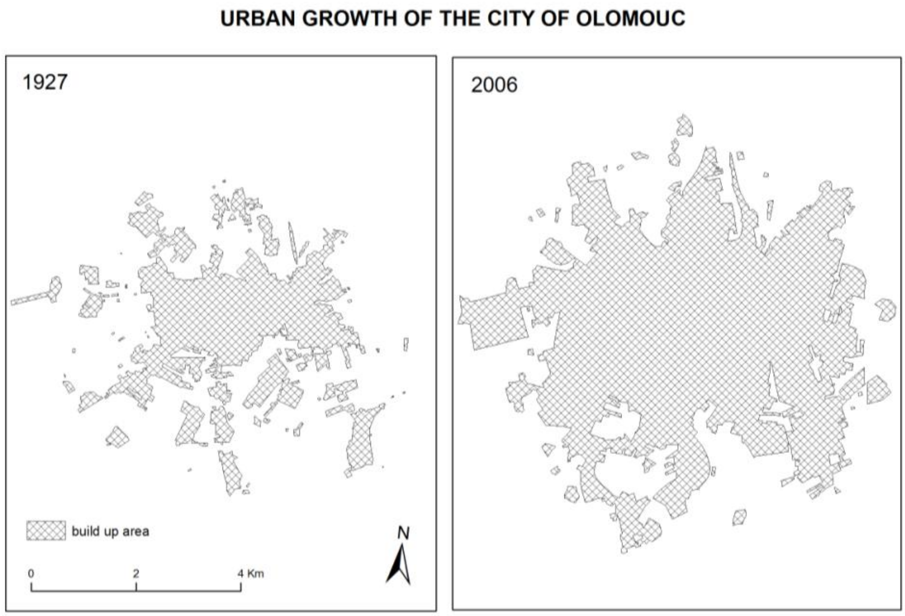

Fig. 2. Urban form of Olomouc in 1927 (left) and 2006 (right).

For case study 2, territory of Olomouc region was used. Its area is approximately 804 km^2 and every single type of LEVEL1 land cover classification is represented. It is necessary to note that CORINE Land Cover dataset from year 2000 was examined. Olomouc region is mainly covered by the agricultural areas, but the north-east part is almost completely covered by forests, because of military area occurrence. Despite this fact, Olomouc region is the most typically agricultural region with a great number of dispersed villages.

CASE STUDY 1 – FRACTAL ANALYSIS OF URBAN GROWTH OF OLOMOUC CITY

Observation of values of fractal dimension of Olomouc as whole is extended by examining the relation between the fractal dimension and other descriptors of shape, namely area and perimeter, which later appeared to be very important. As mentioned above, fractal objects does not have finite perimeter but have finite area, so authors suppose, that there will be relation between fractal dimension and area, but none between fractal dimension and perimeter.

Measured values of fractal dimension of both build-up areas and their boundary are shown in Tab. 1.

Tab. 1. Descriptors of shape of Olomouc

Year	Area (km^2)	D_{Area}	Perimeter (km)	$D_{Perimeter}$
1927	10.485	1.683	106.57	1.363
1971	21.188	1.758	116.61	1.284
1978	23.780	1.780	117.14	1.285
1991	28.028	1.808	108.12	1.268
2001	28.726	1.813	112.29	1.274
2003	29.064	1.816	111.28	1.272
2006	29.639	1.816	112.36	1.272

It is obvious, that both area and its fractal dimension grow constantly in time. Perimeter, and its fractal dimension, on the other hand, does not seem to have a strict trend. This would only support out hypothesis presented in previous text. Plotted values are shown in Fig. 3.

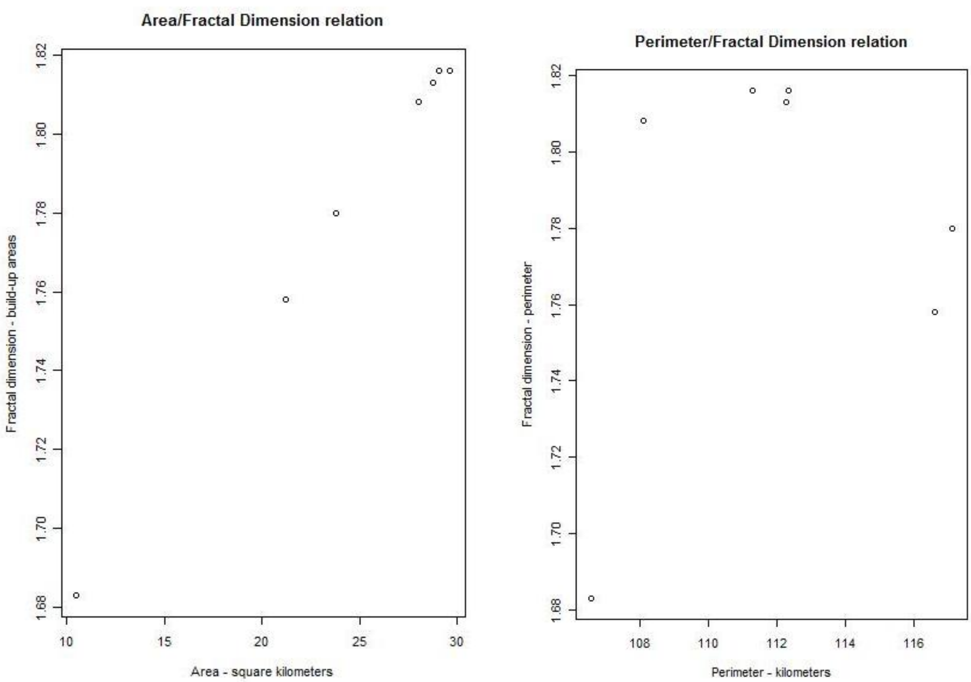

Fig. 3. Relation between area and its fractal dimension (left), and relation between perimeter and its fractal dimension (right).

The relation between area and its fractal dimension is strictly linear (Fig. 3 right). It enables to construct a linear regression model to describe precisely this relation. This model has a form:

*Fractal Dimension = 1.609103 + 0.007081 * Area*

As mentioned above, fractal dimension is a measure of complexity of shape. Although cities are more complex shapes with vertical dimension as well, their cartographical representation is planar and therefore is here examined as planar objects. And thus, plane has a fractal dimension equal to 2 and from the observed trend, it is obvious that growing area will result into fractal dimension equal to 2 – therefore the city will have covered the whole plane. By a simple calculation, the fractal dimension of 2 would correspond with area of 55.2 km^2.

Theoretically, this area value represents critical frontier for Olomouc development. Nowadays, the area is 29.6 km^2, so one can only guess what the future development will be. But there are two possible explanations (considering the hypothesis of linear relation between area and its fractal dimension):

- Predicted area 55.2 km^2 is a limit, which cannot be reached, the city will never grow up to this size,
- Once the city reached predicted area 55.2 km^2, it will continue to grow, but since its complexity in plane cannot grow any longer, the growth will be realized in vertical dimension

Important fact is that while the distance from the center of Olomouc to its peripheries is approximately 4 km, a circle with volume of 55.2 km^2 has radius of 4.2 km. Therefore a natural interpretation would be to expect Olomouc to grow only to 'fill' the non-build up areas within the distance of 4.2 kilometers from the city.

CASE STUDY 2 – FRACTAL ANALYSIS OF LAND COVER WITHIN OLOMOUC REGION

Visualization of land cover in Olomouc region, which has fractal structure typical for landscape, is shown in Fig. 4. Areas with maximal and minimal fractal dimension, both for artificial areas and natural areas, are also outlined. From artificial areas, the maximal fractal dimension ($D = 1.393$) has town Hlubočky (Mariánské Údolí) and the minimal value of fractal dimension has part of Bystrovany municipality ($D = 1.220$). In the first case, the maximal fractal dimension is caused by the topography of the town. Hlubočky (Mariánské Údolí) was built in steep valley on both sides of the river and thus is forced to follow highly irregular topography, which results into observed fractal dimension.

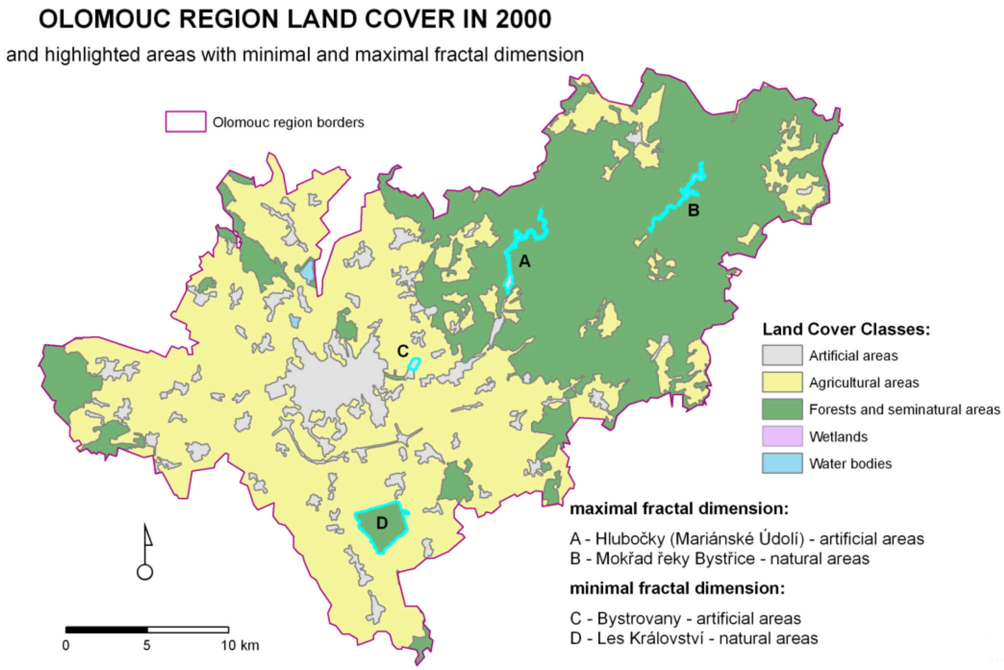

Fig. 4. Olomouc region land cover in 2000 and highlighted areas with minimal and maximal fractal dimension.

On the contrary, part of Bystrovany municipality represents distinct regular shape – almost square. There were no landscape borders or limitation when the settlement was built and regular fabrication of the build-up area (agricultural facility) was, probably, the most logical one. From natural areas, maximal fractal dimension has the wetland area of Bystřice river (*D = 1.396*), which is part of highlands with almost intact landscape. Very regular shape has forest southern from Olomouc called Les Království and its fractal dimension (*D = 1.193*) corresponds with that fact.

At last, join of all areas within class was accomplished and overall fractal dimension calculated. Results are shown in Tab. 2.

Tab. 2. Overall fractal dimension of particular land cover classes in Olomouc region.

Land cover class	Fractal dimension
Artificial areas	1,438574
Agricultural areas	1,385772
Forests and seminatural areas	1,350355
Wetlands	1,395799
Water bodies	1,263722

It is clear from Tab. 2 that highest fractal dimension have artificial areas, which represents in the very most cases man-made build-up areas (villages, towns, various facilities). Although knowledge how to plan and build up the settlement more properly was known long ago, urban sprawl emerged and has great influence on the irregular shape of artificial areas. Wetlands are very specific class, which are fully determined by natural processes and its fractal dimension is the highest among natural areas. On the other hand, water bodies have the lowest overall fractal dimension. It is necessary to note that line objects, which would fall into this class (rivers, streams, channels, etc.), are excluded due to CORINE classification methodology. And that is why the water bodies have this overall fractal dimension – only man-made or man-regulated water bodies were identified by the classification process and consequently analyzed.

To objectively prove the significant statistical difference among the land cover classes, the ANOVA was used. Before that, Shapiro-Wilk test was performed to check up the normality of data. It was confirmed and ANOVA could be used. It was then proven that mean fractal dimension values are significantly different and thus the classes are different too. One can then claim that classes (Tab. 2) originate from diverse processes. To acquire more detailed information, Student's t-test was used to test significant difference only between two selected classes − Artificial areas and Forests and seminatural areas − to objectively prove previously anticipated fact that especially these two classes should be different. Test prove this significance and one can claim that by calculating the fractal dimension of land cover areas it is possible to study, evaluate and interpret the processes lying underneath the current land cover appearance.

According to the CORINE Land cover classification system and acquisition of the dataset in reference scale 1:100,000, influence of generalization on the fractal analysis needs to be taken into account. The more generalized areas in land cover classes, the more regular their shapes. And the results of fractal analyses are less accurate (in sense of capturing objects as much realistically as it is possible). Furthermore, formula (FALCONER, 1999) implies that the longer perimeter of the shape, the higher fractal dimension as a result. And this is very important fact, when calculation using formula (FALCONER, 1999) is used. Fractal analysis results are then influenced by the factors from logic sequence:

reference scale of map/dataset – generalization degree – perimeter of an area – fractal dimension value

CONCLUSION AND DISCUSSION

Changes in urban form of the city of Olomouc by means of fractal dimension were observed. Detailed examination of relations between build-up area, perimeter and their fractal dimension, was made. A dependency between build-up area and its fractal dimension emerged, which may lead to interesting assumption about future development of the city. Consequently, the fractal dimension of the boundary of the city seems to concentrate around value 1.27, which is close value to the one of Koch curve, and thus city's fractal physique is proven. Possible interpretations of the found dependencies were presented and brief discussion was stated. Fractal analysis of the city growth is now frequently used in urban planning and represents robust tool to enhance spatial analyses concerning urban topics.

Furthermore, the use of fractal geometry in evaluating land cover areas was presented. Resulting values of fractal dimension of such areas were commented using expert knowledge of the Olomouc region. Geographical context was mentioned too and proper visualization was made as well. Overall fractal dimension was calculated for comprehension amongst land cover classes. Finally, some important aspects of generalization influence and CORINE classification system on the results were mentioned.

The paper brings to the reader basics of fractal geometry and its possible usage in geospatial analyses. Brief historical facts are also presented and plenty of publications and papers noted. It is obligatory to introduce methodological frame of fractal geometry apparatus, including formulas by which the fractal dimension was calculated. Two original case studies were carried out to demonstrate practical use of fractal geometry and consequence analyses. As mentioned above, fractal analysis built its stable position in various natural sciences, including geoinformatics and geocomputation

Fractal analyses are very sufficient for measuring complexity or irregularity of various objects, but there are other metric characteristics of the shape (e.g. compactness, convexity, roundness, elongation and others) to evaluate objects, respectively areas in this case. But the main difference between fractal geometry and this group of metric characteristics is in use of mathematical apparatus and, what is even more important, in concept of fractal geometry and chaos theory. And that is why the fractal geometry built its position in all kind of geospatial analyses.

REFERENCES

BATTY, M. and LONGLEY, P. (1994): *Fractal Cities: A Geometry of Form and Function*, Academic Press Ltd., London, San Diego, 1994, 394 s.

DE KEERSMAECKER, M.-L., FRANKHAUSER, P., THOMAS I.: *Using fractal dimension for characterizing intra-urban diversity: The example of Brussels*. Paper presented at the ERSA 2003 Congres, Jyvaskyla, Finland, 27-30 September, 2003

FALCONER, K.J.: *Fractal geometry: Mathematical foundations and applications*. Chichester, John Wiley & Sons. 1999

FALCONER, K.J.: *The Geometry of Fractal Sets*. Cambridge University Press, Cambridge, 1985

FRANKHAUSER, P.: *The Fractal Approach. A New Tool for the Spatial Analysis of Urban Agglomerations*, Population: An English Selection, Vol. 10, No. 1, New Methodological Approaches in the Social Sciences (1998), pp. 205-240

GE, M., LIN, Q.: *Realizing the Box-counting Method for Calculating Fractal Dimension of Urban Form Based on Remote Sensing Image*. Geo-spatial Information Science, Volume 12, Issue 4 (1 December 2009), pp 265-270. doi: 10.1007/s11806-009-0096-1 December 2009

GOODCHILD, M.F.: *Fractals and the accuracy of geographical measures*. Math. Geol., Vol 12 (1980) , pp 85–98.

HASTINGS, H. M., SUGIHARA, G.. *Fractals: A User's Guide for the Natural Sciences*. Oxford : Oxford University Press, 1994. 235 s.

IVERSON, L. R. : *Land-use changes in Illinois, USA: The influence of landscape attributes on current and historic land use*, Landscape Ecology vol. 2 no. 1 pp 45-61 (1988), SPB Academic Publishing, The Hague

JENERETTE G. D., WU, J.: *Analysis and simulation of land-use change in the central Arizona - Phoenix region, USA*, Landscape ecology, ISSN 0921-2973 , 2001, vol. 16, no7, pp. 611-626 (1 p.1/4), © 2001 Kluwer Academic Publishers. Dordrecht

KITCHIN, R., THRIFT, N.: *International Encyclopedia of Human Geography*. United Kingdom : Elsevier Science, 2009. 8250 s. (hardcover).

MANDELBROT, B. B. (1967): *How long is the coast of Britain? Statistical self-similarity and fractional dimension*, Science 155 (1967), str. 636-638.

MANDELBROT, B. B. (1989): *Fractal geometry: What is it and what does it do?* In: Fleischmann, M., Tildesey, D. J. a Ball, R. C., 1989, str. 3-16.

MANDELBROT, B.B.: *The Fractal Geometry of Nature*. W. H. Freeman. San Francisco, 1983

McADAMS, M.A.: *Applying GIS and fractal analysis to the study of the urban morpholgy in Istanbul*, GEOMED 2007, held on 5-8 June 2007 in Kemer, Antalya, Turkey.

O'NEILL, R.V. et al.: *Indices of landscape pattern*, Landscape Ecology vol. 1 no. 3 pp 153-162 (1988), SPB Academic Publishing, The Hague

PEITGEN, H.-O., JÜRGENS, H., SAUPE, D.: *Chaos and Fractals : New Frontiers of Science*. New York : Springer, 1992. 984 s.

PEITGEN, H.-O., JÜRGENS, H., SAUPE, D.: *Fractals for the Classroom : Introduction to Fractals and Chaos*. New York : Springer, 1993. 452 s.

REYNOSO, C.: *The impact of chaos and complexity theories on spatial analysis - problems and perspectives*. 24th Research Symposium: Reading Historical Spatial Information from around the World: Studies of Culture and Civilization Based on GIS Data, Kyoto Japan, 7-11 February, 2005

SETO, K. C., FRAGKIAS, M.: *Quantifying spatiotemporal patterns of urban land-use change in four cities of China with time series landscape metrics*, Landscape Ecology (2005) 20: 871–888, Springer 2005.

STANLEY, H.E., OSTROSKY, N.: *On Growth and Form: Fractal and Non-Fractal Patterns in Physics*. Nijhoff, Boston, Mass., 1986.

TANNIER, C., PUMAIN, D.: *Fractals in urban geography: a theoretical outline and an empirical example*, Cybergeo: European Journal of Geography, document 307, Paris, 2005, 24 p.

THEILER, J.: *Estimating fractal dimension*. J. Opt. Soc. Am. A, Vol.7, No. 6 (June 1990), pp. 1055-1071

THE FRACTALYSE [online]. 2010 [cit. 2010-11-21]. Fractalyse - Fractal Analysis Software. Available from WWW: <http://www.fractalyse.org/>

TORRENS, P. M., ALBERTI, M.: *Measuring Sprawl*, Centre for Advanced Spatial Analysis, Paper 27, London, 2000, 43 p.

TURNER, M. G. : *Spatial and temporal analysis of landscape patterns*, Landscape Ecology vol. 4 no. I pp 21-30 (1990) SPB Academic Publishing bv, The Hague

WHITE, R., ENGELEN, G., ULJEE, I. , LAVALLE, C. AND EHRLICH, D. 2000. *Developing an Urban Land Use Simulator for European Cities*. In K. Fullerton (ed.), Proceedings of the 5th EC GIS Workshop: GIS of Tomorrow, European Commission Joint Research Centre: 179-190.

GIS IN MEDIEVAL ARCHAEOLOGY

DERMEKOVA Stanislava and BARTONEK Dalibor

Institute of Geodesy, Faculty of Civil Engineering, Brno University of Technology, Veveří 331/95, 602 00, Brno, Czech Republic
dermekova.s@fce.vutbr.cz

Institute of Geodesy, Faculty of Civil Engineering, Brno University of Technology, Veveří 331/95, 602 00, Brno, Czech Republic
bartonek.d@fce.vutbr.cz

Abstract

GIS in medieval archeology it is the topic of this paper. The aim of this project is a location of community called Kocanov, which disappeared in the Middle Ages in the ArcGIS and creating a prediction, which is based on characteristics of human activity and their relation to space. Estimation of habitual area of the community in the Middle Ages is based on spatial analysis and presents new opportunities in classical archeology. In this work there are described various procedures of making archaeological prediction model. Formation model is to use the features of the hydrological modeling, the distance from water sources, steep terrain, the visibility of the observed points. Result of the analysis is focused on determining the appropriate settlement location. The resulting localization is compared to historical sources and analyzed using the archaeological works. Interpretation and evaluation of results achieved is the starting point for new opportunities, which would lead to more detailed identification of potential archaeological sites.

Keywords: GIS, archaeology, localization, old maps, prediction model, spatial analysis.

INTRODUCTION

Currently, geographic information systems are the main element of a non-destructive approach to the nature of spatial data. Their use in various applied sciences is indispensable nowadays. This may include science and archeology, which work with spatial information associated with historical and contemporary world. The aim of this project is a certain appreciation of the facts as to push the classical archeology at the comprehensive link between past and present world.

This work deals with possibilities to link spatial information in GIS environment with archaeological knowledge of the past, such as search and obtain historical and contemporary documents, evaluation of their use for archaeological prediction.”

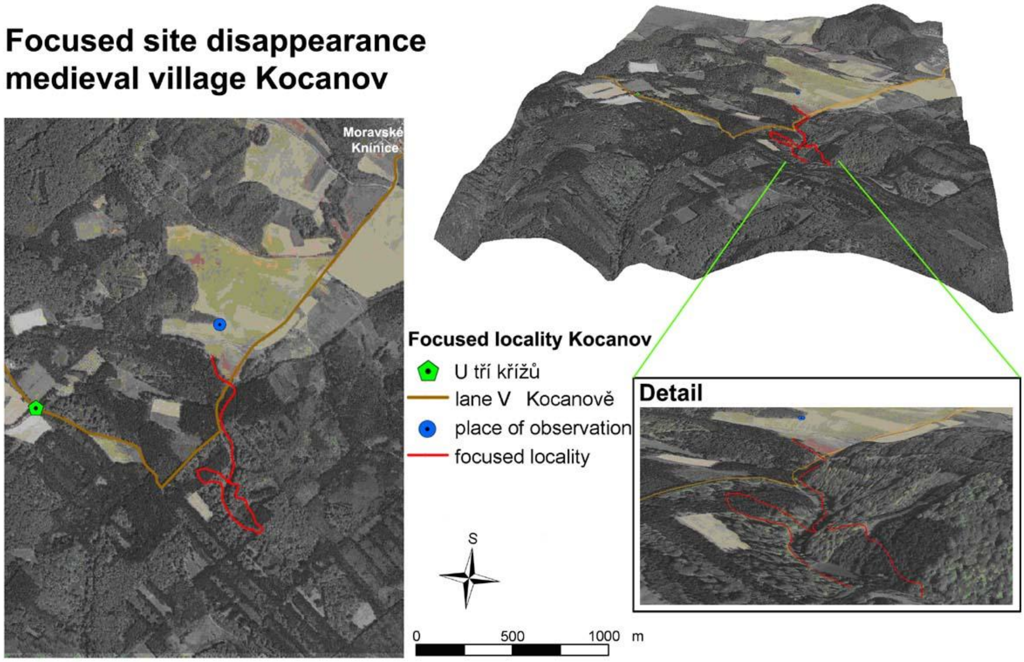

Fig. 1. Overview of the focused locality

The main emphasis is on landscape analysis using GIS spatial analysis and analysis resulting from historical, ethnographic, archaeological and environmental research. The aim is to locate a comprehensive analysis of the defunct medieval villages in the area of Kocanov, Jinačovice set out by municipalities, Moravské Knínice, Chudčice and Rozdrojovice – see Fig. 1. In this paper we deal with verification of each character issue at the site, its archaeological characteristics, reconnaissance, searching for literary documents and map reconstruction. The next part deals with the issue of archaeological prediction model and a procedure for solving spatial analysis. In the final section, we evaluate and interpret the results of tracking a vanished medieval village of Kocanov.

CONCEPTION OF THE PREDICTION MODEL

The first attempt to pragmatically oriented archaeological prediction was recorded in American literature. The solution described in the article was inspired by the projects The archaeological potential of Bohemia: the risk of archaeological research (2000) and Venclová (1995). Prediction Methods in Archaeology can be divided into inductive and deductive. The inductive method works on the basis of already obtained findings (artifacts). In our case we make use of deductive methods to be used for prediction of the sites without archaeological findings. Conception of the prediction model is depicted in Fig. 2. The results in The archaeological potential of Bohemia: the risk of archaeological research (2000) and Venclová (1995) confirmed the generally accepted finding that the location of archaeological findings depends on the parameters of the natural environment (especially the distance from the nearest watercourse, slope of terrain, altitude, possibly on the nature of soils). In addition, there is a strong link to the previous history of the country, which reflected in the ideological motivation: residential areas, even after many centuries of avoiding the areas of earlier sites, which must have had some ritual justification. Furthermore, there is the dependence on settlement processes on social factors. All these facts are reflected in the input parameters of the prediction model

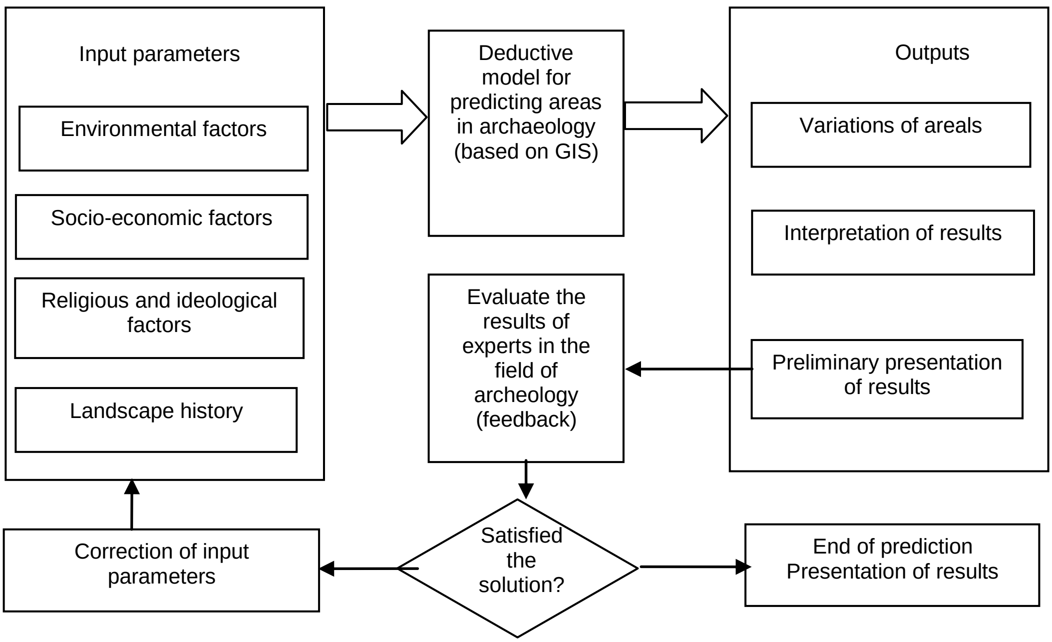

.**Fig. 2.** Conception of the prediction model

All these facts are crucial for the predicting the occurrence of prehistoric sites. If the location of prehistoric sites in addition to the natural environment depends also on the social and ideological factors and the history of the country, then the prediction is obviously difficult, and in some cases even impossible, only the study of natural conditions. It is important to study the relationship of the social dimensions of the settlement areas, determine their structure and history and to make use of GIS tools to achieve these aims. Therefore it has been inserted feedback into the model. Its function is to correct the input parameters of the model. The results obtained by experimenting with the model are tested in the iteration cycle. The test is realized in cooperation with experts in the field of medieval archeology.

PREDICTION MODEL DEVELOPMENT

The project was proposed as a simple prediction model for estimating the potential location of the defunct medieval village of Kocanov. Verification with "technically advanced" software is now pushing forward and offering new possibilities in classical archaeology prediction. APM (Archaeological Predictive Modeling) is the goal (objective) of creating a mere prediction associated with the clarification of human activities on the already documented sites and their relation to space. Next, create APM presents a forecast of unexplained deaths estates context. In developing the archaeological prediction model it is necessary to cooperate with archaeologists themselves or to use literature, which deals with archaeological interpretation. It is necessary to consider the contexts associated with certain factors. Among these factors may include the suitability of the environment, economic factor, factor minimum effort, defensive factor etc. For the considered factors there are certain criteria that effectively create prediction model for the implementation of spatial analysis in ArcGIS.

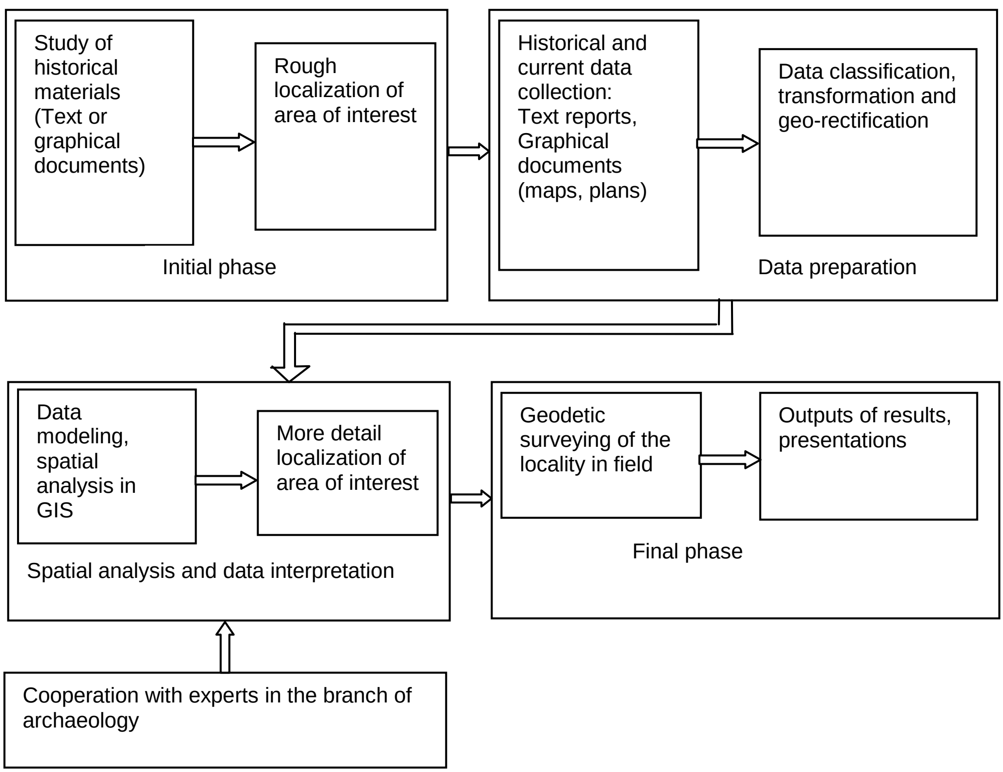

Fig. 3. Development of the prediction model

The whole project consists of 4 phases – see Fig. 3:

1. Initial phase,
2. Data preparation,
3. Spatial analysis and data interpretation,
4. Final phase.

The used model is generalization of methods used in publication Macháček (2008).

The initial phase

The aim of this project is to identify the location of the defunct medieval village of Kocanov. Verification of the existence of a medieval settlement today is feasible only with the help of written historical sources; local names in old maps and documents, especially with reproducible, providing archaeological evidence of the site in question. Historical documents from the Middle Ages are preserved only in the form of literary sources. Therefore, the effort was initially focused on the history of a wide area at municipality of Jinačovice, Moravian Kninice, Chudčice, Rozdrojovice later it has concentrated on Kocanov locality. Reconnaissance issue at the site took place on the ground under the supervision of an archaeologist, where each detail has to be in accordance with archaeological practice. The individual sites were compared with historical map data, which are subsequently transformed in ArcGIS for further technical procedures in the field of spatial data analysis. Very important is the study of historical literature. The previous chapter suggests that successful prediction can't be made without clarification of the fundamental questions what we want to predict or expect and then we have at disposal not only environmental factors, but also a number of historical, social and ideological factors.

Data preparation

Data collection and search are the most important stages of project design for archaeological purposes in ArcGIS environment. Sources of data are essential for building an information system as a prerequisite for spatial analysis. Phase search of suitable substrates is the largest part of the whole work. Among the primary sources may rank surveying, measuring methods of GPS, Remote Sensing (RS), Photogrammetric, etc. The next step includes searching variety of cartographic materials, custom drawings and maps, a database in tabular form, literary, historical text documents, further archaeological and environmental data, data from historical maps, ethnographic research. For the purposes of the project were used both the primary and secondary data sources. Among the evidences supporting archaeological interpretations are primarily historical and ethnographic data. All input data are shown in the Table 1.

Table 1. Input data

Sources	Data source (company)	Datum	Number of sheets	Content	Format
Sources representing spatial features	Czech Office for Surveying and Cadastre	2003	8	Orthophoto	GeoTIFF
		2002	2	Fundamental Base of Geographic Data (3D)	Vector SHP
	Archive of surveying and cadastre	1850-1872	18	Historical maps in the form of mandatory fingerprint scanned imperial stable land of Moravia and Silesia	JPEG
	Military Geography and Hydrometeorology Office, Dobruška	1950,1976	4	aerial survey photos, 8 bit, 1814 dpi	GeoTIFF
Sources representing archaeological features	National Heritage Institute, Brno	2010	1	National Archaeological list of the municipalities a period of prehistory and the Middle Ages, coat areas with archaeological finds	Vector SHP
	Moravian Library, Archaeological Institute of the ASCR (Brno), State District Archive Brno-Country (Rajhrad)	1827-2010	10	loaned archaeological literature	
Sources of the geological character	Research Institute of amelioration and soil conservation, Department of Soil services Brno	2010	1	Digital form a clear map of valuated soil-ecological units at a scale of 1:5000	Vector SHP
	Map Services Public Administration Portal, CENIA	2010	1	Map of potential natural vegetation in Czech Republic	Vector SHP
Source from the climatologically science	Moravian Library	2003	1	Landscape Atlas of the Czech Republic	

When working with the old historical maps we use simple geometric transformations with fewer identical points. The degree of transformation is expressed in polynomial n-th degree. The background raster pixel position is expressed in the system of map coordinates. Geo-referencing process was carried out by using ground control points, which are specific for particular pixel grid coordinates. The quality of input data has been consulted with archaeologists - Archaeological Institute of The Academy of Sciences of the Czech Republic (ASCR), Brno. The low numbers of input data layouts are identical predicting greater emphasis on quality control of data due to the use of rectilinear spatial analysis. Vector bases in the series underwent adjustments which makes it much clearer. Raster documents in digital form are usually created by scanning analogue maps or aerial or satellite acquisition documents, photographic documentation. Most historical documents require the layout type: trimming redundant information, unifying graphic map sheets in the more compact base. All image adjustments were made in Adobe Photoshop Version: 10.0.

Spatial analysis and data interpretation

The core of the project was to exploit the possibilities of spatial analysis in ArcGIS. Spatial analysis of individual housing estate was realized the area of interest using landscape characteristics (landforms, river system, topographical features of the country). In spatial analysis, there were also taken into account other factors such as environmental suitability, economic factor, factor minimum effort, defensive factor, and the cult factor. An important variable and the time factor were observed, because the country and its components are constantly evolving. Therefore it is not possible to examine clearly the linkages between current environment and the environment in the past. It is necessary to set certain targets in the planning of spatial analysis. The primary objective is to find appropriate combinations of spatial analysis in ArcGIS. Another supreme objective was a comprehensive spatial analysis based on documents obtained by the solving site. It was created a digital terrain model, which was applied to each particular analysis of landscape characteristics (terrain slope, shaded relief, exposure area).The substrate that was used for making DMT (Digital Terrain Model) of a given area was ZABAGED (Fundamental Base of Geographic Data) - digital model derived from the vector map image the Base Map 1:10 000 CR (ZM10). Results of landscape features were used for further spatial analysis procedures.

For the spatial analysis it was used multiobjective modeling. The model makes use of quantitative (calculating the area of polygons, the search space with some acreage) and qualitative criteria (reclassification methods - the process of gradient maps defunct settlement likely in the range 0-7% and 7-90%, buffer zones - distance analysis of type distance to the village 150m, 300m from the water source). It was necessary to take into account certain quantitative and qualitative criteria for the landscape component and settlement in the Middle Ages.

For another archaeological prediction model it was used hydrological modeling on the basis of topographic features (water source in solving - the likelihood of human existence in the Middle Ages). Analyses of field elements using data from the general geomorfometry related to hydrology are beneficial to the procedure of the archaeological prediction model (APM). For analysis the hydrological modeling of river network model the smallest streams were made use of, acting as the confluence of several rivers. Hydrological modeling procedure itself consisted of creating a hydrological correct DMT, where various analyses were performed: determine the direction of runoff, accumulated runoff, drainage network, drainage and river length. As a basis for hydrological modeling was used DMT created raster shapefile on waterways and lakes. At the end of the hydrological modeling criteria we have set distances (buffer zones) from the water source, areas within 300m from the water source and the surface to 150m from the water source.

Any action taken as the process of creating maps of slope and hydrological modeling process of moving towards a targeted location solved vanished medieval village. As a result of finished reclassified layers (buffer zones within 150 meters from the water source of hydrological modeling, gradient maps - used interval gradient to 7%), the individual areas of possible occurrence of a medieval settlement were created.

For the final analysis, which aimed to identify the likely site the defunct village of Kocanov, we set a couple of assumptions and criteria. According to literary sources it was identified a clue that has become a precondition for distance analysis. We set the criterion for the likely location of villages within a distance of 1500 meters from the site “U tří křížů”. Around the centre of the site “U tří křížů” buffer zones gradually after 500, 1000 and 1500m has been created. Then we made a breakthrough packaging zones created with the previous results form the basis of topographic and hydrological modeling. In the next stage of spatial analysis it was used the possibility to analyze the visibility. Parameters for the analysis of visibility were chosen according to historical documents. Function visibility may also prove certain inaccuracies in the determination of medieval housing estate, so the height of the likely sites was put 3 m higher. This reasoning implies the existence of possible watchtowers in these points. When using visual scoring points for the creation of village location it was a problem to find a spot in nature. The settlement has the character of surface area; therefore it was necessary to take into account the visibility “lump settlements” which spread out all sides, so the analysis was performed by visualization of line elements, even though the graphic is shown as a point object (point object due to graphic simplicity).

In conclusion, spatial analysis was conducted which resulted in comprehensive analysis of partial results of previous analysis. This comprehensive analysis can determine the existence of potential sites of medieval villages. Consideration of quantitative and qualitative criteria took place again in the ArcGIS environment. Complying places that set criteria were consulted with the experts in the branch of archaeology. We chose those most likely locations for a medieval village and divided them into two categories. The first category, blue ellipse, contains the most likely area. The second one, yellow ellipse, the area contains less likely area. Graphical representation is shown in Fig. 4. All specified areas requiring personal assessment on the ground by the statements of archaeologists in various literary sources.

The focusing of localized settlement has been implemented by manual GPS apparatus – red line in Fig. 1. Used GPS-type apparatus Trimble Recon GPS XC is rugged field computer with an integrated Compact Flash GPS Pathfinder XC receiver. The device is designed for mobile data collection and updating of GIS.

The final phase

The goal was a comprehensive analysis of possible off-targeting to verify village of Kocanov technically. In agreement with the leading job site, we revealed solved and decrypt individual verbal descriptions and statements by archaeologists according to the actual state of the country. Surveying process was preceded by a comprehensive assessment of the conclusions of the analysis in the field. The results of complex analysis can be verified on 3 sites of interest (see Fig. 4 blue oval with serial numbers 1, 2, 3).

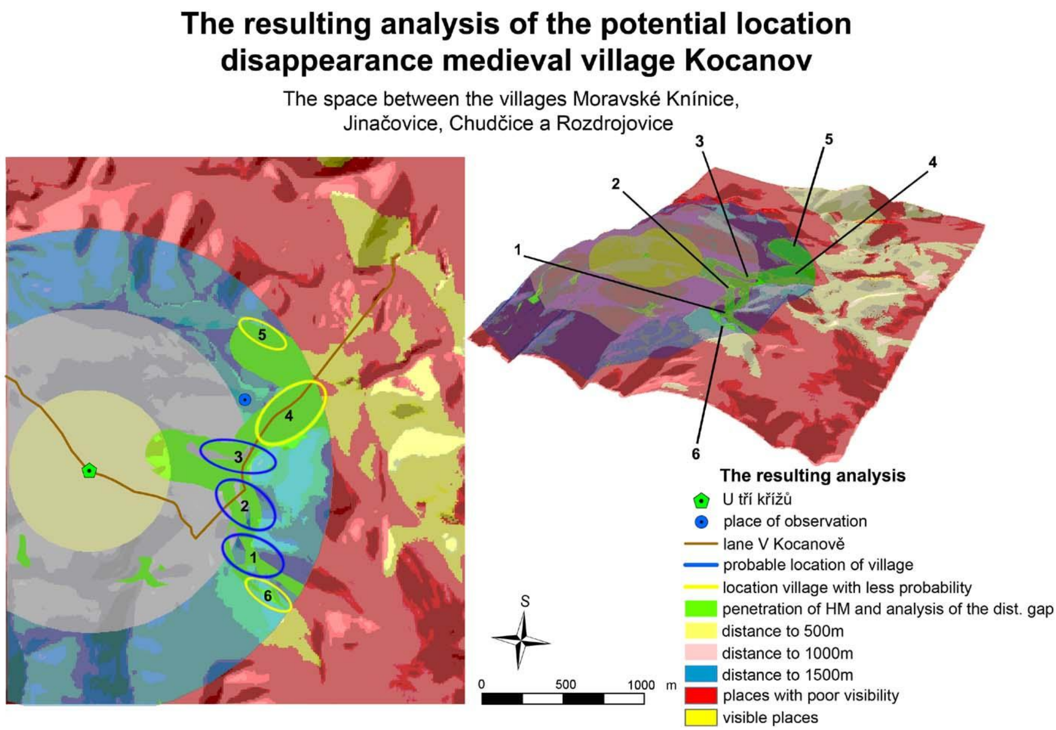

Fig. 4. The result of spatial analysis

Interaction between the general archaeological assumptions medieval village and its incidence is now very important. In conclusion were discussed the connections of results in spatial analysis of landscape elements with factors that follow from historical, ethnographic, archaeological and environmental research. Result of a previous sequence analysis is based on certain assumptions and do not have to be 100%

reliable, which declared that the resulting position estimate is certainly right. Therefore in conclusion, we try to assess the mutual ties between the archeological general assumptions of the medieval village and the result of spatial analysis. Peer assessment of spatial analysis and other factors: evaluation of the analysis of topographic and hydrological features, evaluation of the analysis in terms of natural conditions of the territory, evaluation of the analysis of visibility with signs housing development and evaluation of the overall position of the defunct medieval villages.

BENEFITS AND FURTHER USE OF THE PROJECT

The work presents new possibilities in classical archaeology and thus science is moved forward into other dimensions. On the project cooperated the Archaeological Institute of the ASCR, further institutions dealing with the history of Brno-country in short companies devoted to archaeology. The project demonstrates the technical diversity of today, which can be used in "non-technical" sciences. We propose a roadmap for implementation of spatial analysis and we have tried different results linked to each other with literary sources and historical documents. For the spatial analysis we took advantage of the hydrological and topographic modeling, which resulted in the analysis of relief. In spatial analysis, we consider some quantitative and qualitative criteria, which were set according to historical documents and archaeological sites. For historical documents we have come close to the location of the village with a retrospective exhibition of notion of Kocanov municipality. Retrospectively the development of settlements and the formation of cultural landscapes also took place in the ArcGIS environment. To sum up, this project evaluates results of spatial analysis of factors that issue from historical, ethnographic, archaeological and environmental research. Used method demonstrated new possibilities of data collection and analysis to be verified and archaeological objects, whether found or not. Use of ArcGIS extensions can present complex connection between past and present world. Further usage of the project results serve for the purpose of archival video documentation of the Archaeological Institute of the ASCR Brno-country, the historical archive of municipal offices at Jinačovice and Moravské Knínice to be used for the presentation of the history of communities.

CONCLUSIONS

Finally, it should also be alerted to the dangers which include prediction methods and to be aware of their usage. Firstly, the results of prediction are probabilistic nature: to warn the increased probability (risk) of archaeological sites, but do not guarantee their presence. Second, areas with a high archaeological potential are not automatically seen as the only interesting part of the archaeological landscape. And outside there may be extremely interesting archaeological information in a way more significant that occur in unexpected places. Therefore forecast maps can not replace the expert's opinion, but they can be useful, both for him and the other users too. We are aware that archaeological prediction lead to a narrowing of the space potential of suspected archaeological sites, not their precise delimitation. Even this narrowing can in practice be significant enough to compensate for the costs embedded in the prediction model. We believe that the proposed project could provide valuable assistance in various spheres of public life, government and business.

ACKNOWLEDGEMENTS

The authors thank Mgr. O. Šedo, PhD. from Archaeological Institute of ASCR in Brno for his cooperation and assistance in interpreting the results of spatial analysis. They would also like to thank professor J. Unger from Masaryk University in Brno for consultation in the development of prediction model.

REFERENCES

Allen G., Green S. and E.Zubrow (eds.) (1990): Interpreting Space: GIS and Archaeology. London: Taylor and Francis.

Archeologický potenciál Čech: riziko archeologického výzkumu (The archaeological potential of Bohemia: the risk of archaeological research) (2000). Projekt GAČR, Archeologický ústav AV ČR v Praze, katedra Archeologie ZČU v Plzni a katedra Geoinformatiky PřF UK v Praze.

Belcredi, L., Čižmář, M., Koštuřík, P., Oliva, M., Salaš, M., (1989), Archeologické lokality a nálezy okresu Brno-venkov (Archaeological sites and findings of the district Brno-Country), Brno.

Dreslerová, D., (1996), Modelování prírodných podmínek mikroregionu na základě archeologických dat (Modelling natural conditions on the basis of micro-archaeological data), Archeologické rozhledy 48, Archaeological Institute of the Academy of Science of the Czech Republic in Prague.

Eichler, K., (1891), Paměti panství veverského (Memoirs of Veveří estate), own expense, 1891.

Goláň, J., (2003), Archeologické predikatívní modelování pomocí geografických informačných systémů (Archaeological predictive modeling using geographic information systems), Faculty of Arts of Masaryk University, Brno.

Hosák, L., Šrámek, R., (1970), Místní jména na Moravě a ve Slezsku (Oikonyms in Moravia and Silesia), Academia, Prague.

Klimánek, M. et al., (2008), Geoinformační systémy návody ke cvičením v systému ArcGIS (Geoinformation systems guides the exercises in ArcGIS), Mendel University in Brno.

Macháček, J., (2008), Prostorová archeologie a GIS (Spatial Archaeology and GIS) in: Počítačová podpora archeologie (Computer Aided Archaeology). Masarykova univerzita Brno, 391 pp.

Neustupný, E. (1994): Předvídání minulosti (Predicting the past), Technický magazín 11, 58-60.

Venclová, N, Kuna, M, Haišmanová, L, Křivánek, R, Čišecký, Č. (1995): Predikce archeologických areálů (Prediction of archaeological sites) GA ČR č. 404/95/0523.

Part III

Geoinformation technologies challenges

MODEL GENERALISATION IN THE CONTEXT OF NATIONAL INFRASTRUCTURE FOR SPATIAL INFORMATION

MILDORF Tomas and CADA Vaclav

Department of Mathematics - Section of Geomatics, Faculty of Applied Sciences, University of West Bohemia in Pilsen, Univerzitní 22, 306 14 Pilsen, Czech Republic
mildorf@kma.zcu.cz, cada@kma.zcu.cz

Abstract

Human activity is one of the most important factors that drive the changes of our living environment. Sustainable development aims to eliminate the negative activities and to support the positive ones in a long term approach. The role of infrastructure for spatial information and the advantage of its use to support sustainable development have been demonstrated in a range of projects and studies; e.g. (Corbin 2008) or (ACIL Tasman 2008). Many specialisms including policy, economics, industry and environment profit from the extensive use of infrastructure for spatial information and its components. These are metadata, spatial data sets and spatial data services including the network services and technologies; agreements on sharing, access and use; and coordination and monitoring mechanisms, processes and procedures.

Many processes using spatial information are scale or resolution dependent. Each specialism requires changing degree of detail especially when activities are performed at different levels of abstraction.

This contribution introduces use case from the Czech Republic where model generalisation should play a crucial role – cadastral data model. In the context of the INSPIRE (Infrastructure for Spatial Information in the European Community) and related initiatives it is shown how model generalisation can contribute to better exploitation of cadastral data in connection with spatial planning and other activities. The stress is on model generalisation of cadastral data model into middle scale data model. The aim is to present the ideas of the authors to address an important aspect of the infrastructure for spatial information – model generalisation. This should contribute to long-term research goal of generalisation which is formalising the generalisation problem. As described by (van Oosterom 2009)) the generalisation problem is specifying user needs from the geo-information producers and geo-information users points of view.

Keywords: INSPIRE, model generalisation, cadastral data model, SDI

INSPIRE

INSPIRE (European Parliament 2007) is one of the most important current initiatives on the EU level. It sets the legal framework for establishment of the Infrastructure for Spatial Information in the European Community (INSPIRE). The main purpose is to help Community environmental policies and policies or activities which may have an impact onthe environment. But there are also other initiatives; INSPIRE is not the only one. All of them are interconnected and complementing each other. The following initiatives should be mentioned:

- GEOSS (Global Earth Observation System of Systems) in global dimension;
- service oriented GMES (Global Monitoring for Environment and Security); and
- SEIS (Shared Environmental Information System).

The aim of all these activities is to serve users spatial information with required quality, thematic content and level of detail. The information must be up-to-date and provided in a short time through modern technologies including web services.

GENERALISATION

The International Cartographic Association defined in 1973 generalisation as “the selection and simplified representation of detail appropriate to scale and/or the purpose of a map”. Another definition by McMaster & Shea (1992) says that “digital generalization can be defined as the process of deriving, from a data source, a symbolically or digitally-encoded cartographic data set through the application of spatial data and attribute transformation”.

Generalisation in terms of spatial information can be described as a process responsible for generating visualisations or geographic databases at a coarser level of detail than the original source database, while retaining essential characteristics of the underlying geographic information (Sester et al. 2009). There were many attempts to improve generalisation processes and to integrate them into automated systems in the last decades. Generalisation has created many innovative solutions due to research activities performed in this field.

“An idea is always a generalization, and generalization is a property of thinking. To generalize means to think.” Hegel, Georg

The end users will not be satisfied with generalisation tools and mechanisms until automated generalisation systems will be able to think.

Generalisation in the scope of INSPIRE

INSPIRE addresses the issue of generalisation but it is not in its main scope. Generalisation and its involvement in the Infrastructure for Spatial Information in the European Community were discussed during the Vienna meeting of the Network Services Drafting Team on 19-20 April 2006. The initial idea was to make generalisation as a part of the INSPIRE data transformation services. Because of the immaturity of generalisation the Network Services Drafting Team did not recommend the use of generalisation services, but supported multiple-representation (INSPIRE Drafting Team "Data Specifications" 2008b).

A workshop on multiple-representation and data consistency was held in JRC Ispra on 7-8 November 2006. The main objective was to provide input to the INSPIRE Implementing Rules in the field of data harmonisation. The following recommendations from the workshop should be mentioned:

- “Automatic generalisation methods are not mature enough to be considered as a service in the ESDI. For practical reasons multiple scale representation is generally needed, which can be completed by generalisation.
- Establishing and/or preserving links between different representations contributes to update propagation, thus to data consistency.
- There are different modelling approaches for MRDB (Multiple Representation Databases) that are usually used for linking different Levels of Detail.
- If required, correspondences between the databases can be established by various tools of data matching (data mining, ontologies and formal specifications) and transformations (conflation, generalisation, matching geometries)” (INSPIRE Drafting Team "Data Specifications" 2008b).

As a result Multiple-representations became one of the Data interoperability components (INSPIRE Drafting Team "Data Specifications" 2008a) listed in Fig 1 (component ‘R’) which describes best practices for how data can be aggregated:

- Across time and space;
- Across different resolutions (“generalisation” of data).
- Such aggregation processes are used in particular to create the following results:
- Multiple representations
- Derived reporting (example: typically water samples at 1 km intervals are reported to the European level)

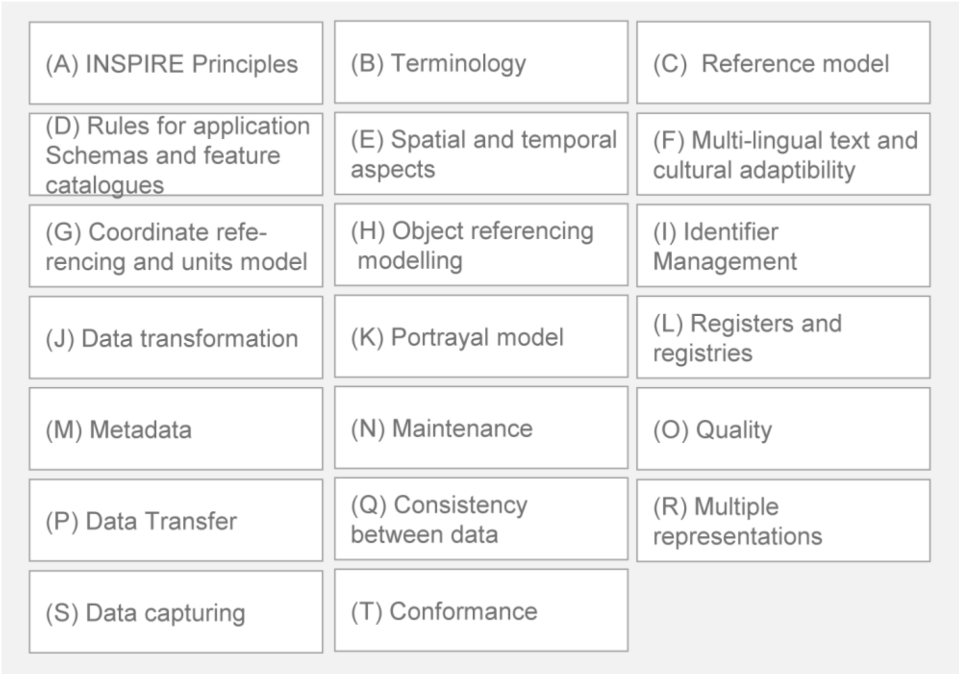

Fig. 1. INSPIRE Data interoperability components (INSPIRE Drafting Team "Data Specifications" 2008a)

Model generalisation

Several theoretical generalisation frameworks have been described in literature within last 40 years. They include division of generalisation, terminology, description of generalisation processes and other aspects. The generalisations concepts differ in these aspects.

There are two main generalisation approaches - cartographic generalisation and model (database) generalisation. While cartographic generalisation is focused on the depiction of objects in map (graphical and visualisation aspects), model generalisation aims at deriving model of lower level of detail that can be used for specific purposes. However, there is not clear distinction between cartographic and model generalisation.

In some literature can be found also object generalisation. It comprises generalisation process while defining and building original database (primary model) of the real world.

“Model generalization as a process of geospatial abstraction aims at modelling real world at different levels of semantic and geometric complexity” (Basaraner 2002).

The role of model generalisation is depicted in Fig 2.

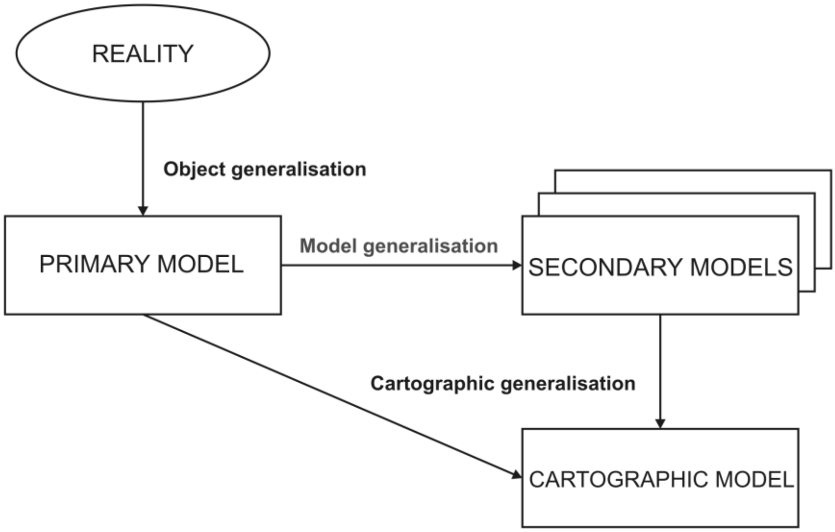

Fig. 2. Role of model generalisation (Gruenreich 1992).

CASE STUDY

The section of Geomatics at the University of West Bohemia in Pilsen contributes to the development of infrastructure for spatial information and its components. Long-term research and development activity of the section of Geomatics is the inclusion of cadastral data in the National Infrastructure for Spatial Information and their better exploitation for various activities including spatial planning.

The generation of complex infrastructure for spatial information is subjected to well-defined data from various sources, institutions or even by various geosciences. The data are essential for decision-making processes in various specialisms including policy, economics, industry and environmental planning. The quality of decision-making processes is highly dependent on the quality of geodata and geospatial information. The International Organization for Stardardization sets out the following data quality elements (International Organization for Standardization 2002) that shall be used to describe how well a dataset meets the criteria set forth in its product specification:

- *completeness*: presence and absence of features, their attributes and relationships;
- *logical consistency*: degree of adherence to logical rules of data structure, attribution and relationships (data structure can be conceptual, logical or physical);
- *positional accuracy*: accuracy of the position of features;

- *temporal accuracy*: accuracy of the temporal attributes and temporal relationships of features;
- *thematic accuracy*: accuracy of quantitative attributes and the correctness of non-quantitative attributes and of the classifications of features and their relationships.

In the Czech Republic cadastral data could be used as one of the base datasets forming the National Infrastructure for Spatial Information. This would ensure consistency and improve integration with datasets of lower levels of detail. It is important to note that it is the only database containing cadastral parcels together with ownership data which plays a crucial role in decision making on all governmental levels (local, regional and national). Cadastral data are captured and maintained at the highest level of detail, covering the entire territory of the Czech Republic. It is a unique data set in terms of completeness, logical consistency and positional, temporal and thematic accuracy.

The exploitation of this unique large scale dataset should be supported by model generalisation to enable integration with other datasets, update of datasets of lower level-of-detail and using cadastral layer as a reference layer for various purposes. Several attempts were already made to delimitate spatial objects from cadastral datasets. As a result a simple feature catalogue was created (see Fig 3). The catalogue forms simple features out of the subjects of content of digital cadastral map (DKM).

CODE								SUBJECT OF CONTENT OF DKM	FEATURE
Code of map symbol	Code of description	Type of land use	Form of exploitation of land	Type of building	Form of exploitation of building	Type of real estate protection	Form of real estate protection		
2.18								inner line	building
4.02				1-4	6			masonry, concrete or iron building	
4.03					19			wood building	
2.19								parcel border	
2.01								state border	territory of Czech Republic
2.03								region border	region territory
2.04								district border	district territopry
2.05								municipal border	municipal territory
2.06								cadastral territory border	cadastral unit
2.19								parcel border	parcel
	18							parcel number (definition point) of land parcel	
	28							parcel number (definition point) of building parcel	

Fig. 3. Example of simple feature catalogue for cadastral dataset (Čada & Mildorf 2005)

Further steps are to define semantic, topology and geometry criteria for data model in lower level-of-detail. The use of model generalisation defining the relations between the two different levels-of-detail is essential.

An example of the use of cadastral data as reference layer is spatial planning. Many issues that are being solved by spatial planners include the legal aspects of the territory being discussed. In particular, the issues of ownership of land and other rights and restrictions.

The INSPIRE Directive addresses spatial planning through spatial data themes, primarily through the spatial data theme Land Use. This theme is defined as territory characterised according to its current and future planned functional dimension or socio-economic purpose (e.g. residential, industrial, commercial, agricultural, forestry, recreational). Spatial planning is becoming part of the INSPIRE and interoperability on all levels is required.

Spatial planning acts in bottom-up and top-down directions between all levels of government. The situation is complicated by the diversity and overall complexity of spatial planning. Spatial planning is a holistic activity. All the tasks and processes must be solved comprehensively with input from many various sources. Several authorities are in charge of single spatially relevant topics (e.g. water management, transport, cadastre, geology, etc.). There is a big diversity in data collection, storing, processing and provision. To combine these sources, to perform an analysis and to ensure valuable results are big challenges in spatial planning (Mildorf 2009). Cadastral data should become a reference layer for the creation of spatial plans and other input data for spatial planning processes. It would ensure the compliance of the legal aspects of land and the spatial plan itself. The schema in Fig 4 shows the role of model generalisation.

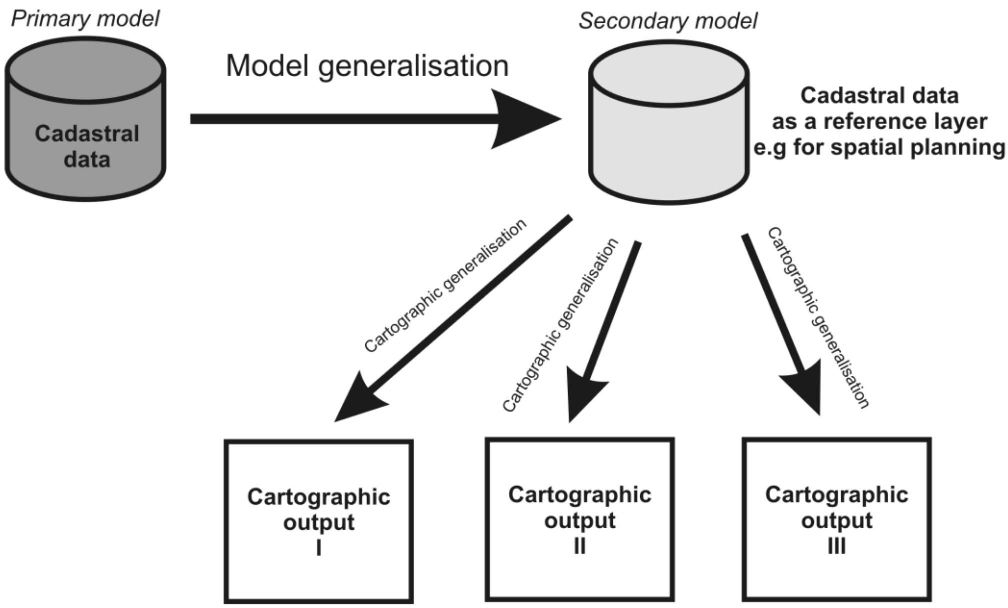

Fig. 4. Simplified schema and the role of model generalisation in the overall process.

CONCLUSIONS AND FUTURE PLANS

This contribution introduces use case from the Czech Republic where model generalisation plays a crucial role – cadastral data model. The context of the INSPIRE and related initiatives is to stress that generalisation plays important role in building Infrastructure for Spatial Information. INSPIRE Directive is a European initiative which has mainly top-down approach. It is a legislative which is transposed and then implemented in Member States on national, regional and local level. The use cases on which the INSPIRE Directive is based on are not always from real situation. The involvement of users and stakeholders and their feedback are therefore essential for further developments.

The Czech use case takes a bottom-up approach and studying the Czech use case contributes to the generalisation problem by enabling us to understand the user requirements in this real situation (van Oosterom 2009). Cadastral data are a unique source of spatial information for National Infrastructure for Spatial Information. Cadastral data are captured and maintained at the highest level of detail and they cover the entire territory of the Czech Republic. The quality of this large-scale dataset has no other equivalent in terms of completeness, logical consistency and positional, temporal and thematic accuracy.

Further developments include the definition of semantic, topology and geometry criteria for the cadastral data model in a lower level of detail. Selected methods for model generalisation will be applied in order to get the target model. The generalisation techniques will be applied to, and tested on, sample cadastral data. The use of model generalisation defining the relations between the two different levels of detail is essential.

ACKNOWLEDGEMENT

The author V. Cada was supported by the Research Plan MSM 4977751301.

REFERENCES

ACIL Tasman, 2008. The Value of Spatial Information, Available at: http://www.crcsi.com.au/uploads/publications/PUBLICATION_323.pdf.

Basaraner, M., 2002. Model Generalization in GIS. In International Symposium on GIS. Istanbul, Turkey.

Čada, V. & Mildorf, T., 2005. Delimitation of reference geodata from land data model. In Proceedings of GIS Ostrava 2005. GIS Ostrava 2005. Ostrava: VŠB - TUO, p. 13. Available at: http://gis.vsb.cz/GIS_Ostrava/GIS_Ova_2005/Sbornik/cz/Referaty/cada.pdf.

Corbin, C., 2008. Public Private Partnerships for building Spatial Data Infrastructures: Summary and recommendations, Available at: http://www.epsiplus.net/content/download/13853/173287/file/PPP4SDI_Report_Part1_V1_1_Final.pdf.

European Parliament, 2007. DIRECTIVE 2007/2/EC OF THE EUROPEAN PARLIAMENT AND OF THE COUNCIL of 14 March 2007 establishing an Infrastructure for Spatial Information in the European Community (INSPIRE). Available at: http://eurlex.europa.eu/JOHtml.do?uri=OJ:L:2007:108:SOM:EN:HTML.

Gruenreich, D., 1992. ATKIS - a topographic information system as a basis for GIS and digital cartography in Germany. In Geologisches Jahrbuch Reihe A. pp. 207-216.

INSPIRE Drafting Team "Data Specifications", 2008a. D2.5: Generic Conceptual Model, Version 3.0, Available at: http://inspire.jrc.ec.europa.eu/reports/ImplementingRules/DataSpecifications/D2.5_v3.0.pdf.

INSPIRE Drafting Team "Data Specifications", 2008b. D2.6: Methodology for the development of data specifications, Available at:

http://inspire.jrc.ec.europa.eu/reports/ImplementingRules/DataSpecifications/D2.6_v3.0.pdf.

International Organization for Standardization, 2002. ISO 19113 - Geographic information - Quality principles.

McMaster, R. & Shea, S., 1992. Generalization in Digital Cartography, Washington D.C.: Association of American Cartographers.

Mildorf, T., 2009. PLAN4ALL - Interoperability of Spatial Planning Information in the Context of the Infrastructure for Spatial Information in the European Community – INSPIRE. In INSPIRE, GMES and GEOSS Activities, Methods and Tools towards a Single Information Space in Europe for the Environment. Riga: Tehnoloģiju attīstības forums, Wirelessinfo. Available at: http://www.earthlook.cz/book/GMES_BOOK.pdf.

van Oosterom, P., 2009. Research and development in geo-information generalisation and multiple representation. Computers, Environment and Urban Systems, 33, pp.303–310.

Sester, M. et al., 2009. Summary report of the Dagsthul seminar 09161 on Generalization of Spatial Information 14-17 April 2009, Dagsthul. Available at: http://ica.ign.fr/dagsthul2009/Dagsthul2009Report.pdf.

THEORETICAL ASPECTS AND OPEN ISSUES IN SDI ESTABLISHMENT WITHIN GEODETIC AND CADASTRAL DOMAIN AT THE SLOVAK UNIVERSITY OF TECHNOLOGY

KLIMENT Tomas, DURACIOVA Renata, GALOVA Linda, CIBULKA Dusan and TUCHYNA Martin

Department of Theoretical Geodesy, Faculty of Civil Engineering, Slovak University of Technology, Radlinskeho 11, 813 68, Bratislava, Slovakia
tomas.kliment@stuba.sk¨

Slovak Environmental Agency, Tajovskeho 28, 975 90, Banska Bystrica, Slovakia
martin.tuchyna@sazp.sk

Abstract

The initiative to establish Spatial Data Infrastructure (SDI) within the Geodetic and Cadastral domain at the Slovak University of Technology aims to implement all principles defined by INSPIRE directive. INSPIRE may be taken into account either as a legal act to force member states to follow its paragraphs or as a "best-practices" in establishing SDI in wider context. Geodetic and Cadastral domain includes geospatial data with a different scale and thematic content and therefore the application of SDI principles is more then appropriate. Therefore, research workers of the Department of Theoretical Geodesy at the Slovak University of Technology propose the project "*Portal of reference data and services for domain of Geodesy and Cartography*". This project is focused on analysis of existing dataset resources that are used within the Geodetic and Cadastral domain and optimization of their workflows (in order to avoid duplication and increase coherency). Realization of the proposed project should ensure interoperable geospatial data discovery, evaluation and consumption in desired quality and quantity. The main objective of the project is data harmonization within selected domain and further implementation of network services that ensure discovery, view, download and processing of these harmonized data. Project has been submitted for approval to the VEGA, a scientific grant agency of the Ministry of Education, Science, Research and Sport of the Slovak Republic and of the Slovak Academy of Sciences, for funding of its realization. There are many opened issues and questions that will most probably arise during the processing of the particular project tasks. All of them are mentioned and described within the grand application, which has been sent for evaluation and review. This paper does not want to find and describe all the answers of those questions, however is trying to outline the actual situation with open issues and consequently propose appropriate solutions based mainly on most economically available applications (cost & benefit considerations), which will be possible to deploy also by the other stakeholders within Geodetic and Cadastral domain, perhaps even in further domains

Keywords: Spatial Data Infrastructure, INSPIRE, Geodetic and Cadastral domain, Initial investigation, Initial metadata profile, Geospatial data

INTRODUCTION

Many times activities focusing on more effective execution of the tasks and better decisions support within the certain domain requires except good will and know-how also strong drivers behind. These drivers can be represented either by legislation force or by strong and accurate identified user needs (Masser, 2005). In the world, where word “spatial” plays significant role we can identify a lot of such drivers in various shapes of networks, initiatives, projects and so on. One of them was recently born in Europe, and its name is INSPIRE.

The proposed project “*Portal of reference data and services for domain of Geodesy and Cartography*” (thereinafter only project) is focused on data flows optimizing. Scope of the project is within the organization level (among the departments, sections, actions...) and thus reducing duplication and improving consistency. It includes design and testing an appropriate structure of the data from the field of geodesy and cadastre. Data flow in this context refers to the chain of operations with data from their production (acquisition) to their use. Within whole process we can identify operations representing inputs into the system for processing and operations acting as distribution of outputs from processing through web services. The Department of Theoretical Geodesy, workplace of project promoter, holds data relating to the region of Slovakia and Central Europe. This data repository contain models of geoid and quasigeoid, data from permanent GNSS stations, geodynamic data from long-term points monitoring, digital elevation model, data from troposphere monitoring and atmospheric moisture, spatial data for prediction of archaeological sites and so on. All data will be shared by access rights for scientific research, educational and other purposes.

The paper describes an approach used to investigate and summarize the current situation within particular departments covering *geodetic and cartographic domain at the Slovak University of Technology in Bratislava* (thereinafter only domain) as well as discuss the open issues and propose the most appropriate solutions considering the personal and financial resources of the public sector: The first section in methods describes INSPIRE and other related realisations of SDI that shall be taken into the consideration within the project proceeding, The second one deals with an approach used to perform *an initial investigation* within the domain to obtain primary information about using data resources. The third section provides a graphical overview of organizational structure of stakeholders within the domain. The fourth section proposes the *initial metadata profile* for existing data resources for catalogue purposes in central domain geo-catalogue. The section with results summarizes the current situation within the domain and shows the examples of data, which are currently used. In the discussion part we describe open issues and raise the questions that should be answered during the project processing. Conclusion and future work provides the proposal how to reach the aims based on investigation results that are described within this paper.

METHODS

INSPIRE and other related works

Main purpose of this initiative driven by the Directive 2007/2/EC of the European Parliament and of the Council is to establish an Infrastructure for Spatial Information in the European Community (INSPIRE) for the purposes of Community environmental policies and policies or activities which may have an impact on the environment. To fulfil this ambitious aim, almost all major domains need to be taken into the consideration as environment is affected by human as well as natural related activities. INSPIRE therefore serves unique opportunity to improve aspects, processes and phenomena, where it was difficult to do it by now.

INSPIRE Directive itself is very generic legal framework defining the five main components, which shall be taken into the consideration by affected stakeholders:

- ***Metadata*** *are descriptive information helping users to navigate and discover, inventory and use the most appropriate spatial data or services. In context of this project proposal plays important role as with the properly structured metadata profile can be spatial data easier described and later on discovered and used according user requirements.*
- ***Data specifications*** *defining structure and content of spatial data according the themes identified in 3 annexes of INSPIRE directive. INSPIRE models can serve important reference base for spatial data identified within the project. When proper mapping and transformation will be executed, compliancy tests can be executed to identify level of conformity with target schema/s. This will enlarge possibility to exchange data in interoperable manner across the various domains.*
- ***Network services*** *specifying the five main type of services used within the INSPIRE architecture (discovery, view, download, transformation and invoke), including definition of spatial data services concept. These services within the project should help make metadata easier discoverable as well as allow to display and properly transform content of spatial data via web browser without*

need for specific software. They should also ensure access to the raw data for further analysis via desktop GIS tools and where possible deploy advanced desktop GIS functionality to the web interface via invoke (for example Web Processing) services,

- ***Data Sharing** is dealing with setting up the rules for spatial data and services access and use.*
- ***Monitoring and reporting** focused on evaluation of spatial data infrastructures evolvement.*

Each of these components comes, or in near future will come with specific set of rules defined in legally binding "Implementing rules" which are accompanied with non legally binding "Guidelines". This set of documentation together with additional INSPIRE documents and registers provide the main base for the implementation within the EU member states. This process just started and according the INSPIRE Roadmap implementation phase fulfilment is foreseen by the 2019, so still long way to go.

Despite of this long term run, there is already a lot of effort and pressure via various pilot implementations and use cases aiming to set up new procedures or adjust existing processes in the various domains utilising spatial data. Their scope is wide from global activities (GSDI, GEOSS), continental (State of play reports, AuScope, Nature SDIplus, oneGeology), through national (géoportail FR, INSPIRE CZ, SK), domain/thematic (Geonet.SK, Geoportal UGKK SR, ENIPI), crossborder (CENTROPE, eSDI-NET+, HUMBOLDT) or regional and local ones (Turistický portál Posázaví, GIS portál Mesta Banská Bystrica).

Examples mentioned above shows only fragments of huge amount and variety of spatial data infrastructures implementations. Each of them are in different level of maturation but when following same principles chance for real interoperability achievement is getting more real.

Approach to investigate the current situation within the domain

The first step of investigation is a general study of data and data workflows in the particular departments, sections and actions within the domain. This study analyzes actual data workflows (which data exists, for what purposes they are used, how they are managed, updated, provided, visualized and shared). From this study there are identified user requirements and then defined future architecture of the system. The result of this step is a metadata inventory describing existing data resources (main identification of all data sources that will be included within the project).

An investigation of the existing data resources (as-is analysis) is performed by interview between the person from research project team and particular person responsible for each data resource (stakeholder). This interview analyzes data resources from several points of view (data theme, format, etc.) to gain information about current state. An interviewer asks individual stakeholders from particular departments questions according to structure, specifically:

- *What sections is a department divided in?*
- *What kinds of actions are realized by those processes (inputs and outputs), data resources (education, research projects, etc.)?*
- *What are the types, themes of datasets used within these actions?*

Furthermore we will get information about current approaches in issues like data search and discovery, maintenance and visualization. Further issues are related to proposals of user requirements for the new system. Received information will be documented for following steps of research project.

Organizational structure of the stakeholders within the domain

The geodetic and cadastral domain at the Faculty of Civil Engineering consists of three departments: Department of Theoretical Geodesy, Department of Surveying and Department of Mapping and Land Consolidation. The results of interview (investigation of data resources) have been modelled in freeware mind mapping program FreeMind (http://freemind.sourceforge.net). FreeMind allows the user to edit a hierarchical structure of any ideas around a central concept as well as provides extensive export capabilities for distribution purposes. Using of this tool brings non-linear approach to map brainstorming outlines and investigation results as ideas are added around the mind map (http://en.wikipedia.org/wiki/FreeMind). Basic structure (Department – Sections - Actions) of individual departments within the domain is mapped using this tool and an example from Department of Theoretical Geodesy is illustrated in Fig 1.

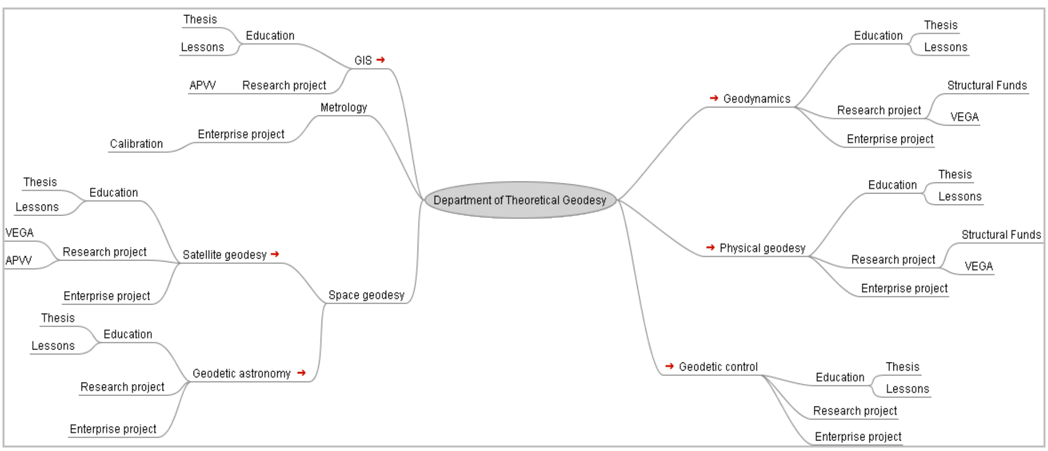

Fig. 16 Department of Theoretical Geodesy – Mapping to Sections and Actions

The data resources mapping from the Department of Theoretical Geodesy is illustrated in Fig. 2 (as an example). Other two departments are mapped in the same way, but the mappings are not included into the paper contents due to extent of the paper.

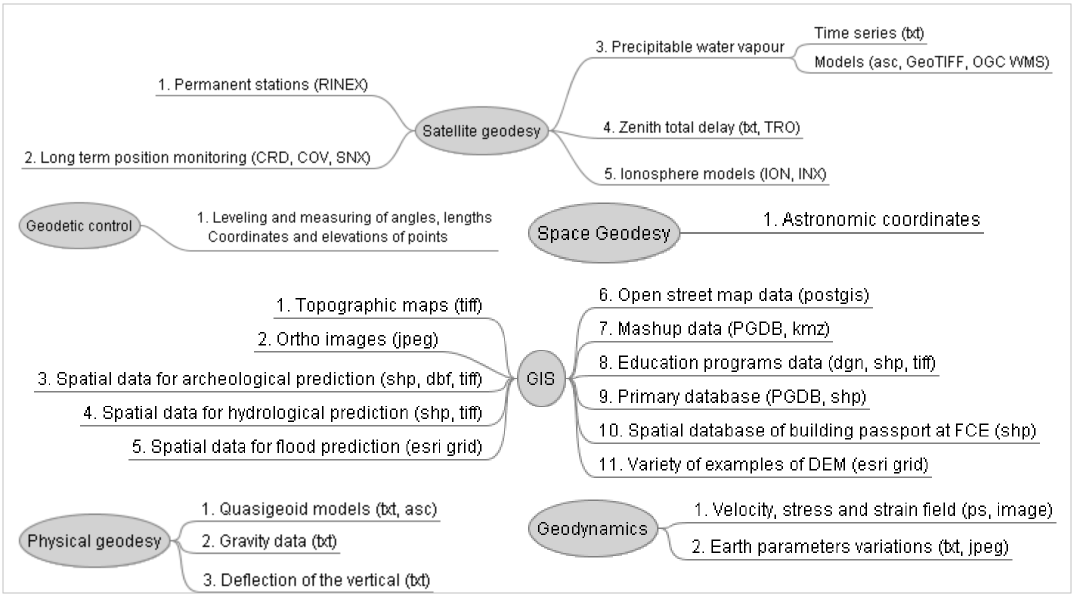

Fig. 17 Department of Theoretical Geodesy – Mapping to data resources

Initial metadata profile

The next investigation step is obtaining the samples of data resources related to particular actions. These samples are further being used to test automatic metadata extraction from them. Software CatMDEdit (http://catmdedit.sourceforge.net/) is used as a tool for extraction. CatMDEditor is an user friendly desktop application for documentation of resources, with focus on geospatial resources. We use this tool to obtain some information from particular data resources (formats) in automatic way as well as to create metadata as XML files defined by ISO (International Organization for Standardization) gmd (ISO, 2007) schema. Content of these metadata will be moreover extended following further interviews with stakeholders to fulfil INSPIRE requirements for metadata defined in metadata regulation (INSPIRE, 2008). Therefore the metadata model defined by INSPIRE regulation is taken into account as the *initial metadata profile* in our work. The initial metadata profile is shown in Fig. 3.

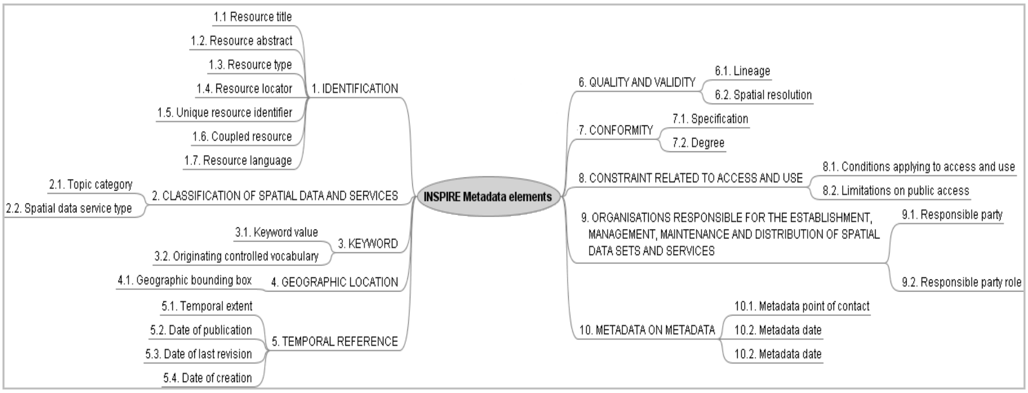

Fig. 18 INSPIRE metadata model (INSPIRE, 2008) – initial metadata profile elements

We will collect all metadata elements illustrated in Fig. 3 on the dataset hierarchy level for discovery purposes. However, the high data diversity within the domain means that INSPIRE metadata may not accommodate all applications. Hence, we will later on extend them again interviewing stakeholders by further elements defined in ISO metadata standard (ISO, 2003) for purposes of evaluation and use. We will create particular community profiles using the rules defined in ISO standard to better serve special stakeholders needs. All metadata records will be created, validated and catalogued using geo-catalogue application to provide web interface for searching, editing and updating of them, as well as to provide discovery service interface endpoint for querying from remote clients.

RESULTS

Overall description of the actual state within the domain

We can say, on the basis of the investigation performed with stakeholders that the data diversity within the domain is in wide range. In the following part we provide summarize tables of actual data resources within the domain with basic metadata like, data format, short abstract and keywords obtained from the stakeholders within the interviews. Table 1 summarizes data resources from the Department of Theoretical Geodesy.

Table 1 Actual data resources of the Department of Theoretical Geodesy (Summary table)

Session	Keywords	Format	Abstract
Geodetic control	control points, coordinates, reference system, reference frame, reference epoch	txt, dgn	Coordinates and elevations of points
Space Geodesy	astronomical coordinates, astronomical catalogue		Astronomical coordinates
Geodynamics	Earth, parameters, polar motions, precession, nutation, lenght of day	txt, jpeg	Earth parameters variations
	velocity, stress field, strain field	ps, image	Velocity, stress and strain fields
GIS	topography, contours,	tiff	Topographic maps
	ortho-imagery	jpeg	Ortho images
	hydrological prediction	shp, dbf, tiff	Spatial data for hydrological prediction
	flood prediction	esri grid	Spatial data for flood prediction
	open street map	postgis database	Open street map data
	mashup, information system	esri pgdb, kmz	Mashup data
	education, training	dgn, shp, tiff	Data for education programs
	primary database for the GIS	esri pgdb, shp	Primary database for the GIS in Slovakia
	passport of building, structure of faculty	shp	Spatial data of Faculty of Civil Engineering passport
	DEM	esri grid	Variety of examples of DEM
Satellite Geodesy	global navigation satellite system	RINEX	Permanent stations measuring data
	global navigation satellite system	CRD, COV, SNX	Long term positions monitoring
	precipitable water vapour, meteorology, monitoring	txt, asc, GeoTIFF, OGC WMS	Precipitable water vapour determination. Time series data and models.
	zenith total delay	txt, TRO	Zenith total delay
	Ionosphere	ION, INX	Ionosphere models
Physical geodesy	Quasigeoid	txt, asx	Quasigeoid models
	Gravity	txt	Gravity data
	Deflection	txt	Deflection of the vertical

Table 2 summarizes data resources from the Department of Surveying and the last table (Table 3) summarizes data resources from the Department of Mapping and Land Consolidation:

Table 2 Actual data resources of the Department of Surveying

Session	Keywords	Format	Abstract
Surveying Engineering surveying Photogrammetry	building, current state	txt, dxf	Measurements of current state
Surveying Engineering surveying	control point	txt, dxf	Setting-out networks, points – control
Surveying Engineering surveying	project data	dwg	Project data – data inputs from architects and planner for geodetic works
Surveying Engineering surveying	hydro meteorological parameters, temperature, atmospheric pressure	doc, txt	Hydro meteorological parameters – temperature (measured), atmospheric pressure, humidity.
Surveying Engineering surveying Photogrammetry	cloud of points	txt, dxf	Cloud of points of measured objects
Surveying Engineering surveying	building tilt	xls,	Measurements of tilts
Surveying Engineering surveying	Cadastre	vgi	Cadastral maps
Engineering surveying	displacement	txt, dxf	Displacements measuring data
Photogrammetry	digital images	jpeg, tiff, raw data	Digital images
	photogrammetry, control points, control feature	txt, dxf	Set of control points, set of control features
	photogrammetry	txt, dxf	New feature collections – edges, lines, polylines, polygons, surfaces
	ortho images	tiff, jpeg	Scaled ortho images
	simulations, animations	avi, wmv	Simulations and animations

Table 3 Actual data resources of the Dept. of Mapping and Land Consolidation

Session	Keywords	Format	Abstract
Cartography	Topographic map	cit, jpeg, dgn, dwg, shp	Digital raster and vector topographic maps
	digital elevation model, elevation	dgn, txt	DEM
	primary database for the GIS	shp	Primary database for the GIS in Slovakia
	thematic map, parcel	jpeg, tiff, shp	Thematic raster and vector cadastral maps
	Imagery	jpeg	Ortho-photographs
	3D model	kmz, SKP	3D models of real objects
Cadastre of Real Estate and Mapping	cadastre, cadastral map, parcel	cit, vgi	Digital raster and vector cadastral maps
	Cadastre	dbf, txt	Descriptive Data File
Land Consolidation	land consolidation, land use, land management	vyk, vgi, dgn, GeoTIFF	Projects of land consolidation
	orto imagery	jpeg	Ortho-photographs

For each obtained data samples is planned to create an Initial metadata record, based on INSPIRE regulation as mentioned above. The example of Initial metadata record was created for one dataset with name **St_Mesto_2010_02_ar_shp**. This metadata records was created by CatMDEdit and online INSPIRE multilingual metadata editor (http://www.inspire-geoportal.eu/EUOSME/userguide/about.html). CatMDEdit was used for automatic metadata extraction from dataset. Automatic metadata extraction procedure does not support full requirements defined by INSPIRE rules. Therefore this metadata record was imported in XML file and extended in INSPIRE multilingual editor. The fragment of XML file is listed in Fig. 4. Dataset described by this metadata record (fragment of XML file) is showed in Fig. 5.

```
<gmd:MD_Metadata xsi:schemaLocation="http://www.isotc211.org/2005/gmd http://schemas.opengis.net/iso/19139/20060504/gmd/gmd.xsd">
 +<gmd:fileIdentifier></gmd:fileIdentifier>
 +<gmd:language></gmd:language>
 +<gmd:characterSet></gmd:characterSet>
 +<gmd:hierarchyLevel></gmd:hierarchyLevel>
 +<gmd:contact></gmd:contact>
 +<gmd:dateStamp></gmd:dateStamp>
 +<gmd:metadataStandardName></gmd:metadataStandardName>
 +<gmd:metadataStandardVersion></gmd:metadataStandardVersion>
 -<gmd:identificationInfo>
   -<gmd:MD_DataIdentification>
     -<gmd:citation>
       -<gmd:CI_Citation>
         -<gmd:title>
             <gco:CharacterString>St_Mesto_2010_02_ar_shp.</gco:CharacterString>
          </gmd:title>
         +<gmd:date></gmd:date>
         -<gmd:identifier>
           -<gmd:RS_Identifier>
             -<gmd:code>
               -<gco:CharacterString>
                   KMPU_Cartography_Thesis_ThematicCadastralMaps_poly_shp
                 </gco:CharacterString>
               </gmd:code>
             </gmd:RS_Identifier>
           </gmd:identifier>
         </gmd:CI_Citation>
       </gmd:citation>
```


Fig. 19 Fragment of XML file for dataset St_Mesto_2010_02_ar_shp

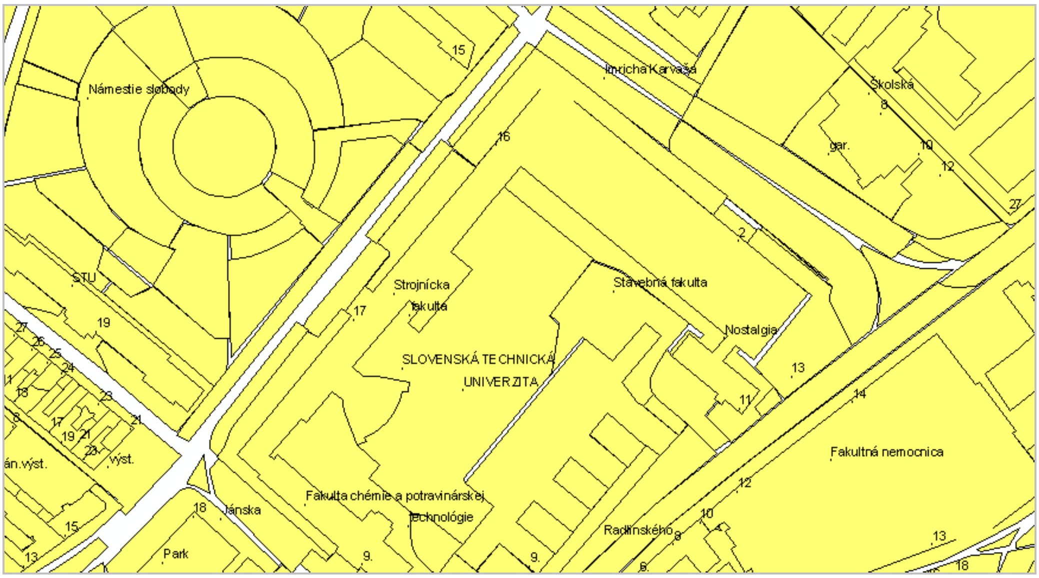

Fig. 20 Sample of dataset portrayal - St_Mesto_2010_02_ar.shp and St_Mesto_2010_02_tx.shp

DISCUSSION

The main objective of the project is data harmonization within selected domain and further implementation of network services that ensure discovery, view, download and processing of these harmonized data. There are many opened issues and questions that will most probably arise during the processing of particular project tasks: (i) Investigation of existing geospatial data resources within the domain – What are the heterogeneities within the data structures? What are the actual data flows? What are the application models used (if there are any)? How to model of existing work flows and propose new? (ii) Modelling of new application models based on reference data specifications (INSPIRE) and user requirements with extensions defined by domain experts – users, data providers and data transformers (producers of value added products based on the data themes of INSPIRE) – Which INSPIRE data specification should be used? How those models should be simplified or extended to ensure user requirements? (iii) Mapping and transformation data resources to the new models and testing the conformance of the mapping process. (iv) Metadata creation – What will be the reference metadata model (INSPIRE)? How to extend this model with specific metadata elements defined in standard ISO 19115 to ensure data resource description according to user requirements for discovery, evaluation and consumption purposes? How to ensure interconnection among related resources (datasets, services) by particular metadata elements? (v) Network services and SDI portal implementation to provide connection between end users and datasets. What types (discovery, view, download, transformation, invoke) of the network services should be implemented regarding to user requirements? How application profiles (OGC, INSPIRE) of particular services should be simplified or extended? What issues need to be taken into account in particular client application (discovery, view, download, transformation) of the final SDI portal development?

CONCLUSION AND FUTURE WORK

To achieve the above mentioned main objective of the project we would propose the following approach of solution:

1. General study (above)

2. Study of user requirements

- Development of highly structured methodology for workflow mapping to aid the final requirements capturing.
- Application of methodology within the organization among the particular data source responsibilities for further advanced user requirements.

  On the base of user requirements study (performed within first step) we will model use cases for developing system using graphic notation of UML language (Unified Modeling Language). For modeling tasks we will use available CASE tools (Select Architect or open source tools like StarUML (http://staruml.sourceforge.net/en/) or ArgoUML (http://argouml.tigris.org/)).

3. System architecture design based on studies performed in previous steps.

Based on use case definition and modelling performed within point 2 we will define the most important entities (data, metadata, services) and their relationships. It will serve as a model to help with understanding the nature of the entities and relationships, their purposes, context and how they could interact to realize use cases and workflows. We will use the same tools mentioned in previous point for system architecture design. The second part will be proposals and evaluation of software tools that could be used for practical implementation of particular system components.

4. Step by step implementation

- Consolidation and harmonization of existing data inventories to the common application models defined by current directions and standards and extended on the base of results from general study realized within the point 1 of this approach. Reference data will be harmonized to common application model based on INSPIRE data specifications.
- Reference data will be described by metadata (metadata creating) and catalogue (metadata management within searchable metacatalogue) in compliance with directives (INSPIRE), standards and implementation specifications (ISO, OGC). Realization of this step will allow organizations to easily discover data sources that are available and gain information like who are responsible persons and what are the licensing conditions.
- An intranet application will be developed that allows users to visualize reference data in accordance with directive (INSPIRE), standards and implementing specifications (ISO, OGC).
- Development of portal extension for download, transformation and geoprocessing facilities based on the study of advanced user requirements.
- Testing phase – pilot services deployment within reference data and service portal, feedback from users.

5. Analysis and development of methods and procedures for processing of spatial data based on WPS (Web Processing Service)

- To develop each process functionality part of WPS based on user requirements. Following current needs service would implement processes to achieve these tasks:

- Functions using models of geoid and quasigeoid for vertical deviation and altitude calculations.

- Geo-kinematics functions and long term monitoring of geodetic points (point stability determination, deformation parameters calculations).
- Functions based on DEM (determinations of altitude, terrain slope, visibility analysis etc.).
- Data conversion among various data formats used within geodetic and cadastral domain.
- Transformations among coordinate systems.

- Methods and procedures for data processing will be developed for facilitate the work with reference data sources for each group of users.

All above mentioned answers and solutions of the proposals probably and even more questions are the main goals of the proposed project. With this paper we would like to point out aspects, which many of the stakeholders will have to consider in near future because of new legislation drivers (INSPIRE) as well as upcoming technology developments and new users expectations.

ACKNOWLEDGEMENT

This paper has been made thanks to VEGA No 1/0894/10.

REFERENCES

INSPIRE (2008) Commission Regulation (EC) No 1205/2008 of 3 December 2008 implementing Directive 2007/2/EC of the European Parliament and of the Council as regards metadata - Metadata Implementing rules, European Commission, Brussels.

ISO (2003) 19115:2003 Geographic information - Metadata, Switzerland.

ISO (2007) 19139:2007 Geographic information – Metadata – XML schema implementation, Switzerland.

Masser, I., (2005) The future of spatial data infrastructures, Proceedings of ISPRS WG IV/1 Workshop on 'Service and Application of Spatial Data Infrastructure' (Hangzhou, China, 2005), http://www.isprs.org/proceedings/XXXVI/4-W6/papers/7-16%20Ian%20Masser-A001.pdf ,

FreeMind, http://freemind.sourceforge.net, October 29, 2010

FreeMind, http://en.wikipedia.org/wiki/FreeMind, October 29, 2010

CatMDEdit, http://catmdedit.sourceforge.net/, October 29, 2010

EUOSME, http://www.inspire-geoportal.eu/EUOSME/userguide/about.html, October 29, 2010

StarUML, http://staruml.sourceforge.net/en/, October 29, 2010

ArgoUML, http://argouml.tigris.org/, October 29, 2010

GSDI, http://www.gsdi.org/, December 30, 2010

GEOSS, http://www.earthobservations.org/geoss.shtml, December 30, 2010

INSPIRE State of play reports, http://inspire.jrc.ec.europa.eu/index.cfm/pageid/6/list/4, December 30, 2010

AuScope, http://www.auscope.org.au/, December 30, 2010

Géoportail, http://www.geoportail.fr/, December 30, 2010

INSPIRE CZ, http://inspire.gov.cz/, December 30, 2010

INSPIRE SK, http://inspire.enviroportal.sk/, December 30, 2010

GEONET.SK, http://www.geonet.sk, December 30, 2010

Geoportal UGKK SR, http://www.geoportal.sk, December 30, 2010

ENIPI, http://isu.enviroportal.sk/index.php/item/enipi, December 30, 2010

CENTROPE, http://pgo.centropemap.org/, December 30, 2010

eSDI-NET+, http://www.esdinetplus.eu/, December 30, 2010

HUMBOLDT , http://www.esdi-humboldt.eu/home.html, December 30, 2010

Turistický portál Posázaví, http://tourist.posazavi.com/cz/mapvylet.asp, December 30, 2010

GIS portál Mesta Banská Bystrica, http://www.uhabb.sk/mapa/htdocs/bystrica.php, December 30, 2010

PLAN4ALL – SPATIAL PLANNING DATA HARMONISATION ACCORDING TO THE INSPIRE DIRECTIVE

SCHRENK Manfred, MILDORF Tomas and NEUSCHMID Julia

CEIT Alanova – Central European Institute of Technology, Institute of Urbanism, Transport, Environment and Information Society, Concorde Business Park 2/F, 2320 Schwechat, Austria
m.schrenk@ceit.at, j.neuschmid@ceit.at

University of West Bohemia, Faculty of Applied Sciences, Department of Mathematics, Section of Geomatics, Univerzitni 22, 306 14 Pilsen, Czech Republic
mildorf@centrum.cz

Abstract

Spatial planning acts between all levels of government so planners face important challenges in the development of territorial frameworks and concepts every day. Spatial planning systems, the legal situation and spatial planning data management are completely different and fragmented throughout Europe. Nevertheless, planning is a holistic activity. All tasks and processes must be solved comprehensively with input from various sources. It is necessary to make inputs interoperable because it allows the user to search data from different sources, view them, download them and use them with help of geoinformation technologies (GIT).

The Plan4all project focuses on the interoperability and harmonisation of spatial planning data. Plan4all is a European project and co-financed by the eContentplus programme of the European Commission. The aims are to define common procedures, methods and standards for spatial planning data management and sharing, to support holistic planning, to support the development of a European network of public and private actors from different levels as well as Spatial Data Infrastructure (SDI). Plan4all is based on existing best practices in European regions and municipalities and the results of current research projects. Plan4all focuses also on implementing the INSPIRE principles into the planning processes. Metadata profiles, data models and networking architecture are developed for seven selected themes from Annex II and III of the INSPIRE Directive. The directive provides common mechanisms for data sharing. The Plan4all standards enable to publish and share spatial planning data from pilot regions on the Plan4all geoportal (http://www.plan4all.eu). The expected results include European forums for SDI in spatial planning, database of best practices and analysis of best practices in terms of organisation, sharing, harmonisation as well as SDI recommendations for spatial planning. The whole sector should profit from the availability of understandable and more transparent planning information across Europe .

Keywords: Spatial planning, Harmonisation, INSPIRE, SDI, Metadata

THE NEED FOR HOLISTIC SPATIAL PLANNING

Spatial planning gives geographical expression to the economic, social, cultural and ecological policies of society. It is at the same time a scientific discipline, an administrative technique and a policy developed as an interdisciplinary and comprehensive approach directed towards a balanced regional development and the physical organisation of space according to an overall strategy (European Regional/Spatial Planning Charter, 1983). Spatial planning strongly influences our society on all levels as it addresses the environment where people live and work, the location of social and economic activities and the way in which processed resources are exploited. Spatial planning includes all levels of land use planning that are urban planning, regional planning, environmental planning, national spatial plans, and European/international cross-border planning.

Today's spatial planning practise is facing major challenges such as decentralisation – following regionalisation on the one hand and globalisation on the other hand, cross-border and transnational planning, vertical and horizontal integration, bottom-up approaches and involvement of multiple actors on different levels with different interests and intentions in the planning process. Often these ideas and concepts are difficult to apply because the legal situation in Europe is fragmented and planning laws are disjointed. Even experts from one country might have problems to understand the planning regulations of the neighbouring country. Especially for investors and decision makers it is almost impossible to compare planning regulations across Europe. Traditionally, standardisation in spatial planning activities has been rather poor. Heterogeneity of datasets and sources, gaps in availability, lack of harmonisation between datasets in different scales, duplication of information as well as loss of time and resources in searching for needed data are characterising for the European situation in spatial planning (Plan4all D.2.1 and Plan4all D.2.2). The idea is not to have isolated information islands, where spatial planning ends at the "coastline", and where planning relevant data is produced and maintained to own standards or even no defined standards at all. Administrative borders should not be knowledge borders. The idea is to support the exchange of compatible spatial planning data and to support the access to the data. Access can be given starting from simply viewing the spatial data, up to even having the right to download it. 'Information islands' need to turn into 'information systems' and 'information infrastructures' that allow different kinds of user access to spatial data from various sources.

PLAN4ALL – THE CONTRIBUTION TO HOLISTIC SPATIAL PLANNING

Goals of Plan4all

Plan4all is a European project running from May 2009 until October 2011 and co-financed by the eContentplus programme of the European Commission. Plan4all focuses on interoperability and harmonisation of spatial planning data in Europe to support holistic spatial planning activities. Data harmonisation means that all member states use a common set of coordinate reference systems, data models, classification schemes, portrayal rules, etc. Interoperability is understood as providing access to spatial datasets through network services, independent from whether the existing dataset is actually changed (harmonised) or just transformed by a service for publication (Plan4all D.2.3 2009). The aim of Plan4all is to support the development of a European spatial data infrastructure (ESDI) and a European network of public and private actors from different levels, i. e. local, regional and national public bodies, stakeholders, ICT industry, organisations dealing with planning issues and regional development, universities and international organisations (see Fig 1). The main objectives are to define the rules for European spatial planning data interoperability, to find consensus about harmonisation of spatial planning data, and to contribute to the establishment of an SDI. Plan4all is based on existing European best practises, the results of current research projects, the INSPIRE directive and the requirements of the users. INSPIRE is a European initiative regulating the development of a European spatial data infrastructure[4]. The directive does not require the collection of new spatial data and it does not establish new infrastructures, moreover it is based on already existing data and infrastructures created by member states that should be made compatible by common implementing rules to guarantee usability in the community and transboundary context.

[4] The acronym INSPIRE refers to the Directive 2007/2/EC of the European parliament and the Council of 14 March 2007 with the aim to establish an Infrastructure for Spatial Information in the European Community. The directive entered into force on 15 May 2007 and will be fully implemented in 2019.

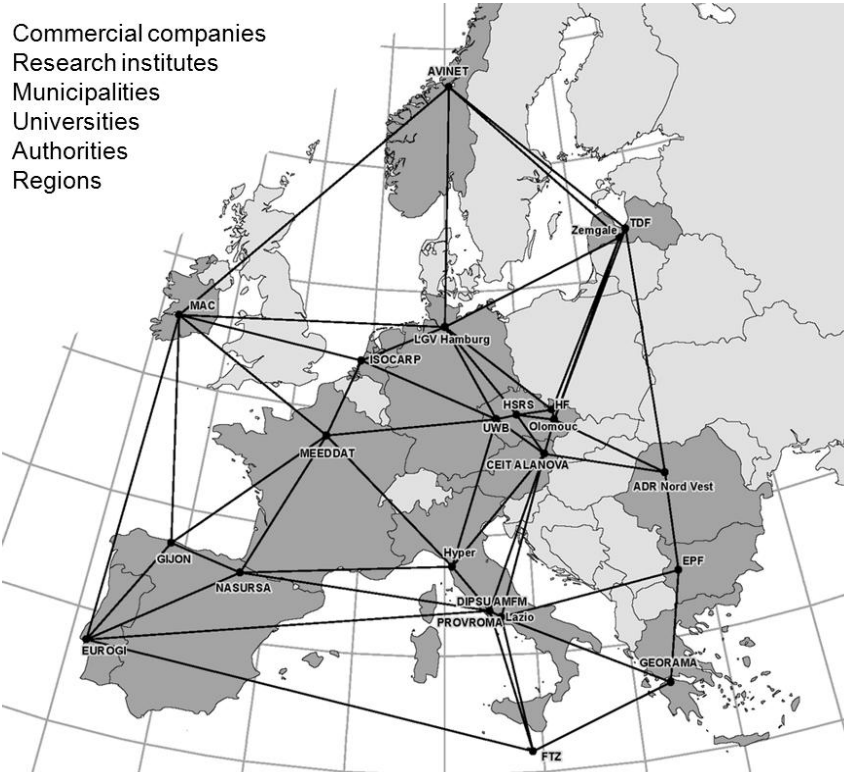

Fig. 1: Network of Plan4all partners

Geoinformation technologies in the spatial planning process

Geoinformation technologies (GIT) in the planning process focus on managing and conveying information to improve the decision-making process. One of the most basic tools for public and private organisations in spatial planning is Geographic Information Systems (GIS) as a decision support tool for both technical experts and decision-makers. GIS allows users to conduct complex geospatial analyses combining data from various sources such as socio-economic statistics, satellite imagery and monitoring data. GIS-based decision support applications are available for fields ranging from transportation, resource management, energy infrastructure, land use planning and disaster management to real estate, business development and marketing. GIS also plays an important role in informing and involving citizens in the planning process. In the past, GIS applications were generally installed locally on a laptop or PC or as an application running on an organisation's network. As the amount of spatial data available and usage of GIS has grown, organisations have become interested in sharing data both internally and with other organisations. This trend has led to the evolution of spatial data structures which rely on Web Services technology and standardised data formats to allow users to access data distributed across various organisations. Such infrastructures are actively supported in Europe through the INSPIRE Directive (Schrenk/Farkas/Brun 2010). In this context Plan4all focuses on the definition of common procedures and methods for spatial planning data interoperability. Into more detail, Plan4all creates metadata profiles and object-oriented data models for data sharing via the Plan4all geoportal.

Plan4all metadata profile

The most common instruments in the European planning systems are the land use local plan for regulating local land use and the regional plan focused on regional development and structure. Nevertheless, planning legislation varies between countries and sometimes even within countries there are significant differences in the terminology associated with planning acts. Especially at the regional level, plans are on different scales and administrative levels (Schrenk/Farkas/Brun 2010). Plan4all metadata profile (Plan4all D.3.2.2 2010) aims at making spatial plans comprehensible and comparable. Spatial plan metadata contains metadata of the spatial plan as a whole and can catalogue spatial plans on any level (regional, state, European). Because one spatial plan consists of many components, e.g. textual documents, maps in paper as well as in digital form, individual components may be optionally described by independent metadata records with links to the corresponding spatial plan. In addition to spatial plan metadata Plan4all metadata profile consists of dataset metadata and service metadata.

The Plan4all metadata profile fulfills the requirements of national metadata regulations, national spatial planning legislation, user requirements for spatial planning metadata and the INSPIRE directive. National and user requirements on metadata were collected using questionnaires. The goal was to compare national metadata regulations and to define common sets of items, which will be used for common metadata sharing. The metadata profile also supports the international standards ISO 19115 (core metadata for geographic datasets), other ISO standards and the standards of the Open Geospatial Consortium (OGC). Plan4all spatial plan metadata and dataset metadata are an extension of the base elements defined by INSPIRE. Additional items – coming from ISO 19115 – have been required by the users as well as national legislation. The service metadata profile was adopted from INSPIRE service metadata profile without extra elements over the INSPIRE profile.

Extensions for spatial plan metadata with multiplicity of ‘1’ are[5]*:*

- File identifier, because every metadata file requires a unique reference (ISO no. 2)

[5] Multiplicity of 1 indicates that each element always needs to be expected in the metadata record and can occur only once.

- Metadata standard name. Phrase "**ISO19115/19119 - Plan4all profile**" shall be used (ISO no. 10)
- Metadata standard version. Phrase "**2003/Cor.1:2006, Plan4all:2010**" shall be used (ISO no. 11)
- Data quality scope; is the level to which data quality information applies (ISO no. 79)

Multiplicity of 1..[6]*:*

- Presentation form; it is required to distinguish hardcopy spatial plans from digital ones. Possible values are: mapDigital – for digital spatial plan; mapHardcopy – for digital plan with maps in paper form; imageDigital – scanned paper maps (ISO no. 368)

Multiplicity of 0..[7]*:*

- Application schema; it is required because it provides information about the conceptual schema of the spatial plan data. It might be used at this level for whole spatial plan structure description or at dataset level for individual corresponding datasets description. (ISO no. 21)
- Reference system information; because different reference systems are in use, information on reference system is required. Example: Codespace: urn:ogc:def:crs:EPSG:: Code: 4326 (ISO no. 13)
- Status; is required because it represents the status of the resource described by metadata. Possible values are in the ISO 19115 code list 'MD_ProgressCode'. It is needed to distinguish if the spatial plan is in design phase (underDevelopment) or if it has already been adopted. Plans after expiration date should be denoted as "obsolete". (ISO no. 28)
- Legal relevance; not every spatial plan is legally binding. The phrase "**NO LEGAL RELEVANCE**" should be used if the spatial plan has no legal relevance. (ISO no. 68)

Multiplicity of 0..1[8]:

- Maintenance and update frequency; users require information on updates frequency. Example: annually. (ISO no. 143)
- Purpose; is required by the users because it summarizes the intentions with which the resource(s) was developed (ISO no. 26)

[6] Multiplicity of 1..* indicates that there shall be at least one instance of this element in a result set.
[7] Mulitplicity of 0..* indicates that the presence of the metadata element in a result set is conditional but the metadata element may occur once or more.
[8] Multiplicity of 0..1 indicates that the presence of the metadata element in a result set is conditional but can occur only once.

Additional items for *dataset metadata* are: file identifier, metadata standard name, metadata standard version, application schema, data quality scope, reference system info and maintenance and update frequency as defined above. In addition the following items were added:

Multiplicity 1..:*

- Spatial representation type, e.g. vector.
- Distribution format; because data is available in different formats, the distribution format is required by the users. In addition it should include information about the format version. Example: shapefile, version 1.0 (ISO no. 271)

Multiplicity 0..:*

- Geometry type; is required because it represents the geometrical type of a spatial dataset which spatial representation type is ‘vector’, and it may assume three possible values: point, polyline or polygon (ISO no. 37,178)
- Image; an image/graphic that illustrates the resource; a legend should be included. (ISO no. 31)
- Character set; character coding used for the dataset. (ISO no. 40)
- Transfer options; number of volumes, data carriers etc. for off-line distribution. Example: Medium: cdRom, volumes: 6 (ISO no. 273)
- Source; because it describes the sources that were used during the production process of the dataset. (ISO no. 85)
- Process step; is useful because it describes the process of data acquisition. Example: e.g. digitalization of analogue orthophotos. (ISO no. 84)

Multiplicity 0..1:

- Parent identifier; file identifier of the metadata to which a metadata is a child. It is used for the identification of spatial plan which the dataset is part of. (ISO no. 5)

Compound elements taken from ISO are metadata about the responsible party for the plan (contact information such as person responsible, address, phone number, email, etc.; ISO 375, 376, 379, 381-386, 390), the process step (e.g. before approval, approval of plan, expiration of plan; 87-90) and the source (e.g. level of the source data, spatial reference system used by the source data, etc.; ISO 93-96). Plan4all metadata records may be multilingual. From the perspective of European spatial planning activities it is recommended to provide metadata at least bilingual – in national language (as metadata language) and English.

The Plan4all metadata profile is an extension of mandatory INSPIRE metadata elements with ISO elements that are required by national metadata profiles and the requirements of the users based on a user requirements assessment. The Plan4all metadata profile is currently tested and validated (December 2010).

Plan4all Data Models

Plan4all develops conceptual data models for seven selected themes from Annexe II and III of the INSPIRE Directive. The themes are land cover, land use, utility and government services, production and industrial facilities, agriculture and aquaculture facilities, area management/restriction/regulation zones and reporting units, and natural risk zones. The data models refer to the INSPIRE documents „Generic Conceptual Model (GCM)“ and „Methodology for the development of data specifications“ which set basic rules for the development of data models. The document GCM describes the basis of Plan4all data models, the General Feature Model, which is a meta-model for the specification and description of spatial object types and their properties. It defines the concept of spatial object type (note that ISO 19101 uses the term “feature type” instead) and several types of properties (attributes, association roles and operations) as well as constraints. It also serves as a meta-model for feature catalogues by providing the structure for representing the semantics of geographic information in these terms (INSPIRE GCM 2010). In addition Plan4all data models respect the requirements of national conceptual models. The object-oriented Plan4all data models are flexible enough to be extended easily with further objects. Each object has a unique identity which is immutable and used only once, even if an object is removed its identity is not assigned to other objects. Also code lists and nomenclatures are extendable. To specify the models in diagrams UML is used. The data models are published on the Plan4all website[9] and are open for validation by affiliated partners. Further, the Plan4all data models will be an input for the development of the INSPIRE data models by the INSPIRE thematic working groups. Especially, there is strong cooperation concerning the land use theme.

Plan4all geoportal

Spatial planning data from pilot regions are being published on the Plan4all geoportal (http://www.plan4all.eu). The geoportal presents geographic information from various sources in a unified way. The Plan4all geoportal has two features that are map and catalogue. The catalogue client allows searching for metadata using OGC Catalogue Service for Web (CSW). The map client allows viewing maps based on OGC Web Services and other formats (Google maps, KML, MapServer, GML). The basic functions are viewing web services (OGC WMS, WFS) selected by user from the catalogue or directly by address; saving user defined map projects on local hard drive a re-loading of this saved composition (OGC WMC); distance and area measurement; searching in the map; inserting user defined objects into the map, large format printing in PDF; showing legends, metadata and querying in the map. The Plan4all geoportal will enable to search and view harmonised spatial planning data from the Plan4all partners with the aim to further extend the network with affiliated partners.

CONCLUSION & OUTLOOK

The three main objectives of Plan4all are the definition of standards for spatial planning data harmonisation according to INSPIRE, the implementation of the Plan4all geoportal that consists of harmonised spatial planning data that can be shared and third, to contribute to a European spatial data infrastructure. Plan4all is a testbed for INSPIRE and supports the distribution of the INSPIRE ideas which are the development of a European spatial data infrastructure and the rising of awareness for this topic to support holistic spatial planning in Europe and its regions. Plan4all develops tools that support geographic information infrastructures; these are the Plan4all metadata profile, data models for seven selected themes from INSPIRE Annex II and III and the Plan4all geoportal. These tools are currently (December 2010) being tested and validated by Plan4all affiliated partners who are external experts. In addition there is an internal verification of results. Validation and verification processes will test if there are any problems with the developed Plan4all standards. It is expected that the Plan4all data models will be an important input for the ongoing activities in the development of INSPIRE data models for the themes from Annex II and III. Plan4all is in close cooperation with INSPIRE Thematic Working Groups.

The implementation of GIT in the spatial planning process faces several challenges. GIT without data, the willingness as well as the knowledge to share it is not fully sufficient. For future developments in SDI bigger efforts are necessary in data collection (quantity and quality) as there are still big disparities between different European Union regions (Plan4all D.2.2 2009). Especially, much metadata information is still incomplete and not collected according to certain standards. Accurate metadata collection clears the way for data networking and SDI building in a European context. Further, interregional, cross-border and transnational cooperation (horizontally) as well as cooperation between the state and regional or local governments (vertically) are key factors for successful data harmonisation. It is of high importance to strengthen the awareness of data providers as well as data users that SDI and data harmonisation are necessary for holistic planning and to point out the advantages of data harmonisation initiatives to keep networks stable and to gain new partners for the future. The planning process depends on continuous input (socio-demographic data, economic data, changes in infrastructure, agriculture and aquaculture, natural risks etc.) to monitor urban, regional and environmental developments, to detect changes and to be able to find strategies to react on these changes. Spatial planning depends

[9] http://www.plan4all.eu/simplecms/?menuID=37&action=article&presenter=Article

on up-to-date geodata. Spatial data infrastructures, consisting of common data models and metadata standards, can contribute as it aims at offering wider access to geospatial data across Europe. Besides promoting the idea of data sharing within the circle of SDI experts, a challenge is to promote new services and technologies also to the users. The big challenge is to bring new GIT, relevant software and services to a wide group of users, which in spatial planning usually are actors from public administrations on all levels – mainly on the local level. Actors working at one of the more than 10.000 municipalities plus public administrations on regional and national level are the end users of GIT.

REFERENCES

European Regional/Spatial Planning Charter, 1983

INSPIRE Directive 2007/2/EC

INSPIRE Generic Conceptual Model (GCM): http://inspire.jrc.ec.europa.eu/reports/ImplementingRules/DataSpecifications/D2.5_v3.1.pdf, accessed in October.2010

INSPIRE Metadata Regulation: http://eur-lex.europa.eu/LexUriServ/LexUriServ.do?uri=OJ:L:2008:326:0012:0030:EN:PDF, accessed in October 2010

INSPIRE Methodology for the Development of Data Specifications: http://inspire.jrc.ec.europa.eu/reports/ImplementingRules/DataSpecifications/D2.6_v3.0.pdf, accessed in October 2010

ISO 19101 Geographic Information – Reference Model

ISO 19109 Geographic Information – Rules for application schema

ISO 19115 Geographic Information – Metadata

Plan4all D.2.1 (2009) Clusters of leading organisations in SDI for spatial planning.

Plan4all D.2.2 (2009) Analysis of innovative challenges

Plan4all D.2.3 (2009) Analysis of INSPIRE requirements.

Plan4all D.3.2.2 (2010) Plan4all metadata profile.

Plan4all geoportal, http://www.plan4all.eu, accessed in October 2010.

Plan4all Newsletter (2009), Issue 1.

Schrenk, Manfred; Andor Farkas; Geoffrey Brun (2010): Scientific Survey. ICT for sustainable development.

CATALOGUE SERVICES LITE - INSPIRE PROFILE

RUZICKA Jan

Institute of geoinformatics, VSB-TU of Ostrava,
17. listopadu 15, 708 33, Ostrava – Poruba, Czech Republic
jan.ruzicka@vsb.cz

Abstract

A very important part of the architecture for GeoWeb services orchestration is a catalogue. It does not matter what kind of a catalogue is used and what type of technology is used for metadata storage. The most important part of the catalogue are two items. The first is a used standard for the description of GeoWeb services and the second one is a standard used for building a catalogue's interface. Interface CSW (Catalogue Services of Web), has shown itself as too complicated for implementation. We have decided to use CSW as a base for building a less-complicated standard for the catalogue used in the architecture for orchestration. In the last year we have published CSW Lite standard. CSW Lite is easy to implement and have all the necessary parts for the architecture of orchestration. CSW Lite is compatible with complete CSW specification. CSW Lite is based on Dublin Core standard for metadata. This seems to be not applicable for several implementations mainly based on INSPIRE directive. We have prepared profile of CSW Lite, that is based on INSPIRE metadata profile. The paper should describe this standard in a brief, but complex way.

Keywords: catalogue, CSW Lite, CSW-L, GeoWeb, INSPIRE, metadata, monitoring

INTRODUCTION

The company that would like to have a CSW compatible catalogue has three possible ways of how to do this. In the commercial sphere, there are several systems that implement CSW specification. Most of them are part of general software solutions that are very expensive. There are only two known system in the area of open source software (GeoNetwork Open Source and Deegree). The third way is based on one's own CSW implementation. All of the options bring challenges. The reason why there are not enough implementations in this area (or they are costly) and why the last way is very difficult for a typical organization is the complexity of the CSW specification. CSW Lite (CSW-L) is a reaction to a quite unnoticed situation in the area of catalogue services for geodata and geoweb services. CSW-L should be a simple specification that could be implemented by a single programmer with basic knowledge of the standards and technologies. CSW-L is compatible with the full CSW 2.0.2

specification and it uses only a minimal set of capabilities of CSW 2.0.2. This simplification should make the CSW more understandable to a general developer. CSW-L is available at (OGCLite, 2010). What is missing in the CSW-L specification is a possibility to encode metadata according to INSPIRE metadata implementation rules. That's why I have created CSW-L INSPIRE Profile implementation specification. The specification is not fully available in this paper, but referenced to external documents at the web (OGCLite, 2010).

DESCRIPTION OF GENERAL CSW-L INSPIRE PROFILE CAPABILITIES

Metadata records are only based on ISO 19115 and ISO 19119 standards.

Communication is based only on HTTP protocol. To make this specification simple enough, other protocols are not supported.

Supported operations are basic methods for catalogue discovery (GetCapabilities, GetRecords, DescribeRecord and GetRecordById). A distributed search is not supported.

GETCAPABILITIES OPERATION

The GetCapabilities operation (OGC 2009) is used as the initial handshake between a client and a service. The service responds with a document that contains a description of the service capabilities (supported operations, formats, etc.).

Request

The GetCapabilities operation is requested via the HTTP GET method with three encoded parameters using KVP (Key-Value Pairs). Values of the parameters are fixed as is shown in the following example.

http://gis.vsb.cz/catalogue/cswl?**REQUEST**=GetCapabilites&**SERVICE**=CSW&**VERSION**=2.0.2

Response

The response is an XML formatted document as is described in the following example. Values marked by –– should be modified, the others should stay untouched. This document specifies which part of the CSW capabilities must be implemented.

<?xml version="1.0" encoding="UTF-8"?>

<csw:Capabilities version="2.0.2" …

Because of space limitations for a paper. The normative example is available at http://www.ogclite.org/cswlite/inspire/capabilities.xml

```
</csw:Capabilities>
```

DESCRIBERECORD OPERATION

The DescribeRecord operation (OGC, 2009) returns the description of a metadata record returned in a response to GetRecords or GetRecordById operations.

Request

The request is XML encoded and transferred via the HTTP POST method. The request is encoded as is described in the following example.

```
<?xml version="1.0" encoding="UTF-8"?>
<DescribeRecord service="CSW"  version="2.0.2" outputFormat="application/xml"
  schemaLanguage="http://www.w3.org/2001/XMLSchema"
  xmlns="http://www.opengis.net/cat/csw/2.0.2">
  <TypeName>gmd:MD_Metadata</TypeName>
</DescribeRecord>
```

Response

The response for this operation is an XML schema that describes (specifies) the structure of the metadata record. The CSW-L compatible service must return document in the following structure.

```
<?xml version="1.0" encoding="UTF-8"?>
<DescribeRecordResponse
  xmlns="http://www.opengis.net/cat/csw/2.0.2">
 <SchemaComponent>content of http://www.isotc211.org/2005/gmd/identification.xsd
file</SchemaComponent>
 <SchemaComponent>content of
http://schemas.opengis.net/iso/19139/20060504/srv/serviceMetadata.xsd
file</SchemaComponent>
</DescribeRecordResponse>
```

There are two elements SchemaComponent, that must contatin content of files specified in the example.

GETRECORDS OPERATION

The GetRecords operation (OGC, 2009) returns metadata records according to specified conditions in a request.

Request

The request is XML encoded and delivered via the HTTP POST method. The request consists of four parts:

- the GetRecords element
- the Query element
- the ElementSetName element
- the Constraint element

The structure of a request is described in the following example.

```
<?xml version="1.0" encoding="UTF-8"?>
<GetRecords
  service="CSW"
  version="2.0.2"
  maxRecords="5"
  startPosition="1"
  resultType="results"
  xmlns="http://www.opengis.net/cat/csw/2.0.2"
  xmlns:csw="http://www.opengis.net/cat/csw/2.0.2"
  xmlns:ogc="http://www.opengis.net/ogc"
  xmlns:gml="http://www.opengis.net/gml">
  <Query typeNames="gmd:MD_Metadata">
    <ElementSetName typeNames="gmd:MD_Metadata">full</ElementSetName>
    <Constraint version="1.1.0">
      <ogc:Filter>
        <ogc:And>
          <ogc:PropertyIsLike escapeChar="\" singleChar="?" wildCard="*">
```

```
<ogc:PropertyName>gmd:identificationInfo/gmd:MD_DataIdentification/gmd:citation/g
md:CI_Citation/gmd:title/gco:CharacterString</ogc:PropertyName>
            <ogc:Literal>*Elevation*</ogc:Literal>
          </ogc:PropertyIsLike>
          <ogc:PropertyIsEqualTo>
 <ogc:PropertyName>gmd:hierarchyLevel/gmd:MD_ScopeCode</ogc:PropertyName>
            <ogc:Literal>service</ogc:Literal>
          </ogc:PropertyIsEqualTo>
          <ogc:PropertyIsGreaterThanOrEqualTo>
<ogc:PropertyName>gmd:identificationInfo/gmd:MD_DataIdentification/gmd:citation/g
md:CI_Citation/gmd:date/gmd:CI_Date/gmd:date/gco:Date[../../gmd:dateType/gmd:CI
_DateTypeCode = 'publication']</ogc:PropertyName>
            <ogc:Literal>2004-03-15</ogc:Literal>
          </ogc:PropertyIsGreaterThanOrEqualTo>
          <ogc:BBOX>
<ogc:PropertyName>gmd:identificationInfo/gmd:MD_DataIdentification/gmd:extent/gm
d:EX_Extent/gmd:geographicElement/gmd:EX_GeographicBoundingBox</ogc:Propert
yName>
            <gml:Envelope>
              <gml:lowerCorner>14.05 46.46</gml:lowerCorner>
              <gml:upperCorner>17.24 48.42</gml:upperCorner>
            </gml:Envelope>
          </ogc:BBOX>
        </ogc:And>
      </ogc:Filter>
    </Constraint>
  </Query>
</GetRecords>
```

The GetRecords Element

The CSW-L compatible service must implement five attributes that are described in the following table.

Table 1. Attributes for the GetRecords element

Attribute	Description
service	Fixed value “CSW”
version	Fixed value “2.0.2”
maxRecords	Maximal count of returned records. Default is 10. 0 means resultType = hits.
startPosition	Index of the first returned record. Starts at 1.
resultType	Hits or results. Option hits must return an empty result set with an identified number of records.

The Query Element

The Query element is fixed as is shown in the previous example.

The ElementSetName Element

The element ElementSetName contains the fixed attribute typeNames as is shown in the previous example. There are three options of the possible value; they are described in the following table.

Table 2. Values for the ElementSetName element

Value	Description
full	Returns a full set of elements for each record in the response.
summary	Returns a selected set of elements described in the Response subchapter for each record in the response.
brief	Returns a selected set of elements described in the Response subchapter for each record in the response.

The Constraint Element

The Constraint element is based on the OGC Filter Implementation Specification (OGC, 2009). It has one fixed attribute and one fixed element ogc:Filter. Specified conditions for searching in a catalogue are found inside ogc:Filter. The structure is described in the previous example. The CSW-L compatible service must support operators described in the following table.

Table 3. Mandatory constraint operators

	Description
And	Conditions can be in a logical And relationship.
Or	Conditions can be in a logical Or relationship.
Not	Conditions can be negated.
PropertyIsEqualTo	Simple equal (==) comparison.
PropertyIsNotEqualTo	Simple not-equal (!=) comparison.
PropertyIsLessThan	Simple lest than (<) comparison.
PropertyIsGreaterThan	Simple greater than (>) comparison.
PropertyIsLessThanOrEqualTo	Simple less than or equal to (<=) comparison.
PropertyIsGreaterThanOrEqualTo	Simple greater than or equal to (>=) comparison.
PropertyIsLike	Like operator including information for: 7. escaping special characters such as quotes (attribute `escapeChar`), 8. wild-card for one letter (attribute `singleChar`), 9. wild-card for more than one letter (attribute `wildCard`).
BBOX	Spatial operator that selects all overlapping envelopes.

Properties can be specified from all metadata elements listed in the Response subchapter.

Response

The response structure (OGC, 2009) depends on two parameters in the request resultType and ElementSetName. When the requested resultType is hit, only then a count of records is returned. When the requested resultType is results, then metadata records are returned.

Structure of each record depends on the ElementSetName parameter. The richest record is returned when the value is full.

Response on hits

Response on resultType=hits returns basic information about the search result, but without any records included. The structure of the response is described in the following example.

<?xml version="1.0" encoding="UTF-8"?>

```
<csw:GetRecordsResponse xmlns="http://www.opengis.net/cat/csw/2.0.2"
  xmlns:csw="http://www.opengis.net/cat/csw/2.0.2">
  <csw:SearchStatus timestamp="2009-10-04T09:05:25"/>
  <csw:SearchResults
      nextRecord="0"
      numberOfRecordsMatched="5"
      numberOfRecordsReturned="5"
  />
</csw:GetRecordsResponse>
```

All elements and attributes included in the example are mandatory. The following table describes attributes.

Table 4. Attributes for response on hits

Value	Description
timestamp	Date and time when the response was created.
nextRecord	Index of the first record from the search result that was not included in the response because of some limits (data size) of the communication. Zero means that all records have been returned in the response.
numberOfRecordsMatched	Number of records that have been matched by specified search criteria.
numberOfRecordsReturned	Number of records that have been returned in the response.

Response on full

Response on resultType=results and ElementSetName=full is the same as response on resultType=hits described above, but it includes records (elements Record) in the SearchResults element. The structure of the Record element is described in the following example. All elements are mandatory. If the information for the element is not available, it must be filled with NULL.

```
<gmd:MD_Metadata ... >
```

Because of space limitations for a paper. The normative example is available at http://www.ogclite.org/cswlite/inspire/dataset.xml

```
</gmd:MD_Metadata>
```

Response on summary

Response on resultType=results and ElementSetName=summary is the same as response on ElementSetName=full described above, but the record element is named SummaryRecord and it includes only selected metadata items (gmd:fileIdentifier, gmd:language, gmd:title, gmd:abstract, gmd:spatialResolution, gmd:distributionInfo and gmd:EX_GeographicBoundingBox).

Response on brief

Response on resultType=results and ElementSetName=brief is the same as response on ElementSetName=full described above, but the record element is named BriefRecord and it includes only selected metadata items (gmd:fileIdentifier, gmd:title and gmd:EX_GeographicBoundingBox).

GETRECORDBYID OPERATION

The GetRecordById operation (OGC, 2009) is KVP encoded and requested via HTTP GET method. It returns a record (records) according to specified id (ids). The same possibility exists to request a full, summary, or brief record from the catalogue.

Request

http://gis.vsb.cz/catalogue/cswl?**REQUEST**=GetRecordById&**SERVICE**=CSW&**VERSION**=2.0.2&**ElementSetName**=full&**id**=
http://gis.vsb.cz/datasets/0015600,http://gis.vsb.cz/datasets/0115600

Parameters REQUEST, SERVICE, and VERSION are mandatory and fixed. The parameter ElementSetName is optional (default is summary). Parameter Id can contain a comma to separate ids and is mandatory.

Response

The response is the same as in the GetRecords operation.

DESCRIPTION OF SERVICES

The CSW-L specification comes from the GeoWeb services orchestration project (GA 205/07/0797) (Růžička, 2009). To make CSW-L specification more clear in a context of GeoWeb services orchestration, it should include information on how to describe specific information about services using ISO 19119/19139.

Service type

One of the most important issues that is connected with service description is an identification of the service type. When searching in the catalogue, a user (client) must have the possibility to find similar services based not only on service interface (WMS), but on data used as well.

For purposes of an orchestration, it is necessary to be able find similar services. This can be managed through several ways. Some of them are described in [Růžička 2008]. The most suitable seems to be the concept based on ontology, where similar services are described as related terms in one branch of the ontology. The service type consists of interface definition, used data, and used algorithms.

The service type is defined by the identifier in the thesaurus. The identifier is constructed from parts of the service description to make the id more human readable. Example of identifier follows.

ogc:WMS:1.1.1/datasets:ZABAGED,DMÚ200/algorithms:simplify

gis.vsb.cz:erosion:0.0.1/datasets:FreeGEOCZ/algorithms:RUSLE

This type identifier is encoded in the serviceTypeVersion element (see 7.3.), because serviceType according to INSPIRE element can contain only selected values: discovery, view, download, transformation, invoke or other.

```
<srv:serviceType>
  <gco:LocalName>view</gco:LocalName>
</srv:serviceType>
<srv:serviceTypeVersion>
<gco:CharacterString>Service/gis.vsb.cz:erosion:0.0.1/datasets:FreeGEOCZ/algorithms:RUSLE</gco:CharacterString>
</srv:serviceTypeVersion>
```

What is still not defined is the dependency of the similarity on a context of a provided process (running orchestra). This should be defined later and included in the CSW-L specification and CSW-L INSPIRE Profile.

Monitoring

For purposes of an orchestration, there are very important measures in service monitoring (Kaszper, 2008). This information can be directly written into the *gmd:MD_Metadata*, but it could make *gmd:MD_Metadata* too complex and it will not be compatible with CSW-L. That is why this kind of information is only referenced via the gmd:onLine element. One of the *gmd:onLine* elements in *gmd:MD_Metadata/gmd:distributionInfo* should (necessary for dynamic orchestration) include a reference to an XML document (static or dynamic). The reference must be done as at the following example where the mandatory and fixed is the name of the onLine resource.

```
<gmd:onLine>
  <gmd:CI_OnlineResource>
    <gmd:linkage>
      <gmd:URL>http://gis.vsb.cz/catalogue/monitor?id=0015647</gmd:URL>
    </gmd:linkage>
    <gmd:protocol>
      <gco:CharacterString>HTTP</gco:CharacterString>
    </gmd:protocol>
    <gmd:name>
      <gco:CharacterString>monitoring</gco:CharacterString>
    </gmd:name>
  </gmd:CI_OnlineResource>
</gmd:onLine>
```

The monitoring document should contain results from monitoring. We have specified three monitoring parameters that should be included, but others can be added to the results. An example of the XML file that describes results from monitoring follows.

```
<?xml version="1.0" encoding="UTF-8"?>
<Service xmlns="http://gis.vsb.cz/monitoring/0.0.1" id="http://gis.vsb.cz/services/0015647">
  <stability>0.95</stability>
  <lastState>ssOK</lastState>
  <speed>1000</speed>
</Service>
```

The stability element contains a float value that describes the long time stability of the service measured in percentage of valid responses according to all valid requests.

The lastState element describes the state of the service from the last monitoring. The possible values are: ssOK, ssWarning, ssCritical, and ssUnknown.

The speed element contains the average time spent on one request-response operation. It is measured in milliseconds.

Full example

The following example describes how a service description should look using ISO 19119/19139.

<gmd:MD_Metadata ... >

Because of space limitations for a paper. The normative example is available at http://www.ogclite.org/cswlite/inspire/service.xml

</gmd:MD_Metadata>

CONCLUSION

The prepared CSW-L INSPIRE Profile specification should be simple enough to be easily implemented by any developer. There are still some open problems with the specification, but not significant. If the specification is not used, it, at least, can help with understanding how to use CSW for INSPIRE.

REFERENCES

GeoNode (2010). CSW_GetRecordById. http://projects.opengeo.org/CAPRA/wiki/CSW_GetRecordById

ISO (2005). ISO 19139. http://www.isotc211.org/2005/

Drafting Team Metadata and European Commission Joint Research Centre (2010) *INSPIRE Metadata Implementing Rules: Technical Guidelines based on EN ISO 19115 and EN ISO 19119*. European Commission Joint Research Centre. Available at: http://inspire.jrc.ec.europa.eu/documents/Metadata/INSPIRE_MD_IR_and_ISO_v1_2_20100616.pdf

Kaszper, R. (2008) *Sledování stavu služeb pro GeoWeb*. Diploma thesis. VŠB-TUO, Ostrava. 2008.

OGC (2009a). http://portal.opengeospatial.org/files/?artifact_id=20555, CSW 2.0.2.

OGC (2009b). http://schemas.opengis.net/csw/2.0.2/.

OGC (2007). http://schemas.opengis.net/iso/19139/20060504/srv/.

OGCLite (2010). http://www.ogclite.org/.

Růžička, J. (2008) ISO 19115 for GeoWeb services orchestration*. P*roceedings from Geoinformatics on CTU 2008. CTU, Prague. Available at: http://geoinformatics.fsv.cvut.cz/wiki/index.php/ISO_19115_for_GeoWeb_services_orchestration

Růžička, J., Šeliga, M. (2010) Catalogue Services Lite. Proceedings from GIS Ostrava 2010. VSB-TUO. Ostrava. Available at: http://gis.vsb.cz/GIS_Ostrava/GIS_Ova_2010/sbornik/Lists/Papers/EN_1_11.pdf

Růžička et al. (2009) Geoweb services orchestration. http://kokos.vsb.cz/wiki/.

PROJECT OPENSTREETMAP AS OPEN AND FREE SOURCE OF GEODATA AND MAPS

BARTA Daniel

DHV CR, spol. s r.o., Černopolní 39, 618 00 Brno, Czech Republic
daniel.barta@dhv.com

Abstract

The article characterizes the fundamentals of the project OpenStreetMap (OSM), which is an original source of open and free geodata. It describes the current state of the project, its usability for geoinformatics technology (GIT) and anticipates its near future. It is compared to similar free and open source projects. As an example, there is given a focus on the representation of the Czech Republic and the local OSM community.

In the first part, there is a description of the project core and associated external community web services. Very interesting is its starting point, the users' motivation and their mapping capabilities like quality, quantity and actuality. OSM is using a specific XML data format and an easy 2D model of geodata. The data are published under a free license. Only a few rules for editing are required, but many recommendations are given. Specific renderers are used for generating thematic maps.

Geodata and maps are importable to traditional GIT and a extension for editing the specific OSM format is developed.

The next part is focused on the Czech Republic. There is a list of externally imported data, basic data sources and completeness layers. Demos of several thematic maps like highway/street map, cycle map, public transport map and other are shown.

It discusses problems concerning the geometric part of geodata - its topology, descriptive part of geodata and semantics. Further are discussed categorizing objects, area completeness and thematic catch of mapping.

The last part is about the project's future. The near future of the project consists in changing the license. The long-term future will be based more on users' than developers' ideas.

Keywords: OpenStreetMap, geodata, crowdsourcing, open and free geodata

INTRODUCITON AND CONTEXT

OpenStreetMap (OSM) is the name of a community project, which's goal is creating and cumulating free and open source geodata. At a glance, it is possible to use this easy analogy:

- public editing + encyclopedia + free = Wikipedia
- public editing + map + free = OpenStreetMap

From the Table 1, which shows founding years of free and open source projects (FOSS) in the field of GIT/IT, it is possible to see, that firstly the idea of FOSS and an appropriate license was formulated. Afterwards, the development of traditional specific software, focused on a small group of specialists, starts. Next comes the development of applications for home and office usage and subsequently it aggregates the creative potential of its consumers (i.e. SETI@home, Wikipedia, OSM).

This evolution comes as an effect of progress in technologies, as military and space survey high technologies (i.e. computer, GPS, internet), which became a part of the daily life of people during the past decades. At the end of this evolution, after 2004, comes a specific phenomenon of the Web 2.0 with the involvement of its users in the process of creation of the project. One of its characteristic features is crowdsourcing, which means in the newspeak, the redistribution of a share of the work to the community.

Presumptions for the functionality of OSM, respectively collaborative mapping, are:

- Absence of user-friendly maps (price, license or technology)
- Low cost and accessible hardware (i.e. PC, GPS receiver), software and services (Internet, GPS)
- Human needs of creativity and its sharing on the free principle (do it yourself)
- Well fulfilled human rights, freedom and free time

Traditionally, mapping is the most costly part of GIT. The rise of OSM is a reaction to the state, that many base maps all over the world are unavailable for ordinary people due to licenses or financial reasons, although many maps are created from public finances. In the Czech Republic, there is an additional problem: many datasets are available for free access or downloading, but they lack appropriate licenses, which would explicitly define the level of freedom for the usage (i.e. at the the organizations ČUZK, ČSÚ, CENIA). The situation in Slovakia is similar.

Positive examples are maps and data created for the government of USA, licensed exclusively under Public domain (i.e. NASA, US Geological Survey, US Census Bureau).

Following users' motivations are technological limitations of actual maps (i.e. paper map, e-paper map, area limited, actuality, accuracy) or the absence of public maps or geodata.

Table 1. Selected free and opensource IT, GIT and community projects.

Starting year[6]	Project	Focused users	Community goal	Note
1983	GNU Project	public	no	long way to end users
1989	GNU/GPL (General Public License), MIT licence, BSD license	IT developers	no	
1990*	GIS Grass	skilled GIT users	no	
1991	GNU Linux	public	no	long way to end users
1995*	PostgreSQL	IT users	no	
1996*	GIMP	public	no	
1999*	Inkscape (first Sodipodi)	public	no	
1998*	Mozilla (later Firefox)	public	no	
1999	SETI@home	public	crowdsourcing	no creativity
2000*	OpenOffice.Org (first StarOffice)	public	no	
2001	Postgis	GIT users	no	
2001	Wikipedia	public	collaboration	limited to articles
2002	Quantum GIS, JUMP GIS	beginner GIT users	no	
2004	OpenStreetMap	public	collaboration	
2009	ODC/ODbL (Open Data Commons/Open Database License)	public	no	

* project is a fork of FOSS

GEOINFORMATICS REFERENCE AND CORE OF PROJECT

OSM uses only a 2-dimensional geographic frame reference WGS84 (EPSG:4326). In its vector model space it is possible to use the following role and elements:

- Node – point (or vertex) with spatial coordinates
- Way – referenced on the nodes
- Area – a way with a specific attribute (at least one from many designated for the area)
- Relation – aggregates elements and describes the relations of one to another

All OSM data, including the history of editing, are saved in PostgreSQL database (db size 1,4 TB) and exchanged and exported in a self-made geodata format *OSM XML format*. The actual version of the last state of the database without history (product named planet) is every week exported into OSM XML format and compressed by bzip2. Its size is 12 GB, every-day changes in OSM XML are compressed by gzip and have cca 50 MB XML. Aside of the model space are appended users' GPS tracklogs in format GPX.

Fig. 1. Czech Republic on the webmap (Mapnik renderer)

The project uses the license *Creative Commons Attribution-ShareAlike 2.0* (CC-BY-SA), but now, it is in migration to a new license *Open Database License* (ODbL). The old license was targeted for multimedia arts; the new license will assure more openness (i.e. creating map compositions from free and license-limited data) with better legal safety of geodatabase. For service software the community it uses mostly the license GNU/GPL.

OpenStreetMap Foundation (OSMF) was founded in 2009 in order to support the project. Money will be used for financing core hardware and promotion. OSMF will support also the OSM meeting *State of the map*, which happens every year since 2007.

The think-tank of project resides in the UK, where OSM was founded in 2004 by Steve Coast, and in Germany, where it became popular in a short time. In both countries reside corporations, which use OSM as a platform for offering commercial services and products: Cloudmade, ITO World, Geofabrik GmbH.

MOTIVATION AND USERS

Users are the engine and the consumer of project, often at the same time. Specifics of the collaborative mapping are:

- Local knowledge (actual and verifiable – see Fig 6.)
- Number of users (theorem: what 1 man does in 100 days, 100 men do in 1 day)
- Liberty in the theme of mapping (minimal rules, often only recommendations)

For community users is typical a low level of organization and uniformity, but a high spontaneity, euphoria and WOW effect. Users have different visions, goals of mapping and methodology. This attitude causes many misunderstandings, mistakes and imperfection. In this collaborative creating, there is expected a positive motivation for any editing and motivation for fixing obtrusive errors.

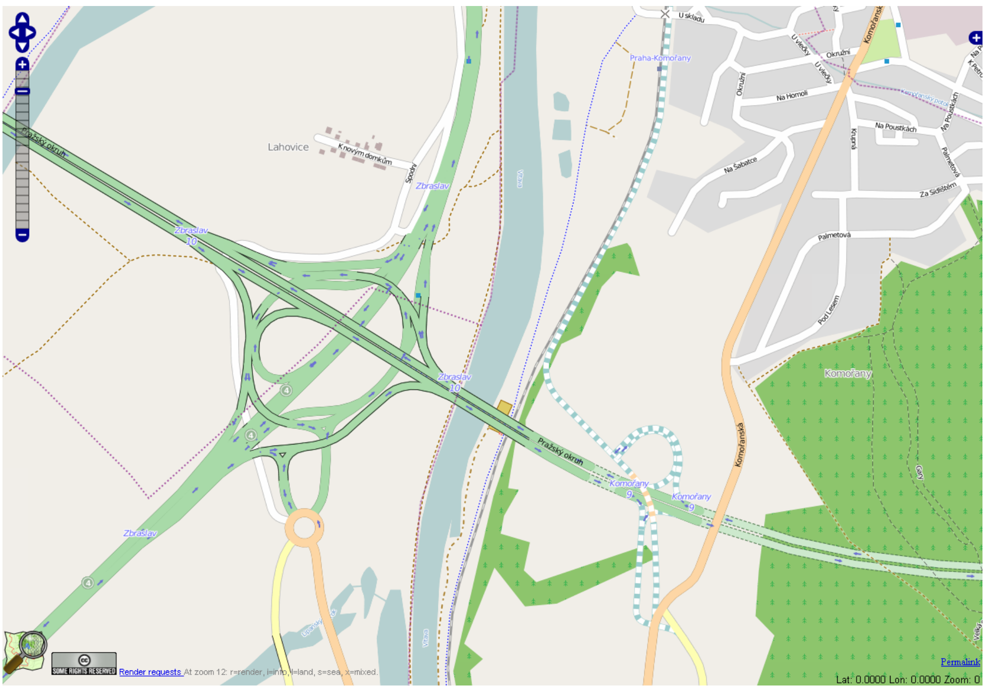

Fig. 6. Flyover junction near Zbraslav and a proposed link to Lahovice on the newly constructed expressway R1, the Prague by-pass. The Prague by-pass has been a part of OSM since 2009. Just on the official opening day, 20. September 2010, its tag has changed from „highway in construction" to „routable way". (Mapnik renderer)

Problematic is to estimate the quality assurance, like spatial and attribute completeness, accuracy, depth of detail and the mapping scale. Spatial completeness in OSM mapping is characterized by the density of inhabitants, which means that the best mapped are urban centers and estates.

In a quantitative evaluation of users we have 300.000 registered from the whole world. Only 5 % were active in the editing of the map in last month. Only 5 % are authors of more than 10 000 nodes (See Table 2).

From the user inquiry it went out that almost all users are men, irrespectively of age groups. 3/4 of users have a university degree and 3/4 of users are working. From the employed almost 3/4 work in commercial sphere. Almost all do the OSM mapping at home, 1/4 of users do it at work or from a mobile device.

Main motivations for users are the *project goal*, *altruism* and *activities in local neighborhood*. About 1/4 of users have experience with GIS, but a majority of them is in the low-activity group.

Table 2. Statistics of OSM users and data.

Criterion	World	Czech Republic	Great Britain	Germany
Number of nodes	810 million	17 million	19 million	49 million
Number of authors of nodes in the actual version	105 068	2 128	9 482	33 767
Number of registered users	310 000	2 930	-	-
Number of authors of more than 10 000 nods	5%	3%	-	-
Number of authors of more than 100 000 nods	0,6%	0,7%	-	-
Number of active users in Sept. 2010:	5%	-	-	-

DATA AND MAPS USEFUL FOR GIS

The internal data type *XML OSM format* of the project is unique and unknown for traditional GIS software. The OSM geodata model includes these primitives: a point and a polyline. A polyline may become a polygon by adding an attribute to it. Since 2007 API version 0.5 was released, extended by a new primitive: *relation*.

Simplified XML file of OSM data with all three primitives:

```
<?xml?>
<osm version="0.6">
  <node id="" lat="" lon="">
    <tag k="" v="" />
  </node>
  <way id="">
    <nd ref="" />
    <tag k="" v="" />
  </way>
```

```
  <relation id="">
    <member type="" ref="" role="" />
    <tag k="" v=""/>
  </relation>
</osm>
```

Table 3. A comparison of the OSM model and a traditional model

Geodata model	Geometry and topology	Geometry validity	Layers	Attribute fixing
Traditional GIS (i.e. ESRI Shapefile)	point polyline polygon	required	by theme and by geometry	by layer
XML OSM	point polyline relation (a group of primitives with roles)	low-level	all in one	no

The export to other formats is nontrivial and ambiguous (See Table 3). In geometry and topology, typical problems occur, which concern multipolygons, roles of elements, aggregations, routing restrictions and routes. A chronic complication is the flow design of attributes, their immediate in ad-hoc changes by users. The improvement of present data exchange between OSM and GIS software depends perhaps on the GIS developers, because big GIS stations are not typical tools in the community.

Real usage in GIS:

- Raster map over slippy maps (i.e. Quantum GIS with plugin, ArcGIS 10 default)
- Raster map via WMS [@1]
- ESRI Shapefiles ready to download [@2,@3] (i.e. layer of road, railway, waterway, buildings, natural and POI, without the information in *relations*)
- PostgreSQL/Postgis (conversion by script Osm2pgsql)

Actually on-line accessible OSM exports to ESRI Shapefiles suffer from these losses:

- big polygons aggregated from multiple parts in relation
- rings composed of polygons
- routes, i.e. cycle, hiking, public transport
- parts of attributes
- many themes, i.e. landuse, traffic accessories, routings data

- many features stored in atypical objects (i.e. a POI saved in a polygon of building, instead of a point)
- areas of administrative terrirorial units are exported only as polylines of borders

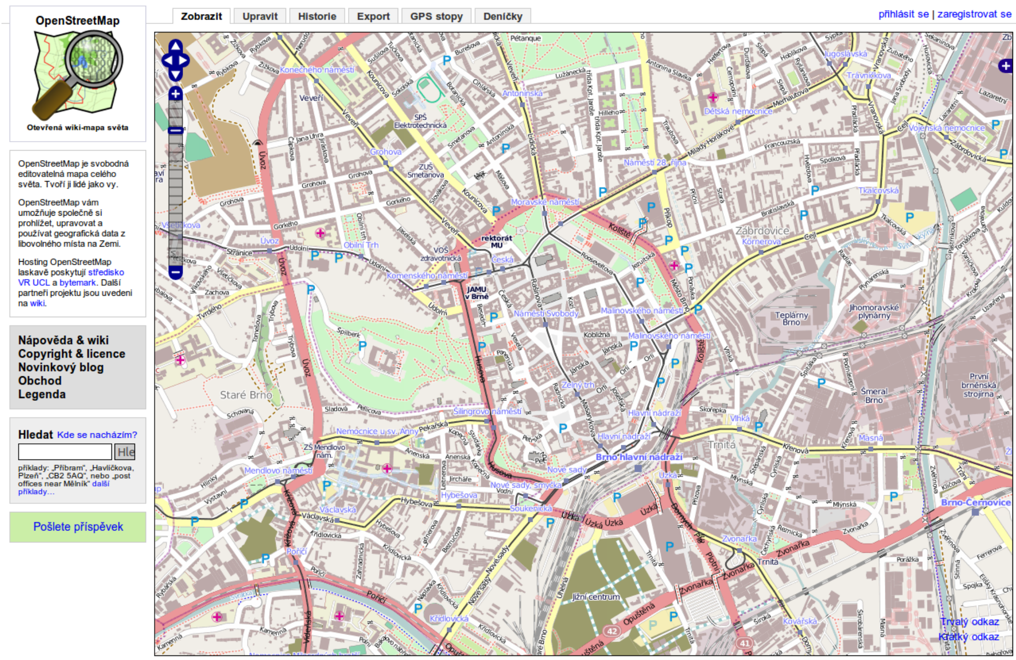

Fig. 2. Detail of the centre of Brno (Mapnik renderer)

For Quantum and ArcGIS, there exist trial plugins for direct editing of OSM data, but their installation and operation is not trivial and have low support in the community.

For the web, for print (PNG, SVG) and mobile devices (typically cell phone or GPS navigation) exist special conversional software or online pre-prepared data.

For the import of free data into OSM there are many special scripts and methodology. A good example is a versatile import utility ogr2osm written in Python, which uses the potential of formats that can be read by the linked library GDAL/OGR. However, reading the OSM format and exporting via GDAL/OGR to other geodata formats is not supported.

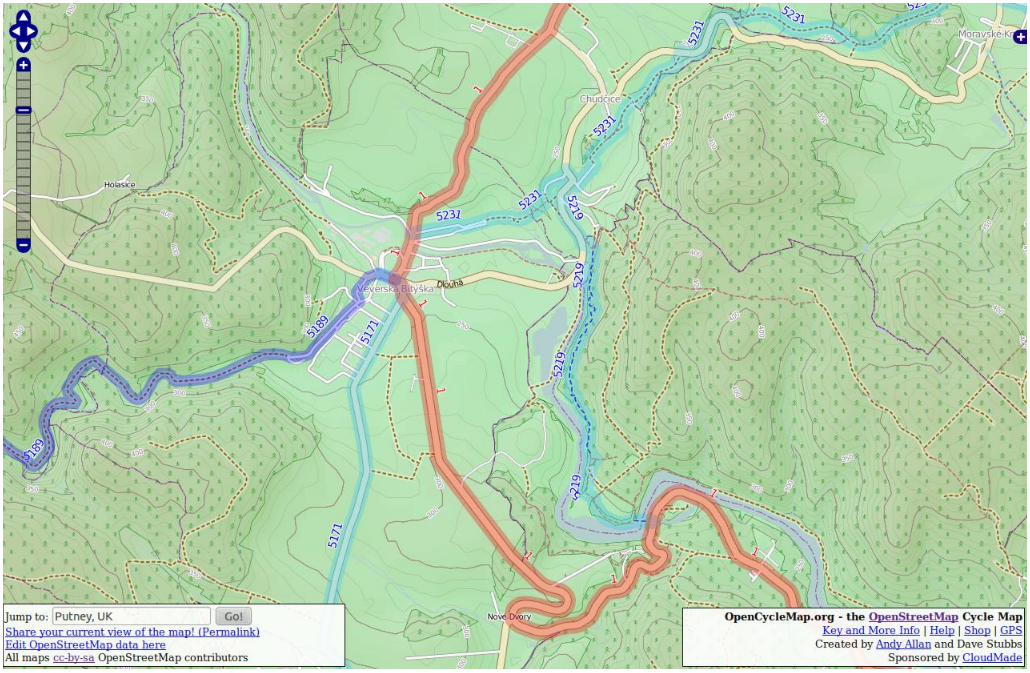

Fig. 3. Detail of cycle route near Brno reservoir (OpenCycleMap renderer)

MAPPING STATE IN THE CZECH REPUBLIC

In every country the state of the map is different, mostly affected by available free datasets for import or creating geodata.

Top data themes

- *Complete* country and regional highways – motorways, expressways and the 1., 2., 3. classes of roads (all in the real course of way). The second class of highways was partially imported from corporation HS-RS. *In progress* - forest tracks and field tracks, village and town residential ways, accessories, options...
- *Complete* railway - main and regional railway with stations. *In progress* - spur, yard, siding track, attributes (electrified, voltage system)
- *Complete* administrative system borders – derived from cadastral territories (CUZK KM), from villages to regions, consecutively the whole republic according to NUTS and LAU standards. *In progress* – fixing the hierarchy.
- *Complete* waterway - imported datasets DIBAVOD (streams, rivers, lakes, basins, marsh). *In progress* – checking and fixing duplicates between old data and import

- *Complete* forest – imported from UHUL layer of forests derived from PUPFL (cadastral parcels primary designated for forest). *In progress* – some fixing of true sizes of forest
- Cca 10% of house addresses – the free part of addresses from UIR-ADR (old version from the ministry MPSV, only former district towns). *In progress* - next 80 % will be imported semi-automatically

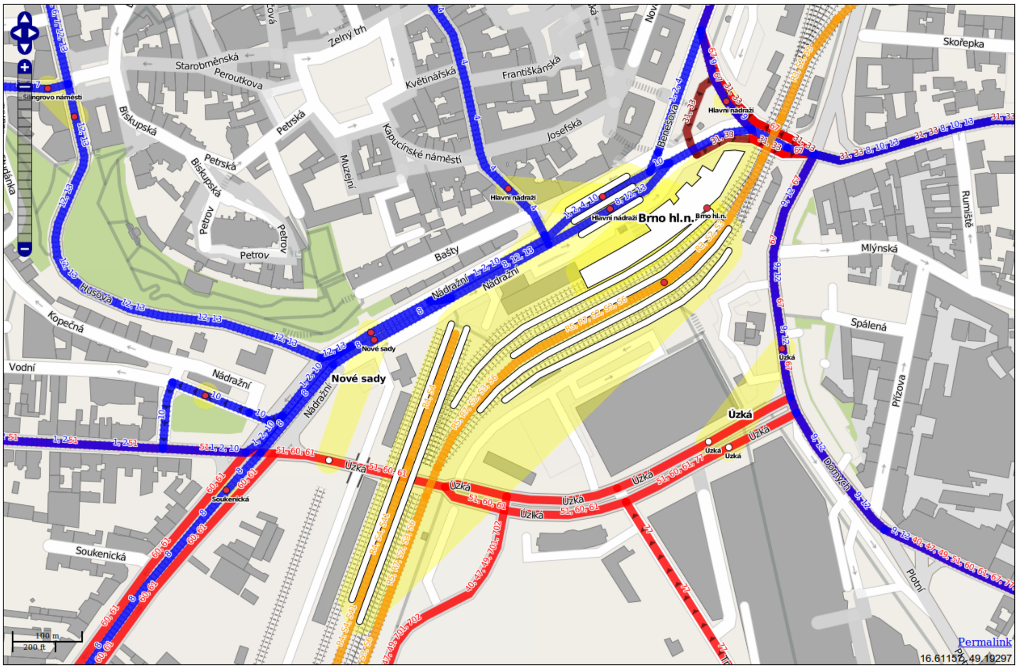

Fig. 4. Detail of public transport map for Brno main station (Öpnvkarte renderer)

Other theme in progress

- Buildings (semi-automatic)
- Hiking, cycle, mountain bike and ski ways
- Public traffic services
- Routing limits
- Landuse/landcover
- High voltage power infrastructure
- Points of interests

Data sources for visual interpretation

- Cadastral map – WMS ČÚZK
- Aerial orthophoto map – WMS UHUL (captured before 2000), spatial resolution 1 meter
- GPS tracks – users’ self-made
- Series of street photo – NORC (only Prague, Brno, Ostrava, Pilsen, Olomouc)
- Satellite orthophoto map – Microsoft Bing (only 16 % of the area of the Czech Republic – i.e. Prague, Brno and surroundings), spatial resolution cca 0,5-1 meter; map composed from satellite images from the company GeoEye, acquired mostly in 2003 or 2007.
- Satellite orthophoto map – Yahoo (only 3 % of the area of the Czech Republic - Prague and surroundings), spatial resolution cca 1 meter, images acquired from the satellite Ikonos in 2007

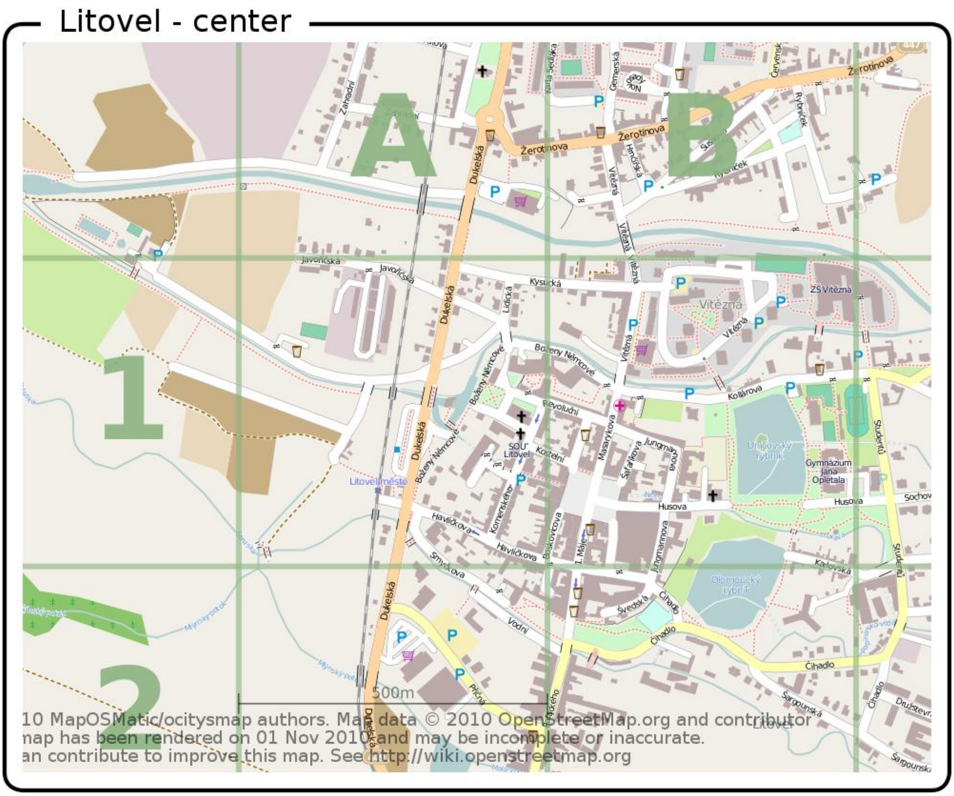

Fig. 5. Detail of the center of Litovel town prepared for print (MapOSMatic via Mapnik renderer)

THEMATIC MAP

For active users' motivation a visual demonstration of their work is very important, because it enables to see their own tile in the mosaics and it brings inspiration for the others. For the other consumers it demonstrates the summary of the database. A typical generalized way from geodata to a webmap comprises OSM XML format > database (PostreSQL) > renderer (Mapnik/Osmarender) > www server + Openlayers.

Lists of online map service, that affect the area of the Czech Republic (OpenStreetMap, 2010):

- Base, street, road map's (See Fig 1, 2 and 6) [@4-@7]:
- Foot, cycle (see Fig 3), hiking, mountain bike, orienteering and wheelchairs map's [@8-@14]
- Power line and grid map [@15]
- Public transport service map (see Fig 4) [@16]
- Road navigation [@17, @18]
- Map with ship navigation feature [@21]
- Isometric map [@19]
- Paper map (see Fig 5) [@20]
- Meta-information map service [@22, @23]
- Map compare [@24]
- Map overlay [@25]

CONCLUSION AND FUTURE

In the present and in the near future a great change of the license is going on. During the next year, secondary map services like routing should be improved. A great theme is now how to match a stabilized attribute system with quality standards and validation, but still open or under the control of the community.

In the present moment, geodata and maps from OSM - compared to other map sources on the Czech market – are interesting foremost by their price, accessibility and actuality. In many geographic themes, the area completeness in general is ready-to-wear in many places (i.e. towns). Nevertheless, a great part of he Czech Republic has a low level of mapping quality.

For a GIS user, OSM can be a valuable help, a secondary or other view of the same place, and may support or complete GIS analyses. For ordinary people OSM represents an effective tool to get and share geographic knowledge in a legal way.

NOTES

[@1] http://www.osm-wms.de/

[@2] http://download.geofabrik.de/osm/europe/

[@3] http://downloads.cloudmade.com/europe/czech_republic

[@4] http://www.openstreetmap.org/

[@5] http://www.openstreetbrowser.org/

[@6] http://www.mapsurfer.net/

[@7] http://open.mapquest.co.uk/

[@8] http://tchor.fi.muni.cz:8080/

[@9] http://hikebikemap.de/

[@10] http://openstreetmap.cz/

[@11] http://opentrackmap.no-ip.org/

[@12] http://gismaster.liberix.cz/osmoverlay.html

[@13] http://www.openpistemap.org

[@14] http://wheelmap.org/

[@15] http://energy.freelayer.net/

[@16] http://openbusmap.org/

[@17] http://www.openrouteservice.org

[@18] http://www.yournavigation.org/

[@19] http://osm.kyblsoft.cz/3dmapa/

[@20] http://maposmatic.org/

[@21] http://www.freietonne.de/seekarte/

[@22] http://www.qualitystreetmap.org/osmqa/

[@23] http://openstreetbugs.schokokeks.org/

[@24] http://tools.geofabrik.de/mc/index.html

[@25] http://sautter.com/map/

REFERENCES

Clinton, S. (2009) Crowdsourcing is radically changing the data landscape: Case study of OpenStreetMap, 24th International Cartographic Conference, 15-21th November 2009, online: http://icaci.org/documents/ICC_proceedings/ICC2009/html/nonref/22_6.pdf

Bárta, D. (2008) Projekt OpenStreetMap z pohledu geoinformatika, Geoinformatics FCE CTU 2008, 18.-19. September 2008, pp. 91-108, online: http://geoinformatics.fsv.cvut.cz/pdf/geoinformatics-fce-ctu-2008-03.pdf

Rapant, P.: Geoinformatika a geoinformační technologie. VŠB-TU Ostrava, 2006. 500 str. ISBN 80-248-1264-9, pp. 304. http://gis.vsb.cz/rapant/publikace/knihy/GI_GIT.pdf

OpenStreetMap, wiki pages, accessed 30. October 2010, http://wiki.openstreetmap.org/wiki/FAQ#Why_are_you_making_OpenStreetMap.3F

OpenStreetMap, wiki pages, accessed 5. December 2010, http://wiki.openstreetmap.org/wiki/WikiProject_Czech_Republic/freemap

Wikipedia, the free encyclopedia, GNU_General_Public_License, GRASS_GIS, Linux, PostgreSQL, Mozilla, SETI@home, OpenOffice.org, PostGIS, Wikipedia, Quantum_GIS, OpenStreetMap, accessed 30. October 2010, http://en.wikipedia.org/

OpenStreetMap, wiki pages, accessed 30. October 2010, http://wiki.openstreetmap.org/wiki/Beginners_Guide_1.3

OpenStreetMap, wiki pages, accessed 30. October 2010, http://wiki.openstreetmap.org/wiki/API_v0.6#Elements_2

OpenStreetMap, wiki pages, accessed 30. October 2010, http://planet.openstreetmap.org/

OpenStreetMap, stats pages, accessed 30. October 2010, http://wiki.openstreetmap.org/wiki/Planet.osm

OpenStreetMap, wiki pages, accessed 30. October 2010, http://munin.openstreetmap.org/openstreetmap/smaug.openstreetmap/postgres_size_openstreetmap.html

OpenStreetMap, wiki pages, accessed 30. October 2010, http://wiki.openstreetmap.org/wiki/OpenStreetMap_License

OpenStreetMap, wiki pages, accessed 30. October 2010, http://www.osmfoundation.org/wiki/Main_Page

OpenStreetMap, wiki pages, accessed 30. October 2010, http://wiki.openstreetmap.org/wiki/State_Of_The_Map

OpenStreetMap, talk-cz archive pages, accessed 30. October 2010, http://www.mail-archive.com/talk-cz@openstreetmap.org/msg05938.html

Gale, G (2010) What's Wrong With OpenStreetMap? Have Your Say, accessed 30. October 2010, http://www.vicchi.org/2010/07/07/whats-wrong-with-openstreetmap-have-your-say/

Chance, T (2010) Political philosophy in Open Street Map, accessed 30. October 2010, http://tom.acrewoods.net/2010/07/16/political-philosophy-in-openstreetmap/

Haklay, M (2010) The tyranny of place and OpenStreetMap, State Of The Map 2010, 9-11th July 2010, http://povesham.wordpress.com/2010/07/10/the-tyranny-of-place-and-openstreetmap/

OpenStreetMap, tool pages, accessed 30. October 2010, http://tagwatch.stoecker.eu/

OpenStreetMap, wiki pages, accessed 30. October 2010, http://wiki.openstreetmap.org/wiki/Stats

Janda, A.: Aktivita uživatelů OpenStreetMap v ČR, accessed 30. October 2010, http://osm.kyblsoft.cz/statistiky/aktivita-uzivatelu

Budhathoki, N.R., Haklay, M., Nedovic-Budic, Z. (2010) Who are the mappers and why do they map in OpenStreetMap? State Of The Map 2010, 9-11th July 2010, http://www.slideshare.net/nbudhat2/nama?from=ss_embed

OpenStreetMap, wiki pages, accessed 30. October 2010, http://wiki.openstreetmap.org/wiki/Osm2pgsql

OpenStreetMap, wiki pages, accessed 30. October 2010, http://wiki.openstreetmap.org/wiki/QGIS_OSM_Plugin

ESRI: ArcGIS Editor for OpenStreetMap, accessed 30. October 2010, http://esriosmeditor.codeplex.com/

OpenStreetMap, wiki pages, accessed 30. October 2010, http://wiki.openstreetmap.org/wiki/Converting_map_data_between_formats

OpenStreetMap, wiki pages, accessed 30. October 2010, http://wiki.openstreetmap.org/wiki/Ogr2osm

OpenStreetMap, wiki pages, accessed 30. October 2010, http://wiki.openstreetmap.org/wiki/Converting_GPS_track_data_between_formats

OpenStreetMap, wiki pages, accessed 30. October 2010, http://wiki.openstreetmap.org/wiki/Import_Adres_%C4%8CR

OpenStreetMap, wiki pages, accessed 30. October 2010, http://wiki.openstreetmap.org/wiki/State_Of_The_Map_2010

OpenStreetMap, map, accessed 30. October 2010, http://www.informationfreeway.org/?lat=49.7957&lon=15.4092&zoom=8&layers=0FB0F0

OpenStreetMap, map, accessed 30. October 2010, http://www.openstreetmap.org/?lat=49.19448&lon=16.6092&zoom=15&layers=M

Moos, M. (2010) Öpnvkarte, accessed 30. October 2010, http://openbusmap.org/?zoom=17&lat=49.19012&lon=16.61099&layers=BT

Allan, A. (2010) OpenCycleMap, accessed 30. October 2010, http://www.opencyclemap.org/?lat=49.2718&lon=16.4494&zoom=14

Petazzoni, T., Petazzoni, M. : MapOSMatic, accessed 30. October 2010, http://maposmatic.org/jobs/20197/IKAojBnIYIClSfsZ#submitmapform

Freemap SK, wiki pages, accessed 30. October 2010, http://wiki.freemap.sk/VojenskeMapyCSLA

OpenStreetMap, wiki pages, accessed 30. October 2010, http://wiki.openstreetmap.org/wiki/List_of_OSM_based_Services

OpenStreetMap, map, accessed 5. December 2010, http://www.informationfreeway.org/?lat=49.98521&lon=14.39959&zoom=16&layers=0FB0F0

OpenStreetMap, wiki pages, accessed 5. December 2010, http://wiki.openstreetmap.org/wiki/Map_Features

OpenStreetMap, wiki pages, accessed 5. December 2010, http://wiki.openstreetmap.org/wiki/Slippy_Map

OpenStreetMap, wiki pages, accessed 5. December 2010, http://wiki.openstreetmap.org/wiki/Mapnik

WORKFLOW FOR CHLOROPHYLL CONCENTRATION MODELING USING MULTISPECTRAL SATELLITE DATA

BRUNCLIK Tomas

Institute of Environmental and Chemical Engineering, Faculty of Chemical Technology,
University of Pardubice, Studentská 573, 53210, Pardubice, Czech Republic
Tomas.Brunclik@upce.cz

Abstract

This paper deals with work in progress to create usable workflow to assess chlorophyll-a concentration from remote sensing data to be used in lake and reservoir water quality monitoring to extend existing monitoring results. The workflow should be practicable with different software tools, and with various multispectral satellite data of suitable spatial resolution. The work is carried on with Landsat data, water quality data from reservoirs by Povodí Labe, a.s. and using Quantum GIS and GRASS GIS open source software. The workflow should use only the satellite data and commonly available geographic data.

Preliminary study showed very good correlation between raw Landsat data and chlorophyll-a concentration for good atmospheric conditions and larger reservoirs, but no agreement of model between various times and reservoirs. Workflows for three use cases are investigated. First use case leads to map of chlorophyll-a concentration for one reservoir and one time, second for multiple water bodies and one time. The third workflow scheme should use time-independent model of chlorophyll-a concentration. The first workflow scheme has been already verified. Details of the other two are being worked on.

Few scripts for preprocessing of Landsat data and for the DOS atmospheric correction were developed in the process of testing various steps of the workflow in GRASS GIS. These and possibly further scripts for other image-based atmospheric correction methods will be published under GPL license.

Keywords: Landsat, Chlorophyll-a, Reservoir, Modeling

INTRODUCTION

The subject of modeling chlorophyll-a concentration and water clarity in inland water using multispectral remote sensing data is widely covered in literature. Most articles focus on developing a model with good correlation between chlorophyll-a concentration and satellite data, usually based on chlorophyll-a concentration measurements in one relatively large lake, bay or reservoir (compared to average lakes and reservoirs in Czech Republic) and single sampling date, i.e.

Proportionally less articles deal with regional scale studies, trying to extend the model over more water bodies and/or multiple sampling dates. An example might be study Olmanson et al. (2002), dealing with modeling Secchi disk depth (SDD) parameter over approx. 12,000 lakes of Minnesota,or approach to retrieve chlorophyll-a concentration from airborne sensor data for 11 lakes in southern Finland.

This article deals with work in progress to create workflow for lake and reservoir chlorophyll-a modeling from satellite multispectral data usable in routine water quality monitoring. One of the objectives is also to verify if the methods used in above mentioned literature are applicable to relatively small reservoirs in the Czech Republic and to find optimal procedure. The work is carried on with Landsat data, water quality data from reservoirs by Povodí Labe, a.s. (east Bohemia region) and using Quantum GIS and GRASS GIS open source software, but the resulting workflow should be as software-independent as possible.

As the correlation used in creating a model is based on data from on-site sampling, the modeling of chlorophyll-a concentrations using remote sensing data could not replace the current monitoring methods, but could extend their results.

USE CASES

Results of conventional chlorophyll-a monitoring are concentrations on the sampling sites from various depths. One reservoir is sampled at 3 to 12 points depending on reservoir size.

If there is suitable satellite image available, taken around the given date of conventional monitoring, there are three possibilities how use it to extend results of conventional chlorophyll-a monitoring:

1. It is possible to create detailed map of chlorophyll-a surface concentration for the reservoir monitored and date of samples collection. Currently, maps are constructed by the catchment area authorities based on the concentration measurements interpolation and knowledge of the water body constellation. The existing maps are constructed in 3D space and published on the web pages, Povodí Labe (2010), but are spatially approximate and less detailed. Maps created using satellite data are more detailed and should be more accurate, although showing only surface concentrations. Map of this type was already created (**Fig. 1**) during the preliminary study mentioned in the next chapter (Šimek, 2010). It may be also possible to combine information from detailed

surface maps and existing 3D maps to create more detailed 3D maps. This possibility should be yet investigated by experts in hydrology.

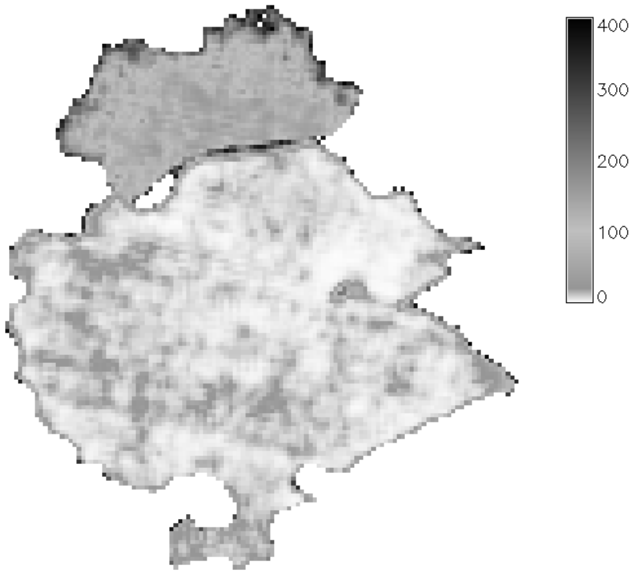

Fig. 1: Detail level of surface chlorophyll-a concentration map

2. It is also possible to create map mentioned in previous chapter for all water areas visible on the satellite image. As it involves applying model created on one or few reservoirs in the image to many different types of lakes, reservoirs and other water bodies, the results should be considered approximate, but they should give insight of the trophic state even of water bodies otherwise not monitored at all. This approach can be beneficial also for routinely monitored reservoirs, where it can add more information about changes in time. One reservoir or group of geographically near reservoirs in the area managed by Povodí Labe a.s. is currently typically monitored about every 50 days. As the monitoring takes place at different times for different reservoirs or groups, creating the map over the whole region of a satellite image should allow to add data more frequently for individual reservoirs or groups.

3. The last possibility is to create a time independent model of chlorophyll-a concentration for given set of reservoirs and satellite sensor. With such model, it would be possible to monitor reservoirs and lakes using satellite data independently on dates of conventional monitoring. Feasibility of this approach for the Czech Republic water bodies has to be yet investigated.

METHODOLOGY

Preliminary study

A preliminary study had been carried on to assess usability of Landsat Thematic Mapper (TM) data for chlorophyll-a concentration modeling (Šimek, 2010). This study, carried on with five on-site measurements of chlorophyll-a content from five reservoirs in eastern Bohemian part of Labe river basin, showed very good correlation between chlorophyll-a concentration and Landsat 5 data for the largest water body, reservoir Rozkoš. Every of the measurements contained results from 6 to 12 sampling points. Best correlation have been achieved with ratio of Landsat bands L1/L3 with the coefficient of determination R^2 = 0.93. The bands and band combinations found to have good correlation are from the range of Landsat TM bands 1-4 (**Table 1**), which corresponds with results commonly found by others.

Table 1: Best correlation of bands and band ratios with log of chlorophyll-a concentration, Rozkoš, 24-jul 2006

Landsat band or ratio	R^2
L1/L3	0.93
L3	0.82
L2/L3	0.82
L4	0.74

With other, smaller reservoirs the best coefficients of determination were ranging from 0.56 to 0.98, but they were for different bands or band combinations for every water body. R^2 for L1/L3 band combination had for other reservoirs and dates values 0.02, 0.12, 0.13, and 0.62. No single band or simple band combination with good coefficients of determination for all water bodies had been found.

The workflow schemes

Every use case mentioned in chapter 0 needs different workflow. Workflow developed in this work should be practicable with various software tools, and with various multispectral satellite data of suitable spatial resolution. The practical testing and development of methods is carried on in Quantum GIS software with GRASS GIS plug-in. The GRASS GIS software is not specialized remote sensing application, but it contains most basic tools needed in this field. The testing and development of methods is done with portability in mind, that is, whenever possible, the methods are carried on using basic tools like map calculator, unsupervised classifier etc. in parallel with specialized or more advanced tools which may be available only in particular software

The workflow schemes mentioned below are just basic steps, the merit of this work lies in details of individual steps and selection of methods with minimal data and software demands. The final results in case of success will be more detailed schemes with particular methods and algorithms, few of which will be mentioned in the next chapter.

The surface concentration map for one reservoir and one time is the simplest case. General workflow for this case, already tested in the preliminary study, consists of few steps:

1. Geometric correction of satellite data (optional, if needed).
2. Import of sampling point locations into GIS as map layer.
3. Reading values of all satellite layers on the sampling point locations into the sampling locations layer attribute table.
4. Examining correlation in a spreadsheet.
5. Using the best regression function to model the surface chlorophyll-a concentration in water.
6. To restrict the analysis to water areas, an existing map of water areas or satellite image classification can be used to create water-only image.

Similar workflow, with small variations, is used in other works. While in the literature is often used atmospheric correction, in this work it is hypothesised that it is not necessary in this type of workflow. The step 1 is not needed with most Landsat images, since most of them are already geometrically corrected with satisfactory precision.

The second use case, constructing the water chlorophyll-a concentration map for the whole area of the satellite image can use similar workflow. If the satellite image is cloud-free and atmospheric conditions (especially haze) is uniform over the whole image, the workflow could be used without change. Unfortunately, absolutely cloud-free, uniform images are quite rare in the Czech Republic territory. If this is the case, the workflow would have additional steps:

1. Geometric correction of satellite data (optional, if needed).
2. Atmospheric correction or normalization (optional, if needed).
3. Masking or otherwise eliminating cloud areas (optional, if needed) and creating water-only image.
4. Import of sampling point locations into GIS as map layer.

5. Reading values of satellite bands on the sampling point locations into the sampling locations layer attribute table.
6. Examining correlation in a spreadsheet.
7. Using the best regression function to model the surface chlorophyll-a concentration in water.

The step 3 can be implemented by classification methods. In this step the water areas for step 7 could be also classified. Generally, various methods could be successfully used for relatively clear and uniform images. Problems to classify an image, not preprocessed by optional step 2, indicate that the image is not uniform in terms of atmospheric haze over the whole area, and step 2 is necessary.

The primary task of step 2 in this workflow is not to convert DN values to absolute reflectance, but to equalize DN values response to surface properties in different areas of the image to compensate spatial non-uniformity of atmospheric conditions, especially of atmospheric haze. This means all methods globally changing all pixels by the same offset or function would not work, while only relative (atmospheric normalization), but spatially sensitive method would be sufficient. The appropriate feasible method of atmospheric correction or normalization for this workflow is still searched for among several possibilities recommended in literature, i.e.

Basic workflow for the last use case (time independent chlorophyll-a model) would be similar to the previous one, but the step 2 is crucial part, not optional one and step 6 would consist of examining data from several reservoirs and sampling times. It may also depend on the step of atmospheric correction or normalization, i.e. some atmospheric correction methods may need to eliminate clouds before the correction. As with previous use case the method of correction of atmospheric effects is still searched for. Unlike the previous use case, here would be of some use even methods assuming uniform atmospheric conditions in the study area.

Partial results

As this is work in progress, no final and detailed workflow has been created so far, but some steps are already semi-finished in more detail.

The first use case general workflow, which is simple and commonly used, had already been confirmed to work well for Labe reservoirs even without atmospheric correction. It had been proved in the preliminary study by constructing the map of chlorophyll-a concentrations and by good to very good levels of correlation between concentration and satellite data without the correction.

For the step of removing clouds and creating water-only image, several classification methods were tested, including the method of two step unsupervised classification recommended in Olmanson et al. (2001). Another quite successful method was supervised classification using GRASS built-in SMAP classifier (Image processing in GRASS GIS, 2010). Both methods worked well for most images, but for other failed – as mentioned earlier, problems with classification indicate inconsistency of atmospheric conditions in various parts of the satellite scene and should be solved by appropriate atmospheric correction. The two methods of classification will be used as alternatives in the final workflow.

In the part of finding correlation between chlorophyll concentrations and satellite bands was found, that best linear correlation for band digital number (DN) or simple band ratio indicated by square of Pearson coefficient R^2 is achieved with logarithm of chlorophyll-a concentration. Using logarithm of band DN, recommended in Luoheng et al. (2005), does not improve the R^2. It was also tried, if preprocessing the satellite data by 3x3 pixels smoothing filter, as recommended in Luoheng et al. (2005), could improve the correlation. In the **Table 2** are results for Landsat bands and reservoir Rozkoš.

Table 2: Influence of 3x3 smoothing on correlation.

Landsat band	L1	L2	L3	L4	L5	L7
R^2, raw DN	0,02	0,43	0,77	0,87	0,25	0,32
R^2, smooth 3x3	0,02	0,54	0,85	0,85	0,41	0,38

As can be seen, for the greatest reservoir Rozkoš there is some improvement of coefficient of determination in most cases, but for the smaller reservoirs the effect was mostly negative. In the final workflow there would be both variants and selection of the better one.

As mentioned earlier, model of chlorophyll-a concentration for reservoir Rozkoš agrees with those found in other works, while other, smaller reservoirs exhibit poor correlation in combinations of bands 1-3 and better correlations in combinations containing bands 5 and 7. Quick test with the 6 processed monitoring samplings from the preliminary study shows strong dependence of correlation of chlorophyll-a - band L3 on range of chlorophyll concentrations in the reservoir (**Fig. 2**). There was not so strong, but still significant, dependence on reservoir size (R^2=0,57).

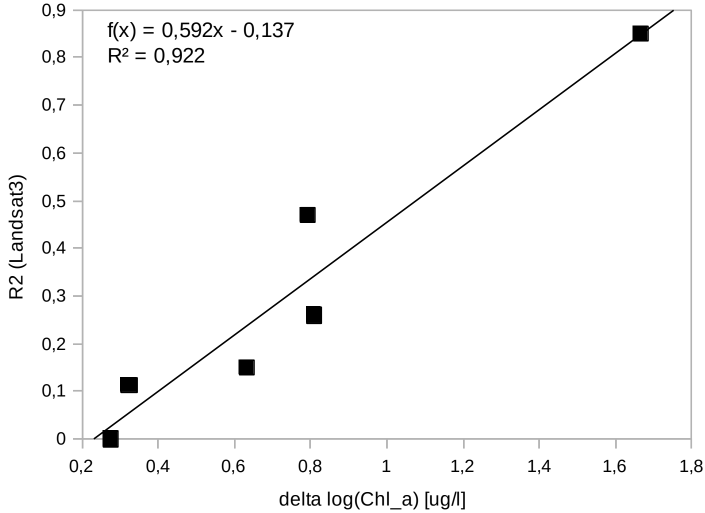

Fig. 2: Dependence of coefficient of determination of model on range of chlorophyll-a concentrations found in the reservoir.

These results are currently in the process of verification using data from more reservoirs and sampling times. If the dependence of correlation between various band combinations and reservoir size, depth or other parameter is confirmed there is possibility to incorporate such dependence into an universal model needed for the second and especially for the third use case workflow.

GRASS scripts

In the process of testing methods of the workflow in the GRASS GIS software, several GRASS scripts were developed as a by-product. Some of these could be generally useable and it is planned to release them under General Public License.

The script i.slcoff.fill fills gaps in the Landsat 7 ETM+ bands caused by Scan Line Corrector (SLC) failure using interpolation. This script is in fact just modified r.fillnulls script which is part of GRASS GIS. The original script was not able to correct Landsat SLC-off bands.

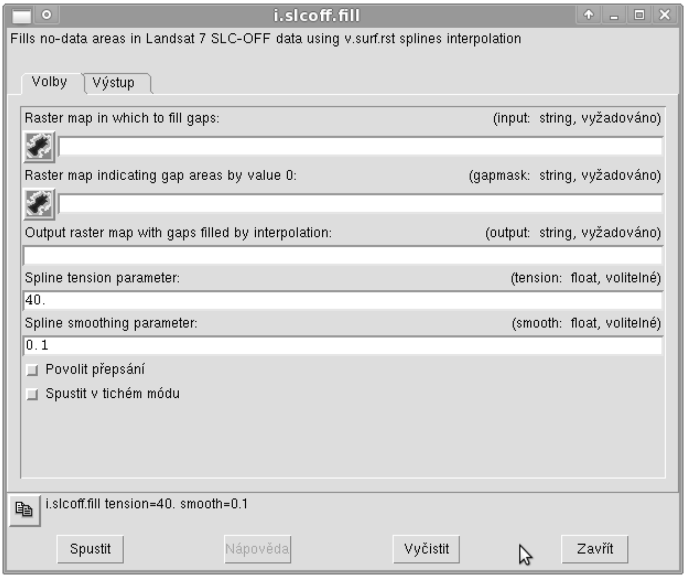

Fig.3: User interface of the i.slcoff.fill script.

The script i.atcorr.dos is intended for quick atmospheric correction of all bands of a scene by well known dark object subtraction (DOS) method. It implements optional moving window averaging of the image before searching for the dark pixel – this approach should eliminate influence of image noise or dead pixels on the results.

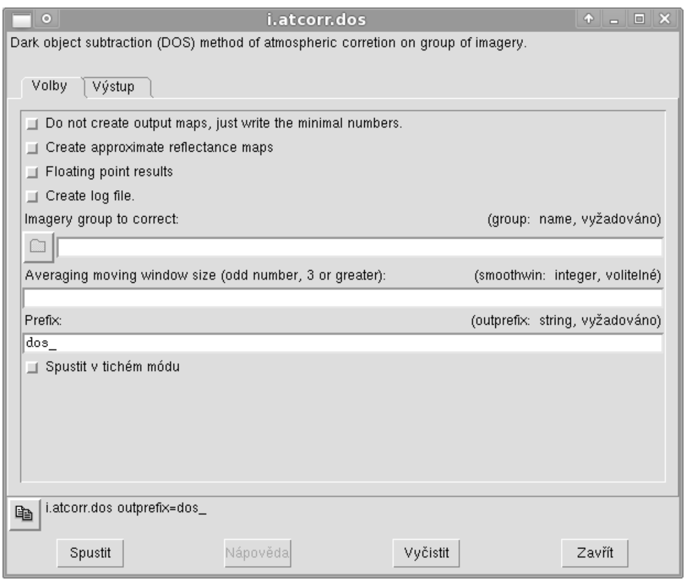

Fig. 4: User interface of the i.atcorr.dos script.

CONCLUSION

Three types of workflows are investigated. The workflow leading to map of chlorophyll-a concentration for single lake and time was confirmed to be feasible for reservoirs in the Czech Republic. Details of other workflows are being worked on, so far two map classification techniques are confirmed to be suitable and satellite image smoothing filter influence tested. Influence of water body parameters on the chlorophyll-a concentration model is being examined, with promising preliminary results. These have to be studied further on a broader data set. As a by-product of testing of the workflow steps in GRASS GIS, two possibly generally useable scripts for this software were created.

ACKNOWLEDGEMENTS

This work was financially supported by the Ministry of Education, Youth and Sports of the Czech Republic by the project MSM 0021627502. This work would not be possible without water monitoring data kindly provided by Povodí Labe, a.s. and Landsat Thematic Mapper data by National Aeronautics and Space Administration, made freely available through United States Geological Survey web service EarthExplorer.

REFERENCES

Luoheng Han, Jordan K..(2005) Estimating and mapping chlorophyll-a concentration in Pensacola Bay, Florida using Landsat ETM+ data. International Journal of Remote Sensing. 26 23, 5245-5254.

Duan H, Zhang Y, Zhang B, Song K, Wang Z. (2006) Assessment of Chlorophyll-a Concentration and Trophic State for Lake Chagan Using Landsat TM and Field Spectral Data. Environ Monit Assess. 129 1-3, 295-308.

Matthews MW, Bernard S, Winter K. (2010) Remote sensing of cyanobacteria-dominant algal blooms and water quality parameters in Zeekoevlei, a small hypertrophic lake, using MERIS. *Remote Sensing of Environment*. 114 9, 2070-2087.

Olmanson LG, Bauer ME, Brezonik PL. (2002) Use of Landsat imagery to develop a water quality atlas of Minnesota's 10,000 lakes. In: Pecora 15/Land Satellite Information IV/ISPRS Commission I/FIEOS 2002 Conference Proceedings.Vol XXXIV. Denver, CO, USA: ISPRS, 10-15 November 2002, pp. 8. Available at: http://www.isprs.org/proceedings/XXXIV/part1/paper/00102.pdf.

Pulliainen J, Kallio K, Eloheimo K, et al. (2001) A semi-operative approach to lake water quality retrieval from remote sensing data. The Science of The Total Environment. 268 1-3, 79-93.

Povodí Labe. Water quality in reservoirs 4.2. http://www.pla.cz/portal/jvn/en/index.htm [Accessed October 31, 2010].

Šimek J. (2010) Využití družicových multispektrálních snímků k hodnocení obsahu chlorofylu ve vodních nádržích. University of Pardubice, Pardubice.

Song C, Woodcock CE, Seto KC, Lenney MP, Macomber SA. (2001) Classification and Change Detection Using Landsat TM Data: When and How to Correct Atmospheric Effects? Remote Sensing of Environment. 75 2, 230-244.

Guanter L, et al. (2010) Atmospheric correction of ENVISAT/MERIS data over inland waters: Validation for European lakes. Remote Sensing of Environment. 114 3, 467-480.

Canty MJ, Nielsen AA, Schmidt M. (2004) Automatic radiometric normalization of multitemporal satellite imagery. Remote Sensing of Environment. 91 3-4, 441–451.

Yuan D, Elvidge C. (1996) Comparison of relative radiometric normalization techniques*. ISPRS Journal of Photogrammetry and Remote Sensing*. 51 3, 117-126.

Olmanson LG, Kloiber SM, Bauer ME, Brezonik PL. (2001) Image processing protocol for regional assessments of lake water quality. Water Resources Centre and Remote Sensing Laboratory, University of Minnesota.

Image processing in GRASS GIS. http://grass.fbk.eu/gdp/html_grass64/imageryintro.html [Accessed November 1, 2010].

Williams DL, Goward S, Arvidson T. (2006) Landsat: yesterday, today, and tomorrow. Photogrammetric engineering and remote sensing. 72 10, 1171.

Part IV

Harmonization and Integration Tools supporting INSPIRE implementation

EDGE-MATCHING POLYGONS WITH A CONSTRAINED TRIANGULATION

LEDOUX Hugo and OHORI Ken Arroyo

Delft University of Technology, GIS technology group

h.ledoux@tudelft.nl

Abstract

While the edge-matching problem is usually tackled by snapping geometries within a certain threshold, we argue in this paper that this method is error-prone and often leads to geometries that are invalid. We present a novel edge-matching algorithm for polygons where vertices are not moved (no snapping is involved); instead gaps and overlaps between polygons are corrected by using a constrained triangulation as a supporting structure and assigning values to triangles. Our approach has three main benefits: (i) no user-defined tolerance needs to be defined, the matching is *adaptative* to the configuration of the polygons; (ii) we can control locally how the polygons should be matched to obtain different results; (iii) we guarantee that the resulting edge-matched polygons are valid (no self-intersection and no gaps/overlaps exist between polygons). We present in the paper our novel algorithm and our implementation, which is based on the stable and fast triangulator in CGAL. We also present some experiments we have made with some real-world cross-boundary datasets in Europe. Our experiments demonstrate that our implementation is highly efficient and permits us to avoid the tedious task of finding the optimal threshold for a dataset, for the polygons are properly edge-matched and we can prove that no gaps/overlaps are left.

Keywords: INSPIRE, EGDE, polygon, snapping

INTRODUCTION

In the context of the INSPIRE Directive, there is an increasing need for tools that can process geographical datasets and harmonise them. One of the main challenges when dealing with datasets produced by different countries is that of the management of the connections of geographical objects at international boundaries, to ensure that objects on both sides are coherent. This issue is often simply called “edge-matching”, and is one aspect of the *geometric conflation* problem, which involves combining multiple datasets in order to make a new one, usually to improve either the spatial extent or the accuracy of the data (Lynch and Saalfeld, 1985). Yuan and Tao (1999) and Davis (n.a.) make a distinction between two types of conflation:

Horizontal conflation refers to edge-matching of neighbouring datasets to eliminate discrepancies at the border region. Country borders defined based on natural features of the terrain are a good example since their continuous nature basically ensures thatindependently produced data will not match at the border (Burrough, 1992). Fig 1 shows an area along the Spanish-Portuguese border with this problem.

Vertical conflation involves combining datasets covering the same area.

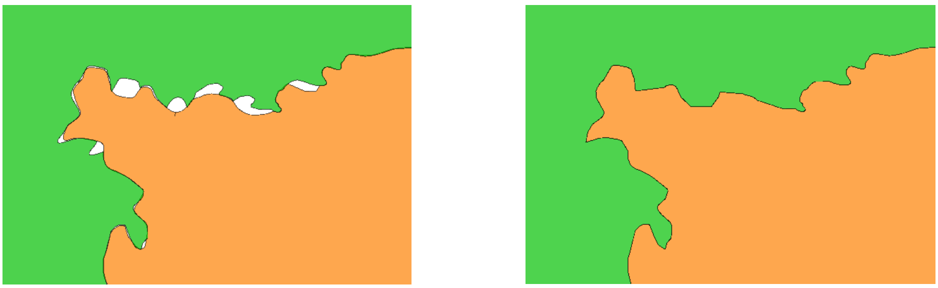

(a) (b)

Fig 1: (a) Part of the polygons representing the Arribes del Duero Natural Park in Spain (orange) and the International Douro Natural Park in Portugal (green). Since the border is defined as a river, the two datasets do not match perfectly (there are gaps and overlaps). **(b)** The polygons after edge-matching has been successfully performed

As explained in Section EDGE-MATCHING WITH THRESHOLD AND SNAPPING, the edge-matching problem has traditionally been tackled almost exclusively by using the concept of a *threshold* (a tolerance). In other words, if two objects (edges or vertices) are closer to each other than a given tolerance, which is usually defined by the user, then they are “equal” and can be *snapped* together so that they become the same object in the resulting dataset. While snapping yields satisfactory results for simple problems, we argue in this paper that for complex ones it is often impossible or impractical to find a tolerance applicable to the whole dataset, and that it is prone to errors that cause invalid geometries. Such invalid geometries might not be visible to the user (for instance tiny gaps and overlaps might be remaining, or a line might self-intersect), but further processing with a GIS requires that datasets be valid. We review in EDGE-MATCHING WITH THRESHOLD AND SNAPPING the previous edge-matching algorithms and we highlight the main pitfalls when snapping geometries.

We present in this paper a novel algorithm to perform edge-matching of one type of geometries: *polygons*. As explained in Section OUR APPROACH USING A CONSTRAINED TRIANGULATION, our algorithm differs from the previous ones since vertices of the geometries are never moved, i.e. no snapping of geometries and no thresholds are involved. Instead, we fill the gaps and fix the overlaps between datasets by using a *constrained triangulation* (CT) as a supporting structure and assigning values to triangles. This approach has in our opinion several advantages: (i) no user-defined tolerance needs to be defined (the triangles permit us to find matching polygons *locally*); (ii) we can control locally how the edges should be matched (in contrast to snapping, which often involves a global tolerance); (iii) we guarantee that the resulting edge-matched polygons will be valid. We report in Section EXPERIMENTS on our implementation of the algorithm (it is based on the stable and fast triangulator in CGAL[10]) and on the experiments we have made with some real-world datasets in Europe. Finally, we discuss in Section CONCLUSIONS the shortcomings of our method and future work.

EDGE-MATCHING WITH THRESHOLD AND SNAPPING

The most common method for edge-matching is based on the concept that polygons *approximately* match each other at their common boundaries (this approximation is based on a threshold). This implies that they should always be within a certain distance of each other along those borders. If, additionally, all parts further apart than this value are known not to be common boundaries, it is possible to snap together polygons that are closer to each other than this threshold, while keeping the rest untouched. Most commercial GISs implement the method (e.g. ArcGIS, FME, GRASS and Radius Topology), and the INSPIRE Directive is explicit about the use of threshold (INSPIRE,):

It will be to each "Thematic Working Group" to define the appropriate thresholds, if required, in a given data product specification, for each case of edge-matching.

Finding the appropriate threshold

The main problem lies in finding an appropriate threshold value for a given dataset. While in theory this value is linked to the accuracy of a dataset, in practice users do not always know how to translate the accuracy into a value, and if they choose the wrong value then their resulting dataset will not be properly edge-matched. In brief, for a successful edge-matching based on snapping, here are some rules:

1. Adjacent polygons should not be further apart than this threshold along any part of their common boundaries (shown as the minimum threshold in Fig 2(a)). Otherwise, gaps are not able to be fixed.

2. Adjacent polygons should not overlap each other in areas which are further inwards than this threshold from their common boundaries (shown as the minimum threshold in Fig 2(b)). Otherwise, overlaps are not able to be fixed.

---

[10]The Computational Geometry Algorithms Library: http://www.cgal.org

3. No vertices of a polygon should be closer to each other than this threshold, including non consecutive vertices (shown as the maximum thresholds in Fig 2). Otherwise, they might be snapped together, creating repeated vertices, disjoint regions, or various topological problems.

4. No vertices of a polygon should be closer than this threshold to any non incident edge. Otherwise, they might be snapped together, creating disjoint regions or various topological problems.

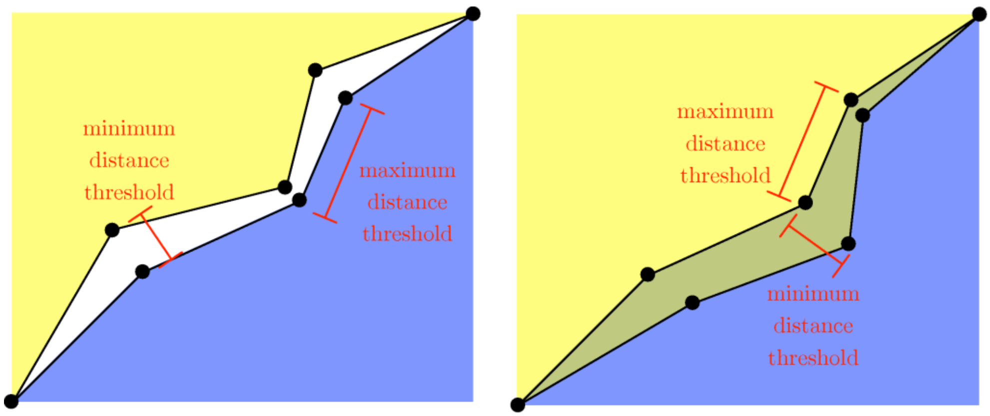

(a) Gaps between polygons (b) Overlapping polygons

Fig 2: Defining a threshold for vertex and edge snapping. The threshold to use should be larger than the largest minimum distance between the matching boundaries, and smaller than the minimum distance between vertices of a single polygon

Furthermore, the threshold value is usually used for a complete dataset while the sizes of the gaps and overlaps between polygons might be different at different locations. What is worse is that sometimes such a “one-size-fits-all threshold” does not even exist (e.g. because point spacing might be in some places smaller than the width of the gaps and overlaps present); in Section EXPERIMENTS we present one such dataset.

Snapping vertices

Even if the aforementioned conditions for a threshold are frequently not met (or are not checked beforehand), snapping is in practice still performed with a trial-and-error tolerance value. We highlight in this section the potential problems that snapping might create, i.e. the creation of invalid polygons and the changes in the topology of existing geometries.

Two examples are shown in Figs 3 and 4.

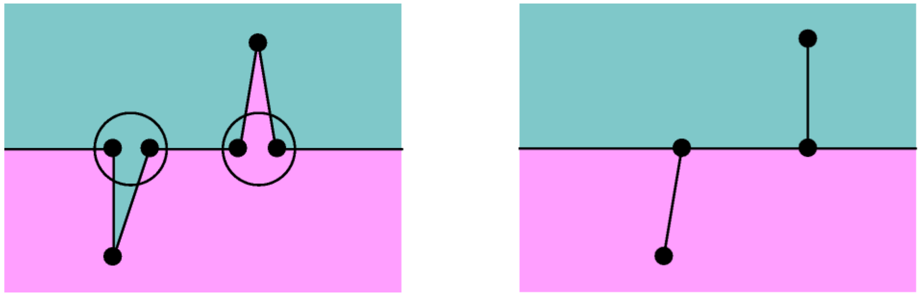

(a) Before snapping (b) After snapping

Fig 3: Spikes and punctures can be created by snapping, since the bases of these elongated forms (encircled) might be narrower than the threshold, but their lengths not

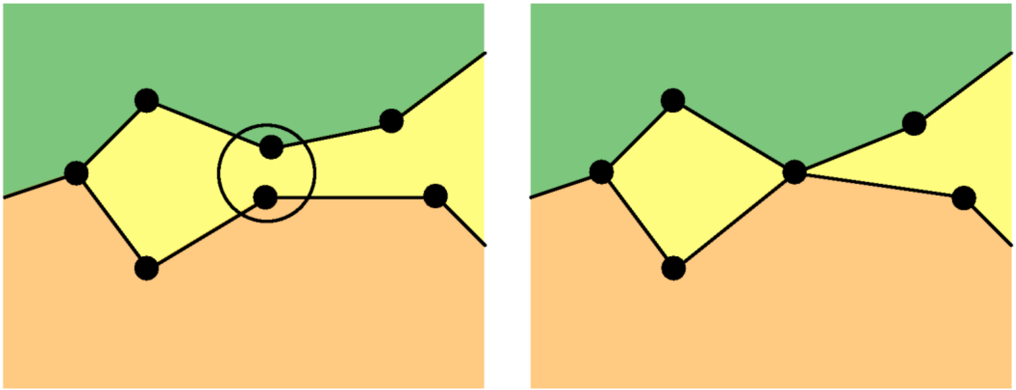

(a) Before snapping (b) After snapping

Fig 4: Polygons can be split by snapping, since some parts might be narrower than the threshold (encircled). While this result does not create an invalid result, it can change the number of polygons present and their topological relations, and can therefore be undesirable

While these examples prove that snapping is not problem-free, it should be said that commercial GIS packages often implement more complex snapping options (such as point-to-edge, edge-to-edge, or using a reference dataset). These options can help solve a problematic case, but can also complicate it by changing the topology of the polygons. One example is the post-processing operations to clean resulting polygons (e.g. disposing of polygons with small areas, removing redundant lines, thresholds for minimum angles, etc.) which might create new gaps and overlaps themselves, requiring an iterative cleaning process.

Another problem is that snapping is an intricate problem in itself, since there are many possible criteria that can be followed for both points and edges (e.g. points to the closest line, points to the closest point, points orthogonally to the closest line). Fig 5 illustrates one example where the resulting polygon is not valid anymore (and thus cannot be processed with a GIS).

Finally, it is worth mentioning that although the edge-matching of two or more polygons *could* be done by snapping and splitting polygons, it might require the use of thresholds so large so as to have no physical basis, and result in polygons that are substantially different from the original data.

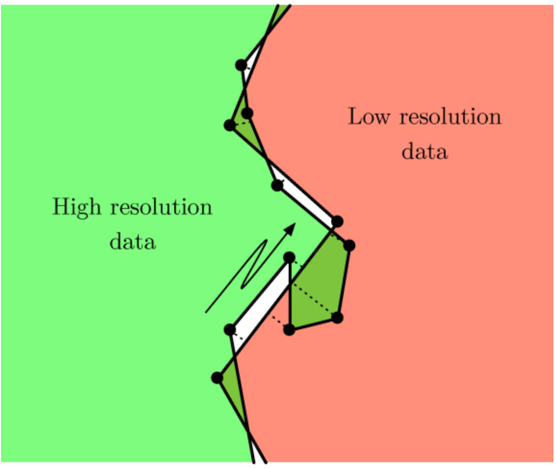

Fig 5: Snapping to the closest line can cause topologically invalid configurations. When two datasets of differing levels of detail are joined together by snapping the vertices of the high resolution dataset to the edges of the low resolution one, a situation where the line reverses on itself is created

OUR APPROACH USING A CONSTRAINED TRIANGULATION

Our approach to the edge-matching of polygons uses a constrained triangulation (CT) as a supporting structure because, as explained below, a CT permits us to fill the whole spatial extent of polygons with triangles, and then these allow us to identify easily the gaps and overlaps between different polygonal datasets. We use the idea of “tagging” each triangle with the label of the polygon it decomposes: gaps will have no labels and regions where polygons overlaps will have more than one label.

The workflow of our approach is illustrated in Fig 6 and is as follows:

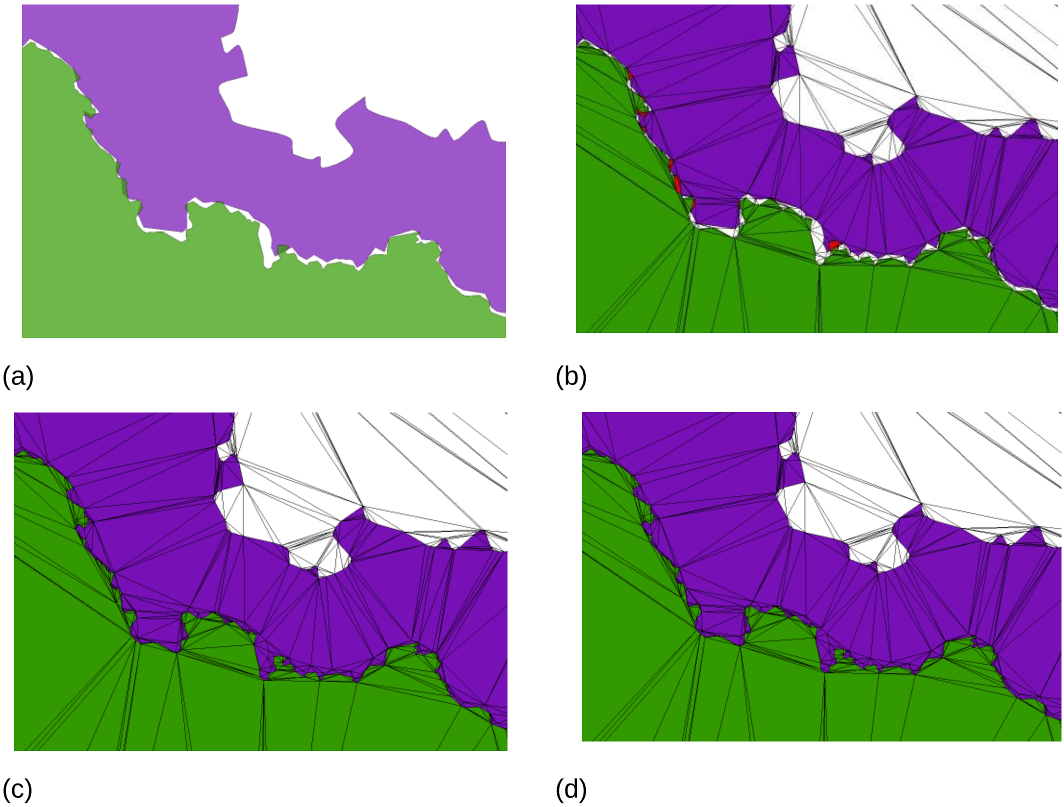

Fig 6: **(a)** Original dataset with two polygons. Notice the gaps (white) and the overlaps (darker green). **(b)** The CT of the input polygons; white triangles have no label, and red ones have >1. **(c)** Triangles are re-tagged such that each triangle has one and only one label. **(d)** The resulting edge-matched polygons.

1. the CT of the input segments forming the polygons is constructed;
2. each triangle in the CT is flagged with the label of the polygon inside which it is located (see Fig 6(b));
3. problems are detected by identifying triangles with no label or more than one label, and by verifying the connectivity between the triangles;
4. gaps/overlaps are fixed locally with the most appropriate tag (see Fig 6(c));
5. edge-matched polygons are returned in a GIS format (e.g. a *shapefile*).

To construct the CT, tag the triangles, repair the problems and recover polygons, we use results we recently obtained for the validation and the automatic repair of planar partitions (such as the CORINE2000 land cover dataset). In Arroyo Ohori (2010) and Ledoux and Meijers (2010) we describe in detail the algorithms used to construct the

CT of a set of polygons, to repair automatically planar partitions and to recover the polygons after the repair. We have modified slightly the algorithms and code so that we can perform the edge-matching of different polygons. We discuss below the main ideas, and we present in the next section some results.

Constrained triangulations.

A constrained triangulation (CT) permits us to decompose an object (a polygon) into non-overlapping triangles, Fig 7 shows an example.

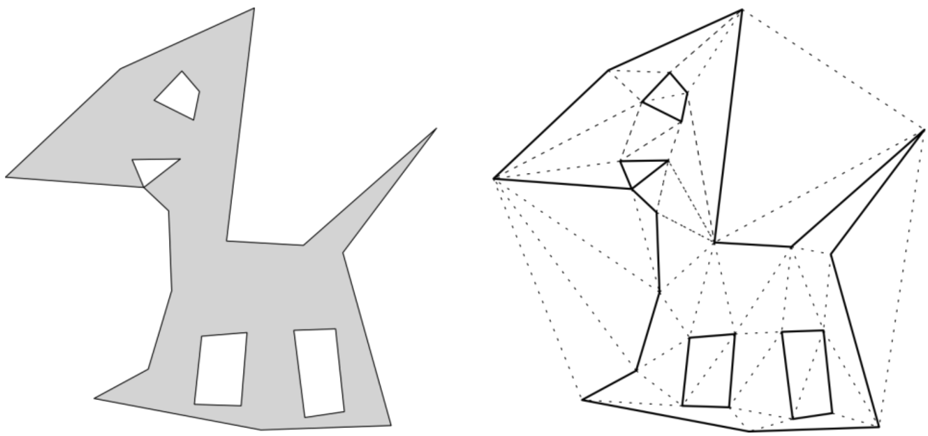

Fig 7: **(a)** A polygon with 4 holes. **(b)** The constrained triangulation of the segments of this polygon

Notice that no edges of the triangulation cross the constraints (the boundaries of the polygon). It is known that any polygon (also with holes) can be triangulated without adding extra vertices (de Berg et al., 2000; Shewchuk, 1997). In our approach, the triangulation is performed by constructing a CT of all the segments representing the boundaries (outer + inner) of each polygon. If two polygons are adjacent by one edge *e*, then *e* will be inserted twice. Doing this is usually not a problem for triangulation libraries because they ignore points and segments at the same location (as is the case with the solution we use, see Section EXPERIMENTS. Likewise, when edges are found to intersect, they are split with a new vertex created at the intersection point.

Tagging triangles.

The labels are assigned to the triangles by tagging the triangles adjacent to the edges of each polygon, and then visiting all the possible triangles with graph-based algorithms (i.e. depth-first search). See Arroyo Ohori (2010) for the details.

Identifying problems: gaps and overlaps.

If the set of input polygons forms a planar partition, then all the triangles will be flagged with one and only one label. Problems (gaps and overlaps) are easily identified: all the triangles are visited and the ones having less or more than one label are returned.

Fixing problems: re-tagging triangles.

Fixing a problem simply involves re-tagging triangles with an appropriate label. (Arroyo Ohori, 2010) proposes different repair operations that can be used to successfully fix gaps and overlaps. Four of them use triangles as a base (i.e. the label assigned is based on that of the 3 neighbouring triangles), which is faster and modifies the area of each input polygon the least. Two of them use regions of adjacent triangles with equivalent sets of tags (Fig 8), which is slower but yields results that are expected when edge-matching polygons.

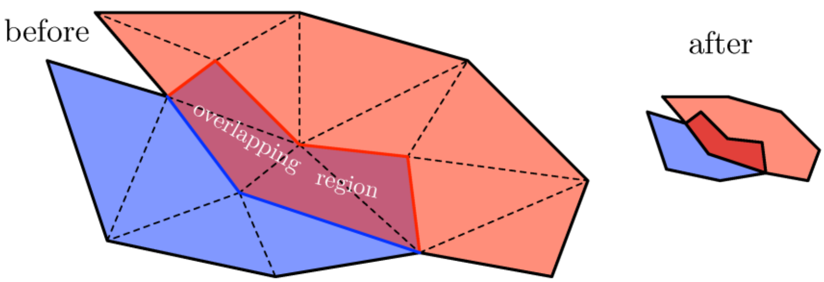

Fig 8: Regions are defined as adjacent triangles with equivalent sets of tags. In this example, the overlapping region between the red and blue polygons is repaired by the tag present along the longest part of the boundary surrounding the region (red

The most interesting repair operation for edge-matching is the one in which a *priority of labels* is used to repair regions, i.e. in case of gaps/overlaps the labels of adjacent polygons are ordered according to a user-defined priority, and the highest priority is assigned to the problematic triangles. We have adapted this operation so that the concept of *reference datasets* for edge-matching can be used. When a reference dataset is used, all the other datasets (we call them *slaves*) are snapped to it, and the reference dataset is not modified. When using a priority list, that means:

- gaps should be filled with slave labels
- overlaps should be fixed with the label of the master polygon.

Notice that in Fig 6(d) this technique was applied, and that the reference dataset (the green polygon) has not been modified. Fig 9 shows the result of edge-matching the polygons of Fig 6 with another criterion.

(a) (b)

Fig 9: (a) The same dataset as Fig 6. **(b)** Edge-matching performed with a repair operation where the label assigned to a problematic region is the one of the adjacent neighbour having the longest common boundary. Notice the differences with Fig 6(d

The main advantage of this approach is that the edge-matching can be performed with a *local* criteria, instead of a global one (the tolerance used is usually for the the whole dataset). It is also an efficient algorithm since only re-tagging triangles is involved to repair gaps and overlaps (which is a local operation).

Validation of results.

If each triangle in the CT has one and only one label, then by definition there are no gaps and/or overlaps between triangles. Observe that triangles not located "between" polygons are ignored; they form the "universe", you can see some at the top-right of Fig 6(d) for instance. The greatest benefit of using a tagged triangulation for edge-matching polygons stems from the fact that while modification operations are performed, the validity of the polygons is always kept, together with the integrity of the data. This comes as a contrast to other methods, where care needs to be taken to ensure that the (geometric or topological) validity is not broken. For instance, if a zero width corridor that joins two regions is created, it should be detected and removed.

EXPERIMENTS

We have implemented the algorithm described in this paper with the C++ programming language, using external libraries for some functionality: the OGR Simple Features Library, which allows input and output from a large variety of data formats common in GIS, and CGAL which has support for many robust spatial data structures and the operations based on them, including polygons and triangulations (Boissonnat et al., 2002). The developed prototype is open source and freely available[11].

We have tested our implementation with two datasets:

1. Fig 10(a): The border between Portugal and Spain along one national park is defined by a river. The Portuguese and the Spanish datasets do not match, see Fig 1 for one example at a larger scale. The two polygons have together about 12 000 points.
2. Fig 10(b): The NUTS boundaries datasets of France and its neighbours. For France, we used the GEOFLA® dataset[12], and for Belgium, Luxembourg, Germany and Italy we used the dataset from UNEP/GRID-Geneva[13]. The larger-scale examples from Figs 6 and 9 are with these datasets. The polygons have together about 6 000 points.

As expected, we have been able to edge-match successfully these datasets, i.e. our output polygons were valid and no gaps/overlaps were present. Because we use an highly-optimised triangulation library, we could obtain results in about 0.3 s for the France dataset, and about 1 s for the Portugal-Spain dataset.

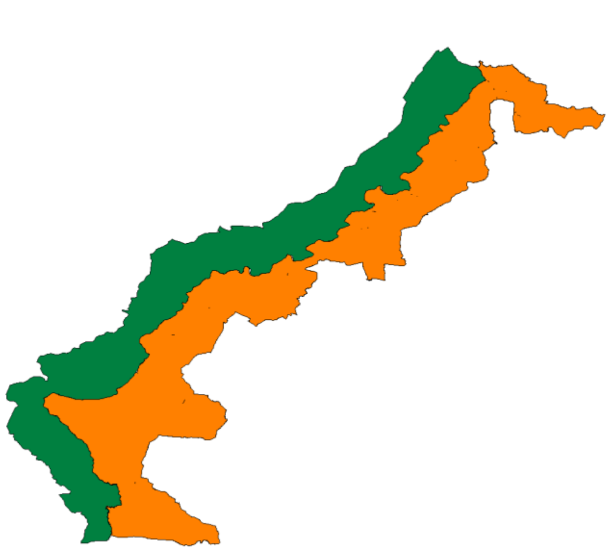

(a) (b)

Fig 10: (a) Border region between Portugal (green) and Spain (orange). **(b)** NUTS regions on the east of France (green), and some of its neighbouring countries (blue is Belgium; orange is Luxembourg; purple is Germany; grey is Italy

[11]On the GDMC website: http://www.gdmc.nl
[12]Freely available from the website of the French IGN: www.ign.fr
[13]Available at http://gcmd.nasa.gov/records/GCMD_GNV00159.html

Comparison with other tools

As a comparison, we used FME[14] and the HUMBOLDT project's Edge Matching Service (EMS)[15] to perform snapping.

FME could perform the matching with a given tolerance in about the same time (about 2 s), since it uses auxiliary data structures to speed up the process. EMS uses a *brute-force* implementation, where all the coordinates are compared with each other for snapping (thus 12 000 times 12 000 comparisons for the Portugal-Spain dataset; a quadratic behaviour), and took around 8 min to edge-match the Portugal-Spain dataset. It should be pointed out here that EMS is a Web-Processing Service (WPS) and that this time includes the conversion to GML and the uploading/downloading of the datasets to a server (we could not evaluate how much of the time was spent for these steps).

However, with both solutions, for both datasets, we could not find an appropriate tolerance with which valid geometries are produced and no gaps/overlaps remain. We applied a trial-and-error method, but as can be seen from Fig 6(a), the size of gaps and overlaps differ substantially. Some tolerance values could fix the gaps, but then other problems were created at different locations in the dataset. One such problem for the dataset Portugal-Spain is illustrated in Fig 11.

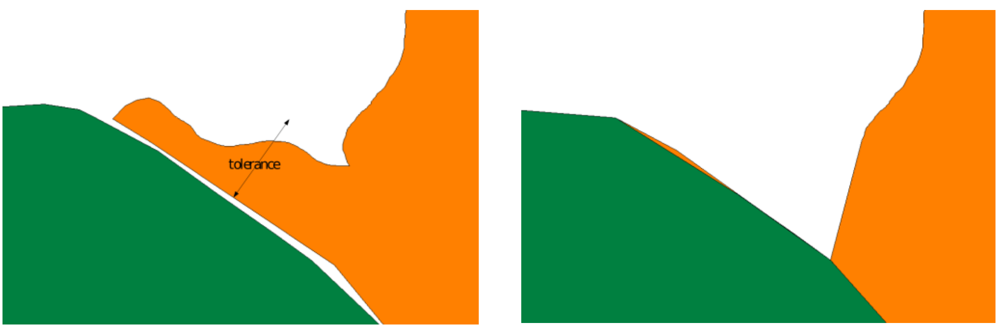

(a) (b)

Fig 11: **(a)** Original dataset, with the tolerance used for snapping. **(b)** Collapsing of part of an polygon

To fix the gaps/overlaps, a large enough tolerance was needed, but this tolerance was also creating topological problems. Notice in Fig 11(b) that the area has been partially collapsed to a line because its width is smaller than the tolerance used; using a smaller tolerance solves that problem but creates others.

[14]www.safe.com
[15]http://community.esdi-humboldt.eu/projects/show/ems

Since no snapping is used in the method we propose, such a problem cannot occur.

CONCLUSIONS

We have proposed a new algorithm to perform the edge-matching of polygons and we have shown that in practice it is highly efficient (since it is based on a highly optimised triangulator and only the tagging of triangles is involved) and it avoids the pitfalls of choosing the appropriate threshold (if it even exists). Anyone who has tried to find this threshold for a given dataset by using trial and error will recognise that our approach has great benefits.

However, it should be said that not everything is perfect, as Fig 12 illustrates.

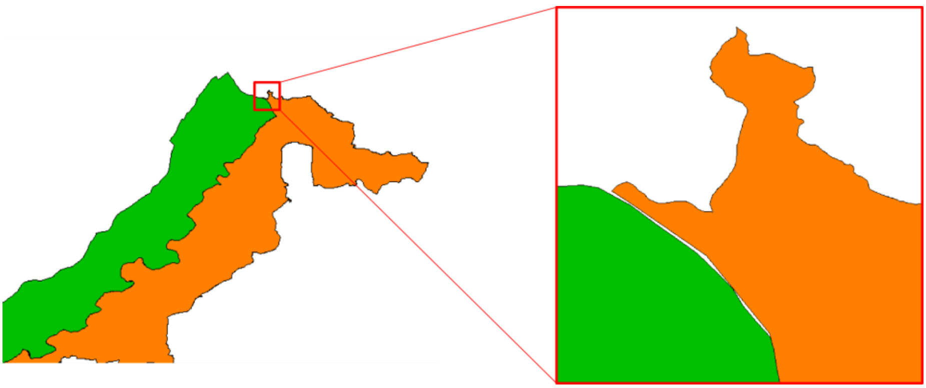

Fig 12: Same dataset as Fig 11, edge-matched with our approach. When polygons do not touch or overlaps, gaps can remain since these are considered part of the universe

If two polygons do not touch or overlap, then the area connected to the universe will not be filled with labelled triangles and the resulting polygons will not be matched. These will happen at the “top” and the “bottom” of the edge-matching edge for two polygons. We are looking for a solution to this problem. One approach involves identifying small triangles, and another involves snapping vertices as a pre-processing step to our approach (but since we use triangles afterwards, we should avoid the problematic cases, e.g. topological errors).

We plan in the future to add more repair functions, particularly one where we can edge-match two polygons without the notion of a master and a slave, i.e. the solution is “in the middle”. Triangles can be used to find the centreline of a region, as Bader and Weibel (1998) showed. We also plan to build a WPS so that everyone can use our implementation.

ACKNOWLEDGEMENTS

We would like to thank the financial support of the HUMBOLDT project. We would also like to thank Roderic Molina for providing the Portugal-Spain dataset and, Jose Ignacio Gisbert for discussion about the implementation of the HUMBOLDT Edge Matching Service.

REFERENCES

K. Arroyo Ohori. Validation and automatic repair of planar partitions using a constrained triangulation. Master's thesis, GIS technology group, Delft University of Technology, the Netherlands, 2010.

M. Bader and R. Weibel. Detecting and resolving size and proximity conflicts in the generalization of polygonal maps. In *Proceedings 18th International Cartographic Conference*, Stockholm, Sweden, 1998.

J.-D. Boissonnat, O. Devillers, S. Pion, M. Teillaud, and M. Yvinec. Triangulations in CGAL. *Computational Geometry-Theory and Applications*, 22: 5–19, 2002.

P. A. Burrough. Are GIS data structures too simple minded? *Computers & Geosciences*, 18(4):395–400, 1992.

M. Davis. Java conflation suite. Technical report, Vivid Solutions, n.a. Available at http://www.vividsolutions.com/jcs/.

M. de Berg, M. van Kreveld, M. Overmars, and O. Schwarzkopf. *Computational geometry: Algorithms and applications*. Springer-Verlag, Berlin, second edition, 2000.

INSPIRE. Methodology for the development of data specifications. Annex I Data Specifications. Document D 2.6, version 3.0.

H. Ledoux and M. Meijers. Validation of planar partitions using constrained triangulations. In *Proceedings of SDH 2010*, Hong Kong, 2010.

M. P. Lynch and A. J. Saalfeld. Conflation: Automated map compilation-a video game approach. In *Proceedings Auto-Carto VII*, pages 343–352, 1985.

J. R. Shewchuk. *Delaunay Refinement Mesh Generation*. PhD thesis, School of Computer Science, Carnegie Mellon University, Pittsburg, USA, 1997.

S. Yuan and C. Tao. Development of conflation components. In *Proceedings of Geoinformatics*, pages 1–13, Ann Harbour, USA, June 1999.

INNOVATION OF THE ARCČR 500 DATA MODEL AND ITS CONVERSION INTO ESRI MAP TEMPLATES

CEJKA Petr, HAJEK Pavel and JEDLICKA Karel

Section of Geomatics, Department of Mathematics, Faculty of Applied Sciences, University of West Bohemia, Univerzitní 22, 306 14, Plzeň, Česká republika
petr.cejka6@gmail.com, pavel.hajek21@gmail.com, smrcek@kma.zcu.cz

Abstract

A need of conversion of existing data into new structures and for other purposes arises in the age of geographic information systems and large geographic databases produced by various organizations and companies. There is also often a need of harmonization of two discrepant data sources into a third one. The paper is thus focused on description of tools suitable for above-mentioned activities, particularly: Free Mind, Geodatabase Diagrammer, ArcGIS Diagrammer, ModelBuilder and ArcGIS Desktop.

These tools are described on two projects realized by authors of the article: "Innovation of the ArcČR 500 data model" and "Conversion of the innovated ArcČR 500 data model into the structure of ESRI Map Templates". The aim of the innovation of the structure of the existing ArcČR 500 geographic database was the conversion of its flat structure into appropriate vertical and richer horizontal structure. The primary data base was created as a flat file structure and the first really geodatabase version was the version 2.0, where datasets and relationships were used. However, the created version 2.1 has a re-structuralized vertical structure and consists of data structures whose allow better exploitation of both spatial and attribute part of the geographic database, namely: more relationships, created topologies, geometric networks, terrain and raster datasets, etc.

The second, following project was focused on conversion of created geographic database ArcČR 500 v 2.1 to several cartographic databases of different scales, whose can be cartographically visualized according to ESRI Map Templates. The aim of this project was to provide the data from Czech Republic into small and medium scales of the ESRI Map Templates.

ArcČR 500 data model vision 2.1 has been currently passed to ARCDATA PRAHA Company, which considers the use of the created data structure for a new version of their ArcČR 500 database. This ArcČR 500 version is planned to publish after data actualization. The data import from ArcČR 500 to ESRI Map Templates is currently (2010 fall) consulted with ESRI.

The goal of the contribution is to present the potential of existing data modeling tools by demonstration of realized projects. The presentation shows, that the core of the data modeling is not in the development of newer and better tools, but in the design of high quality conversion/harmonization model (by using already existing tools).

Authors cooperated with the Czech ESRI distributor (ARCDATA PRAHA) on both projects. The third author was supported by the Research Plan MSM 4977751301. Authors have also used their experiences from their work on data models for themes from INSPIRE annexes, which have gathered from Plan4all project (ECP 318007).

Keywords: *data modeling, harmonization, INSPIRE, Free Mind, Geodatabase Diagrammer, ArcGIS Diagrammer, ModelBuilder, ArcGIS Desktop.*

THE CURRENT SITUATION OF DATA MODELING IN EUROPE

On the present, the INSPIRE directive (more on JRC (2010)) is a leading initiative, which influences architectures of both existing and newly built spatial databases in European Union. INSPIRE directive addresses 34 spatial data themes, whose are described in three Annexes. There are already existing guidelines and data models for themes addressed in Annex I and there are Inspire Thematic Working Groups working on guidelines and data models for themes described in Annexes II and III. Actual results of continuous development in described area can be found at web pages:

- Guidelines: http://inspire.jrc.ec.europa.eu/index.cfm/pageid/2
- UML Model: http://inspire-twg.jrc.ec.europa.eu/inspire-model/

The current situation in European Union is that most of spatial database administrators are, or are going to be, forced to make their geographic data structures interoperable to INSPIRE data models. There can be seen two or three major scenarios.

The first scenario consists in one time data conversion from existing data model to an INSPIRE compliant data model. The second scenario lies in repeated conversion from source to target data model and the conversion can be done in a batch mode or in real time (“on the fly”). Of course there could be also third scenario, which means to built a database from scratch, even if it is rare to build a whole database on a Greenfield.

It is important to deeply discover the data structure of both source and target data models, to understand metadata and the data semantics. These are crucial points whose have to be deal right to successfully undertake the data design or data harmonization. Tools which are used can vary and they are works as the technical background.

Following chapters present two projects recently realized by authors of the article: “Innovation of the ArcČR 500 data model” and “Conversion of the innovated ArcČR 500 data model into the structure of ESRI Map Templates”. The aim of the presentation of these projects is to show them as possible best practices of data model creation or conversion, pointing out the important steps of such a process.

INNOVATION OF THE ARCČR 500 DATA MODEL

The geodatabase ArcČR 500 is a spatial or geographic database in the level of detail 1 : 500 000. Its first version arises out of the classic paper maps of the Czech Republic, whose were digitized into a vector format. Until the version 1.3, the database had just a flat file structure. The actual distribution version 2.0 is stored in ESRI Geodatabase format and takes advantage of a classic Entity-Relationship-Attribute model (ERA model). More about the history of ArcČR can be found in Čejka (2010) or ARCDATA (2010). The ESRI Geodatabase structure is deeply described e.g. in Arctur & Zieler (2004).

The goal of the project *Innovation of the ArcČR 500 data model* was to convert the existing database structure into a new one, which would take the advantage not only from ERA model, but either of other possibilities of the ESRI Geodatabase data format, whose are summarized in Fig 1.

At the start, the ArcČR 2.0 had still flat structure, which was just converted to a database environment. There was just a division into three datasets: admin_clen (administrative division), klady (map layouts) and mapove_prvky (map elements) and there were relationships used in the dataset of administrative division, see left part of fig. 2.

During the conversion process, the approach of a database development described in Longley et al. (2005) was followed:

1. Conceptual Model: model the user view, define objects and their relationships and select geographic representation.
2. Logical Model: match to geographic database types and organize geographic database structure.
3. Physical model: define database schema.

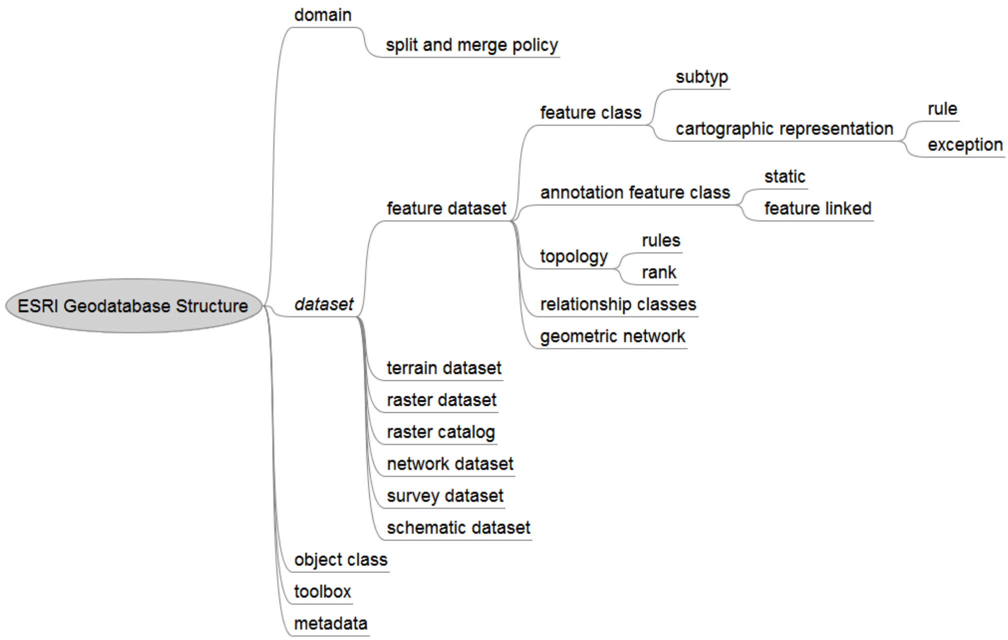

Fig. 1. The structure of ESRI Geodatabase, adopted from Jedlička (2010).

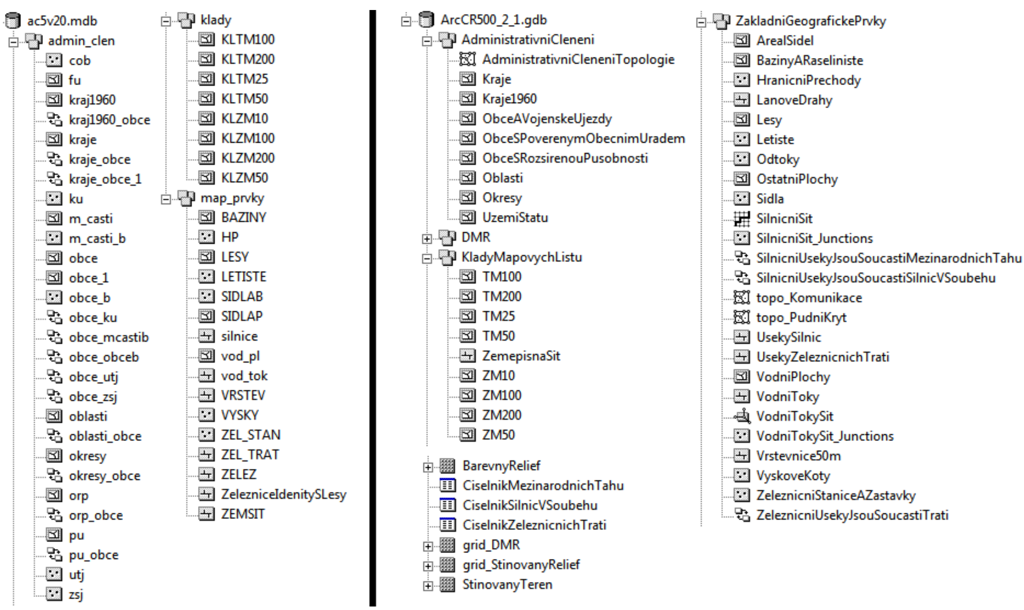

Fig. 2. The starting (at left) and resultant structure of ArcČR 500 (at right).

Naturally some steps were skipped, because in this case it was not about creating a database from scratch. There were some existing data before, even if they had just a flat structure:

The User view: the ArcČR 2.0 was primarily developed and abundantly used for creating of thematic cartographic outputs. Even the data structure allowed basic geographic analysis, the data structure was not sufficient e.g. for downstream analysis. Thus the purpose of development a new version of ArcČR was to improve its structure for geographic analysis, such as: hydrologic analyses, traffic analysis, DEM analysis, etc. Note: according to the database level of detail (LOD), analyses processed on the data have more educational than factual purpose.

At this step, the only used tools were brain, paper and pencil.

Objects were already defined and divided into classes, so their **geographic representation** and later their **geographic database types** were already set and were not changed (up to some exceptions in using specific data structures for both water and transportation networks or terrain).

The main deal was to **organize geographic database structure**, whose would be more convenient to analysis purposes. The whole process is deeply described in Čejka (2010), but the key steps follow.

1. First it was necessary to make a *deep revision of existing data and their structure*. It was necessary not only to understand the basic tree structure depicted at the left side of the Fig 2, but also to understand to existing relationships in administrative division dataset (there was Figd out that they represents spatial relations which can be in GIS modeled in a more suitable way – topologies).

   Next the attribute statistics had to be done and it was Figd out that there was a lot of empty attributes (attributes were not added, because of lack of time, but there was proposed a method how to do such an attribute statistics based on Structured Query Language and mainly the SELECT DISTINCT construct.

   Also it is important to check if the data has some naming convention and choose one in a case of need. The UpperCasseForFirstLetters policy was selected and it was decided to use more descriptive names for datasets, feature classes and attributes. More about naming conventions in geographic database e.g. in Jedlička (2005a,b).

   The ArcGIS software and SQL were used for this step.

2. Second step consisted of a *proposal of new database structure* (the right part of fig 2 and appendix A). Two well known concepts related either to lexical or geographic databases were followed:

- Database normalization – up to third normal form: Table faithfully represents a relation and has no repeating groups. No non-prime attribute in the table is functionally dependent on a proper subset of a candidate key. Every non-prime attribute is non-transitively dependent on every candidate key in the table (http://en.wikipedia.org/wiki/Database_normalization).
- Topology prior to relations – spatial relations should be better represent by topologic rules than entity relationships, except the relationship is useful in often realized attribute queries. Otherwise the entity relationship can be anytime created from spatial relations among objects. Following this concept can save approximately one third of entity relationships in resultant data model (according to author's experiences).

Thus there was proposed to delete relationships in the Administrative division dataset (newly named AdministrativniCleneni) and instead of them it was proposed to use a set of topologic rules. There was also proposed to delete redundant point classes whose represented reference points to polygons (relict from CAD boundary representation). Their attributes were proposed to transfer to appropriate polygon classes.

Layers in the dataset of map layouts (KladyMapovychListu) stayed unchanged; the dataset was just supplemented by lines of geographic network.

Biggest changes were proposed in the dataset of map elements which was renamed into BasicGeographicElements (ZakladniGeografickePrvky). As was already mentioned, al lot of feature classes was proposed to rename to more descriptive names. Next proposals:

- The geometry of roads and railroads should be strictly divided into segments from intersection to intersection. All following structures should be modeled using a many to many relationship: one segment can be a part of multiple roads and of course a road is composed of more than one segment. Additionally, the network dataset structure, which allows an analysis of transportation networks, was proposed to use for road feature class (SilnicniSit).
- Each river has to have a centerline representation. Each centerline has to be downstream oriented. The geometric network structure should be used (for purposes of hydrologic analysis).

- A land cover of the Czech Republic should be completed. Thus it is necessary to add the feature class Other Areas to already existing classes UrbanizedAreas, Woods, WaterAreas and Swamps,
- All above mentioned feature classes has to be of course topologically cleared and with set up topologic rules for further maintenance

Last but not least, the ESRI geodatabase format allows storing raster (raster dataset and raster catalog) and hierarchic triangular irregular networks (terrain dataset). Thus the digital terrain model and imagery should be uploaded directly to database.

The logical model of a geographic database has to be a result of this step. Although it could be still just drawn on a paper, the better way is to use some modeling tool. There of course exist tools based on unified modeling language (UML), but it is not a focus of this paper. Authors used the Geodatabase Diagrammer tool (http://arcscripts.esri.com/details.asp?dbid=13616), which creates an ERA model (including topologies) from existing geodatabase and stores it in Microsoft Visio. The Visio environment allows editing the model and thus proposing the new model.

Unfortunately there does not exist any way to convert the proposed model back to a geodatabase format. This could be seen as a disadvantage, but in many cases is the logical mode still just too much simplified to be used as a blueprint of a database schema. Nevertheless, a two-way tool: ArcGIS Diagrammer (http://kiwigis.blogspot.com/search/label/ArcGIS Diagrammer) can be used.

The last part of the project was to **define the database schema**. It consisted of creating of physical structures of each particular proposal described in previous chapters. Its description would exceed the paper scope, but it is also described in Čejka (2010). Authors use a combination of interactive and batch ArcGIS tools for creating the resultant database schema of ArcČR 500 v 2.1. Mainly ArcCatalog was used for database structure changes, Python scripting for batch processes and also ArcMap for validating the results.

CONVERSION OF ARCČR 500 INTO ESRI MAP TEMPLATES

The following project consists of conversion data between two databases, both with well described structure. The source one is the above described ArcČR 500 v. 2.1 and the target database is a set of geodatabases which underlies the ESRI Map Templates (http://resources.esri.com/maptemplates/).

ESRI Map Templates allows user to take advantage of predefined map design, but the user has to fulfill the condition, that the data has to be in prescribed data structure. In a case of ArcČR 500 v. 2.1 the ESRI Topographic Map Templates for small and medium scales were selected. The right part of a Fig 2 shows the ArcČR 2.1 structure and the Fig 3 depicts the structure of target geodatabase for small scales of topographic maps. Note that the target database also consists of conversion models for each its particular feature class. The visualization of the target geodatabase, using symbology of level of detail 9 (for scales closed to 1 : 1 000 000), is shown in appendix B.

While the left part of Fig 3 depicts the prescribed data structure, the right part shows models whose were developed during the project. These models take the appropriate data from a source database and convert (e.g. combine, filter, transform, etc.) them into a required target feature class. The range of the contribution does not allow describing all of the models. Thus let us focus of one example on which it is possible to show the principles of conversion process.

Fig. 3. Structure of geodatabase structure underlying to ESRI Topographic Map Template – Small Scales.

A road conversion model depicted in Fig 4 is a moderately difficult case. Before the model conversion begins it is important to understand the possible different data semantic between the source and target data model. The semantic problems in our project come mainly from differences between European/national and US data classifications. In this road example it means to match the different classification of roads. Czech terms highway(or motorway) ~ dálnice, speedway ~ rychlostní komunikace, primary roads ~ silnice první třídy, secondary roads ~ silnice druhé třídy, third class roads ~ silnice třetí třídy and other communications ~ ostatní komunikace had to be mapped to codes used in result database whose come from the US classification Motorways (interstate, freeways ~ level 0), trunk (arterial highways ~ level 1), primary (level 2), secondary tertiary, residential, unclassified and service roads. The mapping function for small scales is portrayed in the table 1. Even if the resultant conversion table is simple, the example shows the need of understanding the data semantic. Note the European road classification can be seen e.g. there: http://en.wikipedia.org/wiki/Hierarchy_of_roads and the American classification there: http://wiki.openstreetmap.org/wiki/United_States_Road_Classification.

Table 1. The mapping function for roads in small scales.

Road classification	ArcČR 500 v.2.1	Map Template – small scale
	Dálnice	Level 0
	Rychlostní komunikace	Level 1
	Silnice 1. třídy	Level 2

Processing of the model in Fig 4 starts at its bottom left corner (and later goes from left to right), where a new feature class schema (Roads) is created from a template and stored in appropriate dataset (Layer_4M). Then the features matching level 0-2 are selected from source dataset (highways, speedways and primary roads) and consequently this division is mapped to corresponding levels. Finally other attributes are set to a right parameter (Nation=420 ~ the code of the Czech Republic and the Continent="EU" ~ stands for Europe).

The rest of feature classes (and one raster dataset of course) were built in the same way, which was demonstrated above and which can be divided into several steps:

1. First, it is necessary to understand the target feature class structure and semantic and then seek appropriate data in a source database. Of course, that there can happen a situation, that there is no match in source data.

2. Then a ModelBuilder environment is used for creating a model consisting of sequences of tools, which convert the data into desired structure. Although it is possible to create own script (in Python) or even develop own tool, in our project the standard tools from ArcToolbox were sufficient.

3. There could be a need of geometric match on boundaries of particular national data, while development of a seamless data structure. In that case some method of geometry alignment has to be done. There are generally two possible methods: interactive editing or non residual transformation. Because it was not a goal of this project, it is not described any further.

The used technology (ModelBuilder in ArcGIS) has the advantage that it can be easily implemented in a server environment. Therefore it is possible to offer it even as a kind of a web service, so the conversion can be done on demand.

The conversion process of the Map Template of medium scale is analogous, however models become longer and more complicated, because of a richer content of medium scale map.

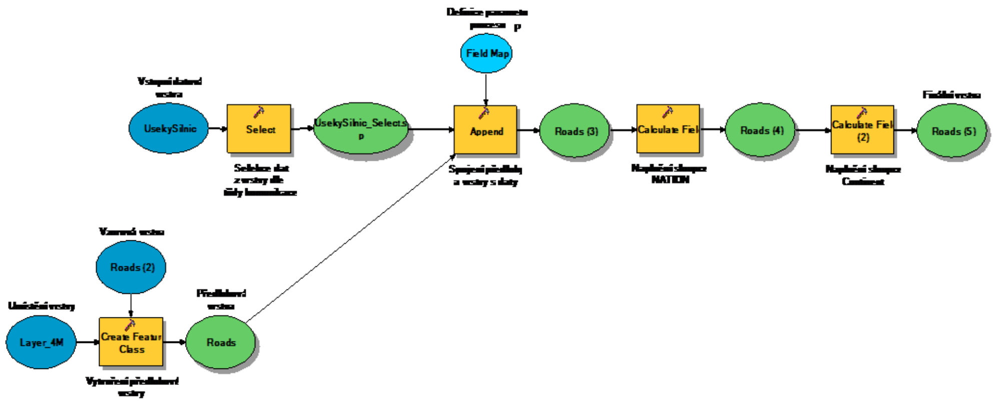

Fig. 4. Conversion of roads – an example of a ModelBuilder Model.

RESULTS AND SUMMARY

Results of project described in this paper are following: ArcČR v 2.1 was developed and well documented in Čejka 2010. ESRI Map Template for small scales was filled with data from the Czech Republic and medium scales have been analyzed, but no yet filled with data, see more in Hájek 2010.

First project shows a scenario of one time conversion process – creating a new structure of existing database (ArcČR 500). Second project show a conversion (harmonization if you want) mechanism from source to target database structure. The ArcČR 500 v 2.1 project has proved the conceptual~logical~physical stages of (geographic) database design. During the work on ESRI Map Templates project, the importance of data semantic and geometric matching appeared. Both of these projects (and several others, whose authors were cooperate, e.g.: data model for ZČE, City of Encinitas data model, geomorphologic database) show that existing tools are sufficient for data modeling, conversion and harmonization and that the core of this domains lies in deep understanding of the data and phenomena whose represent.

REFERENCES

JEDLIČKA, K. (2005a). Konvence v pojmenovávání geodatabáze. 1. část. In ArcRevue. roč.14. č.1. s.21-22. ISSN 1211-2135.

JEDLIČKA, K. (2005b). Konvence v pojmenovávání geodatabáze. 2. část. In ArcRevue. roč.14. č.2. s.25-26. ISSN 1211-2135.

Arctur, D., Zeiler, M. (2004). *Designing Geodatabases – Case studies in GIS Data Modeling*. Redlands. California. ESRI Press. ISBN 158948021X.

Čejka, P. (2010). *Inovace datového modelu ArcČR 500.* Západočeská univerzita v Plzni, Plzeň.

Jedlička, K. (2010). *Geomorfologický informační system.* Vysoká škola báňská, Technická univerzita Ostrava, Ostrava.

Longley, P., A., Goodchild, M., F., Maguire, D., J., Rhind, D., W. (2005). *Geographic information systems and science*. Paul A. Longley [et al.]. Chichester. John Wiley & Sons.

Hájek, P. (2010). Tvorba Map Templates pro databázi ArcČR 500 v. 2.1.Západočeská univerzita v Plzni, Plzeň,

ARCDATA PRAHA, s.r.o., ArcČR 500. http://old.arcdata.cz/data/arccr. 11/6/2010.

European Commission Joint Research Centre (JRC). INSPIRE > Welcome to INSPIRE http://inspire.jrc.ec.europa.eu/. 10/25/2010.

APPENDIX A – THE STRUCTURE OF ARCČR 500 V. 2.1

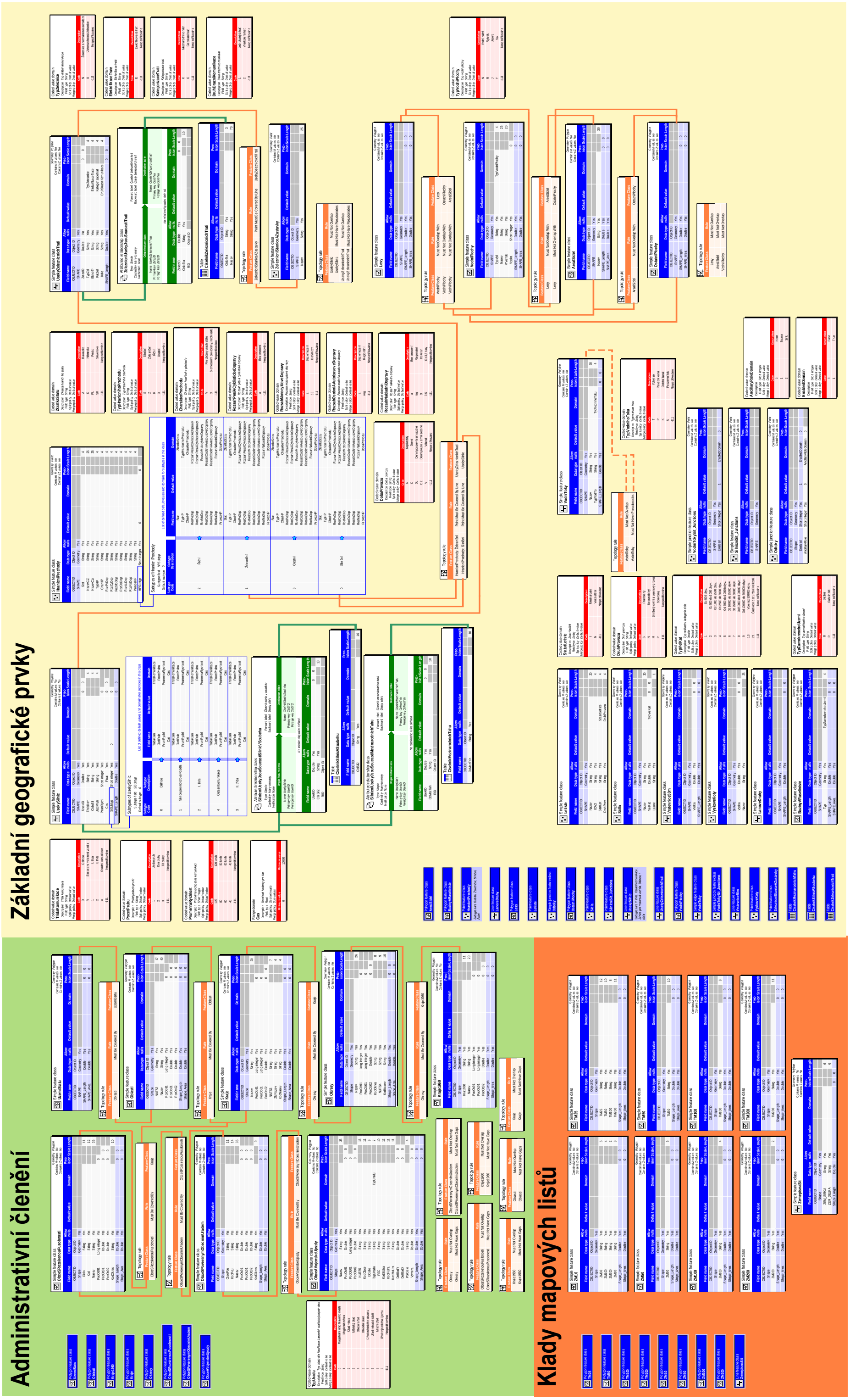

APPENDIX B – TOPOGRAPHIC MAP TEMPLATE – SMALL SCALES

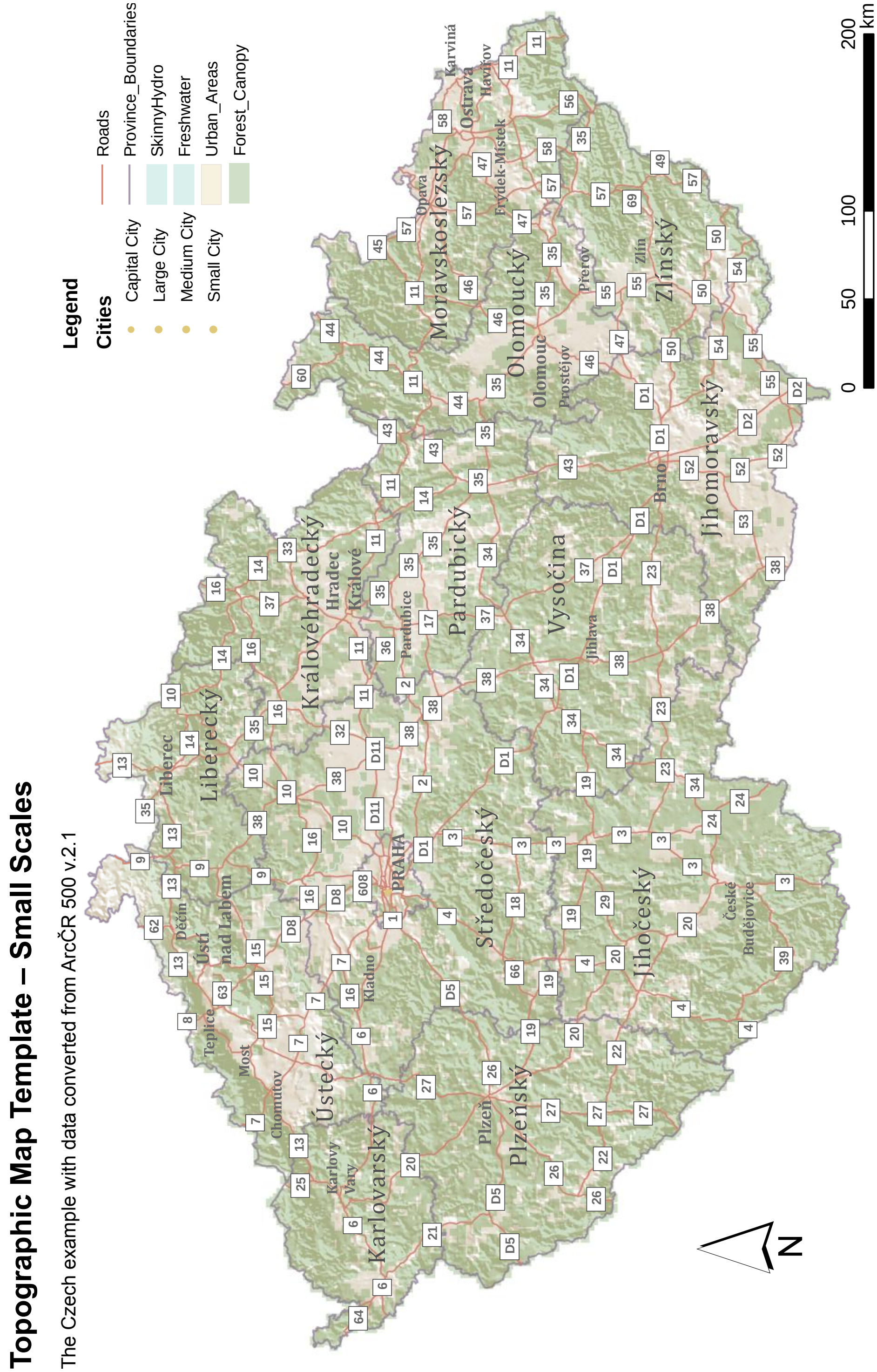

HUMBOLDT ALIGNMENT EDITOR

HORAK Jiri, JURIKOVSKA Lucie, UMLAUF Miroslav, JEZEK Jan,
HANZLOVA Marketa and ZLATANOVA Sisi

Institute of Geoinformatics, HGF, VSB-Technical University of Ostrava, 17.listopadu 15, 70833, Ostrava, Czech Republic
jiri.horak@vsb.cz, lucie.jurikovska@vsb.cz, miroslav.umlauf@vsb.cz

Section of Geomatics, Faculty of Applied Sciences, The University of West Bohemia, Univerzitní 8, 30614, Plzeň, Czech Republic
jezekjan@kma.zcu.cz

GISIG - Geographical Information Systems International Group, Via Piacenza 56, 161 38, Genova, Italy
m.hanzlova@gisig.it

Delft University of Technology, OTB Research Institute, Jaffalaan 9, Build. 30, 2628 BX Delft, Netherlands
S.Zlatanova@tudelft.nl

Abstract

The process of data harmonization starts with a description of data sources and mapping of differences among heterogeneous source and target data sets.

The semantic differences usually include incompatible data schemas (structures, different data types, domains etc.) and differences in content (different values for the same entity). While the second type of differences is difficult to be solved in an automated way, the first type can be described by the new tool HALE, developed within the HUMBOLDT project. The HUMBOLDT Alignment Editor (HALE) allows to interactively specify transformations between models at a conceptual schema level. It is possible to rename attributes, to make reclassification (classification mapping), to change geometric types, to change values using various mathematical expressions, to set default values etc.

The paper presents features, functions and results of testing harmonisation process for selected geodata. The process of data integration into common schemas which are INSPIRE compliant is discussed. The INSPIRE theme Hydrography is used as a core of the solution. Finally the schema transformation performed with HALE is executed with the help of other HUMBOLDT tools (i.e. Conceptual Schema Transformer) to perform required data transformation.

Keywords: Humboldt, harmonisation, data structure, alignment, conflation, WFS, GML, INSPIRE

INTRODUCTION

The purpose of data harmonisation is to resolve heterogeneity in spatial data and make them interoperable. This means that the systems have to be able to provide tools to combine seamlessly all available data. Traditionally three types of data interoperability are identified namely system interoperability, syntax and structure interoperability, and semantic interoperability (Sheth, 1999).

System interoperability reflects operating systems and communications heterogeneity, e.g. the instruction sets, communication protocols, different file systems, naming, file types, operation and so on. As a part of system interoperability it is possible to specify syntactic interoperability. Bishr (1998) and Fonseca et al. (2000) describe syntactic heterogeneity, in which the databases use different paradigms. Stuckenschmidt (2003) explains syntactic heterogeneity for GIS applications using differences in data format.

Structure (schematic) interoperability refers as to data models, data structures, data domains and data representation. Bishr (1998) specifies schematic heterogeneity, in which the same object of the real world is represented using different concepts in a database.

Semantic interoperability is the most complex one and deals with the meaning of the data. Semantics refers to the aspects of meanings that are expressed in a language, code, message or any other form of representation, i.e. semantic interoperability requires that the information system understands the semantics of the users' request and information sources (Sheth 1999). Bishr (1998) and Fonseca et al. (2000) explain semantic heterogeneity, in which a fact can have more than one description. Stuckenschmidt (2003) emphasizes differences in intended meaning of terms within specific context for this type of heterogeneity. Semantic heterogeneity should be solved before schematic and syntactic heterogeneity (Fonseca et al., 2000) using semantic translators (mediators).

It is worth to mention that in the case of datasets overlays a problem of content heterogeneity (different values for the same fact) has to be solved.

Much research has been completed through the years on all aspect of heterogeneity by researchers and standardization organisations. Open Geospatial Consortium (OGC) and ISO (International Standards Organisations) are currently working on standards to solve syntax heterogeneity. Spatial Data Infrastructures (SDI) are being built by different regions, countries and even across national borders (Bernard 2002, Groot and McLaughin 2000, Riecken et al. 2003), are examples of resolving syntax heterogeneity. SDIs support the discovery and retrieval of distributed geospatial data sources and can provide tools to resolve syntax interoperability but only to certain extends (Lutz and Klien 2006). Harmonisation processes represent an important, core part of building SDI. Methods of harmonisation data, metadata, processes, functions, procedures and rules are essential for creating consistent and operational SDI where end-users may access and employ in their systems different data stored in different places in different structures using different rules.

The HUMBOLDT project contributes to solving structural and semantic interoperability and is specifically focussed on the implementation of an European Spatial Data Infrastructure (ESDI). It provides tools, which allow for integration of spatial data sets from the multitude of European organizations. It was the aim of this project to manage and to advance the implementation process of this ESDI. The HUMBOLDT design approach re-uses existing concepts, processes, implementations and experiences as discussed in research articles and standardisation documents. The most important HUMBOLDT tool that deals with structural and semantic heterogeneity is the HUMBOLDT Alignment Editor (HALE). HALE is a desktop application that allows to design data transformations interactively at a conceptual schema level. This paper presents our tests with the HALE tool performed on one of the HUMBOLDT scenarios, i.e. Transboundary catchment.

The paper is organized in the following order: next section elaborates further on SDI and data harmonization issues. Further section presents the overall HUMBOLDT framework for data harmonization. Section HUMBOLDT Alignment Editor presents and discusses the schema mapping tool HALE. Section Case study: Transboundary catchment Roya/Roia river elaborates on the scenario Transboundary catchment and the tests with HALE. The final Section discusses the results.

SDI AND SPATIAL DATA HARMONISATION

Spatial Data Infrastructure (SDI) is the core of any GeoInformation Infrastructure (GII). SDI enables to integrate different spatial data sources and build seamless databases and data-portals providing a central place how to access different data. Roles of metadata, standardisation and geodata sharing (using web services) are essential for SDI design (Nougeras et al., 2005). Ideally SDI should provide means which would hide original data structures, formats and places of storage, and it should offer a transparent access to spatial data (no matter of original way of data storage).

The current implementation of European SDI is closely linked with European initiatives like INSPIRE, GMES and SEIS. The National Geoinformation Infrastructure of the Czech Republic (NGII) has been prepared since the end of 1990, supported by CAGI and Nemoforum (Národní geoinformační infrastruktura České republiky, 2001); nevertheless a significant acceleration of the real SDI establishment was connected with launching the INSPIRE directive (Infrastructure for Spatial Information in Europe, 2007/2/EC). INSPIRE declares necessity to collect data once and maintained it at the level where most effective; and to combine spatial information from different sources seamless and shared between users/applications (Pauknerová, Tryhubová 2006).

Successful implementation of INSPIRE is conditioned by shared data and services compliant to common standards. Main data specifications for INSPIRE can be found on the data specification page (http://inspire.jrc.ec.europa.eu/index.cfm/pageid/2) on the INSPIRE website. Among various documents important for design of INSPIRE compliant systems, it may be worth to note following documents:

- INSPIRE Data Specification on individual domains (e.g. Protected Sites, Hydrography)
- INSPIRE GML Applications Schemas (http://inspire.jrc.ec.europa.eu/index.cfm/pageid/541/downloadid/1707) (available in the "Other Documents" section).

The large requirements for geodata harmonisation lead to extended activities tied up with ways of facilitating the harmonisation process by automating the necessary steps as far as possible. Table 1 provides and overview on some of the harmonisation aspects and the possible implementations, i.e. either off-line of online.

The HUMBOLDT project addresses many of above mentioned issues and concentrates on development of appropriate tools to support automated harmonisation processes. A special attention is dedicated to the usage of web based tools aiming to create an open and distributed system easily integrated to various portals as well as an individual application. Explanations of standard geoweb services can be found in (Lehto, L. and T. Sarjakoski, 2004, Charvát et al., 2007, Šeliga et Růžička, 2005). The interoperability of geoweb services is addressed by several projects; capabilities of semantic oriented geoweb services are introduced in (Vaccari et al., 2009).

Table 1 Review of harmonisation requirements (Vries, de, M. et al, 2010)

Harmonisation goal or purpose	***Offline/pre-publishing (preparation)***	***Online/during use (runtime)***
data (exchange) format	Conversion tools such as FME (Safe Software), export modules of GIS/CAD software, all kinds of image processing and conversion tools	Web services with standardized interfaces that act as 'wrapper' around native formats and produce standard formats (raster of vector) as output (e.g. WMS, WFS, WCS, Web3D)
spatial reference system, reference grids	Beforehand, e.g. have a copy in WGS84 or ETRS89 in case fast retrieval is important	Coordinate transformation by web server of data provider, or by Web processing service, or in client

Harmonisation goal or purpose	***Offline/pre-publishing (preparation)***	***Online/during use (runtime)***
data/conceptual model: structure and constraints	1. defining common model and constraints (UML, OCL, OWL) 2. establishing transformation rules from local to common model (INTERLIS) 3. encoding transformation rules in machine-readable format (sql, XSLT, OWL, QVT/ATL) 4. migration or replication	a. Transform to target model by Web service of data provide or by cascading Web service (WFS-X, mdWFS), b. Or mediate to target model by separate mediator Web service(s), c. or translate to/from target model by client-side software
nomenclature, classification, taxonomy	Defining common nomenclature and classification or taxonomy	Use the standardized classification/taxonomy in: metadata, in search engine (keyword lists), in data content (code lists), for generalization (offline or real-time)
terminology/vocabulary, ontology	Terminology and definitions in thesaurus, data dictionary and/or ontology	
metadata model	Define a ISO 19115 or Dublin Core profile and migrate metadata to that common metadata model	Either centralize the metadata registry, or have distributed registry nodes
scale, amount of detail, aggregation for reporting	MRDB or vario-scale databases, for thematic aggregation: taxonomies and/or ontologies	(cartographic) generalization/refinement in real-time
Portrayal (legend/classification, style)	1. defining standards, e.g. IHO S52, DGIWIG 2. encoding in machine-readable format	Applying rules, e.g. by using SLD or default styling in GML/WFS
Processing functions: their parameters and formulas/algorithms	Agreement on parameters etc. and describe in repositories (possibly same as data and service metadata registries)	e.g. Web processing services that retrieve functions and parameters from repositories
extension (spatial, thematic, temporal)	Data quality actions like edge matching. But also detection of doubles (solve conflation issues)	
data collection procedures	e.g. guidelines for digitizing	

HUMBOLDT FRAMEWORK

A core development within the Humboldt project is the framework for data harmonization. The framework stands for a set of software tools and libraries that helps other developers or advanced GIS users to set up infrastructure for data harmonization. The main concept is described in Fig 1. Humboldt tools are developed in Java programming language and licensed under LGPL (open source license). Humboldt framework consists of desktop application (e.g. HALE), software libraries (e.g. CST) and server-side application (e.g. CST-WPS, Edge Matching Service). From the technical point of view, Humboldt components are standalone modules that are based on Maven build system. Most of the components can be also used as OSGi bundles. The development of Humboldt framework is based on existing ISO and OGC standards and influenced by other projects like CUAHSI (http://www.cuahsi.org/).

The general schema of data harmonisation is depicted in Fig 2 using a data flow diagram. As it can be realised, two basic phases can be distinguished. First, harmonisation steps have to be designed using one of the mapping tools e.g. HALE, WDCS. The next phase solves the actual data transformation (i.e. the transformation of the data sets) according to the harmonisation schema. Data harmonisation implementation utilises other HUMBOLDT tools or other suitable tools.

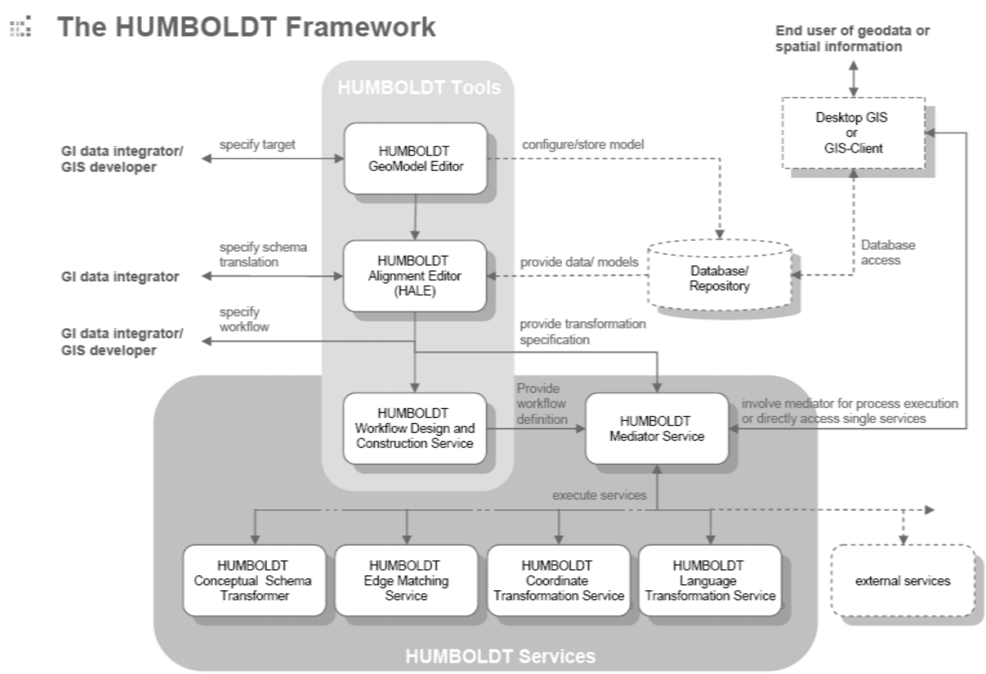

Fig1 Concept of HUMBOLDT Framework

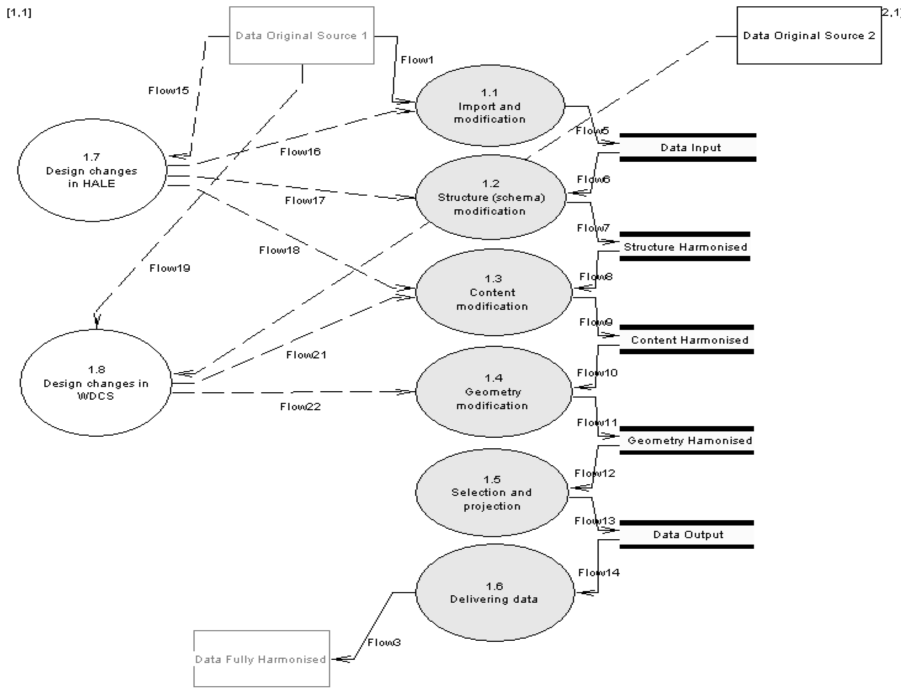

Fig2 Data Flow Diagram of the harmonisation process for the data source 1

It is worth to mention that not all of HUMBOLDT components reached the stable phase of development, but the main goal to prove the concept and establish overall API was achieved. One of the most developed products are HALE (the schema mapper) and CST (the executor of the schema mapping). The status of all components can be tracked on Humboldt community site (http://community.esdi-humboldt.eu/).

The main blockers to reach the stable status are:

- Handling of GML 3.2.1 – this version of GML is required by INSPIRE but has not been yet widely adopted by other GIS software libraries and application. The support of such encodings is nowadays still limited so even if Humboldt framework can generate such outputs there is not many possibilities to use it in other third party software.
- Handling of GML in general – even if GML is a OGC standard, its implementation by third party vendors is not consistent. GML output of different software products (ogr2ogr, Geoserver, Geomedia) has always its specifics. One of the reasons might be high level of complexity of GML (Galdos, 2010).

HUMBOLDT ALIGNMENT EDITOR

The HUMBOLDT Alignment Editor (HALE) is an Eclipse RCP application (Reitz 2010a, Reitz and Kuijper, 2009. HALE allows to interactively define mappings between source and target conceptual schemas. It supports import of schemas (i.e. Eclipse ecore, WFS and GML Application Schemas) and provides tools to indicate mappings between classes, their attributes and relations. Several different cases can be distinguished while mapping classes, relationships and their attributes (Lehto 2007, Reitz 2010b). HALE performs a large number of the specified mappings (see below). As discussed in the HUMBOLDT framework, the defined transformations are stored either locally or in the HUMBOLDT Model Repository and used by the Conceptual Schema Transformer (CST) to perform Schema Transformation on actual geodata. The HALE installer is available on http://community.esdi-humboldt.eu/projects/list_files/hale.

Features

HALE allows resolving several interoperability issues:

- Differences in application schema and terminology. HALE provides mapping rules for the classes and attributes of a source to a target conceptual schema.
- Differences in Metadata. HALE is able to create mapping rules for metadata elements.
- Inconsistency in selected spatial and temporal aspects. HALE enable to define functions for transformation of geometric types.
- Multiple representations. HALE will offer a definition of rules for handling other representations of the same object, i.e. under what circumstances which of the precedence should be used.

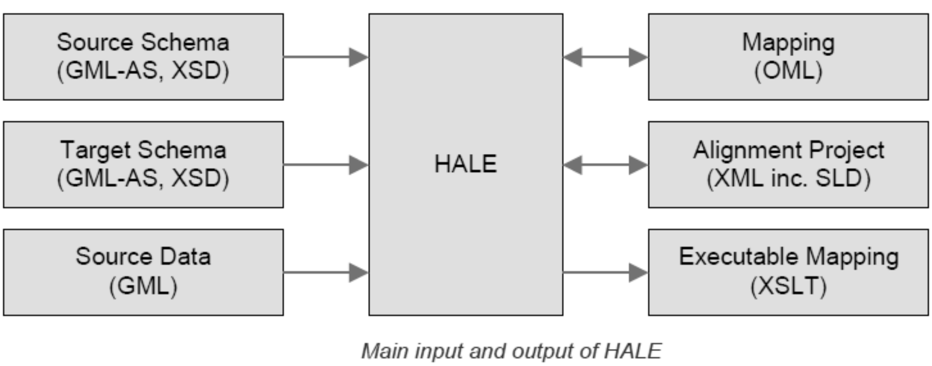

Fig3 Main inputs and outputs of HALE (Reitz, 2010)

The list of proposed functions includes:

1. A simple Attribute Rename Function. It facilitates the change of alphanumeric attributes and also mapping the following geometric types: LineString -- MultiPoint, Polygon -- MultiPoint,
2. A Generic Math Function - calculation of mathematical expressions using source attributes as variables,
3. A Bounding Box Function and a Centroid Function – creation of additional geometry (polygon - minimum bounding rectangle MBR; centroid - point),
4. A Buffer Function – creation of buffer (polygon) around any line or point-type geometry,
5. A Classification Mapping Function – transformation of code lists and classification values.
6. An Ordinates to Point Geometry function that accepts two numerical values as input and will create a point geometry based on that.
7. A Date Extraction Function that allows to extract a date object by specifying the format of that date and to set it in another format.
8. A Create GML Reference Function enables to create a reference to another element in the same data set or a different data set.
9. An INSPIRE Identifier Function enables to create a IdentifierProperty-Type;
10. An INSPIRE Geographic Name Function does the same for Geographic-NamePropertyTypes.

It is possible to classify functions into following main categories: Create new spatial objects, Structure modification and Content modification (Table 2).

Table 2 Classification of HALE functions

Category	Function	HALE function
Create new spatial objects	identification of key attribute	INSPIRE Identifier Function
	geographic name	INSPIRE Geographic name
	MBR	Bounding box function
	point from text	Ordinates to Point Geometry
	point – centroid	centroid function
	buffer	buffer function
Structure modification	attribute name change	rename attribute
	geometry datatypes (i.e. polygon to linestring)	rename attribute
	Integrity constraints change (i.e. adding PK, unique identifiers, null check, referential integrity, user defined IC)	create GML reference function
Content modification	Fill by a given value	Attribute default value
	Fill by NULL value	INSPIRE Nil reason
	Fill by a numerical expression	mathematical expression
	Replace a date (change format)	date extraction
	Replace strings	classification mapping

Not all functions are available in the current version of HALE.

HALE produces three types of outputs:

- GOML files contain information for mapping. It represents an input for HUMBOLDT Conceptual Schema Transformation Service and manages the data scheme transformation.
- XML file containing a configuration for HALE project (used only by HALE).
- SLD file intended for geodata visualisation (used only by HALE).

The mapping can be also saved in OML or XSLT format.

CASE STUDY: TRANSBOUNDARY CATCHMENT ROYA/ROIA RIVER

Water management and hydrological modelling

Water management in transboundary water catchments strongly relies on collaboration of stakeholders from both sides of the border. Any integrated water management requires a joint effort and data interchange to reach adequate decision support.

Hydrological modelling provides various tools which may be successfully exploited in water management.

Principles of numerical modelling of hydrological processes and description of commonly used methods can be found in Bedient and Huber (2001), Maidment (1993) and Beven (2002). A practical evaluation of 18 most frequent numerical modelling systems for water management was provided within the framework of the TANDEM project. The following features were investigated (Horák et al., 2008): embedded models, field of applications, interoperability (linkage to GIS, utilisation of Earth coordinate systems, remote management and control like a macro language or an application programming interface), price and license terms, support (updating, technical support, documentation), software features (operating system, modularity, user interface, provided functions, possibility of integration), input and output (obligatory, conditional, optional). The type of modelling and type of software implementation determine data requirements for numerical hydrological modelling.

Table 3 Main data requirements for hydrological modelling

	Required attributes	**Description**
Digital Elevation Model	Altitude	3D digital representation of the topography
River Network	Width	
Water bodies	Type Altitude	Included Lakes, Reservoirs, etc.
Catchment Area		Catchment boundaries of interest, watershed geometry.
Land Use, Land Cover	Code/CLC Code Vegetation Type	Land cover/Land use data, and other vegetation data (LAI, ...)
Soil	Type	soil data e.g. layer depth, bulk density, porosity, field capacity, saturated conductivity) intended to derive some hydraulic and runoff coefficients

Data required for hydrological modelling

A list of data required for hydrological modelling includes hydrometeorological data (mainly time series of rainfall data, records of river discharge) and geographical data necessary for setting of conditions influencing hydrological processes (i.e. transformation rainfall into a water flow).

Roya/Roia river catchment

The Roya/Roia River basin is one of the internationally shared river basins which crosses France and Italy. The Roya/Roia River catchment covers area about 675 square kilometres. The river springs in an altitude of 1871 m above sea level at Col de Tende on the French-Italian border and runs south about 35 km to Breil-sur-Roya and then another 8 km where it crosses back into Italy and discharges directly to the Mediterranean Sea in Ventimiglia, with an average flow of 15 cubic meters per second. The morphology of the basin is significantly different in France and in Italy. The landscape in France (Upper Roya) is the larger part of the contributing area and is characterized by mountains and valleys with swift rivers, thick forests, and 'Italian-wise' villages. In the southern part, the Italian territory (Lower Roia), the Roia flows in a flood plain area.

Hydrological modelling is required for understanding hydrological processes in the catchment, designing appropriate measures and improving water management (e.g. flash floods, occurring in the surrounding area of Breil Sur Roya, Fig 4).

Fig 4: Roya-Roia and danger of flash floods (Lac de Meshes,Breil sur Roya, Ventimiglia)

As the history shown, Roya basin is exposed for flood hazard and land slide. Some of the significant flood hazards and its consequences happened in the past and giving the corresponding time they are documented by Mitiku (2009).

Data from adjacent (collaborating) countries

Geographical data available from the both countries include contour lines, river network, water bodies, land-use and coast line. The French data were obtained from BD CARTHAGE® database provided by French National Institute of Geography, IGN (Institut Géographique National). The Italian data were provided by Regione Liguria. The French and Italian data obtained were converted into GML files and datasets were made available on Geoserver provided by GISIG to the scenario working group (http://www.gisig.it:8081/geoserver). The French data were obtained in two coordinate reference systems (CRS), recognized under the name "NTF (Paris) / Lambert zone II" (defined by EPSG code 27572) and "RGF93 / Lambert-93" (defined by EPSG code 2154). The Italian CRS is "Monte Mario / Italy zone 1" (defined by EPSG code 3003).

Let us assume requirements for transboundary hydrological modelling originating from the Italian side. It is necessary to transform all French data from their CRS (EPSG code 2154 and 27572) to the Italian coordinate system (EPSG code 3003). Next, the layers with the same CRS have to be matched on borders and joined together. A horizontal conflation (Blasby et al. 2004) is needed for the following layers: contour lines, river network and land-use. This function is available in HUMBOLDT framework under Coverage Alignment (HUMBOLDT Edge Matching Service, see Fig.1). Finally, it is necessary to make transformation of the attribute structure and the attribute content. As described later, there are two basic possibilities of transformation - a one-side transformation from French data to Italian data (and vice versa) or more universal transformation to INSPIRE schema (reference later as two-side transformation) which means data from both countries is transformed into the INSPIRE compliant schema to make them joinable.

Two types of transformation processes were used: renaming attributes and classification mapping function. Only attributes and features necessary for hydrological modelling are adapted in the harmonisation process. The review of the number of required transformation for each layer into the target INSPIRE compliant schema is shown in table 4.

Table 4 Review of harmonisation requirements for hydrological data in the Roia/Roya catchment

Data	**Rename attribute**	**Classification Mapping**
Contour lines	2	-
River Network	4	3
Water Bodies	2(FR), 3(IT)	-
Land-use	3(FR), 2(IT)	2
Coast Line	2	-

Elevation

The digital elevation models are derived from contour lines in both countries. The vertical reference system is Genova 1942 (Italian data, Fig. 5) and NGF-IGN69 (EUREF, 2010) for French data (Fig. 6) and as defined in (IGN, 2002) IGN 1969 pour la France continentale and IGN 1978 pour la Corse. The important information given by this type of dataset is ALTITUDE that represents a mandatory attribute from the hydrological modelling point of view.

Property	Type
the_geom	MultiLineString
tipo	String
quota	Double
id	Long
origine	String
GDO_GEOMET	String

Fig 5: Italian Contour Line dataset preview with listed feature type details

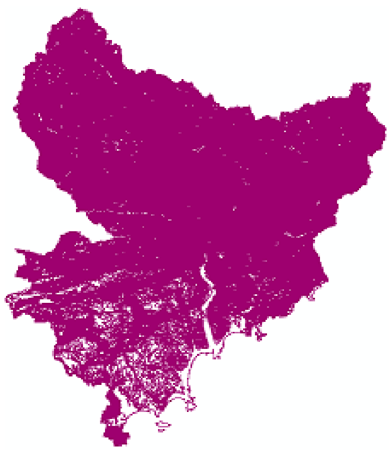

Property	Type
the_geom	MultiLineString
FNODE_	Integer
TNODE_	Integer
LPOLY_	Integer
RPOLY_	Integer
LENGTH	Double
DEP_06_	Integer
DEP_06_ID	Integer
ALTITUDE	String
Object_ID	Integer
Shape_Leng	Double

Fig 6: French Contour Line dataset preview with listed feature type details

River and Water Body

Main differences between the different regions include different classifications of river width and different classifications of watercourse hierarchy. As to the water body layers, there are no polygons, which overlap. The important information given by this type of dataset is WIDTH that represents a recommended attribute from the hydrological modelling point of view. Although, Italian dataset does not provide such information and French dataset classifies such information as follows:

- “1” (from 0 to 15 m),
- “2” (from 15 m to 50 m),
- “3” (more than 50 m).

Land cover (CORINE)

Both datasets are classified according to CORINE nomenclature (3rd level CORINE code) with corresponding land cover description in national language. Example of different attribute names and values: first table is Corine land cover for France, the attribute called NIV3_06 has the same meaning as attribute CLASSE in the second italian table. The values in these two columns are also similar, but use different formats (Fig. 7).

NIV3_06	IDPOL_06	INTIT_06
111	1	Tissu urbain continu
111	2	Tissu urbain continu
111	3	Tissu urbain continu
111	4	Tissu urbain continu
111	5	Tissu urbain continu
111	6	Tissu urbain continu
111	7	Tissu urbain continu
111	8	Tissu urbain continu
111	9	Tissu urbain continu
111	10	Tissu urbain continu
111	11	Tissu urbain continu
111	12	Tissu urbain continu
111	13	Tissu urbain continu
111	14	Tissu urbain continu
111	15	Tissu urbain continu
111	16	Tissu urbain continu
111	17	Tissu urbain continu
111	18	Tissu urbain continu
111	19	Tissu urbain continu

CODICE	CLASSE	DESCRIZION
29	3.2.4	vegetazione bosc. ed arbust in evoluzione
32	3.3.3	vegetazione rada
25	3.1.3	boschi misti
29	3.2.4	vegetazione bosc. ed arbust in evoluzione
32	3.3.3	vegetazione rada
17	2.2.3	oliveti
26	3.2.1	aree a pascolo e praterie naturali
26	3.2.1	aree a pascolo e praterie naturali
25	3.1.3	boschi misti
25	3.1.3	boschi misti
2	1.1.2	tessuto urbano discontinuo
29	3.2.4	vegetazione bosc. ed arbust in evoluzione
29	3.2.4	vegetazione bosc. ed arbust in evoluzione
26	3.2.1	aree a pascolo e praterie naturali
26	3.2.1	aree a pascolo e praterie naturali
29	3.2.4	vegetazione bosc. ed arbust in evoluzione
26	3.2.1	aree a pascolo e praterie naturali
26	3.2.1	aree a pascolo e praterie naturali
21	2.4.3	aree con colture e spazi nat.

Fig 7: Description of the content transformation between French CLC data (let) and Italian CLC data (right)

Required data harmonisation for the Roia/Roya catchment

The top priorities of the harmonisation steps for transboundary catchments are:

- schema transformation, including the Classification Mapping,
- coordinate reference systems transformation,
- layers horizontal conflation (alignment).

Two basic types of transformation have been prepared:

- **one-side transformation**. Transformation of data source from foreign country to match own datasets and append data from the foreign dataset. Here, Italy is assumed to be the home country requiring hydrological modelling due to possessing lower part of the catchment. Thus the harmonisation process "French data ➔ Italian data" is demonstrated (table 5).
- **two-side transformation**. Data from both countries are transformed into the common target schema, which is typically INSPIRE compliant or INSPIRE based. Hereafter such schema is labelled INSPIRE.

Data profiles from both sides of the border, together with common data profiles (INSPIRE inspired), are instrumental for the target schema creation.

Table 5 Example of one-side transformation <French into Italy> for river network data

	Dataset FRANCE	**Transformation process**	**Dataset ITALY**
Dataset	**River network (HYLCOV00_rivers.shp)**		**River network (ELEMENTI_IDRICI.shp)**
Projection	Lambert-93 EPSG:2154	Coordinate transformation	GAUSS BOAGA - ROMA40 EPSG: 3003
Geometry	LINE		LINE
Attribute and Data Types	POSITION [string]	Rename attribute Classification Mapping *(e.g. French data POSITION=1 – Italian data SOTTOPASO=F)*	SOTTOPASO [string]

The harmonised data model (for two-side transformation) is based on specifications of INSPIRE as a key component of current SDI. Following specifications were mainly utilised:

- Hydrography data theme (INSPIRE Annex I) to exchange hydrological information (applied for dataset related to water network, e.g. watercourse, water bodies, etc.),
- Elevation data theme (INSPIRE Annex II) and Geographical Grid Systems (INSPIRE Annex I, 2) for Digital Terrain Model (altitude information necessary for watershed schematisation),
- Land cover data theme (INSPIRE Annex II) for land cover information influencing runoff,

- Environmental Monitoring Facilities data theme (INSPIRE Annex III) and Meteorological Geographical Features data theme (INSPIRE Annex III) for measurements (time series of water discharge, precipitation etc.).

INSPIRE based target schema can be seen on Fig. 8.

It is important to highlight that the data model is INSPIRE based but not fully INSPIRE adopted. This is done by the complexity of the INSPIRE and requirements to maintain more simple attribute implementation.

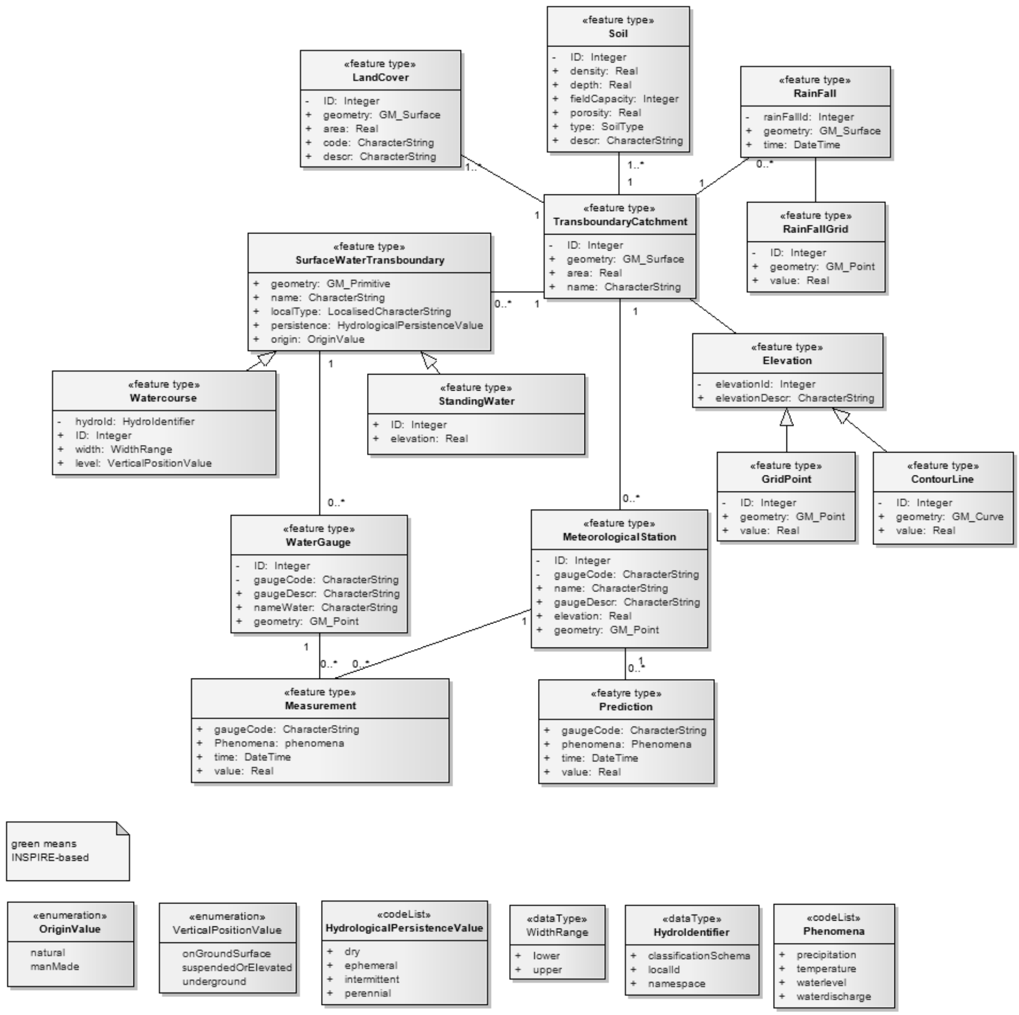

Fig 8: INSPIRE based target schema

HALE workflow

The following workflow description provides a list of required steps how to prepare transformation scheme using HALE. The description is based on the demonstrator prepared by GISIG
(http://www.gisig.it/humboldt/training/level3/protected_areas/demonstrator/test1.html).

1. Loading Schemas and Data: The Source and Target schemas

The first step is to load the source and target schemas in the HALE Schema Explorer. We start with our “source” schema. In the current version of HALE, you can load any XML Schema, including metadata schemas, GML Application Schemas and others. However, the schema import is optimized for GML Application Schemas and supports the following versions: GML 2.1, GML 3.1 and GML 3.2. You can also load a schema from a shapefile (*.shp).

GML Application Schemas have to be available on a WFS server. It is possible to setup your own WFS server or use some existing one.

The source schema is imported from a Web Feature Service's GetCapabilities. To load the schema go to "File", "Open schema", select "Import as source Schema", press the “Change...” button and enter your server's Get- Capabilities request URL into the text field at the top of the appearing window. If the network requires the usage of one proxy server, it is necessary to conFig the proxy server (use the ConFig Menu, click “Network Settings”, enter your HTTP proxy host and port and click “Save settings”). After that all types will be loaded and shown in the list below the button. If used, WFS offers FeatureTypes from more than one namespace, it is now also required to pick one of the namespaces. Finally one sees the namespace of your schema in the left part of the Schema Explorer.

After loading our source schema it is possible to **load** also "**source data"** or “instance data”. This view enables to see a cartographic representation of the reference data for the source schema and the transformed data alongside each other, when you have loaded such data. It can be styled and navigated interactively. If the system cannot clearly identify the used CRS (Coordinate Reference System) from the data, it will request the user to provide either the EPSG code or the Well-Known Text for the used CRS.

Similarly the **target schema** is loaded. The target schema can be also derived from the description of the „home datasets“.

Now it is possible to **explore the source and target models** in the Explorer View. To have a good view of any large schema it is recommended to activate following options in the schema explorer:

- organize feature types as list to have a clear view of the features of the schema,
- repeat inherited properties to explore hidden parts,
- expand complex properties to have a clear vision of all elements.

2. Mapping schema items

The further step is mapping of the items. It means to build a mapping between source and target datasets (schema of classes/attributes changes). We start selecting the items (classes or attributes) we want to map in the Schema Explorer. Next we select a type of transformation during mapping. It is possible to check the details of proposed mapping in the "Mapping" window and split the map viewer to see the transformed geometry. The system offers to apply a specific style to the transformed data. It is recommended to use predefined matching table mappings and apply the transformations in the schema explorer selecting the appropriate mapping function. Usually attribute transformations are applied first.

Let us give an example of using HALE for harmonisation mapping for French Watercourse datasets.

Watercourse transboundary harmonisation

First we transform data from the French watercourse dataset called HYLCOV00_rivers to INSPIRE hydrography schema. After loading our source schema from Web Feature Service´s GetCapabilities (http://www.gisig.it:8081/geoserver/ows?service=WFS&request=GetCapabilities), we have to load target schema for transboundary catchment scenario in *.xsd format. Both schemas (source and target) can be seen in Fig.9. If you want to see your source data in Map Viewer, select File and Open Source Data from the toolbar.

The exploration of matching possibilities between the given dataset and INSPIRE hydrography schema revealed that four attributes have to be transformed. The remaining attributes of the source dataset are not needed and have to be excluded from the transformation process using INSPIRE Nil reason function.

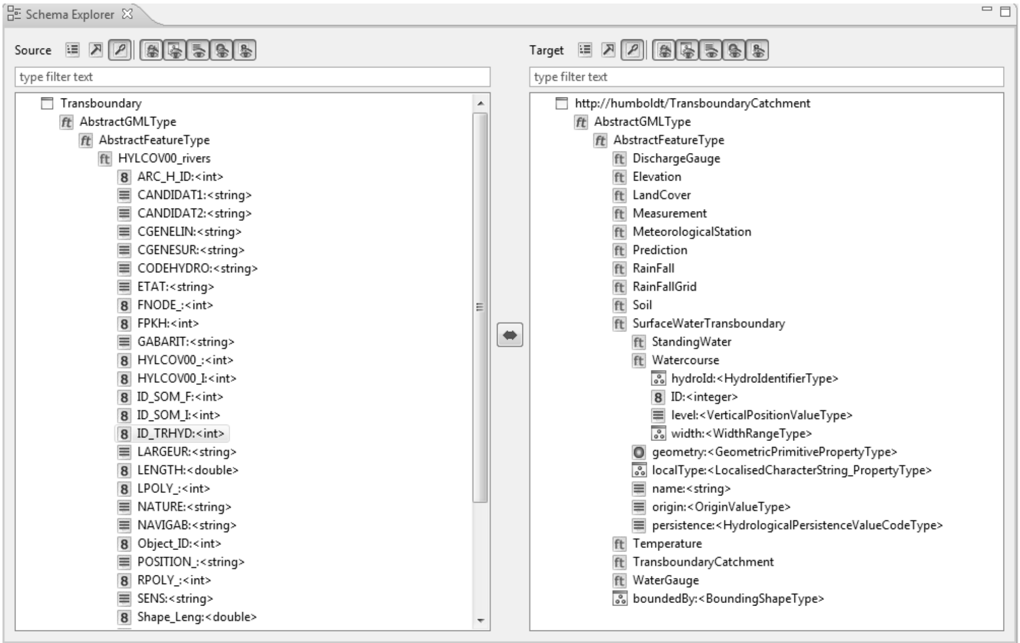

Fig 9: Source and Target schemas in HALE schema explorer

The attribute ID_TRHYD is equivalent to ID in INSPIRE schema (the target schema) (see Fig 9). We use „Rename function" for this transformation. The transformation is repeated for attributes LARGEUR (rename to WIDTH), NATURE (rename to ORIGIN) and POSITION (rename to LEVEL).

It is possible to review the results of your transformations within HALE in the Mapping window (Fig.10).

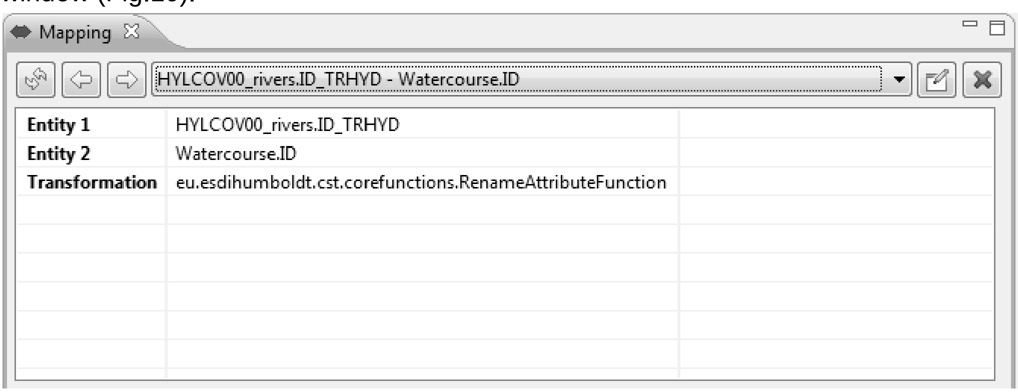

Fig10 Result of renaming function in HALE Mapping window

Next step is to classify some values inside attributes that are mandatory in the watercourse attribute subset of the INSPIRE schema. Classification mapping function allows to map values of a source attribute to fixed values of a target attribute (to reclassify values of a source attribute to the required values of the target). The relation is always a many to one relation, and each code from the source schema can only be mapped once. The function “Classification mapping” is applied to replace values in the attributes LARGEUR, NATURE and POSITION. Matching table can be seen in Table 6.

Table 6 Matching table

France	INSPIRE
LARGEUR 1: from 0 to 15m 2: from 15 to 50m 3: more than 50m	Width width=lower width=upper width=upper
NATURE NATURE=1 NATURE=3 or 4	Origin origin=natural origin=manmade
POSITION POSITION=2 POSITION=1 POSITION=3	Level level=SuspendedorElevated level=onGroundSurface level= underground

Now select both attributes, click the central arrow, and run the “Classification Mapping” function. Select value of target schema from the list and add old value from the source schema in Classification Mapping window. Classification Mapping window is shown in Fig.11. Repeat the procedure for all attributes which you need to classify. The results of classification mapping function can be revised in HALE Mapping window.

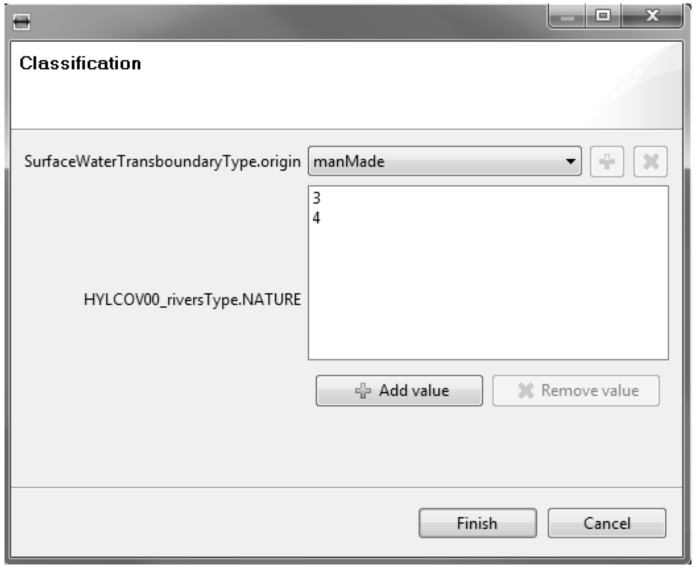

Fig 11: Classification mapping window

When we have no data for some attributes it is recommended to use „Attribute Default Value" function to fill the mandatory fields and „INSPIRE Nil reason“ function for optional attributes. The first function fill the whole attribute with a defined value. The later function sets the attribute unpopulated.

3. Saving the alignment project

After finishing all mappings it is necessary to save the alignment project. This saves an XML and a GOML file with the same name in the same directory or to an alternative mapping file and to an alternative place. GOML is required to make a corresponding data transformation.

Schema translation and transformation to the target schemas

The harmonised schema (described by HALE and saved in an OML file) is used by CTS to implement the required process. The Conceptual Schema Translation Service (CST) is a Web Processing Service for transforming data from one application schema to another (CST, 2010). Note that this tool is currently in testing phase. CST is Java library that is responsible for

- parsing and generating GML,
- parsing OML and
- execution of particular transformation of spatial features.

CST also provides WPS interface for executing the transformation. For this propose pyWPS library was reused where a Java – python binding represents a new contribution. CST internally uses GeoTools library for representing the feature model. CST -WPS provides OGC complaint WPS interface. For simple access to this interface there is also HTML Client (Fig. 12).

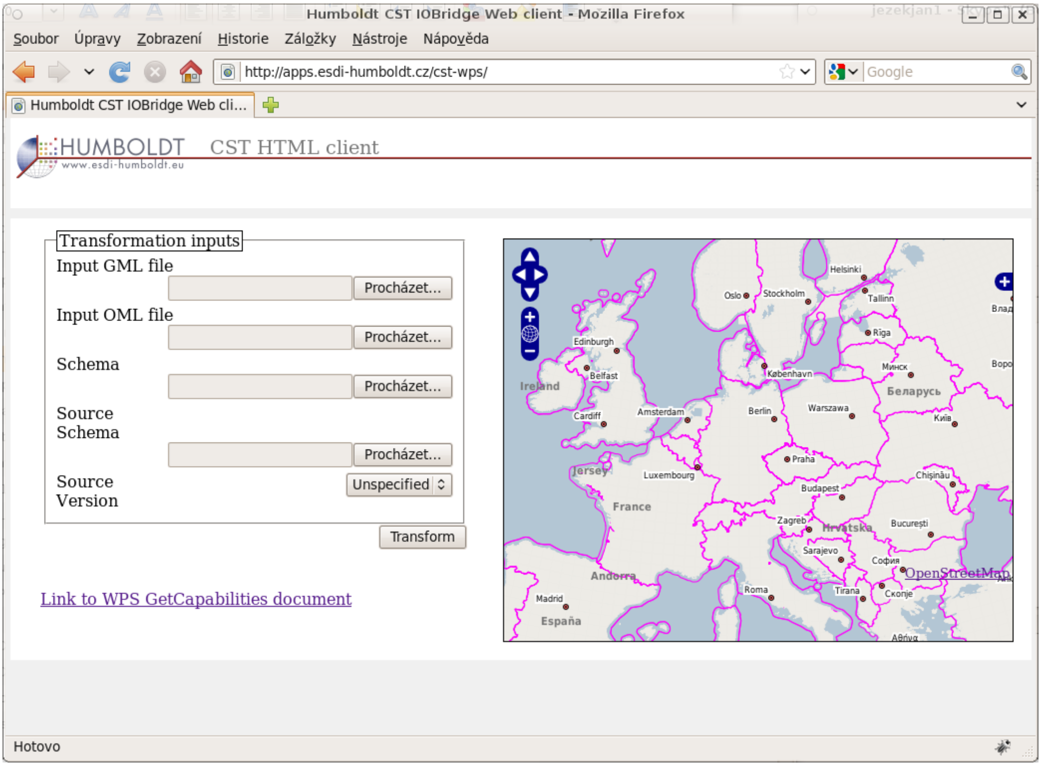

Fig 12: HTML client for WPS interface to CST

DISCUSSION AND CONCLUSION

The HUMBOLDT project contributes to the developments in data harmonisation using web tools and local designing tools, enabling appropriate transformation to create harmonised data sets. As discussed in the paper, such tools are critical for the current implementation phase of INSPIRE. Our experiments have shown that HALE and CST are very promising developments, which close a large gap in the market, i.e. conceptual schema mapping and automatic data transformation. As shows in our paper it is possible to design either one-side transformation (datasets from foreign country to match local datasets) or two-side transformation (where data from both countries are transformed into a common target schema) using HALE. The transboundary scenario is a good demonstration since many of the mentioned data sets are relevant for other cases and scenarios.

Nevertheless, some issues still obstruct full implementation of all proposed tools. One of these drawbacks in the INSPIRE implementation process is the requirement of GML 3.2.1 which is not widely adapted in current applications. Even more existing implementations of GML are not consistent. It may be a critical issue for the wide utilisation of the Humboldt framework.

The Humboldt project is not alone in the aim of facilitating data harmonisation. Standardization of relevant data structures is a subject of many projects. Another important European initiative is the WISE project (http://water.europa.eu/), which provides a repository for a wide range of GIS datasets. These datasets can be compiled by Member States for regulatory reporting as well as the WISE Reference GIS datasets. Information about the reference GIS datasets and data models for themes connected with EU water related directives can be found in documentation of this project namely guidance document No. 22. These data sets can also be used as target schemas when harmonising data sets.

Humboldt framework (based on web services) address successfully future system requirements, especially web portals. The group of water related web services is still growing. TRANSCAT Decision Support System T-DSS (Horak et al., 2006) was one of the first modular web application system build on open sources technologies aimed at water management and utilisation of hydrological modelling. The European project HarmonIT (Gijsbers et al., 2004) addressed issues of spatial and temporal scale differences, unit differences etc. They launched an Open Modelling Interface (OpenMI, http://www.openmi.org) enabling seamless interaction among modelling systems, the integration and combination of their functions. CUAHSI (the Consortium of Universities for the Advancement of Hydrologic Science) community provides a group of web services called WaterOneFlow. CUAHSI web services facilitate the retrieval of hydrologic observations information from online data sources using the SOAP protocol. CUAHSI WaterML is an XML schema defining the format of messages returned by the WaterOneFlow web services (Zaslavsky et al, 2007).

REFERENCES

Bedient, P. and Huber, W. (2001) Hydrology and floodplain analysis, 2nd edition, Prentice Hall, London, 763 pp.

Beven, K. (2002) Rainfall-runoff modelling, The Primer, John Wiley, London, 372 pp.

Blasby D., Davis M., Kim D., Ramsey P. (2004) GIS Conflation using Open Source Tools. A white paper of JUMP project. pp. 32. http://www.jump-project.org/assets/JUMP_Conflation_Whitepaper.pdf

Charvát K., Kocáb M., Konečný M., Kubíček P. (2007): Geografická data v informační společnosti. VÚGTK 2007, 269 pp. ISBN 978-80-85881-28-8.

CST (2010), Conceptual Schema transformer. http://agile2010.dsi.uminho.pt/pen/ShortPapers_PDF/112_DOC.pdf <On-line> Cited 30.10.2010.

EUREF (2010), the IAG Reference Frame Sub-Commission for Europe: http://www.euref.eu/. On-line. Cited 20.10.2010.

Fonseca F.T., Egenhofer M.J., Davis Jr. C. A., Borges K. A. V. (2000) Ontologies and Knowledge Sharing in Urban GIS, Computer, Environment and Urban Systems, vol. 24, pp. 251-271

Galdos Systems Inc.: GML Complexity. Pp.4, <On-line> http://www.galdosinc.com/archives/186, cit. 28.10.2010

Guidance Document No. 22 - Updated Guidance on Implementing the Geographical Information System (GIS) Elements of the EU Water legislation: http://circa.europa.eu/Public/irc/env/wfd/library?l=/framework_directive/guidance_documents&vm=detailed&sb=Title. Appendices to the guidance are available on EEA CIRCA at: http://eea.eionet.europa.eu/Public/irc/eionet-circle/eionettelematics/library?l=/technical_developments/wise_technical_group/updated_2ndedition/appendices_updated&vm=detailed&sb=Title

Horák J., Orlík A., Stromský J. (2008) Web services for distributed and interoperable hydro-information systems. Hydrol. Earth Syst. Sci., 12, 635-644. ISSN 1027-5606. http://www.hydrol-earth-syst-sci.net/12/635/2008/hess-12-635-2008.pdf

Horak J., Unucka J., Stromsky J., Marsik V., Orlik A (2006) TRANSCAT DSS architecture and modelling services. Control & Cybernetics, vol 35, No.1, Warsaw 2006, ISSN 0324-8569, 47-71.

Institut Géographique National (Ed.) (2002) BD CARTHAGE Version 3.0 - Descriptif de contenu (sphère eau), edition 1 (2002).

Lehto, L., 2007, Schema Translations in a Web Service Based SDI, 10th AGILE International Conference on Geographic Information Science 2007Aalborg University, Denmark,

Lehto, L. and T. Sarjakoski, 2004. Schema translations by XSLT for GMLencoded geospatial data in heterogeneous Webservice environment. Proceedings of the XXth ISPRS Congress, July 2004, Istanbul, Turkey, International Archives of thePhotogrammetry, Remote Sensing and Spatial Information Sciences, XXXV (B4/IV):177182, also CDROM.

Lutz M, and E. Klien (2006) Ontology-based retrieval of geographic information. International Journal of Geographical Information Science. Vol. 20, No. 3, March 2006, 233-260.

Maidment, D. (1993) Handbook of Hydrology, 1st edition, McGraw Hill Professional, London, 1424 pp.

Mitiku, A. B., (2009) Modelling of International Transboundary Catchment Area - Roya Basin and Its Data Harmonization Needs, Master thesis, University of Nice Sophia Antipolis. 104 p.

Národní geoinformační infrastruktura České republiky (2001) Program rozvoje v letech 2001-2005. NEMOFORUM, Praha. [on-line] http://www.cuzk.cz/GenerujSoubor.ashx?NAZEV=999-NGII

Nougeras-Iso, J., Medrano, P., Zarazaga-Soria, P. (2005) Geographic Information Metadata for Spatial Data Infrastructures, Springer, Boston.

Pauknerová, Tryhubová (2006) INSPIRE and geoinformation infrastructure in the CR. In Internet ve státní správě a samosprávě. Hradec Králové, 3-4.6.2006, VUGTK.

Reitz, T. (2010a) HUMBOLDT Alignment Editor Manual 2.0.M2. <On-line>

http://community.esdi-humboldt.eu/attachments/72/alignment_editor_manual_2010-03-31-M2.pdf

Reitz, T., (2010b) A Mismatch Description Language for Conceptual Schema Mapping and its Cartographic Representation, Proceedings of the 6th GIScience Conference, Zürich: 2010.

Reitz T. and A. Kuijper, (2009) Applying Instance Visualisation and Conceptual Schema Mapping for Geodata Harmonisation, Advances in GIScience, 2009, S. 173-194.

Sheth A (1999) Changing focus on interoperability in information systems: from system, syntax, structure to semantics. In M.F. Goodchild, M. Egenhofer, R. Fegeas and C.A. Kottman (Eds), Interoperating Geographic Information Systems, pp. 530 (Dordrecht, Netherlands: Kluwer Academic).

Stuckenschmidt H. (2003) Ontology-Based Information Sharing in Weakly Structured Envirnoments. PhD thesis, Vrije Universiteit Amsterdam.

Šeliga M., Růžička J. (2005) Geoinformation systems and web services. Acta Montanistica Slovaca. 2/2005, Technical University of Kosice, the Faculty of Mining, Ecology, Process Control and Geotechnologies (F BERG), Košice 2005, ISSN 13351788. p. 206-212

Vaccari L., Shvaiko P., Marchese M. (2009) A geo-service semantic integration in Spatial Data Infrastructures. International Journal of Spatial Data Infrastructures Research, 2009, vol.4, 24-51.ISSN 1725-0463.

Vries, de, M., Giger, Ch., Iosifescu, I., Laurent, D., Althoff, J.S. (2010) A7.0 D1 Concept of Data Harmonisation Processes. HUMBOLDT project deliverable.

Zaslavsky, I., Valentine, D., Whiteaker, T. (Ed.) (2007) CUAHSI WaterML, Open Geospatial Consortium Inc. http://portal.opengeospatial.org/files/?artifact_id=21743

Author Index

Subject Index

GIS Ostrava 2011

- Advances in Remote Sensing
- Advances in Spatial Modelling
- Geoinformation Technologies Challenges
- Harmonization and Integration Tools supporting INSPIRE implementation

GIS Ostrava 2011 was the 18th event of the series of conferences and symposia held in Ostrava in the fields of geographical information systems, geoinformatics, geomatics, remote sensing and spatial modelling. The aim of the symposia is to provide an international forum for presenting and discussing results of the latest research. The symposium was organised in four main research workshops, a national application session and accompanying events.

ISBN 978-80-248-2406-2

ISBN 978-80-248-2406-2
9 788024 824062 >